Application of Polyacrylamide Gel Electrophoresis for Analysis of Oligopeptide Phosphorylation *In Vitro*

Phosphorylation of synthetic peptides is widely performed in many laboratories for the *in vitro* assay of protein kinases. Most of the assays are based on the incorporation of [γ-^{32}P]ATP into the peptide substrates. In order to detect the incorporated radioactivity, separation of the residual, free [γ-^{32}P]ATP from the generated phosphopeptides is required. Usually a negatively charged phosphocellulose paper is used for separation, as it binds positively charged peptides. Several pitfalls of this method have been reported in the literature. For example, negatively charged peptides do not bind to the phosphocellulose paper at all, and the binding efficiency of oligopeptides with a weak positive charge is insufficient for measuring the peptide phosphorylation. Additionally, oligopeptides with the same net charge differ in their degree of phosphocellulose binding, precluding precise comparative studies. It is generally accepted that the presence of two amino acids with positive charges assures binding. In many proteins, functionally important sequences do not have positively charged amino acids at all. The introduction of additional positively charged amino acids to enhance the binding to phosphocellulose may result in unpredictable conformational changes and could generate false data, especially when short peptides are used as substrates. These problems in analysis of phosphopeptides have been widely discussed (1,3) but have not been eliminated yet.

A polyacrylamide gel electrophoresis (PAGE) system has been used successfully for phosphopeptide mapping (6) and separation of peptides for sequencing (2). Here we report that this method, with a few practical modifications, will circumvent all of the problems resulting from charge and possible conformational changes referred to above, and will allow quantitative stud-

Table 1. The Amino Acid Sequence and the Position of the ζ-Derived Oligopeptides

	Position Within the Zeta Chain	Amino Acid Sequence
p1	ζ[61–67]	PPAYQQG
p2	ζ[69–75]	NQLYNEL
p3	ζ[80–86]	REEYDVL
p4	ζ[106–113]	QEGLYNEL
p5	ζ[119–126]	AEAYSEIG
p6	ζ[138–144]	DGLYQGL
p7	ζ[149–155]	KDTYDAL

The peptides were synthesized by the solid-phase technique and were purified by semipreparative reversed-phase HPLC.

ies of peptide phosphorylation.

The $p56^{lck}$ tyrosine kinase-generated phosphorylation patterns of seven oligopeptides (Table 1), derived from the ζ chain of the T-cell receptor complex, have been studied. Two peptides (p3 and p7) had only one basic amino acid, while the other five (p1, p2, p4, p5 and p6) had none. Six of the seven sequences (p2–p7) are evolutionarily conserved and located in functionally important protein motifs (5).

The $p56^{lck}$ kinase was immunoprecipitated from a human leukemic T-cell line, HPB-ALL. The cells (2×10^7) were washed with phosphate-buffered saline (PBS) and solubilized in 1 mL of kinase lysis buffer (50 mM HEPES pH 7.4, 150 mM NaCl, 20 mM NaF, 200 μM sodium orthovanadate, 1% Triton® X, 1 mM PMSF [phenylmethylsulfonyl fluoride] and 10 μM leupeptin). Immunoprecipitation from postnuclear supernatants was carried out with 10 μL of Protein A Sepharose® CL-4B beads (Pharmacia Biotech, Uppsala, Sweden) coated with 5 μg per sample of a rabbit polyclonal antibody to $p56^{lck}$. The polyclonal antiserum to $p56^{lck}$ was generated in rabbit using the $p56^{lck}$[39-64] oligopeptide coupled to a branched oligolysine carrier, and the immunoglobulin fraction of the antiserum was purified by MAbTrap™ G (Pharmacia Biotech). The immunocomplex was washed twice with kinase lysis buffer and twice with a kinase assay buffer (25 mM HEPES pH 7.4, 100 mM

NaCl, 10 mM $MgCl_2$, 5 mM $MnCl_2$ and 100 μM sodium orthovanadate), and used as a source of kinase in the peptide phosphorylation assay. Stock solutions (15 mM) of peptides were prepared in DMSO, as this solvent was the most efficient in dissolving the peptides and did not affect the kinase reaction in the assay (data not shown). For each sample, the reaction mixture of the *in vitro* phosphorylation assay contained the immunoprecipitated kinase, 20 μL of kinase assay buffer supplemented with 1 μM dithiothreitol (DTT), 1 μL of peptide stock solution and 1 μCi of [γ-^{32}P]ATP (Izinta, Budapest, Hungary). The reaction was carried out at 37°C for 20 min and stopped by cooling the mixture on ice. A two-fold-concentrated peptide sample buffer (250 mM Tris pH 6.8, 12 M urea) was warmed up to 80°C, and 20 μL were added to each sample. The gel was prepared and run as described by West et al. (6) with slight modifications as follows. The gel was 1 mm thick, the stacking gel (3.3% acrylamide, 0.16% bis-acrylamide, 0.125 M Tris-HCl pH 6.8, 0.05% TEMED [*N,N,N′,N′*-tetramethylethylenediamine], 6 M urea, 0.1% ammonium persulfate) was 2 cm long and the resolving gel (40% acrylamide, 0.037% bis-acrylamide, 0.75 M Tris-HCl pH 8.8, 0.035% TEMED, 0.1% ammonium persulfate) was 14 cm long. The reservoir buffer was composed of 0.05 M Tris base and 0.4 M glycine. Electrophoresis was carried out at 10 mA and was stopped when the bromophenol blue tracking dye had migrated 9 cm from the top of the resolving gel (about 12 h). The gel was then soaked in 30% formaldehyde solution for 1 h to fix the peptides. Finally the gel was dried in acetone for 6 h, which caused a slight shrinkage of the gel and resulted in sharper bands than the conventional vacuum drying (4). The dried gel was autoradiographed for 12 h.

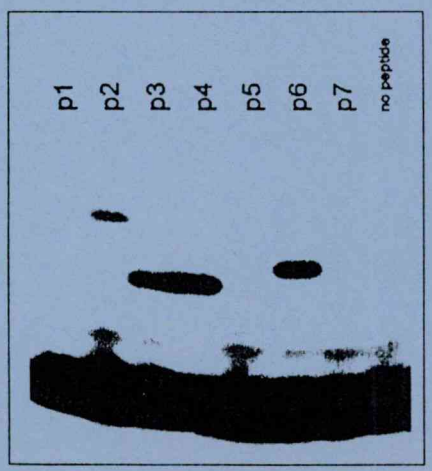

Figure 1. *In vitro* phosphorylation of ζ-derived oligopeptides by p56^{lck}. *In vitro* peptide phosphorylation and PAGE were carried out as described in the text. The oligopeptide substrates used in the individual samples are indicated on the top of the gel.

As shown in Figure 1, six peptides (p2–p7) were phosphorylated by p56^{lck}, while p1 was not. The phosphorylation pattern obtained agrees well with the data published on the function of the six conserved tyrosine residues of the ζ chain (5), which indicates that this method is suitable for phosphorylation studies of functionally important peptide sequences.

The procedure described here allows the analysis of the *in vitro* phosphorylation of very short synthetic oligopeptides without the prior modification of the original sequences and overcomes the limitations imposed by the use of phosphocellulose paper. Additionally, a quantitative estimate of the phosphorylated peptides can be carried out by using a phosphor imager or by counting the gel bands containing the phosphopeptides in a liquid scintillation counter. Due to the simplicity and sensitivity of this *in vitro* peptide phosphorylation assay and polyacrylamide gel electrophoresis system, we recommend its use for the comparative studies of potential phosphorylation sites of proteins.

REFERENCES

1. **Casnellie, J.E.** 1991. Assay of protein kinases using peptides with basic residues for phosphocellulose binding, p. 115-120. *In* T. Hunter and B.M. Sefton (Ed.), Methods in Enzymology, Vol. 200. Academic Press, New York.
2. **Dadd, A.C., R.G. Cook and D.C. Allis.** 1993. Fractionation of small tryptic phosphopeptides by alkaline PAGE followed by amino acid sequencing. BioTechniques *14*:266-273.
3. **Toomik, R., P. Ekman and L. Engstrom.** 1992. A potential pitfall in protein kinase assay: Phosphocellulose paper as an unreliable adsorbent of produced phosphopeptides. Anal. Biochem. *204*:311-314.
4. **Turner, R.J., D.E. Taylor, R.A. Rothery and J.H. Weiner.** 1993. Easy method for SDS-PAGE gel drying and preservation. BioTechniques *14*:200-201.
5. **Weiss, A. and D.R. Littman.** 1994. Signal transduction by lymphocyte antigen receptors. Cell *76*:263-274.
6. **West, M.H.P., R.S. Wu and W.M. Bonner.** 1984. Polyacrylamide gel electrophoresis of small peptides. Electrophoresis *5*:133-138.

This work was supported by the grants OTKA 928, OTKA 5257, OTKA 2734, ETT T03/523 and EEC ERBCI PACT 92 3003.
Address correspondence to Zoltán Hegedûs, Institute of Genetics, Biological Research Center of Hungarian Academy of Sciences, h-6701 Szeged, POB-521, Hungary.

Received 25 October 1994; accepted 29 December 1994.

Z. Hegedûs, I. Andó, G.K. Tóth[1], G. Váradi[1] and É. Monostori
Biological Research Center of Hungarian Academy of Sciences
[1]A. Szent-Györgyi Medical University
Szeged, Hungary

1.2.

BIOCHEMICAL AND BIOPHYSICAL RESEARCH COMMUNICATIONS 242, 474–479 (1998)
ARTICLE NO. RC977989

Conformational Effect of Phosphorylation on T Cell Receptor/CD3 ζ-Chain Sequences

Ilona Laczkó,*[,1] Miklós Hollósi,† Elemér Vass,† Zoltán Hegedüs,‡ Éva Monostori,‡ and Gábor K. Tóth§

*Institute of Biophysics and ‡Institute of Genetics, Biological Research Center, H-6701 Szeged, P.O.B. 521, Hungary; †Department of Organic Chemistry, Eötvös University, H-1518 Budapest 112, P.O.B. 32, Hungary; and §Department of Medical Chemistry, Szent-Györgyi Medical University, H-6720 Szeged Dóm tér 8, Hungary

Received December 5, 1997

The effect of tyrosine-phosphorylation on the conformation of three tyrosine-based immunoreceptor activation motifs, ζ(69-86), ζ(106-126), and ζ(138-155), located in the T cell receptor/CD3 ζ-chain was investigated. Circular dichroism and Fourier-transform infrared spectroscopy of the nonphosphorylated and phosphorylated fragments gave evidence that phosphorylation can alter the secondary structure of the peptides. The most significant—α-helix to β-sheet—conformational change was observed in the case of the ζ(138-155) peptide sequence which may be relevant to recognition by Src homology 2 (SH2) domains of signaling proteins. © 1998 Academic Press

The ζ-chain of the T cell receptor (TCR)/CD3 complex plays a central role in the transduction of antigenic signal to the intracellular signaling pathway. Signaling through the ζ-chain is mediated by triplicate of conserved intracellular sequence motifs, termed Immunoreceptor Tyrosine-based Activation Motifs (ITAMs) with the following amino acid structure: $Y(X)_2I/L(X)_{7-8}Y(X)_2I/L$ (X designates various amino acids) [1-3]. Upon T cell activation the TCR ζ chain is phosphorylated on multiple tyrosine residues [4,5]. *In vitro* experiments revealed that the tyrosines within the ITAMs are phosphorylated by src family tyrosine kinases [6]. Subsequent transmission of the ligand-induced signal is thought to depend on the recognition of the phosphorylated tyrosines by distinct Src homology 2 (SH2) domains of signaling proteins [7]. The major SH2 domain containing protein that associates with the phosphorylated ζ polypeptide is the syk family tyrosine kinase, ζ associated protein 70 (ZAP-70). The two tandemly arranged SH2 domains in ZAP-70 couple to the two phosphorylated tyrosine (pY) residues within one ITAM oligopeptide and the specificity of this interaction is determined by the primary sequence around the phosphotyrosine [8]. It has been shown that both tyrosines in the ITAM must be phosphorylated to measure cooperative, high affinity binding to ZAP-70 [9].

Crystal structure analysis of the complex has revealed that the peptides are oriented roughly perpendicular to the plane of the binding site of SH2, resembling a two-pronged plug (the prongs being pY and the third hydrophobic residue after pY). To interact at both binding sites, the peptides adopt extended conformation [10,11]. That is, the phosphotyrosine- and the hydrophobic-binding pockets on SH2 define a common orientation and secondary structure for bound pY-containing peptides.

Earlier spectroscopic studies on shorter ζ-chain fragments, containing only one tyrosine, revealed that in most cases phosphorylation caused an increase of the β-sheet content [12]. In order to study the effect of tyrosine phosphorylation on the conformation of the longer fragments containing two tyrosine residues, a panel of nonphosphorylated ITAM sequences and also their phosphorylated derivatives were synthesized. The primary sequences and abbreviated name of the peptides are shown in Fig. 1. The secondary structure of the peptides was studied by circular dichroism (CD) and Fourier transform infrared (FTIR) spectroscopy. The main goal of these studies was to establish whether phosphorylation of the different ITAM oligopeptides results in conformational change that may regulate the association with distinct SH2 domain containing signaling molecules.

MATERIALS AND METHODS

Peptide Synthesis

The nonphosphorylated peptides were synthesized by solid-phase technique utilizing Boc chemistry [13]. Side chain protecting groups

[1] Corresponding author. Fax: 36-62-433-133. E-mail: laczko@nucleus.szbk.u-szeged.hu.

0006-291X/98 $25.00

ζ(69-86) H_3N-Asn-Gln-Leu-Tyr(1)-Asn-Glu-Leu-Asn-Leu-Gly-Arg-Arg-Glu-Glu-Tyr(2)-Asp-Val-Leu-NH_2

ζ(106-126) H_3N-Gln-Glu-Gly-Leu-Tyr(1)-Asn-Glu-Leu-Gln-Lys-Asp-Lys-Met-Ala-Glu-Ala-Tyr(2)-Ser-Glu-Ile-Gly-NH_2

ζ(138-155) H_3N-Asp-Gly-Leu-Tyr(1)-Gln-Gly-Leu-Ser-Thr-Ala-Thr-Lys-Asp-Thr-Tyr(2)-Asp-Ala-Leu-NH_2

FIG. 1. Primary sequences of synthesized ITAM peptides from human TCR/CD3 ζ-chain. Tyrosines were phosphorylated in the first (p1) or the second (p2) and both (p1,2) positions.

were as follows: Tos(Arg), Bzl(Thr, Ser), cHex(Glu, Asp), 2BrZ(Tyr) and 2CIZ(Lys). The peptide chains were elongated on p-methyl-benzhydrylamine resin (0.6-0.8 mmol/g) and the syntheses were carried out on an ABI 430 A automatic peptide synthesizer. Couplings were performed with dicyclohexylcarbodiimide (DCC) with the exceptions of Asn, Gln and Arg which were incorporated as their HOBt esters. The completed peptide resins were treated with liquid hydrogenfluoride (HF)/dimethyl sulphide/p-cresol/anisole/p-thiocresol (93:4:1:1:1, vol/vol) on 0°C, 1h. HF was removed and the resulted free peptides were solubilized in 10% aqueous acetic acid, filtered and lyophilized.

The phosphotyrosine containing peptides were synthesized by SPPS-Fmoc methodology. Side chain protecting groups were as follows: Pmc(Arg), Bu^t(Ser, Thr), OBu^t(Glu, Asp) and Boc(Lys). The phenolic hydroxyls of the tyrosine residues were unprotected. The peptides were prepared on trimethyl-benzhydrylamine resin (0.6 mmol/g). After the incorporation of the tyrosine these hydroxyls were phosphitylated using di-tert. butyl-N,N diethyl-phosphoramidite, the latter was prepared in our laboratory from PCl_3, diethylamine and tert. butanol as described [14]. After the oxidation of the phosphite to phosphate using tert. butylperoxide the elongation of the peptide chain was completed. The incorporation of the phosphate moiety was verified by UV spectroscopy. The phosphorylation caused a 10 nm hypsochromic effect on the 278 nm band in the UV spectra recorded during HPLC by using a Hewlett-Packard diode array detector [15]. The phosphopeptide was detached from the resin using trifluoroacetic acid (TFA)/dichloromethane/anisole (62:30:8, vol/vol), on 0°C, 1h and the resulting free peptides were precipitated with diethylether, filtered, dissolved in water and lyophilized.

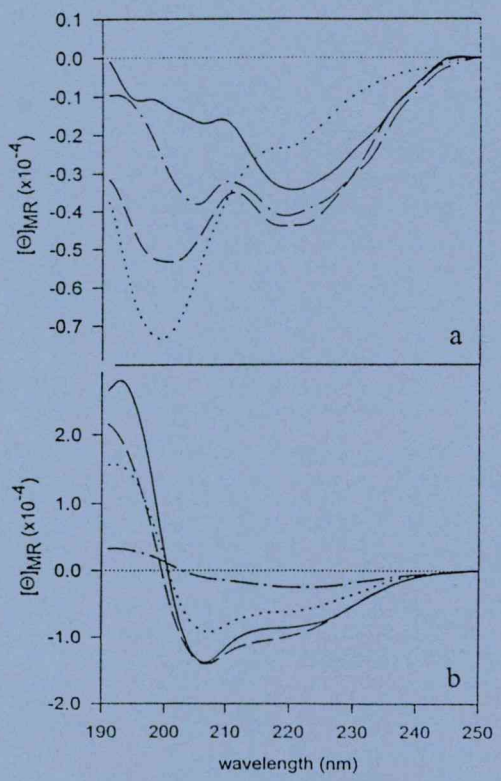

FIG. 2. CD spectra of ζ(69-86)np (· · ·), ζ(69-86)p1 (—), ζ(69-86)p2 (---) and ζ(69-86)p1,2 (-·-) in water (a) and in TFE (b).

TABLE 1

Percentages of Secondary Structural Elements of ITAM Sequences Received from the Deconvolution of the CD Spectra by the Provencher and Glöckner Method [13]

Peptide	α-Helix	β-Sheet	Unordered
ζ(69–86)np	22 (5)	54 (54)	24 (41)
p1	38 (0)	52 (79)	10 (30)
p2	34 (0)	50 (67)	15 (33)
p1,2	0[a] (0)	60[a] (68)	40[a] (32)
ζ(106–126)np	67 (10)	25 (40)	8 (50)
p1	62 (7)	31 (44)	7 (49)
p2	49 (8)	36 (42)	15 (50)
p1,2	60 (7)	30 (40)	10 (52)
ζ(138–155)np	72 (9)	16 (29)	12 (61)
p1	27 (0)	56 (51)	17 (49)
p2	17 (0)	55 (53)	28 (47)
p1,2	0[a] (0)	59[a] (49)	41[a] (51)

Note. In parenthesis: the secondary structure in water.
[a] Deconvolution procedure is not reliable due to the small band intensities caused by aggregation.

Peptide purification. The crude peptides were purified by reverse-phase HPLC on a Lichrosorb RP-18 10 μ column (16×250 mm) using a Knauer HPLC apparatus. The solvent system used was as follows: A: 0.1% TFA in water; B: 0.1% TFA+80% AcN in water; gradient: 0→60% B in 1.5 h; flow rate 3ml/min. The appropriate fractions were pooled and lyophilized. Purity was checked by RP-HPLC. Analytical HPLC investigations were performed on a Vydac C18 column (4×250 mm) at a flow rate of 0.8 ml/min with detection at 220 nm. The solvent system used was as follows: A: 0.1% TFA in water; B: 0.1% TFA+80% AcN in water; gradient: 0→30% B in 20 min.

Peptide characterization. The purified peptides were characterized by mass spectrometry using a Finnigan TSQ 7000 tandem quadrupole mass spectrometer equipped with an electrospray ion source. The calculated and measured masses were in good agreement.

Circular Dichroism

CD spectra were measured by a Jobin-Yvon Mark VI dichrograph. Measurements were carried out at 25°C in water and trifluoroethanol (TFE) in a stoppered optical cell with a path length of 0.02 cm. The peptide concentration was 0.5 mg/ml. Mean residue ellipticity $[\Theta]_{MR}$ was expressed in degrees.cm^2.$dmol^{-1}$, using a mean residue weigth of 110. Percentages of secondary structures were calculated by the Provencher and Glöckner curve analysing algorithm [16].

Infrared Spectroscopy

Fourier transform infrared measurements were performed in TFE on a Bruker IFS-55 FTIR spectrometer at a resolution of 2 cm^{-1} using a 0.02 cm cell with CaF_2 windows. The amide I region of the spectra was decomposed to individual bands by the Levenberg-Marquardt nonlinear curve fitting method using weighted sums of Lorentz and Gauss functions. The choice of starting parameters was

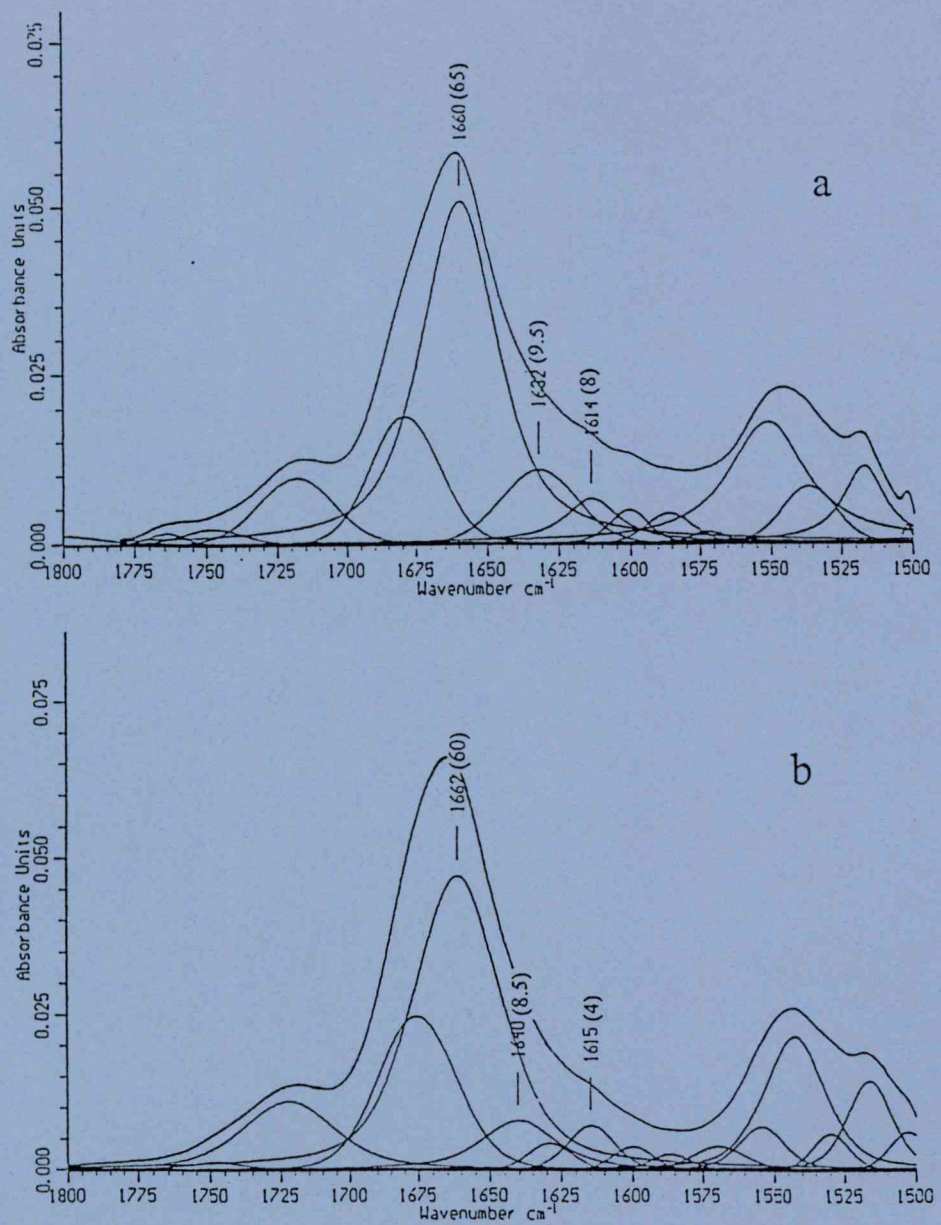

FIG. 3. FTIR spectra of ζ(69-86)np (a), ζ(69-86)p1 (b), ζ(69-86)p2 (c), and ζ(69-86)p1,2 (d) in TFE. In parenthesis: relative intensities percentages.

isted by Fourier self-deconvolution (FSD) [17]. Since the peptides re eluted with a solvent mixture containing TFA, all peptides re present as trifluoroacetate salts. Thus, in the FTIR spectra the nponent at ~1675 cm^{-1} can be correlated with ν_{as} (COO^-) vibra- of TFA [18]. But this band is also contributed by the ν_{as} vibration he guanidinium group of Arg [19].

SULTS

69-86)

The *CD spectra* of the parent and phosphorylated ptides in water and TFE are shown in Fig. 2. In ter, the nonphosphorylated (np) peptide is present in a predominantly random or aperiodic conformation, however, upon phosphorylation of the tyrosine in one (p1 or p2) or both (p1,2) positions the CD spectra show a substantial contribution of β-sheet structures in addition to aperiodic conformation (Fig. 2a). We have to note that the negative contribution of β-sheet (and α-helix) conformation is suppressed by the positive CD band (~225 nm) of the phenolic group of tyrosine. The highest percentage of extended structure was calculated for ζ(69-86)p1 (Table 1).

TFE is well known to have an α-helix or more precisely intramolecular H-bond promoting effect. In this solvent, ζ(69-86)np gave a helical CD spectrum with

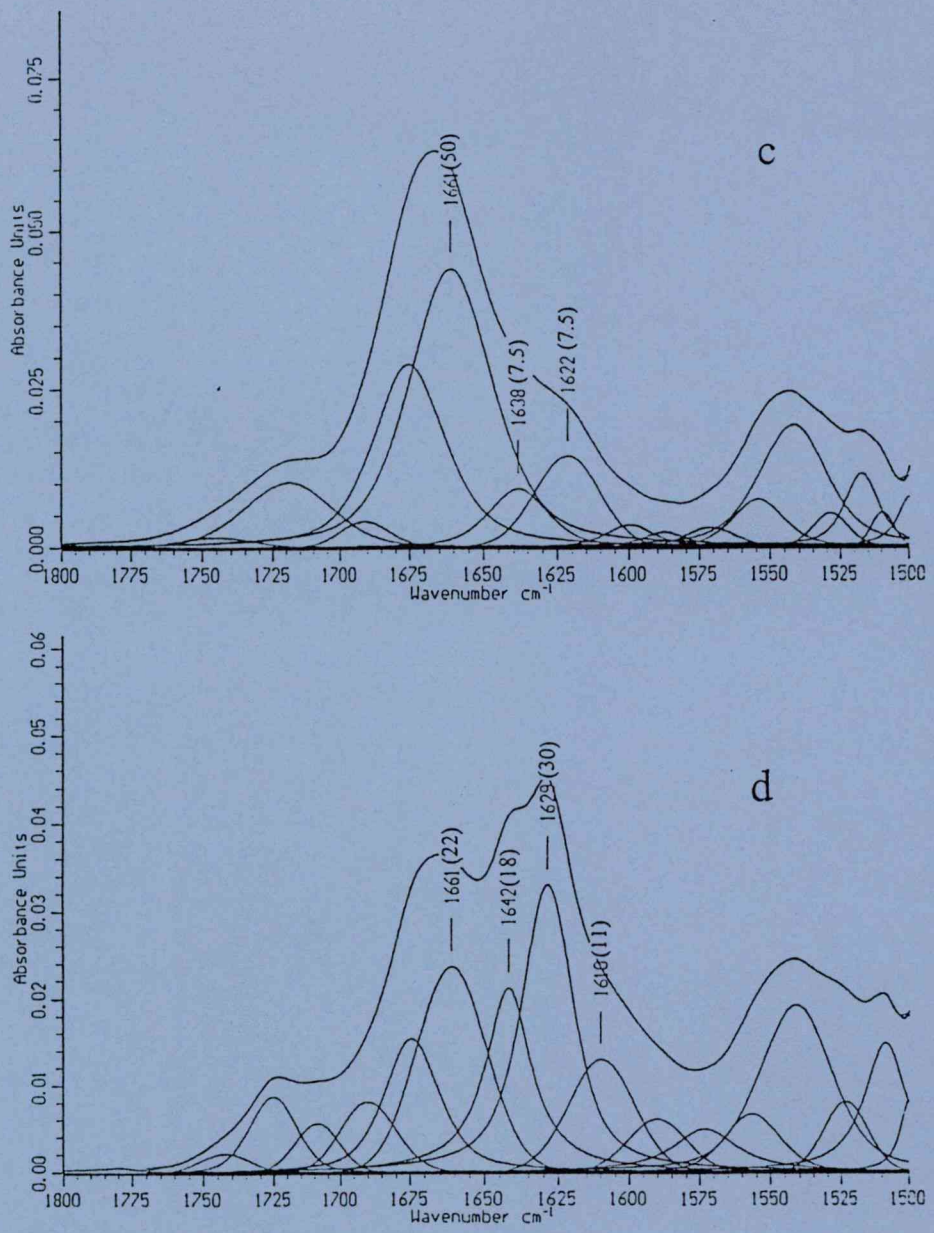

FIG. 3—*Continued*

relatively low intensity bands (Fig. 2b): the curve analysing method resulted in 22% α-helix, 54% β-sheet and 24% unordered conformation (Table 1). In the case of monophospho-derivatives, the increased intensity of the positive and negative bands corresponds to a higher amount of helical conformers. The data in Table 1 show that this increase in the α-helix content occured at the expense of unordered conformation, while the β-sheet content did not change significantly. Diphosphorylation of the peptide entirely changed the shape of the CD spectrum and the decomposition procedure reflected the absence of helical conformers and a considerable increase of aperiodic structures. The cloudy solution of ζ(69-86)p1,2 indicates the formation of aggregates from β-sheets which may account for the decreased band intensities (see also the CD spectrum of ζ(138-155)p1,2!).

FTIR spectra of the ζ(69-86) fragments were measured in TFE and are shown in Fig. 3 together with the characteristic amide I frequencies and their relative intensities received from the FSD-based curve fitting analysis. The bands between 1660 cm^{-1} and 1662 cm^{-1} can be assigned either to solvated aperiodic or weakly H-bonded α-helical peptide segments; these particular conformations cannot be distinguished on the basis of the infrared spectra in the amide I region alone. Comparison of the data of FTIR and CD measurements allows more reliable assignment. Hence, the higher in-

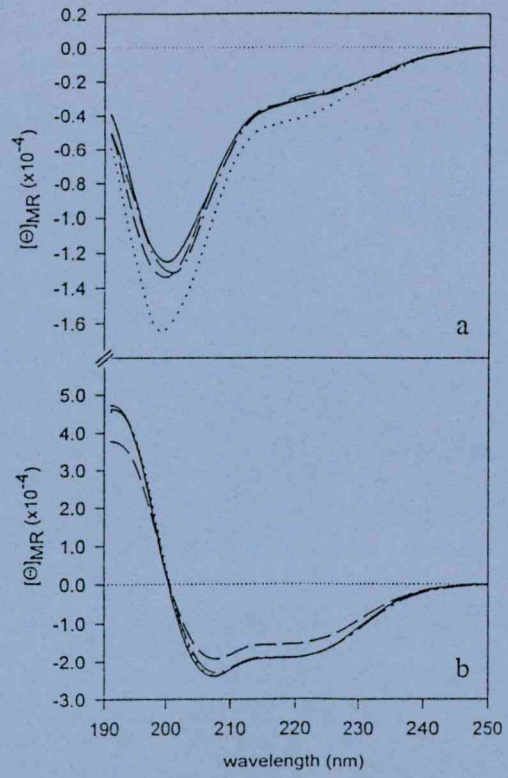

FIG. 4. CD spectra of ζ(106-126)np (· · ·), ζ(106-126)p1 (—), ζ(106-126)p2 (---), and ζ(106-126)p1,2 (-·-) in water (a) and in TFE (b).

tensity of 1660 cm^{-1} band of ζ(69-86)np relative to the monophosphorylated derivatives is due to the increased amount of the aperiodic conformation (calculated from CD spectra, Table 1), and in the case of ζ(69-86)p1,2 the much weaker component at 1661 cm^{-1} belongs to aperiodic rather than helical conformation. The components between 1638 cm^{-1} and 1642 cm^{-1} can be attributed to the acceptor C=O of H-bonded β-turns [20] predicted at the Tyr-Asn, Gly-Arg and Tyr-Asp dipeptide segments. The bands below 1629 cm^{-1} are indicative of the presence of β-sheet and β-aggregation: the differently positioned bands between 1610 and 1629 cm^{-1} reflect stronger and weaker intermolecular hydrogen bondings. The component at 1632 cm^{-1} in the spectra of ζ(69-86)np can be assigned to short extended segments that do not form sheets in a generally defined sense [21]. Based on the FTIR spectra, the double phosphorylated peptide forms the highest amount of β-sheet structure and aggregates which is in agreement with data obtained from CD measurements in TFE.

ζ(106-126)

In water, the peptide adopts unordered conformation irrespective of the absence or presence of phosphoryl group(s) on the tyrosine(s) (Fig. 4a) In TFE, the parent and phosphorylated ζ(106-126) peptides show helical CD spectra (Fig. 4b) with comparable band intensities. Spectral analysis in TFE indicated high amount of α-helix except for the peptide phosphorylated in p2 position, where a decreased helicity was accompanied with increased amount of β-sheet and unordered structures (Table 1). It is worth noting that in our previous study the corresponding phosphorylated shorter fragment, ζ(119-126) showed the highest β-sheet forming tendency [12]. A closer inspection of the primary structure of the ζ (106-126) peptide reveals that it contains amino acids in high percentage with strong α-helix forming potential especially between the $pY(X)_2L/I$ motifs. This may account for the high degree of helicity which is preserved in the phosphorylated forms of the peptide.

ζ(138-155)

As Fig. 5a and the data in Table 1 show, a considerable increase of β-sheet component and a simultaneous decrease of unordered structure is seen in water in the case of phosphorylated derivatives. In TFE, the non-phosphorylated peptide shows a high intensity helical spectrum (Fig. 5b). In contrast to ζ(69-86), selective phosphorylation of the peptide results in a decrease in the α-helix and a considerable increase in the β-sheet content. Phosphorylation of the peptide at both tyrosines caused a complete loss of α-helical conformation with concomitant increase of aperiodic structural elements, while the β-sheet content did not change sig-

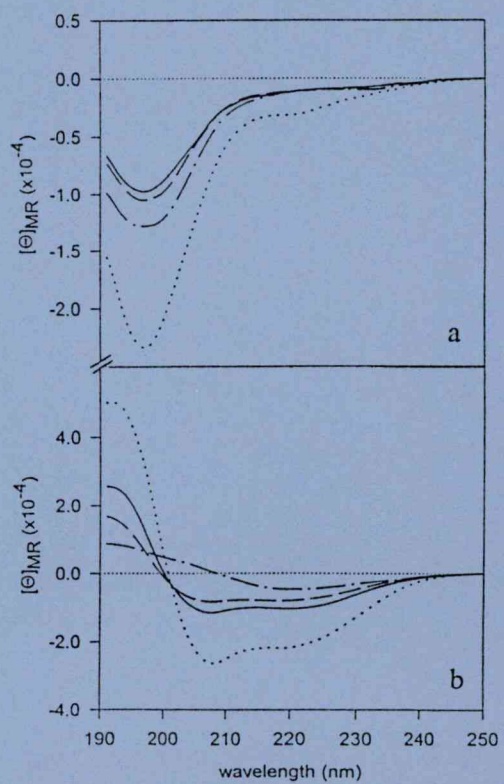

FIG. 5. CD spectra of ζ(138-155)np (· · ·), ζ(138-155)p1 (—), ζ(138-155)p2 (---), and ζ(138-155)p1,2 (-·-) in water (a) and in TFE (b).

nificantly compared to that of the monophosphorylated derivatives. Similar to ζ(69-86)p1,2, the cloudy solution of ζ(138-155)p1,2 indicates β-sheet and subsequent β-aggregate formation. FTIR studies of both the ζ(106-126) and ζ(138-155) peptides (spectra not shown) are in accordance with the CD measurements.

CONCLUSION

In *water*, all the three nonphosphorylated ITAM sequences, ζ(69-86), ζ(106-126) and ζ(138-155) are present as multicomponent mixtures of different conformers. No significant change was observed in the individual conformational elements upon phosphorylating the tyrosines in one or both positions within the ζ(106-126) sequence. Contrary to this, the ζ(69-86) and, in a less considerable extent, the ζ(138-155) fragment suffered an unordered to β-sheet conformational transition upon phosphorylation.

In *TFE*, the nonphosphorylated ζ(69-86)np contains the smallest percentage of α-helix, while the ζ(106-126)np and ζ(138-149)np are present in a predominantly helical conformation. The amount of this secondary structure is increased and more or less maintained in the phosphorylated derivatives of the ζ(69-86) and ζ(106-126) peptides, respectively. However, in the case of ζ(138-155) the phosphorylation events induced an α-helix to β-sheet conformational change either in water or in TFE and no significant differences were detected for the monophosphorylated fragments. As for the diphosphorylated derivatives, aggregation obscured the deconvolution procedure.

From the data presented here, it is obvious that out of the three ITAM sequences, the ζ(138-155) motif displays the most intense - an α-helix to β-sheet - conformational change upon phosphorylation. The relatively high β-sheet content of ζ(69-86)np is further increased upon phosphorylation. The lowest tendency to adopting β-sheet structure upon phosphorylation is shown by ζ(106-126)np.

Several intracellular signaling proteins (ZAP-70, Shc, $p59^{fyn}$ and PI3K subunit, p85) bind to the phosphorylated TCR ζ chain via their SH2 domains [2,22,23]. The binding of these molecules is determined by the primary sequence of the ITAMs and the position of the phosphotyrosine within the motifs [24,25]. The phosphorylation dependent conformational change of the ITAM sequences may be an important modulator of the molecular interactions. Therefore the findings presented in this paper may be of help in better understanding the molecular mechanism of interaction between the phospho-ITAMs and SH2 domain containing proteins.

ACKNOWLEDGMENTS

This work is supported by Hungarian Grants OTKA T0165116 (to I.L.) T017432 (to M.H.), T017838 (to É.M.), and 16156 and ETT672 (to G.K.T.).

REFERENCES

1. Reth, M. (1989) *Nature* 338, 383–384.
2. Iwashima, M., Irving, B., vanOers, N., Chan, A., and Weiss, A. (1994) *Science* 263, 1136–1139.
3. Howe, R., and Weiss, A. (1995) *Trends in Biol. Sci.* 20, 59–64.
4. Patel, M. D., Samelson, L. E., and Klausner, R. D. (1987) *J. Biol. Chem.* 262, 5831–5838.
5. Monostori, E., Desai, D., Brown, M. H., Cantrell, D. A., and Crumpton, M. J. (1990) *J. Immunol.* 144, 1010–1014.
6. Hegedüs, Z., Chitu, V., Tóth, G. K., Finta, Cs., Váradi, Gy., Andó, I., and Monostori, É. Submitted for publication.
7. Sadowski, I., Stone, J. C., and Pawson, T. (1986) *Molec. Cell Biol.* 6, 4396–4408.
8. Koyasu, S., Tse, A., Moingeon, P., Hussey, R., Mildonian, A., Hannisian, J., Clayton, L., and Reinherz, E. (1994) *Proc. Natl. Acad. Sci.* 91, 6693–6697.
9. Waksman, G., Kominos, D., Robertson, S. C., Pant, N., Baltimore, D., Birge, R. B., Cowburn, D., Hanafusa, H., Mayer, B. J., Overduin, M., Resh, M. D., Rios, C. B., Silverman, L., and Kuriyan, J. (1992) *Nature* 358, 646–653.
10. Waksman, G., Shoelson, S. E., Pant, N., Cowburn, D., and Kuriyan, J. (1993) *Cell* 72, 779–790.
11. Songyiang, Z., Shoelson, S., Chaudhuri, M., Gish, G., Pawson, T., Haser, W. G., King, F., Roberts, T., Ratnofsky, S., Lechleider, R. J., Neel, B. G., Birge, R. B., Fajardo, J. E., Chou, M. M., Hanafusa, H., Schaffhausen, B., and Cantley, L. C. (1993) *Cell* 72, 767–778.
12. Tóth, K. G., Laczkó, I., Hegedüs, Z., Vass, E., Hollósi, M., Janáky, T., Váradi, G., Penke, B., and Monostori, É. (1996) *in* Peptides in Immunology (Schneider, C. H., Ed.), pp. 223–230, Wiley, New York.
13. Merrifield, R. B. (1963) *J. Am. Chem. Soc.* 85, 2149–2154.
14. Perich, J. W., and Johns, R. B. (1988) Synthesis, Communications February, pp. 142–144.
15. Turck, C. W. (1992) *Peptide Research* 5, 156–160.
16. Provencher, S. W., and Glöckner, J. (1981) *Biochemistry* 20, 33–37.
17. Surewicz, W. K., and Mantsch, H. H. (1988) *Biochim. Biophys. Acta* 85, 115–130.
18. Holly, S., Majer, Zs., Tóth, G. K., Váradi, Gy., Rajnavölgyi, É., Laczkó, I., and Hollósi, M. (1993) *Biochem. Biophys. Res. Commun.* 193, 1247–1254.
19. Venyaminov, S. Y., and Kalnin, N. N. (1990) *Biopolymers* 30, 1243–1257.
20. Mantsch, H. H., Perczel, A., Hollósi, M., and Fasman, G. D. (1993) *Biopolymers* 33, 201–207.
21. Byler, M., and Susi, H. (1986) *Biopolymers* 25, 469–487.
22. Ravichandran, K. S., Lee, K. K., Songyang, Z., Cantley, L. C., Burn, P., and Burakoff, S. J. (1993) *Science* 262, 902–905.
23. Exley, M., Varticovski, L., Peter, M., Sancho, J., and Terhorst, C. (1994) *J. Biol. Chem.* 269, 1136–1139.
24. Osman, N., Lucas, S., and Cantrell, D. A. (1995) *Eur. J. Immunol.* 25, 2863–2869.
25. Osman, N., Turner, H., Lucas, S., Reif, K., and Cantrell, D. A. (1996) *Eur. J. Immunol.* 26, 1063–1068.

ELSEVIER

Immunology Letters 67 (1999) 31–39

Immunology Letters

Contribution of kinases and the CD45 phosphatase to the generation of tyrosine phosphorylation patterns in the T-cell receptor complex ζ chain

Zoltán Hegedûs [a], Violeta Chitu [a], Gábor K. Tóth [b], Csaba Finta [c], Györgyi Váradi [b], István Andó [a], Éva Monostori [a,*]

[a] *Institute of Genetics, Biological Research Center of Hungarian Academy of Sciences, PO Box 521, Temesvari krt. 62, Szeged H-6701, Hungary*
[b] *Department of Medical Chemistry, A. Szent-Györgyi Medical University, Szeged, Hungary*
[c] *Institute of Biochemistry, Biological Research Center of Hungarian Academy of Sciences, Szeged, Hungary*

Received 18 September 1998; received in revised form 26 October 1998; accepted 29 October 1998

Abstract

The ζ subunit of the T-cell receptor complex plays a crucial role in coupling the antigen binding αβ and γδ heterodimers to the downstream activation pathways. Three tandem amino acid sequence motifs containing pairs of exactly spaced Tyr-X-X-Leu/Ile sequences, designated as Immunoreceptor Tyrosine-based Activation Motifs (ITAMs), control this function. The phosphorylated forms of ITAMs serve as docking sites for several *src* homology 2 (SH2) domain containing signaling proteins. The composition of the assembled signaling complex and the outcome of cell activation depends on the tyrosine phosphorylation pattern of the ζ polypeptide. The mechanism that conducts the generation of various phosphorylated forms has not yet been well established. In this study we have analyzed the ability of *src* family tyrosine kinases and the CD45 tyrosine phosphatase in determining the phosphorylation state of the different ITAMs and the individual tyrosine residues of the TCR ζ chain. The intracellular part of the ζ chain was phosphorylated by *src* family tyrosine kinases, $p56^{lck}$ and $p59^{fyn}$ in vitro. Synthetic oligopeptides representing full-length or half-sized ITAMs with a single tyrosine residue were also phosphorylated by both $p56^{lck}$ and $p59^{fyn}$. In contrast, an additional membrane proximal tyrosine residue in the human ζ chain, located outside of the ITAMs, was not phosphorylated. We also examined the activity of the CD45 phosphatase, using a panel of ITAM derivatives, in which one or both tyrosines were phosphorylated. The efficiency of ITAM dephosphorylation by CD45 was dependent on the primary sequence of the oligopeptides and the position of the phosphotyrosine residues. The in vitro data suggest that the CD45 phosphatase rather than the tyrosine kinase(s) may control the generation of specific phosphorylation patterns of the ζ chain during cell activation.

Keywords: TCR ζ chain; ITAM; Lck; Fyn; ZAP70; CD45

Abbreviations: ATP, adenosine triphosphate; DTT, dithiotreithol; EDTA, ethylenediaminetetraacetic acid; FCS, fetal calf serum; GST, glutathione-*S* transferase; HPLC, high pressure liquid chromatography; ITAM, Immunoreceptor Tyrosine-based Activation Motif; MAP, multiple antigenic peptide; MHC, major histocompatibility complex; NEPHGE, non-equilibrium pH-gradient gel electrophoresis; PAGE, polyacrylamide gel electrophoresis; PMSF, phenylmethhylsulfonyl fluoride; RaMIg, rabbit immunoglobulin to mouse immunoglobulins; SDS, sodium dodecyl sulfate; SH2, *src* homology domain 2; TCR, T-cell receptor complex.

* Corresponding author. Tel.: +36-62-432232; fax: +36-62-433503; e-mail: monos@everx.szbk.u-szeged.hu.

1. Introduction

The TCR is a multimeric complex composed of the polymorphic, antigen binding αβ or γδ heterodimer and a set of invariant components, the TCR ζ chain and the CD3 γ, δ, and ε polypeptides destined for signal transmission [1]. Signaling through the CD3 and ζ chains is mediated by conserved intracellular sequence motifs, termed Immunoreceptor Tyrosine-based Activation

0165-2478/99/$ - see front matter
PII: S0165-2478(98)00138-2

Table 1
The sequence of the $\zeta^{(tc)}$ and the oligopeptide substrates used in the kinase reactions[a]

A

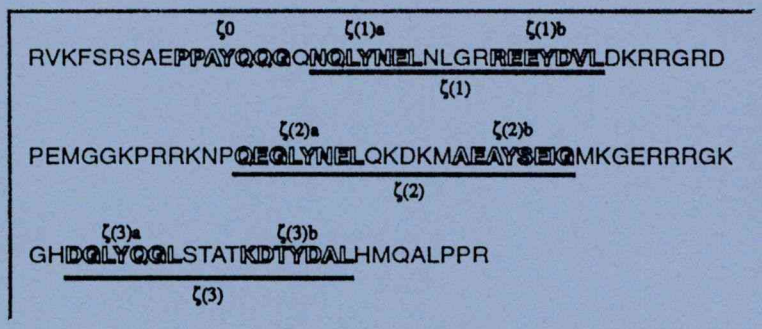

B

ζ0	ζ[61–67]
ζ(1)	ζ[69–86]
ζ(1)a	ζ[69–75]
ζ(1)b	ζ[80–86]
ζ(2)	ζ[106–126]
ζ(2)a	ζ[106–113]
ζ(2)b	ζ[119–126]
ζ(3)	ζ[138–155]
ζ(3)a	ζ[138–144]
ζ(3)b	ζ[149–155]

[a] The aminoacid sequence of the $\zeta^{(tc)}$ and the localization of the oligopeptide substrates. The three tandem ITAMs are underlined and marked as ζ(1), ζ(2), ζ(3). The seven synthetic oligopeptides representing the individual tyrosines of the ζ chain are indicated by using white characters and marked as ζ0, ζ(1)a, ζ(1)b, ζ(2)a, ζ(2)b, ζ(3)a, ζ(3)b. b, Position of the oligopeptide substrates within the ζ chain.

Motif (ITAM). All ITAMs contain two sequence elements (Tyr-X-X-Leu/Ile) with potential tyrosine phosphorylation sites which are separated by seven or eight variable amino acids [2]. The intracellular part of ζ chain contains three ITAMs [1,3] with six tyrosine residues. In addition to the tyrosines in ITAMs, the human ζ chain contains a membrane proximal tyrosine which lies outside of the motifs [4].

Stimulation of T lymphocytes via the TCR or several other cell surface receptors results in rapid phosphorylation of the tyrosines in the ζ chain [5,6]. Two dimensional NEPHGE/SDS-PAGE analysis of the phosphorylated murine and human ζ chains has revealed multiple proteins with molecular masses between 16 and 21 kDa which represent differently phosphorylated forms of the ζ polypeptide [7]. After site specific mutagenesis of any individual tyrosine residues of murine ζ protein phosphorylation of the ζ chain can still occur [8]. The phosphorylated polypeptide promotes the binding of *src* homology 2 (SH2) domain, bearing signaling proteins that are essential for further signal processing. Differently phosphorylated ζ ITAMs associate with distinct sets of proteins in vitro [9,10] and differ in function in vivo. For instance, TCR agonists and antagonists initiate different patterns of ζ chain phosphorylation, resulting in different downstream signals [11–13]. Furthermore, detergent-soluble and cytoskeleton associated TCRs contain differently phosphorylated ζ molecules [14,15].

Three protein tyrosine kinases (PTK) have been implicated in the earliest activation events in T cells: the *src* family kinases $p56^{lck}$ and $p59^{fyn}$, and the *syk* kinase ZAP70. It has been suggested that $p56^{lck}$ is the major tyrosine kinase that phosphorylates the TCR subunits in T lymphocytes in vivo [16,17]. However, both $p56^{lck}$ and $p59^{fyn}$ phosphorylate ζ polypeptide in vitro [18] and the ζ chain is weakly phosphorylated in peripheral T cells in $p56^{lck}$ deficient mice, indicating that another PTK, most likely $p59^{fyn}$, may phosphorylate TCR ζ chain [19]. The syk family kinase, ZAP70, becomes associated with the tyrosine phosphorylated invariant chains after TCR triggering via the tandem SH2 domains of the kinase [19]. After activation, ZAP 70 phosphorylates downstream effector proteins, such as SLP-76 [20,21], LAT [22]. The cytoskeletal protein, tubulin, has also been shown to be a substrate for ZAP70 in vitro [23].

Besides tyrosine kinases, the tyrosine phosphatase CD45 has been implicated in the regulation of ζ chain phosphorylation. It has been shown that the phosphorylated ζ chain is a specific, high affinity substrate for CD45 [24] and that the two molecules are physically associated in vivo [25].

The aim of this work was to analyze, in detail, the role of the tyrosine kinases and the CD45 phosphatase in regulating the phosphorylation pattern of the TCR ζ chain. We defined the target tyrosine residues for the $p56^{lck}$ and $p59^{fyn}$ kinases using substrates representing different parts of the ζ chain. Comparative analysis of the specificity of various kinases showed a similar phosphorylation pattern of the oligopeptide substrate panel. In contrast, in vitro dephosphorylation experiments revealed that the tyrosine phosphatase, CD45 can discriminate between the different phosphorylated derivatives of ITAMs.

2. Materials and methods

2.1. Cells and antibodies

The human T cell line, HPB-ALL, and the B cell line, Raji were cultured in RPMI 1640 (GIBCO) tissue cul-

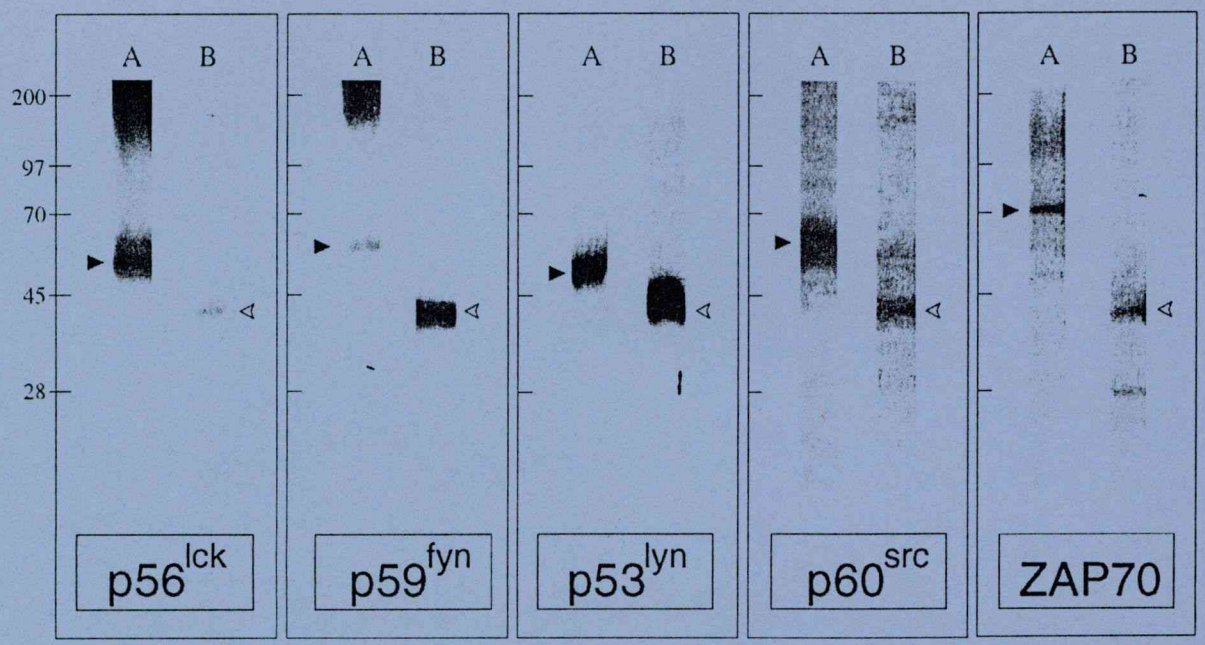

Fig. 1. Demonstration of the specificity of the different antisera and the activity of the immunoprecipitated kinases. $p56^{lck}$, $p53^{lyn}$, $p59^{fyn}$, $p60^{src}$, and ZAP70 kinases were immunoprecipitated and tested by autophosphorylation (A) and by phosphorylation the exogenous substrate, enolase (B). After the kinase reaction the proteins were resolved by SDS-PAGE under reducing (ZAP 70) or non reducing ($p56^{lck}$, $p59^{fyn}$, $p53^{lyn}$, $p60^{src}$) conditions. The molecular weight markers (kDa) and the positions of the different kinases (black arrowheads) and enolase (white arrowheads) are indicated.

Table 2
Sequence and designation of the synthetic phosphopeptide substrates.

ζ(1)y^Py	NQLY(P)NELNLGRREEYDVL
ζ(1)yy^P	NQLYNELNLGRREEY(P)DVL
ζ(1)y^Py^P	NQLY(P)NELNLGRREEY(P)DVL
ζ(2)y^Py	QEGLY(P)NELQKDKMAEAYSEIG
ζ(2)yy^P	QEGLYNELQKDKMAEAY(P)SEIG
ζ(2)y^Py^P	QEGLY(P)NELQKDKMAEAY(P)SEIG
ζ(3)y^Py	DGLY(P)QGLSTATKDTYDAL
ζ(3)yy^P	DGLYQGLSTATKDTY(P)DAL
ζ(3)y^Py^P	DGLY(P)QGLSTATKDTY(P)DAL

ture medium supplemented with 5% heat inactivated FCS (Gen-Inter). Polyclonal antisera were generated by injecting rabbits with branched multiple antigenic peptides (MAPs) [26] of the $p56^{lck}$ (39–64), $p59^{fyn}$ (20–48), and the ZAP70 (485–499) sequences. Immunoglobulin fractions of the antisera were purified by MAbTrap G (Pharmacia, Uppsala, Sweden). The polyclonal rabbit antibody against $p53^{lyn}$ and $p60^{src}$ was kindly provided by Dr René van Lier and was purchased from Oncogene Science, respectively. Monoclonal antibody to CD45, GB3 [27] and CD43, T2/53 [28] was developed in our laboratory. Rabbit immunoglobulin to mouse immunoglobulins (RaMIg) was purchased from DAKO.

2.2. Expression and purification of the intracellular part of the ζ chain as a glutathione- transferase fusion protein

Two synthetic oligonucleotides (5′-tttgcggccgcctggttcctcgtagagtgaagttcagcaggagc-3′ and 5′-aaagaattctgagtggtgaaatcccctggc-3′) were used in PCR with the cDNA of the human ζ chain [4] as a template. The 5′ oligonucleotide primer contained a *Not*I recognition site and sequences coding for the first four amino acids of a thrombin recognition sequence [29]. The resultant fragment coding for the intracellular domain of ζ chain($\zeta^{(ic)}$) was ligated in the *Not*I and *Eco*RI sites of pGEX-KN [30]. The recombinant GST/$\zeta^{(ic)}$ was overproduced in *E. coli* BL21 [31]. The induction and purification of the $\zeta^{(ic)}$ (Table 1) was done with a GST Purification Module (Pharmacia) according to the manufacturer's instructions.

2.3. Synthesis of ζ oligopeptides

The nonphosphorylated peptide substrates (Table 1) were synthesized by solid phase technique utilizing ^{t}Boc chemistry [32]. The peptides were purified by semipreparative reverse phase HPLC and were characterized by amino acid composition and mass spectrometry. The purity of the peptides was above 97% as determined by HPLC. The phosphorylated peptides (Table 2) were prepared using Fmoc [33] technique. The phosphate moiety was incorporated with di-tert. butyl-*N,N'* diethyl phosphoramidite method as described previously [34]. The isolation and characterization were carried out as described for nonphosphorylated peptides except that an additional capillary zone electrophoresis step was included.

2.4. Kinase autophosphorylation and phosphorylation of $\zeta^{(ic)}$ and enolase

The kinases were isolated from HPB-ALL or Raji cells (10^7/sample) by immunoprecipitation as described previously [35]. The autophosphorylation of the immunoprecipitated kinases was carried out in kinase assay buffer (25 mM HEPES pH 7.4, 100 mM NaCl, 10 mM $MgCl_2$, 5 mM $MnCl_2$, 100 μM sodium orthovanadate) containing [γ-^{32}P]ATP (10 μCi) for 10 min at 37°C. The presence of the autophosphorylated enzymes were analyzed using a 10% SDS-polyacrylamide gel. Phosphorylation of $\zeta^{(ic)}$ (1 μg) or enolase (5 μg) was performed under the same conditions for 10 and 45 min, respectively. After the kinase reaction the supernatants consisting the enolase or $\zeta^{(ic)}$ were separated from the immunoprecipitated kinases and were loaded onto SDS-polyacrylamide gel. 10% SDS-polyacrylamide gels were used for the separation of enolase and 15% SDS-polyacrylamide gels were used for the separation of $\zeta^{(ic)}$. The gels were incubated in 1 M KOH at 55°C for 1 h to decrease the unspecific background, then dried and analyzed by autoradiography or by using phosphoimager (Molecular Dynamics 445 SI).

2.5. Peptide phosphorylation assay

The oligopeptide substrates (15 nmol) were phosphorylated by immunoprecipitated kinases prepared as described previously [35]. The enzyme reaction was performed in 20 μl kinase assay buffer containing 1 μCi of [γ-^{32}P]ATP for 20 min at 37°C and was stopped by cooling the samples to 4°C. The phosphorylated peptides were separated in a 40% alkaline polyacrylamide gel [35]. The gel was dried and analyzed by autoradiography or by phosphoimager.

2.6. Immunoprecipitation of CD45 and phosphatase assay

HPB-ALL cells (1×10^7 cells/sample) were lysed for 1 h in ice cold lysis buffer (1% Triton X-100, 20 mM Tris pH 7.5, 150 mM NaCl, 1.0 mM EDTA) supplemented with 10 μg/ml aprotinin, 1 mM PMSF. Postnuclear supernatants were mixed with 10 μl protein

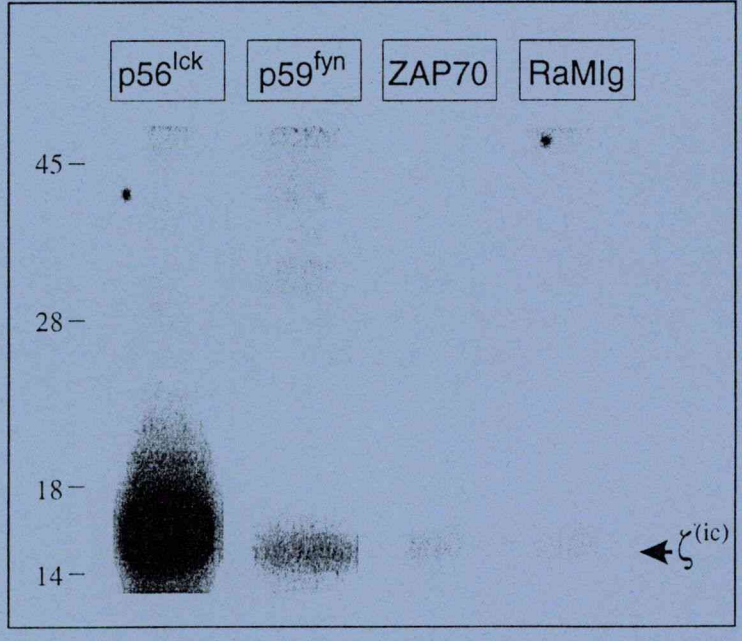

Fig. 2. In vitro phosphorylation of the $\zeta^{(ic)}$ by p56^{lck}, p59^{fyn}, and ZAP70 kinases. The phosphorylation of the $\zeta^{(ic)}$ was analyzed in the presence of immunoprecipitated p56^{lck}, p59^{fyn}, and ZAP70 kinases. RaMIg coated beads were used for controlling the nonspecific background of the kinase assay. After the enzyme reaction the samples were separated by SDS-PAGE. The position of the $\zeta^{(ic)}$ and the molecular weight markers (kDa) are indicated.

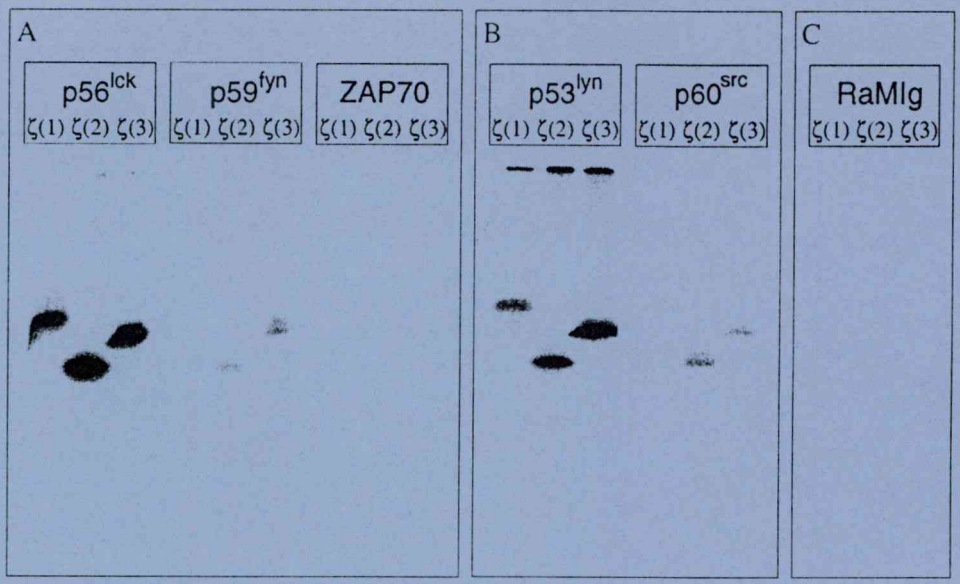

Fig. 3. In vitro phosphorylation of the oligopeptides representing the ITAMs of the ζ chain by $p56^{lck}$, $p59^{fyn}$, $p53^{lyn}$, $p60^{src}$, and ZAP70 kinases. The phosphorylation of the ζ(1), ζ(2), and the ζ(3), oligopeptides were analyzed in the presence of immunoprecipitated $p56^{lck}$, $p59^{fyn}$, and ZAP70 (A) or $p60^{src}$ and $p53^{lyn}$ (B) kinases. RaMIg coated beads were used for controlling the nonspecific background of the kinase reaction (C). The phosphorylated peptide substrates were separated in 40% alkalic acrylamide gels.

G-coupled sepharose beads (Pharmacia) precoated with 20 μg affinity purified anti CD45 mAb and incubated for 1 h at 4°C. The immunoprecipitates were washed two times in lysis buffer and once in phosphatase assay buffer (50 mM Hepes pH 7.0, KCl 100mM, 1% Triton X-100, 1 mM EDTA). The beads were incubated in 10 μl phosphatase assay buffer supplemented with 1 mM DTT and 2.5 nmols phosphopeptide for 1 h at 37°C. The supernatants of the reaction mixtures were transferred into the wells of a 96 well microtiter plate (Falcon) and the amount of the released inorganic phosphatase was determined according to D. H. Ng et al. [36] using malachit green reagent. To determine the amount of the released inorganic phosphate in the samples, we used a potassium dihydrogen phosphate (KH_2PO_4) standard curve in a range of concentration between 0 and 10 nmol.

3. Results

3.1. Phosphorylation of the tyrosine residues of the TCR ζ chain

The TCR ζ chain is phosphorylated on multiple tyrosine residues upon T cell stimulation and *src* family tyrosine kinases, $p56^{lck}$ and $p59^{fyn}$ have been implicated in this process [17]. To compare the specificity of different kinases in the phosphorylation of particular tyrosines of the ζ chain we have carried out in vitro phosphorylation experiments using immunoprecipitated enzymes as the source of kinase activity and substrates representing different parts of the ζ chain. Table 1 shows the ζ chain constructs used in this study: (1) sequence of the cytoplasmic tail of the protein, expressed as GST fusion protein; (2) synthetic ITAM fragments (underlined); (3) one tyrosine containing short oligopeptides (printed in blank). Specificity of the antibodies, used in this work and the activity of the immunoprecipitated enzymes were verified by auto- and enolase phosphorylation experiments (Fig. 1)

The $\zeta^{(ic)}$ derived from a GST fusion protein by thrombin digestion was applied as substrate. Although both $p56^{lck}$ and $p59^{fyn}$ phosphorylated this polypeptide (Fig. 2), $p56^{lck}$ resulted in a much higher phosphorylation of $\zeta^{(ic)}$ than $p59^{fyn}$ did. It was verified in other studies [23] that ZAP70 does not phosphorylate ζ chain therefore we used ZAP70 immunoprecipitate and RaMIg coated Protein-A-Sepharose beads as controls. There was a faint backround phosphorylation detected in both control samples (Fig. 2).

Next we investigated the phosphorylation of the oligopeptides corresponding to the ITAMs of the ζ chain. All ITAM-s (ζ(1), ζ(2), ζ(3)) were phosphorylated by the immunoprecipitates of $p56^{lck}$ and $p59^{fyn}$ (Fig. 3A) compared to the controls, ZAP 70 and RaMIg (Fig. 3C). Both $p56^{lck}$ and $p59^{fyn}$ phosphorylated all three ITAMs with similar patterns. The $p56^{lck}$ phosphorylated the ITAMs more strongly (similarly to ζ^{ic}) than $p59^{fyn}$ did. Two related *src* family kinases, $p53^{lyn}$ and $p60^{src}$, not involved in T cell signalling, were also investigated as to whether they phosphorylated the ζ oligopeptides. As shown on Fig. 3B, these enzymes produced a similar pattern of phosphorylation of the ITAMs as $p56^{lck}$ and $p59^{fyn}$.

To determine which tyrosine residues of the ζ chain were phosphorylated by the different tyrosine kinases, a panel of short oligopeptides containing individual intracellular tyrosines with the neighboring protein sequences were used as substrates. As shown in Fig. 4, six of the seven oligopeptides designated as ζ(1)a, ζ(1)b, ζ(2)a, ζ(2)b, ζ(3)a, and ζ(3)b (Table 1) were phosphorylated by *src* family member kinases, $p56^{lck}$, $p59^{fyn}$, $p53^{lyn}$, and $p60^{src}$, while the ζ0 oligopeptide remained unphosphorylated. The intensity of the phosphorylation obtained by the various enzymes was different, as $p56^{lck}$ gave a much stronger signal than $p59^{fyn}$ $p53^{lyn}$, and $p60^{src}$. When the ZAP70 immunoprecipitate was used, none of the oligopeptides were phosphorylated.

A cell free extract prepared from HPB-ALL cells was also used as a kinase source and the phosphorylation pattern of the short oligopeptides was similar to that obtained with *src* kinases (data not shown).

3.2. Dephosphorylation of the ζ chain by CD45

Differently phosphorylated forms of oligopeptides corresponding to the ITAMs of the ζ chain were synthetized and used as substrates for CD45. The sequence and the designation of the phosphopeptides are indicated in Table 2. The $\zeta(1)y^Py^P$ $\zeta(1)yy^P$, $\zeta(2)y^Py^P$, and $\zeta(2)yy^P$ peptides were the optimal substrates since they were completely dephosphorylated. The $\zeta(2)y^Py$ and $\zeta(3)y^Py^P$ ITAMs were poorer substrates for CD45 and the $\zeta(1)y^Py$, $\zeta(3)y^Py$, and $\zeta(3)yy^P$ were the least efficiently hydrolyzed phosphopeptides (Fig. 5). Using CD43 immunoprecipitate in the phosphatase assay as a

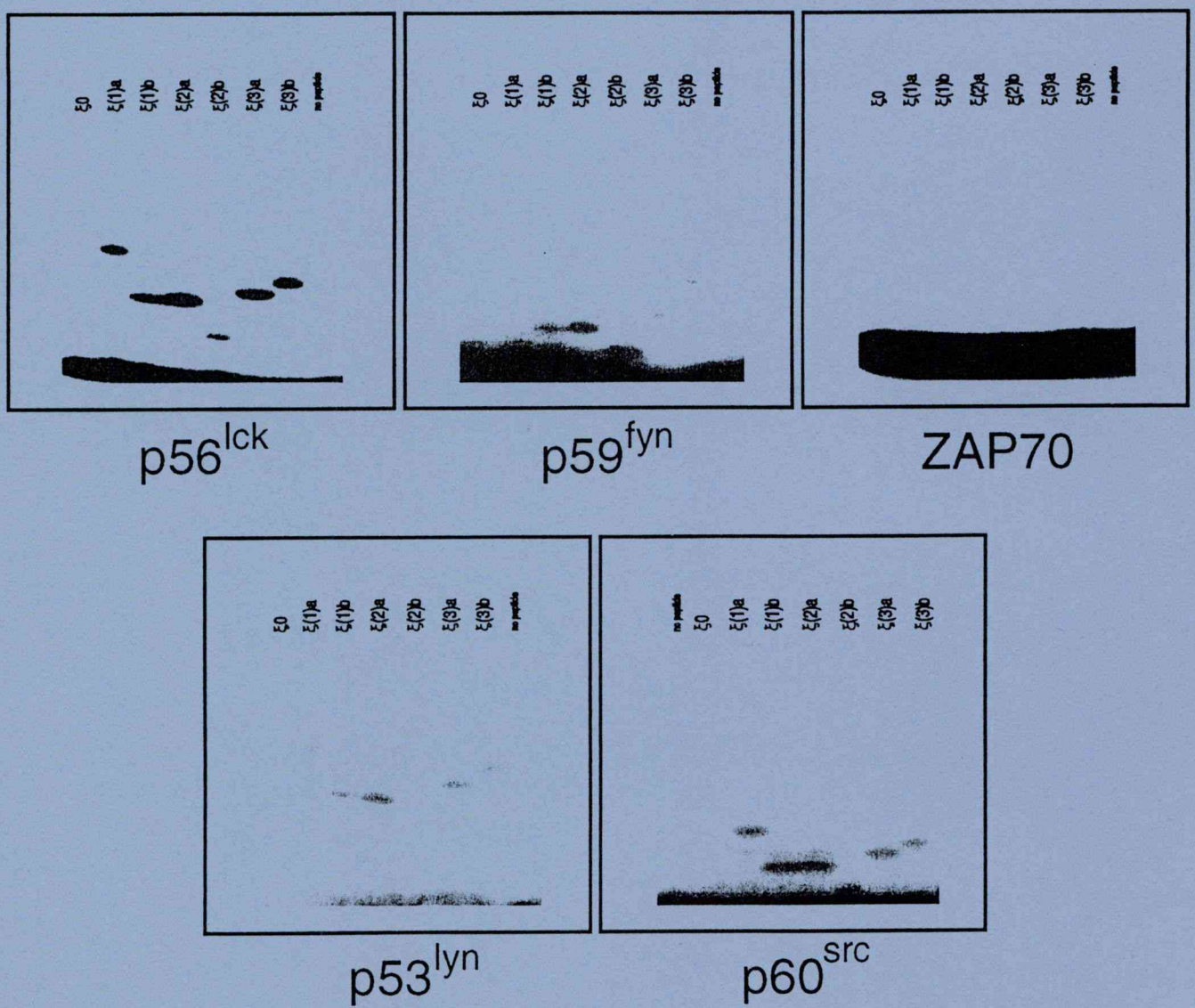

Fig. 4. In vitro phosphorylation of the short ζ oligopeptides by $p56^{lck}$, $p59^{fyn}$, $p53^{lyn}$, $p60^{src}$, and ZAP70 kinases. The phosphorylation of the ζ(1)a, ζ(1)b, ζ(2)a, ζ(2)b, ζ(3)a,. ζ(3)b, and the ζ0 oligopeptides were analyzed in the presence of immunoprecipitated $p56^{lck}$, $p53^{lyn}$, $p59^{fyn}$, $p60^{src}$, and ZAP70 kinases. The phosphorylated peptide substrates were separated in 40% alkalic acrylamide gels.

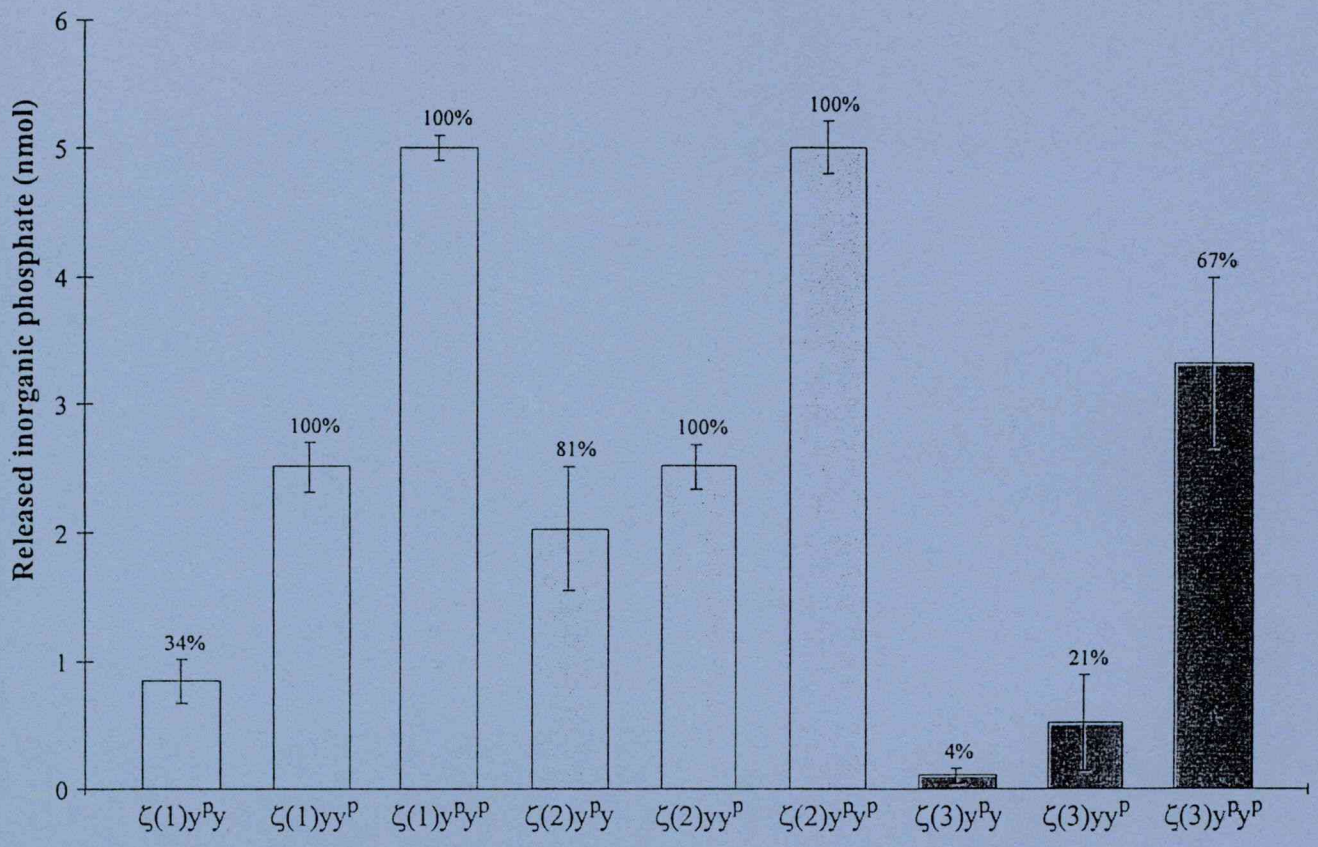

Fig. 5. Dephosphorylation of phosphopeptide substrates representing the differently phosphorylated ITAMs of the ζ chain by CD45. CD45 immunoprecipitates were used for dephosphorylation of the phosphopeptide substrates listed in Table 2. The amount of the released inorganic phosphate was measured as described in Section 2. The mean data and the S.D. from three independent experiments are presented. Above the bars the numerical data represent the released phosphate as the percentage of the starting phosphate content of phosphopeptide substrates.

negative control, no inorganic phosphate release was detected (data not shown).

4. Discussion

Phoshorylation of multiple tyrosine residues within the ζ polypeptide is crucial for the recruitment of effector molecules into the TCR complex. Depending on the phosphorylation pattern of the ζ chain, the T cell receptor may couple to various signaling pathways resulting in different cellular responses, such as activation or energy [11]. However, the mechanism of formation of the distinct phosphorylation pattern and the contribution of the kinases and phosphatases to this process, has not been yet revealed. Therefore, first we have investigated the phosphorylation of a substrate panel derived from the human ζ chain in the presence of different *src* family kinases.

Our results showed that the *src* kinases, $p56^{lck}$ and $p59^{fyn}$, that have been implicated in TCR signalling [17], phosphorylated the ζ chain and related oligopeptides. A higher intensity of overall phosphorylation was detected using $p56^{lck}$ compared to $p59^{fyn}$. These results were consistent with previous findings that under physiological conditions $p56^{lck}$ likely represented the relevant kinase acting in ζ chain phosphorylation [16]. However, it can not be excluded that the detected difference was due to the distinct affinity of the antibodies used for the isolation of the enzymes. Two other *src* kinases, $p53^{lyn}$ and $p60^{src}$, irrelevant in early T cell signaling, also phosphorylated the same set of peptides. The ζ^{ic} was also phosphorylated by $p53^{lyn}$ (unpublished observation). The ability of $p53^{lyn}$ to phosphorylate the ζ-ITAMs is not surprising since $p53^{lyn}$ is involved in the BCR mediated signaling by phosphorylating the ITAMs of the Igα and Igβ proteins [37]. Furthermore, recently a functional homology of *src* family kinases has been suggested based on their high degree of sequence homology in the autophosphorylation site [38] and on their similarity in substrate specificity [39,40].

The experiments concerning the phosphorylation of the seven individual tyrosines located in the intracellular part of the human ζ chain, showed that six of them were phosphorylated by *src* family tyrosine kinases. All tyrosine residues susceptible to phosphorylation were located in the functionally important conserved ITAMs. The non-conserved, membrane proximal tyrosine was not phosphorylated by any of the kinases

used in this work or by cell free extract prepared from HPB-ALL cells, suggesting that this tyrosine did not have phosphorylation dependent function. The pattern of the peptide phosphorylation generated by any of the *src* kinases was identical, suggesting that the *src* kinases may not be the only components regulating the generation of different phosphorylation patterns in the ζ chain.

We have also examined the role of the tyrosine phosphatase, CD45, in controlling the phosphorylation pattern of the ζ chain. The results show that each ITAMs phosphorylated on the N-terminal tyrosine were poorer substrates compared to the identical peptide phosphorylated on C-terminal tyrosine residues. It was observed that the dephosphorylation of the C-terminal phosphotyrosine in ζ(1) and ζ(2) ITAMs was complete, independently of the phosphorylation state of the N-terminal tyrosine residue. In contrast, the hydrolysis of the N-terminal phosphotyrosine in these peptides was enhanced when the C-terminal tyrosine was in phosphorylated form. In general, the ζ(3) phospho-peptides were the weakest substrates, however, the dephosphorylation efficiency of both the C and N-terminal tyrosine was dramatically influenced by the phosphorylation state of the neighboring tyrosine residue.

The different ζ ITAM sequences may be responsible for connecting the TCR to various effector pathways. Several intracellular proteins, such as ZAP70, Shc, Grb2, $p59^{fyn}$, and the p85 subunit of PI3K bind to the phosphorylated TCR polypeptides via their SH2 domains [41–43]. The sequence of the ITAMs and the position of the phosphorylated tyrosine(s) within the motif may affect the binding ability of different signaling proteins. A good example is the C terminal ITAM in the ζ chain that seems to be unique among the TCR ITAMs. It shows the poorest capacity to bind to ZAP and syk [44,45], however it exerts a preferential binding to the actin cytoskeleton [14]. It was also indicated, that the most significant change from α-helix to β-sheet conformation occurs in the ζ3 ITAM upon phosphorylation [46]. These findings suggest that ζ3 ITAM may have a special function in TCR signalling that might also be reflected in the poor dephosphorylation of this ITAM by CD45.

Generation of different ITAM phosphorylation patterns in the TCR may serve as an opportunity for a sophisticated regulation of the TCR signaling. We suggest that the *src* family kinases and the CD45 tyrosine phosphatase may act together in controlling the ζ chain phosphorylation. The ability of the CD45 to distinguish between the various tyrosine residues may play an essential role in the formation of a functional phosphorylation pattern of the ζ chain. The in vivo contribution of the *src* PTKs and CD45 in generation different phosphorylation forms of the TCR ζ chain should be the subject of future studies.

Acknowledgements

We thank Dr René van Lier for his gift of antibody against $p53^{lyn}$ and Dr Tamás Oravecz, and Jenifer Tusz for critically reading the manuscript and for many helpful suggestions. This work was supported by the grants: OTKA 5257, OTKA T-017838, OTKA F-006498, OTKA 16156, ETT T03/672, MKM272, and EEC ERBCI PACT 92 3003. We are grateful to the Bástyai-Holczer Foundation for supporting the cost of the publication of this paper.

References

[1] E.W. Shores, P.E. Love, Curr. Opin. Immunol. 9 (1997) 380–389.
[2] M. Reth, Nature 338 (1989) 383–384.
[3] A. Weiss, D.R. Littman, Cell 76 (1994) 263–274.
[4] A.M. Weissman, D. Hou, D.G. Orloff, W.S. Modi, H. Seuanez, S.J. OqBrien, R.D. Klausner, Proc. Natl. Acad. Sci. USA 85 (1988) 9709–9713.
[5] M. Baniyash, P. Garcia-Morales, E. Luong, L.E. Samelson, R.D. Klausner, J. Biol. Chem. 263 (1988) 18225–18230.
[6] E. Monostori, D. Desai, M.H. Brown, D.A. Cantrell, M.J. Crumpton, J. Immunol. 144 (1990) 1010–1014.
[7] D. Qian, I. Griswold-Prenner, M.R. Rosner, F.W. Fitch, J. Biol. Chem. 268 (1993) 4488–4493.
[8] S. Koyasu, D.J. McConkey, L.K. Clayton, S. Abraham, B. Yandava, T. Katagiri, P. Moingeon, T. Yamamoto, E.L. Reinherz, J. Biol. Chem. 267 (1992) 3375–3381.
[9] N. Osman, S. Lucas, D. Cantrell, Eur. J. Immunol. 25 (1995) 2863–2869.
[10] N. Osman, H. Turner, S. Lucas, K. Reif, D.A. Cantrell, Eur. J. Immunol. 26 (1996) 1063–1068.
[11] J. Madrenas, R.L. Wange, J.L. Wang, N. Isakov, L.E. Samelson, R.N. Germain, Science 267 (1995) 515–518.
[12] V.A. Boussiotis, D.L. Barber, B.J. Lee, J.G. Gribben, G.J. Freeman, L.M. Nadler, J. Exp. Med. 184 (1996) 365–376.
[13] R. Sunder-Plassmann, F. Lialios, M. Madsen, S. Koyasu, E.L. Reinherz, Eur. J. Immunol. 27 (1997) 2001–2009.
[14] M.M. Rozdzial, B. Malissen, T.H. Finkel, Immunity 3 (1995) 623–633.
[15] S. Caplan, M. Baniyash, J. Biol. Chem. 271 (1996) 20705–20712.
[16] N.S. van Oers, N. Killeen, A. Weiss, J. Exp. Med. 183 (1996) 1053–1062.
[17] L.R. Howe, A. Weiss, Trends Biochem. Sci. 20 (1995) 59–64.
[18] M. Raab, C.E. Rudd, Biochem. Biophys. Res. Commun. 222 (1996) 50–57.
[19] N.S. van Oers, N. Killeen, A. Weiss, Immunity 1 (1994) 675–685.
[20] J.B. Wardenburg, C. Fu, J.K. Jackman, H. Flotow, S.E. Wilkinson, D.H. Williams, R. Johnson, G. Kong, A.C. Chan, P.R. Findell, J. Biol. Chem. 271 (1996) 19641–19644.
[21] A.J. da Silva, M. Raab, Z. Li, C.E. Rudd, Biochem. Soc. Trans. 25 (1997) 361–366.
[22] W. Zhang, J. Solan-Lancaster, J. Kitchen, R.P. Tribe, L.E. Samelson, Cell 92 (1998) 83–92.
[23] N. Isakov, R.L. Wange, J.D. Watts, R. Aebersold, L.E. Samelson, J. Biol. Chem. 271 (1996) 15753–15761.
[24] T. Furukawa, M. Itoh, N.X. Krueger, M. Streuli, H. Saito, Proc. Natl. Acad. Sci. USA 91 (1994) 10928–10932.
[25] S. Volarevic, C.M. Burns, J.J. Sussman, J.D. Ashwell, Proc. Natl. Acad. Sci. USA 87 (1990) 7085–7089.

[26] G.K. Toth, G. Varadi, Z. Nagy, E. Monostori, B. Penke, Z. Hegedus, I. Ando, G. Fazekas, I. Kurucz, M. Mak, et al., Pept. Res. 6 (1993) 272–280.
[27] I. Andó, J. Zákány, L. Takács, I. Petri, I. Kaiser, G. Veres, L. Balázs, E.B. Nikolova, P.C.L. Beverley, É. Monostori, in: P. Rohlich, E. Bacsy (Eds.), Tissue Culture and RES, Academic Press, Amsterdam, 1984, pp. 241.
[28] I. Andó, H. Ramadan, G. Bogdán, P. Vilmos, É. Monostori, in: S.F.e. Schlossman (Ed.), Leucocyte Typing V, Oxford University Press, Oxford, 1995, pp. 1711–1712.
[29] J.Y. Chang, Eur. J. Biochem. 151 (1995) 217–224.
[30] D.J. Hakes, J.E. Dixon, Anal. Biochem. 202 (1992) 293–298.
[31] J. Grodberg, J.J. Dunn, J. Bacteriol. 170 (1988) 1245–1253.
[32] R.B. Merrifield, J. Am. Chem. Soc. 85 (1963) 2149–2154.
[33] G.B. Fields, R.L. Noble, Int. J. Pept. Protein Res. 35 (1990) 161–214.
[34] G.K. Tóth, I. Laczkó, Z. Hegedûs, E. Vass, M. Hollósi, T. Janáky, G. Váradi, B. Penke, É. Monostori, in: C.H. Schneider (Ed.), Peptides in Immunology, Wiley and Sons, New York, 1996, pp. 223–230.
[35] Z. Hegedus, I. Ando, G.K. Toth, G. Varadi, E. Monostori, Biotechniques 18 (1995) 631–634.
[36] D.H. Ng, K.W. Harder, I. Clark-Lewis, F. Jirik, P. Johnson, J. Immunol. Methods 179 (1995) 177–185.
[37] A.C. Chan, S.S. Shaw, Curr. Opin. Immunol. 8 (1996) 394–401.
[38] S.K. Hanks, A.M. Quinn, T. Hunter, Science 241 (1988) 42–52.
[39] K.S. Lam, J. Wu, Q. Lou, Int. J. Pept. Protein Res. 45 (1995) 587–592.
[40] R. Schmitz, G. Baumann, H. Gram, J. Mol. Biol. 260 (1996) 664–677.
[41] K.S. Ravichandran, K.K. Lee, Z. Songyang, L.C. Cantley, P. Burn, S.J. Burakoff, Science 262 (1993) 902–905.
[42] M. Iwashima, B.A. Irving, N.S. van Oers, A.C. Chan, A. Weiss, Science 263 (1994) 1136–1139.
[43] M. Exley, L. Varticovski, M. Peter, J. Sancho, C. Terhorst, J. Biol. Chem. 269 (1994) 15140–15146.
[44] M.E. Labadia, R.H. Ingraham, J. Schembri-King, M.M. Morelock, S. Jakes, J. Leukoc. Biol. 59 (1996) 740–746.
[45] J.Y. Bu, A.S. Shaw, A.C. Chan, Proc. Natl. Acad. Sci. USA 92 (1995) 5106–5110.
[46] I. Laczko, M. Hollosi, E. Vass, Z. Hegedus, E. Monostori, G.K. Toth, Biochem. Biophys. Res. Commun. 242 (1998) 474–479.

Conditions for Permeabilization of Cells Used for Intracellular Tyrosine Phosphorylation Studies

BioTechniques 27:435-437 (September 1999)

Permeabilized cells are widely applied for studying the effect of membrane impermeant biomolecules on signaling pathways. After permeabilization with reagents commonly used for this purpose, the architecture of the cells remains essentially intact, and hence, they retain their ability to respond to cell surface receptor stimulation as far as early cellular responses are concerned. Early signaling events, such as tyrosine and serine phosphorylation of cellular proteins (3,6), generation of cAMP (1) or inositol-phosphate hydrolysis (3) can be investigated after the stimulation of permeabilized cells.

Several procedures have been reported to produce permeable cells. These methods apply bacterial toxins such as tetanolysin (1,2,9) and streptolysin-O (SLO) (2,3) or detergents like digitonin (5) and L-α-lysophosphatidyl choline (LPC) (6,8) as permeabilizing agents. However, a common feature of most of the permeabilizing reagents is that they induce a significant tyrosine phosphorylation in most of the leukemic cell lines, which might obscure the regulatory effect of the biomolecules that are tested (References 6 and 9, and unpublished observation).

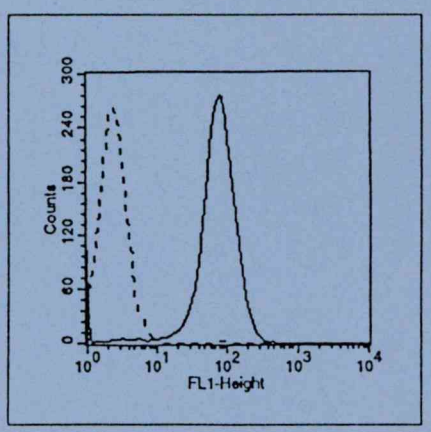

Figure 1. Intracellular staining of permeabilized cells. Intact (dotted line) or LPC-permeabilized J6 cells (continuous line) were stained with a rabbit antibody against a recombinant protein representing the intracellular domain of the CD43 (produced in our laboratory) and subsequent incubation of cells with FITC-labeled, anti-rabbit immunoglobulin (Sigma, St. Louis, MO, USA). The immunofluorescence was analyzed by cytofluorimetry on a FACSVantage™ Instrument (Becton Dickinson, San Jose, CA, USA).

Our aim was to establish a permeabilization procedure that resolves this problem. Therefore, we first compared different reagents, namely SLO, digitonin and LPC and various conditions for permeabilization to select the most efficient system. SLO-mediated permeabilization required a high concentration of SLO (200 IU/mL) and a long time (30 min) to fully permeabilize 10^7 J6 cells or peripheral blood mononuclear cells (PBMC) at 37°C (data not shown). Permeabilization with digitonin also required 10–30 min, and it was not well reproducible. The LPC-mediated permeabilization has turned out to be the most reliable, because it was highly reproducible in the case of different cells (leukemic cell lines, peripheral mononuclear cells), and the permeabilization was completed in a short time. Therefore, the LPC-mediated permeabilization (6) was characterized and optimized for studying the effect of various biomolecules on tyrosine phosphorylation. The amount of LPC, the appropriate time and the optimal temperature required for permeabilization have been established in a series of experiments. The LPC of 50 µg/mL permeabilized a wide variety of cell lines at 10^7–10^8 cell/mL concentration within 1 min (data not shown). Permeabilization carried out at 4° or 37°C was equally efficient (data not shown). Permeability of the cells was assessed in each experiment using trypan blue exclusion. The efficiency of the LPC permeabilization was also assessed by introducing fluorescein isothiocyanate (FITC)-labeled peptides of 2 and 4 kDa molecular mass (data not shown) and FITC-labeled immunoglobulin (150 kDa) into the cells (Figure 1). An antibody recognizing the intracellular domain of the CD43 molecule stained over 95% of the permeabilized cells confirming the successful permeabilization (Figure 1).

The method we finally preferred for permeabilization was as follows: the human leukemic T cells (J6) were centrifuged, washed once with the cell culture medium RPMI (Life Technologies,

manner, were suitable for studying the intracellular tyrosine phosphorylation induced by a membrane impermeable synthetic peptide. A synthetic phosphopeptide (sequence is presented in legend for Figure 3) derived from the TCR ζ subunit (4) and its nonphosphorylated counterpart were introduced into LPC-permeabilized J6 cells. This sequence represented a conserved signal transducing motif, called immunoreceptor tyrosine-based activation motif (ITAM) that was previously shown as an effective modulator of the cell response in permeabilized cells (6,9). As Figure 3 shows, the phospho-peptide induced a high level of phosphorylation compared to that of unstimulated cells or cells stimulated with non-phosphorylated peptide.

The procedure described here allows a fast and efficient permeabilization of a variety of leukemic cell lines without affecting the responsiveness of the cells to external stimuli. Additionally, a wide variety of biomolecules, including antibodies against intracellular antigens, can be introduced into leukemic cells permeabilized in this manner. Due to the simplicity and high efficiency of this procedure, we recommend its use to determine the effect of membrane impermeant biomolecules on tyrosine phosphorylation pathways in leukemic cells. We would like to emphasize the importance of the well-controlled, low temperature during permeabilization, which is a key factor for successful usage of permeabilized cells for signal transduction studies.

REFERENCES

1. **Alava, M.A., K.E. DeBell, A. Conti, T. Hoffmann and E. Bonvini.** 1992. Increased intracellular cyclic AMP inhibits inositol phospholipid hydrolysis induced by perturbation of the T cell receptor/CD3 complex but not by G-protein stimulation. Biochem. J. *284*:189-199.
2. **Bonvini, E., K.E. Debell, M.S. Taplits, C. Brando, A. Aurenza, K. Seamon and T. Hoffman.** 1991. A role for guanine-nucleotide-binding proteins in mediating T-cell-receptor coupling to inositol phospholipid hydrolysis in a murine T-helper (type II) lymphocyte clone. Biochem. J. *275*:689-696.
3. **Graves, J.D., S.C. Lucas, D.R. Alexander and D.R. Cantrell.** 1990. Guanine nucleotide regulation of inositol phospholipid hydrolysis and CD3-antigen phosphorylation in permeabilized T lymphocytes. Biochem. J. *265*:407-413.
4. **Hegedüs, Z., V. Chitu, G.K. Tóth, Cs. Finta, Gy. Váradi, I. Andó and É. Monostori.** 1999. Contribution of kinases and the CD45 phosphatase to the generation of tyrosine phosphorylation patterns in the TCR ζ chain. Immunol. Lett. *67*:31-39.
5. **Jekunen, A.P., D.R. Shalinsky, D.K. Hom, K.D. Albright, D. Heath and S.B. Howell.** 1993. Modulation of cisplatin cytotoxicity by permeabilization of the plasma membrane by digitonin *in vitro*. Biochem. Pharmacol. *45*:2079-2085.
6. **Johnson, S.A., C.M. Pleiman, L. Pao, J. Schneringer, K. Hippen and J.C. Cambier.** 1995. Phosphorylated immunoreceptor signalling motifs (ITAMs) exhibit unique abilities to bind and activate *lyn* and *syk* tyrosine kinases. J. Immunol. *155*:4596-4603.
7. **Laemmli, U.K.** 1970. Cleavage of structural proteins during the assembly of the head of bacteriophage T4. Nature *227*:680-685.
8. **Nomura, S., T. Kamya and M. Oishi.** 1986. A procedure to introduce molecules into living mammalian cells. Exp. Cell Res. *163*:434-444.
9. **Wange, R.L., N. Isakov, T.R. Burke, Jr., A. Otaka, P.P. Roller, J.D. Watts, R. Aebersold and L.E. Samelson.** 1995. F_2 $(Pmp)_2$—$TAM\zeta_3$, a novel competitive inhibitor of the binding of ZAP-70 to the T cell antigen receptor, blocks early T cell signaling. J. Biol. Chem. *270*:944-948.

This work was supported by OTKA T026637, T16156, T29706 and ETT 672. We thank Kinga Székely Szücs for the excellent technical assistance, Mrs. Mária Tóth and András Borka for preparing the photoprints. We are grateful to the Bástyai-Holczer Foundation for contributing to the cost of the publication of this paper. We thank Prof. P.C.L. Beverley for the UCHT1 antibody.

Address correspondence to Dr. Éva Monostori, Institute of Genetics, Biological Research Center of Hungarian Academy of Sciences, H-6701 Szeged, P.O. Box 521, Hungary. Internet: monos@nucleus.szbk.u-szeged.hu

Received 28 December 1998; accepted 3 June 1999.

Violeta Chitu, Dmytro Demydenko, Gábor K. Tóth[1], Zoltán Hegedüs and Éva Monostori
Biological Research Center of the Hungarian Academy of Sciences
[1]A. Szentgyörgyi Medical University
Szeged, Hungary

Gaithersburg, MD, USA), resuspended at 4×10^7 cells/mL in ice-cold permeabilization buffer (6) [10 mM $MnCl_2$, 10 mM $Mg(OAc)_2$, 296 µM $CaCl_2$, 2 mM EGTA, 40 mM HEPES, pH 7.4] and incubated further on ice for 5 min in a cold room. Permeabilization was initiated by adding 1/10 volume of ice-cold LPC stock solution containing 500 µg/mL LPC.

We determined whether permeabilized T cells were able to respond to T cell receptor (TCR) stimulation with an anti-CD3 antibody (UCHT-1) by analyzing the TCR-induced tyrosine phosphorylation and whether this response was comparable to that of intact cells. As Figure 2 shows, a low level of tyrosine phosphorylation was detected in unstimulated cells, either intact or LPC permeabilized (Figure 2, A and B, lanes 1). Moreover, permeabilization did not affect the TCR-induced tyrosine phosphorylation (Figure 2B, lane 2) because it was similar to that of unpermeabilized cells (Figure 2A, lane 2). Similar tyrosine phosphorylation was induced when the stimulant was added 15 min after permeabilization. After 30 min passing permeabilization, the cell response declined, but still a considerable tyrosine phosphorylation was detected upon stimulation (data not shown). Phosphorylation of intracellular substrates was also detected in the presence of [γ-^{32}P]ATP by determining the incorporation of ^{32}P into the proteins upon stimulation of permeabilized cells by the TCR (data not shown). The temperature conditions during permeabilization dramatically influenced the overall tyrosine phosphorylation. In cells permeabilized at 37°C, a high background signal was induced that concealed the effect of TCR stimulation (Figure 2C). When the low temperature was not strictly controlled during the permeabilization, namely the procedure was not done in a cold room, keeping the samples and reagents on ice, the LPC-induced tyrosine phosphorylation in unstimulated cells was always observed (data not shown). We examined whether the composition of permeabilizing buffer used during stimulation affected the phosphate incorporation into cellular substrates or the phosphorylation background of the unstimulated control. Addition of exogenous ATP to the buffer did not improve the efficiency of the phosphate incorporation. The effect of bivalent cations, Ca^{2+}, Mg^{2+} and/or Mn^{2+}, in the permeabilizing buffer to the LPC-induced background phosphorylation at a higher temperature, was also tested. The presence or absence of one or the other ion in the buffer did not affect the background. However, omitting Mg^{2+} and Mn^{2+} simultaneously from the buffer resulted in the dramatic decrease in the inducibility of the tyrosine phosphorylation (data not shown). This result likely reflects the requirement of at least one of these ions for optimal function of the tyrosine kinases.

Next, we analyzed whether the cells, permeabilized in the above-described

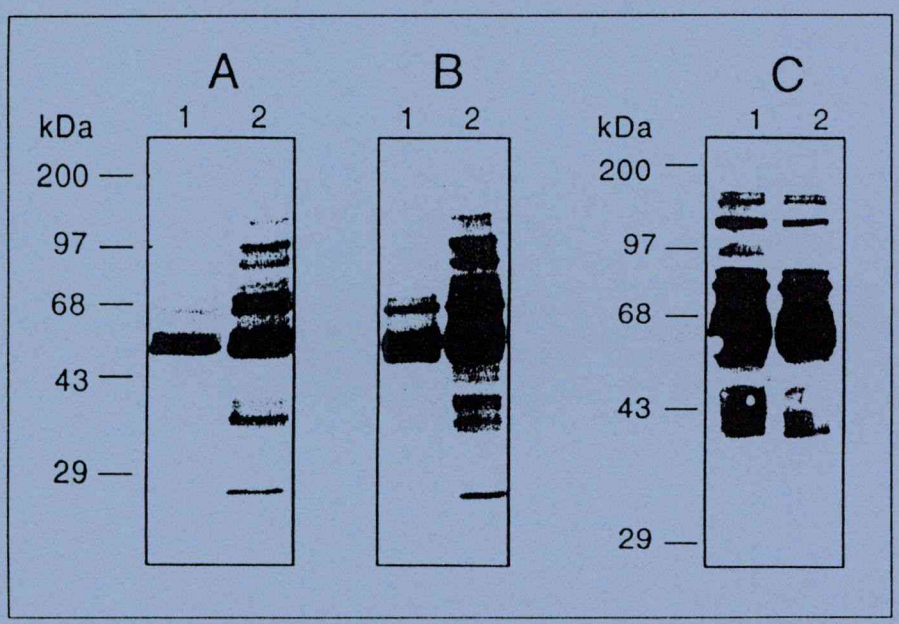

Figure 2. Tyrosine phosphorylation induced by TCR in intact and permeabilized cells. Intact J6 cells (A) or J6 cells permeabilized with LPC (Sigma) on ice (B) or at 37°C (C) were stimulated with 10 µg/mL UCHT-1 for 2 min at 37°C (lanes 2) or were left unstimulated (lanes 1). The activation was stopped by adding 2× ice-cold lysis buffer [50 mM HEPES, pH 7.4, 1% Triton® X-100, 150 mM NaCl, 20 mM NaF, 2 mM sodium orthovanadate, 2 mM EDTA, 10 mM sodium pyrophosphate, 1 mM phenylmethylsulfonylfluoride (PMSF), 10 µg/mL aprotinin and leupeptin]. Postnuclear supernatants were mixed with 2× sodium dodecyl sulfate (SDS) Laemmli buffer (7), boiled for 5 min and loaded onto a 10% SDS polyacrylamide gel. After electrophoresis, proteins were transferred onto nitrocellulose membrane and hybridized with anti-phospho-tyrosine mAb, 4G10 (Upstate Biotechnology, Lake Placid, NY, USA), then peroxidase-labeled, anti-mouse Ig (DAKO, Carpinteria, CA, USA). Finally, the hybridizing protein bands were visualized with enhanced chemiluminescence (ECL) detection system (reagents for ECL were purchased from Sigma).

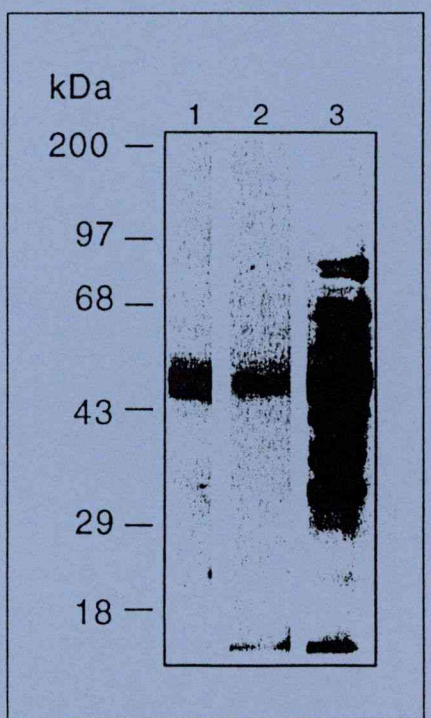

Figure 3. Stimulation of tyrosine phosphorylation by TCR ζ peptides in LPC-permeabilized J6 cells. Cells, permeabilized with LPC were untreated (lane 1) or were treated with synthetic oligopeptide derived from the TCR ζ chain in unphosphorylated (lane 2) or tyrosine-phosphorylated (lane 3) forms. The amino acid sequence of the peptide in single letter code was NQLY*NELNLGRREEY*DVL, where Y* represented tyrosine residues in unphosphorylated or phosphorylated form (4).

1.5.

CO-CLUSTERING OF Fcγ- AND B CELL RECEPTORS INDUCES DEPHOSPHORYLATION OF THE GRB2-ASSOCIATED BINDER 1 DOCKING PROTEIN

Running title: Fcγ receptor IIb-induced dephosphorylation of Gab1

Koncz, Gábor[*], Tóth, K. Gábor[†], Bökönyi, Gyöngyi[‡], Kéri, György[‡], Pecht, Israel[§], Gergely, János[*], and Sármay, Gabriella[¶]

[*]Research Group of the Hungarian Academy of Science at the Dept. of Immunology, Loránd Eötvös University, Göd, [†]Dept. of Medical Chemistry, A. Szentgyörgyi University, Szeged, [‡]Dept. of Medical Chemistry, Semmelweis University of Medicine, Budapest, [§]Dept. of Immunology, The Weizmann Institute of Science, Rehovot, Israel, and [¶]Dept. of Immunology, of Loránd Eötvös University, Göd, Hungary

Corresponding author: Gabriella Sármay, Dept. of Immunology, Loránd Eötvös University, Jávorka Sándor u. 14., Göd 2131, Hungary. Tel/Fax: 36 27 345 147

E-mail: sar7197@mail.iif.hu

Keywords: human, B lymphocytes, Fcγ receptors IIb, signal transduction

Abstract

The Immunoreceptor Tyrosine-based Inhibitory Motif (ITIM) of human type IIb Fcγ receptor (FcγRIIb) is phosphorylated on its tyrosine upon co-clustering with the B cell receptor (BCR). The phosphorylated ITIM (p-ITIM) binds SH2 domain containing phosphatases, the protein tyrosine phosphatase, SHP-2, and the polyphosphoinositol 5-phosphatase (SHIP), which then may recruit further signaling molecules. We investigated the involvement of the human FcγRIIb p-ITIM assembled multimolecular complex in the activation of SHP-2 and its induced dephosphorylation of the Grb2-associated binder 1 (Gab1) docking protein. As a model compound for the p-ITIM-SHIP complex, we synthesised a bisphosphopeptide, combining the sequences of p-ITIM and the N-terminal tyrosine phosphorylated motif of SHIP. This compound bound to the recombinant SH2 domains of SHP-2 with an approximately 10 fold higher affinity than p-ITIM and activated the phosphatase. This result indicates that the FcγRII-SHIP complexes formed in the intact cells may activate SHP-2. Gab1 is a multisite docking protein which becomes tyrosine-phosphorylated in response to antigen receptor signaling, and in turn binds SH2 domains of SHP-2 and the p85 regulatory subunit of phosphatidyl inositol 3- kinase (PI3-K). The tyrosine phosphorylated Gab1 is a potential SHP-2 substrate in activated B cells. We show here, that Gab1 is part of the multiprotein complex assembled by FcγRIIb upon its co-clustering with BCR, furthermore, SHP-2, activated upon interaction with FcγRIIb-SHIP complexes, dephosphorylates Gab1. This results in the dissociation of the Gab1-recruited PI3-K and ultimately in the inhibition of PI3-K dependent activation pathways.

Introduction

Clustering of B cell receptors (BCR) activates protein tyrosine kinases (PTK) associated with the BCR signal transducing Igα/Igβ chains (1, 2). This leads to the phosphorylation of tyrosine residues of Immunoreceptor Tyrosine-based Activation Motif (ITAM) present in the cytoplasmic tail of Igα/Igβ, consequently triggering cell activation (3). B cell activation is further regulated by multiple molecular interactions inside the cell, many of these involve binding of tyrosine phosphorylated motifs to SH2 domains of adaptor proteins and enzymes (4, 5), resulting in the translocation of cytoplasmic molecules to the cell membrane, activation of kinases and phosphatases, and amplification or inhibition of the signal (6). Docking/scaffolding proteins with multiple tyrosine phosphorylated interaction sites produce the signal coupling complexes and target these to the cell membrane (7, 8). A recently identified member of the docking protein family is the Grb-2 associated binder 1 (Gab1), which is mostly found located in the membrane enriched fraction of activated B cells (9, 10). Gab1 has a plekstrin homologue (PH) domain, multiple potential phosphorylation sites and several proline rich sequences. Gab1 becomes tyrosine phosphorylated in response to diverse signals, e.g. by EGF, insulin, cytokine or antigen receptors, and interacts with SH2 domain containing SHIP, SHP-2, Shc, and the p85 regulator subunit of PI3-K. Tyrosine phosphorylated Gab1 recruits these cytosolic proteins to the cell membrane, where their substrates reside (11, 12, 13, 14). Thus Gab1 was proposed to play a pivotal role in multiple BCR-triggered signaling pathways.

FcγRIIb of B cells is the first identified member of the inhibitory receptor superfamily, characterized by an ITIM (15, 16, 17, 18). Co-aggregating FcγRIIb and BCR induces phosphorylation of ITIM and the tyrosine phosphorylated ITIM (p-ITIM) then recruits SH2 domain containing phosphatases and further signalling proteins, targeting them to the BCR

proximity. We have reported earlier that in human B cells FcγRIIb p-ITIM interacts with SHP-2, the adaptor molecule Shc, and with the p85 regulatory subunit of PI3-K (19, 20, 21). We have also pointed out that SHP-2 plays a central role in FcγRIIb dependent regulation of human B cells (22, 23). Membrane targeting of molecules assembled by FcγRIIb p-ITIM transfers these cytoplasmic proteins into a compartment where they can modulate the cell's response.

The biological significance of FcγRIIb dependent B cell inhibition caused by IgG containing immune complexes is in controlling antibody synthesis (24, 25, 26). The mechanism of the inhibition in the human B cell is not fully clarified and controversial data were reported for various in vitro models. In order to examine the potential interactions among molecules present in the FcγRIIb p-ITIM associated multiprotein complex, we synthesised phosphopeptides consisting of the tyrosine phosphorylated motifs of human FcγRIIb and various signaling molecules (Shc, SHIP and Gab1) and identified the proteins binding to these phosphopeptides. Furthermore, we have composed a bisphosphopeptide combining the N-terminal tyrosine phosphorylated motif of SHIP with FcγRIIb p-ITIM by a flexible linker and tested its binding to and activation of SHP-2. Finally, we monitored the molecules associated to the Gab1 docking protein in BCR activated and in FcγRIIb-BCR co-clustered cells. Based on the results we suggest that the FcγRIIb p-ITIM-assembled multimolecular complex activates SHP-2, which in turn dephosphorylates the adaptor protein Gab1. Thus co-aggregation of BCR and FcγRIIb results in the dissociation of PI3-K and possible other molecules from Gab1, leading to the disruption of multiple downstream signaling pathways.

Materials and methods

Reagents

Monoclonal human IgG κ chain specific antibody was developed in our laboratory, and characterized as IgG1. Biotinylated anti-murine IgG, HRPO-conjugated $F(ab)_2$ fragments of anti-mouse and anti-rabbit IgG $F(ab)_2$ specific antibodies (Axell), CD32 specific mAb (PharMingen), Sepharose CL 4B and GammaBind G beads (Pharmacia). SHP-2 and SHP-1 specific rabbit antibodies (Santa Cruz), phosphotyrosine, Shc, SHP-2 or Lyn specific monoclonal antibodies (Transduction) or PI3-K specific antibody (UBI), ECL detection reagent (Pierce). SHIP specific rabbit antibody was a kind gift of J.Cambier, Denver, USA. All the other reagents were purchased from Sigma.

Phosphopeptide synthesis

The phosphotyrosine containing peptides were synthesized by SPPS-Fmoc methodology (27). The peptide chain were elongated on a p-alcoxybenzylalcohol resin (0.48 mmol/g), and the syntheses were carried out using an ABI 430A automatic machine with certain minor modifications on the standard protocol. Side chain protecting groups were as follows: Glu(OBut), Asp(OBut), His(Trt), Tyrosine(But), Thr(But), and Ser(But). The phenolic hydroxyl group of the tyrosine residue subjected to phosphorylation was unprotected. Couplings were performed with N,N'-dicyclohexylcarbodiimide and 1-hydroxybenzotriazole. After the incorporation of the tyrosines, their hydroxyls were phosphytilated using di-tert. butyl- N,N diethyl-phosphoramidite which proved to be the optimal reagent in our laboratory (28). The di-tert. butyl- N,N diethyl-phosphoramidite was prepared in our laboratory from PCl3, diethylamine, and tert. butanol as described (29). After the oxidation of the phosphite to phosphate using tert. butylperoxide, the elongation of the

peptide chain was completed, the free amino function of the protected phosphopeptide on the resin was acylated with biotinamidocaproate N-hydroxysuccinimide ester. After the labelling step, the resulted crude biotinylated phosphopeptide was detached from the resin using TFA/DCM/anisole mixture (62:30:8, vol/vol), at 0oC, 1 h. The resulting free peptides were precipitated with diethylether, filtered, dissolved in water, and lyophilized. The crude peptides were purified by reverse-phase HPLC. The appropriate fractions were pooled a lyophilized. The purified peptides were characterized by mass spectrometry using a Finnigan TSQ 7000 tandem quadrupol mass spectrometer equipped with electrospray ion source. Peptide purities were above 97% (HPLC) and the measured Mw values were good agreement with the calculated ones in all cases.

Surface plasmon resonance (SPR)

SPR measurements were performed on BIAcore (Pharmacia, Uppsala, Sweden). The glutathione S-transferase (GST)-SHP-1.SH2(NC) and GST-SHP-2.SH2(NC) were kindly provided by B. Neel (Boston, USA), the GST-SHIP.SH2 was a gift of M. Daeron (Paris, France). The fusion proteins were purified from Escherichia Coli DH5α lysates (30). The protein purity was controled by SDS-PAGE.

The biotinylated phosphopeptides (10 ng/ml) were bound to the streptavidin coated sensor chips (Biacore, Uppsala, Sweden) at low ligand densities, ranging between 30-60 resonance units (RU). The presence of accessible phosphopeptide was also confirmed by using anti-phosphotyrosine antibodies, and resulted in 800-1700 RU using 5 μg/ml anti-phosphotyrosine. The experiments were carried out at six different concentrations (from 250 nM to 8 nM) of the various SH2 domains, and each experiments were repeated 3-4 times. The surface of the chips were regenerated by 0.1 M HCl between the measurements with different

SH2 domains. The data were analysed by BIAevaluation 3.0 software. For the kinetic measurements the calculated observed association rates (k_{obs}) were plotted as the function of the concentration of the SH2 domains. The plots were linear between 60 to 8 nM concentration. The slope of each plot was taken as k_{on} and the y intercept was taken as k_{off} (31).

Cell stimulation

5×10^7 BL41 cells were stimulated by 10 μg of anti human κ chain mAb, or treated with 4 μg/ml CD32, and 10 μg/ml anti-κ chain mAb, then co-clustering was induced by 4 μg anti-murine IgG. After 2-5 min stimulation at 37°C, the cells were sedimented for 20 sec and immediately frozen in liquid nitrogen.

Preparation of cell lysates

5×10^7 BL41 cells were solubilized in 1ml lysis buffer containing, 50 mM HEPES [pH7.4], 1% Triton X-100, 100 mM NaF, 10 mM EDTA, 2 mM sodium orthovanadate, 10 mM sodium pyrophosphate, 10% glycerol and 10 μg/ml aprotinin, 5 μg/ml leupeptine and 0.2 mM phenylmethylsulphonyl fluoride. After 30 min incubation on ice, cell lysates were centrifuged at 15,000 g for 20 min and the postnuclear supernatants were used.

Affinity isolation and Western blotting

Affinity isolation was carried out using either human Fcγ fragments covalently coupled to Sepharose beads, CD32 mAb coated GammaBind G beads, or 10μg/sample bitotinylated synthetic peptides (summarized in Table I.) coupled to Streptavidine-agarose beads as insoluble supports. After continous mixing for 1 h at 4°C the beads were washed 4 times

with lysis buffer and the bound components were eluted by incubation in 40 µl reducing SDS-PAGE sample buffer for 5 min at 95 ^{o}C. The eluted samples were separated on 8.5 or 10 % SDS-PAGE gel, then the proteins were transferred onto nitrocellulose membranes, and consecutively probed with various antibodies. Immunoblots were developed by using HRPO conjugated second antibodies, followed by ECL detection. The membranes were stripped according to the manufacturers instruction and re-probed with a different antibody.

Phosphatase activity assays

SHP-2 was affinity purified by using specific antibodies coupled to GammaBind G beads from samples in lysis buffer without phosphatase inhibitors, then washed and incubated at 37^{o}C for 1 h in phosphatase buffer containing 20 mM HEPES, [pH 7.0], 5% glycerol, 0,05 % Triton X-100, 2.5 mM $MgCl_2$, aprotinin [10 µg/ml] and leupeptin [10 µg/ml]. The beads were washed twice. Dephosphorylation of synthetic phosphopeptides by affinity isolated SHP-2 was tested by ELISA based on phosphotyrosine detection in the biotinylated phosphopeptides. 50 µl of 0.02-0.1 µg/ml biotinylated phosphopeptides (listed in Table I) were preincubated at 37^{o}C for one hour in the presence of various dilutions of immunoisolated SHP-2. All samples were isolated from equivalent amounts ($2x10^{6}$) of cells. The mixtures of phosphatase and biotinylated peptides were then transferred to avidin-precoated ELISA plates in duplicates, and were further incubated at 4^{o}C overnight. After several rinsing steps, the plates were developed using phosphotyrosine specific mAb and peroxidase conjugated anti murine IgG $F(ab)_2$.

Results

Binding affinities of FcγRIIb, SHIP and Shc phosphopeptides to the recombinant SH2 domains of SHP-1, SHP-2 and SHIP

We have analysed the interactions between the phosphopeptides listed in Table I., and recombinant proteins consisting of the SH2 domains of SHP-1, SHP-2 and SHIP, respectively, by using surface plasmon resonance (SPR). The phosphopeptides were biotinylated and bound to the streptavidin coated biosensor chips. Typical association and dissociation curves are shown on Fig.1. Both dimeric SH2 domains of SHP-2 and monomeric SH2 of SHIP bound the p-ITIM peptide with high affinity (K_D=104x10^{-9} M, and 40x10^{-9} M, respectively). In contrast, SHP-1 SH2 domains exhibited rather low affinity to p-ITIM (K_D=10^{-3} M) (Fig 1. a) and did not bind to any of the other phosphopeptides tested. SHP-2 and SHIP SH2 domains bound to all phosphopeptides, with apparent K_D of 60-305x10^{-9} M and 14-145x10^{-9} M, respectively (Fig. 1b, 1c). The K_D values calculated from the kinetic measurements are summarised in Table II. None of the SH2 domains reacted with tyrosine phosphorylated peptides corresponding to the PI3-K binding consensus sequences of CD19.

In order to establish a model for studying the possible interaction of the phosphorylated FcγRIIb-SHIP complexes with SHP-2 a bisphosphopeptide was synthesised, combining FcγRIIb p-ITIM with the N-terminal phosphopeptide of SHIP by a 50 A long flexible linker consisting of 15 A-G dimer repeats. This SHIP-p-ITIM peptide is potentially capable to engage both SH2 domains of the recombinant SHP-2 protein. Indeed, SPR measurements of the interaction between this compound and SHP-2 SH2 domains established an apparent K_D=9x10^{-9} M, i.e. an approximately 10 times higher affinity constant than that of the p-ITIM for these domains and a 30 times increase as compared to the K_D of the

corresponding SHIP peptide. Examining closer the association-dissociation curves, a considerably higher K_{on} rate was observed between the bisphosphopeptide and SHP-2, as compared to the K_{on} between the monophosphopeptides and SHP-2 (Table 2., Fig. 1d). SHP-2 and SHIP bound to the bisphosphopeptide with a similar affinity.

Activation of SHP-2 by the SHIP-p-ITIM bisphosphopeptide

Catalytic activity of SHP-2 has been shown to increase dramatically upon occupancy of both its SH2 domains by bisphosphorylated tyrosine-based motifs. This was rationalised by the disruption of the interaction between SHP-2 phosphatase domain and the N-terminal SH2 domain (37, 38). We have shown previously that the p-ITIM peptide bound to an insoluble matrix precipitated from BL41 cell lysates considerable tyrosine phosphatase activity (21, 22, 23). The catalytic activity of immunoisolated SHP-2 was now tested on different phosphopeptides substrates by ELISA measurements of their remaining phosphotyrosine content. The immunoprecipitated SHP-2 samples exhibited a single protein band corresponding to SHP-2 by Western blot detection. This band was not recognised by SHP-1 specific antibody. Comparing the phosphotyrosine content of the non-treated phosphopeptide samples with those treated with various dilutions of SHP-2, 60% dephosphorylation of SHIP-p-ITIM bisphosphopeptide was obtained by as high as a 70 fold dilution of SHP-2 immunoisolated from $2x10^6$ BL41 cells-equivalent lysate. A 10 and 20 fold dilution was required to dephosphorylate the various monophosphopeptides at the same rate. Similar differences were observed comparing SHP-2 dilutions required for 20% dephosphorylation of the phosphopeptides (Fig.2). These results indicate that the SHIP-p-ITIM bisphosphopeptide significantly enhances the catalytic activity of SHP-2.

Binding of Grb2 and Gab1 to the phosphopeptides of FcγRIIb, SHIP and Shc

Recently the tyrosine phosphorylated Grb2-binding, docking protein, Gab1 was

reported to play a role in translocation of the SH2 domain containing SHP-2, PI3-K, and Shc to the cell membrane of activated B cells (10). We have tested the binding from BL41 cell lysate samples of Gab1 and Gab1-associated molecules to p-ITIM and to phosphopeptides identical with the tyrosine phosphorylated motifs of p-ITIM-recruited proteins (Fig.3). As controls, tyrosine phosphorylated peptides corresponding to the CD19 C-terminal sequence were used. Both CD19 phosphopeptides bound PI3-K (data not shown), but did not react with any other SH2 domain containing signaling molecules, such as SHP-2, SHIP, Shc, and Grb2. FcγRIIb p-ITIM, SHIP-p-ITIM bisphopshopeptide and the C- terminal phosphopeptides of SHIP bound Shc, while SHIP-p-ITIM and the N-terminal phosphopeptide of SHIP, as well as both the C- and N-terminal Shc peptides bound Grb-2. Binding of Grb-2 to p-ITIM was also observed after longer incubation times. Pre-clearance immunoprecipitation by 2 μg Gab1 specific antibodies /5*10^6 cells considerably reduced Shc and Grb2 binding to SHIP-p-ITIM (Fig.3a).

The binding of SHP-2 and Grb2 to the bisphosphopeptide, SHIP-p-ITIM was also tested in a competition experiment. Only the p-ITIM peptide decreased the binding of SHP-2 to SHIP-p-ITIM, while the N-terminal SHIP and Shc phosphopeptides competed for Grb-2 binding (Fig.3b). Thus binding of Grb2 to p-ITIM may be indirect.

Since SHP-2, Shc, and Grb2 were detected in samples precipitated by the p-ITIM and SHIP-p-ITIM phosphopeptides from cell lysates, we tested whether Gab1 is present in the p-ITIM bound complex. Though Gab1 lacks an SH2 or phosphotyrosine binding (PTB) domains, it did bind to both p-ITIM, and SHIP-p-ITIM phosphopeptides. Moreover, it reacted with the N-terminal phosphopeptide of SHIP and with the C-terminal phosphopeptide of Shc (Fig.3c). These results indicate that the binding of Gab1 to these tyrosine phosphorylated peptides is indirect, probably mediated by molecules with multiple SH2 or

PTB domains.

Interaction between Gab1 and SHP-2

In order to examine the interaction between Gab1 and SHP-2, we have synthesised three phosphopeptides, two of which corresponded to the assumed SHP-2 binding motifs of Gab1 (Ingham et al. 1998)). Binding of these phosphopeptides to PI3-K was also monitored and compared with that of p-ITIM. All three phosphopeptides bound SHP-2, while only the N-terminal phosphopeptide (Q - C), containing the YLLL motif bound both PI3-K and SHP-2. The p-ITIM peptide bound SHP-2 most efficiently. The peptide containing the phosphorylated tyrosine 626 (YLDL) was a strong SHP-2 binder, the C-terminal phosphopeptide (YVVV) bound weakest, while the N-terminal phosphopeptide showed intermediate binding ^{177}Q-^{189}C (Fig.4a). The level of tyrosine phosphorylation was similar in all peptides as controled by ELISA.

The phosphopeptides corresponding to three tyrosine phosphorylation motifs of Gab1 were also compared for their SHP-2 activation capacity, which was found to correlate with their SHP-2 binding. One of them (^{621}GDQVEYLDLDLD^{632}) was the most efficient one as evidenced by its complete dephosphorylation (Fig. 4b).

FcγRIIb-BCR co-clustering induces Gab1 dephosphorylation and its dissociation from PI3-K

FcγRIIb and Gab1 were affinity purified from untreated, BCR activated or BCR-FcγRIIb co-clustered BL41 cells. The isolated proteins were analysed after SDS-PAGE by immunoblotting. Both Gab1 and Grb2 were detected in FcγRIIb precipitates obtained from BCR clustered and FcγRIIb-BCR co-clustered cells after 2 min treatment, while the untreated control samples and cells treated only for 30 sec were negative (Fig.5a).

In order to examine the influence of BCR-FcγRIIb co-aggregation on the state of Gab1 tyrosine phosphorylation, affinity purified Gab1 samples immunoisolated from resting

cells, or from BCR clustered and BCR-FcγRIIb co-clustered cells after 5 min treatment were separated by electrophoresis and immunoblotted with phosphotyrosine specific antibodies. Tyrosine phosphorylation of the 110 kDa protein corresponding to Gab1 significantly decreased upon co-clustering FcγRIIb and BCR, as compared to the BCR activated samples, indicating that Gab1 undergoes dephosphorylation (Fig.5b, left panel).

Association of Gab1 with SHP-2 was tested by analysing affinity purified SHP-2 samples obtained from resting, BCR-activated and BCR-FcγRIIb co-clustered BL41 cells. The level of bound Gab1 was the same in the latter two samples, indicating that co-clustering of antigen and FcγRIIb receptors on human B cells does not influence the Gab1 association with SHP-2 induced by BCR clustering (Fig. 5b, right panel).

To asses whether the tyrosine phosphorylation state of Gab1 affects its binding to PI3-K, this interaction was tested in immunoisolated PI3-K samples. BCR-FcγRIIb co-aggregation abolished the association between the p85 subunit of PI3K and Gab1, as monitored by both phosphotyrosine and Gab1 specific antibodies. The same result was obtained in the reverse experiment, we could not observe PI3-K in the immunoisolated Gab1 samples obtained from FcγRIIb-BCR co-clustered cells (data not shown). Thus co-clustering of the BCR and FcγRIIb induces dephosphorylation of Gab1 and the dissociation of p85 PI3-K from Gab1 (Fig. 5c).

Discussion

The aim of this study was to investigate the intermolecular interactions within the human FcγRIIb p-ITIM recruited protein complex. FcγRIIb is tyrosine phosphorylated on its ITIM upon co-clustering with the BCR, resulting in its binding to SH2 domain containing SHP2, SHIP, Shc, and PI3-K (22, 23). SHIP and Shc are also phosphorylated on their tyrosines upon BCR clustering, thus the phosphorylated SHIP and/or Shc might interact with the available SH2 domains of other proteins within the FcγRIIb assembled multimolecular complex. SHIP was suggested to play a dominant role in the regulation of FcγRIIb mediated inhibition on mouse B- and mast cells (32), although the high affinity binding of SHP-2 to mouse FcγRIIb p-ITIM peptide was also observed (33). SHIP activity may reduce the binding of Btk PH domain to phosphatidylinositol (3,4,5)- trisphosphate (PIP_3) in the cell membrane via its hydrolysis to phosphatidyl inositol (3,4)- bisphosphate (PIP_2). This may lead to the inhibition of Btk mediated PLCγ activation and consequently to reduced inositol trisphosphate (IP_3) production and Ca^{2+} mobilization (17, 34). Furthermore, SHIP recruitment also attenuates FcγRIIb induced proapoptotic signal by inhibiting the membrane location and activation of Btk (35).

We have previously shown that in contrast to the mouse B cells, where only SHIP was found to bind to the tyrosine phosphorylated FcγRIIb, in human B cells SHP-2 co-precipitates with the BCR-co-clustered FcγRIIb (23, 22). Since we observed that SHIP and Shc were released from the p-ITIM-recruited complexes as a result of the bound phosphatase activity, we suggested that SHP-2 plays a crucial role in FcγRIIb dependent B cell inhibition, by dephosphorylating SHIP, Shc, and presumably, other potential substrates (23).

Here we provide evidence that SHP-2 plays a critical role in the FcγRIIb-mediated regulation of human B cells by dephosphorylating the docking protein Gab1, disrupting

thereby its recruited signaling complex. This emerged from results of a model system established to study the FcγRIIb-SHIP complexes using combined sequences of the tyrosine phosphorylated motif of SHIP and the FcγRIIb p-ITIM. Binding of this bisphosphopeptide to SHP-2 was analysed and compared with that of the monophosphopeptides. P-ITIM peptide bound SHP-2 and SHIP SH2 domains at nanomolar range, (K_D=104 nM and 40 nM, respectively), while the apparent affinity constant for SHP-1 was 2 mM. This is in agreement with previous findings, suggesting that SHP-1 binds to p-ITIM with the lowest K_D as compared to SHP-2, and SHIP, furthermore, with data showing that SHP-1 is dispensable for FcγRIIb dependent B cell inhibition (33, 36). Since p-ITIM bound complexes contain tyrosine phosphorylated proteins, including SHIP and Shc, we supposed that these molecules may also interact with the SH2 domains of SHP-2. Indeed, the SHIP and Shc phosphopeptides bound to SHP-2 SH2 domains with a 60-300 nM and to SHIP SH2 with 14-116 nM affinity constants. Interestingly, SHIP phosphopeptides also bound to the autologous SH2, suggesting that phosphorylated SHIP might inhibit the interactions of its own SH2 domain.

In spite of the high affinity binding of recombinant SHP-2 SH2 domains to the biosensor coated with SHIP and Shc phosphopeptides, the same molecules did not bind native SHP-2 from the cell lysates suggesting that tyrosine phosphorylated motifs of SHIP and Shc cannot bind to the free C-terminal SH2. However, they may react with the N-terminal SH2 domain of SHP-2, which becomes accessible in the native molecule only after the occupation of the C-terminal SH2 domain by the phosphopeptide ligand, such as p-ITIM. Crystallographic data have shown that the activation of SHP-2 is initiated by the phosphopeptide binding of C SH2, localizing the second tyrosine containing motif in the proximity of N-terminal SH2 domain (37). These phosphorylated ligands then would achieve

a sufficient local concentration to compete for the binding to N SH2, thus liberating the catalytically active site. Recent data have also shown that the two SH2 domains of SHP-2 are widely spaced and oppositely oriented, thus a ligand with a spacer larger than 50 intervening amino acids between the two tyrosines would be suitable for the bidental binding (38). The latter authors concluded that the two activating phosphotyrosines do not have to be located on the same protein. Thus, we expected that following the binding of p-ITIM to the C-terminal SH2 domain of SHP-2, an other phosphotyrosine containing protein(s) in the same p-ITIM associated complex maybe in a position to react with the N-terminal domain and activate the phosphatase. The results of the SHP-2 activity assays have shown that indeed, this is the case: phosphatase activity of affinity purified SHP-2 was approximately 10 times higher when measured using the bisphosphopeptide, as compared to the monophosphopeptide substrates. On the basis of these results, we suggest that the FcγRIIb p-ITIM bound multimolecular complex, containing multiple tyrosine phosphorylated motifs, is able to activate SHP-2 via interacting sequentially with both the C- and the N-terminal SH2 domains. Thus FcγRIIb-SHIP complexes may switch the adaptor function of SHP-2 into a catalytically active phosphatase function.

The adaptor protein Shc when phosphorylated binds Grb2 via its SH2 domain and translocates it to the cell membrane, where Grb2 interacting with SOS, induces GDP-GTP exchange of ras (39). Monitoring the molecules isolated from the cell lysate samples by the biotinylated bisphosphopeptide, we have found that SHIP-p-ITIM precipitated a significant amount of Grb2. Binding of Grb2 to SHIP-p-ITIM was inhibited by the N-terminal monophosphopeptide of Shc, and SHIP as well. Since the N-terminal phosphopeptide of SHIP bound Grb2, while only the C-terminal SHIP phosphopeptide bound Shc, we suggest that SHIP-Grb2 as well as Shc-Grb2 complexes may interact with p-ITIM.

The Grb2 binding docking/scaffolding protein, Gab1 was also suggested earlier to play role in the Grb2 translocation to the inner leaflet of the cell membrane (10). When tyrosine phosphorylated upon BCR clustering, Gab1 translocates to the plasma membrane and recruits SHP2, Grb2, SHIP, Shc, and PI3-K to the vicinity of their substrates, regulating thereby the activity of these proteins (10, 40). We detected Gab1 in samples isolated by p-ITIM, SHIP-p-ITIM, N-terminal SHIP and Shc peptides and also identified Gab1 in immunoisolated FcγRIIb samples obtained from BCR activated and BCR- FcγRII co-clustered cells. Since Gab1 has no SH2 or PTB domains the results indicate that these interactions may be mediated by the free SH2 domain of Shc, SHP-2 or the p85 subunit of PI3-K.

Gab family docking proteins are known as a potential substrates of SHP-2 (40). When tyrosine phosphorylation of the Gab1 was monitored after an extended time of BCR-FcγRIIb co-clustering, a marked decrease in tyrosine phosphorylation of a 110 kDa protein, corresponding to Gab1 was observed. This result indicates that Gab1 is dephosphorylated, at least partially in BCR-FcγRIIb co-clustered B cells. In order to control whether SHP-2 is indeed responsible for dephosphorylating Gab1, we have employed synthetic peptides corresponding of three tyrosine phosphorylated motifs of Gab1 as possible substrates of affinity isolated SHP-2. All phosphopeptides bound SHP-2, though to a different extent, and one of them containing the tyrosine 626, was completely dephosphorylated by SHP-2 suggesting that this peptide efficiently activated the phosphatase.

The tyrosine phosphorylated state of Gab1 is a pre-requisite for binding SH2 domain containing proteins. PI3-K binds to Gab1 in BCR activated cells via the SH2 domains of the p85 regulatory subunit (40). Membrane targeting was shown to be sufficient for PI3-K activation and triggering multiple signal transduction pathways (19, 41). Gab1 is recruited to the cell membrane via its PH domain binding specifically to PIP_3, a product of PI3-K. Thus

PI3-K apparently functions as both an upstream modulator and a downstream effector of Gab1 (42). We have shown here that PI3-K binding to Gab1 is diminished in the BCR-FcγRII co-clustered cells. Interfering with the PI3-K translocation to the cell membrane by dephosphorylating Gab1 may result in the inactivation of PI3-K. Thus PIP_3 level in the cell membrane might be downregulated, resulting in the abolished binding of Gab1 PH domain, and the release of Gab1 from the membrane. Moreover, since Gab1 regulates ras activation via Shc-Grb2-SOS complexes, disruption of the Gab1 bound signaling complex may also lead to the inhibition of the ras pathway. We may conclude that Gab1 dephosphorylation might be responsible for the previously observed inhibition of both the PI3-K- and the ras-dependent activation pathways in FcγRIIb-BCR co-clustered cells (19, 20, 43).

The level of PIP_3 in the cell membrane is regulated by two enzymes: SHIP, which hydrolyses PIP_3 to yield phosphatidylinositol 3,4 phosphate, and PI3-K, which phosphorylates phosphatidylinositol (4, 5) bisphosphate at position 3, resulting PIP_3 (34, 44). Therefore both the recruitment of SHIP to the cell membrane as well as the inactivation of PI3-K may result in a decreased level of PIP_3, consequently, an insufficient binding of both Btk and Gab1 PH domains. Thus, taken together, our data suggest that SHIP has a double role in course of regulating B cell activation. Beside dephosphorylating PIP_3, SHIP co-operates with the phosphorylated FcγRIIb and by activating SHP-2 promotes dephosphorylation of Gab1. This results in the dissociation of Gab1 bound signaling molecules, leading to the inactivation of PI3-K, and a reduced Btk and PLCγ activity.

Acknowledgements

The authors wish to thank for the vectors containing GST -SHP-1.SH2(NC) and GST-SHP-2.SH2(NC) to B. Neel, Boston, USA and for GST-SHIP.SH2 to M. Daeron (Paris, France). We thank for preparing the recombinant proteins to R. Philosof-Oppenheimer (Rehovot, Israel).

Figure legends

Fig. 1. Affinity measurements between the SH2 domains of SHP-1, SHP-2 and SHIP and the biotinylated phosphopeptides of FcγRIIb, Shc and SHIP. A, Real-time association and dissociation of 31.2 nM SH2 domains of SHP-1 (Δ), SHP-2 ( ) and SHIP (■) to biotinylated human p-ITIM peptide. B, Comparison of the binding and dissociation of 31.2 nM SHIP SH2 domains and C, SHP-2 SH2 domain to the various phosphopeptides. D., Binding and dissociation SHP-2 (thick line) and SHIP (thin line) SH2 domains at 62.5 nM (■), 31.2 nM (Δ), and 15.8 nM (∇) concentrations to the bisphosphopeptide corresponding to the combined sequence of the tyr phosphorylated motif of SHIP and of human FcγRIIb ITIM. Background signal of theSH2 domains flowing through an empty chip was subtracted from each curves. Typical curves out of three independent experiments are shown.

Fig. 2. SHP-2 phosphatase activity measured using different phosphopeptide substrates. The biotinylated tyrosine phosphorylated peptides were treated with various dilutions of affinity purified SHP-2 at 37° for 1 hour, then the samples were transferred onto streptavidine coated ELISA plate. After an overnight incubation the remaining phosphotyrosine contents of the bound peptides were detected by ELISA using phosphotyrosine specific antibodies. Shown are the dilutions of the immunoprecipitated, 10^6 cell equivalent SHP-2 required for dephosphorylation of 20 % (open columns) and 60 % (hatched columns) of each phosphopeptides (50 pM). Mean +/- SD of 3-4 independent experiments.

Fig. 3. Binding of Shc, Grb2 and Gab1 from BCR activated BL41 cell lysates to the biotinylated, tyrosine phosphorylated peptides of FcγRIIb, Shc , SHIP, SHIP-p-ITIM, and CD19 coupled to Streptavidine-agarose beads as insoluble matrices. A., Lysate samples were precipitated by the corresponding phosphopeptides or with Gab1 specific antibodies (last

lane), or pre-cleared for Gab1, then precipitated by SHIP-p-ITIM (third lane). The bound components were separated by SDS-PAGE, and transfered to nitrocellulose membranes. Western blotting of the same membranes were done sequentially by Shc and Grb2 specific antibodies. B., SHP-2 and Grb2 binding to the biotinylated SHIP-p-ITIM bisphosphopeptide. The precipitation was carried out in the absence, or presence of 50 nM soluble peptides, as indicated. C., activated BL41 cell lysate samples were incubated with different biotinylated phosphopeptides bound to Streptavidine coated beads, and the precipitated samples were analysed after electrophoresis and Western blotting by Gab1 specific antibodies. Typical experiments out of three or four.

Fig. 4. Binding to and activation of SHP-2 by Gab1 phosphopeptides. A., PI3-K and SHP-2 binding to Gab1 and p-ITIM phosphopeptides. The samples were treated and immunoprecipitated as described for Fig. 2. B., Activation of SHP-2 by Gab1 phosphopeptides ^{653}ADERVDYVVVDQ^{664} (•), ^{177}QEDPQDYLLLINC^{189}(■) and ^{621}GDQVEYLDLDLD^{632} (▲). The experiments were carried out as described in the legend to Fig. 3. Percentage of residual phosphorylation of each peptides is plotted as function of SHP-2 dilution, taking the phosphotyrosine contents of the untreated phosphopeptide as 100 %.

Fig. 5. Association and dephosphorylation of Gab1 by CD32. A., FcγRIIb were immunoprecipitated by a CD32 specific mAb from untreated, BCR activated (for 30 and 120 sec, respectively), or BCR and CD32 co-clustered BL41 cell lysates. The samples were first Western blotted with Gab1-, then by Grb2-specific antibodies. B., left panel: Tyrosine phosphorylation of affinity isolated Gab1 and the Gab1 associated proteins from untreated, BCR activated and BCR-FcγRIIb co-clustered samples. The arrow shows the posititon of Gab1. B., right panel: SHP-2-Gab1 association is not affected by BCR-FcγRIIb co-

clustering. C., PI3-K was immunoprecipitated by specific antibodies, and the membrane was Western blotted with phosphotyrosine, Gab1, and PI3-K specific antibodies.

Footnotes

[1] This work was supported by the Hungarian National Science and Research Developmental Foundation (OTKA T017173 and 026637) and by the Foundation for the Development of Graduate Education and Research (FKFP 0135/1997).

[2] Corresponding author: Gabriella Sármay, Dept. of Immunology, Loránd Eötvös University, Jávorka Sándor u. 14., Göd 2131, Hungary. E-mail: sar7197@mail.iif.hu

[3] Abbreviations: BCR, B cell receptor ; FcγRIIb, Fc gamma receptor type II; Grb2 associated binder 1, Gab1; ITAM, Immunoreceptor Tyrosine-based Activation Motif; ITIM, Immunoreceptor Tyrosine-based Inhibitory Motif; PI3-K, phosphatidylinositol 3-kinase; PIP_3 , phosphatidylinositol(3,4,5)trisphosphate; PTB, phosphotyrosine binding ; SH2, src homologue; SHIP, polyphosphoinositol 5-phosphatase; SPR, surface plasmon resonance

References

1. Gold, M.R.,Law, D.A., and DeFranco, A.L. 1990. Stimulation of protein tyrosine phosphorylation by the B-lymphocyte antigen receptor. *Nature, 345: 810.*

2. Campbell, K.S., Hager, E.J., Friedrich, R.J., and Cambier, J.C. 1991. IgM antigen receptor complex containes phosphoprotein products of B29 and mb-1 genes. *Proc. Natl. Acad. Sci. 88: 3982.*

3. Campbell, K.S. 1999. Signal transduction from the B cell antigen receptor. *Curr. Opin. in Immunol. 11: 256.*

4. Pawson, T.1995. Protein modules and signalling networks, *Nature, 373: 573.*

5. Cohen, G.B., Ren, R., and Baltimore D. 1995. Modular binding domains in signal transduction proteins. *Cell, 80: 237.*

6. DeFranco, A.L. 1997. The complexity of signaling pathways activated by the BCR. *Curr. Opin. Immunol. 9: 296.*

7. Lemmon, M.A., Ferguson, K.M., and Schlessinger, J. 1996. PH domains: diverse sequences with a common fold recruit signalling molecules to the cell surface. *Cell, 85: 621.*

8. Panchamoorthy, G., Fukazawa, T., Miyake, S., Soltoff, S., Reedquist, K., Druker, B., Shoelson, S., Cantley, L., and Band, H. 1996. p120cbl is a major substrate of tyrosine phosphorylation upon B cell antigen receptor stimulation and interacts in vivo with Fyn and Syk tyrosine kinases, Grb2 and Shc adaptors, and the p85 subunit of phosphatidylinositol 3-kinase. *J.Biol Chem. 271: 3187.*

9. Holdago-Madruga, M., Emlet, D.R., Moscatello, D.K., Godwin, A.K., Wong, A.J. 1996. A Grb2-associated docking protein in EGF and insulin receptor signaling. *Nature, 379: 560.*

10. Ingham, R.J., Holdago-Madruga, M., Siu, C., Wong, A.J. Gold, M.R. 1998. The Gab1 protein is a docking site for multiple proteins involved in signaling by the B cell antigen receptor. *J. Biol. Chem. 273: 30630.*

11. Rocchi, S., Tartara-Deckert, S., Murdaca, J., Holdalgo-Madruga, M., Wong, A.J., and Van Obberghen, E. 1998. Determination of Gab1 (Grb2 associated binder) interaction with insulin receptor signaling molecules. *Mol. Endocrinol. 12: 914.*

12. Takahashi-Tezeuka, M., Yoshida, Y., Fukada, T., Ohtani, T., Yamanaka, Y., Nishida, K. , Nakajima, K., Hibbi, M, and Hirano, T. 1998. Gab1 acts as an adapter molecule linking the cytokine receptor GP130, to ERK mitogen activated proteine kinase. *Mol. Cell. Biol. , 18: 4109.*

13. Lecoq-Lafon, C, Verdier, F., Fishelson, C, Chretien S., Gisselbrecht S., and Lacombe C. 1999. Erythropoietin induces the tyrosine phospohrylation of Gab. *Blood, 93: 2578.*

14. Lehr, S., Kotzka, J., Klein, E., Siethoff, C., Knebel, B., Noelle, V., Brüning, J.C., Klein, H.W., Mever, H.E., Krone, W., and Müller-Wieland, D. 1999. Identification of phosphorylation sites in human Gab1 protein by EGF receptor kinase in vitro. *Biochemistry, 38: 151.*

15. Amigorena, S., Bonnerot, C., Drake, J., Choquet, D., Hunziker, W., Guillet, J. G., Webster, P., Sautes, C., Mellman, I. and Fridman W. H. 1992. Cytoplasmic domain heterogeneity and functions of IgG Fc receptors in B lymphocytes. *Science, 256: 1808.*

16. Muta, T., Kurosaki, T., Misulovin, Z., Sanchez, M., Nussenzweig, M. C. and Ravetch, J. V. 1994. A 13 amino-acid motif in the cytoplasmic domain of FcγRIIb modulates B cell receptor signalling. *Nature 368: 70.*

17. Scharenberg, A. M. and Kinet, J. P. 1996. The emerging field of receptor mediated inhibitorysignaling: SHP or SHIP. *Cell, 87: 961.*

18. Daeron, M. 1996. Building up the family of ITIM-bearing negative coreceptors. *Immunol. Lett. 54: 73.*

19. Sármay, G., Koncz, G., and Gergely, J. 1996. Human type II Fcγ receptors inhibit B cell activation by interacting with the p21ras-dependent pathway. *J.Biol. Chem. 271: 30499.*

20. Sármay, G., Koncz, G. and Gergely, J. 1996. Integration of activatory and inhibitory signals in human B cells. *Immunol. Lett. 54: 93.*

21. Sármay G., Koncz G., Pecht, I., and Gergely J. 1997. Fcγ receptor IIb induced recruitment of inositol and protein phosphatases to the signal transductory complex of human B-cell. *Imm. Lett. 57: 159.*

22. Sármay G, Koncz G, Pecht I, and Gergely J. 1999. Cooperation between SHP-2, phosphatidyl inositol 3- kinase and phosphoinositol 5-phosphatase in the FcRIIb mediated B cell regulation. *Imm. Letters, 68: 25.*

23. Koncz, G., Pecht, I., Gergely, J., and Sármay, G. 1999. Fcγreceptor mediated inhibition of human B cell activation: the role of SHP-2 phosphatase. *Eur. J. Immunol. 29: 1980.*

24. Chan, P. L., and Sinclair, N. R. S. C. 1971. Regulation of the immune response. V. An analysis of the function of the Fc portion of antibody in suppression of an immune response with respect to interaction with components of the lymphoid system. *Immunology, 21: 967.*

25. Ono, M., Bolland, S., Tempst, P. and Ravetch, J. V. 1996. Role of inositol phosphatase SHIP in negative regulation of the immune system by FcγRIIb. *Nature, 383: 263.*

26. Takai, T., Ono, M., Hikida, M., Ohmori, H., and Ravetch, J.V. 1996. Augmented humoral and anaphylactic responses in FcγRII defficient mice. *Nature, 379: 346.*

27. Fields, G. B., and Noble, R. L. 1990. SPPS utilizing 9-fluorenylmethoxycarbonyl amino acids. *Int. J. Peptide Protein Res. 35: 161.*

28. Laczkó, I., Hollósi, M., Vass, E., Hegedus, Z., Monostori, É., and Tóth, G. K. 1998. Conformational effect of phosphorylation on T cell receptor/CD3 zeta chain sequences *Biochem. Biophys. Res. Commun. 242: 474.*

29. Perich, J. W., and Johns, R. B. 1988. Di-tert-butyl N,N-Diethylphosphoramidite. A New Phosphitylating Agent for the Efficient Phosphorylation of Alcohols. *Synthesis,* 142.

30. Vely, F., Olivero, S., Olcese, L., Moretta, A., Damen, J., Liu, L., Krystal, G., Cambier, J.C., Dearon, M., and Vivier, E. 1997. Differential association of phosphatases with hemopoietic co-receptors bearing immunoreceptor tyrosine based inhibition motifs. *Eur.J. Immunol. 27: 1994.*

31. Tridandapani, S., Pradhan, M., LaDine, J.R., Garber,S., Anderson, C.L., and Coggeshall, K.M. 1999. Protein interaction of Src homology 2 (SH2) domain containing inositol phosphatase (SHIP): Association with Shc displaces SHIP from FcγRIIb in B cells. *J. Immunol. 162: 1408.*

32. Daeron, M. 1997. Fc receptor biology. *Ann. Rev. Immunol. 15: 203.*

33. Famiglietti, S.J., Nakamura, K., and Cambier, J.C. 1999. Unique features of SHIP, SHP-1 and SHP-2 binding to FcγRIIb revealed by surface plasmon resonance analysis. *Immunol. Lett. 68: 35.*

34. Bolland, S., Pearse, R.N., Kurosaki, T., and Ravetch, J.V. 1998. SHIP modulates immune receptor responses by regulating membrane association of Btk. *Immunity, 8: 509.*

35. Ono, M., Okada, H., Bolland, S., Yanagi, S., Kurosaki, T. and Ravetch, J.V. 1997. Deletion of SHIP or SHP-1 reveals two distinct pathways for inhibitory receptor signaling. *Cell, 90: 293.*

36. Nadler, M. J. S., Chen, B., Anderson, J. S, Wortis, H. H, and Neel, B. G. 1997. Protein tyrosine phosphatase SHP-1 is dispensable for FcgammaRIIb-mediated inhibition of B cell antigen receptor activation. *J. Biol. Chem. 272: 20083.*

37. Hof, P., Pluskey, S., Dhe-Paganon, S., Eck, M.J., Shoelson, S.E. 1998. Crystal structure of the tyrosine phosphatase SHP-2. *Cell, 92: 441.*

38. Ottinger, E. A., Botfield, M.C., and Shoelson, S. E. 1998. Tandem SH2 domains confer high specificity in tyrosine kinase signaling. *J. Biol. Chem. 273: 729.*

39. Saxton, T., M., van Oostveen, I., Bowtell, D., Aebersold, R., and Gold, M. R. 1994. B cell antigen receptor cross-linking induces phosphorylation of the p21ras oncoprotein activators Shc and mSOS1 as well as assembly of complexes containing Shc, Grb2, mSOS1, and a 145 kDa tyrosine- phosphorylated protein. *J. Immunol. 153: 623.*

40. Nishida, K., Yoshida, Y., Itoh, M., Fukada, T., Ohtani, T., Shirogane, T., Atsumi, T., Takahashi- Tezuka, M., Ishihara, K., Hibi, M., and Hirano, T. 1999. Gab-family adapter proteins act downstream of cytokine and growth factor receptors and T and B antigen receptors. *Blood,*

93: 1809.

41. Klippel, A., Reinhard, C., Kavanaugh, W. M., Appel, G., Escobedo,M., Williams, L.T. 1996. Membrane localization of phosphatidylinositol 3-kinase is sufficient to activate multiple signal-transducing kinase pathways. *Mol. Cell. Biol. 16: 4117.*

42 . Rodrigues, G.A., Falasca, M., Zhang, Z., Ong, S.H., Schlessinger, J. 2000. A novel positive feed-back loop mediated by the docking protein Gab1 and phosphatidylinositol 3 kinase in epidermal growth factor receptor signaling. *Mol.Cell.Biol. 20 (4):1448.*

43. Buhl, E.M., and Cambier, J.C. 1999. Phosphorylation of CD19 Y484 and Y515, and linked activation of phosphatidylinositol 3-kinase, are required for B cell antigen receptor mediated activation of Bruton's tyrosine kinase. *J. Immunol. 162:4438.*

44. Scharenberg, A. M., El-Hillal, O., Fruman, D.A., Beitz, L.O., Li, Z., Lin, S., Gout, I., Cantley, L.C., Rawlings, D.J., and Kinet, J.P. 1998. Phosphatidylinositol-3,4,5,-trisphosphate (PtdIns-3,4,5-P3) /Tec kinase-dependent calcium signaling pathway: a target for SHIP- mediated inhibitory signals. *EMBO J. 17:1961.*

Table I.

SYNTHETIC PHOSPHOPEPTIDES[1]

^{908}TEIINPN**Y**MGVG^{919}	SHIP(1)
^{1013}EMFENPL**Y**GSLS^{1026}	SHIP(2)
^{233}EPPDHQ**Y**YNDFPG^{245}	SHC-(3)
^{306}ELFDDPS**Y**VNVQNL^{319}	SHC-(4)
^{242}AENTIT**Y**SLLMHP^{254}	p-ITIM hu
TEIINPN**Y**MGVG(AG)$_{15}$- -AENTIT**Y**SLLMHP	SHIP-p- ITIM
^{177}QEDPQD**Y**LLLINC^{189}	Gab1(1)
^{621}GDQVE**Y**LDLDLD^{632}	Gab1(2)
^{496}GSQS**Y**EDMRG^{505}	Gab1(3)
^{527}DADS**Y**ENMDN^{536}	CD19 (1)
^{653}ADERVD**Y**VVVDQ^{664}	CD19 (2)

[1] Phosphorylated tyrosine residues are bold and underlined, bold letters stand for amino acids having a role in the binding to Src homology 2, or phosphotyrosine binding domains

Table II.

Association, dissociation and affinity constants of various tyrosine phosphorylated peptides[2]

SH2 domains	SHP-2			SHIP		
tyr phospho-peptides	K_{on} $M^{-4}s^{-1}$	K_{off} s^{-1}	K_D nM	K_{on} $M^{-4}s^{-1}$	K_{off} s^{-1}	K_D nM
p-ITIM	0.6446±0.0615	0.0067±0.0004	**104**	0.9199±0.1730	0.0037±0.0014	**40**
Shc YYND	1.3490±0.1762	0.0083±0.0006	**61**	1.781±0.1088	0,0026±0,0008	**14**
Shc YVNV	0.5300±0.0156	0.0091±0.0001	**172**	1.602±0.0983	0.0232±0.0008	**145**
SHIP T-G	0.4387±0.0081	0.0134±0.0001	**305**	2.733±0.3709	0.0041±0.0030	**15**
SHIP E-S	0.9311±0.3275	0.0110±0.0012	**118**	1.241±0.0158	0.0016±0.0001	**13**
SHIP (T-G) -p-ITIM	4.158± 0. 6027	0.0038± 0.0012	**9**	2.814 ± 0.0402	0.0026± 0.0001	**10**

[2] The observed association rates for the SH2 domains of SHP-2 or SHIP binding to the phosphopeptides were plotted as a function of the concentration. The slopes of the plots were taken as K_{on} and the y intercepts were taken as K_{off} and K_D values were calculated.

A)

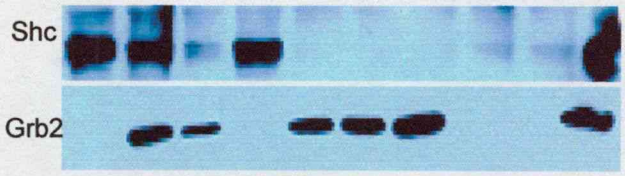

p-ITIM	SHIP-pITIM		SHIP		Shc		CD19		Gab1
	+	-	1	2	3	4	1	2	

B)

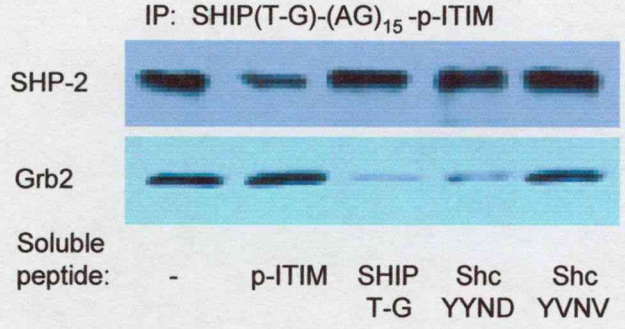

C)

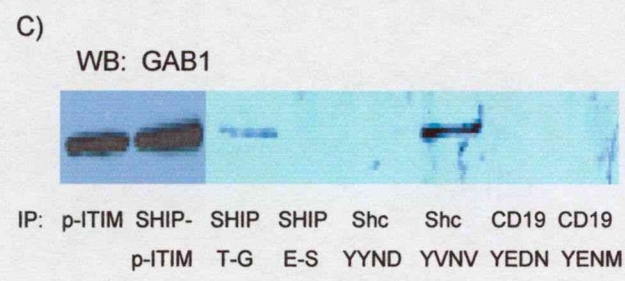

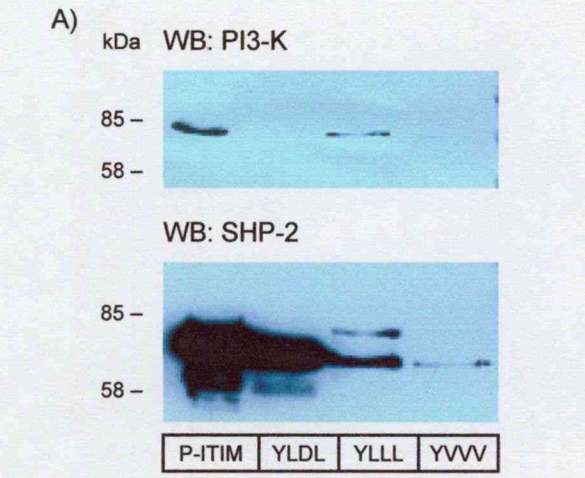
A)
kDa
WB: PI3-K
85 –
58 –
WB: SHP-2
85 –
58 –
P-ITIM
YLDL
YLLL
YVVV

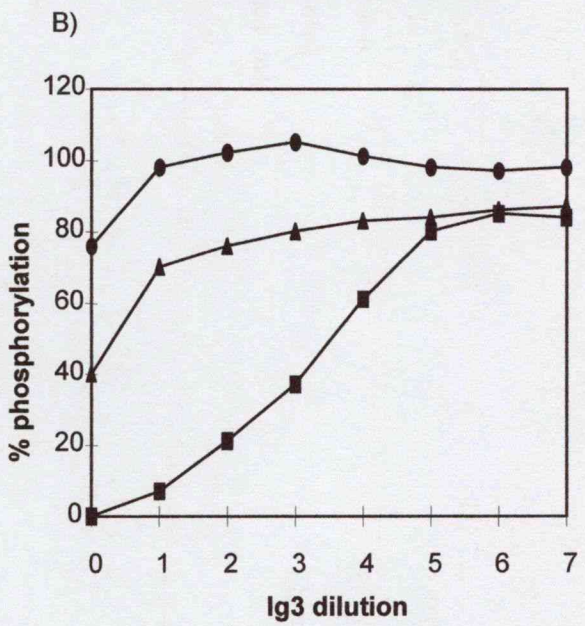
B)
120
100
80
60
40
20
0
% phosphorylation
0
1
2
3
4
5
6
7
Ig3 dilution

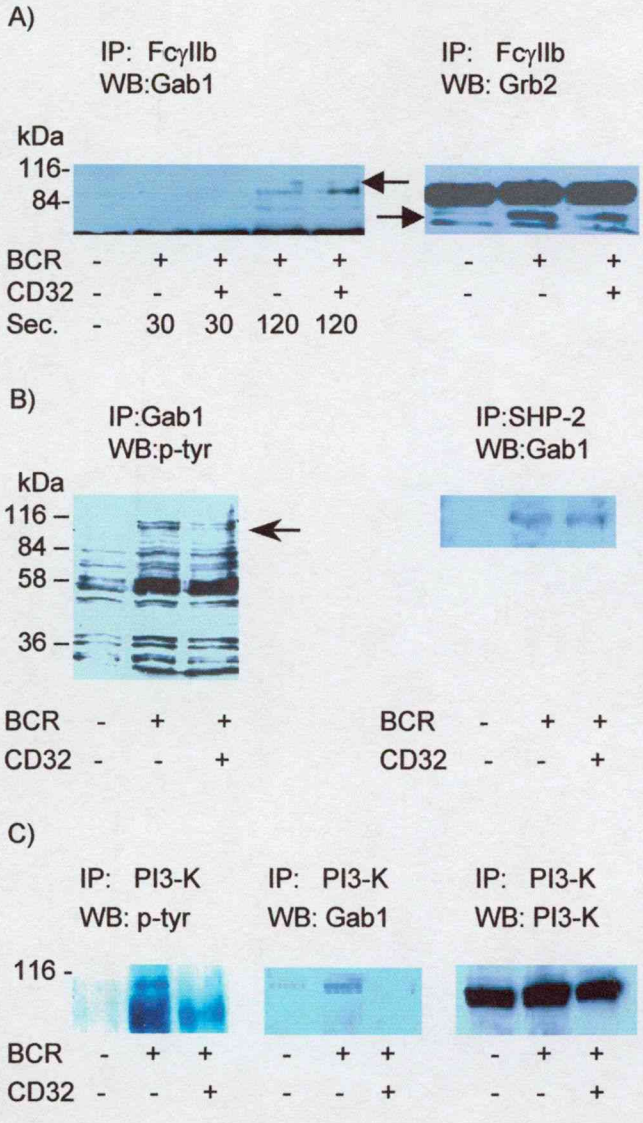
A)
IP: FcγIIb
WB:Gab1
IP: FcγIIb
WB: Grb2
kDa
116-
84-
BCR - + + + + - + +
CD32 - - + - + - - +
Sec. - 30 30 120 120
B)
IP:Gab1
WB:p-tyr
IP:SHP-2
WB:Gab1
kDa
116 –
84 –
58 –
36 –
BCR - + +
CD32 - - +
BCR - + +
CD32 - - +
C)
IP: PI3-K
WB: p-tyr
IP: PI3-K
WB: Gab1
IP: PI3-K
WB: PI3-K
116 -
BCR - + + - + + - + +
CD32 - - + - - + - - +

Synthesis of phosphotyrosine-containing peptides: Comparison of different methods and their use to investigate cell signalling *via* the T-cell receptor

G.K. Tóth[a], G. Váradi[a], T. Janáky[a], B. Penke[a], M. Mák[b], E. Láng[c], L. Ötvös[c], Z. Hegedüs[d] and É. Monostori[d]

[a] *Department of Medical Chemistry, A. Szent-Györgyi Medical University, H-6720 Szeged, Hungary*

[b] *Central Research Institute of Chemistry, Budapest, Hungary*

[c] *The Wistar Institute, Philadelphia, PA 19104, U.S.A.*

[d] *Institute of Genetics, Biological Research Center, H-6726 Szeged, Hungary*

Introduction

The phosphorylation of protein tyrosine residues is one of the main steps in the regulation of various cell processes. Therefore, there has been much interest in the establishment of efficient chemical methods for the synthesis of Tyr-phosphate-containing peptides. For the preparation of phosphotyrosine containing peptides many different strategies have been considered. The use of phosphochloridates (either for the synthon or global approaches) or the different phosphoramidite derivatives offers many possibilities for the phosphopeptide synthesis. The ζ-chain of the TCR/CD3 complex plays a central role in cell signalling *via* the TCR. Following receptor stimulation, the ζ-chain is phosphorylated on multiple tyrosine residues present in the intracellular region of this molecule. However, it has not yet been revealed which of the seven tyrosines present in the ζ-polypeptide are phosphorylated. The functional consequences of the particular tyrosine phosphorylation events are also unknown. Six short peptide fragments and the corresponding phosphorylated derivatives of the ζ-subunit were synthesized in order to investigate the role of individual phosphotyrosine residues in the biochemical process of T-cell activation.

Results and Discussion

The peptides were synthesized by the solid-phase technique utilizing Boc or Fmoc chemistry. The peptides were synthesized on TMBHA or MBHA resins, respectively. Couplings were performed with DCC. The final peptide resins were phosphated or treated with the appropriate cleavage reagent. The resulting crude peptides were purified by semipreparative RP-HPLC. Phosphorylation with dibenzyl phosphochloridate failed both in the solid and in the liquid phase. Only the phenolate seems to be sufficiently nucleophilic, but its preparation from the protected peptide resin was not feasible. The use of the commercially available Fmoc-Tyr(PO_3Me_2)-OH is a safe but rather expensive method and the deprotection of the phosphate moiety can lead to partially deprotected by-products. The purity of the resulting phosphopeptide is not high due to the drastic cleavage conditions. The preparation of di-*tert*-butyl-diethylphosphoramidite can be carried out with a good yield and this product can be used successfully for the phosphorylation of protected peptides both in the liquid and in the solid phase (phosphitylation and subsequent oxidation with *tert*-butyl-peroxide). In the case of partially protected peptides (free carboxyl functions) the phosphorylation failed. For the temporary protection of the carboxyl functions *tert*-butyldimethylsilyl chloride seems to

be suitable, but owing to low reactivity, this reaction needs careful optimization. The method described for the liquid-phase phosphorylation of N-protected tyrosine (reaction with *tert*-butyldimethylsilyl chloride and subsequent phosphorylation with phosphoramidite) cannot be applied for this purpose due to the low reactivity of the *tert*-butyldimethylsilyl chloride. In contrast with data reported in the literature, the formation of the silyl ester required a 24 to 36 h reaction time at ambient temperature, and not 3 min as indicated by other authors. After formation of the *tert*-butyldimethylsilyl ester, the phosphoramidite method becomes suitable for this purpose. The global method of SPPS can be applied with good results, but only in the case of the Fmoc strategy. The synthesized phosphotyrosine-containing peptides were characterized by RP-HPLC, AAA, UV spectra and Fab mass spectrometry. The immunological investigations concerning the role of the phosphated ζ-peptides are currently in progress.

Conclusions

All the synthetic methods summarized previously (synthon method or global phosphorylation in liquid or solid phase) are suitable for the synthesis of Tyr-phosphate-containing peptides. The phosphochloridate method, which gives excellent results for Ser- and Thr-containing peptides, is not applicable in the case of tyrosine. The global phosphoramidite method seems consistently better than the synthon method.

Acknowledgments

This work was supported by grants OTKA 2734 and ETT T03/523.

References

1. Ötvös Jr., L., Elekes, I. and Lee, V.M.-Y., Int. J. Pept. Protein Res., 34(1989)129.
2. Valerio, R.M., Alewood, P.F., Johns, R.B. and Kemp, B.E., Int. J. Pept. Protein Res., 33(1989)428.
3. Turek, C.W., Pept. Res., 5(1992)156.
4. Perich, J.W., Ruzzene, M., Pinna, L.A. and Reynolds, E.C., Int. J. Pept. Protein Res., 43(1994)39.
5. Perich, J.W. and Johns, R.B., Synthesis, (1988)142.
6. Andrews, D.M., Kitchin, J. and Seale, P.W., Int. J. Pept. Protein Res., 38(1991)469.
7. De Bont, H.B.A., Van Boom, J.H. and Liskamp, R.M.J., Tetrahedron Lett., 31(1990)2497.
8. Bannwarth, W. and Trzeciak, A., Helv. Chim. Acta, 70(1987)175.
9. Corey, E.J. and Venkateswarlu, A., J. Am. Chem. Soc., 94(1972)6190.
10. Wissner, A. and Grudzinskas, C.V., J. Org. Chem., 43(1978)3972.
11. Lalonde, M. and Chan, T.H., Synthesis, (1985)835.
12. Samelson, L.E. and Klausner, R.D., J. Biol. Chem., 267(1992)24913.
13. Isakov, N., Mol. Immunol., 30(1993)197.

Peptides: Chemistry, Structure and Biology
Pravin T.P. Kaumaya and Robert S. Hodges (Eds.)
Mayflower Scientific Ltd., 1996

188
Synthesis of Phosphotyrosine-containing T-cell Receptor ζ-Subunit Peptides: Conformational and Immunological Studies

G.K. Tóth[1], I. Laczkó[2], Z. Hegedűs[2], E. Vass[3], M. Hollósi[3], T. Janáky[1], G. Váradi[1], B. Penke[1] and É. Monostori[2]

[1]*Department of Medical Chemistry, A. Szent-Györgyi Medical University, Hungary*
[2]*Institute of Genetics and Biophysics, Biological Research Center, Szeged, Hungary*
[3]*Department of Organic Chemistry, Eötvös University, Budapest, Hungary*

Introduction

The ζ-chain of the TCR/CD3 complex plays a central role in cell signalling *via* the TCR [1, 2]. On receptor stimulation, the ζ-chain is phosphorylated on tyrosine residues in the intracellular region of this molecule. It has not yet been revealed which of the seven tyrosines present in the ζ-polypeptide are phosphorylated nor which kinase is involved in this event [3, 4]. Dephosphorylation of the protein is necessary for the downregulation of T-cell activation, but the phosphatases participating in dephosphorylation have not yet been identified [5]. Different peptide fragments and the corresponding phosphorylated derivatives of the ζ-subunit were synthesized in order to investigate the roles of the individual phosphotyrosine residues in the biochemical process of T-cell activation. The phosphorylated ζ-peptides were also applied to establish whether any of them are substrates for CD45, a lymphocyte-specific transmembrane tyrosine phosphatase.

Results and Discussion

Both the synthon approach and the global method were applied in the synthesis of seven short phosphorylated (and non-phosphorylated) fragments of the TCR, CD3 ζ-chain. Of the separation methods applied for the purity control MECC seemed best. Preliminary experiments revealed that six short ζ-related peptides, corresponding to the conservative sequences of the ζ-polypeptide are substrates for the src kinases, and one of the seven peptides (PPAYQQG), which lies outside the conservative motifs, is not a target for *in vitro* phosphorylation by the src kinases used (lck and fyn) [6]. CD45, a lymphocyte surface protein, which has tyrosine phosphatase activity, seems to be responsible for the dephosphorylation of the ζ-chain. It has been demonstrated that CD45 dephosphorylates

PPAY(*P*)QQG, 61P; NQLY(*P*)NEL, 69P; REEY(*P*)DVL, 80P; QEGLY(*P*)NEL, 106P; AEAY(*P*)SEIG, 119P; DGLY(*P*)QGL, 138P; KDTY(*P*)DAL, 149P

Figure 1. *The structures of the synthesized peptides.*

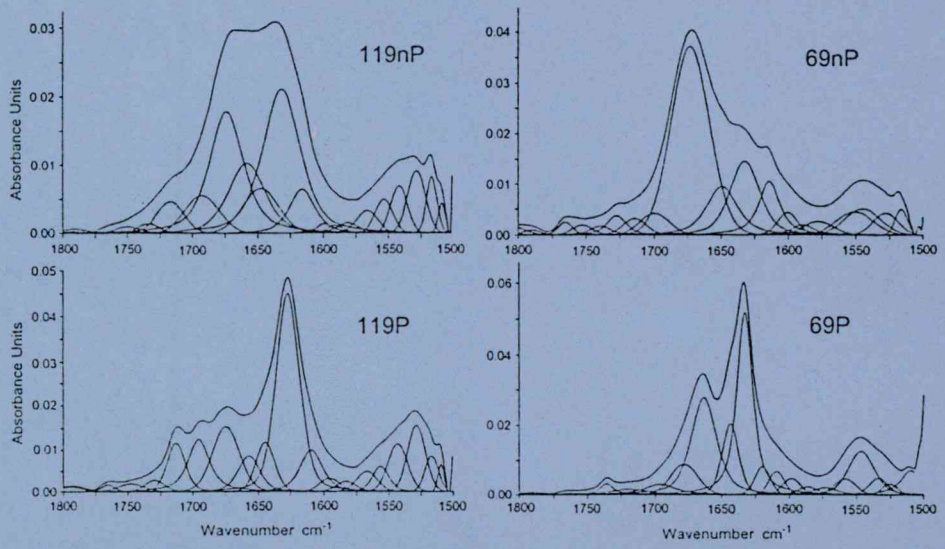

Figure 2. *The FT-IR spectra of several peptides. Band at 1633 cm^{-1} indicates ß-sheet formation.*

phosphorylated ζ- oligopeptides, indicating that this tyrosine phosphatase may play a role in the downregulation of T-cell activation. In water, both the non-phosphorylated (nP) and phosphorylated (P) peptides give CD spectra characteristic of a predominantly random conformation (strong negative band below 200 nm). In TFE solution, the peptides exist as mixtures of conformers, and the CD spectra reflect more than one prevailing secondary structure. The conformational investigations of these phospho-peptides by means of CD and FTIR spectroscopy supported the idea that the phosphorylation event can change the conformations of the parent peptides, mostly leading to an increase in the ß-sheet conformation.

Acknowledgments

This work was supported by the following grants: OTKA T 016156 and ETT T03/523 to GKT, OTKA T 005159 to TJ and OTKA T 005257 to EM.

References

1. June, C.H., Fletcher, M.C., Ledbetter, J.A., Schieven, G.L., Siegel, A.F., Phillips, A.F. and Samelson, L.E., *Proc. Natl. Acad. Sci. USA*, 87 (1990) 7722.
2. Irving, B.A. and Weiss, A., *Cell*, 64 (1991) 891.
3. Barber, E.K., Dasgupta, J.D., Schlossman, S.F., Trevillyan, J.M. and Rudd, C.E., *Proc. Natl. Acad. Sci. USA*, 86 (1989) 3277.
4. Samelson, L.E. and Klausner, R.D., *J. Biol. Chem.*, 267 (1992) 24913.
5. Isakov, N., *Mol. Immunol.*, 30 (1993) 197.
6. Hegedüs, Z., Andó, I., Tóth, G.K., Váradi, G. and Monostori, É., *BioTechniques*, 18 (1995) 632.

Synthesis of Phosphotyrosine-Containing Peptides: Immunological and Conformational Investigations

GÁBOR K. TÓTH[1], ILONA LACZKÓ[2], ZOLTÁN HEGEDÜS[2], ELEMÉR VASS[3], MIKLÓS HOLLÓSI[3], TAMÁS JANÁKY[1], GYÖRGYI VÁRADI[1], BOTOND PENKE[1] and ÉVA MONOSTORI[2]

[1] Department of Medical Chemistry, A. Szent-Györgyi Medical University, Szeged, Hungary
[2] Institute of Genetics and Biophysics, Biological Research Center, Szeged, Hungary
[3] Department of Organic Chemistry, Eötvös University, Budapest, Hungary

Abstract: The ζ-chain of the T-cell receptor (TCR)/CD3 complex plays a central role in cell signalling via the TCR. Following receptor stimulation, the ζ-chain is phosphorylated on multiple tyrosine residues present in the intracellular region of this molecule. However, it has not yet been revealed which of the seven tyrosines present in the ζ-polypeptide are phosphorylated. The functional consequences of the particular tyrosine-phosphorylation events are also unknown. Seven short peptide fragments and the corresponding phosphorylated derivatives of the ζ-subunit were synthesized by solid-phase methodology. Both the synthon approach and the global method were applied for phosphorylation. The resulting peptides and corresponding phosphopeptides were used in *in vitro* experiments to study the role of the phosphorylation of the individual ζ-phosphotyrosines in T-cell signal transduction. The conformational consequences of the phosphorylation were investigated by CD and IR spectroscopy.

INTRODUCTION

Phosphorylation of protein tyrosine residues is one of the main steps in the regulation of various cell processes. There has therefore been much interest in the establishment of efficient chemical methods for the synthesis of Tyr-phosphate-containing peptides. For the preparation of phosphotyrosine-containing peptides, many different strategies have been considered [1–6]. The ζ-chain of the T-cell receptor (TCR)/CD3 complex plays a central role in cell signalling via the TCR [7,8]. Following receptor stimulation, the ζ-chain is phosphorylated on multiple tyrosine residues present in the intracellular region of this molecule (Fig. 1). However, it has not yet been revealed which of the seven tyrosines present in the ζ-polypeptide are phosphorylated. It is also unknown which kinase is involved in this event [9–12]. Dephosphorylation of this protein is necessary for the down-regulation of T-cell activation, but the phosphatases that participate in the dephosphorylation have not yet been identified [13]. Seven short peptide fragments and the corresponding phosphorylated derivatives of the ζ-subunit were synthesized in order to investigate the roles of the individual phosphotyrosine residues in the biochemical process of T-cell activation. The phosphorylated ζ-peptides were also used to establish whether any of them are substrates for CD45, a lymphocyte-specific transmembrane tyrosine phosphatase.

Peptides in Immunology. Edited by C.H. Schneider

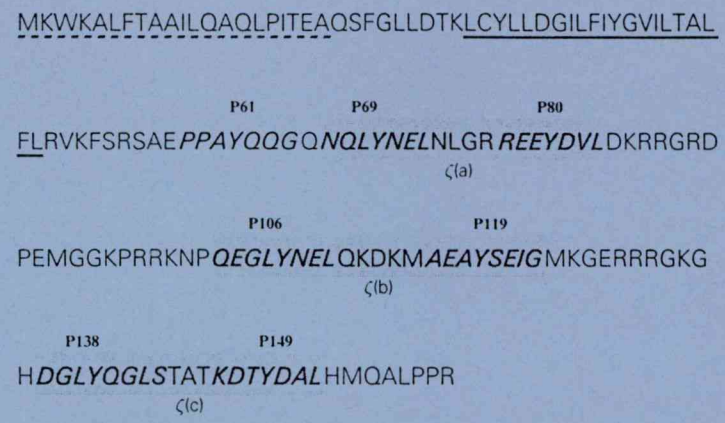

Fig. 1 Primary structure of the ζ-subunit.

MATERIALS AND METHODS

Dichloromethane (DCM), dimethylformamide (DMF), di-isopropylethylamine (DIEA), methanol (MeOH), trifluoroacetic acid (TFA) and HPLC-grade acetonitrile (AcN) were purchased from E. Merck (Darmstadt, Germany) and were used without further purification. Fluka (Buchs, Switzerland) supplied puriss-grade dicyclohexylcarbodiimide (DCC). Protected amino acid derivatives were from Bachem Inc. (Torrance, CA, USA). 1-Hydroxybenzotriazole (HOBt), piperidine, *p*-cresol and dimethyl sulphide were purchased from Aldrich (Steinheim, Germany). Hydrogen fluoride (HF) was obtained from UCAR (Olen, Belgium).

Peptide Synthesis

The peptides were synthesized by a solid-base technique, utilizing ^{t}Boc or Fmoc chemistry. The peptides were synthesized on TMBHA or MBHA resins respectively. Couplings were performed with DCC, with the exceptions of Asn, Gln and Arg, which were incorporated as their HOBt esters. Amino acid incorporation was monitored with the ninhydrin test. The completed peptide resins were phosphated or treated with the appropriate cleavage reagent (liquid HF or TFA) and the resulting free peptides were solubilized in 10% aqueous acetic acid, filtered and lyophilized. The details of the syntheses will be published elsewhere.

Peptide Purification and Characterization

The crude peptides were purified by reverse-phase HPLC (RP-HPLC) on a Lichrosorb RP-18 10 μ column (16 × 250 mm) using a Knauer HPLC apparatus (Berlin, Germany). The solvent system used was as follows: A: 0.1% TFA in water; B: 0.1% TFA+80% AcN in water; gradient: 0 → 60% B in 1.5 h; flow 3 ml/min. The appropriate fractions were pooled and lyophilized. Purity was checked by RP-HPLC. Analytical HPLC investigations were performed on a Vydac C_{18} column (4 × 250 mm; 218TP54; Hesperia, CA, USA), at a flow rate of 0.8 ml/min, with detection at 220 nm; the solvent system used was as follows: A: 0.1% TFA in water; B: 0.1% TFA + 80% AcN in water; gradient: 0 → 30% B in 20 min.

Capillary electrophoresis. A fused silica capillary with an effective length of 45.5 cm was used for micellar electrokinetic chromatography (MECC) using a Biofocus 3000 (BioRad) apparatus. Before each run, the capillary was rinsed for 8 min with the appropriate running buffer. The separation was carried out in 0.01 M sodium borate

Table 1 Mass spectrometry of phosphorylated peptides.

Peptide sequences	Mass spectra		Code
	Calc.	Found	
PPAY(P)QQG	838.81	839.2	61P
NQLY(P)NEL	971.96	972.7	69P
REEY(P)DVL	1001.99	1002.0	80P
QEGLY(P)NEL	1044.02	1044.6	106P
AEAY(P)SEIG	917.86	918.4	119P
DGLY(P)QGL	843.83	845.1	138P
KDTY(P)DAL	903.88	904.1	149P

buffer, pH 8.5, containing 0.005 M sodium phosphate and 0.05 M SDS. Samples were made up as 1 mg/mL solutions in water. Buffer and samples were filtered through a 0.45 μm pore filter (Millipore) and degassed prior to use. Injection of the samples was accomplished by pressure injection for 2 s. The running voltage was 15 kV, with a maximal current of 80 μA, and the polarity was towards the cathode. All electropherograms were detected at 200 nm. During runs, the capillary temperature was set to 20°C (water cooling).

UV spectroscopy and mass spectrometry. The incorporation of the phosphate moiety was verified by using UV spectroscopy. The phosphorylation caused a 10 nm hypsochromic effect in the UV spectra recorded from the HPLC by using a Hewlett–Packard diode array detector [14].

The mass spectra were recorded on a VG ZAB SE Fab mass spectrometer or on a Finnigan TSQ 7000 tandem quadrupole mass spectrometer equipped with an electrospray ion source. The results are given in Table 1.

Dephosphorylation of Phosphopeptides

CD45 tyrosine phosphatase was isolated as described previously [15]. Phosphopeptides (15 nM) were added to the CD45 immunoprecipitates in 60 mM Tris/HCl, pH 7.2, containing 5 mM EDTA, 50 mM NaCl and 10 mM dithiothreitol for 30 min at 37°C.

Conformational Investigations

CD measurements were carried out in water and trifluorethanol (TFE) on a Jasco J720 dichrograph. The peptide concentration was 0.5 mg/ml, and the cell length was 0.2 mm. Mean residue ellipticity $[\theta]_{MR}$ was expressed in degrees·cm^2·dmol^{-1}, using a mean residue weight of 110. IR spectra were recorded on a Bruker IFS55 instrument at a resolution of 2 cm^{-1}.

RESULTS AND DISCUSSION

Peptide Synthesis and Structure Proof

Seven short phosphorylated (and non-phosphorylated) fragments of the TCR CD 3ζ-chain were synthesized. Both the synthon approach and the global method were applied. The global method using phosphoramidites gave significantly better results than the synthon approach in this case [6].

Di-*t*-butyl diethylphosphoramidite can be prepared in good yield and can be used successfully for the phosphorylation of protected peptides in both liquid and solid phases (phosphitylation and subsequent oxidation with *t*-butyl peroxide).

Different separation methods were used for the purity control of these phosphopeptides;

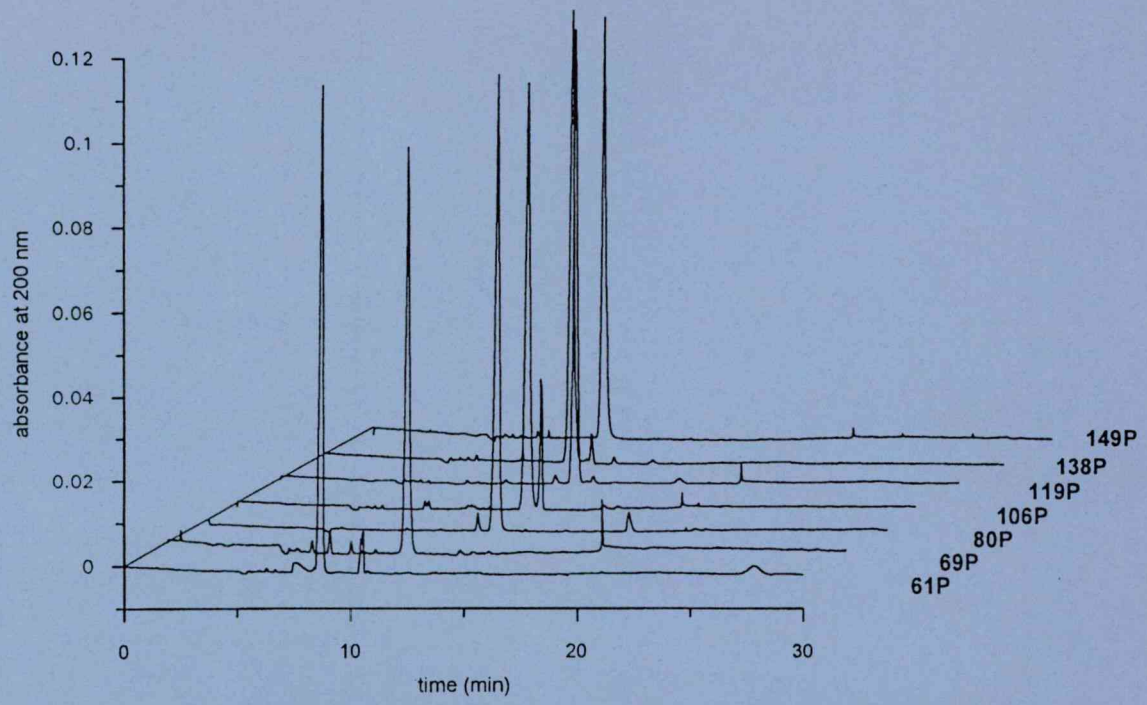

Fig. 2 Micellar electrokinetic chromatograms of the synthesized phosphopeptides.

MECC appeared to be the best. Although all the synthesized and HPLC-purified phosphopeptides appeared to be pure when RP-HPLC and capillary-zone electrophoresis (CZE) were applied, the use of MECC in some cases revealed low percentages of impurities, as shown in Fig. 2.

The use of UV spectroscopy is a fast and easy way of proving the incorporation of the phosphate moiety, although the protected phosphate group-containing peptides gave practically the same spectra. To verify the structure, mass spectrometry is necessary.

Immunological Investigations

Several tyrosine kinases such as those belonging to the *src* oncogene family, $p59^{fyn}$ and $p56^{lck}$ or the syk family member ZAP 70, may be responsible for the ζ-chain phosphorylation that follows T-cell activation. Preliminary experiments revealed that six short ζ-related peptides, corresponding to the conservative sequences of the ζ-polypeptide, are substrates for the *src* kinases, and one of the seven peptides (PPAYQQG), which lies outside the conservative motifs, is not a target of *in vitro* phosphorylation by the *src* kinases used (lck and fyn) [16].

CD45, a lymphocyte surface protein that has tyrosine phosphatase activity, appears to be responsible for the dephosphorylation of the ζ-chain. Preliminary investigations involving capillary electrophoresis and chemically phosphorylated peptides as substrates support this hypothesis (Fig. 3). It has been demonstrated that CD45 dephosphorylates phosphorylated ζ-oligopeptides indicating that this tyrosine phosphatase may play a role in the downregulation of T-cell activation [17].

Conformational Investigations

In water, both the non-phosphorylated (nP) and phosphorylated (P) peptides give CD

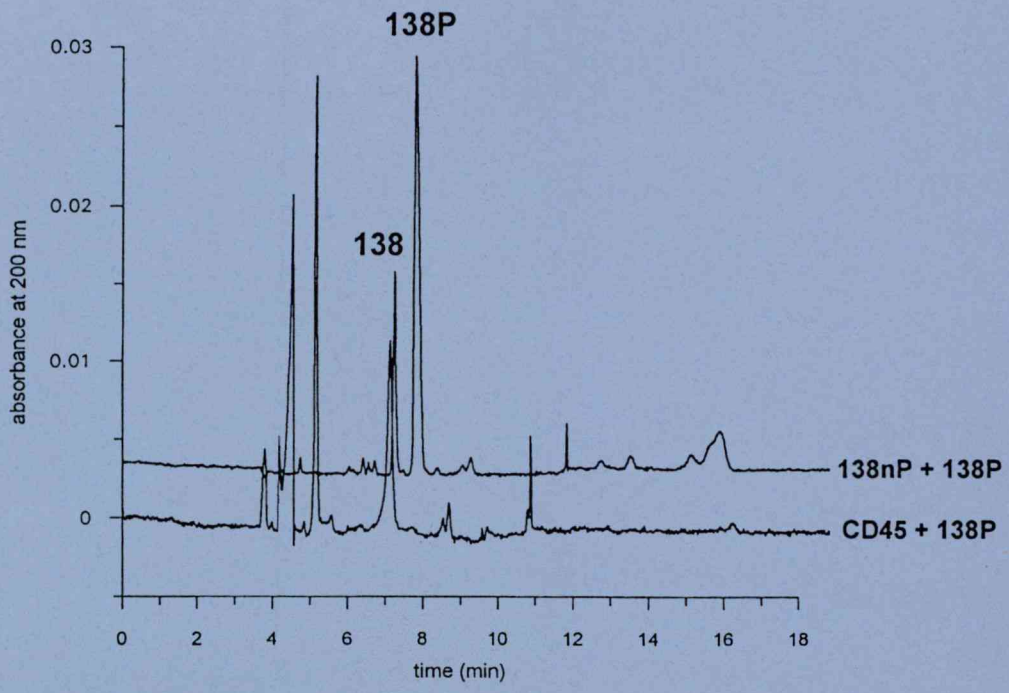

Fig. 3 Capillary electropherogram of a CD45-treated phosphopeptide (138P)

spectra characteristic of a predominantly random conformation (strong negative band below 200 nm). In TFE solution, the peptides exist as mixtures of conformers, and the CD spectra reflect more than one prevailing secondary structure. As regards the changes in the CD spectra of the phosphorylated peptides relative to the non-phosphorylated ones in TFE, four groups of peptides can be distinguished.

(1) 61nP, 61P; 69nP, 69P. The strong negative $\pi\pi^*$ band at around 200 nm and the weaker negative $n\pi^*$ band at 220–230 nm in the CD spectra of the nP peptides indicate the presence of an unordered and type I or type III β-turn conformation. Introduction of the negative $PO_3H_2^-$ on the Tyr group alters the spectra dramatically. The low band intensities are probably due to the overlapping of the bands of the unordered conformation with the bands of the β-sheet conformation (see Fig. 4). The stability of the β-sheet conformation of 69P in TFE is demonstrated by adding water to the TFE solution of the peptide. The β-sheet character of the spectrum is still preserved at 50% TFE, while in the case of the non-phosphorylated peptide (69nP) the turn structure (stabilized in 100% TFE) is destroyed at 75% TFE.

The FITR spectra of 69nP and 69P (Fig. 5) clearly illustrate the shifts in the conformational equilibrium upon phosphorylation. A characteristic feature of the spectrum of 69nP is the intense amide I band at 1632 cm^{-1}, which represents a mixture of β-sheet and β-turn conformers, while the component band at 1649 cm^{-1} is indicative of the undordered conformation. The strong component band at 1673 cm^{-1} can be attributed to the antisymmetric COO^- stretching vibration of trifluoroacetate ions. In the spectrum of the phosphorylated peptide, this band is practically absent. The negatively charged phosphate group presumably prevents the binding of TFA to the peptide. In the spectrum

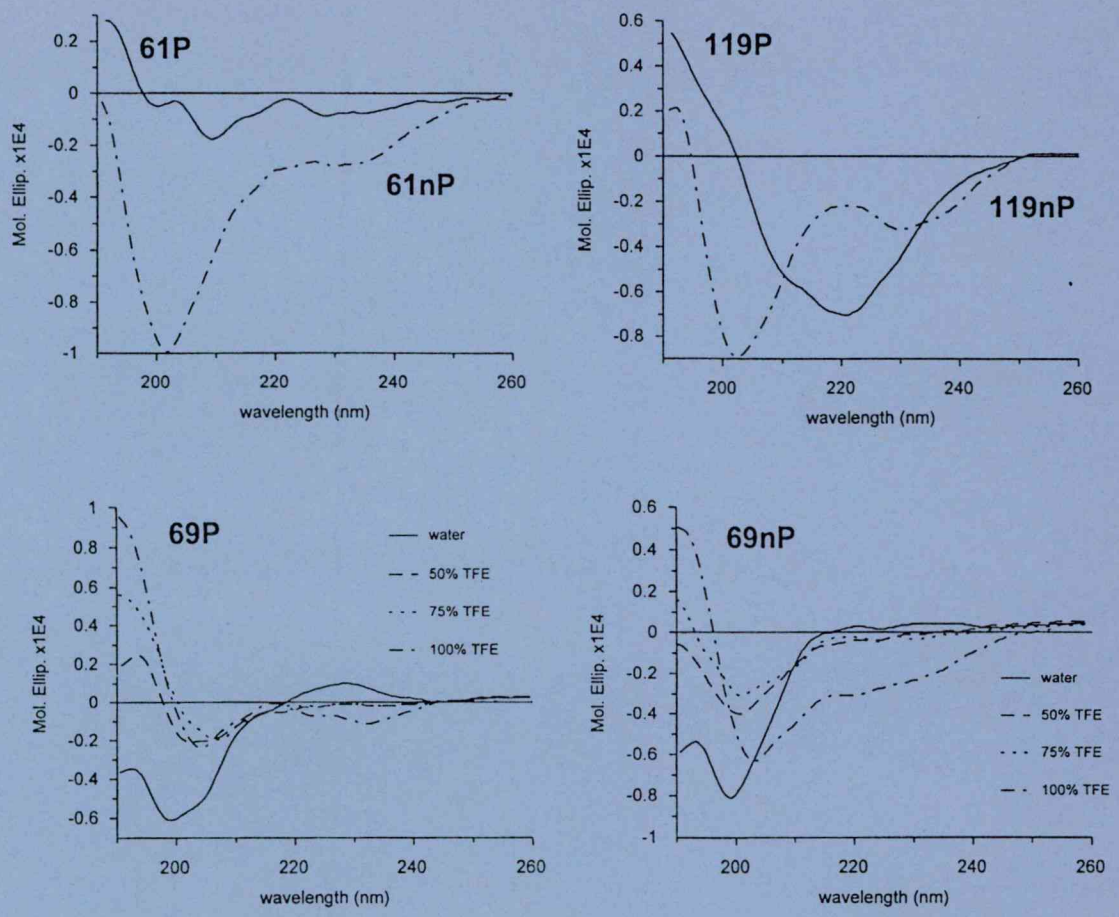

Fig. 4 CD spectra of several ζ-subunit-related peptides (61P and 61nP; 69P and 69nP; 119P and 119nP).

of 69P, the very intense component band at 1633 cm^{-1} reflects a substantial amount of the β-sheet structure, while the band at 1643.6 cm^{-1} relates to the unordered conformation. The band at 1663 cm^{-1} indicates the presence of solvated amide carbonyls.

(2) 119nP, 199P. Similar changes upon phosphorylation can be observed for the 119 fragment. The well-expressed β-sheet character of the CD spectrum of 119P (negative $n\pi^*$ band at 215 nm) reflects that, compared with the 61 and 69 peptides, a higher amount of β-sheet conformation is formed upon phosphorylation. Of the seven ζ-peptide fragments studied, this exhibits the highest β-sheet-forming tendency upon phosphorylation.

(3) 149nP, 149P. The CD spectrum of the 149nP fragment indicates a β-turn/unordered conformer mixture. This conformational equilibrium is shifted towards the unordered structure upon phosphorylation.

(4) 80nP, 80P; 106nP, 106P; 138nP, 138P. Even the non-phosphorylated peptides contain substantial amounts of β-turn and/or β-sheet structures, and the proportion of the ordered

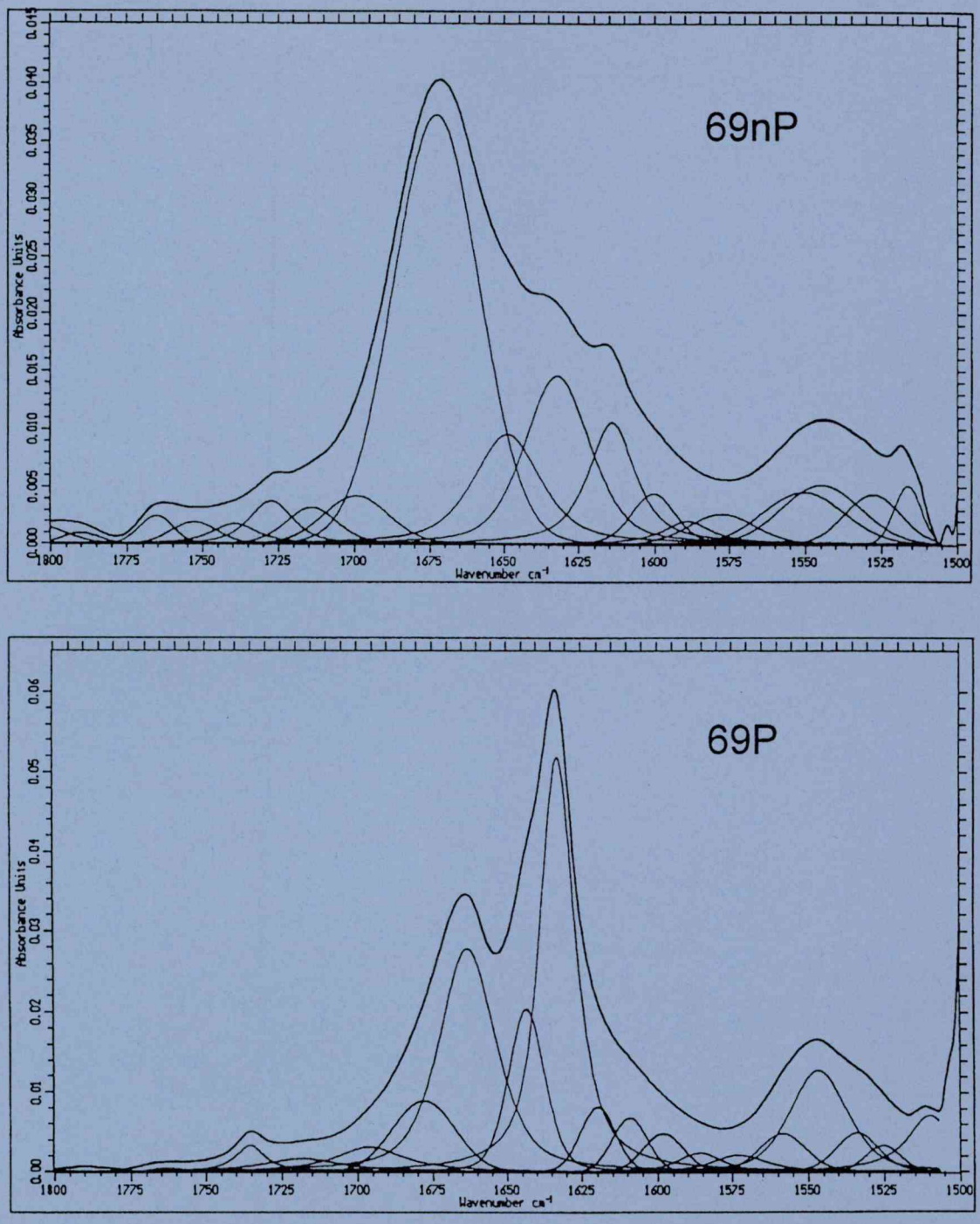

Fig. 5 FTIR spectra of a ζ-peptide fragment in phosphorylated (69P) and non-phosphorylated (69nP) forms.

conformation relative to the unordered one is further increased in the phosphorylated fragments (see e.g. 80nP and 80P).

The conformational investigations of these phosphopeptides means of CD and FTIR spectroscopy supported the idea that the phosphorylation event can change the conformations of the parent peptides, mainly leading to an increase in the β-sheet conformation.

ACKNOWLEDGEMENTS

This work was supported by the following grants: OTKA 2734, OTKA T 016156 and ETT T03/523. The authors are indebted to Dr. M. Mák and Mr Z. Kele for the MS measurements and Ms É. Dósai-Molnár and Mr A. Szász for skilful technical assistance.

REFERENCES

1. R.M. Valerio, P.F. Alewood, R.B. Johns and B.E. Kemp (1989). Synthesis of O-phosphonotyrosyl peptides. *Int. J. Pept. Protein Res. 33*, 428–438.
2. J.W. Perich, M. Ruzzene, L.A. Pinna and E.C. Reynolds (1994). Efficient Fmoc/solid-phase peptide synthesis of O-phosphotyrosyl-containing peptides and their use as phosphatase substrates. *Int. J. Pept. Protein Res. 43*, 39–46.
3. D.M. Andrews, J. Kitchin and P.W. Seale (1991). Solid-phase synthesis of a range of O-phosphorylated peptides by post-assembly phosphitylation and oxidation. *Int. J. Pept. Protein Res. 38*, 469–475.
4. N. Mora, J.M. Lacombe and A.A. Pavia (1994). A new approach to phosphoserine, phosphothreonine and phosphotyrosine synthons and to thiophospho analogs. *Int. J. Pept. Protein Res. 45*, 53–63.
5. R. Hofmann, W.O. Wachs, R.G. Berger, H.-R. Kalbitzer, D. Waidelich, E. Bayer, W. Wagner-Redeker and M. Zeppezauer (1994). Chemical phosphorylation of the peptides GGXA (X=S,T,Y): an evaluation of different chemical approaches. *Int. J. Pept. Protein Res. 45*, 26–34.
6. G.K. Tóth, G. Váradi, T. Janáky, B. Penke, M. Mák, E. Láng, L. Ötvös, Z. Hegedüs and É. Monostori in: *Peptides 1994*, H.L.S. Maia, Ed., p. 743-744, ESCOM, Leiden 1995.
7. C.H. June, M.C. Fletcher, J.A. Ledbetter, G.L. Schieven, J.N. Siegel, A.F. Phillips and L.E. Samelson (1990). Inhibition of tyrosine phosphorylation prevents T cell receptor mediated signal transduction. *Proc. Natl. Acad. Sci. USA 87*, 7722-7726.
8. B.A. Irving and A. Weiss (1991). The cytoplasmic domain of the T cell receptor ζ chain is sufficient to couple to receptor-associated signal transduction pathways. *Cell 64*, 891–901.
9. E.K. Barber, J.D. Dasgupta, S.F. Schlossman, J.M. Trevillyan and C.E. Rudd (1989). The CD4 and CD8 antigens are coupled to a protein-tyrosine kinase (p56lck) that phosphorylates the CD3 complex. *Proc. Natl. Acad. Sci. USA 86*, 3277–3281.
10. A.C. Chan, M. Iwashima, C.W. Turck and A. Weiss (1992). ZAP-70: A70 kd protein-tyrosine kinase that associates with the TCR ζ chain. *Cell 71*, 649–662.
11. L.E. Samelson and R.D. Klausner (1992). Tyrosine kinases and tyrosine-based activation motifs. Current research on activation via the T cell antigen receptor. *J. Biol. Chem. 267*, 24913–24916.
12. L.E. Samelson, A.F. Philips, E.T. Loung and R.D. Klausner (1990). Association of the fyn protein tyrosine kinase with the T cell antigen receptor. *Proc. Natl. Acad. Sci. USA 87*, 4358–4362.
13. N. Isakov (1993). Tyrosine phosphorylation and dephosphorylation in T lymphocyte activation. *Mol. Immunol. 30*, 197–210.
14. C.W. Turck (1992). Identification of phosphotyrosine residues in peptides by high performance liquid chromatography on-line derivative spectroscopy. *Peptide Research 5*, 156–160.
15. É. Monostori, Z. Hartyáni, I. Ocsovszky, Z. Hegedüs, T. Oravecz, M. Kálmán and I. Andó (1994). Effect of phytohaemagglutinin on CD45 in T cells. *Immunol. Lett. 42*, 197–201.
16. Z. Hegedüs, I. Andó, G.K. Tóth, G. Váradi and É. Monostori (1995). Application of polyacrylamide gel electrophoresis for analysis of oligopeptide phosphorylation *in vitro*. *Bio Techniques 18*, 632–634.
17. J.F. Dawson, M.P. Boland and F.B. Holmes (1994). A capillary electrophoresis-based assay for protein kinases and protein phosphatases using peptide substrates. *Anal. Biochem. 220*, 340–345.

Volume 26 · Number 1 · 1997

European Biophysics Journal

with Biophysics Letters

26/1
97

EBSA

Structure and Dynamics of Biological Macromolecules

Membrane Biophysics and Ion Channels

Cell Biophysics and Organisation

Macromolecular Assemblies

Biophysical Methods and Instrumentation

An International Journal of Biophysics published by
Springer-Verlag
and the
European Biophysical Societies' Association

Springer

1-74

CONFORMATIONAL CONSEQUENCES OF THE PHOSPHORYLATION OF THE T-CELL RECEPTOR COMPLEX ζ-CHAIN. I. Laczkó, M. Hollósi, É. Monostori, G.K.Tóth.

The ζ-chain of the T-cell receptor (TCR)/CD3 complex plays a central role in cell signalling via the TCR. Following receptor stimulation, the ζ-chain is phosphorylated on tyrosine residues in certain positions in the intracellular region of this molecule. However, it has not yet been revealed which of the tyrosines are phosphorylated.

In order to study if the phosphorylation of the shorter and longer fragments of ζ-chain causes comparable conformational changes, the following short peptide fragments (P69, P80, P106, P119, P138, P149), three longer fragments containing the P69+P80 (ζa), P106+P119 (ζb), P138+P149 (ζc) sequences and the corresponding phosphorylated derivatives were synthesized by solid-phase methodology:

P69 P80 P138 P149
ζ(a): *NQLYNEL*NLGR*REEYDVL*, ζ(c) *DGLYQGLS*TAT*KDTYDAL*,

P106 P119
ζ(b): *QEGLYNEL*QKDKM*AEAYSEIG*

The secondary structures of peptides were studied by circular dichroism (CD) and Fourier transform infrared (FTIR) spectroscopy in water and trifluoroethanol (TFE) solutions. The non-phosphorylated short peptides are mainly present as a β-turn/unordered conformer mixture in TFE. This conformational equilibrium is shifted in most cases towards the β-sheet structure upon phosphorylation. Selective phosphorylation of one or the other tyrosine of the longer peptides results in the predominance of α-helical conformation. However, a substantial amount of β-sheet structure is formed phosphorylated the peptides on both tyrosines.

Institute of Biophysics, Biological Research Center, H-6701 Szeged, P.O.Box 521, Hungary

1-75

SOLUTION STRUCTURE OF DROSOMYCINE, AN INSECT POTENT ANTIFUNGAL PROTEIN

C. Landon, P. Sodano, P. Fehlbaum, C. Hetru and M. Ptak

In response to a septic injury, larvae and adults of *Drosophila* produce a considerable amount of drosomycin, a 44-residue protein containing 4 disulfide bridges. This protein, inactive against bacteria, exhibits potent antifungal activity, and shows significant homologies with plant antifungal proteins isolated from the seeds of radish. Its three-dimensional solution structure was established from two-dimensional NMR data and molecular modeling. Its fold involves a helix fastened to a three stranded beta-sheet by two disulfide bridges defining a CSαβ motif. This motif was previously described in insect defensin, plant defensin, γ-thionin and scorpion toxin structures. Comparison of high resolution solution structures of drosomycin with γ-thionin structures reveals the structural importance of some residues such as Ser4, Tyr7, Gly9, Gly31 and the probable functional importance of Glu26 and Lys38. The use of programm 'cavité' which aims at delineating cavities in protein structures, revealed the presence of a hydrophobic pocket of moderate dimensions and compatible with a water molecule size, inside the protein core. This solvent molecule should be important to the protein three dimensional structure stability.

Centre de Biophysique Moléculaire, CNRS, rue Charles Sadron, 45071 Orléans Cédex 02 (France)

1-76

A NEW CONCEPT TO EXPLAIN THE RESISTANCE OF A THERMOPHILIC PROTEIN TO HEAT, COLD and PRESSURE.

E. Mombelli[a], P. Tortora[b], M. Afshar[c], N. Bec[a] and R. Lange[a]

Ribonuclease P2 (7 kDa) from *S. solfataricus* is extremely resistant to pressure and heat. This protein has a large hydrophilic mantle and a hydrophobic core which contains three aromatic residues (Phe5, Phe31 and Tyr33). A molecular dynamics simulation reveals that these residues are arranged in a fish-bone geometry and have strong van der Waals interaction energies. For an understanding of the structural basis of its stability, we studied the thermodynamics of the heat, cold and pressure induced protein conformational changes of the wild type and of the F31A and F31Y mutants, by analyzing the protein UV absorbance in the fourth derivative mode. By this method we probed the properties of the hydrophobic aromatic core. Heat and cold denaturation of both mutants, as well as denaturation by pressure of the F31A mutant led to strong blue shifts of the derivative spectrum, indicating increased solvent exposure of Tyr33. For the F31Y mutant, high pressure protected the protein against thermal denaturation. In contrast, the hydration of the core of the wild type protein did not change under extreme conditions of temperature (-20 to +90°C) and pressure (500MPa). In comparison, a much lower stability and shallow transitions had been observed previously for the overall protein structure (Knapp et al., 1996, J. Mol. Biol., 264, 1132). The response of P2 to extreme conditions may be explained by a gradual multi-stage unfolding mechanism of larger peripheral parts of the protein. However, the melting is not complete, since the outer parts are linked to a very stable, stone-like hydrophobic core, which is stabilized by particular aromatic interactions.

[a]INSERM U128, BP5051, F-34033 Montpellier [b] Dipartimento di Fisiologia e Biochemical generali, Università di Milano, Milano, Italy, [c]Protein Structure Group, University of York, Y015DD, UK.

1-77

STABILITY OF THE DIMERIC PROAEROLYSIN AND THE AEROLYSIN HEPTAMER.

C.Lesieur, J.T.Buckley, R.Kellner, G.van der Goot.

Proaerolysin is secreted by *Aeromonas hydrophila* as a soluble dimeric protoxin. C-terminal cleavage leads to activation of the toxin. Heptamerization and pore formation then occur inducing cell lysis. Transition from dimer to heptamer certainly involves folding/unfolding processes. To decipher this mechanism, we have analyzed the unfolding of dimeric proaerolysin and heptameric aerolysin in urea and GuHCl. The results showed that proaerolysin unfolds in two steps and that the two disulfides bridges significantly contribute to the stability of the protein. By disturbing the bridges either with DTT or by mutagenesis, we could show that the elongated C-terminal domain unfolds first. Therefore, the N-terminal domain appears to be the most stable part of the protoxin, and perhaps maintains the two monomers together. The aerolysin heptamer remained assembled and fully folded even in 8 M urea illustrating its uncommon stability. Partial unfolding could be observed in GuHCl. To investigate which part of the protein maintains the heptamer assembled, we have searched for limited digests that did not affect assembly. A 200Kda complex was obtained after treatment of the heptamer in SDS with trypsin. N-terminal sequencing showed that the N-terminal domain had been removed. This truncated oligomer still migrated as a complex on SDS gels, indicating that it does not require the N-terminal domain to remain assembled. In conclusion, the N-terminal domain of proaerolysin is the most stable part of the protoxin but it is not required to maintain the heptamer assembled.

Dept of Biochemistry, Univ of Geneva, Geneva, CH-1211

Peptides 1998
Sándor Bajusz and Ferenc Hudecz (Eds.)

Synthesis of Phosphorylated T-cell Receptor/CD3 ζ-chain Sequences - Conformational Effects and Immunological Investigations

GÁBOR K. TÓTH[1], ILONA LACZKÓ[2], MIKLÓS HOLLÓSI[4], VIOLETA CHITU[3], ZOLTÁN HEGEDÜS[3] and ÉVA MONOSTORI[3]

[1]*Department of Medical Chemistry, Albert Szent-Györgyi Medical University, Szeged*
[2]*Institute of Biophysics and* [3]*Institute of Genetics, Biological Research Center, Szeged*
[4]*Department of Organic Chemistry, Eötvös University Budapest, Hungary*

Introduction

The ζ-chain of the TCR/CD3 complex plays a central role in the transduction of antigenic signal to the intracellular signaling pathway. Following receptor stimulation, the .-chain is phosphorylated on multiple tyrosine residues present in the intracellular region of this molecule. The functional consequences of the particular tyrosine phosphorylation events are unknown. Three conservative motifs - Immunoreceptor Tyrosine-based Activation Motifs (ITAMs) containing two tyrosine residues and the corresponding phosphorylated derivatives of the .-subunit were synthesized by solid-phase methodology applying Fmoc-chemistry.

MKWKALFTAAILQAQLPITEAQSFGLLDTKLCYLLDGILFIYGVILTAL

FLRVKFSRSAE ***PPAYQQG*** Q ***NQLYNEL***NLGR ***REEYDVL***DKRRGRD
ζ(1)

PEMGGKPRRKNP ***QEGLYNEL***QKDKM***AEAYSEIG*** MKGERRRGKG
ζ(2)

H***DGLYQGL***STAT***KDTYDAL***HMQALPPR
ζ(3)

Figure 1. *The sequence of the ζ subunit and the synthetized fragments*

Peptide Synthesis and Purification

The nonphosphorylated peptides were synthesized by solid phase technique utilizing ^{t}Boc chemistry. The peptide chain were elongated on MBHA resin (0.6-0.8 mmol/g). The phosphotyrosine containing peptides were synthesized by SPPS-Fmoc methodology. Side chain protecting groups were as follows: Arg(Pmc), Ser(Bu^t), Thr(Bu^t), Glu(OBu^t), Asp(OBu^t) and Lys(Boc). The phenolic hydroxyls of the tyrosine residues were unprotected. The peptides were prepared on TMBHA resin (0.6 mmol/g) using an ABI 430 A synthesizer and a modified synthesis protocol. After the incorporation of the tyrosine

their hydroxyls were phosphytilated using di-tert. butyl- N,N diethyl-phosphoramidite [1] which proved to be the optimal in our laboratory earlier [2]. After the oxidation of the phosphite to phosphate using tert. butylperoxide the elongation of the peptide chain was completed, the resulted crude phosphopeptide was detached from the resin using TFA/ DCM/anisole mixture (62:30:8, vol/vol), on 0°C, 1 h. and the resulting free peptides were precipitated with diethylether, filtered, dissolved in water and lyophilized. The crude peptides were purified by reverse-phase HPLC . The appropriate fractions were pooled and lyophilized. Purity was checked by RP-HPLC, the structure was confirmed by mass spectrometry.

Conformational Investigations

The conformational consequences of the phosphorylation were investigated by CD and IR spectroscopy and gave evidences that phosphorylation can alter the secondary structures [3,4]. The most significant α helix to β sheet conformational change was observed in the case of ζ(138-155) peptide sequence ζ(3). In TFE the nonphosphorylated ζ(2) and ζ(3) are present in a predomonantly helical conformation which is in case of ζ(138-155) changed to mainly β sheet conformation upon phosphorylation. In water, all the three nonphosphorylated ITAM sequences are present as multicomponent mixtures of different conformers, and in case of ζ(2) no significant change was observed upon phosphorylation.

Immunological Results

Comparative analysis of the kinase activities showed similar phosphorylation of the different ITAMs by *src* family kinases, $p56^{lck}$ and $p59^{lyn}$ but no phosphorylation by syk family kinase, ZAP70 [5]. *In vitro* dephosphorylation experiments [6] revealed that the tyrosine phosphatase CD45 can discriminate between different phosphorylated derivatives of ITAMs. These results show that *src* family kinases and the CD45 phosphatase may control together the specific phosphorylation pattern of the ζ-chain during T-cell activation.

References

1. Perich, J.W. and Johns, R.B. *Synthetic Communications*, (1988) 142.
2. Tóth, G.K., Laczkó, I., Hegedüs, Z., , Vass, E., Hollósi, M., Janáky, T., Váradi, G., Penke, B. and Monostori, I. In Schneider, C.H. (Ed.) *Peptides in Immunology*, Wiley & Sons Ltd 1996. p. 223.
3. Wade, J.D., Perich, J.W., McLeish, M.J., Ötvös, L. jr. and G.W. Tregear. *Letters in Peptide Science*, 2 (1995) 71.
4. Laczkó, I., Hollósi, M., Vass, E., Hegedüs, Z., Monostori, I. and Tóth, G. K., *Biophys. Biochem. Research Communication*, 242 (1998) 474.
5. Hegedüs, Z., Andó, I., Tóth, G.K., Váradi, G. and Monostori, I. *BioTechniques*, 18 (1995) 632.
6. Ng, D.H., Harder, K.W., Clark-Lewis, I., Jirik, F. and Johnson, P. *J Immunol Methods*, 179 (1995) 177.

Pergamon

Tetrahedron Letters 41 (2000) 4457–4461

TETRAHEDRON LETTERS

Preparation of an asymmetrically protected phosphoramidite and its application in solid-phase synthesis of phosphopeptides

Zoltán Kupihár,[a] Györgyi Váradi,[a] Éva Monostori[b] and Gábor K. Tóth[a,*]

[a]*Department of Medical Chemistry, University of Szeged, H-6720 Szeged, Dóm tér 8, Hungary*
[b]*Institute of Genetics, Biological Research Center of Hungarian Academy of Sciences, H-6726 Szeged, Temesvári krt. 62, Hungary*

Received 15 March 2000; accepted 10 April 2000

Abstract

O-tert-Butyl-*O'*-β-cyanoethyl-*N,N*-diisopropylphosphoramidite as a new global phosphorylation reagent and its application for solid-phase phosphopeptide synthesis via monoprotected phosphate-peptide ester during peptide synthesis are described. © 2000 Elsevier Science Ltd. All rights reserved.

Keywords: peptide; solid-phase synthesis; phosphorylation; phosphoramidite; phosphopeptide.

Protein phosphorylation has been recognized as one of the most important elements of cell regulation and signal transduction. For studying the role of the phosphorylation/dephosphorylation event in biological functions or investigating its conformational consequence, the isolation of the appropriate phosphorylated protein is not usually feasible. Therefore, the efficient chemical synthesis of the related phosphopeptide is a valuable alternative. There are two major strategies for the preparation of phosphopeptides: the synthon and the global approach. The synthon method[1–4] (both in liquid and solid-phase) requires appropriately protected phosphorylated derivatives—these derivatives are often not commercially available and their syntheses are multistep, complicated and expensive procedures. Sometimes the synthesis of the appropriate building block itself can be a challenge for the synthetic chemist. On the other hand, this approach is a safe and simple method to synthesize phosphate containing peptides. The global approach requires appropriate reagents for the phosphorylation (practically phosphitylation and subsequent oxidation to phosphate, or alternatively, reaction with phosphochloridate[5,6]) and experience in handling these reagents which are not routine chemicals for peptide chemists. For phosphitylation, usually symmetrical phosphoramidite derivatives[7–11] are used which produce symmetrically bis-protected phosphate derivatives. However, while this method can be applied with good yield in

* Corresponding author. Tel: +36 62 54 51 39; fax: +36 62 42 52 62; e-mail: toth@ovrisc.mdche.u-szeged.hu

0040-4039/00/$ - see front matter
PII: S0040-4039(00)00615-8

the case of phosphotyrosine containing peptides, for phosphoserine and phosphothreonine containing peptides the treatment with piperidine during the standard deprotection cycle leads to β-elimination with loss of the phosphate moiety and formation of the corresponding dehydropeptide.[12] Removal of the protecting groups from the phosphate moiety would hinder this reaction,[13] but the resulting free acidic hydroxyl functions can cause other side reactions such as pyrophosphate formation.[14] The monoprotected derivatives of these hydroxyl group-containing amino acid phosphate esters seem to be the optimal choice, but to date only the synthon method has been applied for this purpose utilizing Fmoc-Ser[PO(OBn)OH]-OH and Fmoc-Thr[PO(OBn)OH]-OH monomers.[13] The global approach, being applicable for any hydroxyl group-containing residue, would offer a more general method. However, the application of the unsymmetrically protected phosphoramidite reagent needed for this has not yet been reported. Here we describe the synthesis of a novel unsymmetric phosphoramidite reagent and its application for the synthesis of a phosphoserine containing peptide by the global approach.

Our aim was to develop a phosphitylation reagent which can convert a hydroxyl group-containing peptide to the corresponding monoprotected phosphopeptide. The reason for this was the need for the phosphorylated derivative of the QDGVRQSRASDKQTLLPNDQ peptide. This peptide is a fragment of the CD3 γ-chain of the T-cell receptor complex, namely the 117–136 fragment phosphorylated on the Ser-126 residue. Phosphorylation of this serine residue has been implicated in the regulation of the TCR signalling by the involvement in the downmodulation of the receptor complex from the cell surface. The standard synthesis applying the routine amidite reaction resulted in a very complex crude product and the desired phosphopeptide could be isolated with a very low yield (below 1%).

Earlier, we successfully used the symmetrical di-*tert*-butyl-*N*,*N*-diisopropylphosphoramidite for synthesis of phosphotyrosine containing peptides[15] which affords an efficient, fast, convenient and symmetrical phosphitylation. The *tert*-butyl group is easily removable at the end of the peptide synthesis.[12] Based on these data, we designed a novel unsymmetric compound in which one of the *tert*-butyl groups is replaced by a β-cyanoethyl group. This latter group, well known in oligonucleotide chemistry,[16] is removable with 1,8-diazabicyclo[5.4.0]undec-7-ene (DBU)[17,18] by β-elimination to afford the desired monoprotected phosphopeptide. In addition, DBU also removes the Fmoc *N*-protecting group[19] of the Ser/Thr residue; therefore, a subsequent deprotection step is not necessary.

O-*tert*-Butyl-*O'*-β-cyanoethyl-*N*,*N*-diisopropylphosphoramidite was prepared from *O*-β-cyanoethyl-*N*,*N*-diisopropylchlorophosphite,[20] by a literature method.† Peptide synthesis was carried out on Rink amide resin using standard Fmoc protocol. Phosphitylation was carried out in tetrahydrofuran (THF) at room temperature for 30 min using 1*H*-tetrazole as activator and the subsequent

† To a stirred solution of *tert*-butanol (0.1 mol) and *N*,*N*-diisopropylethylamine (0.24 mol, 2.4 equiv.) in dry DCM (50 ml) a solution of *O*-β-cyanoethyl-*N*,*N*-diisopropylchlorophosphite (0.12 mol, 1.2 equiv.) in dry DCM (10 ml) was added at 0°C. After 1 h, the reaction mixture was extracted with 5% aq. $NaHCO_3$ (2×50 ml) and the organic layer was dried and concentrated in vacuo. The residue was distilled at 100–114°C/2–4 mmHg to give the desired product as a colourless oil (6.0 g, 55%). ^1H NMR ($CDCl_3$, 500 MHz, δ, ppm): 1.16–1.19 (m, 12H, $CH(CH_3)_2$), 1.36 (s, 9H, $(CH_3)_3$), 2.61 (t, 2H, 6.6 Hz, CH_2CN), 3.61 (m, 2H, CH), 3.68–3.81 (m, 2H, CH_2O). ^{13}C NMR ($CDCl_3$, 125 MHz, δ, ppm, assignment based on *J*-modulated spin–echo and HMQC experiments): 21.05 (d, $^3J_{CP}=7.0$ Hz, CH_2CN), 24.84 (d, $^3J_{CP}=7.7$ Hz, $CH(CH_3)_2$), 25.30 (d, $^3J_{CP}=7.2$ Hz, $CH(CH_3)_2$), 31.53 (d, $^3J_{CP}=8.1$ Hz, $C(CH_3)_3$), 43.85 (d, $^3J_{CP}=12.7$ Hz, CH); 58.44 (d, $^2J_{CP}=17.6$ Hz, CH_2O), 76.09 ($C(CH_3)_3$), 118.52 (CN). ^{31}P NMR ($CDCl_3$, 200 MHz, δ, ppm, proton-decoupled spectrum): 139.84. The compound is too unstable to be characterized by elemental analysis or high resolution mass spectrometry.

oxidation was performed by 15% *tert*-butyl hydroperoxide in THF. Simultaneous cleavage of β-cyanoethyl and Fmoc groups was performed by 20% DBU in dichloromethane (DCM) (Scheme 1).

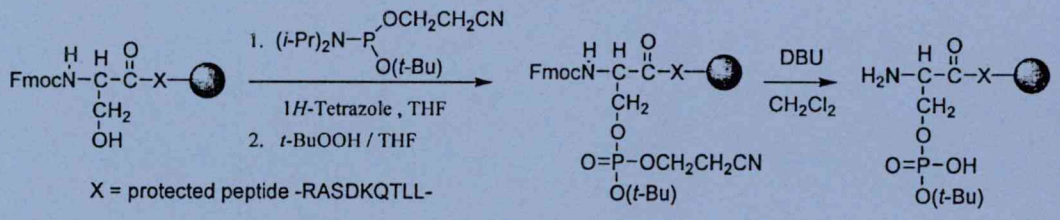

Scheme 1.

DBU, being a strong base, could also promote the β-elimination resulting in the loss of the phosphate group. To investigate this possible side reaction, an aliquot of the peptide-resin after phosphorylation followed by DBU deprotection was cleaved from the resin with trifluoroacetic acid (TFA).‡ As can be seen in Fig. 1, the crude cleavage mixture contained one main product. According to ESI-MS analysis, this product has the M_W of the desired phosphopeptide.§ All these data suggest that the β-cyanoethyl group is a better leaving group than the phosphate moiety and the resulting monoprotected phosphate is not subject to further elimination.

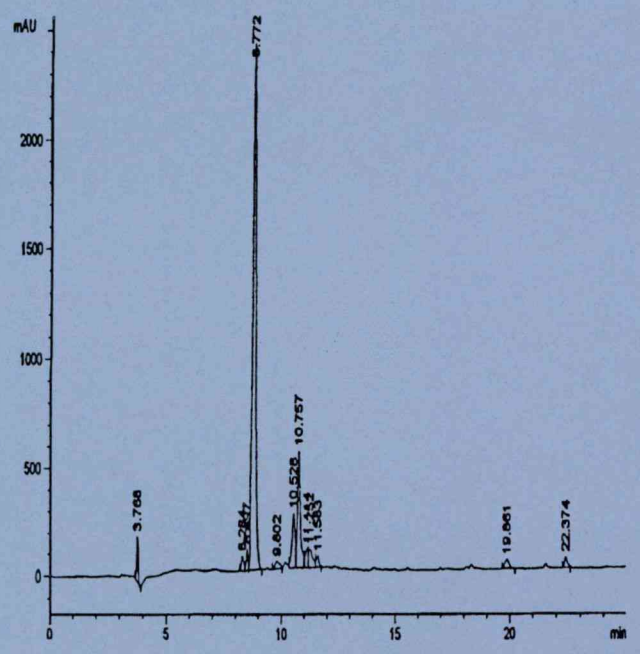

Figure 1. HPLC chromatogram of the crude S(PO_3H_2)DKQTLLPNDQ peptide

‡ Conditions of the final deprotection and the cleavage of the peptide from the resin: 87.5% TFA, 5% H_2O, 2.5% 1,4-DL-dithiothreitol, 5% phenol, 2 h at O°C.

§ M_W of the S(PO_3H_2)DKQTLLPNDQ peptide: calcd 1337.3; found 1337.1.

After completion of the elongation of the peptide chain, the protecting groups were removed and the peptide was detached from the resin using TFA.‡ The mass spectrum of the final crude product can be seen in Fig. 2.

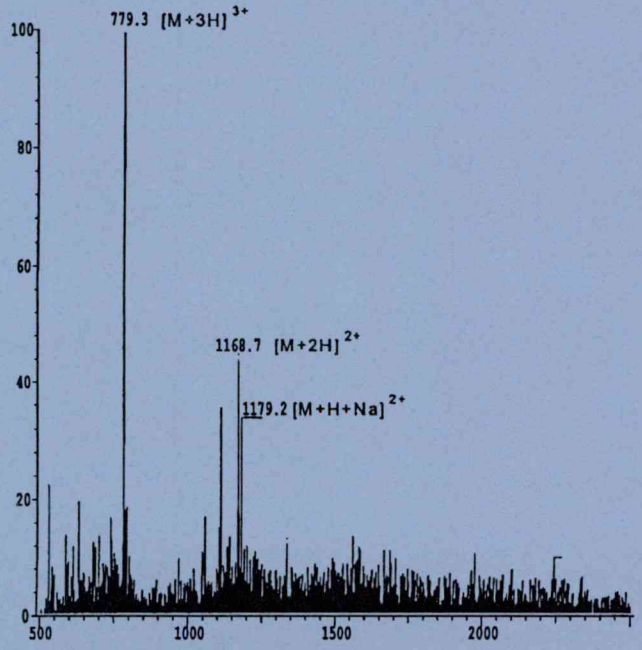

Figure 2. ESI-MS spectrum of the crude QDGVRQSRAS(PO_3H_2)DKQTLLPNDQ peptide M_W (calcd): 2335.4

In conclusion, we have introduced a new phosphitylation reagent which affords the synthesis of Ser/Thr containing phosphopeptides by the global approach without the undesired phosphate loss. Application of this new reagent has the following advantages: the phosphite incorporation is practically quantititive and removal of the β-cyanoethyl group does not require an additional step if DBU is used for the Fmoc deprotection. Furthermore, final removal of the *tert*-butyl group from the phosphate can be performed under milder conditions compared to those required for the previously described OBn containing synthons. TFA, normally used for final cleavage in Fmoc peptide synthesis, also removes the *tert*-butyl group and, therefore, an additional deprotection step is not necessary. The major advantage of this method is that the reagent is universally applicable for the phosphorylation of any hydroxyl group-containing compound without the same time-consuming multistep synthesis of the corresponding synthons.

Acknowledgements

The authors' thanks are due to the OTKA Foundation (grant Nos. T022540 and T022551) for the financial support and Ms Katalin Nagy for skillful technical assistance.

References

1. Perich, J. W.; Valerio, R. M.; Johns, R. B. *Tetrahedron Lett.* **1986**, *27*, 1377–1380.
2. Valerio, R. M.; Alewood, P. F.; Johns, R. B.; Kemp, B. E. *Int. J. Pept. Protein Res.* **1989**, *33*, 428–438.
3. Kitas, E. A.; Knorr, R.; Trzeciak, A.; Bannwarth, W. *Helv. Chim. Acta* **1991**, *74*, 1314–1328.

4. Perich, J. W.; Ruzzene, M.; Pinna, L. A.; Reynolds, E. C. *Int. J. Pept. Protein Res.* **1994**, *43*, 39–46.
5. Ötvös Jr., L.; Elekes, I.; Lee, V. M.-Y. *Int. J. Pept. Protein Res.* **1989**, *34*, 129–133.
6. Hoffmann, R.; Wachs, W. O.; Berger, R. G.; Kalbitzer, H. R.; Waidelich, D.; Bayer, E.; Wagner-Redeker, W.; Zeppezauer, M. *Int. J. Pept. Protein Res.* **1994**, *45*, 26–34.
7. Bannwarth, W.; Trzeciak, A. *Helv. Chim. Acta* **1987**, *70*, 175–186.
8. Perich, J. W.; Johns, R. B. *Tetrahedron Lett.* **1988**, *29*, 2369–2372.
9. de Bont, H. B. A.; van Boom, J. H.; Liskamp, R. M. J. *Tetrahedron Lett.* **1990**, *31*, 2497–2500.
10. Starker, G.; Jakobsen, M. H.; Olsen, C. E.; Holm, A. *Tetrahedron Lett.* **1991**, *32*, 5389–5392.
11. Andrew, D. M.; Kitchin, J.; Seale, P. W. *Int. J. Pept. Protein Res.* **1991**, *38*, 469–475.
12. Lacombe, J. M.; Andramanampisoa, F.; Pavia, A. A. *Int. J. Pept. Protein Res.* **1990**, *36*, 275–280.
13. Wakamiya, T.; Saruta, K.; Yasuoka, J.; Kusumoto, S. *Chemistry Lett.* **1994**, 1099–1102.
14. Ottinger, E. A.; Xu, Q.; Barany, G. *Peptide Res.* **1996**, *9*, 223–228.
15. Laczkó, I.; Hollósi, M.; Vass, E.; Hegedüs, Z.; Monostori, É; Tóth, G. K. *Biophys. Biochem. Res. Comm.* **1998**, *242*, 474–479.
16. Letsinger, R. L.; Oglilvie, K. K.; Miller, P. S. *J. Am. Chem. Soc.* **1969**, *91*, 3360–3365.
17. Xu, Y. Z.; Swann, P. F. *Nucleic Acids Res.* **1990**, *18*, 4061–4065.
18. Tosquellas, G.; Bologna, J. C.; Morvan, F.; Rayner, B.; Imbach, J. L. *Bioorg. Med. Chem. Lett.* **1998**, *8*, 2913–2918.
19. Wade, J. D.; Bedford, J.; Sheppard, R. C.; Tregear, G. W. *Peptide Res.* **1991**, *4*, 194–199.
20. Sinha, N. D.; Biernat, J.; Köster, H. *Tetrahedron Lett.* **1983**, *24*, 5843–5846.

2.1.

Peptides 1992
C.H. Schneider and A.N. Eberle (Eds.)

Synthesis of ANP and related compounds: The active center of the central effects

Gábor K. Tóth[a], Botond Penke[a], Amelia Bidzseranova[b] and Gyula Telegdy[b]

[a]Department of Medical Chemistry and [b]Department of Pathophysiology, A. Szent-Györgyi Medical University, Dóm tér 8, H-6720 Szeged, Hungary

Introduction

The recently discovered natriuretic peptide family is an important regulatory factor both in the periphery and in the brain. These peptides regulate the sodium balance and extracellular fluid volume and the blood pressure. As neuromodulator, ANP may be directly involved in the central control of the water-mineral balance and cardiovascular functions. However, the exact mechanism of this action and the active centers for different physiological effects are still poorly understood and determined.

Results and Discussion

Human and rat ANP(1–28), porcine CNP(1–22) and 11 shorter fragments of the upper peptides were synthesized by solid-phase methodology applying t-Boc chemistry [1]. Side chain protecting groups were as follows: Arg(Tos), Asp(OcHex), Cys(Meb), Lys(2ClZ), and Ser(Bzl). The peptide chains were elongated on Boc-Tyr(2BrZ)-Pam or Boc-Cys(Meb)-Pam resins (0.87–0.51 mmol/g, respectively) and the syntheses were carried out manually. CNP and its shorter fragments were made on benzyl ester resin (0.67 mmol/g). Several shorter fragments were prepared on MBHA resin (0.77 mmol/g). Couplings were performed with DCC, with the excep-

Table 1 *The sequences of the synthesized peptides*

α-rANP(1–28)	S	L	R	R	S	S	C	F	G	G	R	I	D	R	I	G	A	Q	S	G	L	G	C	N	S	F	R	Y
rANP(13–22)													D	R	I	G	A	Q	S	G	L	G						
rANP(12–23)												I	D	R	I	G	A	Q	S	G	L	G						
hANP(11–28)											R	M	D	R	I	G	A	Q	S	G	L	G	C	N	S	F	R	Y
hANP(16–28)																G	A	Q	S	G	L	G	C	N	S	F	R	Y
hANP(13–17)													D	R	I	G	A											
hANP(17–22)																	A	Q	S	G	L	G						
hANP(21–28)																					L	G	C	N	S	F	R	Y
rANP(7–23)							C	F	G	G	R	I	D	R	I	G	A	Q	S	G	L	G	C					
rANP(17–23)																	A	Q	S	G	L	G	C					
α-hANP(1–28)	S	L	R	R	S	S	C	F	G	G	R	M	D	R	I	G	A	Q	S	G	L	G	C	N	S	F	R	Y
CNP(1–22)		G	L	S	K	G	C	F	G	L	K	L	D	R	I	G	S	M	S	G	L	G	C					
CNP(14–22)															I	G	S	M	S	G	L	G	C					
CNP(18–22)																			S	G	L	G	C					

Table 2 *Effects of α-rANP(1–28) and some related compounds on consolidation of passive avoidance learning*

Peptide		Avoidance latency (Mean SEM)	Activity (%)	Significance
α-rANP(1–28)	(30)	182.4 ± 18.1	100	*
rANP(5–27)	(11)	168.2 ± 11.0	92	*
rANP(5–28)	(12)	188.2 ± 11.5	103	*
hANP(11–28)	(8)	175.1 ± 4.4	96	*
hANP(16–28)	(8)	158.9 ± 9.4	87	*
hANP(21–28)	(12)	113.2 ± 9.1	62	NS
rANP(7–23)	(10)	172.2 ± 11.0	94	*
rANP(17–23)	(10)	120.8 ± 9.0	66	NS
α-hANP(1–28)	(12)	226.2 ± 18.0	124	*
pBNP(1–32)	(14)	204.6 ± 9.5	112	*
pBNP(7–32)	(8)	207.7 ± 5.0	114	*
vs. control	(19)	101.7 ± 7.5		

tion of Asn, Gln and Arg which were incorporated as their HOBt-esters. Amino acid incorporation was monitored by the ninhydrin test [2]. The completed peptide resins were treated with liquid HF/dimethyl sulfide/*p*-cresol (88:6:4, v/v), at 0 °C for 1 h, in order to split off the peptide. HF was removed and the resulting free peptides were solubilized in 10% aqueous acetic acid, filtered and folded by stirring in air (with the exception of some shorter fragments containing only one cysteine residue) and lyophilized.

Purification was carried out by RPHPLC on a C_{18} column (16 × 250 mm). The peptides were eluted with a liner gradient of acetonitrile (0% → 76% in 90 min). The appropriate fractions were pooled and lyophilized. The structures of the resulting purified peptides were confirmed by amino acid analysis and FABMS.

The central effects of these peptides were characterized by electroconvulsive shock induced amnesia [3] and passive avoidance behavior [4] tests. The preliminary results concerning 11 peptides showed that the ring (7–23 fragment) is fully active and the C-terminal half of the molecule is almost fully active. The CNP proved less active than ANP and BNP in different central tests.

The cyclic structure of the peptides proved to be unnecessary and the minimum active sequence consists of approximately eight amino acids in the center of the molecule. The determination of the active centers for other biological effects needs further investigation.

References

1. Merrifield, R.B., Biochemistry, 3(1964)1385.
2. Kaiser, E., Colescott, R.L., Bossinger, C.D. and Cook, P.I., Anal. Biochemistry, 34(1970)595.
3. Bidzseranova, A. Penke, B. Tóth, G.K. and Telegdy, G., Neuropeptides, 19(1991)103.
4. Bidzseranova, A., Tóth, G.K. and Telegdy G., Pharmacol. Biochem. Behav., 40(1991)237.
5. Bidzseranova, A., Gueron, J., Penke, B., Tóth, G.K. and Telegdy, G., Brain Res. Bull., 28(1992)767.
6. Bidzseranova, A., Tóth, G.K. and Telegdy, G., Neuropeptides, 20(1991)163.
7. Koller, K.J., Lowe, D.G., Bennett, G.L., Minamino, N., Kangawa, K., Matsuo, H. and Goeddel, D.V., Science, 252(1991)120.

NEUROPEPTIDES

Neuropeptides (1991) 20, 163-167

The Effects of Atrial Natriuretic Peptide on the Open-Field Activity of Rats. The Role of Neurotransmitters

A. BIDZSERANOVA, G. TÓTH* and G. TELEGDY

*Institute of Pathophysiology and *Institute of Medical Chemistry, Albert Szent-Györgyi Medical University, Szeged, POB 531, Hungary (Reprint requests to GT)*

Abstract—In the present study, four doses (50, 100, 200 or 500 ng per animal) of rat atrial natriuretic peptide ($rANP_{1-28}$) were tested on the open-field activity of rats following i.c.v. application of the peptide. ANP in doses of 200 ng or 500 ng/rat significantly increased the ambulation activity 15 min after the treatment. However, the effect was transitory; 30 min after application it was no longer observed. When the experimental animals were pretreated with different receptor blockers in doses which per se could not affect the behavioral paradigm, the effect of ANP was completely blocked by haloperidol (a dopaminergic blocking agent), phenoxybenzamine (an α-adrenergic blocker) and propranolol (a β-adrenergic blocker). Atropine, naloxone, bicuculline and methysergide were ineffective.

These results suggest that dopaminergic and adrenergic transmitter systems are involved in the ANP-induced locomotor activity of rats.

Introduction

The presence of ANP and its receptors in the brain is well established (12, 14, 17, 23). The peptide has central effects on the cardiovascular system (10, 15, 16), hormone release (6, 9, 18) and water-salt homeostasis (7, 8, 13). These data prompted us to investigate whether ANP might be involved in behavioral reactions related to memory functions and learning processes. Our previous studies demonstrated that fear-motivated learning-associated memory formation can be facilitated by ANP (1, 2, 4). In this respect the peptide exerts its actions via dopaminergic and cholinergic mediations. It has also been shown that electroconvulsive shock-induced partial amnesia can be prevented by ANP (3). This mechanism is mediated by dopaminergic, cholinergic and β-adrenergic systems. Since the above observations can also be related to a changed locomotion, in the present investigation the following problems were studied:

1. Has ANP any effect on open-field behavior and, if so, at what time after administration can it be observed?
2. What are the roles of the different neuro-

Date received 25 July 1991
Date accepted 21 June 1991

transmitter systems in the effects of ANP on this activity?

Materials and Methods

Animals. Adult CFY rats weighing 180 ± 35 g were used. The animals were kept on a standard illumination schedule (lights on at 6 a.m.). Food and tap water were given ad libitum. The experiments were carried out daily between 8 a.m. and noon.

Surgery. The rats were anaesthetized with pentobarbital-Na (Nembutal, 35 mg/kg i.p.). A stainless cannula was placed into the right lateral cerebroventricle and was fixed to the skull with dental cement. The animals were used for the experiments after a 5-day recovery period. Correct positioning of the cannula was checked by injecting methylene blue after the experiments were completed.

Drugs. The rat ANP_{1-28} was purchased from Bachem (CA, USA) and was synthesized by G. Tóth. It was dissolved in 0.9% saline and administered i.c.v. in a volume of 2 µl in four doses (50, 100, 200 or 500 ng per rat). The receptor blockers were used 30 min before the peptide administration as follows: 1) haloperidol (G. Richter, Budapest), 10 µg/kg i.p.; 2) atropine sulphate (EGYT, Budapest), 2 mg/kg i.p.; 3) propranolol hydrochloride (Imp. Chem. Indust. Ltd, UK), 10 mg/kg i.p.; 4) phenoxybenzamine hydrochloride (Smith, Klein and French, UK), 2 mg/kg i.p.; 5) methysergide hydrogenmaleinate (Sandoz, D), 5 mg/kg i.p. Another two blockers (naloxone hydrochloride (Endo Lab. Inc., USA), 0.3 mg/kg, and bicuculline methiodide (Sigma, USA), 1 mg/kg) were applied subcutaneously 20 min before ANP administration.

Behavioral method. The animals were placed in an open-field box consisting of 36 squares (10 × 10 cm). The activity was characterized by the total number of the squares explored and defecation boluses during 3-min sessions. The open-field behavior was measured 5, 15 and 30 min after peptide treatment.

Statistical evaluation. Statistical analysis of the results was performed by one-way ANOVA followed by the Dunnett and Tukey tests. A probability level of 0.05 was accepted as significant for the differences between the different groups. Values are given as means ± SEM.

Results

From our previous experience with the effects of ANP on fear-motivated activity, we selected a four-dose range (50 ng, 100 ng, 200 ng or 500 ng per rat) for the present experiments. For the time of appearance of the effect, the open-field locomotion 5, 15 and 30 min after application was tested (Table 1). The peptide in the doses of 200 or 500 ng increased the locomotion at 15 min (ANOVA $F(3.1) = 8.56$ and $F(3.9) = 3.5$ respectively, Dunnett ($p < 0.05$)), but at 5 min the peptide was ineffective and at 30 min the effect was no longer observed.

From this experience, a time of 15 min following administration of ANP was used to test the open-field activity in further experiments, i.e., ambulation, rearing, grooming and defecation boluses. Only the 200 ng and 500 ng ANP doses were effective, and only on ambulation, (ANOVA $F(4.15) = 7.12$ and $F(4.15) = 7.12$ respectively, Dunnett ($p < 0.05$)). There was no action on the other open-field parameters (grooming, rearing or defecation boluses). (Table 2).

Table 1 The effects of ANP on the ambulatory activity of rats on the 5th, 15th and 30th min after application

Dose ng	*Total number of squares 5 min*	*Total number of squares 15 min*	*Total number of squares 30 min*
50	46.2 ± 11.8 (6)	57.2 ± 7.6 (6)	60.2 ± 7.6 (6)
100	49.8 ± 5.5 (18)	60.1 ± 6.2 (18)	63.0 ± 6.7 (18)
200	42.7 ± 6.4 (18)	85.0 ± 4.2* (18)	50.2 ± 11.2 (6)
500	44.0 ± 11.6 (6)	91.7 ± 16* (6)	52.3 ± 12.1 (6)

Mean ± standard errors. Numbers in brackets represent the number of animals used. * $p < 0.05$ vs control (ANOVA-Dunnett).

Table 2 Effects of ANP on the open-field activity 15 min following administration in rats

Dose ng	*Total number of squares*		*Total number of rearings*		*Total number of groomings*		*Defecation boluses*	
	control	*treated*	*control*	*treated*	*control*	*treated*	*control*	*treated*
50	60.9 ± 11.8 (10)	56.6 ± 5.5 (10)	15.5 ± 3.1 (10)	11.5 ± 1.6 (10)	2.8 ± 0.5 (10)	5.1 ± 0.8 (10)	2.9 ± 0.6 (10)	3.0 ± 0.65 (10)
100	51.8 ± 5.1 (36)	60.1 ± 7.9 (30)	11.1 ± 1.1 (36)	12 ± 1.2 (30)	4.5 ± 0.5 (36)	5.2 ± 0.6 (30)	3.0 ± 0.4 (36)	1.7 ± 3.0 (30)
200	45.7 ± 6.7 (24)	85.0 ± 7.2* (24)	13.1 ± 2.2 (24)	15.5 ± 1.6 (24)	4.5 ± 0.8 (24)	4.8 ± 8.0 (24)	2.6 ± 0.5 (24)	2.3 ± 0.4 (24)
500	49.3 ± 2.2 (10)	90.9 ± 7.7* (10)	11.8 ± 1.8 (10)	15.2 ± 1.2 (10)	3.3 ± 1.1 (10)	5.4 ± 1.1 (10)	3.7 ± 0.9 (10)	2.8 ± 0.9 (10)

Mean ± standard errors. Numbers in brackets represent the number of animals used. * $p < 0.05$ vs control (ANOVA-Dunnett).

In order to investigate the possible involvement of different receptors in the action of ANP on ambulation, the animals were pre-treated with different receptor blockers which effectively modified the action of different peptides in previous studies (21). The doses selected from this experience did not change the behavioral paradigm per se. In the groups pre-treated with haloperidol, phenoxybenzamine or propranolol, the effect of ANP on ambulation (or the horizontal activity) was inhibited significantly (ANOVA $F(3.36) = 5.25$; $F(3.36) = 6.6$ and $F(3.56) = 3.65$ respectively. Dunnett ($p < 0.05$)) (Table 3), whereas the other four blockers (atropine, methysergide, bicuculline and naloxone were ineffective (Table 3).

Discussion

It has been reported that the highest concentrations of ANP in the CNS are to be found in the hypothalamus and septum, followed by the midbrain, cortex, olfactory bulb, thalamus and pontine medullary region (12, 19, 23). These findings indicated that ANP might also have central effects besides its known peripheral effects (6, 13, 15).

In previous experiments we observed that $rANP_{1-28}$, when given into the lateral brain ventricle before or immediately after the learning trial, delayed the passive avoidance response, which was interpreted as facilitating learning and consolidation of memory in passive avoidance behavior (1, 4). When it was given immediately after the last learning trial, the peptide delayed the extinction of the active avoidance reflex (2). These results suggested a possible participation of ANP in the processes of fear-induced motivated behavior. The active and passive avoidance effects caused by ANP strengthened the supposition that the observed responses are related to learning and not to locomotion. Despite this evidence, in the present study we followed the action of ANP on open-field behavior, with the doses found effective in the previous experiments. From the data obtained it was obvious that ANP caused only a transitory increase in locomotion activity, the maximum of which was at 15 min after application and which was no longer present at 30 min. From these data, it is clear that the delayed extinction or lengthened passive avoidance response cannot be caused by ANP action on locomotion.

Nakamura and co-workers (13) reported no significant increase in locomotor activity 30 min after i.c.v. application of a 5 μg doses of α-hANP, although a tendency was observed: 259 ± 35 active counts for the control vs 336 ± 56 counts for the peptide group. Our data clearly show that the action of the peptide is only transitory, and 30 min following administration significant action can no longer be observed.

ANP can influence the neurotransmitter metabolism or the action of neurotransmitters. Marin-Grez et al. (11) reported that dopamine receptor antagonists inhibited the natriuretic effect of the peptide. Israel, Torres and Barbella (7) found that haloperidol and domperidon prevented the natriuretic and diuretic responses to centrally administered ANP. Our observations suggested

Table 3 The effects of different receptor blockers pre-treatment on the number of ambulances 15 min after ANP treatment in rats

Blockers		*Total number of squares*	*Significance*
Haloperidol (10 mg/kg)			
control	(10)	54.3 ± 8.9	
200ng ANP	(10)	91.8 ± 5.3.	* F(3.36) = 5.25
haloperidol	(10)	57.4 ± 7.9	
halop. + ANP	(10)	68.5 ± 7.0	
Phenoxybenzamine (2mg/kg)			
control	(10)	60.1 ± 7.9	
200ng ANP	(10)	88.5 ± 5.6	* F(3.36) = 6.6
phenoxybenz.	(10)	55.9 ± 3.9	
phenox. + ANP	(10)	62.6 ± 4.6	
Propranolol (10mg/kg)			
control	(18)	60.7 ± 4.3	
200ng ANP	(18)	85.7 ± 5.6	* F(3.56) = 3.65
propranolol	(8)	54.9 ± 11.9	
propr. + ANP	(16)	60.1 ± 9.6	
Bicuculline (1 mg/kg)			
control	(21)	58.8 ± 4.7	
200ng ANP	(22)	81.9 ± 3.7	* F(3.66) = 5.43
bicuculline	(9)	57.2 ± 10.0	
bicuc + ANP	(18)	76.2 ± 4.5	* F(3.66) = 6.3
Atropine (2mg/kg)			
control	(10)	59.2 ± 7.1	
200ng ANP	(10)	90.6 ± 9.4	* F(3.36) = 5.7
atropine	(10)	52.7 ± 5.8	
atr. + ANP	(10)	92.2 ± 11.2	* F(3.66) = 5.7
Naloxone (0.3mg/kg)			
control	(20)	57.5 ± 4.9	
200ng ANP	(20)	82.2 ± 5.8	* F(3.76) = 10.37
naloxone	(16)	45.9 ± 4.4	
nalox. + ANP	(24)	76.4 ± 4.7	* F(3.76) = 10.37
Methysergide (5mg/kg)			
control	(14)	54.2 ± 5.4	
200ng ANP	(13)	82.4 ± 4.9	* F(3.4) = 4.65
methysergide	(9)	59.6 ± 8.8	
meth. + ANP	(9)	82.6 ± 10.7	* F(3.4) = 4.65

Mean ± standard errors. Numbers in brackets represent the number of animals used. * $p < 0.05$ vs control (ANOVA-Dunnett).

that the centrally induced action of the peptide is also mediated by transmitters. The ANP-induced delayed extinction in the active avoidance paradigm and the delayed response in the passive avoidance paradigm could both be blocked by dopaminergic and cholinergic receptor blockers (2.4). The antiamnesic action of ANP could also be blocked by haloperidol, atropine and propranolol (3).

The present study demonstrates that the increased locomotion caused by ANP can be blocked by dopaminergic and α- and β-adrenergic blockers. Other receptor blockers, such as atropine, naloxone, bicuculline and methysergide, which were effective in the same doses in previous experiments, e.g., atropine and haloperidol in (4), methysergide in self-stimulation behavior (29), naloxone on LH-RH action (personal communication) or bicuculline in (5), were ineffective. It seems that the ANP-induced behavioral action is mediated by different neurotransmitters and that different neurotransmitter systems are involved in the organization of the behavioral reaction.

References

1. Bidzseranova, A., Telegdy, G. and Penke, B. (1991). The effects of atrial natriuretic peptide on passive avoidance behavior in rats. Brain Res. Bul. 26, 1: 177-180.
2. Bidzseranova, A., Gueron, J., Penke, B. and Telegdy, G. (1990). The effects of atrial natriuretic peptide on active avoidance behavior in rats. The role of the transmitter systems. Pharmacol. Bioch. Behav. (submitted).
3. Bidzseranova, A., Penke, B. and Telegdy, G. (1990). The effects of atrial natriuretic peptide on electroconvulsive shock-induced amnesia in rats: transmitter mediated action. Neuropeptides (in press).
4. Bidzseranova, A., Telegdy, G. and Toth, G. (1990). The effects of receptor blockers on atrial natriuretic peptide-induced action on passive avoidance behavior in rats. Pharmacol. Biochem. Behav. (submitted)
5. Guidotti, A. and Hanbauer, I. (1986). Participation of GABA Benzodiazepine Receptor System in the Adrenal Chromaffin Cell Function. In: GABA and Endocrine Function. Eds G. Racagni and A. O. Donoso, Raven Press, 165-172.
6. Iitake, K., Share, L., Crofton, J., Brooks, D.P., Ouchi, Y., Blain, E. (1986). Central atrial natriuretic factor reduces vasopressin secretion in the rat. Endocrinology 119: 1, 438-440.
7. Israel, A., Torres, M., Barbella, Y. (1989). Evidence for a dopaminergic mechanism for the diuretic and natriuretic action of centrally administered atrial natriuretic factor. Cell Mol. Neurobiol. 9: 3, 365-378.
8. Itoh, H., Nakao, K., Katsuura, G., Morii, M., Shiono, S., Sakamoto, M., Sugawara, A., Yamada, T., Saito, Y., Matsushita, A. and Imura, H. (1986). Centrally infused atrial natriuretic polypeptide attenuates exaggerated salt appetite in spontaneously hypertensive rats. Circulat. Res. 59: 342-347.

9. Lamacz, M., Netchitailo, P., Tonon, M., Feuilloley, M., Ling, N., Pelletier, G. and Vaudary, H. (1987). Atrial natriuretic factor (ANF) stimulates the releases of α-MSH from the frog neurointermediate lobes in vitro. Interaction with dopamine, GABA and Neuropeptide Y. Life sci. 40: 1853-1857.
10. Levin, E., Weber, M. and Mills, S. (1988). Atrial natriuretic factor-induced vasodepression occurs through central nervous system. Am. J. Physiol. 255 (Heart Circ. Physiol. 24): 616-622.
11. Marin-Grez, M., Briggs, J., Shubert, G., Schnermann, J. (1985). Dopamine receptor antagonists inhibit the natriuretic response to atrial natriuretic factor (ANF). Life sci. 36: 2171-2176.
12. Morii, N., Nakao, K., Sugawara, A., Sakamoto, M., Suda, M., Shimokura, M., Kiso, J., Kihara, M., Yamori, Y. and Imura, H. (1985). Occurence of atrial natriuretic polypeptide in brain. Biochem. Biophys. Res. Commun. 127: 413-419.
13. Nacamura, M., Katsuura, G., Nakao, K. and Imura, H. (1985). Antidisogenic action of α-human atrial natriuretic polypeptide administered intracerebroventricularly in rats. Neurosc. Lett. 58: 1-6.
14. Quirion, R., Dalpe, M., De Len, A., Gutkowska, J., Caitin, M. and Genest, J. (1984). Atrial Natriuretic Factor (ANF) binding sites in brain and related structures. Peptides 5: 1167-1172.
15. Sills, M. A., Nguyen, K. O. and Jacobowitz, D. M. (1985). Increases in heart rate and blood pressure produced by microinjections of atrial natriuretic factor into AV3V region of the rat brain. Peptides 6: 1037-1042.
16. Smimizu, T., Katsuura, G., Nacamura, M., Nakao, K., Morii, N., Itoh, Y., Shiono, S. and Imura, H. (1986). Effect of icv atrial natriuretic polypeptide on blood pressure and urine production in rats. Life sci. 39: 1263-1270.
17. Skofitsch, G. and Jacobowitz, D. (1988). Atrial natriuretic peptide in the central nervous system of the rat. Cell Mol. Neurobiol. 4: 339-391.
18. Takao, T., Hashimoto, K. and Ota, Z. (1988). Effect of atrial natriuretic peptide on acetylcholine-induced release of corticotropin releasing factor from rat hypothalamus in vitro. Life sci. 2: 1199-1203.
19. Tanaka, I., Misono, K. S. and Inagami, T. (1984). Atrial natriuretic factor in rat hypothalamus, atria and plasma: Determination of specific radioimmunoassay. Biochem. Biophys. Res. Commun. 124: 663-668.
20. Vécsei, L., Schwarzberg, H., Telegdy, G. (1983). The effect of somatostatin on self-stimulation behavior in atropine- and methysergide-pretreated rats. Eur. J. Pharm. 91: 89-93.
21. Telegdy, G. (1987) in: Neuropeptides and Brain Function, Karger, Basel, p. 1-332.
22. Zamir, N., Skofitsch, G., Eskay, R. L. and Jacobowitz, D. M. (1986). Distribution of immunoreactive atrial natriuretic peptides in the central nervous system of the rat. Brain Res. 365: 105-111.

2.3.

NEUROPEPTIDES

Neuropeptides (1991) 19, 103-106

The Effects of Atrial Natriuretic Peptide on Electroconvulsive Shock-Induced Amnesia in Rats. Transmitter-Mediated Action

A. BIDZSERANOVA, B. PENKE, G. TÓTH and G. TELEGDY

Department of Pathophysiology and Department of Medical Chemistry, Szent-Györgyi A. University Medical School, Szeged, POB 531, Hungary. (Reprints to GT)

Abstract—Electroconvulsive shock (ECS) applied immediately after passive avoidance learning in rats caused partial amnesia. This could be prevented by administering r-ANP into the lateral brain ventricle. The effects of pre-treatment with different receptor blockers: (haloperidol, atropine, phenoxybenzamine, propranolol, naloxone, bicuculline and methysergide) on the ANP-induced antiamnesia were investigated. The receptor blockers per se in the doses selected had no influence on the ECS-induced amnesia. Haloperidol, atropine and propranolol blocked the antiamnestic action of the peptide, while phenoxybenzamine, naloxone, bicuculline and methysergide were ineffective. The results confirm our previous observations that ANP might play a role in learning and memory processes and also suggest that the antiamnestic action of the peptide is mediated by dopaminergic, cholinergic and beta-adrenergic mediator systems.

Introduction

Atrial natriuretic peptide (ANP) is present not only in the heart, but also in a variety of rat brain regions, in the circumventricular organs, the telencephalic, diencephalic and mesencephalic regions, the medulla oblongata and the spinal cord (17). This wide distribution of the peptide suggests a versatile action. Intracerebroventricularly administered ANP was found to inhibit water drinking in rats (1, 8, 7). Samson (13) has shown that icv. applied ANP inhibits the vasopressin release induced in rats by dehydration and haemorrhage. Further icv. application of the peptide attenuates the hypertension induced by angiotensin II (6).

Very little is known about the effects of ANP on the processes of learning, retention of learning and memory formation.

As a continuation of our former work, the goal of the present study was to establish the effects of ANP on electroconvulsive shock-induced amnesia in rats, based on passive avoidance learning. An attempt has also been made to follow the possible involvement of the transmitter systems in this action.

Date received 13 November 1990
Date accepted 29 January 1991

Methods

Animals. The experiments were performed on male CFY rats weighing 150-250g. They were kept at constant room temperature in artificial 12h light (started at 6a.m.), 12h dark periods. Commercial food and tap water were given ad libitum. The experiments started at 8a.m. and were concluded by noon.

Surgery. The rats were anaesthetized with pentobarbital-Na (Nembutal, 35mg/kg, i.p.) and a cannula was placed into the lateral cerebroventricle and fixed to the skull with dental cement. The operated animals were used after a recovery period of 5 days. The correct positioning of the cannula was checked by injecting methylene blue through the cannula and by subsequent dissection of the brain.

Electroconvulsive shock (ECS)-induced amnesia. The experimental apparatus consisted of an illuminated platform (7 × 30cm) attached to a dark box (25 × 37 × 30cm). The animals were placed on the platform facing away from the entrance and were allowed to enter the box. Since rats prefer dark to light, they normally entered within 15s. Two additional sessions were given on the following day. After the second session unavoidable electric shocks (0.75mA, 2s) were delivered through the grid floor of the dark compartment. After this single learning trial, the animals were immediately removed from the apparatus. Retrograde amnesia was performed by ECS, using a MINICOMA (AC 190V, 50Hz, 0.5s duration, position 2) apparatus immediately after the learning trial (15).

Pre-treatment. The following receptor blockers were used. Haloperidol (G. Richter, Budapest). (10μg/kg, i.p.), atropine (EGYT, Budapest) (2mg/kg i.p.): propanolol (Imp Chem Ind Ltd, Great Britain) (10mg/kg i.p.) phenoxybenzamine (Smith, Kline and French), (2mg/kg, i.p.), methysergide (Sandoz), (5mg/kg, i.p.): All the above mentioned drugs were given 30 min before the learning trial. Naloxone (Endo Lab Inc, USA) (0,3mg/kg, s.c.) and bicuculline (Serva) (1mg/kg, s.c.), were given 20 min before the learning trial.

Treatment. The peptide was dissolved in 0.9% saline and injected in a volume of 2μl into the lateral ventricle in doses of 0.2, 0.5 and 1μg per rat, immediately after the ECS-induced amnesia, except in the case of phenoxybenzamine, which was given 20 min after the blocker.

Statistical analysis. For statistical evaluation of the data, the U-test of Mann-Whitney (MW test) and one-way ANOVA tests were used. A probability level of 0.05 or less was accepted as statistically relevant.

Results

The experiments were begun with the lowest dose of the peptide, i.e., 0.2μg per rat, as this dose had proved to be effective in our previous studies on passive avoidance learning in rats (2). Overall, the average latency of entering without electric foot-shock was 7s. The avoidance latency of the animals treated with foot-shock and saline icv. was approximately 120s (mean). If the rats received ECS the avoidance latency decreased significantly (p 0.001 vs foot-shock + saline, MW and ANOVA tests). The animals treated with 0.2μg ANP immediately after the ECS did not display a significant improvement in avoidance response.

Table 1 The effects of ANP on electroconvulsive shock-induced amnesia in rats

Groups	*Avoidance latency*	*Significance*
Control (30)	121.0 + 12.5	
Amnesia (30)	45.9 + 3.8	vs. control $p < 0.05$
Amnesia + 200ng/ANP (18)	67.8 + 9.3	vs. amnesia $p < 0.05$
Amnesia + 500ng/ANP (12)	110.7 + 6.2	vs. amnesia $p < 0.002$
Amnesia + 1μg/ANP (12)	153.5 + 13.7	vs. amnesia $p < 0.001$

+ Mean ± standard errors. Numbers in brackets represented the number of animals used

The 0.5 and 1.0 μg doses of ANP, given icv. immediately after the ECS, blocked the ECS-induced amnesia (p 0.001 vs ECS (Table 1)). For convenience, in subsequent experiments we chose the dose of 0.5 μg ANP per rat.

Pre-treatment with blockers. The doses of the different receptor blockers were chosen to lie in the range that did not influence the task itself. This pre-treatment with a blocker modified the action of the peptide. Haloperidol, atropine and propra-

Table 2 The effects of different receptor blockers on antiamnesic action of ANP in rats

Blockers	*Avoidance latency*	*Significance*	
Haloperidol (10 μg/kg)			
Control (36)	92.4 ± 5.9+		
Amnesia (15)	64.9 ± 10.1	vs. cont	$p < 0.05$
Amnesia + haloperidol (17)	57.5 ± 9.0	vs. cont	$p < 0.05$
Amnesia + 500 μg/rat ANP (17)	118.1 ± 9.7	vs. amnesia	$p < 0.05$
Amn + haloperidol + ANP (15)	66.0 ± 7.6	vs. (amn. ANP)	$p < 0.05$
Atropin (2 mg/kg ip.)			
Control (12)	81. 5 ± 19.5		
Amnesia (12)	36.4 ± 7.1	vs. cont	$p < 0.05$
Amn + Atropine (12)	39.5 ± 7.8		
Amnesia + 500 ng ANP (12)	116.5 ± 9.4	vs. amnesia	$p < 0.05$
Amn + Atropine + ANP (12)	58.4 ± 7.5	vs. (amn + ANP)	$p < 0.05$
Propranolol (10 mg/kg ip.)			
Control (6)	99.0 ± 13.5		
Amnesia (6)	55.0 ± 11.3	vs. cont	$p < 0.05$
Propranolol + Amn (6)	69.6 ± 15.6		
Amn + 500 ng ANP (6)	129.0 ± 17.0	vs. amn	$p < 0.05$
Amn + propranolol + ANP (6)	58.6 ± 13.6	vs. (amn + ANP)	$p < 0.05$
Phenoxybenzamine (2 mg/kg ip.)			
Control (6)	101.16 ± 12.1		
Amnesia (6)	49.0 ± 3.2	vs. cont	$p < 0.05$
Amn + phenoxybenzamine + Amn (6)	58.5 ± 10.8		
Amnesia + 500 ng ANP (6)	124.1 ± 13.8	vs. amn	$p < 0.05$
Amn + phenoxybenzamine + ANP (6)	106.8 ± 12.3		
Naloxone (0.3 mg/kg)			
Control (6)	80.8 ± 18.8		
Amnesia (6)	48.8 ± 4.8	vs. cont	$p < 0.05$
Amn + naloxone (6)	42.1 ± 4.2		
Amn + 500 ng ANP (6)	127.5 ± 13.3	vs. amn	$p < 0.05$
Amn + naloxone + ANP (6)	122.0 ± 4.9		
Bicuculline (1 mg/kg ip.)			
Control (6)	92.3 ± 7.8		
Amnesia (6)	56.0 ± 5.6	vs. cont	$p < 0.05$
Amn + bicuculline (6)	44.5 ± 9.5		
Amn + 500 ng ANP (6)	117.1 ± 4.7	vs. amn	$p < 0.05$
Amn + bicuc + ANP (6)	104.0 ± 12.7		
Methysergide (5 mg/kg ip.)			
Control (6)	100.5 ± 16.4		
Amnesia (6)	47.6 ± 5.5	vs. cont	$p < 0.05$
Amn + methysergide + Amn. (6)	53.1 ± 13.1		
Amn + 500 ng ANP (6)	120.8 ± 8.8	vs. amn	$p < 0.05$
Amn + methyserg + ANP (6)	112.3 ± 9.2		

+ Mean ± standard errors. Numbers in brackets represent the number of animals used

nolol significantly inhibited the ANP-induced antiamnesia (Table 2), whereas phenoxybenzamine, naloxone, bicuculline and methysergide (Table 2) did not change the antiamnestic effect of the peptide.

Discussion

In our previous study with ANP showed, that the peptide can improve the learning and consolidation of a passive avoidance response (2) and delay the extinction of the active avoidance reflex (3). It seems that these responses can be modified by dopamine, and cholinergic receptor blockers (4).

A number of previous studies in our Department (14) have shown that some peptides exert antiamnesic potency. Electro-shock-induced amnesia can be prevented by somatostatin in the same paradigm and the antiamnesic action can be blocked by propranolol and phenoxybenzamine but not by haloperidol and atropine (5, 16).

The present study clearly showed that ANP prevents amnesia and this action can be mediated by dopaminergic and cholinergic transmission. Since ACTH and vasopressin display similar action (11, 12) one might suppose that ACTH or vasopressin could be also a mediator in these processes. However, most of the data indicate that ANP depresses the release of vasopressin (9) and does not affect ACTH (10). Thus the involvement of ACTH or vasopressin as mediators in these processes is unlikely.

References

1. Antunes-Rodrigues, J., McCann, S.M., Rogers, L.C. and Samson, W.K. (1985). Atrial natriuretic factor inhibits dehydration and angiotensin II-induced water intake in the conscious, unrestrained rat. Proc. Natl. Acad. Sci. USA 82: 8720-8723.
2. Bidzseranova, A. and Telegdy, G. (1990). The effects of atrial natriuretic peptide on passive avoidance behaviour in rats. Brain Res. Bull. (in press).
3. Bidzseranova, A., Telegdy, G. and Penke, B. (1990). The effects of atrial natriuretic peptide on passive avoidance behaviour in rats. Brain Res. Bull. (in press).
4. Bidzseranova, A., Telegdy, G. and Tóth, G. (1990). The effects of receptor blockers on atrial natriuretic peptide-induced action on passive avoidance behaviour in rats. Neuropharmacology (in press).
5. Bollók, I., Vécsei, L. and Telegdy, G. (1983). The effects of interaction between propranolol and somatostatin on the active avoidance behaviour, open-field activity and electroconvulsive shock-induced amnesia of rats. Neuropeptides 3: 263-270.
6. Itoh, H., Nakao, K. and Morii, N. et al. (1986). Central action of atrial natriuretic polypeptide on blood pressure in conscious rats. Brain Res. Bull. 16: 745-749.
7. Masotto, G. and Negro-Vilar, A. (1985). Inhibition of spontaneous or angiotensin II-stimulated water intake by atrial natriuretic factor. Brain Res. Bull. 15: 523-526.
8. Nakamura, M., Katsuura, G., Nakao, K. and Imura, H. (1985). *Antidipsogenic action of alfa-human atrial* natriuretic polypeptide administered intracerebroventricularly in rats. Neurosci. Lett. 58: 1-6.
9. Obana, K., Naruse, M. and Inagami, T. et al. (1985) Atrial natriuretic factor inhibits vasopressin secretion from rat posterior pituitary. Biochem Biophys. Res. Commun. 132: 1088-1094.
10. Ohashi, M., Fujio, N., Kato, K., Nawata, H., Ibayashi, H. and Matsuo, H. (1986). Effect of human α-atrial natriuretic polypeptide on adrenocortical function in man. J. Endocr. 110: 287-292.
11. Rigter, H., van Riezen, H. and de Wied, D. (1974). The effects of ACTH and vasopressin analogues on CO_2-induced retrograde amnesia in rat. Physiol. Behav. 13: 381-388.
12. Rigter, H., Elbertse, R. and van Riezen, H. (1975). Time-dependent anti-amnesic effect of ACTH 4-10 and desglycin-amide-lysine vasopressin, in: Hormones, Homostasis and the Brain (W. H. Gispen, Tj. B. van Wimersma Greidanus, B. Bohus and D. de Wied eds.). Prog. Brain Res. Elsevier Amsterdam 42: 163-171.
13. Samson, W. K. (1985). Atrial natriuretic factor inhibits dehydration and hemorrhage-induced vasopressin release. Neuroendocrinology 40: 227-229.
14. Telegdy, G. (1987). Neuropeptide and Brain Function Karger, Basel pp. 1-332.
15. Vécsei, L., Bollók, I. and Telegdy, G. (1983). Intracerebroventricular somatostatin attenuates electroconvulsive shock-induced amnesia in rats. Peptides 4: 293-295.
16. Vécsei, L., Bollók, I. and Telegdy, G. (1984). Phenoxybenzamine antagonizes somatostatin-induced antiamnesia in rats. Eur. J. Pharmacol. 99: 325-328.
17. Zamir, N., Skofitsch, G., Eskay, R. L. and Jacobowitz, D. M. (1986). Distribution of immunoreactive atrial natriuretic peptides in the central nervous system of the rat. Brain Res. 365: 105-111.

Pharmacology Biochemistry & Behavior, Vol. 40, pp. 237–239. © Pergamon Press plc, 1991. Printed in the U.S.A. 0091-3057/91 $3.00 + .00

The Effects of Receptor Blockers on Atrial Natriuretic Peptide-Induced Action on Passive Avoidance Behavior in Rats

AMELIA BIDZSERANOVA, GABOR TOTH* AND GYULA TELEGDY[1]

*Departments of Pathophysiology and *Medical Chemistry, University Medical School H-6701, Szeged, P.O. Box 531, Hungary*

Received 8 March 1991

BIDZSERANOVA, A., G. TOTH AND G. TELEGDY. *The effects of receptor blockers on atrial natriuretic peptide-induced action on passive avoidance behavior in rats.* PHARMACOL BIOCHEM BEHAV 40(2) 237–239, 1991.—In previous experiments, it was shown that rat atrial natriuretic peptide ($rANP_{1-28}$) is able to increase the passive avoidance latency in a dose-dependent manner in the learning and consolidation phase (3). In order to clarify whether ANP has a direct action on this behavioral paradigm, or whether the action is mediated by neurotransmitters, rats were pretreated with different receptor blockers. The selected doses of the different receptor blockers could themselves not influence the behavioral paradigms. Haloperidol or atropine blocked the action of ANP on the consolidation of the passive avoidance response. Phenoxybenzamine, propranolol, methysergide, bicuculline and naloxone were ineffective. The data suggest that dopaminergic and cholinergic mediations are involved in the action of ANP on the passive avoidance response.

Atrial natriuretic peptide Receptor blockers Avoidance behavior

THE extract of the rat atria possesses natriuretic, diuretic and vasorelaxant activity (4). This discovery led to the isolation of atrial natriuretic peptide from both rats and humans (5,8). ANP has been demonstrated to be present independently in the periphery and in the brain (9, 12, 18). Specific ANP receptors have been found in the central nervous system (14).

Centrally administered ANP is able to increase the blood pressure (17). However, angiotensin II-induced hypertension is attenuated by centrally administered ANP (16). The exaggerated salt appetite in spontaneous hypertensive rats is blunted by centrally administered ANP (7). Central administration of ANP causes diuresis and natriuresis (6), diminishes vasopressin release (15) and has antidipsogenic action (2).

In previous experiments we have shown that ANP administered into the lateral brain ventricle is able to facilitate the passive avoidance response in a one-trial learning paradigm, when the peptide is given before or immediately after the learning trial. It was less effective, or even ineffective, when it was given before the retention testing (3).

In order to elicit the possible involvement of neurotransmitters in the ANP-induced action, animals were pretreated with different receptor blockers which were effective in modifying the action of a number of peptides in the same paradigm (20).

METHOD

CFY adult male rats weighing 150–250 g were used. All animals had access to commercial food and tap water ad lib and were kept at a constant room temperature (20–22°C) and on a standard 12-h light-12-h dark cycle (lights on at 6 a.m.). Experiments were carried out daily between 9 a.m. and noon.

The animals were anesthetized with pentobarbital (35 mg/kg, IP), and a cannula was placed into the lateral cerebroventricle and fixed to the skull with dental cement. The animals were used 7 days following operation. The correct positioning of the cannula was checked individually by the injection of methylene blue after the experiments had been completed. Animals with incorrect placement of the cannula were discarded and excluded from the statistical evaluations.

The experimental apparatus consisted of an illuminated platform (30 × 7 cm) attached to a large, dark compartment (40 × 30 × 30 cm) with a grid floor. In this apparatus, one-trial learning step-through passive avoidance behavior was measured according to Ader and De Wied (1). Rats were placed on the platform and allowed to enter the dark compartment. Since rats prefer dark to light, they normally entered within 15 s. Two additional trials were given on the following day. After the second one, unavoidable electric footshocks (0.75 mA, 2 s) were delivered through the grid floor. The animal could not escape the footshock. After this single learning trial, the rats were immediately removed from the apparatus. Passive avoidance behavior was tested 24 h after the learning trial: the rats were placed on the platform and the latency to enter the dark compartment was measured up to a maximum of 300 s. Animals were treated with

[1]Request for reprints should be addressed to G. Telegdy, Department Pathophysiology, University Medical School, Szeged, P.O. Box 531, Hungary.

TABLE 1

EFFECTS OF ATROPINE AND HALOPERIDOL ON ANP-INDUCED ACTION ON PASSIVE AVOIDANCE BEHAVIOR

Blocker		Avoidance Response (s) Mean ± SEM	Significance
Haloperidol			
Control	(27)	106.6 ± 12.6	
ANP 200 ng	(27)	200.7 ± 16.8	$p<0.002$ vs. contr.
Halop. 2.5 μg/kg	(9)	96.6 ± 9.3	
Halop. 5 μg/kg	(9)	104.9 ± 12.3	
Halop. 10 μg/kg	(18)	106.7 ± 19.9	
Halop. 2.5 μg/kg+ANP	(9)	169.3 ± 10.7	$p<0.01$ vs. contr.
Halop. 5 μg/kg+ANP	(9)	139.3 ± 14.7	
Halop. 10 μg/kg+ANP	(18)	89.6 ± 13.0	$p<0.01$ vs. ANP
Atropine			
Control	(26)	102.0 ± 10.5	
ANP 200 ng	(27)	205.4 ± 12.7	$p<0.001$ vs. contr.
Atropine 0.5 mg/kg	(8)	106.6 ± 9.2	
Atropine 1 mg/kg	(8)	100.8 ± 8.3	
Atropine 2 mg/kg	(18)	114.2 ± 13.0	
Atr. 0.5 mg/kg+ANP	(8)	191.5 ± 18.0	$p<0.001$ vs. contr.
Atr. 1 mg/kg+ANP	(8)	171.5 ± 11.6	$p<0.001$ vs. contr.
Atr. 2 mg/kg+ANP	(19)	99.8 ± 15.2	$p<0.001$ vs. ANP

Numbers in parentheses represent the number of the animals used.

TABLE 2

EFFECTS OF NALOXONE, BICUCULLINE, PHENOXYBENZAMINE, PROPRANOLOL AND METHYSERGIDE ON ANP-INDUCED ACTION ON PASSIVE AVOIDANCE BEHAVIOR

Blocker		Avoidance Response (s) Mean ± SEM	Significance
Naloxone (0.3 μg/kg, IP)			
Control	(18)	84.8 ± 13.5	
ANP 200 ng	(16)	200.6 ± 20.3	$p<0.01$ vs. contr.
Naloxone	(12)	113.8 ± 27.9	
ANP + Nalox.	(12)	195.3 ± 38.1	
Bicuculline (1 mg/kg, SC)			
Control	(18)	105.9 ± 10.9	
ANP 200 ng	(17)	202.5 ± 18.2	$p<0.01$ vs. contr.
Bicuculline	(11)	102.8 ± 31.2	
ANP + Bicucul.	(10)	229.2 ± 35.3	
Phenoxybenzamine (2 mg/kg, IP)			
Control	(6)	92.0 ± 13.5	
ANP 200 ng	(6)	195.8 ± 30.1	$p<0.05$ vs. contr.
Phenox.	(6)	120.0 ± 18.6	
ANP + Phenox.	(6)	163.6 ± 11.2	
Propranolol (10 mg/kg, IP)			
Control	(18)	100.5 ± 21.9	
ANP 200 ng	(19)	202.0 ± 18.9	$p<0.03$ vs. contr.
Propranolol	(19)	131.1 ± 18.4	
ANP + Propran.	(19)	154.4 ± 21.9	
Methysergide (5 mg/kg, IP)			
Control	(24)	101.5 ± 13.5	
ANP 200 ng	(22)	204.3 ± 19.2	$p<0.001$ vs. contr.
Methysergide	(23)	102.1 ± 15.2	
ANP + Methyser.	(24)	167.1 ± 17.3	

Numbers in parentheses represent the number of the animals used.

the peptide immediately after the learning trial.

Rat atrial natriuretic peptide (1–28) was purchased from Bachem (Torrance, CA) and also synthesized by one of us (G. Toth) by solid phase technique, utilizing ^{t}Boc (tert. butyloxycarbonyl) chemistry. The product was compared to authentic sample of rat ANP (American Peptide Co. Inc., Santa Clara, CA). Peptide purity was above 97% (HPLC). The peptide (200 ng) was dissolved in 0.9% saline and administered in a volume of 2 μl to freely moving animals. The control animals received the same amount of 0.9% saline.

The following receptor blockers were used: atropine (atropine sulphate, EGIS, Hungary) 2, 1 and 0.5 mg/kg IP; haloperidol (G. Richter, Hungary) 10, 5 and 2.5 μg/kg IP; propranolol (ICI, Macclesfield, England) 10 mg/kg IP; phenoxybenzamine (phenoxybenzamine HCl, Smith, Kline and French) 2 mg/kg IP; methysergide (Deseryl, Sandoz) 5 mg/kg IP. All receptor blockers listed above were administered 30 min before the peptide treatment. Bicuculline (bicuculline methiodide, Serva) 2 mg/kg SC and naloxone (Narcan, Winthrop) 0.3 mg/kg SC, were administered 20 min before the peptide. The doses of the receptor blockers were selected according to our previous experience, in which the receptor blocker itself did not influence the passive avoidance paradigm but was able to block a number of neuropeptide-induced actions (20).

Statistical analysis was done by Kruskal-Wallis test.

RESULTS

The effects of haloperidol on the ANP-induced increased mean passive avoidance latency are shown in Table 1. ANP in a dose of 200 ng [selected from our previous study (3)] facilitated the avoidance response when it was given immediately after the learning trial. Haloperidol in a dose of 10 μg/kg, given 30 min before the peptide administration, blocked the action of the peptide. While haloperidol in the doses of 2.5 and 5.0 μg/kg showed a tendency to modify the action. Haloperidol alone had no effect on the passive avoidance response.

Atropine in a dose of 2 mg/kg, given IP under similar conditions, also blocked the action of ANP on the passive avoidance learning. Smaller doses (0.5 and 1.0 mg/kg) were ineffective (Table 1).

Naloxone in a dose of 0.3 mg/kg IP did not antagonize the action of ANP on the passive avoidance response (Table 2).

Bicuculline (1 mg/kg), phenoxybenzamine (2.0 mg/kg), propranolol (10 mg/kg), and methysergide (5 mg/kg) were also ineffective, although there was tendency to suppress the response of ANP, the action was not significant statistically (Table 2).

DISCUSSION

In the present experiments, we have demonstrated that in a passive avoidance paradigm ANP is able to increase the mean passive avoidance latency when it is given immediately after the learning trial, confirming our previous findings (3). In addition, it is demonstrated that, when the animals are pretreated with certain receptor blockers in a dose which itself cannot alter the passive avoidance response, these are able to modulate the action of the peptide. Haloperidol (a dopamine receptor blocker), in a dose of 10 μg/kg and atropine (a cholinergic receptor blocker), in a dose of 2 μg/kg, are each able to block the ANP response completely. Smaller doses showed a tendency to modify the action in a dose-dependent manner. Other receptor blockers such as phenoxybenzamine and propranolol, showed a tendency

to decrease the response, but the change was not significant statistically. Other receptor blockers such as methysergide, naloxone and bicuculline were ineffective in the doses used. The same doses of receptor blockers were able to block successfully the action of other peptides in the same experimental paradigm (20).

It has already been reported that ANP is able to bring about a biological action via transmitter mediation. The diuretic and natriuretic action of ANP might be mediated via central dopaminergic activation, since dopamine antagonists can prevent ANP action (11, 13, 21). In frog ANP stimulates α-MSH release from the neurointermediate lobes in vitro. Dopamine, GABA and NPY suppressed the action of ANP (10).

As regards interactions with the cholinergic system, the coexistence of ANP-immunoreactivity cells with choline acetyltransferase-like immunoreactivity has been shown in the lateral dorsal tegmental and pedunculopontine nuclei (19). Whether this morphological finding has any relevance to our observation concerning the participation of the cholinergic system in the ANP-induced action on the passive avoidance response remains to be seen.

REFERENCES

1. Ader, R.; Weijnen, J. A. W. M.; Moleman, P. Retention of a passive avoidance response as a function of the intensity and duration of electric shock. Psychosom. Sci. 26:126–128; 1972.
2. Antunes-Rodriges, J.; McCann, S. M.; Rogers, L. C.; Samson, W. K. Atrial natriuretic factor inhibits dehydration and angiotensin II-induced water intake in the conscious, unrestrained rat. Proc. Natl. Acad. Sci. USA 82:8720–8724; 1985.
3. Bidzseranova, A.; Telegdy, G.; Penke, B. The effects of atrial natriuretic peptide on passive avoidance behavior in rats. Brain Res. Bull. 26:177–180; 1991.
4. De Bold, A. J.; Borenstein, H. B.; Veress, A. I.; Sonnenberg, H. Rapid and potent natriuretic response to intravenous injection of atrial myocardial extract in rats. Life Sci. 28:83–94; 1981.
5. Flynn, T. D.; De Bold, M. L.; De Bold, A. J. The amino acid sequence of an atrial peptide with potent diuretic and natriuretic properties. Biochem. Biophys. Res. Commun. 117:859–865; 1983.
6. Israel, A.; Barbella, Y. Diuretic and natriuretic action of rat atrial natriuretic peptide (6–33) administered intracerebroventricularly in rats. Brain Res. Bull. 17:141–144; 1986.
7. Itoh, H.; Nakao, K.; Katsuura, G.; Morii, N.; Shiono, S.; Sakamoto, M.; Sugawara, A.; Yamada, T.; Saito, Y.; Matsushita, A.; Imura, H. Centrally infused atrial natriuretic polypeptide attenuates exaggerated salt appetite in spontaneously hypertensive rats. Circ. Res. 59:342–347; 1986.
8. Kangawa, K.; Matsuo, H. Purification and complete amino acid sequence of α-human atrial natriuretic polypeptide (α-hANP). Biochem. Biophys. Res. Commun. 118: 131–139; 1984.
9. Kawata, M. K.; Nakao, K.; Morii, N.; Kiso, Y.; Yamashita, H.; Imura, H. Atrial natriuretic polypeptide: Topographical distribution in the rat brain by radioimmunoassay and immunohistochemistry. Neuroscience 16:521–546; 1985.
10. Lamacz, M.; Netchitailo, P.; Tonon, M. C.; Feuilloley, M.; Ling, M.; Pelletier, G.; Vaudry, H. Atrial natriuretic factor (ANF) stimulates the release of α-MSH from frog neurointermediate lobes in vitro. Interaction with dopamine, GABA and neuropeptide Y. Life Sci. 40:1853–1857; 1987.
11. Marin-Grez, M.; Briggs, J. P.; Schubert, G.; Schnermann, J. Dopamine receptor antagonists inhibit the natriuretic response to atrial natriuretic factor (ANF). Life Sci. 36:2171–2176; 1985.
12. Morii, N.; Nakao, K.; Sugawara, A.; Sakamoto, M.; Suda, M.; Shimokura, M.; Kiso, Y.; Kihara, M.; Yamori, Y.; Imura, H. Occurrence of atrial natriuretic polypeptide in brain. Biochem. Biophys. Res. Commun. 127:413–419; 1985.
13. Petterson, A.; Hedner, J.; Hender, T. The diuretic effect of atrial natriuretic peptide (ANP) is dependent on dopaminergic activation. Acta Physiol. Scand. 126: 619–621; 1986.
14. Quiron, R.; Dalpe, H.; De Lean, A.; Gutkowska, J.; Cantin, M.; Genest, J. Atrial natriuretic factor (ANF) binding sites in brain and related structures. Peptides 5:1167–1172; 1984.
15. Samson, W. K. Atrial natriuretic factor inhibits dehydration and hemorrhage-induced vasopressin release. Neuroendocrinology 40: 277–279; 1985.
16. Shimizu, T.; Katsuura, G.; Nakamura, M.; Nakao, K.; Morii, N.; Itoh, Y.; Shiono, S.; Imura, H. Effect of i.c.v. atrial natriuretic polypeptide on blood pressure and urine production in rats. Life Sci. 39:1263–1270; 1986.
17. Sills, M. A.; Nguyen, K. O.; Jacobowitz, D. M. Increases in heart rate and blood pressure produced by microinjections of atrial natriuretic factor into AV3V region of the rat brain. Peptides 6:1037–1042; 1985.
18. Siono, S.; Nakao, K.; Morii, N.; Yamada, T.; Itoh, H.; Sakamoto, M.; Sugawara, A.; Saito, Y.; Katsuura, G.; Imura, H. Nature of atrial natriuretic polypeptide in rat brain. Biochem. Biophys. Res. Commun. 135:728–734; 1986.
19. Standaert, D. G.; Saper, C. B.; Rye, D. B.; Weiner, B. H. Atrial colocalization and atriopeptin-like immunoreactivity with cholineacetyltransferase and substance P-like immunoreactivity in the pedunculopontine and laterodorsal tegmental nuclei in the rat. Brain Res. 382:163–168; 1986.
20. Telegdy, G. Neuropeptides and brain function. Basel: Karger; 1987: 1–332.
21. Webb, R. L.; Dellapuca, R.; Manniello, J.; Robson, R. D.; Zimmerman, M. B.; Chai, R. D. Dopaminergic mediation of the diuretic and natriuretic effects of ANF in the rat. Life Sci. 38:2319–2327; 1986.

European Journal of Pharmacology 211 (1992) 411–414
© 1992 Elsevier Science Publishers B.V. All rights reserved 0014-2999/92/$05.00

2.5.

EJP 52277

Effect of atrial natriuretic peptide on apomorphine-induced stereotyped cage-climbing behavior in mice

Amelia Bidzseranova, Jony Gueron, Gábor Tóth [a], Botond Penke [a] and Gyula Telegdy

Institute of Pathophysiology and [a] Institute of Medical Chemistry, Albert Szent-Györgyi Medical University, Szeged, Hungary

Received 27 September 1991, revised MS received 13 November 1991, accepted 19 November 1991

In previous experiments, it was observed that rat atrial natriuretic peptide-(1–28) (ANP-(1–28)) participated in fear-induced learning and memory processes via dopaminergic and cholinergic mediation. Since cage-climbing behavior is described as a simple test for studying dopaminergic activity in the central nervous system, a systemic study was carried out with ANP-(1–28) in order to confirm or to exclude the possible involvement of dopamine in the ANP-induced action in the brain. The present study demonstrates that ANP-(1–28) facilitated cage-climbing behavior in mice in a dose-dependent manner. When combined with apomorphine, the peptide potentiated the effect of the dopamine agonist. The effect of ANP-(1–28) in combination with apomorphine could be antagonized by a selected dose of haloperidol. These data suggest that ANP might be regarded as a dopamine agonist-modulating agent and that a dopaminergic mechanism is a possible mode of action of ANP in the fear-induced learning studied earlier.

ANP (atrial natriuretic polypeptide); Apomorphine-induced stereotyped cage-climbing behavior; Apomorphine; Haloperidol

1. Introduction

Atrial natriuretic peptide (ANP) is generally considered to be a neuropeptide which can regulate the extracellular fluid volume and electrolyte balance via central and peripheral mechanisms (De Bold et al., 1981; Masotto and Negro-Vilar, 1985; Nakamura et al., 1985; Antunes-Rodrigues et al., 1986; Itoh et al., 1986; Israel et al., 1989; etc.). Nevertheless, its exact role in the CNS is not completely understood. ANP-(1–28) is widespread in various brain regions in mammals (rat, guinea pig, monkey, etc.) (Quirion, 1988; Skofitsch and Jacobowitz, 1988). It affects the release of some hormones, e.g. it decreases the secretion of renin (Obana et al., 1985), vasopressin (Yamada et al., 1986; Iitake et al., 1986), and aldosterone (Atarashi et al., 1984) and increases LH, FSH and CRF secretion in superfused anterior lobe cells of the pituitary (Horváth et al., 1986). However, no information is available about the possible involvement of this peptide in behavioral reactions related to memory function and learning processes. We studied the effects of rANP-(1–28) on fear-motivated learning behavior in rats (Bidzseranova and Telegdy, 1990; Bidzseranova et al., 1991a; in press). In these experiments, we observed that the peptide, when administered into the lateral brain ventricle in doses of 200 or 500 ng per rat, facilitated the consolidation and learning of passive avoidance behavior and delayed the extinction of an active avoidance reflex in rats. When the animals were pretreated with different receptor blockers, these effects of the peptide could be blocked completely by dopaminergic and cholinergic blocking agents (haloperidol and atropine).

Apomorphine-induced stereotyped cage-climbing behavior is an accepted test for studying dopamine (DA) activity in the brain (Wilcox et al., 1980). We used this method in order to confirm our observations that the DA system is activated by the ANP-(1–28) action exerted on learning behavioral tasks. Since the dopaminergic agonist, apomorphine, induces activation of dopamine neurotransmission in the CNS, thereby facilitating apomorphine-induced cage-climbing (Protais et al., 1976), we investigated the possible effects of ANP-(1–28) on cage-climbing behavior alone and in combination with apomorphine and haloperidol.

2. Material and methods

2.1. Experimental animals

Adult male CFLP mice of an inbred strain were used. The animals weighed 25–30 g and were housed

Correspondence to: G. Telegdy, Institute of Pathophysiology, Albert Szent-Györgyi Medical University, Semmelweis u. 1, P.O.B. 531, Szeged 6701, Hungary. Tel./fax 36.62.10 651.

10 per cage. They were kept under a standard 12 h illumination schedule (lights on at 6:00 a.m.). Commercial food and tap water were available ad libitum.

2.2. *Surgery*

The animals were anesthetized with pentobarbital-Na (Nembutal, 35 mg/kg) and a guiding stainless cannula was placed into the lateral cerebroventricle and fixed to the skull with dental cement (Vécsei et al., 1985). The mice were used after a recovery period of at least 5 days. Correct positioning of the cannula was checked by injection of methylene blue through it and dissection of the brain after the experiments had been completed.

2.3. *Cage-climbing behavior*

The apomorphine-induced cage-climbing behavior was measured according to Protais et al. (1976). The mice were given apomorphine hydrochloride (0.5 or 1.0 mg/kg s.c.) and were then placed individually into a wire-meshed cage. After a habituation period of 5 min, cage-climbing was observed for the next 10 min. The behavior was scored by means of the time (in s) that the animal spent with all four paws holding on to the walls of the cage. Experiments were carried out daily between 8:00 a.m. and noon. The observations were 'double blind' and done by two independent persons.

2.4. *Drugs*

Rat ANP-(1–28) was purchased from Bachem (Calif.) and was synthesized by one of us (G. Tóth). It was dissolved in 0.9% saline and administered i.c.v. in a volume of 2 μl in three doses (0.2, 0.5 or 1 μg per mouse) 20 min prior to the test. Apomorphine hydrochloride (Sigma) was dissolved in saline and administered s.c. in two doses (1 or 0.5 mg/kg) 5 min prior to the test. Haloperidol (G. Richter, Budapest) was administered i.p. in two doses (10 or 20 μg/kg) 30 min prior to the peptide (table 1).

2.5. *Statistical analysis of the data*

One-way analysis of variance (ANOVA) was used to analyze the differences between groups. Comparison with the control group was made with Dunnett's test; comparison within the groups was made with Tukey's test. The level of significance was accepted to be at $P < 0.05$.

3. Results

The doses of the peptide, the DA agonist and the DA antagonist were selected on the basis of our previous findings (Bidzseranova and Telegdy, 1990; Bidzseranova et al., 1991a,b, in press; Kovacs et al., 1981). The results shown in table 2 were obtained.

TABLE 1

Scheme of treatments for measuring apomorphine-induced stereotyped cage-climbing behavior in mice.

Groups	Treatment			
	0 min	30 min	45 min	50-60
(1) Control	Saline	Saline	Saline	Testing
(2) Apomorphine (A)	Saline	Saline	0.5 mg/kg s.c.	Testing
(3) A	Saline	Saline	1 mg/kg s.c.	Testing
(4) Haloperidol (H)	10 μg/kg i.p.	Saline	Saline	Testing
(5) H	20 μg/kg i.p.	Saline	Saline	Testing
(6) H + A	10 μg/kg i.p. (H)	Saline	1 mg/kg s.c. (A)	Testing
(7) H + A	20 μg/kg i.p. (H)	Saline	1 mg/kg s.c. (A)	Testing
(8) ANP	Saline	200 ng i.c.v. (ANP)	Saline	Testing
(9) ANP	Saline	500 ng i.c.v. (ANP)	Saline	Testing
(10) ANP	Saline	1000 ng i.c.v. (ANP)	Saline	Testing
(11) ANP + A	Saline	200 ng i.c.v. (ANP)	1 mg/kg s.c. (A)	Testing
(12) ANP + A	Saline	500 ng i.c.v. (ANP)	1 mg/kg s.c. (A)	Testing
(13) ANP + A	Saline	500 ng i.c.v. (ANP)	0.5 mg/kg s.c. (A)	Testing
(14) ANP + A	Saline	1000 ng i.c.v. (ANP)	0.5 mg/kg s.c. (A)	Testing
(15) H + ANP	10 μg/kg i.p. (H)	1000 ng i.c.v. (ANP)	Saline	Testing
(16) H + ANP	20 μg/kg i.p. (H)	1000 ng i.c.v. (ANP)	Saline	Testing
(17) H + ANP	10 μg/kg i.p. (H)	500 ng i.c.v. (ANP)	Saline	Testing
(18) H + ANP	20 μg/kg i.p. (H)	500 ng i.c.v. (ANP)	Saline	Testing
(19) H + ANP + A	10 μg/kg i.p. (H)	500 ng i.c.v. (ANP)	1 mg/kg s.c. (A)	Testing
(20) H + ANP + A	20 μg/kg i.p. (H)	500 ng i.c.v. (ANP)	1 mg/kg s.c. (A)	Testing

TABLE 2

Effect of ANP on apomorphine-induced stereotyped cage-climbing behavior in normal and haloperidol pretreated mice.

Groups [a]	N of animals	Score (s)
1) Saline	49	204.1 ± 27.2 [b]
2) Apomorphine (A) 0.5 mg/kg	20	247.6 ± 59.1
3) A 1 mg/kg	14	536.1 ± 23.7 [c]
4) Haloperidol (H) 10 μg/kg	31	197.1 ± 36.2
5) H 20 μg/kg	32	177.7 ± 38.0
6) H 10 μg/kg + A 1 mg/kg	17	312.9 ± 63.8 [d]
7) H 20 μg/kg + A 1 mg/kg	22	180.5 ± 48.6 [d]
8) ANP 200 ng	15	207.3 ± 56.9
9) ANP 500 ng	13	238.9 ± 61.5
10) ANP 1 μg	30	328.6 ± 36.5 [c]
11) ANP 200 ng + A 1 mg/kg	15	515.2 ± 31.0 [c]
12) ANP 500 ng + A 1 mg/kg	12	531.3 ± 25.9 [c]
13) ANP 500 ng + A 0.5 mg/kg	20	384.9 ± 54.7 [c,d]
14) ANP 1 μg + A 0.5 mg/kg	46	427.6 ± 33.2 [c,d]
15) H 10 μg/kg + ANP 500 ng	14	214.6 ± 37.3
16) H 20 μg/kg + ANP 500 ng	14	184.7 ± 50.7
17) H 10 μg/kg + ANP 1 μg	14	330.4 ± 72.6
18) H 20 μg/kg + ANP 1 μg	16	247.8 ± 46.9
19) H 10 μg/kg + ANP 500 ng + A 1 mg/kg	12	536.1 ± 33.2 [c]
20) H 20 μg/kg + ANP 500 ng + A 1 mg/kg	20	321.4 ± 49.3 [d]

[a] For exact scheme and doses of treatment see table 1. [b] Mean ± S.E. [c] $P < 0.05$ ANOVA (Dunnett's test). [d] $P < 0.05$ ANOVA (Tukey's test).

In order to check the method, two doses of apomorphine were used to measure cage-climbing behavior: 0.5 or 1.0 mg/kg s.c. The dose of 1.0 mg/kg apomorphine, selected on the basis of our previous observations (Kovács et al., 1981), significantly increased the time spent by the animals on the wall of the cage (ANOVA – $F(5,1) = 7.6$; $P < 0.05$ vs. control, Dunnett's test), while the dose of 0.5 mg/kg increased this time only slightly, without reaching statistical significance.

Haloperidol alone in two doses (10 or 20 μg/kg i.p.) had no significant effect, but was able to decrease or completely block the effect of 1 mg/kg apomorphine (ANOVA – $F(5,1) = 7.6$, $P < 0.05$ vs. 1 mg/kg apomorphine, Tukey test). ANP-(1–28) induced a dose-dependent increase in cage-climbing behavior. The lower dose (1.0 μg) exerted a statistically significant effect (ANOVA – $F(3,1) = 9.3$, $P < 0.05$ vs. control, Dunnett's test).

ANP-(1–28) in combination with apomorphine potentiated the otherwise ineffective 500 ng ANP or 0.5 mg/kg apomorphine alone (ANOVA – $F(7,2) = 4.8$, $P < 0.05$ vs. 500 ng ANP and vs. 0.5 mg/kg apomorphine, Tukey's test).

Haloperidol at the lower dose (10 μg/kg) was unable to block the effect of ANP (1 μg), while the dose 20 μg/kg showed a tendency to block this action. The dose of 10 μg/kg haloperidol was also unable to modify the potentiating effect of ANP (500 ng) when combined with apomorphine (1 mg/kg), but the dose 20 μg/kg haloperidol significantly diminished the combined action of ANP and apomorphine (ANOVA – $F(3,6) = 5.8$, $P < 0.05$ vs. 500 ng ANP + 1 mg/kg AM, Tukey's test).

4. Discussion

Apomorphine-induced stereotyped cage-climbing behavior is an accepted test for studying DA activity in the brain. We used this method to confirm our observation that the dopaminergic system is activated during ANP action exerted on passive and active avoidance behavior.

The present study demonstrated that ANP facilitated apomorphine-induced stereotyped cage-climbing behavior in mice in a dose-dependent manner. Since the dose of 1 mg/kg apomorphine, which elicits climbing, is considered a relatively high dose and since it is believed that, at such a dose, apomorphine stimulates postsynaptic DA receptors, ANP might modulate the effect of the agonist either by making postsynaptic DA receptors more sensitive to apomorphine or by increasing the DA efflux from the presynaptic stores, and as a result the released DA potentiates the effect of apomorphine.

Data on ANP interactions with DA are controversial. Nakao et al. (1986) reported decreased levels of DA and its metabolite in septum and hypothalamus, after central administration of ANP-(1–28) in doses of 2 or 5 μg. On the other hand, Israel et al. (1989) reported that the DA blockers, haloperidol and domperidone, prevent the diuretic and natriuretic response

) the centrally administered peptide. Marin-Grez et l. (1985) also reported a complete blocking effect of aloperidol and chlorpromazine on peripherally administered semi-purified atrial extract or synthetic α-ANP-(1-28).

We reported earlier a blocking effect of haloperidol the effects of rANP-(1–28) on fear-motivated learng behavior in rats (Bidzseranova and Telegdy, 1990; dzseranova et al., 1991a, in press). This finding, gether with our results from the present study, led us the conclusion that ANP could be regarded as a DA onist-modulating agent. The interaction with DA urotransmission seems to occur at a receptor level. rther studies are needed, however, to find whether is is a pre-/or postsynaptic interaction.

ferences

tan-s Rodriguez, L., S.V. McCann and W.K. Samson, 1986, Central administration of atrial natriuretic factor inhibits saline preference in rat, Endocrinology 118, 1726.

nash, K., P.J. Marlow, R. Franco-Suenz, R. Snaider, J. Rapp, 1981, Inhibition of aldosterone production by an atrial extract, Science 224, 992.

zseranova, A. and G. Telegdy, 1990, The effects of receptor blockers on atrial natriuretic peptide-induced action on passive avoidance learning in rats, Acta Physiol. Hung. 75 (Suppl.), 35.

zseranova, A., G. Telegdy and B. Penke, 1991a, The effects of atrial natriuretic peptide on passive avoidance behavior in rats, Brain Res. Bull. 26, 177.

zseranova, A., B. Penke, G. Tóth and G. Telegdy, 1991b, The effects of atrial natriuretic peptide on electroconvulsive shock induced amnesia in rats, Transmitter-mediated action, Neuropeptides 19, 107.

zseranova, A., J. Gueron, B. Penke and G. Telegdy, The effects of atrial natriuretic peptide on active avoidance behavioral in rats. The role of the transmitter systems, Pharmacol. Biochem. Behav. (in press).

Bold, A.J., H.B. Borenstein, A.T. Veress and H.A. Sonnenberg, 1981, Rapid and potent natriuretic response to intravenous injection of atrial myocardial extract in rats, Life Sci. 28, 83.

vath, T.L., T. Ertl and A.V. Schally, 1986, Effects of atrial natriuretic peptide on gonadotropin release in superfused rat pituitary cells, Proc. Natl. Acad. Sci. U.S.A. 83, 3444.

Iitake, K., I. Sharre, J. Crofton, P. Brooks, Y. Ouchi and E. Blaine, 1986, Central atrial natriuretic factor reduced vasopressin secretion in the rat, Endocrinology 119 (1), 438.

Israel, A., M. Torres, J. Barbella, 1989, Evidence for a dopaminergic mechanism for the diuretic and natriuretic action of centrally administered Atrial Natriuretic Factor, Cell. Mol. Neurobiol. 9 (3), 369.

Itoh, H., K. Nakao, G. Katsuura, M. Morii, S. Shiono, M. Sakamoto, A. Sugawara, T. Yamada, Y. Saito, A. Matsushita and H. Imura, 1986, Centrally infused atrial natriuretic polypeptide attenuates exaggerated salt appetite in spontaneously hypertensive rats, Circ. Res. 59, 342.

Kovács, G., G. Szabo, B. Penke and G. Telegdy, 1980, Effects of cholecystokinin octapeptide on striatal dopamine metabolism and on apomorphine-induced stereotyped cage-climbing in mice, Eur. J. Pharmacol. 69, 313.

Marine-Grez, M., J.P. Briggs, G. Schubert and Schnerman, 1985, Dopamine receptor antagonists inhibit the natriuretic response to atrial natriuretic factor (ANF), Life Sci. 36, 2171.

Masotto, C. and A. Negro-Vilar, 1985, Inhibition of spontaneous or angiotensin-II-stimulated water intake by atrial natriuretic factor, Brain Res. Bull. 15, 523.

Nakamura, M., G. Katsuura, K. Nakao and H. Imura, 1985, Antidipsogenic action of α-human atrial natriuretic polypeptide administered intracerebroventricularly in rats, Neurosci. Lett. 58, 1.

Obana, K., M. Naruse, T. Inagami, A.B. Brown, R. Naruse, F. Kurimoto, H. Sakurai, H. Demura and K. Shizume, 1985, Atrial natriuretic factor inhibits vasopressin secretion from rat posterior pituitary, Biochem. Biophys. Res. Commun. 138, 1088.

Protais, P., J. Constentin and J.C. Schwartz, 1976, Climbing behavior induced by apomorphine in mice: a simple test for the study of dopamine receptors in striatum, Psychopharmacology 50, 1.

Quirion, R., 1988, Atrial natriuretic factors and the brain: an update, Trends Pharmacol. Sci. 11 (2), 58.

Shohtsch, G. and D. Jacobowitz, 1988, Atrial natriuretic peptide in the central nervous system of the rat, Cell. Mol. Neurobiol. 8 (4), 339.

Vécsei, L., G. Telegdy, I. Bollók and A.V. Schally, 1985, The role of central dopaminergic systems in the behavioral effects of H-Phe-Ile-Tyr-His-Ser-Tyr-Lys-OH, Neuropeptides 6, 183.

Wilcox, R., E.E. R.V. Smith, J.A. Anderson and W. Riffee, 1980, Apomorphine-induced stereotyping cage-climbing in mice as a model for studying changes in dopamine receptor sensitivity, Pharmacol. Biochem. Behav. 12, 29.

Yamada, T., K. Nacao, N. Morii, H. Itoh, S. Shiono, M. Sakamoto, A. Sugawara, Y. Saito, H. Ohno, A. Kanai, G. Katsuura, M. Eigio, A. Matsushita and H. Imura, 1986, Central effect of atrial natriuretic polypeptide on Angiotensin II-stimulated vasopressin secretion in conscious rats, Eur. J. Pharmacol. 125, 453.

NEUROPEPTIDES

Neuropeptides (1992) 23, 61–65

Structure-activity Studies on the Effects of Atrial Natriuretic Peptide, Brain Natriuretic Peptide and Their Analogs on Fear-motivated Learning Behavior in Rats

A. BIDZSERANOVA, J. GUERON, G. TÓTH*, J. VARGAt and G. TELEGDY

*Institute of Pathophysiology, *Institute of Medical Chemistry, Albert Szent-Györgyi Medical University, Szeged, POB 531, Hungary, †American Peptide Company, Santa Clara, CA, USA (Reprint requests to GT)*

Abstract — Our previous studies have demonstrated that rat atrial natriuretic peptide (rANP 1-28) and porcine brain natriuretic peptide (pBNP 1-32) administered into the lateral brain facilitate the consolidation of a passive avoidance response and delay the extinction of an active avoidance response in fear-motivated learning in rats.

To study the structure-activity relationships in the same learning processes, the effects of several fragments related to ANP and BNP were investigated following their intracerebroventricular administration to rats. The following peptides were studied: rANP 1-28, rANP 5-28, rANP 5-27, rANP 7-23 (ring), rANP 17-23, hANP 10-28, hANP 15-28, hANP 20-28, hANP 1-28, pBNP 1-32 and pBNP 7-32. The peptides were used in equimolar concentration. Two of the peptides studied, ANP 20-28 and ANP 17-23, were ineffective on the extinction of active avoidance behavior and on the consolidation of passive avoidance learning. They exhibited similar actions.

The results showed that small fragments of ANP and BNP can carry the biological activity of ANP and BNP on the central nervous system (CNS). It is likely that the biological active center for ANP lies between amino acids 15 and 23 and it is suspected that the ring structure is not absolutely important for the CNS activity.

Introduction

The family of natriuretic peptides is known to consist of three members: atrial natriuretic peptide (ANP), first isolated from atrial cardiocytes (5) and later discovered in the brain (8–10, 14, 17, 18), brain natriuretic peptide (BNP) and the C type natriuretic peptide, both recently isolated from the porcine brain (12, 13). Generally, they are considered to be intimately involved in the maintenance and regulation of fluid volume homeostasis.

In earlier experiments we demonstrated that intracerebroventricularly (i.c.v.) administered ANP and BNP facilitated the consolidation of a passive avoidance response and delayed the extinction of an

Date received 27 February 1992
Date accepted 18 May 1992

active avoidance response in rats (2–4), i.e. both peptides were effective in the fear-motivated learning behavior of rats.

The present study was undertaken to determine structure-activity relationships in the effects of ANP, BNP and their fragments on fear-motivated learning behavior following i.c.v. administration. To enable a comparison of the effects, the peptides were used in equimolar concentrations.

Materials and Methods

Animals

The experiments were performed on male CFY rats (LATI Gödöllő, H) weighing 150–250 g. The animals were used 6 per cage at room temperature (20–21°C). They were kept in artificial 12-hour light (started at 6 a.m.), 12-hour dark periods. Commercial food and tap water were given ad libitum. All observations were carried out between 8 a.m. and 4 p.m.

Peptides

Rat ANP (rANP 1-28) was purchased from Bachem (CA, USA) and also synthesized by G. Tóth. All the ANP fragments and the human ANP-1-28 were also synthesized by a solid-phase technique, utilizing Boc (fert.-Butyloxycarbonyl) chemistry. The following peptides were used: rANP 1-28, rANP 5-28, rANP 5-27, rANP 7-23 (ring), rANP 17-23, hANP 10-28, hANP 15-28, hANP 20-28, hANP 1-28. Porcine BNPs (pBNP 1-32 and pBNP 7-32) were kindly donated by the American Peptide Company (Santa Clara, CA, USA) via Janos Varga.

The peptides were diluted with 0.9% saline to equimolar concentrations before administration in a volume of 2 µl into the lateral brain ventricle.

Surgery

The rats were anesthetized with pentobarbital-Na (Nembutal, 35 mg/kg, i.p.) and a cannula was placed into the lateral cerebroventricle and fixed to the skull with dental cement. The stereotaxic coordinates of Fifkova and Marsala (6) were used (AP: + 1.0, L: 1.5, V: 3.0). The operated animals were taken for the experiment after a recovery period of 5 d. The correct positioning of the cannula was checked by injecting methylene blue through the cannula and subsequent dissection of the brain. Animals with incorrect placement of the cannula were discarded and excluded from the statistical evaluations.

Behavioral methods

Fear-motivated learning behavior was studied, using the following tests:

1. *Passive avoidance test*—one-trial learning step-through passive avoidance behavior was measured according to Ader et al (1). Briefly, rats were placed on a platform and allowed to enter a dark compartment. Since rats prefer dark to light, they normally entered within 15 s. On the following day two additional trials were given. After the second trial, unavoidable electric footshocks (0.75 mA, 2 s) were delivered through the grid floor during the learning trial. Having entered the box, the animals could not escape the footshock. After this single learning trial, the rats were immediately removed from the apparatus and were treated with peptide. Consolidation of passive avoidance behavior was tested 24 h later: every rat was placed on the platform and the latency to enter the dark compartment was measured up to a maximum of 300 s.
2. *Active avoidance test*—this was performed according to the method described in detail by Telegdy et al (15, 16). Briefly, the experimental apparatus consisted of a 'bench-jumping' conditioning box. The conditional stimulus was the light of a 45 W bulb. The unconditional stimulus was an electric shock of 1 mA AC, delivered through the grid floor. Daily experimental sessions were performed, with a duration of 10 min each. Every session consisted of 10 trials with a mean intertrial interval of 60 s (range 50–70 s). The conditioning stimulus was presented for a maximum of 15 s. If the rat jumped onto the bench during the first 10 s (conditioned avoidance response (CAR)), the conditioning stimulus was terminated. Non-occurrence of the CAR was associated with termination of the unconditional stimulus in the last 5 s of the conditioning stimulus period. The learning criterion was 80% or more CARs measured on the third day of training. After having reached the criterion of learning, the animals were treated with peptide i.c.v.

and their effects in the extinction of the active avoidance behavior were studied after 3, 6 and 24 h. During the extinction trials, the conditional stimulus was not followed by electric shock. The results are expressed as the sum of the 3-day measurement.

Statistical analysis

The non-parametric ranking tests of Kruskal-Wallis (KW) (for the passive avoidance test) and Mann-Whitney (MW) (for the active avoidance) were used for the analysis of the data. A probability level of 0.05 or less was accepted as the level of significance.

Results

The structures of the different peptides are shown in Figure 1.

For the first series of experiments on the activities of the compounds in the passive avoidance consolidation of learning, a previously selected dose of 0.065 nmol, corresponding to 200 ng of ANP per rat, was used (2–4). Each analog was administered in equimolar concentration, corresponding to this dose. It can be seen from Table, that only two analogs (hANP 20-28 and rANP 17-23) did not facilitate the consolidation of the passive avoidance response, i.e. they were ineffective. Shortening ANP molecule of the ANP from the N-end resulted in a gradual decline in the activity of the compounds. The ring structure (rANP 7-23), however, still preserved high activity (94%). Shortening of the molecule from the same end, within the ring, further lessened the activity, and when only 7 amino acids remained (rANP 17-23) no effect was observed, i.e. the response was the same as that in the control group.

Similar results were obtained in the second series of experiments, concerning the effect of the peptides and their analogs on the extinction of the active avoidance learning behavior. Here the dose was selected to be 0.16 nmol.

Figure 2 demonstrates the overall activity of the experimental animals in the three test situations (3, 6 and 24 h following administration of the peptides).

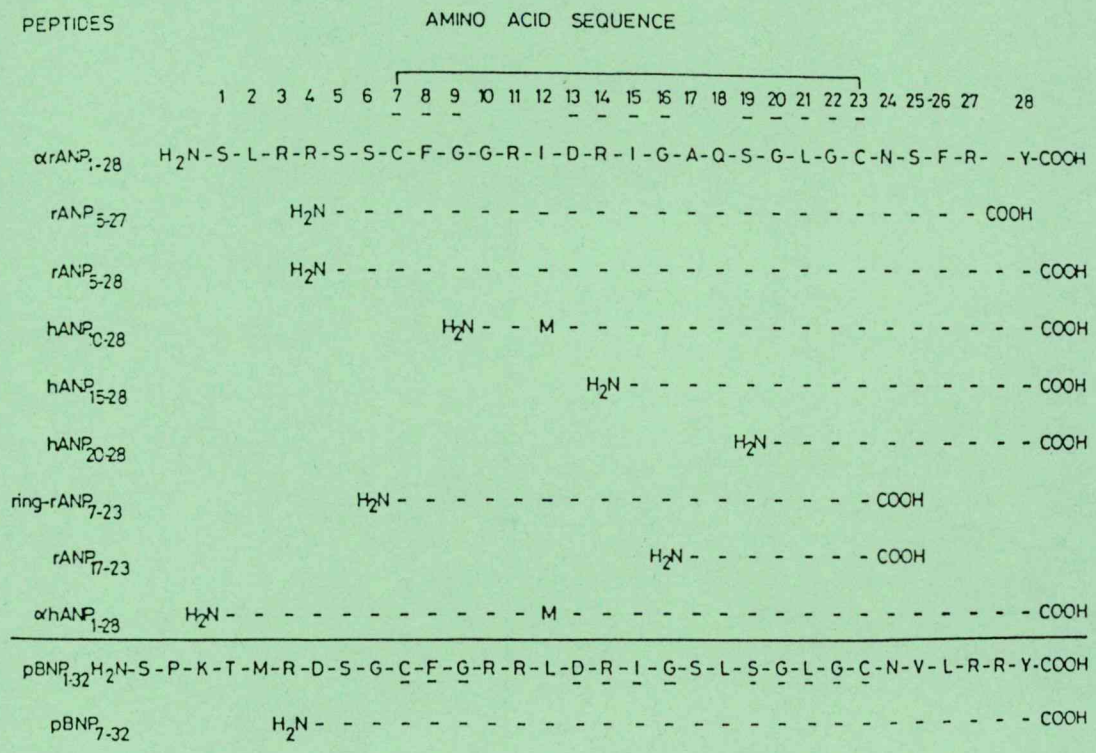

Fig. 1 The structure of ANP and related peptides. The underlined amino acids represent the identical residue of ANP and BNP.

Table Effects of α-rANP 1-28 and related compounds on the consolidation of passive avoidance learning.

Peptide	*Avoidance latency Mean ± SEM*	*Activity %*	*Significance*
α-rANP 1-28 (30)	182.4 ± 18.1	100	*
rANP 1-27 (11)	168.2 ± 11.0	92	*
rANP 5-28 (12)	188.2 ± 11.5	103	*
hANP 10-28 (8)	175.1 ± 4.4	96	*
hANP 15-28 (8)	158.9 ± 9.4	87	*
hANP 20-28 (12)	113.2 ± 9.1	62	NS
rANP 7-23 (10)	172.2 ± 11.0	94	*
rANP 17-23 (10)	120.8 ± 9.0	66	NS
α-hANP 1-28 (12)	226.2 ± 18.0	124	*
pBNP 1-32 (14)	204.6 ± 9.5	112	*
pBNP 7-32 (8)	207.7 ± 5.0	114	*
Control (19)	101.7 ± 7.5		

( ) Number of animals used. * vs Control p 0.05

The means were summarized and compared by the Mann-Whitney test. The same two fragments as previously were ineffective in delaying the extinction of the avoidance response ($p < 0.05$, MW).

Discussion

In 1986 Itoh et al (7), using reverse-phase–high performance liquid chromatography (RP-HPLC) coupled with radioimmunoassay (RIA), reported that the predominant forms of ANP in the rat brain were α-rANP 4-28 and α-rANP 5-28. They also suggested that the molecular form of ANP as a brain peptide differs from the circulating (hormonal) peptide form. These data promted us to investigate the actions of ANP, BNP and a number of synthetic fragments related to them for their behavioral effects on fear-motivated learning. What we have learned from these observations is as follows:

rANP 1-28, hANP 1-28 and BNP F-32 had similar equipotential actions in the two tests. This indicates that presumably the same type of response is due to the identical amino acids in the same positions i.e. positions 15, 16, 19, 20, 21, 22 and 23. Since hANP 10-28 and hANP 15-28 were also active, despite the fact that the ring structure is not present, the ring is probably not an essential structural element for the biological activity measured.

Since rANP 17-23 was not effective, but rANP 15-28 was, while ANP 7-23 with the ring structure retained full biological activity, the effective biological active center of the peptide in fear-motivated behavior might be between amino acids 15 and 23.

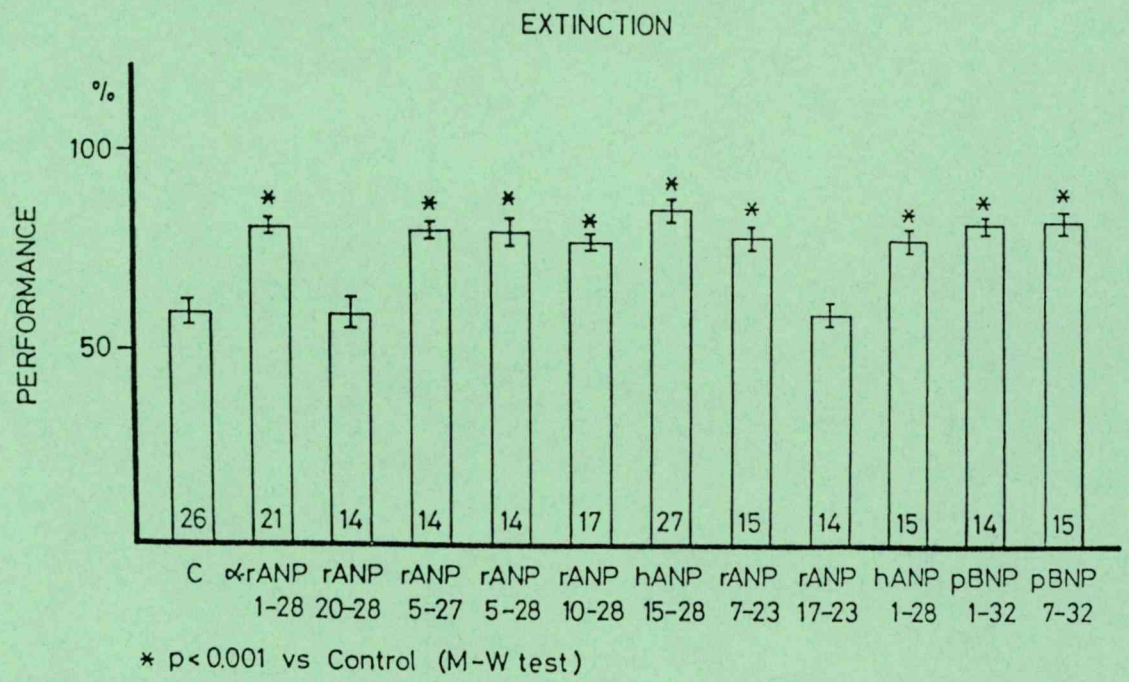

Fig. 2 The effects of ANP 1-28 and related peptides on the extinction of active avoidance behavior.

References

1. Ader, R., Weijnen, J. A. W. M. and Moleman, P. (1972). Retention of a passive avoidance response as a function of the intensity and duration of electric shock. Psychosom. Sci. 26: 126–128.
2. Bidzseranova, A., Telegdy, G. and Penke, B. (1991). The effects of atrial natriuretic peptide on passive avoidance behavior in rats. Brain Res. Bull. 26: 177–180.
3. Bidzseranova, A., Telegdy, G. and Tóth, G. (1991). The effects of receptor blockers on atrial natriuretic peptide-induced action on passive avoidance behavior in rats. Pharm. Bioch. Behav. 40 (2) (in press).
4. Bidzseranova, A., Gueron, J., Penke, B. and Telegdy, G. (1991). The effects of atrial natriuretic peptide on active avoidance behavior in rats. The role of the transmitter systems. Pharmacol. Bioch. Behav. 40 (1): 61–64.
5. DeBold A. J., Borenstein, H. B., Veress A. T. and Sonnenberg, H. (1981). A rapid and potent natriuretic response to intravenous injection of atrial myocardial extract in rats. Life Sci. 28: 83–94.
6. Fifkova, E. and Marsala, J. (1967). Stereotaxic atlases for the cat, rabbit and rat. In: Electrophysiological Methods in Biological Research (Bures, J., Petrán, M., Zacher, J., Eds.). Publishing House of the Czechoslovak Academy of Sciences, Prague. 653–731.
7. Itoh, H., Nakao, K., Katsura, G. et al (1986). Atrial natriuretic polypeptides: Structure-activity relationship in the central action—a comparison of their antidipsogenic action. Neurosc. Lett. 74: 102–106.
8. Kawata, M. K., Nakao, K., Morii, N., Kiso, J., Jamashita, H., Imura, H. and Sano, J. (1985). Atrial natriuretic polypeptide: Topographical distribution in the rat brain by radioimmunoassay and immunohistochemistry. Neuroscience 16: 521–546.
9. Morii, N., Nakao, K., Sugawara, A., Sakamoto, M., Suda, M., Shimokura, M., Kiso, J., Jamori, J. and Imura, H. (1985). Occurrence of atrial natriuretic polypeptide in brain. Biochem. Biophys. Res. Commun. 127: 413–419.
10. Quirion, R., Dalpe, H., DeLean, A., Gutkowska, J., Cantin, M. and Genest, J. (1984). Atrial natriuretic factor (ANF) binding sites in brain and related structures. Peptides 5: 1167–1172.
11. Quirion, R. (1988). Atrial natriuretic factors and the brain: an update. TINS, 11. 2: 58–62.
12. Sudoh, T., Kangawa, K., Minamino, N. and Matsuo, H. (1988). A new natriuretic peptide in porcine brain. Nature 332: 78–81.
13. Sudoh, T., Minamino, N., Kangawa, K. and Matsuo, H. (1990). C-type natriuretic peptide (CNP): a new member of natriuretic peptide family identified in porcine brain. Biochem. Biophys. Res. Commun. 168: 863–870.
14. Tanaka, I., Misono, K. S. and Inagami, T. (1984). Atrial natriuretic factor in rat hypothalamus, atria and plasma: Determination of specific radioimmunoassay. Biochem. Biophys. Res. Commun. 124: 663–668.
15. Telegdy, G., Hadnagy, J. and Lissák, K. (1968). The effect of gonads on conditioned avoidance behavior of rats. Acta Physiol. Acad. Sci. Hung. 37: 439–444.
16. Telegdy, G. (1987). In: Neuropeptides and Brain Function. Karger, Basel. pp. 1–332.
17. Skofitsch, G. and Jacobowitz, D. (1985). Atrial natriuretic peptide in the central nervous system of the rat. Cell. Moll. Neurobiol. 4: 339–391.
18. Zamir, N., Skofitsch, G., Eskay, R. L. and Jacobowitz, D. M. (1986). Distribution of immunoreactive atrial natriuretic peptides in the central nervous system of the rat. Brain Res. 365: 105–111.

Brain Research Bulletin, Vol. 28, pp. 767–768, 1992
Printed in the USA.

0361-9230/92 $5.00 + .00

Effect of Atrial Natriuretic Peptide on DOPA Potentiation in Mice

AMELIA BIDZSERANOVA,* JONY GUERON,* GÁBOR TÓTH,† BOTOND PENKE† AND GYULA TELEGDY*[1]

**Institute of Pathophysiology and †Institute of Medical Chemistry, Albert Szent-Györgyi Medical University, Szeged, Hungary*

Received 6 May 1991

BIDZSERANOVA, A., J. GUERON, G. TÓTH, B. PENKE AND G. TELEGDY. *Effect of atrial natriuretic peptide on DOPA potentiation in mice.* BRAIN RES BULL 28(5) 767–768, 1992.—The effect of rat atrial natriuretic peptide (ANP_{1-28}) on the pargyline–DOPA potentiation test was studied following its administration into the lateral brain ventricle in mice. Thirty minutes after pargyline pretreatment, three doses of ANP (200, 500, or 1,000 ng/mouse) were administered simultaneously with DOPA and animals were then observed for 2 h. ANP in doses of 500 and 1,000 ng markedly enhanced the effect of DOPA. The maximum intensity of the effect was registered 30–45 min following administration of the peptide. The data suggest that ANP might be regarded as a dopaminergic-modulating agent in the CNS.

Atrial natriuretic peptide Pargyline DOPA potentiation

IN previous experiments, we demonstrated that atrial natriuretic peptide (ANP) participates in fear-induced learning processes via dopaminergic and cholinergic mediation (1,4,5). We confirmed the supposition that ANP might be considered a modulatory peptide of dopamine (DA) mediation by describing its effect on apomorphine-induced stereotyped cage-climbing behavior in rats (2). The present work provides more experimental data in this respect. The effect of ANP on pargyline–DOPA potentiation in mice was studied following its administration into the lateral brain ventricle. The pargyline–DOPA mouse test of Plotnikoff et al. (9), which has been used to screen new substances for antidepressant action, was explored to demonstrate the effect of ANP on DA mediation.

METHOD

Adult CFLP mice of an inbred strain were used. Animals weighed 25–30 g and were housed 10 per cage. They had access to commercial food and tapwater ad lib and were kept on a standard 12 L:12 D cycle (lights on at 6:00 a.m.). Experiments were carried out daily between 8:00 a.m. and noon.

Mice were anesthetized with pentobarbital-Na (nembutal, 35 mg/kg, IP) and a cannula was placed into the right lateral cerebroventricle and fixed to the skull with dental cement. Animals were used 5 days following operation. The correct positioning of the cannula was checked individually by injection of methylene blue after experiments had been completed. Only those with right positioning of the cannula were included in the statistical evaluation.

The DOPA response potentiation test in mice, as developed and described by Plotnikoff et al. (10), was used with modification to have a quantitative evaluation for statistical analysis. The method consists of pretreating animals with pargyline HCl (40 mg/kg, IP) (6,10) 30 min before DOPA and then observing them for 1–2 h. Observation was done in a double-blind manner and the behavior was scored every 15 min. Potentiation of the DOPA-induced response was scored by means of the changes in the expression of five different indexes—piloerection, salivation, jumping, squeaking, and aggressive fightings—using a four-degree scoring scale for each of them (0 stands for no DOPA effect, 1 for slight DOPA effect, 2 for moderate one, and 3 for marked

TABLE 1

SCHEME OF TREATMENTS FOR MEASURING DOPA POTENTIATION IN MICE

Groups	Treatment (min)		
	0	30	30–150
Control	Paragyline*	DOPA† + saline	Testing
200 ng ANP	Paragyline	DOPA + ANP	Testing
500 ng ANP	Paragyline	DOPA + ANP	Testing
1,000 ng ANP	Paragyline	DOPA + ANP	Testing

* Paragyline 40 mg/kg IP.
† L-DOPA 100 mg/kg IP.

[1] Requests for reprints should be addressed to Gyula Telegdy, Institute of Pathophysiology, A. Szent-Györgyi Medical University, Semmelweis u. 1, POB 531, Szeged 6701, Hungary.

TABLE 2

EFFECT OF ANP ON DOPA POTENTIATION IN MICE

$rANP_{1-28}$ (ng/mouse, ICV)	n	Test Periods (min)					
		45	60	75	90	120	150
Control	24	0.63 ± 0.16	0.79 ± 0.16	1.46 ± 0.23	1.41 ± 0.23	0.63 ± 0.13	0.00 ± 0.00
200	16	0.75 ± 0.18	1.00 ± 0.16	1.69 ± 0.24	1.43 ± 0.20	0.94 ± 0.14	0.00 ± 0.00
500	16	0.94 ± 0.17*	1.88 ± 0.20*	2.75 ± 0.11*	2.25 ± 0.17*	1.19 ± 0.16*	0.38 ± 0.18*
1000	16	1.70 ± 0.15*	2.75 ± 0.11*	2.81 ± 0.10*	2.13 ± 0.18*	1.75 ± 0.17*	0.75 ± 0.14*

Data are means ± SEM of individual scores.
* $p < 0.05$ vs. control (ANOVA, Dunnett).

one). The response of animals from the control group (treated with pargyline, DOPA, and saline), consisting of piloerection and slight salivation, was scored as a behavioral rating of 1. Moderate and marked increase in the above-mentioned activities were scored with 2 and 3, respectively. When there was no DOPA effect observed or it disappeared, the score was 0. For convenience in the statistical evaluation, the individual data are given as mean of all five index scores.

Rat ANP_{1-28} was purchased from Bachem (Bubendorf, Switzerland) and also synthesized by two of us (G.T. and B.P.). The peptide was dissolved in 0.9% saline and administered in doses of 200, 500, or 1,000 ng per animal in a volume of 2 μl ICV to freely moving animals simultaneously with L-DOPA (EGYS, Budapest) (100 mg/kg, IP). The control group received the same amount of 2 μl ICV saline and L-DOPA (10).

Statistical analysis of the results was performed by analysis of variance (ANOVA), followed by Dunnett's test.

RESULTS

Table 1 shows the scheme of treatment in the different groups. The entire experiment lasted 150 min. Animals were observed for 120 min in their home cages.

The effect of three doses of ANP on the DOPA potentiation test is demonstrated in Table 2. The dose of 200 ng had almost no influence on the behavior of mice. The doses of 500 and 1,000 ng ANP effectively potentiated the DOPA response, with maximal intensity of the increase 30–45 min following administration of the peptide [ANOVA, $F(3, 7) = 26.7$ and $F(3, 7) = 13.3$, $p = 0.0001$, Dunnett test, $p < 0.05$ vs. control]. Forty-five minutes after administration of ANP, the effect gradually declined and at the end of the first hour of observation only a slight (500 ng) or moderate–slight (1,000 ng) increase remained. At the end of the second hour, there was still a slight degree of DOPA potentiation at the highest dose.

DISCUSSION

In the present study, ANP administered intracerebroventricularly in doses of 500 or 1,000 ng/mouse was found active in the DOPA potentiation test. Our earlier studies suggested ANP might exert a modulatory effect in the processes of fear-induced learning via dopaminergic mediation (1,4,5). This peptide potentiated the effect of apomorphine (a DA agonist) in inducing stereotyped cage-climbing behavior in mice (2). All effects of ANP studied by us could be blocked by haloperidol (a DA blocking agent) (1,3,5). Others also reported a DA blockade on central and peripheral effects of the peptide (7,8).

Little is known about the mechanism in which ANP interacts with the dopaminergic neurotransmission. ANP may act pre- or postsynaptically on dopaminergic neurons in the hypothalamus or other brain structures to augment the combined effects of pargyline–DOPA. It may interact with dopaminergic receptors in appropriate brain structures involved in the performance of the DOPA potentiation test. There is no literature available answering this question at present time. Our data confirm our earlier observations that the action of ANP on active and passive avoidance behavior is mediated via dopaminergic transmission (1,3,5); however, the actual site of its action, that is, whether it is acting pre- or postsynaptically or at receptor site, remains to be clarified.

REFERENCES

1. Bidzseranova, A.; Gueron, J.; Penke, B.; Telegdy, G. The effects of atrial natriuretic peptide on active avoidance behavior in rats. The role of the transmitter systems. Pharmacol. Biochem. Behav. 40: 61–64; 1991.
2. Bidzseranova, A.; Gueron, J.; Tóth, G.; Penke, B.; Telegdy, G. Effect of atrial natriuretic peptide on apomorphine-induced stereotyped cage-climbing behavior in mice. Eur. J. Pharmacol. (in press).
3. Bidzseranova, A.; Penke, B.; Telegdy, G. The effects of atrial natriuretic peptide on electroconvulsive shock-induced amnesia inrats: Transmitter mediated action. Neuropeptides 19:103–106:1990.
4. Bidzseranova, A.; Telegdy, G.; Penke, B. The effects of atrial natriuretic peptide on passive avoidance behavior in rats. Brain Res. Bull. 26:177–180; 1991.
5. Bidzseranova, A.; Telegdy, G.; Tóth, G. The effects of receptor blockers on atrial natriuretic peptide-induced action on passive avoidance behavior in rats. Pharmacol. Biochem. Behav. 40:237–239; 1991.
6. Fekete, M.; Telegdy, G.; Schally, A. V.; Coy, D. Effects of β-/TYR^9/ melanotropin-/9-18/ decapeptide on catecholamine disappearance and serotonin accumulation in discrete brain regions of rats. Neuropeptides 1:377–382; 1981.
7. Israel, A.; Torres, M.; Barbella, Y. Evidence for a dopaminergic mechanism for the diuretic and natriuretic action of centrally administered atrial natriuretic factor. Cell Mol. Neurobiol. 9(3):365–378; 1989.
8. Marin-Grez, M.; Briggs, I. P.; Schubert, G.; Schnermann, J. Dopamine receptor antagonists inhibit the natriuretic response to atrial natriuretic factor (ANF). Life Sci. 36:2171–2176; 1985.
9. Plotnikoff, N. P.; Kastin, A.; Anderson, M.; Schally, A. DOPA potentiation by a hypothalamic factor, MSH release-inhibiting hormone (MIF). Life Sci. 10:1279–1283; 1971.
10. Plotnikoff, N. P.; Prange, A.; Breese, G.; Wilson, I. Thyrotropin releasing hormone: Enhancement of DOPA activity in thyroidectomized rats. Life Sci. 14:1271–1278: 1974.

Learning and Memory

neuroReport

NeuroReport 3, 283–285 (1992)

Behavioral effects of atrial and brain natriuretic peptides in rats

Amelia Bidzseranova, Jony Gueron, Gábor Tóth,[1] Botond Penke,[1] János Varga[2] and Gyula Telegdy[CA]

Institute of Pathophysiology and [1]Institute of Medical Chemistry, Albert Szent-Györgyi Medical University, Szeged, POB 531, Hungary; [2]American Peptide Company, Santa Clara, CA 95051, USA

[CA] Corresponding Author

The effects of intracerebroventricular administration of rat atrial natriuretic peptide (rANP-1-28) and porcine brain natriuretic peptide-32 (pBNP-32) on passive and active avoidance behavior and on electroconvulsive shock-induced amnesia were studied in rats. The dose range for both peptides was selected to lie between 0.016 and 0.32 nmol. The two peptides were found to facilitate consolidation of the passive avoidance response, to delay extinction of the active avoidance response, and to prevent electroconvulsive shock-induced amnesia in a similar way. It is suggested that some modulatory functions in the central nervous system of the rat, so far attributed to ANP, may in fact involve a dual control by both ANP and BNP, and there is no difference in the biological activity of the two peptides as far as fear-motivated learning behavior is concerned.

Key words: Atrial natriuretic peptide; Brain natriuretic peptide; Avoidance behavior

Introduction

Atrial natriuretic peptide (ANP) is a peptide of 28 amino acid residues which was identified in mammalian atria 10 years ago,[1] and later in mammalian brains.[2] Brain natriuretic peptide (BNP) is a peptide of 26 amino acid residues, recently identified in porcine brain.[3] A form extended by six amino acids at the *N*-terminal was also discovered in porcine brain.[4] The six additional amino acids are reported not to change the intrinsic bioactivity of BNP.[4] The peptides ANP, BNP-26 and BNP-32 share substantial sequence homology and have similar potency in their natriuretic, diuretic and vasorelaxant activities.[5]

Despite the fact that these peptides are generally considered to participate in a control mechanism for maintaining the homeostatic balance of body fluids and electrolytes in mammals, their roles in the functions of the central nervous system still remain uncertain. In order to clarify the existence of physiological functions of the natriuretic peptide family, related to learning and memory processes, we compared the effects of rat ANP (rANP-1-28) and of porcine BNP (pBNP-32) on three different fear-motivated learning tasks in rats, following their intracerebroventricular (i.c.v.) administration. The tests were as follows: passive avoidance, active avoidance behavior, and electroconvulsive shock (ECS)-induced amnesia.

Materials and Methods

Animals: The experiments were performed on male CFY rats (LATI, Gödöllö, Hungary), weighing 150–250 g. They were kept at constant room temperature in artificial 12 h light (started at 6 a.m.), 12 h dark periods. Commercial food and tap water were given *ad libitum*. The experiments started at 8 a.m. and were concluded by noon.

Surgery: The rats were anesthetized with sodium pentobarbital (Nembutal, 35 mg kg^{-1}, i.p.) and a cannula was introduced into the lateral cerebroventricle and fixed to the skull with dental cement. The operated animals were used after a recovery period of 5 days. The correct positioning of the cannula was checked by injecting methylene blue through the cannula and subsequent dissection of the brain. Animals with incorrect placement of the cannula were discarded and excluded from the statistical evaluations.

Behavioral methods: (1) Passive avoidance test; one-trial learning step-through passive avoidance behavior was measured according to Ader *et al.*[6] Briefly, rats were placed on a platform and allowed to enter a dark compartment. Since rats prefer dark to light, they normally entered within 15 s. Two additional trials were given on the following day. After the second trial, unavoidable electric footshocks (0.75 mA, 2 s) were delivered through the grid floor. Having entered the box, the animals could not escape the footshock. After this single learning trial, the rats were immediately removed from the apparatus and were treated with peptide. Consolidation of passive avoidance behavior was tested 24 h later: every rat was placed on the platform and the latency to enter the dark compartment was measured up to a maximum of 300 s.

(2) ECS-induced amnesia; the method is based on a passive avoidance test. After the footshock (learning trial), the animal was immediately removed from the apparatus and retrograde amnesia was effected, using a Minicoma set (a.c. 190 V, 50 Hz, 0.5 s duration, pos-

ition 2). Twenty-four hours later, the consolidation of the passive avoidance response was measured as already described.

(3) **Active avoidance test**; this was performed as described previously.[7] Briefly, the experimental apparatus consisted of a 'bench-jumping' conditioning box. The conditional stimulus was the light of a 45 W bulb. The unconditional stimulus was an electric shock of 1 mA a.c., delivered through the grid floor. Experimental sessions were performed daily, with a duration of 10 min each. Each session consisted of 10 trials, with a mean inter-trial interval of 60 s (range 50–70 s). The conditioning stimulus was presented for a maximum of 15 s. If the rat jumped onto the bench during the first 10 s (conditioned avoidance response [CAR]), the conditioning stimulus was terminated. Non-occurrence of a CAR was associated with termination of the unconditional stimulus in the last 5 s of the conditioning stimulus period. The learning criterion was 80% or more CARs measured on the third day of training. After having reached the criterion of learning, the animals were treated with peptide i.c.v., and its effect was measured after 3, 6 and 24 hours, i.e. the effect of the peptide on extinction of active avoidance behavior was studied. The control group received the same volume of saline. During the extinction trials, the conditional stimulus was not followed by electric shock.

Peptides: rANP-1-28 was purchased from Bachem (Cal., USA) and also synthesized by G. Tóth and B. Penke. pBNP-32 was kindly donated by J. Várga from the American Peptide Company, Santa Clara, California, USA. The peptides were dissolved in 0.9% saline and injected in a volume of 2 µl into the lateral brain ventricle of the animals in doses of 0.016, 0.032, 0.065, 0.16 or 0.32 nmol per rat.

Statistical analysis: For statistical evaluation of the data, the one-way analysis of variance (ANOVA) test, followed by the Tukey test, was used. A probability level of 0.05 was accepted as statistically relevant.

Results

The effects of five doses of rANP-1-28 or pBNP-32 (0.016, 0.032, 0.065, 0.16, and 0.32 nmol) on the consolidation of passive avoidance behavior in rats are shown in Table 1A. The dose of 0.065 nmol was the lowest which caused a statistically significant increase in the avoidance latency for both peptides. The doses of 0.16 and 0.32 nmol further facilitated consolidation of the learning task for the two peptides, showing a similar dose-dependence.

Thus, the doses of 0.065, 0.16 and 0.32 nmol were selected for further series of experiments. As shown in Table 1B, the antiamnesic effects of rANP-1-28 and

Table 1. Behavioral responses induced by rANP-1-28 and pBNP-32

(A) Consolidation of passive avoidance behavior

Peptide	Control group (saline) 99.5 ± 5 (64)				
	0.016 nmol	0.032 nmol	0.065 nmol	0.16 nmol	0.32 nmol
rANP-1-28	139.4 ± 21 (33)	131.1 ± 21 (18)	206.8 ± 25* (13)	228.0 ± 17* (12)	240.3 ± 22* (12)
pBNP-32	114.6 ± 12 (9)	128.8 ± 26 (9)	193.8 ± 12* (9)	210.0 ± 13* (11)	211.3 ± 27* (8)

(B) Antiamnesic action based on passive avoidance behavior
Amnesia group (saline + amnesia) 53.1 ± 4 (36)

rANP-1-28			67.8 ± 9 (18)	110.7 ± 6* (12)	153.5 ± 14* (12)
pBNP-32			87.2 ± 14 (10)	128.2 ± 7* (10)	173.5 ± 18* (8)

(C) Extinction of active avoidance behavior

rANP-1-28					
3h			71.9 ± 6 (32)	89.2 ± 6* (24)	88.5 ± 5* (9)
6h			63.0 ± 8 (32)	81.3 ± 4* (24)	82.5 ± 5* (9)
24h			57.5 ± 8 (32)	77.0 ± 5* (24)	79.3 ± 6* (9)
pBNP-32					
3h			73.0 ± 6 (10)	82.7 ± 4* (11)	85.5 ± 4* (11)
6h			62.8 ± 8 (10)	76.4 ± 4* (11)	78.3 ± 5* (11)
24h			60.0 ± 7* (10)	73.7 ± 4* (11)	75.6 ± 5* (11)
Control group	Saline				
3h	62.5 ± 3 (36)				
6h	49.2 ± 3 (36)				
24h	46.1 ± 4 (36)				

* $p < 0.05$ (ANOVA, Tukey test).
The results are represented as means ± s.e.m. Numbers in brackets are the numbers of animals used.

pBNP-32 in doses of 0.16 and 0.32 nmol were statistically significant ($p < 0.05$, Tukey test).

The same results were obtained in the active avoidance test. In both cases, the peptides in doses of 0.16 and 0.32 nmol significantly delayed extinction of the active avoidance response ($p < 0.05$, Tukey test) (Table 1C). The results are expressed as percentage.

Discussion

The recently isolated pBNP-32 not only shows a structural resemblance to ANP,[5] but also exerts similar diuretic, natriuretic and vasorelaxant effects.[5,8,9] Furthermore, pBNP-32 has been found to elicit biological activity comparable to that induced by pBNP-26.[4,10] Since rANP-1-28, pBNP-26 and pBNP-32 share a substantial sequence homology and bioactivity,[5] we designed series of behavioral experiments to clarify the roles of two of these natriuretic peptides in learning processes and memory functions.

The present report demonstrates that rANP-1-28 and pBNP-32 have rather similar effects in the fear-motivated learning tests studied. They both facilitated consolidation of the passive avoidance response, prevented the ECS-induced amnesia and delayed extinction of the active avoidance response when administered into the lateral brain ventricle in selected equimolar doses.

We have previously reported the involvement of ANP in learning processes.[11-15] Itoh *et al*,[8] demonstrated a central effect of BNP, inhibiting angiotensin-stimulated water intake in rats after i.c.v. administration, in a manner comparable to that of ANP. Controversially, Aburaya *et al*[16] reported that a substantial amount of ir-BNP was not detected in the rat central nervous system, except in the spinal cord, suggesting the possibility that the peptide in the rat brain functions not as a neuropeptide, but mainly as a circulating hormone.

Conclusion

In conclusion, the findings to date lead us to suggest that some physiological functions in the central nervous system of the rat, so far attributed to ANP, may in fact involve a dual control by both ANP and BNP, as far as fear-motivated learning behavior is concerned. Both peptides affect the learning processes in a similar way, so that a neuromodulatory function for both ANP and BNP, connected with learning processes, might be quite feasible. However, the effects described in this paper are not unique since similar results have been published for other peptides also.[17]

References

1. De Bold AJ, Borenstein HB, Veress AT *et al*. *Life Sci* 28, 83-94 (1981).
2. Tanaka I, Misono KS, Inagami T. *Biochem Biophys Res Commun* 124, 663-668 (1984).
3. Sudoh T, Kangawa K, Minamino N *et al*. *Nature* 332, 78-81 (1988).
4. Sudoh T, Minamino N, Kangawa K *et al*. *Biochem Biophys Res Commun* 155, 726-732 (1988).
5. Sudoh T, Minamino N, Kangawa K *et al*. *Biochem Biophys Res Commun* 168, 863-870 (1990).
6. Arlet R, Weijnen JA, Moleman P. *Psychosom Sci* 26, 126-128 (1972).
7. Telegdy G, Hadnagy J, Tissak K. *Acta Physiol Acad Sci Hung* 339, 439-446 (1968).
8. Itoh H, Nakao K, Saito J *et al*. *Biochem Biophys Res Commun* 158, 120-128 (1989).
9. Saper C, Hurley K, Muga M *et al*. *Neuroscience lett* 96, 29-34 (1989).
10. Tordo T, Nazarali A, Saavedra J. *Biochem Biophys Res Commun* 159, 1032-1038 (1989).
11. Bidzseranova A, Telegdy G. *Acta Physiol Hungarica* 75, (Suppl) 35-36 (1990).
12. Bidzseranova A, Telegdy G, Penke B. *Brain Res Bull* 26, 177-180 (1990).
13. Bidzseranova A, Penke B, Toth G *et al*. *Neuropeptides* 19, 103-106 (1991).
14. Bidzseranova A, Gueron J, Penke B *et al*. *Pharmacol Bioch Behav* (in press) (1991).
15. Bidzseranova A, Telegdy G, Toth G. *Pharmacol Biochem Behav* (in press) (1991).
16. Aburaya M, Minamino N, Hino J *et al*. *Biochem Biophys Res Commun* 165, 880-887 (1989).
17. Telegdy G. *Neuropeptides and Brain Function*. Karger 1987; 332.
18. Ueda S, Minamino N, Sudoh T *et al*. *Biochem Biophys Res Commun* 155, 733-739 (1988).

Received 10 January 1992; accepted 28 January 1992

2.9.

Life Sciences, Vol. 52, pp. PL 19-24 Pergamon Press
Printed in the USA

PHARMACOLOGY LETTERS

Accelerated Communication

ANP(1-28), BNP(1-32) AND CNP(1-22) INCREASE THE SEVERITY OF PICROTOXIN-KINDLED SEIZURE SYNDROME IN RATS

Andrey M. Mazarati[1], Éva Halászi[1], Gyula Telegdy[1], Gábor Tóth[2] and János Varga[3]

Institutes of [1]Pathophysiology and [2]Medical Chemistry, A.Szent-Gyorgyi Medical University, Szeged, P.O.B. 531, H-6701, Hungary and [3]American Peptide Company, Santa Clara, Ca 95051, USA.

(Submitted September 3, 1992; accepted September 28, 1992; received in final form November 12, 1992)

Abstract. The administration of rANP(1-28) in doses of 1.0 and 2.0 nmol (but not 0.2 nmol) into the lateral cerebral ventricle (i.c.v) of rats preliminarily kindled with picrotoxin resulted in an increase of the severity of picrotoxin-kindled convulsions 24 hrs after injection of the peptide. I.c.v. injection of pBNP(1-32) also resulted in a proepileptic effect when it was applied in the same doses with a similar time course; the increased seizure severity was observed 48 hrs after injection of pBNP in a dose of 2 nmol. I.c.v. administration of CNP(1-22) in a dose of 2 nmol induced an increase in the severity of picrotoxin-kindled convulsions 24 and 48 hrs after application of the peptide. None of the peptides influenced the seizure syndrome immediately after the injections. It is presumed that the delayed proepileptic properties of the three natriuretic peptides could be caused by some of their stable fragments which accumulate during their metabolism.

Introduction

The family of natriuretic peptides contains the atrial (ANP), brain (BNP) and C-type (CNP) natriuretic peptides; all of them have been shown to be present in the central nervous system (CNS) of mammals (1-6) and to participate not only in the regulation of the homeostasis of the fluid, electrolytic balance and blood pressure (7,8), but also in the activity of the CNS, and in particular, in the processes of learning and memory (9-11).

There are as yet no clinical or experimental data on the involvement of these peptides in the mechanisms of certain CNS disorders. With regard to their central effects, it was of interest to study their influence on the kindling model of epilepsy, the basic mechanisms of which are close to the mechanisms of learning and memory (12), and which is now regarded as one of the most relevant epileptic syndrome models (13).

Correspondence should be sent to Prof. G.Telegdy, Inst. of Pathophysiology, A.Szent-Györgyi Medical University, Szeged, P.O.B. 531, H-6701, Hungary.

0024-3205/93 $6.00 + .00

Materials and Methods

The experiments were performed on male CFY rats weighing 200-250 g. The animals were kept at constant room temperature in artificial light with 12-hr light - 12-hr dark cycles. Standard diet and tap water were available ad libitum.

The animals were kindled by means of 20-25 daily i.p. picrotoxin (Sigma) injections at a dose of 1.5 mg/kg (14). The severity of the convulsions was evaluated on a 6-stage scale: 0 - absence of convulsions; 1 - facial tremor or clonic jerks of separate muscles; 2 - repeated total-body clonic convulsions; 3 - repeated total-body clonic convulsions with rearings; 4 - generalized clonic-tonic convulsions with rearings and fallings; 5 - repeated or lethal generalized clonic-tonic convulsions.

Two-five days after the last picrotoxin administration, stainless guide cannulas were implanted stereotaxically into the right lateral brain ventricle according to the rat brain atlas (15), with the animals under pentobarbital anaesthesia (Ceva, France, 35 mg/kg i.p.)

Five-seven days after the surgery, the animals were injected with picrotoxin (1.5 mg/kg) and the convulsion severity was evaluated in animals in individual boxes for 60 min after picrotoxin administration. 24 hrs later, rANP(1-28) (Bachem, Switzerland), pBNP(1-32) (American Peptide Company CA, USA) or CNP(1-22) (synthesized in the Institute of Medical Chemistry, Szent-Györgyi Medical University, Szeged, Hungary) was administered i.c.v. into animals 1 in doses 0.2, 1 or 2 nmol in 2 mcl of 0.9% NaCl under conditions of free behavior. Control animals received an equal volume of saline. Within 10 min after the injections of the peptides, picrotoxin (1.5 mg/kg) was administered i.p. and the convulsion severity was evaluated as mentioned above. Picrotoxin administration was also performed 24 and 48 hrs after the peptide microinjection.

After the experiments, the animals were sacrificed with an overdose of nembutal and the placement of the cannulas was identified by comparing the tracks with the pictures from the atlas (16). The data were analyzed by using the Friedman test, followed by the Wilkoxon signed rank test where appropriate (comparison of the convulsion severity in the same animal before and after peptide injection).

Results

I.c.v. administration of saline had no effect upon the severity of the picrotoxin-kindled seizure syndrome (Tables I-III).

The effects of rANP(1-28) upon the severity of the picrotoxin-kindled convulsions are presented in Table I. When applied in doses of 1 and 2 nmol, rANP(1-28) resulted in a significant increase in the severity of the convulsions, which was revealed only 24 hrs after administration of the peptide. The procipleptic affect of rANP(1-28) was expressed in a increase in the number of animals with convulsions in stages 3-5.

Table II presents the effects of pBNP(1-32) upon the picrotoxin kindled convulsive syndrome. BNP in doses of 1 and 2 nmol also induced an increase in the severity of the

TABLE I
Effects of Administration of rANP(1-28) Into Lateral Brain Ventricle upon Severity of Picrotoxin-Kindled Convulsions in Rats.

Dose of ANP nmol	Number of rats	Time of testing, hrs to ANP injection	Number of rats with convulsions of						P values (vs -24 hrs)
			stage 0	stage 1	stage 2	stage 3	stage 4	stage 5	
Saline	14	-24	0	3	2	9	0	0	-
		0	1	6	1	5	1	0	>0.05
		+24	1	3	3	4	3	0	>0.05
		+48	0	3	2	6	3	0	>0.05
0.2	11	-24	0	4	0	7	0	0	-
		0	0	7	1	1	2	0	>0.05
		+24	0	5	0	3	3	0	>0.05
		+48	0	4	1	4	2	0	>0.05
1.0	16	-24	0	4	2	9	1	0	-
		0	0	4	4	7	1	0	>0.05
		+24	0	0	2	11	2	1	<0.05
		+48	0	5	2	4	5	0	>0.05
2.0	10	-24	0	4	1	4	1	0	-
		0	0	5	0	1	3	1	>0.05
		+24	0	3	0	2	2	3	<0.05
		+48	1	3	0	0	2	4	>0.05

convulsions 24 hrs after its i.c.v. application. The proepileptic effect of BNP also persisted 48 hrs after its administration.

CNP(1-22) enhanced the seizure severity only if applied in a high dose (2 nmol). It increased the number of animals with convulsions in stages 3-5, and this effect was observed 24 and 48 hrs after peptide administration (Table III).

Discussion

These studies showed that, when administered in equimolar concentrations i.c.v., all three natriuretic peptides resulted in an increase in the behavioral manifestations of the

picrotoxin-kindled seizure syndrome, with both common and specific features of action with respect to the time course and dose-dependent effects.

TABLE II
Effects of Administration of pBNP(1-32) Into Lateral Brain Ventricle upon Severity of Picrotoxin-Kindled Convulsions in Rats.

Dose of BNP nmol	Number of rats	Time of testing, hrs to BNP injection	Number of rats with convulsions of						P values (vs -24 hrs)
			stage 0	stage 1	stage 2	stage 3	stage 4	stage 5	
Saline	22	-24	1	8	2	7	4	0	-
		0	0	7	6	7	1	1	>0.05
		+24	2	5	4	9	2	0	>0.05
		+48	1	5	4	7	4	1	>0.05
0.2	8	-24	0	2	0	6	0	0	-
		0	0	2	0	4	2	0	>0.05
		+24	0	2	1	4	1	0	>0.05
		+48	0	3	0	2	3	0	>0.05
1.0	19	-24	0	7	5	6	1	0	-
		0	0	5	3	9	1	1	>0.05
		+24	0	5	2	10	1	1	>0.05
		+48	0	1	3	5	6	4	<0.05
2.0	20	-24	1	9	5	5	0	0	-
		0	1	5	6	7	1	0	>0.05
		+24	0	5	3	12	0	0	<0.05
		+48	0	4	2	11	1	2	<0.05

First of all, none of the peptides influenced the convulsive syndrome immediately after its administration. The proconvulsive effect was observed at least 24 hrs after injection of the peptides. ANP increased the seizure severity in doses of 1 and 2 nmol and this effect was absent 48 hrs after its application. While having similar dose-dependent proconvulsive properties, BNP in the high dose (2 nmol) provided prepileptic action for at least 48 hrs after its administration. Finally, although CNP displayed the same effect only in the highest of the used doses (2 nmol), its effect also persisted for 48 hrs after administration.

TABLE III
Effects of Administration of CNP(1-32) into
Lateral Brain Ventricle upon Severity of Picrotoxin-Kindled Convulsions in Rats.

Dose of CNP nmol	Number of rats	Time of testing, hrs to CNP injection	Number of rats with convulsions of						P values (vs -24 hrs)
			stage 0	stage 1	stage 2	stage 3	stage 4	stage 5	
Saline	9	-24	1	3	1	4	0	0	-
		0	1	3	1	3	1	0	>0.05
		+24	2	4	0	2	1	0	>0.05
		+48	3	1	2	2	1	0	>0.05
0.2	10	-24	1	4	4	1	0	0	-
		0	2	3	1	4	0	0	>0.05
		+24	0	2	1	7	0	0	>0.05
		+48	1	2	1	6	0	0	>0.05
1.0	10	-24	0	6	1	3	0	0	-
		0	1	6	2	1	0	0	>0.05
		+24	0	4	0	4	1	1	>0.05
		+48	0	3	1	2	1	3	>0.05
2.0	10	-24	0	6	2	2	0	0	-
		0	2	4	2	2	0	0	>0.05
		+24	0	2	0	6	1	1	<0.05
		+48	0	1	2	4	2	1	<0.05

It was earlier shown that rANP, pBNP and CNP facilitate learning and memory in passive and active avoidance tasks, and that these effects are realized via modulator action upon certain brain neurotransmitter systems, particularly the dopaminergic and cholinergic systems (9-11,16). As mentioned above, kindling represents the model not only for epilepsy, but also for learning and memory (12). Thus, the increase in the behavioral manifestations of kindled seizure syndrome under the conditions of application of these peptides could be regarded from this aspect as a result of activation of the mechanisms underlying learning and memory.

The time course of the effects of ANP, BNP and CNP is of interest. The fact that their effects could be observed only 24 hrs later, but not immediately after their

administration suggests that the described effects could be caused not by the peptides themselves, but by some of their fragments which accumulate as a result of sequenation of the original molecules. It should be stressed that the three peptides contain sequences which are common to all of them, in particular Cys-Phe-Gly, Asp-Arg-Ile-Gly and Ser-Gly-Leu-Gly-Cys(5). It is possible that one of the fragments determines the observed proconvulsive effect of ANP, BNP and CNP.

Acknowledgement

The work has been supported by the Ministry of Social and Welfare of Hungary (T-70/1990) and OTKA (T/3, 1354).

References

1. W.K.SAMSON, Endocrinology and Metabolism Clinics of North America, Vol.16, Atrial Natriuretic Factor, M.Rosenblat and J.W.Jakobs (eds), 145-161, Saunders, Philadelphia, 1987.
2. A.J. DE BOLD, Science 230 767-770 (1985).
3. T.SUDOH, K.KANGAWA, N.MINAMINO & H.MATSUO, Nature 332 78-81 (1988).
4. T.SUDOH, N.MINAMINO, K.KANGAWA & H.MATSUO, Biochem. Biophys. Res. Commun. 155 726-732 (1988).
5. T.SUDOH, N.MINAMINO, K.KANGAWA & H.MATSUO, Biochem. Biophys. Res. Commun. 168 863-870 (1990).
6. N.MINAMINO, Y.MAKINO, H.TATEYAMA, K.KANGAWA & H.MATSUO, Biochem. Biophys. Res. Commun. 179 535-542 (1991).
7. K.KANGAWA & H.MATSUO, Biochem. Biophys. Res. Commun. 118 131-139 (1984).
8. M.FURUYA, N.OHNUMA, M.TAKEHISA, Y.HAYASHI, T.ISHIARA, N.MINAMINO, K.KANGAWA & H.MATSUO, European J. Pharmacol. 200 233-237 (1991).
9. A.BIDZSERANOVA, G.TELEGDY & B.PENKE, Brain Res. Bull. 26 177-180 (1991).
10. A.BIDZSERANOVA, J.GUERON, G.TÓTH, B.PENKE, J.VARGA & G.TELEGDY, Neuroreport 3 283-285 (1992).
11. A.BIDZSERANOVA, J.GUERON, B.PENKE & G.TELEGDY, Pharmacol. Biochem. Behav. 40 61-64 (1991).
12. J.MAJKOWSKY, Acta Neurol. Scand. 74 suppl. 109 97-108 (1986).
13. R. S. FISHER, Brain Research Reviews 14 245-278 (1989).
14. G.N.KRYZHANOVSKY, A.A.SHANDRA, L.S.GODLEVSKY, R.F.MAKULKEN & A.M.MAZARATI, Bull. Exp. Biol. 108 17-21 (1989).
15. G.PAXINOS & CH.WATSON, The rat brain in stereotaxic coordinates. Academic Press Inc, Sydney, 1982.
16. A.BIDZSERANOVA, G.TÓTH & G.TELEGDY, Pharmacol. Biochem. Behav, 40 237-239 (1991).

Physiology & Behavior, Vol. 53, pp. 325–328, 1993
Printed in the USA.

2.10.

0031-9384/93 $6.00 + .00

The Effects of Atrial Natriuretic Peptide on Food-Reinforced Conditioning in Rats. Interactions with Neurotransmitters

AMELIA BIDZSERANOVA,* JONY GUERON,* GABOR TÓTH† AND GYULA TELEGDY*[1]

**Institute of Pathophysiology and †Institute of Medical Chemistry, Albert Szent-Györgyi Medical University, Szeged, POB 531, Hungary*

Received 21 January 1992

BIDZSERANOVA, A., J. GUERON, G. TÓTH AND G. TELEGDY. *The effects of atrial natriuretic peptide on food-reinforced conditioning in rats. Interactions with neurotransmitters.* PHYSIOL BEHAV 53(2) 325–328, 1993.—The effects of two doses of rat atrial natriuretic peptide (rANP-1–28), 200 and 500 ng, on 6-day acquisition and extinction of food-reinforced conditional learning (conditional stimulus: light) were studied in rats following administration into the lateral cerebroventricle. With the higher dose, there was a tendency for facilitated acquisition and significantly delayed extinction of the positively reinforced learning task. In order to clarify whether the effect of the peptide is obtained through the involvement of neurotransmitters, the experimental animals were pretreated with different receptor blockers in selected doses that did not influence the behavioral test. Haloperidol, atropine, phenoxybenzamine, and propranolol blocked the action of ANP on extinction of the food-reinforced conditioning, whereas naloxone, bicuculline, and methysergide were ineffective. The results suggest that ANP might be considered a modulating agent in a positively reinforced conditional learning task, and that its action might involve dopaminergic, cholinergic, and α- and β-adrenergic mechanisms.

Atrial natriuretic peptide Positive reinforcement Conditional learning Behavior Neurotransmitters

THE presence of atrial natriuretic peptide (ANP) and its receptors in the central nervous system is well documented (6–11). Although the functions of this peptide in the brain are generally connected with water-salt homeostasis, the presence of ANP in motivation-emotion-related structures (10) makes it reasonable to look for possible central effects of ANP on learning processes and memory formation.

We earlier studied the effects of ANP on fear-motivated (negatively reinforced) learning in rats (1–4). The peptide facilitated consolidation of a passive avoidance response and delayed extinction of an active avoidance response in a dose-dependent manner.

In the present study, the effect of ANP on food-reinforced (positively reinforced) conditional learning behavior in rats was investigated. To examine the involvement of neurotransmitters in the ANP-induced action, the animals were pretreated with different receptor blockers that had earlier been proven effective in modifying the action of a number of peptides in the same behavioral paradigm (13).

METHOD

Animals

Male rats of the CFY albino strain, weighing 180–250 g at the beginning of the experiments, were used. They were housed six per cage under standard conditions: constant room temperature, an artificial 12 h light–12 h dark cycle (lights on at 0600) and free access to tap water. A 22-h food deprivation (+2-h feeding schedule) was initiated 3 days before the experiments. Behavioral sessions were carried out between 0800 and 1600.

Surgery

The rats were anesthetized with pentobarbital-Na (Nembutal, 35 mg/kg) intraperitoneally and a 20 ga 1-½" Luer cannula was introduced into the right lateral cerebroventricle and fixed to the skull with dental cement (Spofa Cs). The stereotaxic coordinates of Fifkova and Marsala (5) were used (AP: +1.0, L: 1.5, V: 3.0). A volume of 2 μl per animal was injected through the cannula, using a microinjector (Mauser, BRD) and tubing. The animals were used after a recovery period of 5 days. The correct positioning of the cannula was verified by injecting methylene blue after the experiments were completed. Data from animals with incorrectly positioned cannulae were excluded from statistical evaluation.

Behavioral Method

The experimental apparatus was a conditioning box, measuring 12 × 20 × 40 cm, with a 2 × 2 cm slip-in feeding tray at

[1] Requests for reprints should be addressed to Prof. G. Telegdy, Inst. of Pathophysiology, Medical University, Szeged, POB. 531, Hungary 6701.

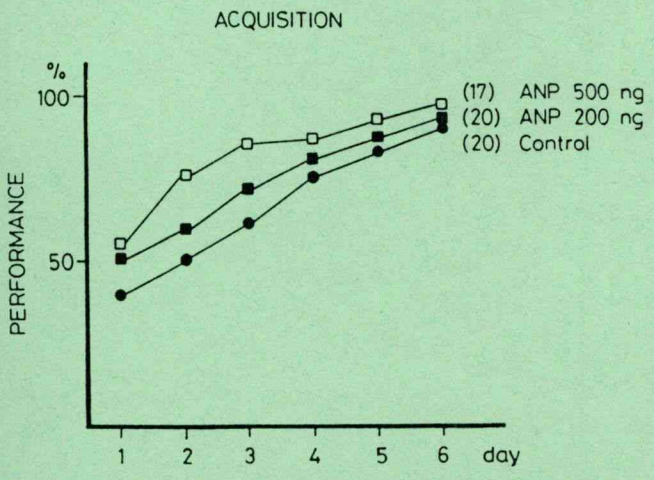

FIG. 1. Effects of two doses of ANP on acquisition of food-reinforced conditioning in rats. The numbers in parentheses are the numbers of animals used.

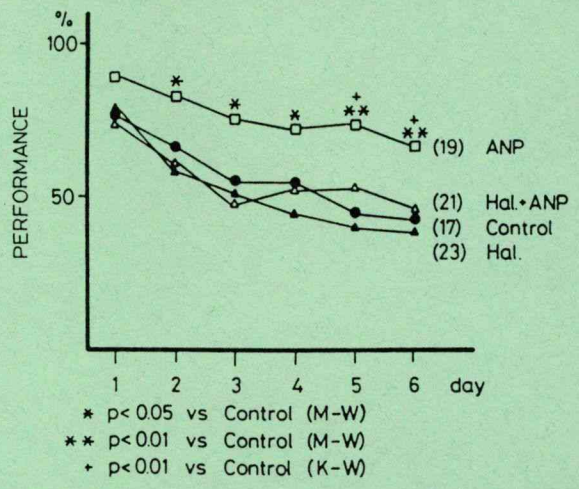

FIG. 3. Effect of haloperidol (10 μg/kg IP) on ANP-induced action (500 ng/animal) on extinction of food-reinforced conditioning in rats. The numbers in parentheses are the numbers of animals used.

one end. Above the tray, there was a 15 W bulb. At this end of the box, there was a 4 × 4 cm Plexiglas window for observation. The conditioning stimulus was light from the bulb for 10 s, and this was associated with food reinforcement of one oat grain in the feeding tray (12). Three animals were conditioned simultaneously in three adjacent boxes. On the fourth day of the deprivation schedule, 22-h food-deprived rats were placed in the conditioning boxes, with the feeding tray full of grain and the light on for 10 min. During this habituation period, all rats generally found the food and ate. On the following day, experimental sessions began. Each 10-min behavioral session consisted of 10 trials, with a mean intertrial interval of 60 s (range 50–70 s). The conditional stimulus (light) and the food reinforcement were presented for a maximum of 15 s or until the rat picked up the oat grain from the tray. After each behavioral session, standard rat chow was given to the animals for 2 h. Conditioning was carried out for 6 days. The criterion of learning was eight or more conditioned feeding responses (CFR) during 3 consecutive days (80% or more performance). After the rats had reached the criterion of learning, extinction began. During extinction the conditional stimulus was not associated with food and the positive response was recorded. Extinction session was also carried out for 6 days.

Peptide

Rat ANP (rANP-1–28) was purchased from Bachem. (Cal., USA) and also synthesized by G. Tóth. The ANP obtained from two sources were chemically (HPLC) identical. The peptide was given in a volume of 2 μl ICV, in two doses, 200 and 500 ng/rat, every day, 20 min prior to the conditioning or extinction trials.

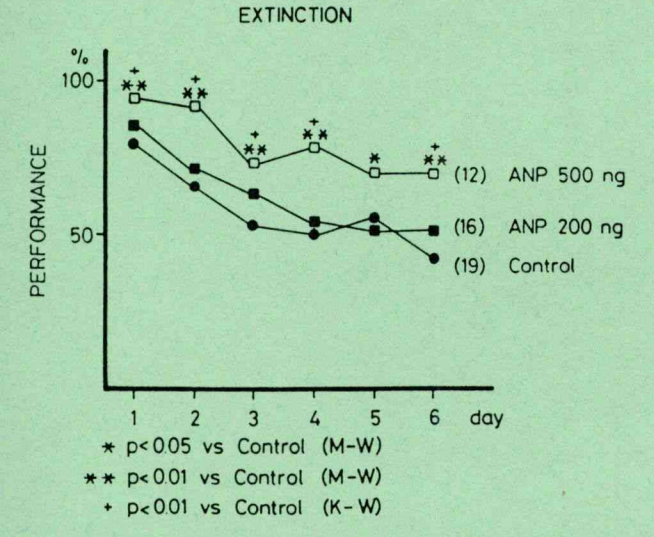

FIG. 2. Effect of two doses of ANP on extinction of food-reinforced responding in rats. The numbers in parentheses are the numbers of animals used.

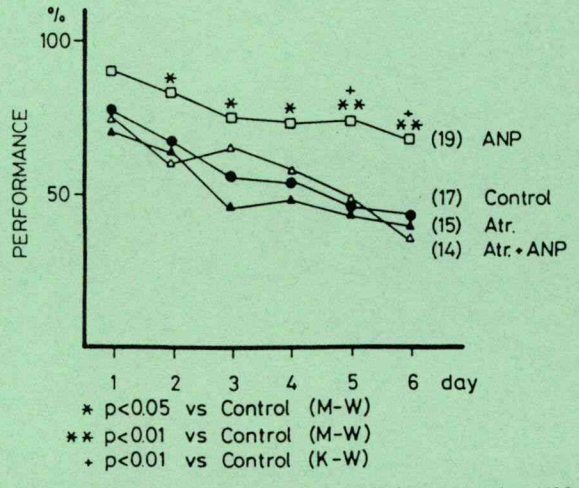

FIG. 4. Effect of atropine (2 mg/kg IP) on ANP-induced action (500 ng/animal) on extinction of food-reinforced conditioning in rats. The numbers in parentheses are the numbers of animals used.

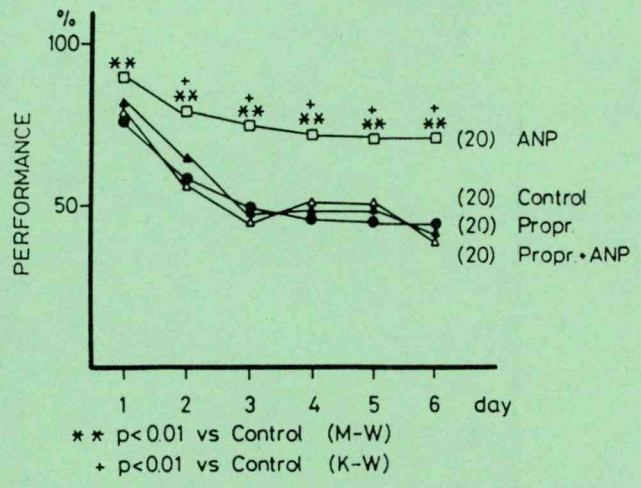

FIG. 5. Effect of propranolol (10 mg/kg IP) on ANP-induced action (500 ng/animal) on extinction of food-reinforced conditioning in rats. The numbers in parentheses are the numbers of animals used.

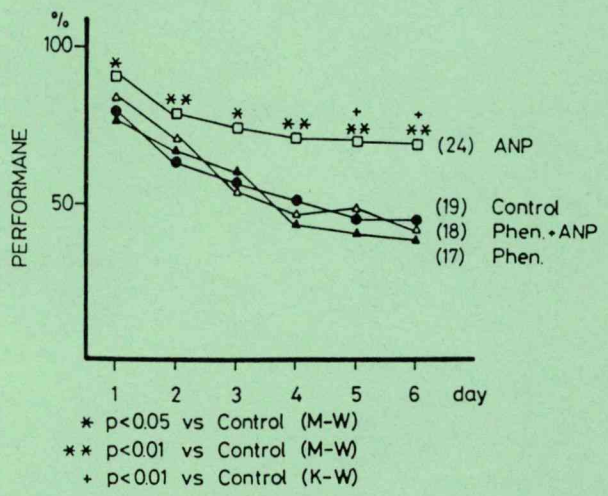

FIG. 6. Effect of phenoxybenzamine (2 mg/kg IP) on ANP-induced action (500 ng/animal) on extinction of food-reinforced conditioning in rats. The numbers in parentheses are the numbers of animals used.

Pretreatment

Pretreatment was performed with the following receptor blockers: haloperidol (G. Richter, Budapest) (10 μg/kg, IP), atropine (EGIS, Budapest) (2 mg/kg, IP), propranolol (I.C.I. Ltd., GB) (10 mg/kg, IP), phenoxybenzamine (Smith, Kline and French, GB) (2 mg/kg, IP), methysergide (Sandoz) (5 mg/kg, IP). All the above-mentioned drugs were given 30 min before the peptide. Naloxone (Endo Lab. Inc.) (0.3 mg/kg, SC) and bicuculline (Serva) (1 mg/kg, SC) were given 20 min before the peptide. The treatment was carried out only before the extinction trial.

Experimental Groups

In the first series of experiments, the animals were divided into three groups: a control group (which received 2 μl saline ICV) and two dose groups, which received 200 or 500 ng ANP per rat in a volume of 2 μl ICV every day, 20 min prior to the acquisition or the extinction trials.

In the following experiments, the animals were allocated into four groups:

1. Control groups: saline pretreatment (20–30 min prior saline, SC or IP) plus treatment with 2 μl saline ICV 20 min prior to the trial.
2. Blocker-treated groups: receptor-blocker pretreatment (20 or 30 min prior to saline SC or IP) plus treatment with 2 μl saline ICV) 20 min prior to the trial.
3. Peptide-treated groups: saline pretreatment (20 or 30 min prior to the peptide SC or IP) plus treatment with 200 or 500 ng ANP in a volume of 2 μl ICV, 20 min prior to the trial.
4. Blocker plus peptide-treated groups: blocker pretreatment plus treatment with ANP.

Statistical Analysis

Statistical evaluation of the data was performed with the nonparametric tests of Kruskal–Wallis (KW) followed by Mann–Whitney (MW). A probability level of 0.05 or less was considered significant.

RESULTS

The doses of 200 and 500 ng/rat of ANP were selected on the basis of previous experience (1–4). As shown in Fig. 1, with the higher dose there was a tendency for more rapid acquisition of the food-reinforced conditioning, but this did not reach statistical significance. In Fig. 2, the effects of these two doses of ANP on extinction of the conditioning can be seen. The dose of 500 ng/rat significantly delayed extinction of the conditioned response during all 6 days of testing (KW and MW tests at $p < 0.001$). The lower dose was ineffective. In the receptor blocker combined study, only 500 ng/rat ANP was used.

When the animals were pretreated with different receptor blockers in appropriate doses, the following results were obtained: haloperidol (Fig. 3) in a dose of 10 μg/kg IP, administered 30 min before the peptide every day, significantly blocked the delaying effect of ANP on extinction of the conditioned response

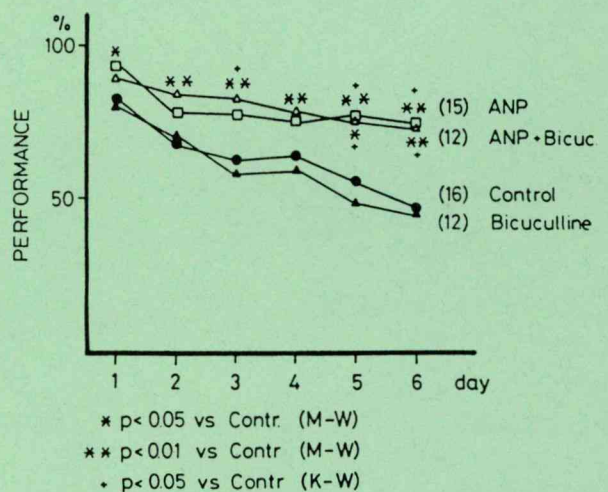

FIG. 7. Effect of bicuculline (1 mg/kg SC) on ANP-induced action (500 ng/animal) on extinction of food-reinforced conditioning in rats. The numbers in parentheses are the numbers of animals used.

on most days (on second, third, and fourth days, $p < 0.05$, MW, and on the fifth and sixth days, $p < 0.001$, KW and MW).

In a similar way, atropine, phenoxybenzamine, and propranolol (Figs. 4, 5, and 6) modulated the effect of the peptide. The other three receptor blockers (naloxone, bicuculline, and methysergide) were ineffective (only the results obtained with bicuculline are shown in Fig. 7).

DISCUSSION

The present study demonstrates that ANP is effective in a positively reinforced learning task. When administered ICV in a dose of 500 ng/rat, 20 min prior to the daily acquisition or extinction sessions, it transitorily enhanced acquisition, and significantly delayed extinction of the food-reinforced conditioning during all 6 days on which extinction of the conditional response was measured.

These results confirm our previous observations that ANP might be considered a neuropeptide with a regulatory function in learning processes, because in some fear-motivated learning tests (negatively reinforced learning) the peptide successfully facilitated consolidation of passive avoidance learning and delayed extinction of active avoidance learning (1–4).

As we have shown in our previous negatively reinforced experiments that ANP lengthened the passive avoidance response, delayed the extinction of active avoidance conditioning, and ANP cannot have an affect on locomotion in 24 h test (4), made our position strong enough to suppose that ANP has an effect on learning and memory function (1–3). The present paper is a continuation of the previous experiments demonstrating that the extinction of a positively reinforced conditioning can also be delayed. Of course, one has to be aware of the fact that the delayed extinction alone cannot be interpreted as an index of memory formation. Because food intake cannot be influenced by ANP (6), the motivation for food intake—hunger drive—can be ruled out. Taking together, the results of the negatively reinforced experiments with the present one, we feel that the evidences altogether are strong enough to suppose that ANP acting on learning and memory formation connected with positively reinforcement of the conditioning also.

Regarding the transmitters involved in the positively reinforced conditioning, it seems that, in contrast to the negatively reinforced conditioning, in which dopaminergic and cholinergic transmitters were involved here, not only dopaminergic and cholinergic but α- and β-adrenergic neurotransmitters may be involved also. This will give an important difference in organization of between the negatively and positively reinforced learning processes modulated by ANP.

ACKNOWLEDGEMENTS

The work has been supported by the Ministry of Social and Welfare of Hungary (T-70/1990) and OTKA (T/3, 1354).

REFERENCES

1. Bidzseranova, A.; Telegdy, G.; Penke, B. The effects of atrial antriuretic peptide on passive avoidance behavior in rats. Brain Res. Bull. 26:177–180; 1991.
2. Bidzseranova, A.; Telegdy, G.; Tóth, G. The effects of receptor blockers on atrial natriuretic peptide-induced action on passive avoidance behavior in rats. Pharmacol. Biochem. Behav. 40:237–239; 1991.
3. Bidzseranova, A.; Gueron, J.; Penke, B.; Telegdy, G. The effects of atrial natriuretic peptide on active avoidance behavior in rats. The role of the transmitter systems. Pharmacol. Biochem. Behav. 40(1): 61–64; 1991.
4. Bidzseranova, A.; Tóth, G.; Telegdy, G. The effects of atrial natriuretic peptide on the open-field activity of rats. The role of neurotransmitters. Neuropeptides 20:163–167; 1991.
5. Fifkova, E.; Marsala, J. Stereotaxic atlases for the cat, rabbit and rat. In: Bures, J.; Petrán, M.; Zachar, J., eds. Electrophysiological methods in biological research. Prague: Publishing House of the Czechoslovak Academy of Sciences; 1967:653–731.
6. Inagami, T.; Tanaka, I. K.; McKezie, J. C.; Nakamura, M.; Takayanagi, R.; Imada, T.; Pochet, R.; Resibois, A.; Naruse, M.; Naruse, K.; Shibasaki, T. Discovery of atrial natriuretic factor in the brain: Its characterization and cardiovascular implication. Cell. Mol. Neurobiol. 9(1):75–85; 1989.
7. Kawata, M. K.; Nakao, K.; Morii, N.; Kiso, J.; Jamashita, H.; Imura, H.; Sano, J. Atrial natriuretic polypeptide: Topographical distribution in the rat brain by radioimmunoassay and immunohistochemistry. Neuroscience 16:521–546; 1985.
8. Morii, N.; Nakao, K.; Sugawara, A.; Sakamoto, M.; Suda, M.; Shimokura, M.; Kiso, J.; Jamori, J.; Imura, H. Occurence of atrial natriuretic polypeptide in brain. Biochem. Biophys. Res. Commun. 127:413–419; 1985.
9. Quirion, R.; Dalpe, H.; De Lean, A.; Gutkowska, J.; Cantin, M.; Genest, J. Atrial natriuretic factor (ANF) binding sites in brain and related structures. Peptides 5:1167–1172; 1984.
10. Skofitsch, G.; Jacobowitz, D. Atrial natriuretic peptide in the central nervous system of the rat. Cell Mol. Neurobiol. 4:339–391; 1988.
11. Tanaka, I.; Misono, K. S.; Inagami, T. Atrial natriuretic factor in rat hypothalamus, atria and plasma: Determination of specific radioimmunoassay. Biochem. Biophys. Res. Commun. 124:663–668; 1984.
12. Telegdy, G.; Hadnagy, J.; Lissák, K. The effect of gonads on conditioned avoidance behavior of rats. Acta Physiol. Acad. Sci. Hung. 37:439–444; 1968.
13. Telegdy, G. Neuropeptides and brain function. Basel: Karger; 1987: 1–332.
14. Zamir, N.; Skofitsch, G.; Eskay, R. L.; Jacobowitz, D. M. Distribution of immunoreactive atrial natriuretic peptides in the central nervous system of the rat. Brain Res. 365:105–111; 1986.

NEUROPEPTIDES

Neuropeptides (1995) 29, 215–220

Involvement of Neurotransmitters in the 'Anxiolytic-like' Action of Atrial Natriuretic Peptide in Rats

É. BÍRÓ*, G. TÓTHt and G. TELEGDY*

**Department of Pathophysiology and †Department of Medical Chemistry, Albert Szent-Györgyi Medical University, Semmelweis 1, 6701 Szeged, P.O.B. 531, Hungary (Reprint requests to GT)*

Abstract—Effects of centrally administered rat atrial natriuretic peptide (ANP_{1-28}) in different doses (50, 100, 150, 200, 500 or 1000 ng) were examined in rats with respect to anxiolytic properties in an elevated plus-maze model. In doses of 100, 150 and 200 ng, ANP_{1-28} abolished the normal preference for the closed arms of the maze, and increased the percentage of time spent on the open arms; this is consistent with an 'anxiolytic-like' effect. Doses of 50, 500 and 1000 ng of $rANP_{1-28}$ produced no behavioral effects in the elevated plus-maze model. Pretreatment with a dopaminergic blocker, an α-adrenoreceptor or a β-adrenoreceptor antagonist antagonized the effect of 200 ng ANP_{1-28} in the elevated plus-maze test. A muscarinergic cholinergic blocker, a GABA receptor antagonist, a 5-HT receptor antagonist and an opiate antagonist were not able to modulate the 'anxiolytic-like' effects of ANP_{1-28}. These results suggest that a multiple neurotransmitter system activation might be responsible for the ANP_{1-28}-induced 'anxiolytic-like' activity.

Introduction

The atrial natriuretic peptides were first isolated from rat atrial secretory granules.[1] Atrial natriuretic peptide (ANP), a 28 amino acid peptide with biologically active 4–28 and 5–28 congeners, plays an important role in regulation of the fluid and electrolyte balances, as demonstrated by its potent natriuretic, vasorelaxant and aldosterone secretion-inhibiting activity. The presence and widespread distribution of immunoreactive ANP in the rat brain have been revealed by radioimmunnoassay[2] and immunohistochemistry.[3] ANP binding sites in the rat brain have been localized by autoradiographic techniques.[4] Furthermore, immunoreactive ANP is released from the rat hypothalamus[5] and ANP mRNA transcripts have been identified in the rat hypothalamus and porcine brain stem.[6] ANP exerts a central inhibitory effect on vasopressin and oxytocin release. Secretagogue-evoked ACTH secretion in vitro and corticotropin releasing-factor (CRH)-stimulated secretion of ACTH and cortisol in humans are suppressed by

Date received 7 March 1995
Date revised 10 April 1995
Date accepted 1 May 1995

Correspondence to: Prof. G. Telegdy, Department of Pathophysiology, Albert Szent-Györgyi Medical University, Semmelweis 1, 6701 Szeged, POB 531, Hungary. Tel. and Fax: (36)-62-310651.

atriopeptins. Dopaminergic and cholinergic neurotransmission have been detected in the behavioural responses to ANP: the delayed extinction in the active avoidance paradigm and the delayed response in the passive avoidance paradigm.[7] Dopaminergic, cholinergic and α-adrenergic neurotransmission have been found in the antiamnestic action of ANP.[8]

In the present study, an investigation was made of whether rat atrial natriuretic peptide (ANP_{1-28}) has any effect in the elevated plus-maze paradigm, and if so, what the roles of the different neurotransmitter systems are.

Materials and methods

Adult male Wistar rats, weighing 200–250 g were used. The animals were housed five per cage at room temperature and kept on a standard illumination schedule (lights on at 06:00). They had access to commercial food and tap water ad libitum.

In order to allow intracerebroventricular drug administration, all rats were implanted with a unilateral cannula aimed at the right lateral brain ventricle. Under pentobarbital anesthesia (Nembutal 35 mg/kg intraperitoneally, i.p.). the stainless steel cannula was stereotaxically inserted into the ventricle according to the coordinates found in the atlas of Pellegrino et al.[9] Cannulas were secured with dental acrylic cement. The adequancy of placement was checked by injecting methylene blue solution. Only data from animals with accurate placement were considered for further investigations. Rats were allowed a minimum of 5 days to recover from surgery before treatment with drugs began.

ANP_{1-28} was purchased from Bachem (CA, USA) or was synthetized by G. Tóth. It was dissolved in 0.9% saline and was injected icv in a volume of 2 μl in six doses (50, 100, 150, 200, 500 or 1000 ng per animal) to conscious, freely-moving rats, 30 min before the start of the experiment. The control animals received the same volume of 0.9% saline. The transmitter antagonists were injected i.p. 30 min before peripheral peptide or vehicle administration, as follows: haloperidol (G. Richter, Budapest), 5 μg/kg; phenoxybenzamine hydrochloride (Smith, Klein and French, UK), 2 mg/kg; propranolol hydrochloride (Imp. Chem. Indust. Ltd, UK), 10 mg/kg; atropine sulphate (EGYS, Budapest), 2 mg/kg; bicuculline methiodide (Sigma, USA), 1 mg/kg; methysergide hydrogenmaleinate (Sandoz, D), 5 mg/kg; naloxone hydrochloride (Endo Lab. Inc., USA), 0.1 mg/kg. Control animals received the same volume of 0.9% saline.

The elevated plus-maze model has been validated pharmacologically, behaviorally and biochemically as a test of animal anxiety.[10] The wooden maze consisted of two open and two enclosed arms, which were connected by a 10 × 10 cm central square and elevated to a height of 50 cm above the floor. Arms of the same type were positioned opposite each other. Rats were placed individually onto the central square of the maze, facing one of the open arms and allowed to explore the maze for 5 min. During this test period, the behavior of the rat was recorded by an observer sitting 1 m from the center of the maze, who scored the following measures: the numbers of entries into open and enclosed arms and the times spent in open and closed arms. These scores were converted into percentage values. The rationale is that the open arms are more fear-provoking, causing a decrease in the time spent in the open arms or the number of open arm entries. Anxiolytic compounds increase the percentage in time spent in, and the percentage number of entries into the open arms. Anxiogenic compounds have the opposite effect. The total number of entries into the arms provided a measure of the overall activity. The percentage of time spent in the open arms provided a measure of any changes in general activity. The maze was cleaned with a damp cloth between each trial.

Statistical analysis of the results was performed by one-way ANOVA followed by Tukey's test. A probability level of 0.05 was accepted as significant for the differences between the different groups. Values are given as means ± SEM of the percentage of time spent in and the number of entries in to open arms.

Results

Figure 1 shows the effects of icv administration of ANP_{1-28} (50, 100, 150, 200, 500 or 1000 ng) to rats tested in the elevated plus-maze paradigm. The 100 ng, 150 ng and 200 ng doses of ANP_{1-28} significantly

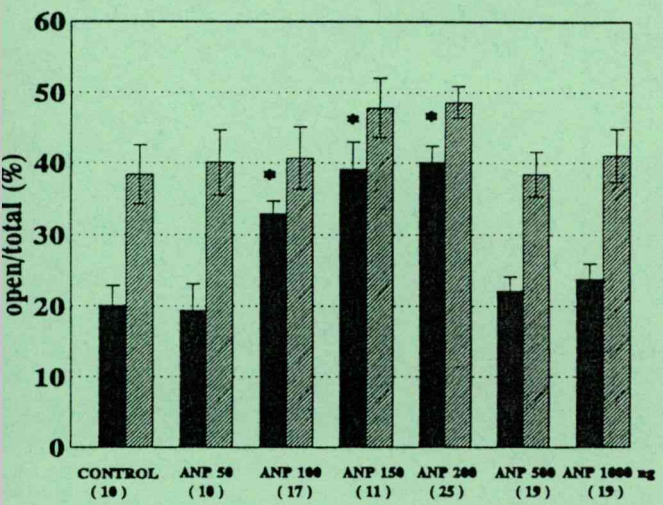

ig. 1 The effects of different doses of ANP on anxiety state of ats in the elevated plus-maze paradigm. Results are presented s mean ± SE *$P < 0.05$ (ANOVA, Tukey's test). Numbers in rackets represent the number of animals used.

ncreased the percentage of time spent in the open rms as compared with saline treated (control) nimals. The doses of 50, 500 and 1000 ng of ANP_{1-28} were ineffective (ANOVA $F_{6,110} = 12.81$, $P < 0.0001$, Tukey's test). A statistically significant ncrease in the percentage number of entries onto he open arms of the elevated plus-maze test was ot observed at any dose (ANOVA $F_{6,110} = 1.51$, $P < 0.18$, Tukey's test). From this experience the 00 ng dose of ANP_{1-28} was used to test the anxi-lytic activity in the elevated plus-maze paradigm.

In order to investigate the possible involvement f different receptors in the action of ANP_{1-28}, the ats were pretreated with different receptor block-rs, in doses which did not themselves change the ehavioral paradigm. The effects of different neuro-ransmitter antagonists relative to the control rats re shown in Figure 2. Haloperidol (5 μg/kg i.p.) retreatment prevented the 'anxiolytic-like' activity f ANP_{1-28}: there was not a statistically significant ifference in the percentage of time spent on the pen arms (ANOVA $F_{3,45} = 24.82$, $P < 0.0001$, ukey's test) and in the percentage number of ntries into the open arms of the elevated plus-maze st (ANOVA $F_{3,45} = 0.6$, $P < 0.61$, Tukey's test) s compared with vehicle-treated rats. The results f pretreatment with phenoxybenzamine (2 mg/kg, p.) 30 min before ANP_{1-28} administration revealed at the significant 'anxiolytic-like' activity of ANP_{1-28} was blocked. There was no increase in the ercentage of time spent in the open arms (ANOVA $F_{3,39} = 22.25$, $P < 0.0001$, Tukey's test), and no increase either in the percentage number of entries into the open arms (ANOVA $F_{3,39} = 1.77$, $P < 0.16$, Tukey's test) as compared with control rats. Following propranolol pretreatment (10 mg/kg, i.p.), there was no increase in the percentage of time spent in the open arms (ANOVA $F_{3,46} = 23.6$, $P < 0.0001$, Tukey's test) or in the percentage number of entries into the open arms (ANOVA $F_{3,46} = 3.99$, $P < 0.013$, Tukey's test) as compared with control animals. In the atropine pretreated group, there was a significant increase in the percentage of time spent in the open arms (ANOVA $F_{3,33} = 11.14$, $P < 0.0001$, Tukey's test) and a marked but not statistically significant increase in the percentage number of entries into the open arms of the elevated plus-maze paradigm as compared with control rats (ANOVA $F_{3,33} = 6.79$, $P < 0.0012$, Tukey's test). Pretreatment with the GABA receptor antagonist bicuculline (1 mg/kg, i.p.) did not block the increase in the percentage of time spent in the open arms (ANOVA $F_{3,36} = 5.51$, $P < 0.0001$, Tukey's test) or the increase in the percentage number of entries into the open arms of the maze (ANOVA $F_{3,36} = 0.85$, $P < 0.18$, Tukey's test) as compared with control animals. The increase in the percentage of time spent in the open arms was not affected by methysergide (0.5 mg/kg, i.p.) pretreatment (ANOVA $F_{3,36} = 16.02$, $P < 0.0001$, Tukey's test), nor was the increase in the percentage number of entries into the open arms (ANOVA $F_{3,36} = 2.66$, $P < 0.0001$, Tukey's test) as compared with control rats. Naloxone (0.1 mg/kg, i.p.) pretreatment did not block the increase in the percentage of time spent in the open arms (ANOVA $F_{3,29} = 10.43$, $P < 0.0004$, Tukey's test), nor the increase in the percentage number of entries into the open arms of the elevated plus-maze (ANOVA $F_{3,29} = 4.64$, $P < 0.01$, Tukey's test) as compared with control animals.

Discussion

The present results demonstrate that treatment with ANP_{1-28} in doses of 100, 150 or 200 ng increases the time spent in the open arms of the elevated plus-maze, indicating an anxiolytic response. This is in agreement with previous studies which dem-

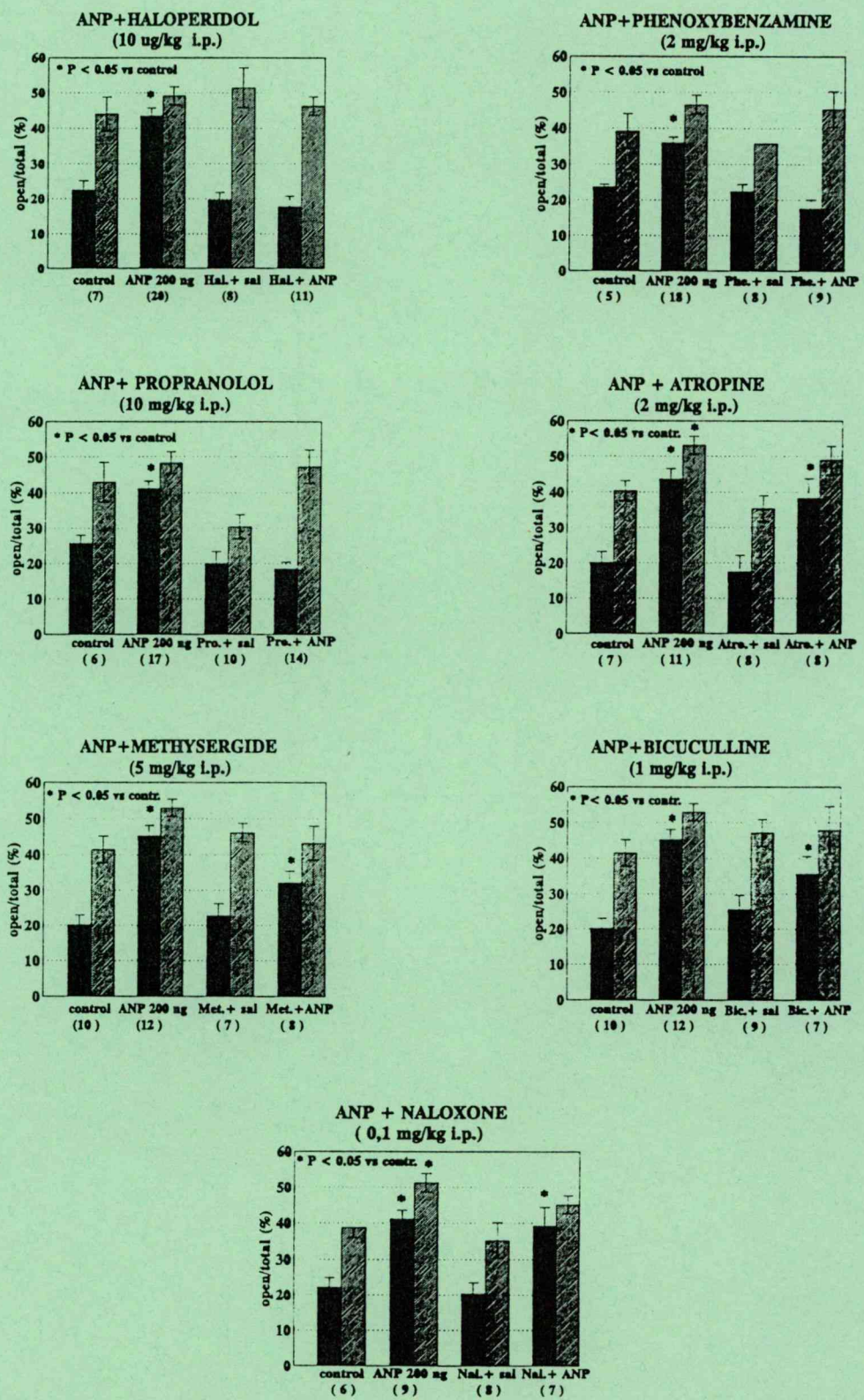

Fig. 2 The effects of different receptor blockers on ANP induced 'anxiolytic-like' state in rats scored in the elevated plus-maze paradigm. Results are presented as mean $\pm$ SE $^*P < 0.05$ (ANOVA, Tukey's test). Numbers in brackets represent the number of animals used.

onstrated 'anxiolytic' responses. Similar increases n general activity have been found for other 'anxiolytic' compounds, such as chlordiazepoxide, diazepam and phenobarbitone,[10] both in the elevated plus-maze test and in most other tests of anxiety. The elevated plus-maze test has an advantage over other conflict tests in that it requires only the spontaneous activity of the animals. Doses of 50, 500 or 1000 ng administered centrally were without effect. The 'anxiolytic-like' effect of 200 ng ANP_{1-28} was blocked by pretreatment with dopaminergic, or α- or β-adrenoreceptor antagonists. The muscarinergic cholinergic blocker, GABA receptor blocker and 5-HT receptor antagonists and the opiate antagonist were ineffective in modulating the 'anxiolytic-like' activity of ANP_{1-28}. None of the transmitter antagonists alone produced any behavioral changes in the doses used.

ANP has been reported to influence the hypothalamo-pituitary-adrenal axis. It has been found that intravenous injection of ANP inhibits hemorrhage-induced ACTH release in rat[11] and also inhibits the CRH-stimulated secretion of ACTH and cortisol in man.[12] Consonant evidence from in vivo immunoneutralization studies suggests that ANP exerts an inhibitory effect on ACTH release and plasma corticosterone concentrations.[13] It has been shown that in isolated perifused rat anterior pituitary cells atriopeptin 1–28 and 5–28 potently suppress the corticotropin secretion elicited by the 41-residue corticotropin-releasing factor and arginine-vasopressin at concentrations which are in the range of those in the hypophyseal portal vessel blood.[14] Nuclei involved in the regulation of anterior pituitary hormone secretion contain cells immunoreactive for ANP, suggesting that ANP may moderate pituitary hormone release. Consistent with this hypothesis, ANP has been shown to be released from rat hypothalamic fragments in vitro,[15] to bind to anterior pituitary cells[16] and to increase the cellular content of cCMP. In addition, ANP_{1-28} may act through circumventricular organs and not only on the pituitary gland.

Besides altering the release of stress hormones, ANP can influence the neurotransmitter metabolism or the action of neurotransmitters. It has been reported that peripherally (intravenously) administered dopamine receptor blockers such as haloperidol or chlorpromazine in a dose of 50 μg inhibit the natriuretic response to atrial natriuretic factor.[17] Haloperidol and domperidone prevented the natriuretic responses to centrally administered ANP.[18] It has been found that centrally administered ANP has an inhibitory effect on the dopaminergic neurotransmission in the central nervous system of rats.[19] The other catecholaminergic systems are involved in the action of ANP. It has been shown that the basal release of irANP is a product of the activation and α- and β-adrenoreceptors by their endogenous ligands.[20] The hypothalamic CRF release induced by acetylcholine in rats was blocked by continuous administration of ANP.[21] The roles of different neurotransmitter systems in mediating the behavioral effects of ANP in rats have been examined. The involvement of dopaminergic and cholinergic systems in ANP-induced delayed extinction in the active avoidance paradigm, and delayed response in the passive avoidance paradigm was observed.[7] Peripheral pretreatment with a dopaminergic (haloperidol), a β-adreno- (propranolol) or a cholinergic (atropine) receptor blocker inhibited the antiamnestic action of ANP.[8]

In summary, the present study appears to demonstrate that the 'anxiolytic-like' activity caused by ANP_{1-28} can be inhibited by dopaminergic, or α- or β-adrenoreceptor antagonists. We found no evidence of the involvement of cholinergic, GABAergic, serotoninergic or opiate neurotransmission in mediation of the 'anxiolytic-like' effect of ANP_{1-28}. Our experiments appear to indicate the involvement of different neurotransmitter systems in the mediation of ANP-induced behavioral action.

Acknowledgements

The work has been supported by the Ministry of Social and Welfare of Hungary T-11-549/1993. OTKA (T.3. 1354. T-6084) and FEFA 1008.

References

1. De Bold, A. J., Borenstein, H. B., Veress, A. T. and Sonnenberg, H. A rapid and potent natriuretic response to intravenous injection of atrial myocardial extract in rats. Life Sci. 1981; 28: 89–94.
2. Tanaka, I., Misono, K. S. and Inagami, I. Atrial natriuretic factor in rat hypothalamus, atria and plasma. Determination by specific radioimmunoassay. Biochem. Biophys. Res. Commun. 1984; 124: 663–668.

3. Sapre, C. B., Standaert, D. G., Currie, M. G., Schwartz, D., Geller, D. M. and Needleman, P. Atriopeptin-immunoreactive neurons in the brain: Presence in cardiovascular regulatory areas. Science 1985; 227: 1047–1049.
4. Gibson, T. R., Wildey, G. M., Manaker, S. and Glembotski, C. C. Autoradiographic localisation of atrial natriuretic peptide binding sites in the rat central nervous system and adrenal gland. J. Neurosci. 1986; 6: 2004–2011.
5. Yeung, V. T. F., Lai, C. K., Cockram, C. S. et al. Atrial natriuretic peptide in the central nervous system. Neuroendocrinology 1991; 53: 18–24.
6. Gardner, D. G., Vlasuk, G. P., Baxter, J. D., Fiddes, J. C. and Lewicki, J. A. Identification of atrial natriuretic gene transcripts in the central nervous system of the rat. Proc. Natl. Acad. Sci. USA 1987; 84: 2175–2199.
7. Bidzseranova, A., Varga, J. and Telegdy, G. The effect of receptor blockers on brain natriuretic peptide-32-induced action on passive avoidance behaviour in rats. Neuropeptides 1992; 22: 107–110.
8. Bidzseranova, A., Telegdy, G. and Tóth, G. The effects of receptor blockers on atrial natriuretic peptide-induced action on passive avoidance behaviour in rats. Pharmacol. Biochem. Behav. 1991; 40: 237–239.
9. Pellegrino, L. J., Pellegrino, A. S. and Cushman, A. J. A stereotactic atlas of the rat brain. New York: Plenum, 1979.
10. Pellow, S., Chopin, P., File, S. E. and Briley, M. Validation on open:closed arm entries in an elevated plus-maze as a measure of anxiety in the rat. J. Neurosci. Methods 1985; 14: 149–167.
11. Hattori, T., Hashimoto, K., Inouge, H. et al. Effect of synthetic natriuretic peptide on haemorrhage-induced adrenocorticotropin secretion of the rat. Endocrinol. Japn 1986; 33(5): 533–539.
12. Kellner, M., Wiedmann, K. and Holsboer, F. Atrial natriuretic factor inhibits the CRH-stimulated secretion of ACTH and cortisol in man. Life Sci. 1992; 50: 1835–1842.
13. Dayanithi, G. and Antoni, F. A. Atriopeptins are potent inhibitors of ACTH secretion by rat anterior pituitary cells in vitro: involvement of atrial natriuretic factor receptor domain of membrane-bound guanyl-cyclasem. J. Endocrinol. 1990; 125: 39–44.
14. Fink, G., Dow, R. C., Casley, D. et al. Atrial natriuretic peptide is a physiological inhibitor of ACTH release: evidence from immunoneutralization in vivo. J. Endocrinol. 1991; 131: R9–12.
15. Shibasaki, T., Naruse, M., Naruse, K., et al. Atrial natriuretic factor is released from rat hypothalamus in vitro. Biochem. Biophys. Res. Comm. 1986; 136: 590–596.
16. Quiron, R., Dalphe, M., De Lean, A., Gutkowska, S., Cantin, M. and Genert, J. Atrial natriuretic factor (ANF) binding sites in brain and related structures. Peptides 1984; 5: 1167–1170.
17. Martin-Grez, M., Briggs, J. P., Schubert, G. and Schnermann, J. Dopamine receptor antagonists inhibit the natriuretic response to atrial natriuretic factor (ANF). Life Sci. 1985; 36: 2171–2176.
18. Israel, A., Torres, M. and Barbella, Y. Evidence for dopaminergic mechanism for the diuretic and natriuretic action of centrally administered atrial factor. Cell. Mol. Neurobiol. 1989; 9(3): 365–378.
19. Nakao, K., Katsumura, G., Mari, N. et al. Inhibitory effect of centrally administered atrial natriuretic polypeptide on the brain dopaminergic system in rats. Eur. J. Pharmacol. 1986; 131: 171–177.
20. Bush, A. J., Huang, W., Copolov, D. L. and Lim, A. T. W. Hypothalamic atrial natriuretic peptide secretion plasticity: differential modulation of alpha and beta adrenoreceptors. Neuroendocrinology 1990; 52: 65–69.
21. Takao, T., Hashimoto, K. and Ota, Z. Effect on atrial natriuretic peptide on acethylcholine-induced release of corticotropin-releasing factor from rat hypothalamus in vitro. Life Sci. 1988; 42: 1199–1203.

NEUROPEPTIDES

Neuropeptides (1995) 29, 145–149

C-type Natriuretic Peptide can Modify the Acute and Chronic Effects of Morphine

E. BABARCZY, Z. VÍZI, G. TÓTH* and G. TELEGDY

*Department of Pathophysiology and *Department of Medical Chemistry, Albert Szent-Györgyi Medical University, Szeged, POB 531, Hungary*

Abstract—Different doses (0.2–200 ng) of C-type natriuretic peptide (CNP) were administered into the lateral brain ventricle, and morphine (5 mg/kg) was injected subcutaneously. The analgesic effect was measured in a tail-flick test, in CFLP mice. CNP administered centrally did not itself affect pain sensitivity, but it depressed the acute antinociceptive effect of morphine 30 min after icv (0.2, 2 or 20 ng) CNP administration and the 2 and 20 ng doses also decreased this action after 60 min. CNP in a 0.2 or 200 ng dose blocked the development of acute tolerance to morphine after 30 min, as did the 200 ng dose at 60 min. CNP in a 0.2 ng dose blocked the development of chronic tolerance to morphine after 30 min, but there was no effect at 60 min. Morphine withdrawal signs were studied by injecting naloxone (1 mg/kg sc). There was no significant difference in symptoms between the tolerant group and the animals treated with CNP.

Introduction

The natriuretic peptide family consists of atrial natriuretic peptide (ANP), brain natriuretic peptide (BNP) and C-type natriuretic peptide (CNP). CNP was originally isolated from porcine brain.[1] When injected intravenously into rats,[1] CNP was not so hypotensive, diuretic or natriuretic as ANP and BNP. Komatsu et al have demonstrated that the tissue distribution of CNP in the central nervous system is different from those of ANP and BNP.[2] The concentration of CNP in the human brain[3] and also in human cerebrospinal fluid[4] is higher than those of ANP and BNP. Thus, CNP is thought to act mainly as a neuropeptide.

Previously, the effects of ANP and BNP on the development of analgesic tolerance to and dependence on morphine were investigated. It was found that centrally administered ANP[5] and BNP (Babarczy et al unpublished data) diminish the development of acute and chronic morphine tolerance. A continuation of those experiments, results relating to the antinociceptive effect in male CFLP mice of the other member of the natriuretic peptide family, CNP, are now presented.

Date received 11 February 1995
Date accepted 28 February 1995

Correspondence to Prof. Gyula Telegdy, Dept. of Pathophysiology, A. Szent-Györgyi Med. Univ., Semmelweis u. 1., POB 531, Szeged 6701, Hungary.

Materials and methods

Animals. Male CFLP mice (30 ± 5 g) of an outbred strain (LATI, Gödöllő, Hungary) were used. They were kept under a standard light-dark cycle (lights on between 6.00 a.m. and 6.00 p.m.) with food and water available ad libitum. At least 1 week of habituation was allowed before the beginning of the experiments. The animals were kept and treated according to the rules of the Ethical Committee for the Protection of Animals in Research (Albert Szent-Györgyi Medical University).

Surgery. For icv cannulation, mice were anesthetized with sodium pentobarbital (Nembutal, CEVA, France; 50 mg/kg intraperitoneally), and a polyethylene cannula was inserted into the right lateral cerebral ventricle. The experiments started 4 days after intracerebroventricular (icv) cannulation. Upon conclusion of the experiments, 10 μl methylene blue was injected into the ventricle of the decapitated animals and the position of the cannula was inspected visually. Animals with an improper cannula placement were excluded from the final statistical analysis.

For chronic tolerance and withdrawal studies, animals were lightly anesthetized with ether, and a morphine pellet was implanted subcutaneously (sc) into the sacral area through a small section in the neck area.

Treatments. CNP was synthetized by one of the authors (G. Tóth). For icv treatment, the peptide was dissolved in artificial cerebrospinal fluid and injected in a volume of 2 μl. In all experiments involving measurement of the antinociceptive effect, morphine-HCl (Alkaloida, Tiszavasvári, Hungary; 5 mg/kg sc) was used. In acute tolerance studies, 100 mg/kg of morphine-HCl (sc) was used as a tolerance-inducing dose. In chronic tolerance and withdrawal studies, pellets containing 35 mg morphine were implanted. The precipitated withdrawal syndrome was induced with naloxone-HCl, 1 mg/kg sc (Sigma, St Louis, USA).

Procedures. All experiments were started with an initial tail-flick latency measurement, pain sensitivity being measured immediately before and 15, 30, 60 and 120 min after the test morphine challenge. The heat-radiant tail-flick method of D'Amour and Smith[6] was used. The antinociceptive effect was expressed according to the equation:

$$\text{antinociceptive effect} = \frac{TF_n - TF_0}{TF_{max} - TF_0} \times 100$$

where TF_0 is the tail-flick latency in the preliminary test mentioned above, or (in all tolerance studies) before the injection of the test dose of morphine, TF_n is the value of a repeated corresponding measurement n (15, 30, 60 or 120) min after morphine injection, and TF_{max} indicates the cut-off time (20 s). The control tail-flick latencies (TF_0) were between 2.5 and 3.0 s in all groups.

The following experiments were conducted:

1. The effects of CNP on pain sensitivity were studied.
2. In studies with CNP on the acute antinociceptive effect of a single dose of morphine, the peptide was given icv 60 min prior to the test dose of morphine (5 mg/kg sc), and the pain sensitivity was assessed 30 and 60 min later.
3. In acute tolerance studies, animals were pretreated with the peptide and 60 min later a tolerance-inducing dose of morphine (100 mg/kg sc) was injected; 6 h later, a test dose of morphine (5 mg/kg) was used to assess the antinociceptive effect.
4. In chronic tolerance and withdrawal studies, the peptide was given 60 min before the morphine-containing pellets were implanted. The peptide treatment was repeated three times 24 h apart. On day 4, a test dose of morphine (5 mg/kg) was given and the antinociceptive effect was determined. 3 h later, the animals received naloxone (1 mg/kg sc) and the precipitated withdrawal signs were assessed. The precipitated abstinence syndrome was measured by scoring the latency of the appearance of stereotyped jumping from a circular platform 35 cm in diameter and 70 cm high. A cut-off time of 900 s was used.[7] The body temperatures and weights of all animals were measured 30 and 60 min after the injection of naloxone, and the changes in both parameters were calculated.

Statistical analysis. Statistical analysis of the data was made by ANOVA. For significant ANOVA

Table 1 Effects of CNP on pain sensitivity

Time (min)	*Control*	*C-type natriuretic peptide*			
		0.2 ng	*2 ng*	*20 ng*	*200 ng*
15	−8.4±6.3	0.6±2.1	−1.0±0.8	−0.1±0.6	0.8±0.8
30	−9.9±7.2	−1.0±1.0	−0.4±1.1	−0.2±0.4	0.6±0.4
60	−9.1±7.2	−1.7±0.8	−2.4±0.4	−0.7±0.4	−0.4±0.9
120	−9.1±9.6	−1.6±1.3	−3.6±0.9	−0.2±0.8	−0.5±0.8

Values are means±SEM for treated animals; numbers of animals per group: control: 8; 0.2 ng CNP: 6; 2 ng CNP: 7; 20 ng CNP: 7; 200 ng CNP: 6.

values, groups were compared by Tukey's test for multiple comparisons with unequal cell size. A probability level of 0.05 was accepted as indicating significant differences.

Results

Effects of CNP on tail-flick latency

Graded doses of CNP (0.2, 2, 20 or 200 ng) 15, 30, 60 or 120 min after icv administration had no analgesic effect: $F(4,29) = 1.35$, $P < 0.2$ (Table 1).

Effects of CNP on challenge dose of morphine

A single dose of morphine caused a near-maximal analgesic effect. In doses of 0.2, 2 or 20 ng, CNP inhibited morphine analgesia 30 min after the narcotic challenge: $F(4,124) = 8.81$, $P < 0.01$; doses of 2 or 20 ng decreased this action after 60 min too: $F(4,124) = 6.7$, $P < 0.01$ (Fig. 1).

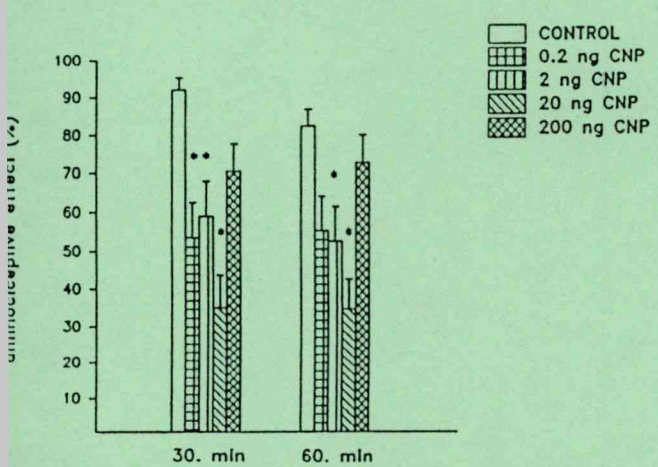

Fig. 1 Effects of CNP icv on acute antinociceptive action of morphine (5 mg/kg) in tail-flick test. The peptide was given icv 0 min prior to the test dose of morphine and the pain sensitivity was assessed 30 and 60 min later. Numbers of animals per group: control, 32; 0.2 ng CNP, 25; 2 ng CNP, 23; 20 ng CNP, 23; 200 ng CNP, 26. Values shown are means±SEM (*: $P < 0.01$).

Effects of CNP on acute morphine tolerance

Acute tolerance was observed 6 h after a tolerance-inducing dose of morphine was given. CNP in doses of 0.2 or 200 ng blocked the development of acute tolerance to morphine 30 min after the administration of a test dose of morphine: $F(5,82) = 5.87$, $P < 0.01$; and a dose of 200 ng also did so after 60 min: $F(5,82) = 3.57$, $P < 0.01$ (Fig. 2).

Effects of CNP on chronic tolerance and withdrawal

Chronic tolerance to morphine was observed in animals implanted with morphine pellets. CNP in a dose of 0.2 ng blocked the development of chronic tolerance to morphine 30 min after the administration of a test dose of morphine: $F(5,92) = 16.1$, $P < 0.01$; but there was no effect after 60 min, except for a significant difference between the control and

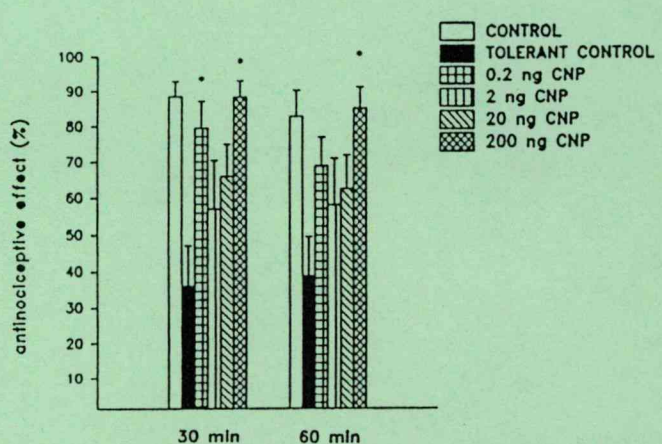

Fig. 2 Effects of CNP icv on development of acute tolerance to morphine. Animals were pretreated with the peptide and 60 min later a tolerance-inducing dose of morphine (100 mg/kg sc) was injected; 6 h later, a test dose of morphine (5 mg/kg) was used to assess the antinociceptive effect. Numbers of animals per group: control, 17; tolerant control, 15; 0.2 ng CNP, 18; 2 ng CNP, 11; 20 ng CNP, 14; 200 ng CNP, 13. Values shown are means±SEM (*: $P < 0.01$).

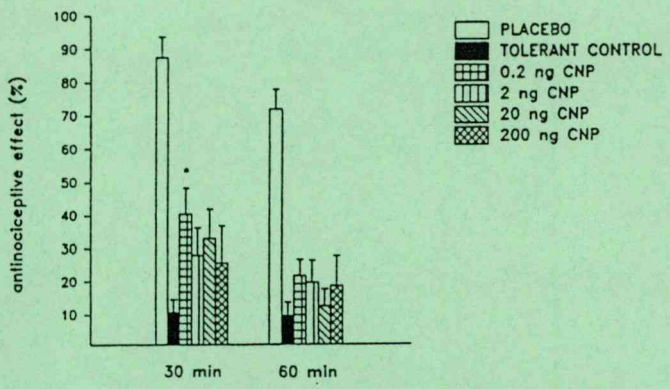

Fig. 3 Effects of CNP icv on development of chronic tolerance to morphine. The peptide was given 60 min before the morphine-containing pellets were implanted. The peptide treatment was repeated three times 24 h apart. On day 4, a test dose of morphine (5 mg/kg) was given and the antinociceptive effect was determined. Numbers of animals per group: placebo, 22; tolerant control, 19; 0.2 ng CNP, 18; 2 ng CNP, 15; 20 ng CNP, 13; 200 ng CNP, 11. Values shown are means ± SEM (*: $P < 0.01$).

tolerant control groups: $F(5,92) = 19.13$, $P < 0.01$ (Fig. 3).

In naloxone-precipitated withdrawal studies, there was no significant difference in symptoms between the tolerant group and animals treated with CNP.

Discussion

The present results revealed an interaction between centrally administered CNP and morphine. Dose-related studies were carried out to determine the effects of CNP on pain sensitivity, acute morphine analgesia, acute and chronic tolerance and withdrawal. CNP did not affect pain perception when it was given alone icv. This might indicate the lack of an acute interaction of CNP at the opiate receptor site. However, when CNP was injected before a challenge dose of morphine, it caused an attenuation in pain sensitivity. CNP inhibited the development of acute and chronic tolerance to morphine, but naloxone-precipitated withdrawal symptoms were not affected by CNP.

Previous data are available from our laboratory on the effects of other neuropeptides on pain sensitivity. It has been found that two members of the natriuretic peptide family, ANP and BNP, diminish the development of acute and chronic morphine tolerance, suggesting a potential endogenous role for these peptides in narcotic addiction[5] (Babarczy et al unpublished data). Similar doses of natriuretic peptides administered icv had no analgesic effects themselves. However, when these peptides were injected before a challenge dose of morphine they caused a dose-related attenuation in pain sensitivity. ANP and BNP caused changes basically similar to those of CNP, although several differences were observed. Graded doses of peptides were used in these studies, and not linear dose-effect plots, but rather an inverted bell-shaped dose-response relationship was observed. The inverted bell-shaped dose-effect phenomenon is known from the literature.[8,9] In acute studies, a 20 ng dose of ANP, the same dose of CNP, and then again a 0.2 ng dose of BNP produced the most prominent block in the nociceptive effect. In the effects of these peptides on acute morphine tolerance, different responses were observed. ANP and CNP were the most effective in the 200 ng dose, as was BNP in the 20 pg dose. BNP exhibited a bell-shaped dose-response curve. All three peptides influenced chronic morphine tolerance: it was blocked by 20 or 200 ng ANP, 0.2, 2 or 200 ng BNP, and also by CNP, but this peptide displayed a significant effect only in the 0.2 ng dose. The effects of the natriuretic peptides were investigated on the development of naloxone-precipitated withdrawal syndromes. Neither naloxone-induced jumps nor changes in body weight and temperature were affected by central administration of natriuretic peptides. The development of a tolerance to and the development of a dependence upon narcotic analgesics do not necessarily occur in parallel[10] and it is likely that these peptides act differently on these processes. The amino acid sequences of the three peptides are known to be highly homologous, with a common ring frame formed by a disulfide linkage,[1] which explains why this action of CNP displays a similar profile to those of ANP and BNP.

Acknowledgements

The work was supported by the Hungarian Ministry of Social Affairs and Health (T-11, 549/93) and OTKA (T/3, 1354, and T 006084).

References

1. Sudoh, T., Minamino, N., Kangawa, K. and Matsuo, H. C-type natriuretic peptide (CNP): a new member of natriuretic peptide family identified in porcine brain. Biochem. Biophys. Res. Commun. 1990; 168: 863–870.

2. Komatsu, Y., Nakao, K., Suga, S. et al. C-type natriuretic peptide (CNP) in rats and humans. Endocrinology 1991; 129: 1104–1106.
3. Ogawa, Y., Nakao, K., Nakagawa, O. et al. Human C-type natriuretic peptide: characterization of the gene and peptide. Hypertension 1992; 19: 809–813.
4. Kaneko, T., Shirakami, G., Nakao, K. et al. C-type natriuretic peptide (CNP) is the major natriuretic peptide in human cerebrospinal fluid. Brain Res. 1993; 612: 1–2: 104–109.
5. Azarov, A., Szabó, G. and Telegdy, G. Effects of atrial natriuretic peptide on acute and chronic effects of morphine. Pharmacol. Biochem. Behav. 1992; 43: 193–197.
6. D'Amour, F. E. and Smith, D. L. A method for determining loss of pain sensation. J. Pharmacol. Exp. Ther. 1941; 72: 74–79.
7. Kovács, G. L., Szontágh, L., Baláspiri, L., Hódi, K., Bohus, P. and Telegdy, G. On the mode of action of an oxytocin derivative (Z-Pro-D-Leu) on morphine dependence in mice. Neuropharmacology 1981; 20: 647–651.
8. Kovács, G. L., Borthaiser, Z. and Telegdy, G. Oxytocin reduced intravenous heroin self-administration in heroin tolerant rats. Life Sci. 1985; 37: 17–26.
9. Sarnyai, Z., Babarczy, E., Kriván, M. et al. Selective attenuation of cocaine-induced stereotyped behavior by oxytocin: putative role of basal forebrain target sites. Neuropeptides 1991; 19: 51–56.
10. Levine, R. R. The pharmacologic aspects of drug abuse and drug dependence. In: Levine, R. R., ed. Pharmacology, drug action and drug reactions. Boston: Little, Brown and Co. 1978: 341–370.

2.13.

Neuropeptides (1996) 30 (1), 59–65

Effect of receptor blockers on brain natriuretic peptide and C-type natriuretic peptide caused anxiolytic state in rats

Éva Bíró[1], Gábor Tóth[2], Gyula Telegdy[1]

[1]Department of Pathophysiology, Albert Szent-Györgyi Medical University, Szeged, Hungary.
[2]Department of Medical Chemistry, Albert Szent-Györgyi Medical University, Szeged, Hungary.

Summary Effect of different doses of centrally administered brain natriuretic peptide (BNP) and C-type natriuretic peptide (CNP) were examined in rats with respect to anxiolytic properties in an elevated plus-maze model. BNP in doses of 100, 200 and 400 ng, and CNP in doses of 100 and 200 ng abolished the normal preference for the closed arms of the maze, and increased the percentage time spent in the open arms; this is consistent with an 'anxiolytic-like' effect. Doses of 50 and 1000 ng BNP, and of 25, 50, 400 and 1000 ng CNP produced no behavioural effects in the elevated plus-maze model. Pretreatment with an α-adrenoreceptor antagonist or a muscarinergic cholinergic blocker, antagonized the effect of 200 ng BNP in the elevated plus-maze test. The 'anxiolytic-like' effects of a BNP were not modulated by a dopaminergic blocker, an α-adrenoreceptor antagonist, a GABA receptor antagonist, a 5-HT receptor antagonist or an opiate antagonist. The 'anxiolytic-like' effect of CNP was prevented by a dopamine receptor antagonist, or an α- or β-adrenoreceptor blocker but not by a muscarinergic cholinergic blocker, a GABA receptor, a 5-HT receptor antagonist or an opiate receptor antagonist. These results suggest that multiple neurotransmitter system activation might be responsible for the BNP and CNP-induced 'anxiolytic-like' activity.

INTRODUCTION

The natriuretic peptide system consists of the atrial (ANP), BNP and CNP natriuretic peptides; at least three subtypes of receptors exist in the central nervous system of mammals and participate not only in the regulation of the homeostasis of the fluid, electrolytic balance and blood pressure, but also in the activity of the central nervous system.[1] BNP and CNP share similar cysteine-ring structures with ANP,[2–4] and the interpretation of previous physiological studies using ANP antibodies has been rendered more difficult by the discovery of these peptides. Intravenous administration of synthetic BNP into anesthetized rats elicits natriuretic, diuretic and hypotensive activities comparable to those induced by α-hANP.[5] Intracerebroventricular (i.c.v.) administration of BNP antagonized the central endothelin-induced pressor response, plasma catecholamine and ACTH secretion.[6] Polymerase chain reaction and in situ hybridization analysis demonstrated that ANP and CNP mRNA are coexpressed (and potentially colocalized) in several hypothalamic loci, suggesting an interaction in the regulation of the reproductive, adrenocortical and neurohypophyseal axes.[7] In our previous work, an 'anxiolytic-like' action of ANP was found in an elevated plus-maze model of anxiety, with increased corticotropin releasing factor like immunoreactivity (CRF-LI) in different hypothalamic and extrahypothalamic brain regions after central ANP administration in rats (unpublished results).

In the present study to establish the involvement of neurotransmitters in the BNP and CNP-induced anxiolytic action, the animals were pretreated with different

Received 26 June 1995
Accepted 11 September 1995

Correspondence to: Prof. G. Telegdy, Department of Pathophysiology, Albert Szent-Györgyi Medical University, Semmelweis 1, 6701 Szeged, P.O. Box 531, Hungary. Tel. and Fax. (36)-62-310-651.

receptor blockers which had earlier been proved to be effective in modifying the action of a number of peptides in the same paradigm.

MATERIALS AND METHODS

Animals

Adult male Wistar rats (LATI, Gödöllö, Hungary) weighing 180–220 g were used. They were housed 5 per cage with food and water available ad libitum in an environmentally controlled facility (12-h light/12-h dark cycle with lights on at 06.00). Rats were handled daily for 1 week before the experiment to minimize the effects of non-specific stress.

Surgery

In order to allow i.c.v. peptide administration, all rats were implanted with a unilateral cannula aimed at the right lateral brain ventricle. The stainless steel cannula was inserted stereotaxically into the ventricle according to the coordinates found in the atlas of Pellagrino et al,[8] under pentobarbital (Nembutal 35 mg/kg, i.p.) anesthesia. The cannula was secured with dental acrylic cement. Rats were allowed a minimum of 5 days to recover from surgery before peptide treatment began.

Rat BNP and CNP were purchased from Bachem (CA, USA) or were synthesized by G. Tóth. They were dissolved in 0.9% saline and injected i.c.v. in a volume of 2 µl in different doses (25, 50, 100, 200, 400 or 1000 ng per animal) to conscious, freely-moving rats. The control animals received the same volume of 0.9% saline.

The transmitter antagonists were injected intraperitoneally (i.p.) 30 min before peptide or saline administration, as follows: haloperidol (G. Richter, Budapest), 5 µg/kg; phenoxybenzamine hydrochloride (Smith, Klein and French, UK), 2 mg/kg; propranolol hydrochloride (Imp. Chem. Indust. Ltd, UK), 10 mg/kg; atropine sulphate (EGYS, Budapest), 2 mg/kg; bicucullinemethiodide (Sigma, USA), 1 mg/kg; methysergide hydrogenmaleinate (Sandoz, D), 5 mg/kg; naloxone hydrochloride (Endo Lab. Inc., USA), 0.1 mg/kg. Control animals received the same volume of 0.9% saline.

Behavioural testing

The elevated plus-maze model has been validated pharmacologically, behaviourally and biochemically as a test of animal anxiety.[9] The wooden maze consisted of two open and two enclosed arms, which were connected by a 10x10 cm central square and elevated to a height of 50 cm above the floor. Arms of the same type were positioned opposite each other. Rats were placed individually onto the central square of the maze, facing one of the open arms, and were allowed to explore the maze for 5 min. During this test period, the behaviour of the rat was recorded by an observer sitting 1 m from the centre of the maze, who scored the numbers of entries into the open and enclosed arms and the times spent in the open and closed arms. These scores were converted into percentages. The rationale is that the open arms are more fear-provoking, causing a decrease in the time spent in the open arms or the number of open arm entries. Anxiolytic compounds increase the percentage time spent in, and the frequency of entries into the open arms. Anxiogenic compounds have the opposite effect. The total number of entries into the arms provided a measure of the overall activity. The percentage time spent in the open arms provided a measure of any changes in general activity. The maze was cleaned with a damp cloth after each trial.

Statistical analyses

All data are presented as means ± SEM. Data were analysed by one-way ANOVA followed by Tukey's test. A probability level of 0.05 was accepted as indicating a statistically significant difference.

RESULTS

Table 1 shows the effects of i.c.v. administration of BNP (50, 100, 200, 400 or 1000 ng) to rats tested in the elevated plus-maze paradigm. The 100 ng, 200 ng and 400 ng doses of BNP significantly increased the percentage of time spent in the open arms as compared with control animals. The doses of 50 ng and 1000 ng of BNP were ineffective (ANOVA F5, 57=5.83, $P<0.0002$, Tukey's test). A statistically significant increase in the frequency of entries into the open arms of the elevated plus-maze test was not observed at any dose (ANOVA F5, 57=0.81, $P<0.547$, Tukey's test).

The 200 ng dose of BNP was selected to test the anxiolytic activity in the elevated plus-maze test. In order to investigate the possible involvement of different receptors in the action of BNP, the rats were pretreated with different receptor blockers, in doses which did not themselves change the behavioural paradigm; these blockers are shown in Table 2. Pretreatment with the dopaminergic receptor blocker haloperidol (10 µg/kg i.p.) did not prevent the 'anxiolytic-like' activity of BNP: there was a statistically significant difference in the percentage time spent in the open arms (ANOVA F3, 36=5.93, $P<0.0024$, Tukey's test) and a marked but not statistically significant increase in the frequency of entries into the open arms of the elevated plus-maze test (ANOVA F3, 36=1.29, $P<0.295$, Tukey's test) as compared with the control

Table 1 Effects of different doses of CNP on anxiety state of rats tested in the elevated plus-maze paradigm. Results are presented as means ± SE[a] $P < 0.05$ (ANOVA. Tukey's test)

Groups	No. of animals	Open/total time %	Open/total entries
Control (saline)	7	29.53 ± 2.48	48.21 ± 5.74
25 ng CNP	7	26.65 ± 2.68	35.48 ± 3.86
50 ng CNP	9	38.98 ± 3.90	41.88 ± 5.65
100 ng CNP	9	54.51 ± 7.46[a]	46.16 ± 4.68
200 ng CNP	9	66.69 ± 3.48[a]	54.31 ± 4.48
400 ng CNP	9	58.3 ± 6.35	54.29 ± 5.53
1000 ng CNP	9	31.45 ± 3.71	41.81 ± 3.5

Table 2 Effects of neurotransmitter blockers on CNP-induced anxiolytic state in rats. Results are presented as means ± SE[a] $P < 0.05$ (ANOVA, Tukey's test)

Groups	No. of animals	Open/total time %	Open/total entries
Haloperidol (10 μg/kg i.p.)			
Control (saline)	6	23.20 ± 2.89	35.56 ± 3.98
CNP (200 ng i.c.v.)	7	50.14 ± 4.13[a]	56.19 ± 6.24
Haloperidol + saline	6	28.3 ± 4.13	41.67 ± 4.77
Haloperidol + CNP	7	35.64 ± 6.45	50.00 ± 5.59
Phenoxybenzamine (2 mg/kg.i.p.)			
Control (saline)	6	24.94 ± 1.97	47.92 ± 4.2
CNP (200 ng i.c.v.)	8	44.85 ± 5.97[a]	41.49 ± 3.43
Phenoxybenzamine + saline	7	29.87 ± 3.04	55.17 ± 6.49
Phenoxybenzamine + CNP	7	49.52 ± 3.12	49.52 ± 4.01
Propranolol (10 mg/kg i.p.)			
Control (saline)	6	24.81 ± 1.78	40.20 ± 4.75
CNP (200 ng i.c.v.)	8	44.41 ± 3.06[a]	47.44 ± 3.72[a]
Propranolol + saline	7	25.44 ± 3.99	35.66 ± 7.32
Propranolol + CNP	9	25.38 ± 1.90	47.59 ± 5.25
Atropine (2 mg/kg i.p.)			
Control (saline)	7	22.32 ± 2.43	41.77 ± 4.47
CNP (200 ng i.c.v.)	7	52.72 ± 6.32[a]	47.72 ± 5.04
Atropine + saline	8	19.5 ± 2.73	40.73 ± 5.30
Atropine + CNP	8	52.16 ± 2.16[a]	37.17 ± 2.18
Methysergide (5 mg/kg i.p.)			
Control (saline)	7	20.92 ± 2.14	41.43 ± 3.84
CNP (200 ng i.c.v.)	8	50.96 ± 2.73[a]	43.58 ± 3.81
Methysergide + saline	7	19.03 ± 0.78	43.55 ± 4.68
Methysergide + CNP	7	50.75 ± 3.38[a]	48.62 ± 4.76
Bicuculline (1 mg/kg i.p.)			
Control (saline)	7	20.29 ± 3.85	38.5 ± 4.58
CNP (200 ng i.c.v.)	8	44.69 ± 5.13[a]	44.11 ± 2.58
Bicuculline + saline	8	22.00 ± 3.15	45.89 ± 4.46
Bicuculline + CNP	7	50.35 ± 2.16[a]	43.81 ± 5.22
Naloxone (0.1 mg/kg i.p.)			
Control (saline)	6	21.13 ± 2.87	40.24 ± 2.82
CNP (200 ng i.c.v.)	8	47.89 ± 2.74[a]	45.77 ± 2.63[a]
Naloxone + saline	7	23.67 ± 3.16	41.30 ± 4.39
Naloxone + CNP	7	45.87 ± 3.81[a]	43.79 ± 4.56

rats. Pretreatment with phenoxybenzamine, an α-adrenoreceptor antagonist, in a dose of 2 mg/kg i.p., 30 min before BNP administration did not modify the 'anxiolytic-like' activity of BNP. There was an increase in the percentage time spent in the open arms (ANOVA F3, 33=4.05, $P<0.0156$, Tukey's test), and a marked increase in the frequency of entries into the open arms (ANOVA F3, 33=1.38, $P<0.266$, Tukey's test) as compared with the control rats. Following pretreatment with the β-adrenoreceptor blocker propranolol 10 mg/kg, i.p. there was no increase in the percentage time spent in the open arms (ANOVA F3, 37=3.49, $P<0.026$, Tukey's test) or in the frequency of entries into the open arms (ANOVA F3, 37=3.97, $P<0.015$, Tukey's test) as compared with control animals, indicating the blocking effect of the β-adrenergic system. In the group pretreated with the muscarinergic acetylcholine receptor blocker atropine, there was not a significant increase in the percentage time spent in the open arms (ANOVA F3, 32=12.33, $P<0.0001$, Tukey's test) or in the frequency of entries into the open arms of the elevated plus-maze paradigm as compared with the control rats (ANOVA F3, 32=3.99, $P<0.017$, Tukey's test). Pretreatment with the GABA receptor blocker bicuculline (1 mg/kg i.p.) did not block the increase in the percentage time spent in the open arms (ANOVA F3, 36=5.51, $P<0.0035$, Tukey's test), nor the increase in the frequency of entries into the open arms of the maze (ANOVA F3, 36=0.85, $P<0.47$, Tukey's test) as compared with the control animals. The increase in the percentage time spent in the open arms was not affected by pretreatment with the 5-HT receptor blocker methysergide (5 mg/kg i.p.) (ANOVA F3, 29=7.36, $P<0.001$, Tukey's test); nor was the marked increase in the frequency of entries into the open arms (ANOVA F3, 29=0.85, $P<0.0479$, Tukey's test) as compared with the control rats. Pretreatment with the endogenous opioid system blocker naloxone (0.1 mg/kg i.p.) pretreatment did not block the increase in the percentage time spent in the open arms (ANOVA F3, 33=6.54, $P<0.0016$, Tukey's test), nor the increase in the frequency of entries into the open arms of the elevated plus-maze (ANOVA F3, 33=1.89, $P<0.15$, Tukey's test) as compared with the control animals.

Table 3 shows the effects of i.c.v. administration of CNP (25, 50, 100, 200, 400 or 1000 ng) to rats tested in the elevated plus-maze paradigm. The 100 ng, 200 ng and 400 ng doses of CNP significantly increased the percentage time spent in the open arms as compared with the control animals. The doses of 25, 50 and 1000 ng CNP were ineffective (ANOVA F6, 58=10.32, $P<0.0001$, Tukey's test). A statistically significant increase in the frequency of entries into the open arms of the elevated plus-maze test was not observed at any dose (ANOVA F6, 58=1.96, $P<0.088$, Tukey's test). The 200 ng dose of CNP was selected to test the anxiolytic activity.

The effects of different neurotransmitter antagonists relative to the control rats are shown in Table 4. Pretreatment with the dopaminergic receptor blocker haloperidol (10 μg/kg i.p.) blocked the 'anxiolytic-like' activity of CNP: there was no statistically significant difference in the percentage time spent in the open arms (ANOVA F3, 25=6.16, $P<0.0033$, Tukey's test); it prevented the increase in the frequency of entries into the open arms of the elevated plus-maze test (ANOVA F3, 25=2.86, $P<0.06$, Tukey's test) as compared with the control rats. Pretreatment with the α-adrenoreceptor antagonist phenoxybenzamine (2 mg/kg i.p.) blocked the 'anxiolytic-like' activity of CNP. There was no increase in the percentage time spent in the open arms (ANOVA F3, 27=5.92, $P<0.0036$, Tukey's test), nor in the frequency of entries into the open arms (ANOVA F3, 27=1.57, $P<0.22$, Tukey's test) as compared with the control rats. Pretreatment with the β-adrenoreceptor blocker propranolol (10 mg/kg i.p.) also prevented an increase in the percentage time spent in the open arms (ANOVA F3, 30=13.2, $P<0.0001$, Tukey's test) and the increase in the frequency of entries into the open arms (ANOVA F3, 30=1.36, $P<0.27$, Tukey's test) as compared with the con-

Table 3 Effects of different doses of CNP on anxiety state of rats tested in the elevated plus-maze paradigm. Results are presented as means ± SE[a] $P<0.05$ (ANOVA, Tukey's test)

Groups	No. of animals	Open/total time %	Open/total entries
Control (saline)	7	29.53 ± 2.48	48.21 ± 5.74
25 ng CNP	7	26.65 ± 2.68	35.48 ± 3.86
50 ng CNP	9	38.98 ± 3.90	41.88 ± 5.65
100 ng CNP	9	54.51 ± 7.46[a]	46.16 ± 4.68
200 ng CNP	9	66.69 ± 3.48[a]	54.31 ± 4.48
400 ng CNP	9	58.3 ± 6.35	54.29 ± 5.53
1000 ng CNP	9	31.45 ± 3.71	41.81 ± 3.5

Table 4 Effects of neurotransmitter blockers on CNP-induced anxiolytic state in rats. Results are presented as means ± SE[a] $P < 0.05$ (ANOVA, Tukey's test)

Groups	No. of animals	Open/total time %	Open/total entries
Haloperidol (10 µg/kg i.p.)			
Control (saline)	6	23.20 ± 2.89	35.56 ± 3.98
CNP (200 ng i.c.v.)	7	50.14 ± 4.13[a]	56.19 ± 6.24
Haloperidol + saline	6	28.3 ± 4.13	41.67 ± 4.77
Haloperidol + CNP	7	35.64 ± 6.45	50.00 ± 5.59
Phenoxybenzamine (2 mg/kg.i.p.)			
Control (saline)	6	24.94 ± 1.97	47.92 ± 4.2
CNP (200 ng i.c.v.)	8	44.85 ± 5.97[a]	41.49 ± 3.43
Phenoxybenzamine + saline	7	29.87 ± 3.04	55.17 ± 6.49
Phenoxybenzamine + CNP	7	49.52 ± 3.12	49.52 ± 4.01
Propranolol (10 mg/kg i.p.)			
Control (saline)	6	24.81 ± 1.78	40.20 ± 4.75
CNP (200 ng i.c.v.)	8	44.41 ± 3.06[a]	47.44 ± 3.72[a]
Propranolol + saline	7	25.44 ± 3.99	35.66 ± 7.32
Propranolol + CNP	9	25.38 ± 1.90	47.59 ± 5.25
Atropine (2 mg/kg i.p.)			
Control (saline)	7	22.32 ± 2.43	41.77 ± 4.47
CNP (200 ng i.c.v.)	7	52.72 ± 6.32[a]	47.72 ± 5.04
Atropine + saline	8	19.5 ± 2.73	40.73 ± 5.30
Atropine + CNP	8	52.16 ± 2.16[a]	37.17 ± 2.18
Methysergide (5 mg/kg i.p.)			
Control (saline)	7	20.92 ± 2.14	41.43 ± 3.84
CNP (200 ng i.c.v.)	8	50.96 ± 2.73[a]	43.58 ± 3.81
Methysergide + saline	7	19.03 ± 0.78	43.55 ± 4.68
Methysergide + CNP	7	50.75 ± 3.38[a]	48.62 ± 4.76
Bicuculline (1 mg/kg i.p.)			
Control (saline)	7	20.29 ± 3.85	38.5 ± 4.58
CNP (200 ng i.c.v.)	8	44.69 ± 5.13[a]	44.11 ± 2.58
Bicuculline + saline	8	22.00 ± 3.15	45.89 ± 4.46
Bicuculline + CNP	7	50.35 ± 2.16[a]	43.81 ± 5.22
Naloxone (0.1 mg/kg i.p.)			
Control (saline)	6	21.13 ± 2.87	40.24 ± 2.82
CNP (200 ng i.c.v.)	8	47.89 ± 2.74[a]	45.77 ± 2.63[a]
Naloxone + saline	7	23.67 ± 3.16	41.30 ± 4.39
Naloxone + CNP	7	45.87 ± 3.81[a]	43.79 ± 4.56

trol animals. In the group pretreated with the muscarinergic acetylcholine receptor blocker atropine, the significant increase in the percentage time spent in the open arms was not prevented (ANOVA F3, 29=25.06, $P < 0.0001$, Tukey's test) and the frequency of entries into the open arms was not modified as compared with the control rats (ANOVA F3, 29=0.98, $P < 0.41$, Tukey's test). Pretreatment with the GABA receptor blocker bicuculline (1 mg/kg i.p.) did not block the increase in the percentage time spent in the open arms (ANOVA F3, 29=15.99, $P < 0.0001$, Tukey's test) and it did not affect the marked increase in the frequency of entries into the open arms of the maze (ANOVA F3, 29=0.55, $P < 0.65$, Tukey's test) as compared with the control animals.

The increase in the percentage time spent in the open arms was not affected by pretreatment with the 5-HT receptor blocker methysergide (0.5 mg/kg i.p.) (ANOVA F3, 28=51.73, $P < 0.0001$, Tukey's test), and nor was the marked increase in the frequency of entries into the open arms (ANOVA F3, 28=0.5, $P < 0.68$, Tukey's test) as

compared with the control rats. Pretreatment with the endogenous opioid system blocker naloxone (0.1 mg/kg i.p.) did not block the increase in the percentage time spent in the open arms (ANOVA F3, 27=19.8, $P<0.0001$, Tukey's test), nor the increase in the frequency of entries into the open arms of the elevated plus-maze (ANOVA F3, 27=1.89, $P<0.46$, Tukey's test) as compared with the control animals.

DISCUSSION

The present results demonstrate that central administration of BNP and CNP in different doses caused an 'anxiolytic-like' effect in an elevated plus-maze paradigm. BNP in doses of 100, 200 and 400 ng, and CNP in doses of 100 and 200 ng abolished the normal preference for the closed arms of the maze, and increased the percentage time spent in the open arms; this is consistent with an 'anxiolytic-like' effect. Doses of 50 and 1000 ng BNP, and doses of 25, 50, 400 and 1000 ng CNP produced no behavioural effects in the elevated plus-maze model. This is in agreement with the results of previous studies which demonstrated 'anxiolytic' responses. Similar increases in general activity have been found for other 'anxiolytic' compounds, such as chlordiazepoxide, diazepam and phenobarbitone,[9] both in the elevated plus-maze test and in most other tests of anxiety. Pretreatment with a β-adrenoreceptor antagonist or a muscarinergic cholinergic blocker antagonized the effect of 200 ng BNP in the elevated plus-maze test. A dopaminergic blocker, an α-adrenoreceptor antagonist, a GABA receptor antagonist, a 5-HT receptor antagonist and an opiate antagonist did not modulate the 'anxiolytic-like' effects of BNP. A dopamine receptor antagonist, or an α- or β-adrenoreceptor blocker prevented the anxiolytic effect of CNP, while a muscarinergic cholinergic blocker, a GABA receptor antagonist, a 5-HT receptor antagonist and an opiate receptor antagonist did not block the effect of CNP. The elevated plus-maze test has an advantage over other conflict tests in that it requires only the spontaneous activity of the animals.

A variety of evidence suggests that members of the natriuretic peptide family affect numerous neuroendocrine systems, including the hypothalamo-pituitary-adrenocortical and hypothalamo-neurohypohyseal axes. ANP can inhibit the basal and CRF-induced release of corticotropin,[10] and of vasopressin, the most potent cofactor of CRF in pituitary ACTH secretion.[11] In a previous study, we found an 'anxiolytic-like' action of ANP in an elevated plus-maze model of anxiety, and increased CRF-LI levels in different hypothalamic and extrahypothalamic brain regions after central ANP administration in rats (unpublished results). ANP, BNP and CNP are of potential importance in neuroendocrine regulation, acting as neurotransmitters or neuromodulators in the brain, regulating hormonal and cardiovascular functions. It was previously reported that centrally administered endothelin-induced activation of the hypothalamo-pituitary-adrenocortical axis (increased ACTH secretion) was attenuated by BNP.[6] The inhibitory effects of BNP on angiotensin II-induced dipsogenic, behaviour, pressor response and vasopressin secretion were reported recently.[12] Anatomical localization indicates that CNP is contained in neuronal circuits having a direct relevance to several neuroendocrine systems. The heaviest concentration of CNP mRNA was observed in the anteroventral periventricular nucleus (AVPv), a region known to regulate the hypothalamopituitary-gonadal axis (LHRH release) and vasopressin release from the hypothalamo-neurohypophyseal system. In addition, localization of CNP to the hypothalamic arcuate nucleus, the medial, median and periventricular preoptic area, the supraoptic, dorsomedial, ventral premamillary and lateral mamillary nuclei, and the posterior hypothalamic area[7] has implications as concerns the hypothalamo-pituitary-gonadal function and the regulation of pituitary-adrenocortical secretion.

ANP[13,14] and BNP[15,16] participate in the processes of learning and memory. ANP, BNP and CNP have been found to increase the severity of picrotoxin-kindled seizure syndrome in rats.[17]

In summary, the present study appears to demonstrate that the 'anxiolytic-like' activity caused by BNP can be inhibited by pretreatment with a β-adrenoreceptor antagonist or a muscarinergic cholinergic blocker.

A dopaminergic blocker, an α-adrenoreceptor antagonist, a GABA receptor antagonist, a 5-HT receptor antagonist and an opiate antagonist did not modulate the 'anxiolytic-like' effects of BNP. A dopamine receptor antagonist, or an α- or β-adrenoreceptor blocker inhibited the anxiolytic effect caused by CNP, but a muscarinergic cholinergic blocker, a GABA receptor antagonist, a 5-HT receptor antagonist and an opiate receptor antagonist did not block the effect of CNP. Our experiments appear to indicate the involvement of different neurotransmitter systems in the mediation of BNP and CNP-induced behavioural action.

ACKNOWLEDGEMENTS

This work was supported by grants from the Hungarian Ministry of Social Affairs and Health (T-11 549/93) and OTKA (T/3, 1354 and T 6084, F 016864) and FEFA (1008/1).

REFERENCES

1. Imura, H., Nakao, K., Itoh, H. The natriuretic peptide system in the brain: implications in the central control of cardiovascular and neuroendocrine functions. Frontiers in Neuroendocrinology 1992; 13 (3): 217–249.
2. Sudoh, T., Minamino, N., Kangawa, K., Matsuo, H. C-type natriuretic peptide (CNP): A new member of natriuretic peptide family identified in porcine brain. Biochem. Biophys. Res. Comm. 1990; 168: 863–870.
3. Kojima, M., Minamino, N., Kangawa, K., Matsuo, H. Cloning and sequence analysis of cDNA encoding a precursor for rat brain natriuretic peptide. Biochem. Biophys. Res. Comm. 1989; 159: 1420–1426.
4. Kojima, M., Minamino, N., Kangawa, K., Matsuo, H. Cloning and sequence analysis of cDNA encoding a precursor for rat C-type natriuretic peptide (CNP). FEBS Lett. 1990; 276: 209–213.
5. Itoh, H., Nakao, K., Yamada, T., et al. Antidipsogenic action of novel peptide 'brain natriuretic peptide' in rats. Eur. J. Pharmacol. 1988; 150: 193–196.
6. Makino, S., Hashimoto, K., Hirasawa, R., Hattori, T., Kageyama, J., Ota, Z. Central interaction between endothelin and brain natriuretic peptide on pressor and hormonal responses. Brain. Res. 1990; 534: 117–121.
7. Hermann, J. P., Langub, M. C., Watson, R. E. Localization of C-type natriuretic peptide mRNA in rat hypothalamus. Endocrinol. 1993; 133 (4): 1903–1906.
8. Pellegrino, L. J., Pellegrino, A. S. and Cushman, A. J. A stereotactic atlas of the rat brain. Plenum, New York, 1979.
9. Pellow, S., Chopin, P., File, S. E. and Briley, M. Validation of open: closed arm entries in an elevated plus-maze as a measure of anxiety in the rat. J. Neurosci. Methods 1985; 14: 149–167.
10. Shibasaki, T., Naruse, M., Yamauchi, N., et al. Rat natriuretic factor suppresses proopiomelanocortin-derived peptide secretion from both anterior and intermediate lobe cells and growth hormone release from anterior lobe cells of rat in vitro. Biochem. Biophys. Res. Comm. 1986; 135 (3): 1035–1041.
11. Bardeleben, U., Holsboer, F., Stalla, G. K., Müller, O. A. Combined administration of human corticotropin-releasing factor and lysine vasopressin induced cortisol escape from dexamethazone suppression in healthy subjects. Life Sci. 1985; 37: 1613–1618.
12. Yamada, T., Nakao, K., Itoh, H., et al. Intracerebroventricular injection of brain natriuretic peptide inhibits vasopressin secretion in conscious rats. Neurosci. Lett. 1988; 95: 223–228.
13. Bidzseranova, A., Telegdy, G., Penke, B. The effects of natriuretic peptide on passive avoidance behaviour in rats. Brain. Res. Bull. 1991; 26: 117–118.
14. Bidzseranova, A., Penke, B., Tóth, G., Telegdy, G. The effects of atrial natriuretic peptide on electroconvulsive shock-induced amnesia in rats. Transmitter-mediated action. Neuropeptides 1991; 19: 103–106.
15. Bidzseranova, A., Varga, J., Telegdy, G. The effects of receptor blockers on brain natriuretic peptide-32-induced action on passive avoidance behaviour in rats. Neuropeptides 1992; 22: 107–110.
16. Bidzseranova, A., Varga, J., Telegdy, G. The effects of brain natriuretic peptide-32 on electroconulsive shock-induced amnesia in rats. The role of neurotransmitters. Eur. J. Pharmacol. 1993; 232: 305–309.
17. Mazarati, A., Halászi, É., Telegdy, G., Tóth, G., Varga, J. ANP 1-28, BNP 1-32 and CNP 1-22 increase the sensitivity of picrotoxin-kindled seizure syndrome in rats. Life Sci. 1992; 52: 19–24.

2.14.

ELSEVIER

Life Sciences, Vol. 59, No. 16, pp. 1351-1356, 1996

0024-3205/96 $15.00 + .00

PII S0024-3205(96)00460-2

THE EFFECTS OF ATRIAL NATRIURETIC PEPTIDE (ANP_{1-28}) ON CORTICOTROPIN RELEASING FACTOR IN BRAIN OF RATS

Éva Biró, János Gardi*, Miklós Vecsernyés*, János Julesz*, Gábor Tóth#, Gyula Telegdy

Department of Pathophysiology, *Endocrine Unit of First Department of Medicine and #Department of Medical Chemistry, Albert Szent-Györgyi Medical University, Szeged, Hungary

(Received in final form August 15, 1996)

Summary

We have shown that ANP has anxiolytic-like effects in behavioral studies.Since CRF is thought to be involved in emotional state of the brain, the present study was undertaken to follow the possible alterations in corticotropin-releasing factor-like immunoreactivity (CRF-LI) in different regions of the brain in rats following ANP treatment.CRF-LI immunoreactivity was determined in hypothalamic and extrahypothalamic brain areas after central injection of atrial natriuretic peptide 1-28 (ANP_{1-28}) in rats. After various doses of ANP_{1-28} administration the CRF-LI significantly increased in the hypothalamus,the hippocampus and the frontal cortex. In the amygdala, ANP caused a marked but nonsignificant CRF-LI enhancement. In the basal forebrain, the CRF-LI decreased. These results suggest that ANP_{1-28} may moderate activation of the CRF-ergic system in the brain which could be related to the neuroendocrine and behavioral action.

Key Words: atrial natriuretic peptide, corticotropin-releasing factor-like immunoreactivity, brain metals

ANP binding sites in rat brain are distributed in the hypothalamic nuclei, hippocampus, septum, circumventricular organs and cerebellum (1). The widespread occurrence of ANP-like immunoreactivity suggests its involvement in the regulation of central nervous autonomic and neuroendocrine functions (2). Numerous studies suggest that the peptide can inhibit the stress-induced release of corticotropin (3, 4) and other pro-opiomelanocortine-derived peptides such as ß-lipotropin, ß-endorphin, and α-MSH as well as prolactin, growth hormone and thyroid stimulating hormone, which are released during stress (5,6) In additon, ANP has an inhibitory effect on the release of vasopressin (VP), the most potent cofactor of CRF in pituitary ACTH secretion (7,8).

Only few data were published on the relationship of the CRF and ANP in the brain; CRF and ANP colocalized in the

All correspondance should be sent to: Prof.Gyula Telegdy,Dept. Pathophysiology, Albert Szent-Györgyi Medical University, Semmelweis 1, 6701 Szeged, POBox 531, Hungary. Tel and Fax (36)-62-310651,Email:Telegdy@patph.szote.u-szeged.hu.

paraventricular nuclei (9), and ANP can inhibit the acetylcholine (10) and noradrenalin (11) induced release of CRF.

Our previous findings demonstrated that ANP prevents the stress-induced neuroendocrine and behavioral responses (12), and centrally administered ANP caused anxiolytic-like behavioral effects in rats (13). As the central CRF-ergic system plays a critical role in anxiety and other behavioral stress responses (14); these above mentioned findings suggest to investigate the effects of central application of various doses of ANP on the CRF-LI levels in different brain regions.

Methods

Adult male Wistar rats (LATI, Gödöllö, Hungary) weighing 180-220 g were used. They were housed 5 per cage with food and water available ad libitum in an environmentally controlled facility (12-h light/12-h dark cycle with lights on at 06.00 h). Rats were handled daily for a week before the experiment to minimalize the effects of nonspecific stress. In order to allow intracerebroventricular (icv) peptide administration, all rats were implanted with a unilateral cannula aimed at the right lateral brain ventricle. The stainless steel cannula was stereotaxically inserted into the ventricle according to the coordinates found in the atlas of Pellegrino et al (15), under pentobarbital (Nembutal 35 mg/kg, i.p.) anesthesia. Cannulas were secured with dental acrylic cement. Rats were allowed a minimum of 5 days to recover from surgery before peptide treatment begun.

The rat ANP_{1-28} was purchased from Bachem (CA, USA) or was synthetized by G. Tóth. It was dissolved in artificial cerebrospinal fluid and was injected icv in a volume of 2 ul in three doses (100, 200 or 400 ng per animal) to conscious, freely-moving rats. The control animals received the same volume of artificial cerebrospinal fluid.

Animals were sacrificed in a separate room 30 min after icv injection of artificial cerebrospinal fluid and of different doses of ANP_{1-28}. After decapitation, the brains were quickly removed and various brain regions were isolated from the both hemispheres on ice by a modification of the technique of Glowinski and Iversen (16). The hypothalamus was defined as the tissue within 3 mm of the ventral surface of the brain. The anterior extreme was the optic chiasm; the posterior extreme was the mamillary bodies; the lateral extremes were the lateral hypothalamic sulci. The hippocampus was removed as a whole. The amygdaloid complex was dissected from below the base of the caudate putamen, excluding the adjacent cortical surface. The anterior and posterior borders of the amygdaloid complex were defined by the genu of the corpus callosum and the optic chiasm. The basal forebrain area (tuberculum, nucleus accumbens and septal area) was removed from the anterior-ventral part of the telencephalon as a trapezoid from tissue sliced by razor cuts. This complex was bordered by the frontal cortex anteriorly, and by a razor cut at the level of the anterior commissure posteriorly. The dorsal border of the basal forebrain complex was the corpus callosum and the lateral borders were the internal walls of the lateral ventricules laterally to the ventral surface of the anterior telencephalon. The frontal cortex was

obtained by a razor cut at the level of the genu of the corpus callosum.

For radioimmunoassay (RIA) to determine the CRF-LI, each area was homogenized with ultrasound (Soniprep 150 MSE, Great Britain) in HCl (100 mM) containing 1 mM ascorbic acid, and an aliquot was sampled for protein measurement. The residual homogenates were centrifuged at 6,000 g for 20 min, at 4 C, and aliquots were taken and lyophilized for RIA. The CRF antiserum (kindly donated by Paul Vecsei, Dept. of Pharmacology, University of Heidelberg, Germany) was obtained from a rabbit immunized with hCRF. The CRF antibody (17) was specific for the C-terminal region of the CRF_{41} molecule since it did not cross-react with fragments of CRF_{1-20} or CRF_{6-33}. The CRF tracer was prepared by using a modified iodogen method in order to minimize damage to the iodinated peptide (18). The labeled material was purified via two steps of reverse-phase chromatography (19), a gradient HPLC system being applied in the second step. The specific radio-activity of the purified tracer was 1700-2900 Ci/mmol. The freeze-dried residues were redissolved in a 1 ml assay buffer (50 mM phosphate, pH 7.4, containing 0.25% human serum albumin and 0.1% Triton X-100) and 200 ml aliquots were subjected to RIA. The assay standard was a synthetic h/rCRF preparation (Bachem, Budendorf, Switzerland). The procedure involved a nonequilibrium system: a 16-h preincubation of the samples or standards with antiserum (100 ml, working dilution 1:10,000) was followed by a 24-h incubation with CRF tracer (100 ml, 10,000 cpm). The immunologically bound and free fractions were separated with a second antibody (raised in sheep against whole rabbit IgG in our laboratory) and subsequently by polyethyleneglycol 6000 precipitation (FERAK Laborit. Gmbh, Berlin, Germany) by the DAB/PEG method. The lower limit of assay detection was 7-8 pg/tube. The intra- and interassay coefficients of variation were 4.0 and 13.8%, respectively. CRF-LI in the brain extracts subjected to HPLC has been shown to chromatograph with synthetic r/h CRF (Gardi et al., unpublished observation). The CRF-LI is expressed in pg/mg protein.

All data are presented as mean ± S.E.M. Data were analysed by one-way ANOVA followed by Dunnett's test. A probability level of 0.05 was accepted as indicating a statistically significant difference.

Results

The results of the present study are shown in Table I. Icv administration of ANP resulted in a significant, dose-dependent increase in the CRF-LI in the hypothalamus ($F_{3,18}$=12.66, P<0.0001; 100 ng ANP_{1-28}: P<0.0001 vs. artificial cerebrospinal fluid, 248%; 200 ng ANP_{1-28}: P<0.0001 vs. artificial cerebrospinal fluid, 367%; 400 ng ANP_{1-28}: P<0.0001 vs. artificial cerebrospinal fluid, 220%). In the basal forebrain ANP caused a decrease in the CRF-LI ($F_{3,19}$=3.81, P<0.02; 100 ng ANP_{1-28}: P<0.05 vs. artificial cerebrospinal fluid, 75%; 200 ng ANP_{1-28}: P<0.02 vs. artificial cerebrospinal fluid, 35%; 400ng ANP_{1-28}: P<0.02 vs. artificial cerebrospinal fluid, 115%). In the hippocampus, ANP_{1-28} administration led to significant, dose-dependent increase in the CRF-LI ($F_{3,21}$=3.06, P<0.05; 100 ng ANP_{1-28}: P>0.05 vs. artificial cerebrospinal fluid, 166%; 200 ng ANP_{1-28}: P<0.05 vs. artificial cerebrospinal fluid, 461%; 400 ng ANP_{1-28}: P<0.05 vs. artificial cerebrospinal fluid, 455%). A similar effect was observed in the

frontal cortex ($F_{3,19}$=11.33, P<0.0002; 100 ng ANP_{1-28}: P<0.0002 vs. artificial cerebrospinal fluid, 171%; 200 ng ANP_{1-28}: P<0.0002 vs. artificial cerebrospinal fluid, 409%; 400 ng ANP_{1-28}: P<0.0002 vs. artificial cerebrospinal fluid, 295%). In the amygdala, ANP caused

TABLE I

Effects of ANP_{1-28} on Corticotropin-Releasing Factor-like Immunoreactivity (CRF-LI pg/mg protein ± S.E.M) in Different Brain Areas.

BRAIN REGION	CONTROL	100 ng ANP	200 ng ANP	400 ng ANP
HYPOTHALAMUS	1052±348	2611±580*	3868±671*	2321±178*
BASAL FOREBRAIN	308± 37	230± 76*	109± 11*	354± 53*
HIPPOCAMPUS	18± 7	30± 14*	83± 14*	82± 28*
FRONTAL CORTEX	21± 5	36± 3*	86± 11*	62± 8*
AMYGDALA	732±273	1100±310	972±151	1069±241

Each group containes 5-7 animals. * p< 0.05 vs. control by ANOVA followed by Dunnett's test.

a marked but not significant increase in the CRF-LI ($F_{3,22}$=0.39, P=0.76; 100 ng ANP_{1-28}: P=0.76 vs. artificial cerebrospinal fluid,150%; 200 ng ANP_{1-28}: P=0.76 vs. artificial cerebrospinal fluid,133%; 400 ng ANP_{1-28}: P=0.76 vs. artificial cerebrospinal fluid,146%).

Discussion

The results of the present study with regard to the distribution of basal CRF-LI in saline-treated, nonstressed, handled rats are similar to those of previous RIA studies (20, 21) and to our previous studies. (22, 23).

The present results show that centrally administered ANP_{1-28} increases the levels of CRF-LI in the hypothalamus, hippocampus and frontal cortex . Although measurement of the IR-CRF concentration alone does not distinguish between changes in synthesis, release, storage or degradation of the peptide, the increase in the IR-CRF level in certain brain area might indicate a decreased release of these peptide. To support this interpretation it was found earlier, that ANP colocalized with CRF in the paraventricular nucleus (9); inhibits the release of CRF from the hypothalamus in vitro (10, 11), and suppress the stress-induced HPA-axis activation (3, 4, 24).

It is well known, that the alterations of the activity of the central CRF-ergic system correlate with the behavioral changes of the anxiolytic and "emotional" states; e.g. acute cocaine administration increases the CRF level in the amygdala (22). Cocaine withdrawal, which resulted in a strong anxiety-like behavior (25) in cocaine treated rats, decreases the CRF concentrations in this area (23). Our previous findings were that the ANP caused anxiolytic-like behavioral state demonstrated by increased plus maze scores (13). These data favor the idea that the

inhibition of the CRF neurotransmission might be involved in the mediation the anxiolytic-like behavioral response of centrally administered ANP.

The peptide treatment produced a significant reduction in IR-CRF in the basal forebrain structures. It may be hypothesized that the decrease in the CRF level in this region reflects the increased release and subsequent degradation of the CRF. It has been published that central administration of ANP results in an increase of locomotor activity of rats (26). It is known that microinfusion of CRF into the basal forebrain caused an intense locomotor activity (27), and it could be hypothesized that CRF release in basal forebrain regions may contribute to the expression of ANP-induced locomotor activity.

In conclusion, different actions of ANP on the CRF-LI in different brain structures of the rat have been reported, suggesting that ANP altered the brain CRF-ergic system activity. This may be one of the mechanisms mediating the neuroendocrine and behavioral responses to ANP.

Acknowledgements

The work has been supported by the Ministry of Social and Welfare of Hungary (T-70/1990), OTKA (T/3, 1354, T-6084) and FEFA-1008.

References

1. V.T.F. YEUNG, C.K. LAAI, C.S. COCHRAM, R. TEOH, J.D. YOUNG, T.G. YANDLE and M.G. NICHOLLS, Neuroendocrinology 53 18-24 (1991).
2. L.Y. MA, M.L. ZHANG, X.D. YANG, D.R. TIAN, J.S. QI and D.M. ZHANG, Neuroendocrinology 53 12-17 (1991).
3. T. HATTORI, K. HASHIMOTO, H. INOUE, M. SUGAWARA, S. SUEMARU, J. KAGEYAMA and Z. OTA, Endocrinol. Japon 33 533-539 (1986).
4. G.A. WITTERI, A. ESPINER, A.M. RICHARDS, R.A. DONALD, J.H. LIVESEY and T.G. YANDLE, Clin. Endocrinol. 38 183-189 (1993).
5. C.R. FRANCI, J. ANSELMO-FRANCI and S.M. MCCANN, Proc. Natl. Acad. Sci. USA 89 11391-11395 (1992).
6. T. SHIBASAKI, M. NARUSE, N. YAMAUCHI, A. MASUDA, T. IMAKI, K. NARUSE, H. DEMURA, N. LING, T. INAGAMI and K. SHIZUME, Biochem. Biophys. Res. Comm. 135 1035-1041 (1986).
7. U. BARDELEBEN, F. HOLSBOER, G.K. STALLA and O.A. MÜLLER, Life Sci. 37 1613-1618 (1985).
8. G.E. GILLIES, E.A LINTON and P.J. LOWRY, Nature 299 355-357 (1982).
9. M. PALKOVITS, R.L. ESKAY and F.A. ANTONI, Neuroendocrinology 46 542-544 (1987).
10. T. TAKAO, K. HASHIMOTO and Z. OTA, Life Sci. 42 1199-1203 (1988).
11. J. IBANEZ-SANTOS, S. TSAGARAKIS, L.H. REES, G.M. BESSER and A. GROSSMAN, J.Endocrinol. 126 223-228 (1990).
12. É. BIRÓ, G. TÓTH and G. TELEGDY, J. Clin. Invest. 16 (Suppl.1 to 8) C.27 (1993).
13. É. BIRÓ, G. TÓTH and G. TELEGDY, Neuropeptides 29 215-220 (1995).

14. A.J. DUNN and C.W. BERRIDGE, Brain Res. Rev. 21 71- 100 (1990).
15. L.J. PELLEGRINO, A.S. PELLEGRINO and A.J. CUSHMAN, A Stereotic Atlas of the Rat Brain. 8-57, Plenum Press, New York (1979).
16. J. GLOWINSKI and L.L. IVERSEN, J. Neurochem. 13 655-669 (1966).
17. C. MASER-GLUTH and P. VECSEI, Clin. Endocrinol. 30 405-412 (1989).
18. E.A. LINTON and P.J. LOWRY, Neuropeptides 3 45-52 (1982).
19. T. JANÁKY, G. TÓTH, B. PENKE, K. KOVÁCS and F.A. LÁSZLÓ, J. Liquid Chromatography 5 1499-1507 (1982).
20. P.B. CHAPPELL, M.A. SMITH, C.D. KILTS, G. BISETTE, J. RITCHIE, C. ANDERSON and C.B. NEMEROFF, J. Neurosci. 6 2908-2914 (1986).
21. T. INOUE, T. KOYAMA, T. MURAKI and I. YAMASHITA, Prog. Neuro-Psychopharmacol. Biol. Psychiat. 17 161-170 (1993).
22. Z. SARNYAI, É. BIRÓ, J. GARDI, M. VECSERNYÉS, J. JULESZ and G. TELEGDY, Brain Res. 616 315-319 (1993).
23. Z. SARNYAI, É. BIRÓ, J. GARDI, M. VECSERNYÉS, J. JULESZ and G.TELEGDY, Brain Res. 675 89-97 (1995).
24. G. FINK, R.C. DOW, D. CASLEY, C.I. JOHNSTON, A.T. LIM, D.L.COPOLOV, J. BENNIE, S. CARROLL and H. DICK, J. Endocrinol. 131 R9-R12 (1991).
25. X.M. YANG, A.L. GORMAN, A.J. DUNN and N.E. GOEDERS, Pharmacol. Biochem. Behav. 41 643-650 (1992).
26. A. BIDZSERANOVA, G. TÓTH and G. TELEGDY, Neuropeptides 20 163-167 (1991).
27. A. TAZI, N.R. SWERDLOW, M. LE MOUL, J. RIVIER, W. VALE and G.F. KOOB, Life Sci. 41 41-49 (1987).

Life Sciences, Vol. 60, No. 23, pp. 2111-2117, 1997

0024-3205/97 $17.00 + .00

PII S0024-3205(97)00198-7

THE EFFECTS OF BRAIN AND C-TYPE NATRIURETIC PEPTIDES ON CORTICOTROPIN-RELEASING FACTOR IN BRAIN OF RATS

János Gardi, Éva Bíró*, Miklós Vecsernyés, János Julesz, Tibor Nyári**, Gábor Tóth*** and Gyula Telegdy*

Endocrine Unit, *Department of Pathophysiology, **Department of Medical Informatics and ***Department of Medical Chemistry, Albert Szent-Györgyi Medical University, Szeged, Hungary

(Received in final form March 3, 1997)

Summary

The central corticotropin-releasing factor (CRF)-ergic system plays a critical role in anxiety and other behavioral stress responses. It has been shown that atrial (ANP), brain (BNP) and C-type (CNP) natriuretic peptides exert anxiolytic-like effects in behavioral studies. Our previous findings demonstrated that various doses of centrally administered ANP selectively altered the CRF content in different brain areas. In the present study, CRF immunoreactivity was determined in hypothalamic and extrahypothalamic brain regions after central injection of BNP or CNP in rats. A high dose (400 ng) of BNP significantly increased the CRF-like immunoreactivity (CRF-LI) in the hypothalamus and amygdala, while only a tendency towards an increase was found in the hippocampus. In the hypothalamus, the CRF-LI decreased after a high dose (400 ng) of CNP. The CRF-LI increased in the basal forebrain after a low dose (100 ng) of CNP. These results suggest that CRF may be involved in the mediation of some neuroendocrine and behavioral responses to BNP and CNP.

Key Words: brain natriuretic peptide, C-type natriuretic peptide, CRF-like immunoreactivity, hypothalmus

The family of natriuretic peptides contains the atrial (ANP), brain (BNP) and C-type (CNP) natriuretic peptides. All of them are distributed in discrete brain regions, which suggests the involvement of these peptides in the regulation of neuroendocrine and some other central nervous system functions (1). While much is known of the central nervous system (CNS) actions of ANP (2,3), few data have been reported on the CNS actions of the other cerebral natriuretic peptides, BNP and CNP (4-6). Numerous studies indicate that ANP can inhibit the secretion of ACTH (7,8), other POMC-derived peptides, prolactin (Prl), growth hormone and thyroid-stimulating hormone, which are released during stress (9,10). Centrally administered BNP attenuates the endothelin-induced ACTH secretion (11). Although some of the reported actions of CNP in the brain are similar to those of ANP (12-15), effects that oppose those of ANP have also been described. As an example, while ANP inhibits Prl secretion in the hypothalamus (16,17), CNP acts within the same region to stimulate Prl secretion (18). ANP inhibits the release of corticotropin-releasing factor (CRF) from the hypothalamus in vitro (19,20). Our previous findings showed that after the administration of various doses of ANP the CRF-like

All correspondence should be sent to: Dr. János Gardi, Endocrine Unit, Albert Szent-Györgyi Medical University, Korányi fasor 8, 6701 Szeged, P.O.B. 744, Hungary. Tel/Fax: 36-62-455211, E-mail: gardi@endoc.szote.u-szeged.hu

immunoreactivity (CRF-LI) was selectively altered in different brain areas (21). Similarly to ANP (22) centrally administered BNP and CNP evoked anxiolytic-like behavioral effects in rats (23). As the central CRF-ergic system plays a critical role in anxiety and other behavioral stress responses (24) and ANP is able to change the activity of the brain CRF system (21), the present investigation was undertaken to clarify how BNP and CNP, two peptides structually related to ANP with anxiolytic effects too (23), would influence the CRF-LI in certain brain areas which might explain their anxiolytic actions.

Methods

Adult male Wistar rats (LATI, Gödöllő, Hungary) weighing 180-220 g were used. They were housed 5 per cage with food and water available ad libitum in an environmentally controlled facility (a 12-h light/12-h dark cycle with lights on at 06.00 a.m.). Rats were handled daily for a week before the experiment to minimize the effects of nonspecific stress. In order to allow intracerebroventricular (icv.) peptide administration, all rats were implanted with a unilateral cannula aimed at the right lateral brain ventricle. The stainless steel cannula was stereotaxically inserted into the ventricle according to the coordinates found in the atlas of Pellegrino et al. (25), under pentobarbital (Nembutal 35 mg/kg, ip.) anaesthesia. Cannulas were secured with dental acrylic cement. Rats were allowed a minimum of 5 days to recover from surgery before peptide treatment began.

Rat BNP and CNP were synthetized by G. Tóth. They were dissolved in 0.9% saline and injected icv. in a volume of 2 μl in three doses (100, 200 or 400 ng per animal) to conscious, freely-moving rats. The control animals received the same volume of artificial cerebrospinal fluid.

Animals were sacrificed in a separate room 30 min after icv. injection of artificial cerebrospinal fluid or different doses of BNP or CNP. After decapitation, the brains were quickly removed and various brain regions were isolated from both hemispheres on ice by a modification of the technique of Glowinski and Iversen (26), as described previously (27).

For radioimmunoassay (RIA) of CRF-LI, each area was homogenized with ultrasound (Soniprep 150 MSE, Great Britain) in HCl (100 mM) containing 1 mM ascorbic acid, and an aliquot was sampled for protein measurement (28). The residual homogenates were centrifuged at 6000 g for 20 min, at 4°C, and aliquots were taken and lyophilized for RIA. The CRF antiserum (kindly donated by Paul Vecsei, Dept. of Pharmacology, University of Heidelberg, Germany) was obtained from a rabbit immunized against hCRF. The CRF antibody (29) was specific for the C-terminal region of the CRF_{41} molecule since it did not cross-react with the fragment $CRF_{1\text{-}20}$ or $CRF_{6\text{-}33}$. The RIA procedure was performed as described earlier (27). The lower limit of assay detection was 7-8 pg/tube. The intra- and interassay coefficients of variation were 4.0 and 13.8%, respectively. CRF-LI in the brain extracts subjected to HPLC has been shown to chromatograph identically with synthetic r/hCRF (Gardi et al., unpublished observation). The CRF-LI is expressed in pg/mg protein.

All data are presented as means$\pm$S.E.M. Data were analysed by one-way ANOVA, followed by Duncan's test. A probability level of 0.05 was accepted as indicating a statistically significant difference.

Results

The results of the present study are shown in Figures 1 and 2. After icv. administration of a high dose (400 ng) of BNP, the CRF-LI increased significantly in the hypothalamus ($F=3.07$, $p<0.05$), and amygdala ($F=11.55$, $p<0.001$), while a tendency towards an increase was found in the hippocampus ($F=2.23$, $p=0.12$). In the hypothalamus, the CRF-LI decreased ($F=3.90$, $p<0.05$) after a high dose (400 ng) of CNP. The CRF-LI increased in the basal forebrain ($F=3.13$, $p<0.05$) after a low dose (100 ng) of CNP. At all other examined doses, the CRF-LI contents of the investigated brain regions did not exhibit any marked alteration.

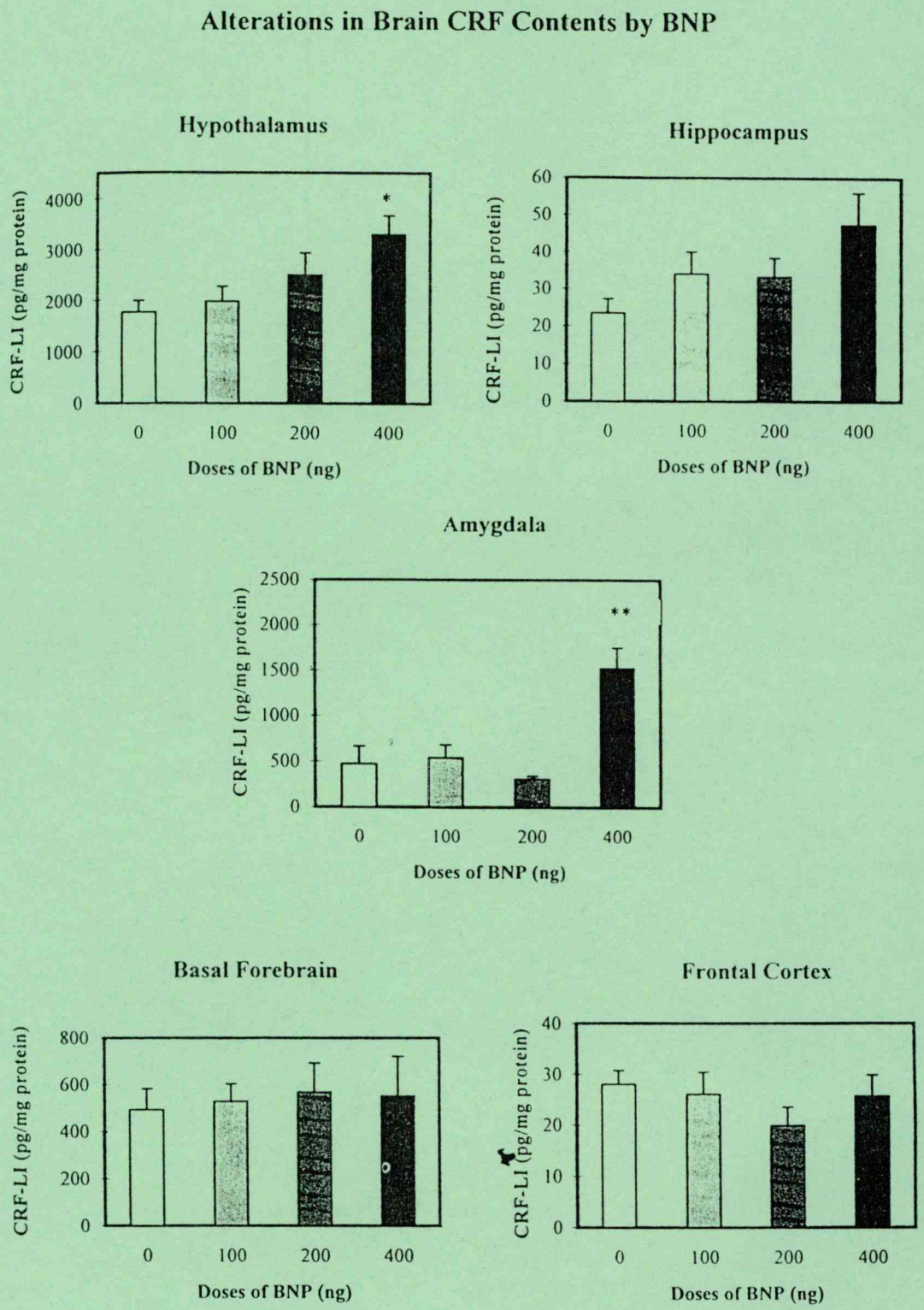

Fig. 1.

Effects of icv. administered BNP on CRF-LI (pg/mg protein ± S.E.M.) in various brain areas. Each group contain 5-8 animals. $^{*}p < 0.05$ vs. control, $^{**}p < 0.001$ vs. control.

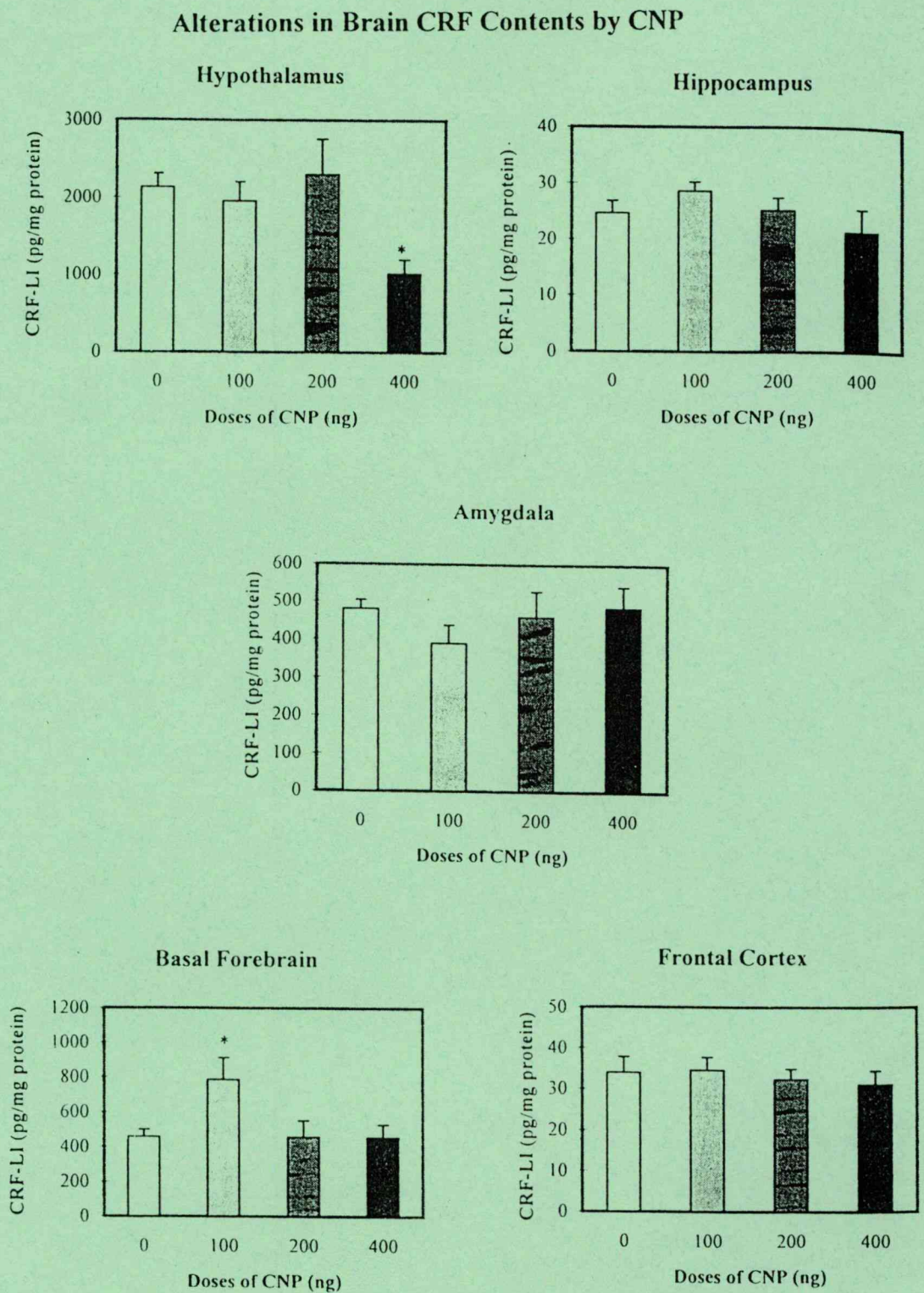

Fig. 2.

Effects of icv. administered CNP on CRF-LI (pg/mg protein±S.E.M.) in various brain areas. Each group contain 5-8 animals. *$p<0.05$ vs. control.

Discussion

The present data demonstrate that centrally administered BNP increases the levels of CRF-LI in the hypothalamus and amygdala. Although the measurement of peptide concentration alone cannot distinguish between synthesis, release or degradation, an increase in regional brain neuropeptide concentration might indicate an increased accumulation due to the decreased release of the peptide. Various evidence suggests that members of the natriuretic peptide family affect numerous neuroendocrine systems, including the hypothalamo-pituitary-adrenal axis. ANP is a potent inhibitor of ACTH secretion in the conscious male rat, and it is a hypothalamic neurohormone which is likely to play an important inhibitory role in the neural control of ACTH release (30). Further, BNP inhibits the ACTH secretion induced by endothelin (11). Our results on the CRF-LI-increasing effects of ANP (21) and BNP in the hypothalamus indicate that the inhibitory actions of ANP and BNP on ACTH secretion could be caused by the inhibition of hypothalamic CRF release.

CRF provokes a behavioral state that resembles fear or anxiety (31). Lesion of the central nucleus of the amygdala blocked this effect of CRF, demonstrating that both the amygdala and CRF are critically involved in fear and anxiety (32). BNP caused an anxiolytic--like behavioral state, revealed by increased plus maze scores (23). In light of the behavioral events mentioned above, the present data on the BNP-induced activation of the intra-amygdaloid CRF raise the possibility that the CRF release in the amygdala may be involved in the mediation of the anxiolytic-like behavioral response of centrally administered BNP.

Several lines of evidence suggest that ANP, BNP and CRF are all involved in the modulation of learning and memory processes (33-38). ANP dose-dependently facilitated passive avoidance behavior (33). Icv. injection of ANP antiserum immediately after the learning trial attenuated passive avoidance behavior; it also facilitated extinction of an active avoidance response (33). BNP has the same effect on avoidance behavior (38,39). Peripheral administration of low doses of CRF was found to facilitate passive avoidance behavior, whereas high doses had the opposite effect (40). The attenuating effect was predominant following central (icv.) administration. Our previous (21) and present results demonstrate that ANP and BNP increase the CRF-LI in the hypothalamus, hippocampus and amygdala. These brain regions play a critical role in learning and memory processes (39). It could be hypothesized that the alterations of the hypothalamic, hippocampal and amygdaloid CRF by ANP and BNP constitute important mediators of the learning and memory processes.

In contrast with the actions of ANP (21) and BNP, CNP decreased the CRF-LI in the hypothalamus. A decrease in the immunoreactive peptide level in a certain brain area usually reflects an increased release and subsequent degradation of the neuropeptide (41). The CNP--induced reduction of the hypothalamic CRF-LI was probably due to the increased release of CRF, whereas the ANP-induced enhancement of CRF-LI in the hypothalamus (21) may be a result of a decreased release. Similarly, ANP and CNP counteract each other in their effects influencing Prl release in the hypothalamus: ANP inhibits and CNP stimulates Prl secretion (16,18). These results raise the possibility that ANP and CNP may exert opposite effects on the hormones released during stress.

The present publication reports effects of BNP and CNP on the CRF contents of various brain structures. These data suggest that CRF neurotransmission may be involved in the mediation of some neuroendocrine and behavioral responses to natriuretic peptides.

Acknowledgements

This work was supported by the Ministry of Social Affairs and Welfare of Hungary (T-11-592/1993), OTKA (T-6084), FEFA 1008 and MHB "A Magyar Tudományért" Foundation. Dr. Paul Vecsei is to be acknowledged for the generous donation of the CRF antiserum.

References

1. H. IMURA, K. NAKAO AND H. ITOH, Front. Neuroendocrinol. 13 217-249 (1992).
2. W.K. SAMSON, Trends Endocrinol. 3 86-90 (1992).
3. E.A. ESPINER, J. Int. Med. 235 527-541 (1991).
4. N. MINAMINO, Y. MAKINO, H. TATEYAMA, K. KANGAVA AND H. MATSUO, Biochem. Biophys. Res. Comm. 179 535-542 (1991).
5. N. MINAMINO, M. ABURAYA, M. KOJIMA, K. MIYAMOTO, K. KANGAVA AND H. MATSUO, Bioochem. Biophys. Res. Comm. 197 326 -335 (1993).
6. M. ABURAYA, N. MINAMINO, J. HINO, K. KANGAWA AND H. MATSUO, Biochem. Biophys. Res. Comm. 165 880-887 (1989).
7. T. HATTORI, K. HASHIMOTO, H. INOUE, SUGAWARA, M., S. SUEMARU, J. KAGEYAMA AND Z. OTA, Endocrinol. Japon. 33 533-539 (1986).
8. G.A. WITTERT, A. ESPINER, A. M. RICHARDS, R.A. DONALD, J.H. LIVESEY AND T.G. YANDLE, Clin. Endocrinol. 38 183-189 (1993).
9. C.R. FRANCI, J. ANSELMO-FRANCI AND S.M. MCCANN, Proc Natl. Acad. Sci. USA 89 11391-11395 (1992).
10. T. SHIBASAKI, M. NARUSE, N. YAMAUCHI, A. MASUDA, T. IMAKI, K. NARUSE, H. DEMURA, N. LING, T. INAGAMI AND K. SHIZUME, Biochem. Biophys. Res. Comm. 135 1035-1041 (1986).
11. S. MAKINO, K. HASHIMOTO, R. HIRASAWA, T. HATTORI, J. KAGEYAMA AND Z. OTA, Brain Res. 534 117-121 (1990).
12. W.K. SAMSON, M.C. AGUILA AND R. BIANCHI, Endocrinology 122 1573-1582 (1988).
13. W.K. SAMSON, Neuroendocrinology 40 277-279 (1985).
14. G. SHIRAKAMI, H. ITOH, S. SUGA, Y. KOMATSU, N. HAMA, K. MORI AND K. NAKAO, Neurosci. Lett. 159 25-29 (1993).
15. W.K. SAMSON, K.D. SKALA, F.L.S. HUANG AND R.J. FULTON, Endocrinology 132 504-509 (1993).
16. W.K. SAMSON, R. VIANCHI AND R.J. MOGG, Can. J. Physiol. Pharmacol. 66 301-305 (1988).
17. W.K. SAMSON, R. VIANCHI AND R.J. MOGG, Neuroendocrinology 47 268-270 (1988).
18. F.L.S. HUANG, K.D. SKALA AND W.K. SAMSON, J. Neuroendocrinol. 4 325-330 (1992).
19. J. IBANEZ-SANTOS, S. TSAGARAKIS, L.H. REES, G.M. BESSER AND A. GROSSMAN, J. Endocrinol. 126 223-228 (1990).
20. T. TAKAO, K. HASHIMOTO AND Z. OTA, Life Sci. 42 1199-1203 (1988).
21. É. BÍRÓ, J. GARDI, M. VECSERNYÉS, J. JULESZ, G. TÓTH AND G. TELEGDY, Life Sci. 59 1351-1356 (1996).
22. É. BÍRÓ, G. TÓTH AND G. TELEGDY, Neuropeptides 29 215-220 (1995).
23. É. BÍRÓ, G. TÓTH AND G. TELEGDY, Neuropeptides 30 59-65 (1996).
24. A.J. DUNN AND C.W. BERRIDGE, Brain Res. Rev. 15 71-100 (1990).
25. L.J. PELLEGRINO, A.S. PELLEGRINO AND A.J. CUSHMAN, A Stereotic Atlas of the Rat Brain, 8-57, Plenum Press, New York (1979).
26. J. GLOWINSKI AND L.L. IVERSEN, J. Neurochem. 13 65-69 (1966).
27. Z. SARNYAI, É. BÍRÓ, J. GARDI, M. VECSERNYÉS, J. JULESZ AND G. TELEGDY, Brain Res. 616 315-319 (1993).
28. O.H. LOWRY, N.J. ROSEBROUGH, A.L. FARR AND R.J. RANDALL, J. Biol. Chem. 193 265-275 (1951).
29. C. MASER-GLUTH AND P. VECSEI, Clin. Endocrinol. 30 405-412 (1989).
30. G. FINK, R.C. DOW, D. CASLEY, C.I. JOHNSTON, A.T. LIM, D.L. COPOLOV, J. BENNIE, J. CARROLL AND H. DICK, J. Endocrinol. 131 R9-R12 (1991).
31. M. DAVIS, The Amygdala: Neurobiological Aspects of Emotion, Memory and Mental Dysfunction, J. Aggleton (Ed.), 255-305, Wiley, New York (1992).
32. K.C. LIANG, K.R. MELIA, S. CAMPEAU, W.A. FALS, M.J.D. MISERENDINO AND M. DAVIS, J. Neurosci. 12 2313-2320 (1992).
33. A. BIDZSERANOVA, J. GUERON, L. BALÁSPIRI AND G. TELEGDY, Peptides 13 957-960 (1992).

34. A. BIDZSERANOVA, B. PENKE, G. TÓTH AND G. TELEGDY, Neuropeptides 19 103-106 (1991).
35. E.H. LEE, H.C. HUNG, K.T. LU, W.H. CHEN AND H.Y. CHEN, Peptides 13 927-937 (1992).
36. E.H. LEE AND W.R. LIN, Life Sci. 48 1333-1340 (1991).
37. M.F. CHEN, T.H. CHIU AND E.H. LEE, Psychoneuroendocrinology 17 113-124 (1992).
38. G. TELEGDY, Rev. Neurosci. 5 309-315 (1994).
39. G.L. KOVÁCS AND D. DE WIED, Pharmacol. Rev. 46 269-292 (1994).
40. H.D. VELDHUIS AND D. DE WIED, Pharmacol. Biochem. Behav. 21 707-713 (1984).
41. Z. SARNYAI, É. BÍRÓ, M. VECSERNYÉS, F. LACZI, G. SZABÓ AND G.L. KOVÁCS, Neuropeptides 23 27-31 (1992).

Pergamon

Peptides, Vol. 16, No. 7, pp. 1167–1172, 1995

0196-9781/95 $9.50 + .00

0196-9781(95)02007-J

Synthesis of Two Peptide Scorpion Toxins and Their Use to Investigate the Aortic Tissue Regulation

GÁBOR K. TÓTH,*[1] JÁNOS PATARICZA,† TAMÁS JANÁKY,* MARIANNA MÁK,‡ MÁRTA ZARÁNDI,* JULIUS GY. PAPP† AND BOTOND PENKE*

**Department of Medical Chemistry, †Department of Pharmacology, Albert Szent-Györgyi Medical University, H-6720 Szeged, Hungary, and ‡Central Research Institute of Chemistry, H-1025 Budapest, Hungary*

Received 17 January 1995

TÓTH, G. K., J. PATARICZA, T. JANÁKY, M. MÁK, M. ZARÁNDI, J. GY. PAPP AND B. PENKE. *Synthesis of two peptide scorpion toxins and their use to investigate the aortic tissue regulation.* PEPTIDES 16(7) 1167–1172, 1995.—The 37 amino acid residue polypeptides iberiotoxin and charybdotoxin, which contain three disulfide bridges, were chemically synthesized and characterized. The physiological effectiveness of these peptides was tested on rabbit aorta in vitro.

Charybdotoxin Iberiotoxin Scorpion toxins Solid-phase synthesis Formation of disulfide bridges Aortic tissue regulation

CHARYBDOTOXIN, a polypeptide containing three disulfide bridges, was isolated from the venom of the scorpion *Leiurus quinquestriatus* by Miller et al. (25,27). The three-dimensional structure of the isolated 37-mer polypeptide was investigated by 2D NMR (3–5,32). A polypeptide with 68% homology to charybdotoxin (Fig. 1) was recently isolated and characterized from the venom of the scorpion *Buthus tamulus* by Galvez et al. (14,18). This peptide, which has been named iberiotoxin, displays similar biological activities as concerns the Ca^{2+}-activated K^+ channels (30,33). Recently, Murphy et al. (13) synthesized it and characterized its 3D structure by 2D ^{1}H-NMR spectroscopy (13,20). However, several successful syntheses of these peptides are described in the literature (22,23,31); the methods used are rather expensive (mainly Fmoc chemistry) and the described yields are quite low (approx. 1%). The synthesis of the appropriate hexasulfhydryl peptide chains can be carried out with better yields and simpler methods, but the refolding of the synthetic polypeptides containing multiple disulfide bonds remains one of the most challenging problems to surmount in the production of biologically active peptides and proteins.

Calcium-activated potassium channels have been shown to play an important role in the regulation of the arterial tone (29). The presence of a large or "big" conductance type (BK_{Ca}) of these channels was demonstrated in the smooth muscle cell membrane of the rabbit aorta with electrophysiological (17) and pharmacological methods (12). Depolarization of the cell membrane (11) and enhancement of intracellular calcium ($[Ca^{2+}]_i$) (8) activate BK_{Ca} channels. Contraction of rabbit aorta elicited either by depolarization or by receptor stimulation was shown to be enhanced by a partially purified toxin of *Leiurus quinquestriatus* venom (9) and, subsequently, by nanomolar concentrations of pure charybdotoxin (10). BK_{Ca} is the only known potassium channel in arterial smooth muscle that is blocked by charybdotoxin (29) and, therefore, the increased tone of the rabbit aorta by the toxin can be accepted as a blocking action on BK_{Ca} channels (30). In our experiments, isolated aortic tissue of rabbits was used as a tool for comparing the functional effectiveness of charybdotoxin and that of its more selective derivative, iberiotoxin (15). The effect of the toxins was measured on basal and

Charybdotoxin:

Glp-Phe-Thr-Asn-Val-Ser-Cys-Thr Thr-Ser-Lys-Glu-Cys-Trp-Ser-Val-Cys-Gln-Arg-
-Leu-His-Asn-Thr-Ser-Arg-Gly-Lys-Cys-Met-Asn-Lys-Lys-Cys-Arg-Cys-Tyr-Ser-OH

Iberiotoxin:

Glp-Phe-Thr-Asp-Val-Asp-Cys-Ser-Val-Ser-Lys-Glu-Cys-Trp-Ser-Val-Cys-Lys-Asp-
-Leu-Phe-Gly-Val-Asp-Arg-Gly-Lys-Cys-Met-Gly-Lys-Lys-Cys-Arg-Cys-Tyr-Gln-OH

FIG. 1. Primary structure of the two scorpion toxins.

[1] Requests for reprints should be addressed to Dr Gábor K. Tóth, Department of Medical Chemistry, Albert Szent-Györgyi Medical University, H-6720 Szeged, Dóm tér 8, Hungary.

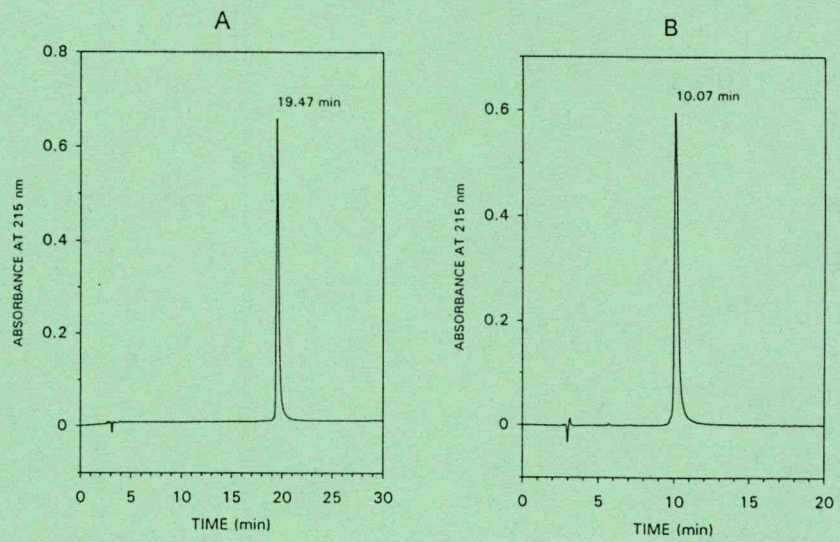

FIG. 2. HPLC profiles of the purified toxins. HPLC conditions: 4.6 × 250 mm 5 μ C18 column (Vydac 218TP54) at a flow rate of 1.0 ml/min with the solvents A (0.1% aqueous TFA) and B (0.1% TFA in 80% aqueous MeCN) in linear gradient mode (gradient: 16.5–30.0% MeCN in 20 min for iberiotoxin, and 6.0–21.0% MeCN in 30 min for charybdotoxin). (A) Charybdotoxin and (B) iberiotoxin.

phenylephrine (PE)-induced isometric tone of aortic ring preparations.

METHOD

Synthesis of Peptides

The peptides were synthesized by a solid-phase technique, utilizing *t*-Boc chemistry (26). Side-chain protecting groups were as follows: Arg(Tos), Glu(OcHex), Asp(OcHex), His(Z), Tyr(2BrZ), Lys(2ClZ), Cys(Meb), Thr(Bzl), and Ser(Bzl). Glp, Met, and Trp were unprotected. The peptides were synthesized on 1.0 g Boc-Gln-Pam resin (0.56 mmol/g) and 1.5 g Boc-Ser(Bzl)-Pam resin (0.37 mmol/g), respectively, and the syntheses were carried out manually. Couplings were performed with DCC, with the exception of Gln and Arg, which were incorporated as their HOBt esters. After the coupling of the first Met or Trp, 0.5% of dithiothreitol was added to the cleavage mixture; this reagent proved to be sufficient to prevent side reactions under the acidolytic cleavage conditions (35). Amino acid incorporation were monitored by the ninhydrin test (21). The peptide resins obtained (3.98 g of iberiotoxin and 4.4 g of charybdotoxin) were divided into two aliquot parts and treated with 6 ml dimethyl sulphide, 2 ml *p*-cresol, 2 ml *p*-thiocresol, 2 ml anisole, and 80 ml HF at 0°C for 1 h. After evaporation of HF under high vacuum, the mixture of the peptide and the resin was washed with dry diethyl ether, and the whole of the remainder was then solubilized without isolation in 2 *M* urea, 0.1 *M* glycine, 0.1 *M* NaCl buffer, pH 8.7, 2000 ml volume, and folded (oxidized) by stirring overnight in air. The resulting folded crude peptides containing disulfide bridges were purified on a SHIMADZU LC8A preparative HPLC system. The resin was filtered off and the whole 2000-ml solution was pumped onto the column and separations were achieved on a 47 × 300 mm column packed with C18 silica gel (300 Å pore size, 15–20 μm particle size) with solvents A (0.1% aqueous TFA) and B (0.1% TFA in 80% aqueous MeCN) using a gradient of 13–26% MeCN in 32 min for the iberiotoxin and 7–20% MeCN in 32 min for the charybdotoxin. The flow rate was 80 ml/min and the column eluate was monitored at 220 nm.

Materials

Phenylephrine hydrochloride (PE) and pentobarbital sodium were purchased from Sigma Chemical Co. (St. Louis, MO). PE was dissolved in double-distilled water for obtaining 1 mmol/l stock solution and stored at −20°C. Dilutions were freshly made every day using Krebs–Henseleit solution. Stock solutions of charybdotoxin and iberiotoxin (each 3 μmol/l concentrations) were prepared in double-distilled water and stored at −20°C. All concentrations indicated in the text and in figures are expressed as final concentrations. The Krebs–Henseleit solution consisted of (mmol/l): NaCl 120, KCl 4.2, $CaCl_2$ 1.5, $NaHCO_3$ 20, $MgCl_2$ 1.2, KH_2PO_4 1.2, and glucose 11.

Preparation of Isolated Rabbit Aorta

White New Zealand rabbits of either sex were anesthetized with 35 mg/kg pentobarbital sodium and then exsanguinated. The thoracic aorta was carefully removed, dissected free of adjoining connective tissue, and immersed in a room-temperature bath of Krebs–Henseleit solution. The aorta was cut into 5-mm rings and suspended in 100-ml organ chambers filled with Krebs–Henseleit solution (bubbled with 95% O_2 and 5% CO_2 gas mixture; pH 7.4 at 37°C).

Measurement of Isometric Tension

Rings were mounted in a recording chamber with a volume of 2 ml for isometric tension recording (Hugo Sachs Elektronic,

FIG. 3. Fab mass spectra of the synthesized peptides. (a) Charybdotoxin, (b) charybdotoxin after reduction of the disulfide bridges, and (c) iberiotoxin.

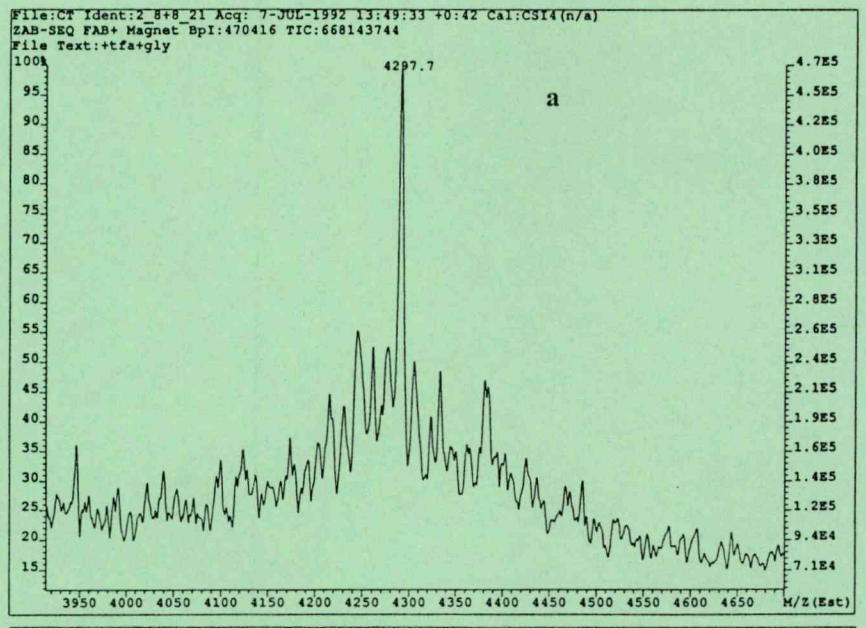
File:CT Ident:2_8+8_21 Acq: 7-JUL-1992 13:49:33 +0:42 Cal:CSI4(n/a)
ZAB-SEQ FAB+ Magnet BpI:470416 TIC:668143744
File Text:+tfa+gly
4297.7
a
M/Z(Est)

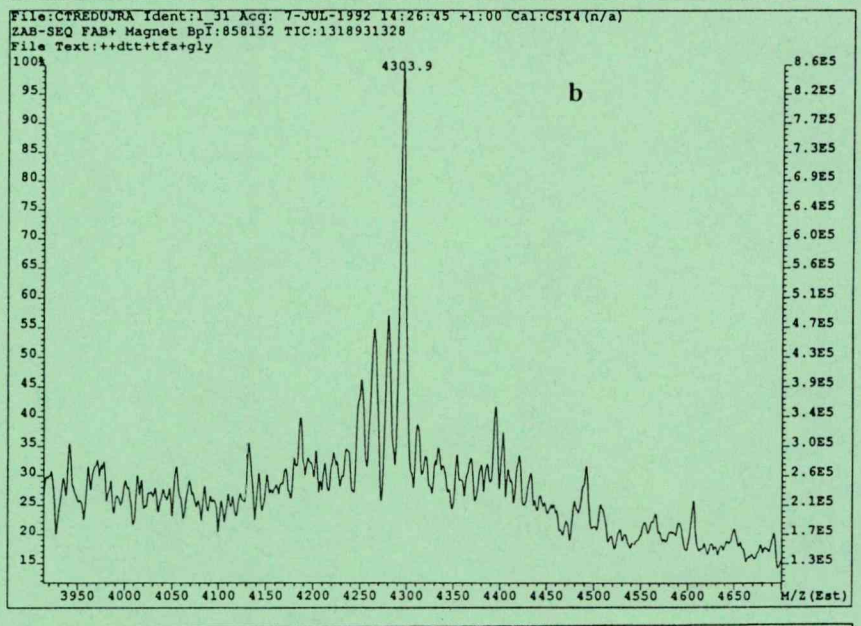
File:CTREDUJRA Ident:1_31 Acq: 7-JUL-1992 14:26:45 +1:00 Cal:CSI4(n/a)
ZAB-SEQ FAB+ Magnet BpI:858152 TIC:1318931328
File Text:++dtt+tfa+gly
4303.9
b
M/Z(Est)

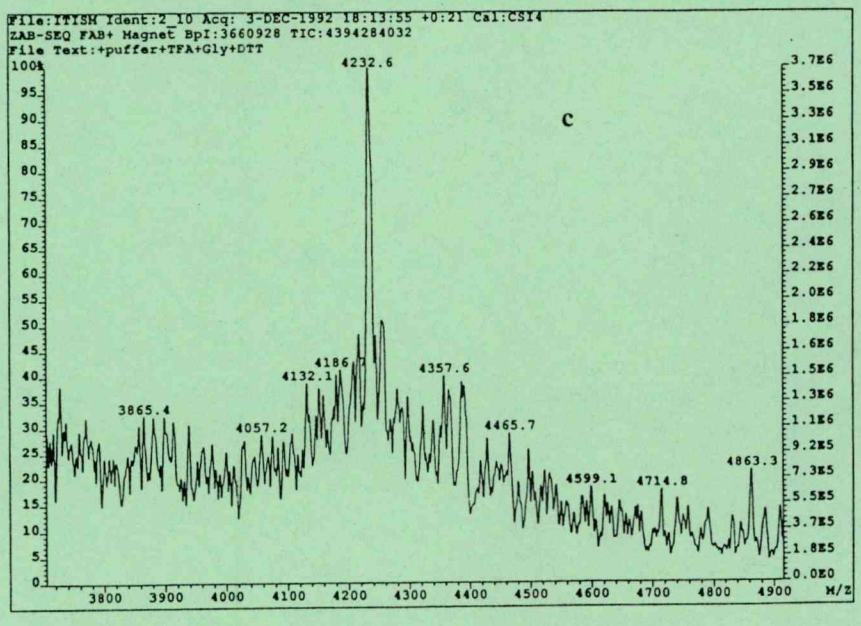
File:ITISH Ident:2_10 Acq: 3-DEC-1992 18:13:55 +0:21 Cal:CSI4
ZAB-SEQ FAB+ Magnet BpI:3660928 TIC:4394284032
File Text:+puffer+TFA+Gly+DTT
4232.6
c
3865.4
4057.2
4132.1
4186.7
4357.6
4465.7
4599.1
4714.8
4863.3
M/Z

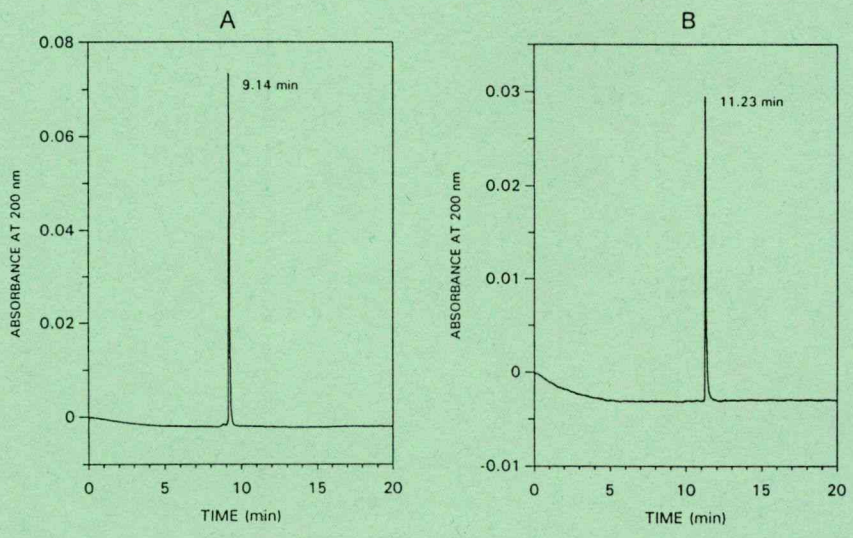

FIG. 4. Capillary electropherogram of the purified toxins. Conditions: BioRad Biofocus 3000 apparatus, 50 μm × 50 cm uncoated capillary using 0.1 *M* phosphate buffer (pH 2.5) and 18 kV voltage. Detection was in 200 nm in single wavelength mode. (A) Charybdotoxin and (B) iberiotoxin.

Type F30, Germany). The recording chamber contained Krebs–Henseleit solution. A resting tension of 10 mN was applied to the tissues, which were equilibrated for 45 min. Mechanical responses of arterial rings were displayed on a pen recorder (KUTESZ Type 175, Hungary).

Two intact arterial rings from the same aorta were separately mounted on two isometric force transducers: one was used for detecting the constricting effect of PE and the other for measuring the action of charybdotoxin or iberiotoxin on PE-induced increase of arterial tone. A cumulative concentration–effect curve was constructed on both rings for PE (15–160 nmol/l), allowing a stable contractile response to develop before progressing to the next concentration of the contractile agent; 90 nmol/l charybdotoxin or iberiotoxin was applied in 62 μl volume 30 min prior to the addition of the first PE dose. In the control (without charybdotoxin or iberiotoxin), 62 μl of distilled water was incubated for 30 min.

Statistical Analysis

Changes in the baseline tension and in PE-induced contractions were expressed in millinewtons. In the text, a minus symbol indicates a decrease of baseline tension compared to the initial resting tension. Values are given as mean ± SEM. Statistical evaluation of the data was performed by one-way analysis of variance (ANOVA) followed by Newman–Keuls multiple range test. Significance was accepted at the 95% confidence interval.

RESULTS

The peptides thus obtained (35.6 mg iberiotoxin and 15.9 mg charybdotoxin from one aliquot) were judged by using a Hewlett–Packard HP-1090 liquid chromatograph to be substantially (>97%) pure. The peptides were chromatographed on a 4.6 × 250 mm 5 μ C18 column (Vydac 218TP54) at a flow rate of 1.0 ml/min with the solvent system mentioned above in linear gradient mode. The retention time for iberiotoxin was 10.07 min (gradient: 16.5–30.0% MeCN in 20 min) and that for charybdotoxin was 19.47 min (gradient: 6.0–21.0% MeCN in 30 min) (Fig. 2). The electropherogram of the upper peptides were made on a BioRad Biofocus 3000 apparatus in 50 μm × 50 cm uncoated capillary using 0.1 *M* phosphate buffer (pH 2.5) and 18 kV voltage. Detection was in 200 nm in single wavelength mode (Fig. 4). Amino acid analyses were: iberiotoxin: Asp 4.3, Glu 3.1, Ser 2.7, Gly 2.7, Arg 2.0, Tyr 1.0, Cys 5.0, Val 4.0, Phe 1.9, Leu 1.0, Lys 4.6, Met 1.1, Thr 1.1; charybdotoxin: Asp 2.9, Glu 2.7, Ser 3.7, Gly 1.0, Arg 2.6, Tyr 0.8, Cys 4.5, Val 2.0, Phe 1.1,

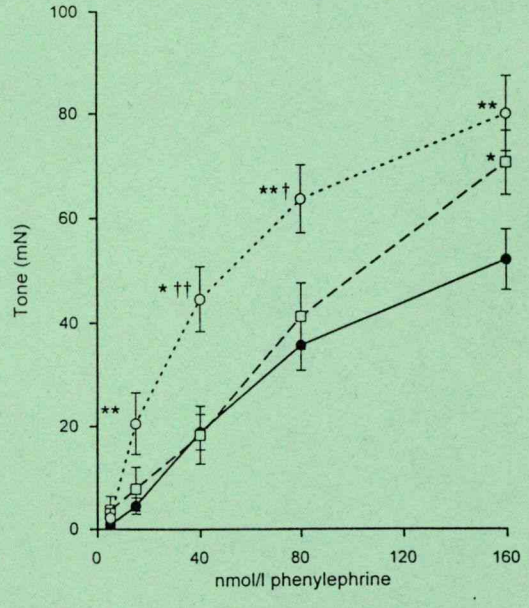

FIG. 5. Effect of charybdotoxin and iberiotoxin on phenylephrine-induced tone in isolated rabbit aorta. Charybdotoxin (□, n = 10) and iberiotoxin (○, n = 8) increased the tone of aortic ring preparations compared to control without toxins (●, n = 16). *$p < 0.05$ and **$p < 0.01$ represent significant differences compared to control; †$p < 0.05$ and ††$p < 0.01$ refer to significant differences between iberiotoxin and charybdotoxin.

Leu 0.9, Lys 3.2, Met 1.0, Thr 2.8, His 0.9, Pro 1.4. Both peptides were coeluted with natural reference standards and proved to be identical.

The FAB-MS experiments were performed with a VG ZAB-2SEQ type hybrid tandem mass spectrometer, equipped with an LSIMS source (Cs^+ ion gun used at 30 keV). Results: iberiotoxin: calculated M + H: 4231.9, found: 4232.6 ± 0.5 [Fig. 3(c)]; charybdotoxin: calculated M + H: 4296.9, found: 4297.7 ± 0.5 [Fig. 3(a)]; after reduction of the disulfide bridges with dithiothreitol: calculated M + H: 4303.0, found: 4303.9 ± 0.5 [Fig. 3(b)].

Pharmacological Measurements

Baseline tension of isolated aorta was not significantly changed after 30-min incubation of rabbit aortic rings with 90 nmol/l charybdotoxin compared to the control treated with solvent (control = −0.18 ± 0.14 mN, charybdotoxin = 1.10 ± 0.82 mN, n = 10, NS). Similarly, 90 nmol/l iberiotoxin also did not change the resting tension of the rings during a 30-min incubation period (control = 0.0 ± 0.0 mN, iberiotoxin = 0.20 ± 0.14 mN, n = 8, NS). When PE, as a contracting agent, was added to the organ bath the BK_{Ca} inhibitors enhanced the amplitude of contraction expressed in mN (Fig. 5). Charybdotoxin increased the effect of 160 nmol/l PE only whereas iberiotoxin significantly increased 15, 40, 80, and 160 nmol/l PE-induced tone. Iberiotoxin was more effective than charybdotoxin against 40 and 80 nmol/l PE.

DISCUSSION

Peptide Synthesis and Purification

The Boc syntheses of the scorpion toxins gave at least comparable results as the described Fmoc syntheses; however, the cost of a Boc synthesis is far lower than the Fmoc synthesis. The overall yield of the synthetic process mentioned above is higher than the described ones. The key step of the production was finding the proper conditions for the formation of the three disulfide bridges by appropriate folding. After the HF cleavage, the solubilization and subsequent lyophilization of the crude unfolded peptide was avoided, because this procedure resulted in an enormous amount of side products. Different pH values were tried for the oxidation. In the first experiments, 0.1 *M* NH_4OH and 2 *M* urea containing solutions were used, but the pH value was not stable during stirring the reaction mixtures in air to form the disulfide bridges. Therefore, in the latter experiments glycine-NaOH buffers were used. According to our findings the best pH for the folding is 8.7. For the folding, mainly the simple air oxidation method was used. The formation of disulfide bridges using oxidized/reduced glutathione gave similar results. The peptide purification proved to be the most effective, if we made separation only in the last step. The isolation of the hexasulfhydryl peptide is unnecessary, and time and work consuming. In some cases an appropriately pure product was resulted in only one-step preparative RP-HPLC purification—in contrast of the described methods.

Aortic Tissue Regulation

In the present study, the functional effectiveness of charybdotoxin and iberiotoxin was tested on the mechanical activity of rabbit aorta in vitro. The two toxins serve as important pharmacological tools for evaluating the role of calcium-activated potassium channels in regulatory pathways of different tissues. Rabbit aorta was used to test the efficiency of the chemical synthesis because only one charybdotoxin-sensitive potassium channel, BK_{Ca}, is located in the smooth muscle of the arterial tissues (29). The role of BK_{Ca} channels in the regulation of rabbit aortic tension has recently been demonstrated in detail (2). This study supported the presence of BK_{Ca} channels in a single smooth muscle cell by using patch clamp method and 50 nmol/l charybdotoxin was able to increase the tone of the blood vessel when 100–200 nmol/l PE was used as contractile agent. We also used PE, a specific α_1-adrenergic receptor agonist. Stimulation of the α_1 receptor results in depolarization (19) and increase of $[Ca^{2+}]_i$ (16,34) in rabbit aorta, both of which can open BK_{Ca} channels (6,8,11). Charybdotoxin (90 nmol/l), which corresponded to the magnitude of concentrations used by others for blocking BK_{Ca} channels in rabbit aorta (2,12) and in other arterial preparations (1,7), increased 160 nmol/l PE-induced contraction but did not affect the baseline tension. In another study, basal tone of rabbit aorta was also not changed by charybdotoxin (28), supporting 1) the lack of a nonspecific contractile action of the toxin, and 2) the absence of functional BK_{Ca} channels in resting smooth muscle. Iberiotoxin also did not influence basal tone and was more effective than charybdotoxin against low concentrations of the contractile agent (40 and 80 nmol/l PE). The latter result is in agreement with the finding that iberiotoxin enhances smooth muscle tone more potently than charybdotoxin (24).

It is important to note that the effectiveness of the toxins in a functional model does not mean selectivity on a particular potassium channel. Charybdotoxin also blocks calcium-activated potassium channels other than BK_{Ca} (15). Pharmacological agonist–antagonist interactions cannot be performed because no specific agonists for BK_{Ca} channels are available at present. However, the charybdotoxin-sensitive potassium channel is a well-characterized channel in rabbit aorta, and the mechanical responses of this tissue to selected concentrations of these toxins can be considered as antagonism on BK_{Ca} channels (30). In conclusion, our synthetic charybdotoxin and iberiotoxin are potent and valuable pharmacological tools for assessing the possible involvement of hyperpolarizing, calcium-activated potassium channels in the physiological and pathologic regulation of tissue responses.

ACKNOWLEDGEMENTS

The authors are indebted to Mr. R. Ferenci, Ms. É. Dósai-Molnár, and Ms. M. Fehér for skillful technical assistance and to Bachem California for financial support.

REFERENCES

1. Asano, M.; Masuzawaito, K.; Matsuda, T.; et al. Functional role of charybdotoxin-sensitive K^+ channels in the resting state of cerebral, coronary and mesenteric arteries of the dog. J. Pharmacol. Exp. Ther. 267:1277–1285; 1994.
2. Bolotina, V. M.; Najibi, S.; Palacino, J. J.; Pagano, P. J.; Cohen, R. A. Nitric oxide directly activates calcium-dependent potassium channels in vascular smooth muscle. Nature 368:850–853; 1994.
3. Bontems, F.; Roumestand, C.; Boyot, P.; et al. Three-dimensional structure of natural charybdotoxin in aqueous solution by ^{1}H-NMR. Charybdotoxin possesses a structural motif found in other scorpion toxins. Eur. J. Biochem. 196:19–28; 1991.
4. Bontems, F.; Roumestand, C.; Gilquin, B.; Menez, A.; Toma, F. Refined structure of charybdotoxin: Common motifs in scorpion toxins and insect defensins. Science 254:1521–1523; 1991.

5. Botems, F.; Roumestand, C.; Gilquin, B.; Menez, A.; Toma, F. New data on the 3D structure of natural charybdotoxin show that scorpion toxins and insect defensins share a common structural motif. In: Smith, J. A.; Rivier, J. E., eds. Peptides, chemistry and biology. Leyden: Escom Science Publishers B. V.; 1992:195–199.
6. Brayden, J.; Nelson, M. T. Regulation of arterial tone by activation of calcium-dependent potassium channels. Science 256:532–535; 1992.
7. Calder, J. A.; Schachter, M.; Sever, P. S. Ion channel involvement in the acute vascular effects of thiazide diuretics and related compounds. J. Pharmacol. Exp. Ther. 265:1175–1180; 1993.
8. Castle, N. A.; Haylett, D. G.; Jenkinson, D. H. Toxins in the characterization of potassium channels. Trends Neurosci. 12:59–65; 1989.
9. Cook, N. S. Effect of some potassium channel blockers on contractile responses of the rabbit aorta. J. Cardiovasc. Pharmacol. 13:299–306; 1989.
10. Cooke, J. P.; Rossitch, E., Jr.; Andon, N. A.; Loscalzo, J.; Dzau, V. J. Flow activates an endothelial potassium channel to release an endogenous nitrovasodilator. J. Clin. Invest. 88:1663–1671; 1991.
11. Cook, N. S. The pharmacology of potassium channels and their therapeutic potential. Trends Pharmacol. Sci. 9:21–28; 1988.
12. Cowan, C. L.; Palacino, J. J.; Najibi, S.; Cohen, R. A. Potassium channel-mediated relaxation to acetylcholine in rabbit arteries. J. Pharmacol. Exp. Ther. 266:1482–1489; 1993.
13. Flinn, J. P.; Murphy, R.; Johns, R. B.; Kunze, W. A. A.; Angus, J. A. Synthesis and biological characterisation of a series of iberiotoxin analogues. Int. J. Pept. Protein Res. 45:320–325; 1995.
14. Galvez, G.; Gimenez-Gallego, G.; Reuben, J. P.; Roy-Constancin, L.; Feigenbaum, P.; Kaczorowski G. J.; Garcia, M. L. Purification and characterization of a unique, potent, peptidyl probe for the high conductance calcium-activated potassium channel from venom of the scorpion *Buthus tamulus*. J. Biol. Chem. 265:11083–11090; 1990.
15. Garcia, M. L.; Galvez, A.; Garcia-Calvo, M.; King, V. F.; Vazqe, J.; Kaczorowski, G. J. Use of toxins to study potassium channels. J. Bioenerg. Biomembr. 23:615–646; 1991.
16. Gelband, C. H.; Ishikawa, T.; Post, J. M.; Keef, K. D.; Hume, J. R. Intracellular divalent cations block smooth muscle potassium channels. Circ. Res. 73:24–34; 1994.
17. Gelband, C. H.; Lodge, N. J.; van Breemen, C. A Ca^{2+}-activated K^+ channel from rabbit aorta. Eur. J. Pharmacol. 167:201–210; 1989.
18. Giangiacomo, K. M.; Sugg, E. E.; Garcia Calvo, M.; et al. Synthetic charybdotoxin-iberiotoxin chimeric peptides define toxin binding sites on calcium-activated and voltage-dependent potassium channels. Biochemistry 32:2363–2370; 1993.
19. Haeusler, G.; DePeyer, J-E. Rabbit aorta: Electrical properties and agonist-induced depolarization. Eur. J. Pharmacol. 166:175–182; 1989.
20. Johnson, B. A.; Sugg, E. E. Determination of the three-dimensional structure of iberiotoxin in solution by ^1H nuclear magnetic resonance spectroscopy. Biochemistry 31:8151–8159; 1992.
21. Kaiser, E.; Colescott, R. L.; Bossinger C. D.; Cook, P. J. Color test for detection of free amino groups in the solid-phase synthesis of peptides. Anal. Biochem. 34:595–598; 1970.
22. Lambert, P.; Kuroda, H.; Chino, N.; Watanabe, T. X.; Kimura, T.; Sakakibara, S. Solution synthesis of charybdotoxin (ChTX), a K^+ channel blocker. Biochem. Biophys. Res. Commun. 170:684–690; 1990.
23. Lambert, P. F.; Kuroda, H.; Chino, N.; Watanabe, T. X.; Kimura, T.; Sakakibara, S. Solution-phase syntheses of the K^+ channel blocker, charybdotoxin. In: Giralt, E.; Andreu, D., eds. Peptides 1990. Leyden: Escom Science Publishers B. V.; 1991:111–112.
24. Laurent, F.; Michel, A.; Bonnet, P. A.; Bompart, J.; Chapat, J. P.; Boucard, M. Effects of toxins, apamine, charybdotoxin and iberiotoxin on the smooth muscle relaxant activity of an imidazo (1,2-a) pyrazine derivative. C R Seances Soc. Biol. Fil. 187:526–535; 1993.
25. MacKinnon, R.; Miller, C. Mutant potassium channels with altered binding of charybdotoxin, a pore-blocking peptide inhibitor. Science 245:1382–1385; 1989.
26. Merrifield, R. B. The synthesis of a tetrapeptide. Solid phase peptide synthesis. J. Am. Chem. Soc. 85:2149–2154; 1963.
27. Miller, C.; Moczydlowski, E.; Philips, M. Charybdotoxin, a protein inhibitor of single Ca^{2+}-activated K^+ channels from mammalian skeletal muscle. Nature 313:316–318; 1985.
28. Najibi, S.; Cowan, C. L.; Palacino, J. J.; Cohen, R. A. Enhanced role of potassium channels in relaxations to acetylcholine in hypercholesterolemic rabbit carotid artery. Am. J. Physiol. 266:H2061–H2067; 1994.
29. Nelson, M. T.; Patlak, J. B.; Worley, J. F.; Standen, N. B. Calcium channels, potassium channels, and voltage dependence of arterial smooth muscle tone. Am. J. Physiol. 259:C3–C18; 1990.
30. Sugg, E. E.; Garcia, M. L.; Reuben, J. P.; Patchett, A. A.; Kaczorowski, G. J. Synthesis and structural characterization of charybdotoxin, a potent peptidyl inhibitor of the high conductance Ca^{2+}-activated K^+ channel. J. Biol. Chem. 265:18745–18748; 1990.
31. Sugg, E. E.; Garcia, M. L.; Johnson, B. A.; Kaczorowski, G. J.; Patchett, A. A.; Reuben, J. P. Synthetic studies on the K^+ channel antagonist charybdotoxin. In: Rivier, J. E.; Marshall, G. R., eds. Peptides, chemistry, structure and biology. Leyden: Escom Science Publishers B. V.; 1990:1069–1070.
32. Takashima, H.; Kobayashi, Y.; Tamaoki, H.; et al. Solution structure of charybdotoxin determined by NMR and distance geometry calculations. In: Giralt, E.; Andreu, D., eds. Peptides 1990. Leyden: Escom Science Publishers B. V.; 1991:557–559.
33. Vita, C.; Bontems, F.; Roumestand, C.; et al. Solid-phase synthesis, structural and functional characterisation of charybdotoxin and of two truncated analogues. In: Schneider, C. H.; Eberle, A. N., eds. Peptides 1992. Leyden: Escom Science Publishers B. V.; 1993:641–642.
34. Yoshitake, K.; Hirano, K.; Kanaide, H. Effects of glibenclamide on cytosolic calcium concentrations and on contraction of the rabbit aorta. Br. J. Pharmacol. 102:113–118; 1991.
35. Zarándi, M.; Tóth, G. K.; Váradi, G.; Janáky, T.; Varga, J. R.; Penke, B. Comparative solid-phase synthesis of caerulein. In: Epton, R., ed. Innovation and perspectives in solid phase synthesis II. UK: Intercept;, 1992:503–506.

2.17.

J. Pharm. Pharmacol. 1995, 47: 921–925
Received January 26, 1995
Accepted July 20, 1995

Effect of Selective Inhibition of Potassium Channels on Vasorelaxing Response to Cromakalim, Nitroglycerin and Nitric Oxide of Canine Coronary Arteries

JANOS PATARICZA, GABOR K. TOTH*, BOTOND PENKE*, JOZSEF HOHN AND JULIUS GY. PAPP

*Department of Pharmacology and *Department of Medical Chemistry, Albert Szent-Gyorgyi Medical University, H-6701 Szeged, Dom ter 12, Hungary*

Abstract

A comparative study was performed on the sensitivity of in-vitro vasorelaxation by nitroglycerin and cromakalim to block glibenclamide, a blocker of ATP-sensitive potassium channels, and iberiotoxin, a selective inhibitor of large-conductance calcium-activated potassium channels.

In isolated canine coronary arteries preconstricted with 25 μM prostaglandin $F_{2\alpha}$, nitroglycerin (0·005–1·8 μM) and cromakalim (0·15–9·6 μM) produced dose-dependent vasodilations. Glibenclamide (30 μM) had no significant effect on relaxation of the dose-response curve to nitroglycerin and almost completely abolished the relaxation by cromakalim, a known opener of ATP-sensitive potassium channels. Iberiotoxin (90 nM) decreased the maximal response to nitroglycerin and had no effect on the vasodilation induced by cromakalim. The effect of iberiotoxin on the vasorelaxing action of nitric oxide, the active metabolite of nitroglycerin, was also examined. In a low potassium chloride (14·4–20·4 mM) medium, as a contractile stimulus, iberiotoxin inhibited relaxations by exogenous nitric oxide (100–200 nM). Enhancement of potassium concentrations to 35·4–40·4 mM significantly decreased relaxation by nitric oxide and under these conditions the inhibitory action of iberiotoxin disappeared.

The present study demonstrated that in canine coronary arteries, the functional role of two potassium channels can be separated by pharmacological means. Nitroglycerin-induced vasorelaxation may be mediated, at least in part, by its enzymatic breakdown product, nitric oxide that activates large-conductance calcium-activated potassium channels.

A change in potassium conductance of the smooth-muscle cell membrane that accompanies relaxation of blood vessels to pharmacological agents is currently the focus of several studies. The heterogeneous distribution of different potassium channels in different vascular preparations determines the subtypes of those channels involved in the mechanism of action of a particular drug (Atwal 1992). Agents that open ATP-sensitive potassium channels (K_{ATP}) such as cromakalim, pinacidil and nicorandil, hyperpolarize the vascular smooth muscle and cause relaxation (Weston 1989). Although the mechanism of vasodilating action of cromakalim, the known representative of this class of drugs, is generally considered specific for opening K_{ATP} (Weston 1989), evidence for the involvement of calcium-activated potassium channels has also been shown (Gelband et al 1989; Cowan & Cohen 1992).

Calcium-activated potassium channels of the large-conductance type (BK_{Ca}) have been identified in smooth-muscle cells from coronary arteries by using patch-clamp techniques (Fujino et al 1991; Taniguchi et al 1993). BK_{Ca} channels were found to be inhibited by scorpion toxins such as charybdotoxin and more selectively by iberiotoxin (Garcia et al 1991), a 37-amino acid peptide produced by the scorpion *Buthus tamulus* (Galvez et al 1990). In isolated canine coronary arteries, agents that elevate guanosine 3′,5′-cyclic monophosphate (cGMP) concentration have been suggested to activate BK_{Ca} channels (Taniguchi et al 1993). Previously, a high concentration (10 μM) of nitroglycerin was found to increase the open probability of a calcium-activated potassium channel with large conductance (300 picosiemens) in cultured smooth muscle of porcine coronary artery (Fujino et al 1991). In epicardial coronary arteries, however, the functional effect of a selective blocker of BK_{Ca} channels on nitroglycerin-induced relaxation has not been demonstrated.

The objective of this investigation was to characterize and compare the effect of the potent and selective blocker of BK_{Ca} channels, iberiotoxin, and that of a blocker of K_{ATP}, glibenclamide, on the in-vitro vasorelaxations induced by cromakalim and nitroglycerin in isolated canine coronary arteries. Further, because nitric oxide is thought to mediate vasodilation by nitroglycerin, the effect of iberiotoxin on the relaxation induced by nitric oxide was also investigated.

Correspondence: J. Pataricza, Department of Pharmacology, Albert Szent-Gyorgyi Medical University, H-6701 Szeged, Dom ter 12, Hungary.

Materials and Methods

Measurement of isometric tension

Mongrel dogs of either sex, 9–15 kg, were anaesthetized with sodium pentobarbitone (30 mg kg^{-1}, i.v.) and heparinized (1000 int. units kg^{-1}). The heart was excised and placed into a Krebs-Henseleit solution of the following composition (mM): NaCl 120, KCl 4·2, $CaCl_2$ 1·5, $NaHCO_3$ 20, $MgCl_2$ 1·2, KH_2PO_4 1·2 and glucose 11. Rings (1·1–1·9 mm o.d., 5 mm widths) from the descending and circumflex branches of left coronary artery were isolated from the heart.

Endothelium was removed by gently rubbing the endothelial surface with a stainless steel wire covered with a cotton swab. Preparations were then mounted in water-jacketed baths containing 2 mL Krebs-Henseleit solution bubbled with 95% O_2-5% CO_2 gas mixture at 37°C. The isometric tension was recorded with a force-displacement transducer (Hugo Sachs Elektronic, Type F30, Germany). Rings were stretched up to 10 mN and allowed to stabilize for 45 min. This tension was readjusted to 10 mN during equilibration. Following equilibration, contractions were induced by 25 μM prostaglandin (PG) $F_{2\alpha}$ and at the maximum amplitude of contraction 1 μM acetylcholine was applied. Only those arterial preparations were used for the experiments that responded with contraction after addition of 1 μM acetylcholine. This protocol served as evidence for functionally de-endothelialized arterial preparations. Indomethacin (10 μM) was used in all experiments to exclude the effect of endogenous prostaglandins on the arterial tone.

Effects of glibenclamide and iberiotoxin on nitroglycerin- and cromakalim-induced relaxation

Two parallel rings isolated from the same branch of a coronary artery were used for measurement of contraction and relaxation. After checking the functional denudation with acetylcholine, the rings were then washed with Krebs-Henseleit solution. One arterial ring was exposed to solvent and served as a control while the other was exposed to a potassium channel blocker (90 nM iberiotoxin or 30 μM glibenclamide) for 30 min. Contractions were induced again by the addition of 25 μM $PGF_{2\alpha}$ to both rings. At the steady state of contraction cromakalim or nitroglycerin was applied in cumulative fashion. The same arterial rings were used for further contractions.

Effect of iberiotoxin on nitric oxide-induced relaxation

In another series of experiments the contraction of the rings was induced with low (14·4–20·4 M) or higher (35·4–40·4 M) concentrations of depolarizing potassium chloride (KCl). Elevation of potassium concentration in the solution was made by substituting NaCl with equimolar KCl in the Krebs-Henseleit medium. Experiments were started with 14·4 mM KCl medium and, if it was necessary, replaced with higher concentrations of KCl until it was enough to induce contraction. Relaxation by exogenous nitric oxide in the presence and absence of 90 nM iberiotoxin was examined.

Preparation of nitric oxide solution

A saturated solution of nitric oxide (about 1·6 mM) in double-distilled water was prepared using a slight modification of a previously described method (Menon et al 1991). Water in a 10-mL Vacutainer tube was deoxygenated by purging with 100% nitrogen for 1 h and then bubbled with nitric oxide for 20 min. For diluting nitric oxide, 100 μL of this solution was transferred with a gas tight syringe (Hamilton, Bonaduz, Switzerland) to another tube containing 10 mL deoxygenated water and used for experiments within 1.5 h. Relaxation with nitric oxide (100–800 nM) was induced at the steady state of KCl contraction in control rings and in rings pretreated with iberiotoxin as described above.

Drugs

Prostaglandin $F_{2\alpha}$, indomethacin and glibenclamide were obtained from Sigma (St Louis, MO, USA). Nitric oxide gas (99·8% pure) was purchased from Messer Griesheim Co. (Düsseldorf, Germany) and nitroglycerin from G. Pohl-Boskamp Gmbh & Co. (Hohenlockstedt, Germany). Cromakalim (BRL 34915) was obtained from Beecham Pharmaceuticals (Harlow, UK). Iberiotoxin was synthesized by Gabor K. Toth (Department of Medicinal Chemistry, Szeged, Hungary). Prostaglandin $F_{2\alpha}$ was dissolved in 70% ethanol (stock solution 10·5 mM), indomethacin was dissolved in 96% ethanol at a concentration of 1 mM. Stock solution of glibenclamide was prepared in dimethylsulphoxide and cromakalim in 70% ethanol to give a concentration of 10 mM. Iberiotoxin was dissolved in double-distilled water to give a concentration of 3 μM. Nitroglycerine was dissolved in 99·8% ethanol (4·4 mM). All stock solutions, except nitroglycerin, were stored frozen at −20°C. From these stock solutions the appropriate concentrations were obtained by diluting with Krebs-Henseleit solution.

Statistical analysis

Enhancement or reduction of arterial tone was calculated as percent maximum increase or decrease of contractile force compared with the pre-drug values. Results are expressed as mean ± s.e.m. and n refers to the number of experiments. Student's *t*-test for paired data or analysis of variance was used to determine the significance of differences between mean values. $P < 0.05$ was taken as statistically significant. EC50 values were calculated by fitting the individual values to the logistic equation of 100*x / (x + b).

Results

In the first part of the experiments, the effect of cromakalim and nitroglycerin was studied in the absence and presence of glibenclamide. The activator of K_{ATP} channels, cromakalim, produced a dose-dependent relaxation of coronary arterial rings in a concentration range of 0·15–9·6 μM (Fig. 1A). The calculated EC50 of cromakalim was 0·41 μM in the absence of glibenclamide. Preincubation of coronary rings for 30 min with 30 μM glibenclamide did not affect the resting tone of the arteries (control = 0·8 ± 1·1%, glibenclamide = 1·7 ± 2·0%, n = 7, $P > 0.05$; percent increase of tone compared with the amplitude of steady-state contraction induced by $PGF_{2\alpha}$) nor was there an effect on the magnitude of contraction induced by $PGF_{2\alpha}$ (control = 49·4 ± 6·0 mN, glibenclamide = 53·8 ± 7·4 mN, n = 7, $P > 0.05$). However, glibenclamide almost completely inhibited the relaxation induced by cromakalim. Cumulative addition of nitroglycerin (0·005–1·8 μM) relaxed the coronary arteries with an EC50 of 0·15 μM (Fig. 1B). Preincubation of arterial preparations with 30 μM glibenclamide for 30 min did not significantly modify the relaxation induced by nitroglycerin. The EC50 value of nitroglycerin in the presence of glibenclamide was 0·17 μM.

In the second part of the experiments, the vasorelaxing effect of cromakalim and nitroglycerin was studied in the absence and presence of 90 nM iberiotoxin, the specific inhibitor of BK_{Ca} channels (Fig. 2). At the end of the 30-min incubation period with iberiotoxin, the resting tone of

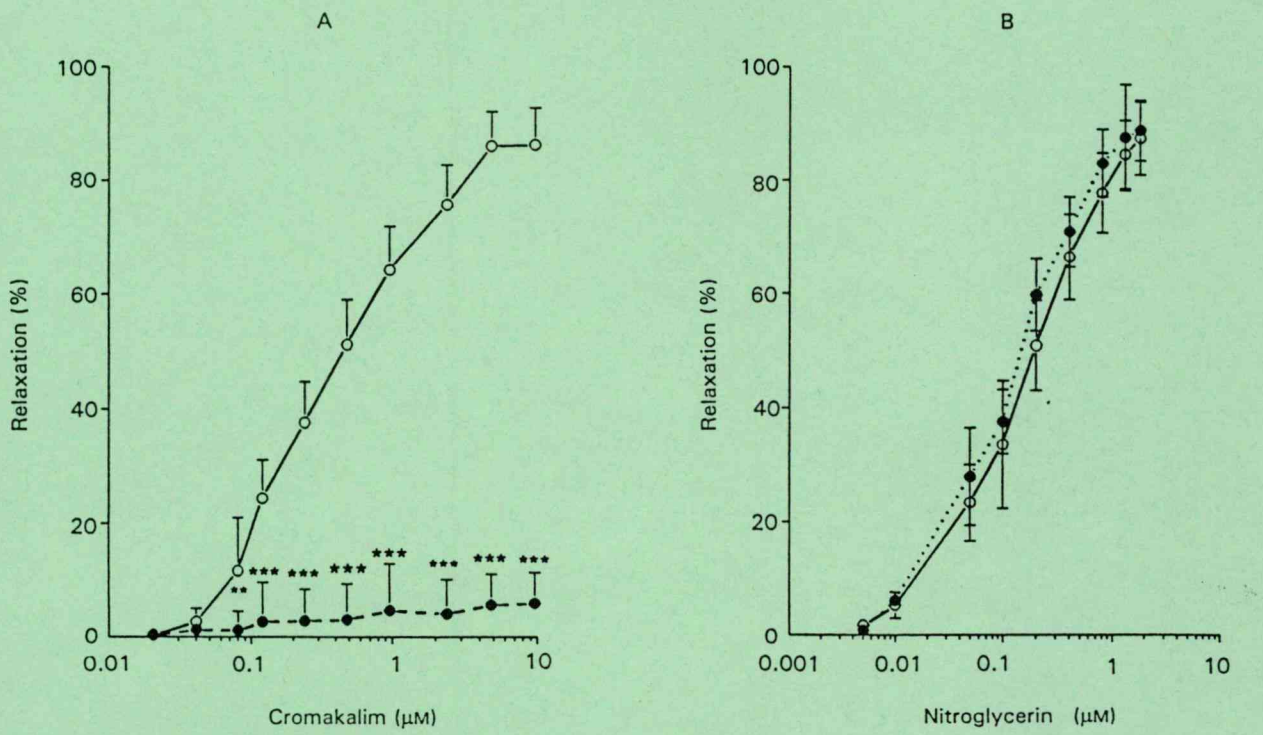

FIG. 1. Effect of glibenclamide on the relaxant responses to cromakalim (A) and nitroglycerin (B) in isolated rings of canine coronary arteries. Paired arterial rings prepared from the same heart were pretreated with either 30 μM glibenclamide (●) or the corresponding volume of vehicle (○) 30 min before addition of 25 μM $PGF_{2\alpha}$. At the steady-state contraction induced by $PGF_{2\alpha}$ cromakalim or, in two different rings from the same heart, nitroglycerin was applied cumulatively. Each value represents the mean of percent relaxation obtained in seven coronary rings from different dogs. Vertical lines show the s.e.m. $^{**}P < 0.01$, $^{***}P < 0.001$ compared with vehicle-treated group.

the arteries was slightly but significantly increased compared with control (control = 1·2 ± 1·2%, iberiotoxin-treated = 10·4 ± 2·5%, n = 7, $P < 0.05$). The maximum contraction amplitude produced by $PGF_{2\alpha}$ did not differ between the iberiotoxin-treated group and the control (control = 55·6 ± 5·3 mN, iberiotoxin-treated = 53·3 ± 7·8 mN, n = 7, $P > 0.05$). Preincubation of coronary arteries with iberiotoxin for 30 min did not change the vasodilating potency of cromakalim (EC50 cromakalim = 0·43 μM, EC50 cromakalim + iberiotoxin = 0·42 μM, Fig. 2A). When the isolated rings were preincubated with iberiotoxin, a significant decrease of maximum relaxation by nitroglycerin at the doses of 1·3 and 1·8 μM was seen (Fig. 2B). Because only the maximum relaxation of the drug was affected by iberiotoxin, the EC50 value for nitroglycerin was not calculated.

In the third part of the experiments, exogenous nitric oxide was added to the coronary rings partially depolarized with KCl. Threshold concentration of KCl necessary to induce contraction varied between 14·4 and 20·4 mM. When the KCl concentration was 14·4–20·4 mM, iberiotoxin significantly enhanced the amplitude of contraction (control = 11·6 ± 4·3 mN, KCl = 25·3 ± 3·7 mN, n = 7, $P < 0.05$). The results obtained with nitric oxide are summarized in Table 1. Relaxation by 100 and 200 nM nitric oxide was significantly inhibited by iberiotoxin. The effect of higher concentrations (400–800 nM) of nitric oxide was not influenced by the toxin. Depolarization of the artery with 35·4–40·4 mM KCl resulted in a contraction amplitude of 35·7 ± 7·0 mN (control) that did not differ from that of the iberiotoxin pretreated group (38·4 ± 4·7 mN, n = 6, $P > 0.05$ compared with control). Amplitudes of relaxation by nitric oxide were significantly smaller in higher KCl concentrations and the inhibitory effect of iberiotoxin on nitric oxide-induced relaxation disappeared at higher concentrations of depolarizing KCl.

Discussion

This study provides a comparative analysis in coronary arterial smooth muscle of the sensitivity of vasorelaxation to cromakalim and nitroglycerin as well as to the specific antagonists of potassium channels, K_{ATP} and BK_{Ca} in-vitro. Glibenclamide almost completely inhibited the relaxation response to cromakalim and did not influence the cumulative dose-response curve induced by nitroglycerin in canine coronary vessels. In conscious dogs, a similar functional distinction in coronary dilations by pinacidil, another K_{ATP} opener, and sodium nitroprusside, another cGMP-elevating substance, has been performed (Duncker et al 1993). Iberiotoxin, the most selective inhibitor of BK_{Ca} channels (Garcia et al 1991), did not modify vasorelaxation to cromakalim. Some observations support (Strong et al 1989; Green et al 1991) while others contradict (Gelband et al 1989; Okabe et al 1990) this finding, suggesting the possibility that K_{ATP} and BK_{Ca} channels are not functionally distinct entities in some blood vessels. In our study, the basal tone was also differentially affected by glibenclamide and iberiotoxin, supporting the hypothesis that the two potassium channels can be separated by pharmacological means in epicardial coronary arteries.

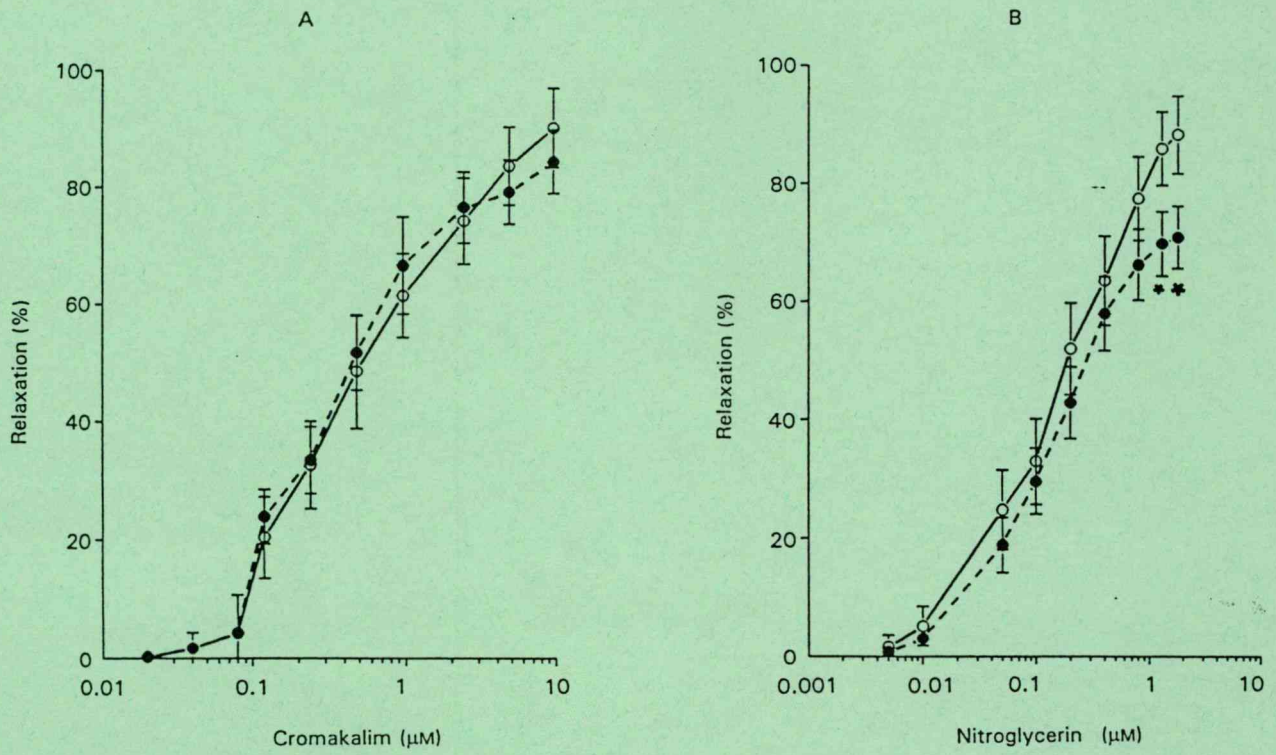

FIG. 2. Effect of iberiotoxin on the relaxation induced by cromakalim (A) and by nitroglycerin (B) in isolated rings of canine coronary arteries. One of two arterial rings was pretreated with 90 nM iberiotoxin (●) and the other was exposed to the solvent of iberiotoxin (○). After 30 min preincubation with iberiotoxin, contraction was induced with 25 μM $PGF_{2\alpha}$. At the steady-state of contraction, cromakalim was added in a cumulative fashion. Experiments were repeated with nitroglycerin in two other arteries prepared from the same heart. Values are mean ± s.e.m. each representing seven coronary preparations obtained from different dogs. $^{*}P < 0.05$ compared with vehicle-treated group.

It is generally accepted that nitroglycerin increases cGMP in the smooth-muscle cell which is associated with relaxation (Ignarro & Kadowitz 1985). In coronary arteries, the open probability of large-conductance calcium-activated potassium channels was increased by nitroglycerin, 8-bromo-cGMP (Fujino et al 1991) as well as by cGMP-dependent protein kinase (Taniguchi et al 1993), suggesting a connection between BK_{Ca} channels and the cGMP-messenger system. Although a large density of this potassium channel was measured in the isolated smooth muscle cells of canine coronary arteries (Wilde & Lee 1989; Taniguchi et al 1993), the functional effect of nitroglycerin, as a major coronary dilator, on BK_{Ca} channels has not yet been investigated. In the current study, iberiotoxin, the most selective inhibitor of BK_{Ca} channels, significantly inhibited the maximum relaxation by nitroglycerin. This is in agreement with the observation that 1 μM nitroglycerin decreased the amplitude of the action potential evoked by tetraethylammonium (Harder et al 1979), a nonselective inhibitor of BK_{Ca} channels (Nelson et al 1990). However, the vascular action of submicromolar concentrations of nitroglycerin was not sensitive to the inhibitory effect of the toxin. Many proposals have been made concerning other mechanisms. These include the inhibition of phospholipase C and the subsequent decrease of inositol 3′,5′-triphosphate formation, the inhibition of Ca^{2+} release by the sarcoplasmic reticulum, the activation of

Table 1. Effect of iberiotoxin on nitric oxide-induced relaxation in depolarizing potassium chloride (KCl) solution.

Agonist	Relaxation (%)			
Nitric oxide (nM)	100	200	400	800
14·4–20·4 mM KCl	30·0 ± 5·2	50·8 ± 4·6	71·3 ± 3·6	89·6 ± 4·1
+ iberiotoxin	12·0 ± 4·9**	28·3 ± 6·0**	67·8 ± 5·5	92·5 ± 3·3
35·4–40·4 mM KCl	3·2 ± 2·0++	13·4 ± 4·1++	41·3 ± 6·90+	67·4 ± 6·6+
+ iberiotoxin	5·3 ± 3·3	17·2 ± 5·2	46·0 ± 4·7	59·1 ± 5·7

Data are mean ± s.e.m. Number of experiments was six in the low-potassium medium and seven in the high-potassium medium. $^{**}P < 0.01$ compared with the corresponding 14·4–20·4 mM KCl, $^{+}P < 0.05$, $^{++}P < 0.01$ compared with values obtained in 14·4–20·4 mM KCl.

the Ca^{2+} pump ATPase in cellular and subcellular membranes and dephosphorylation of the myosin light chain. These mechanisms are all known to be mediated by cGMP (Rapoport 1986; Ahlner et al 1991; Ignarro 1991). Thus, opening of an iberiotoxin-sensitive potassium channel by nitroglycerin represents only a part of the complex mechanism by which the drug decreases coronary tone. Because the relaxation by cromakalim was not affected by iberiotoxin at all and cromakalim did not influence cyclic nucleotides (Taylor et al 1988), we hypothesized a functional connection between BK_{Ca} channels and nitric oxide, the active metabolite of nitroglycerin.

Nitroglycerine is converted into nitric oxide in coronary arteries (Chung & Fung 1993) and nitric oxide has also been found to open BK_{Ca} channels (Bolotina et al 1994). In our experiments, the effect of 100 and 200 nM but not 400 and 800 nM nitric oxide was decreased by iberiotoxin in a medium of low potassium (< 20·4 mM KCl). Elevation of potassium concentration to 35·4–40·4 mM significantly depressed the relaxation by nitric oxide and, under this condition, the iberiotoxin-sensitive component disappeared. These findings support the importance of the membrane potential in the vasorelaxing mechanism of nitric oxide (Tare et al 1990) and also show that most of the relaxations, similar to nitroglycerin, are not sensitive to the high concentration of iberiotoxin.

In conclusion, there are at least two potassium channels, K_{ATP} and BK_{Ca}, that can be activated or inhibited in epicardial coronary arteries of dogs. We have demonstrated for the first time that nitroglycerin and its active metabolite, nitric oxide possess an iberiotoxin-sensitive mechanism in their acute vasodilator action in-vitro. This mechanism involves a large-conductance potassium channel (BK_{Ca}) that mediates a part of the relaxation induced by nitroglycerin and nitric oxide. Further studies are necessary for exploring the significance of this hyperpolarizing potassium channel, known to be a protective mechanism against depolarization overload in the smooth muscle (Brayden & Nelson 1992).

Acknowledgements

This study was supported by the Hungarian National Scientific Foundation (OTKA T 12848). The authors are grateful to Maria Feher for her valuable technical assistance.

References

Ahlner, J., Andersson, R. G. G., Torfgard, K., Axelsson, K. L. (1991) Organic nitrate esters: clinical use and mechanisms of actions. Pharmacol. Rev. 43: 351–423

Atwal, K. S. (1992) Modulation of potassium channels by organic molecules. Med. Res. Rev. 12: 569–591

Bolotina, V. M., Najibi, S., Palacino, J. J., Pagano, P. J., Cohen, R. A. (1994) Nitric oxide directly activates calcium-dependent potassium channels in vascular smooth muscle. Nature 368: 850–853

Brayden, J. F., Nelson, M. T. (1992) Regulation of arterial tone by activation of calcium-dependent potassium channels. Science 256: 532–535

Chung, S.-J., Fung, H.-L. (1993) Relationship between nitroglycerin-induced vascular relaxation and nitric oxide production. Biochem. Pharmacol. 45: 157–163

Cowan, C. L., Cohen, R. A. (1992) Different mechanisms of relaxation of pig coronary artery to bradykinin and cromakalim are distinguished by potassium channel blockers. J. Pharmacol. Exp. Ther. 260: 248–253

Duncker, D. J., Van Zon, N. S., Altman, J. D., Pavek, T. J., Bache, R. J. (1993) Role of K^+_{ATP} channels in coronary vasodilation during excercise. Circulation 88: 1245–1253

Fujino, K., Nakaya, S., Wakatsuki, T., Miyoshi, Y., Nakaya, Y., Mori, H., Inoue, I. (1991) Effects of nitroglycerin on ATP-induced Ca^{++}-mobilization, Ca^{++}-activated K channels and contraction of cultured smooth muscle cells of porcine coronary artery. J. Pharmacol. Exp. Ther. 256: 371–377

Galvez, A., Gimenez-Gallego, G., Reuben, J. P., Contancin, L., Fiegenbaum, P., Kaczorowski, G. J., Garcia, M. L. (1990) Purification and characterization of a unique, potent, peptidyl probe for high-conductance calcium activated potassium channel from venom of the scorpion *Buthus tamulus*. J. Biol. Chem. 265: 11083–11090

Garcia, M. L., Galvez, A., Garcia-Calvo, M., King, V. F., Vazque, J., Kaczorowski, G. J. (1991) Use of toxins to study potassium channels. J. Bioenerg. Biomembr. 23: 615–646

Gelband, C. H., Lodge, N. J., van Breemen, C. (1989) A Ca^{2+}-activated K^+ channel from rabbit aorta. Eur. J. Pharmacol. 167: 201–210

Green, K. A., Foster, R. W., Small, R. C. (1991) A patch clamp study of K^+-channel activity in bovine isolated tracheal smooth muscle cells. Br. J. Pharmacol. 102: 871–878

Harder, D., Belardinelli, L., Sperelakis, N., Rubio, R., Berne, R. M. (1979) Differential effects of adenosine and nitroglycerin on the action potentials of large and small coronary arteries. Circ. Res. 44: 176–182

Ignarro, L. J. (1991) Signal transduction mechanisms involving nitric oxide. Biochem. Pharmacol. 41: 485–490

Ignarro, L. J., Kadowitz, P. J. (1985) The pharmacological and physiological role of cyclic GMP in vascular smooth muscle relaxation. Annu. Rev. Pharmacol. Toxicol. 25: 171–191

Menon, N. K., Pataricza, J., Binder, T., Bing, R. J. (1991) Reduction of biological effluents in purge and trap micro reaction vessels and detection of endothelium-derived nitric oxide (Edno) by chemiluminescence. J. Mol. Cell. Cardiol. 23: 389–393

Nelson, M. T., Patlak, J. B., Worley, J. F., Standen, N. B. (1990) Calcium channels, potassium channels, and voltage dependence of arterial smooth muscle tone. Am. J. Physiol. 259: C3–C18

Okabe, K., Kajioka, S., Nakao, K., Kitamura, K., Kuriyama, H., Weston, A. H. (1990) Actions of cromakalim on ionic currents recorded from single smooth muscle cells of the rat portal vein. J. Pharmacol. Exp. Ther. 252: 832–839

Rapoport, R. M. (1986) Cyclic guanosine monophosphate inhibition of contraction may be mediated through inhibition of phosphatidylinositol hydrolysis in rat aorta. Circ. Res. 58: 407–410

Strong, P. N., Weir, S. W., Beech, D. J., Hiestand, P., Kocher, H. (1989) Effects of potassium channel toxins from *Leiurus quinquestriatus hebraeus* venom on responses to cromakalim in rabbit blood vessels. Br. J. Pharmacol. 98: 817–826

Taniguchi, J., Furukawa, K.-I., Shigekawa, M. (1993) Maxi K^+ channels are stimulated by cyclic guanosine monophosphate-dependent protein kinase in canine coronary artery smooth muscle cells. Pflugers Arch. 423: 167–172

Tare, M., Parkington, H. C., Coleman, H. A., Neild, T. O., Dusting, G. J. (1990) Hyperpolarization and relaxation of arterial smooth muscle caused by nitric oxide derived from the endothelium. Nature 346: 69–71

Taylor, S. G., Southerton, J. S., Weston, A. H., Baker, J. R. J. (1988) Endothelium-dependent effects of acetylcholine in rat aorta: a comparison with sodium nitroprusside and cromakalim. Br. J. Pharmacol. 94: 853–863

Weston, A. H. (1989) Smooth muscle K^+ channel openers, their pharmacology and clinical potential. Pflugers Arch. 414: S99–S105

Wilde, D. W., Lee, K. S. (1989) Outward potassium currents in freshly isolated smooth muscle cell of dog coronary arteries. Circ. Res. 65: 1718–1734

2.18.

Acta Physiologica Hungarica, Volume 84 (3), pp. 293–294 (1996)

NITRIC OXIDE ACTIVATES AN IBERIOTOXIN-SENSITIVE POTASSIUM CHANNEL IN HUMAN SAPHENOUS VEIN

J. Hőhn, J. Pataricza+, G. K. Tóth*, Á. Balogh, J. Gy. Papp+

Department of Surgery, +Department of Pharmacology and *Department of Medical Chemistry, Albert Szent-Györgyi Medical University, Szeged, Hungary

Abstract: Synthetic iberiotoxin (IBTX), an inhibitor of large conductance calcium-activated potassium channel (BKCa), was used to study the possible involvement of a specific hyperpolarizing ion channel in nitric oxide (NO)-induced venodilation. Serotonin (0.125 μM)-induced contraction of isolated human saphenous vein was dose-dependently relaxed with 50–1550 nanoM exogenous NO. 30 min preincubation of venous preparations with 90 nanoM IBTX decreased vasorelaxation induced by NO. In conclusion, a hyperpolarizing potassium channel, BK_{Ca}, may be involved in the venodilator effect of endogenous NO.

Keywords: nitric oxide, iberiotoxin, saphenous vein, human

Introduction

The precise mechanism by which nitric oxide (NO) dilates venous blood vessels is still not known. Recent investigations have presented evidences at cyclic GMP elevating drugs are able to activate BK_{Ca}, a hyperpolarizing potassium channel (1, 2). Synthetic IBTX (3), the known most selective inhibitor of large conductance calcium activated potassium channel (BK_{Ca}), has been shown to decrease acute venodilatation induced by nitroglycerine (4). In the present study, the possible involvement of BK_{Ca} channels in venous dilatation by NO was investigated using isolated human saphenous veins.

Methods

Saphenous veins were prepared from patients suffered from varicose vein disease and put into ice-cold Krebs-Henseleit solution (KHS). The veins were cleared of connective tissues and cut into 5 mm rings. Then, rings were put into KHS bubbled with 95% O_2 and 5% CO_2 gas mixture; pH 7.4 at 37 °C. Nitric oxide was obtained by reducing $NaNO_2$ in the following medium: 140 mM Na_2SO_4, 100 mM NaI, and 270 μl concentrated H_2SO_4 in 50 ml double distilled water. This solution was then bubbled with 95% N_2 and 5% CO_2 gas mixture for 45 min in an air-tight vacutainer tube. $NaNO_2$ was injected into this O_2 free solution to result in 100 μM stock solution. Rings were suspended on a force transducer to measure the isometric contractions. In parallel measurements, two rings prepared from the same vein were streched up with 10 mN in 2 ml recording chambers containing KHS. Equilibration of the rings lasted for 60 min. Mechanical responses of venous preparations were displayed on a pen recorder. After 30 min equilibration of the two venous preparations with 90 nM IBTX and with the corresponding volumes of solvent contractions were induced with serotonin (0.125 μM). At the steady state of contractions, cumulative concentrations of NO (50–1550 nM) were applied. For statistics one-way analysis of variance (ANOVA) was used. ED_{50} values were calculated by fitting the equation of A/(1+exp(b*(x–c))) to the mean values.

For correspondence: József Hőhn, Department of Surgery, Albert Szent-Györgyi Medical University, H–6720 Szeged, P.O. Box 464, Hungary

0231–424X/96/$ 5.00

Results

NO in a concentration range of 50–1550 nanoM dose-dependently relaxed both IBTX pretreated and control saphenous rings. Significant differences have been found between the corresponding values of NO and IBTX+NO (Table 1). The calculated IC_{50} values of NO were 1471.9 nanoM (with IBTX) and 952.7 nanoM (at the control), respectively.

Table 1

Effect of iberiotoxin on nitric oxide-induced relaxation of human saphenous vein

	Relaxation (%)				
	50	150	350	750	1550
			nitric oxide (nanoM)		
Serotonin	1.0 ±1.0	5.5 ±1.2	16.8 ±4.2	29.9 ±3.1	65.5 ±6.9
Serotonin +IBTX	0.0 ±0.0	0.0 ±0.0*	4.5 ±1.7*	15.4 ±3.6*	34.8 ±7.3*

Number of preparations=6. Data are mean ± S.E.M., *$p<0.05$ between the corresponding values of serotonin and serotonin + IBTX

Conclusion

In the light of these observations, we suppose that BK_{Ca} channels exist in the smooth muscle membrane of human saphenous vein. From these and from our previous findings (4, 5) we can conclude that vasodilation by nitroglycerine in some blood vessels may be mediated through NO-induced opening of BK_{Ca} channels.

References

1. Robertson, B. E., Schubert, R., Hescheler, J., Nelson, M. T.: cGMP-dependent protein kinase activates Ca-activated K channels in cerebral artery smooth muscle cells. Am. J. Physiol. 265, C299–C303, 1993
2. Khan, S. A., Mathews, W. R., Meisheri, K. D.: Role of calcium-activated K+ channels in vasodilation induced by nitroglycerine, acetylcholine and nitric oxide. J. Pharmacol. Exp. Ther. 267, 1327–1335, 1993
3. Tóth, G. K., Pataricza, J., Janáky, T., Mák, M., Zarándi, M., Papp, J. Gy., Penke, B.: Synthesis of two peptide scorpion toxins and their use to investigate the aortic tissue regulation. Peptides 16/7, 1167–1172, 1995
4. Höhn, J., Pataricza, J., Tóth, G. K., Balogh, Á., Papp, J. Gy.: Nitroglycerine activates an iberiotoxin-sensitive potassium channel in human saphenous vein. J. Mol. Cell. Cardiol. 27/6, A143, 1995
5. Pataricza, J., Tóth, G. K., Penke, B., Höhn, J., Papp, J. Gy.: Effect of selective inhibition; of potassium channels on vasorelaxing response to cromakalim, nitroglycerin and nitric oxide of canine coronary arteries. J. Pharm. Pharmacol. 47, 921–925, 1995

Supported by the Hungarian Health Science Council (T-06521/93) and by OTKA (T-12848)

Eur. J. Biochem. 206, 421–425 (1992)
© FEBS 1992

3.1.

Conformational and functional properties of peptides covering the intersubunit region of influenza virus hemagglutinin

Miklos HOLLÓSI[1], Ashraf A. ISMAIL[2], Henry H. MANTSCH[2], Botond PENKE[3], Istvan G. VARADI[3], Gabor K. TOTH[3], Ilona LACZKÓ[4], Istvan KURUCZ[5], Zoltan NAGY[6], Gerald D. FASMAN[7] and Eva RAJNAVÖLGYI[6]

[1] Department of Organic Chemistry, Eötvös University, Budapest, Hungary
[2] Steacie Institute for Molecular Sciences, NRC, Ottawa, Canada
[3] Department of Medical Chemistry, A. Szentgyörgyi Medical University, Szeged, Hungary
[4] Institute of Biophysics, Biological Research Center, Szeged, Hungary
[5] Institute for Drug Research, Budapest, Hungary
[6] Department of Immunology, Eötvös University, God, Hungary
[7] Department of Biochemistry, Brandeis University, Waltham, USA

(Received November 12, 1991, February 17, 1992) – EJB 91 1525

The functionally active part of influenza virus hemagglutinin was investigated through the synthesis of a series of peptides representing different parts of the intersubunit region. Secondary structure prediction, circular dichroism and Fourier transform infrared spectroscopic studies were undertaken to investigate the secondary structure of these peptides. The peptide fragments were found to adopt multiple conformations, depending on their concentration in solution, the presence of the non-ionic detergent octyl-β-D-glucoside and the polarity of the solvent. The results of biological studies with these peptide fragments are discussed in relation to their conformation, as inferred from the spectroscopic analysis.

Hemagglutinin, the envelope glycoprotein of the influenza virus, is a trimer of molecular mass 224 640 Da. It is an integral membrane protein characterized by a three-domain structure [1]. A basic requirement for the infectivity of the virus is the post-translational enzymic cleavage of the external domain of hemagglutinin which, by elimination of Arg329 results in two subunits, which we refer to as hemagglutinin 1 (HA1) and hemagglutinin 2 (HA2) (see Scheme 1 for the amino acid sequence of these fragments). This separation exposes the N-terminal of HA2, the so-called fusion peptide [1–3]. It is this peptide which, after a pH-dependent conformational change, enables the fusion of the virus envelope with the endosomal membrane of the host cell. According to earlier circular dichroism and fluorescence spectroscopic studies [4], the 20-amino-acid fragment, but not the 16-amino-acid fragment from the N-terminal fusogenic region of HA2 adopts a helical conformation when bound to vesicles. Using circular dichroism spectroscopy, Wharton et al. [5] found a correlation between fusogenicity and α-helix content of a 23-amino-acid fragment of HA2.

To elucidate whether the conformation of this part of hemagglutinin plays a role in T-cell and B-cell recognition, a series of peptides representing the intersubunit region (IP), the fusion peptide (FP1) and the remnant of the hemagglutinin intersubunit (HA1C-Arg) were synthesized, along with analogues that contain a D-Arg in the central position [D-Arg13]IP, lack an arginine at the N-terminal peptide (HA1C), or contain arginines at both ends of the fusion peptide (FP3; see Scheme 1). As B-cell recognition is highly dependent on determinant conformation [6, 7] and T cell epitopes are characterized by restricted conformational requirements [8], the conformational characterization of these peptides was of particular interest.

Circular dichroism and Fourier-transform (FT-IR) spectroscopic studies were undertaken to explore the secondary structure adopted by these synthetic peptides in solution. The conformation of the peptides was investigated in aqueous solution and in trifluoroethanol, a structure-promoting organic solvent. Changes in peptide conformation are discussed in terms of their impact on antibody and T-cell recognition.

MATERIALS AND METHODS

Peptide synthesis

The hemagglutinin peptide fragments shown in Scheme 1 were all synthesized by solid-phase techniques. Side chain-protecting groups were as follows: Arg (tosyl), Glu (cyclohexyl), Thr and Ser (benzyl). Peptides were synthesized on *p*-methylbenzhydrylamine resin (0.65 mmol/g) and synthesis was carried out manually. Couplings were performed by use of dicyclohexylcarbodiimide, with the exception of Gln, Asn and Arg, which were incorporated as their *N*-hydroxybenzotriazole esters. Amino acid incorporation was monitored by the ninhydrin test. The completed peptide resins were treated with liquid HF/dimethylsulphide/*p*-cresol (88:6:4, by vol.) at 0°C for 1 h. HF was then removed and the free peptides solubilized in 10% aqueous acetic acid. The crude peptides were purified by semipreparative reverse-phase HPLC on a C_{18} column (16 mm × 250 mm). Peptides were

Correspondence to H. H. Mantsch, Steacie Institute for Molecular Sciences, National Research Council of Canada, Ottawa, Canada K1A 0R6

Abbreviations. FT-IR, Fourier transform infrared; IP, intersubunit peptide; FP, fusion peptide; HA, hemagglutinin.

	1	13	25
IP	Val-Thr-Gly-Leu-Arg-Asn-Ile-Pro-Ser-Ile-Gln-Ser-Arg-Gly-Leu-Phe-Gly-Ala-Ile-Ala-Gly-Phe-Ile-Glu-Gly		
FP1		Gly-Leu-Phe-Gly-Ala-Ile-Ala-Gly-Phe-Ile-Glu-Gly	
FP3		Arg-Gly-Leu-Phe-Gly-Ala-Ile-Ala-Gly-Phe-Ile-Glu-Gly-Arg	
HA1C	Val-Thr-Gly-Leu-Arg-Asn-Ile-Pro-Ser-Ile-Gln-Ser		
HA1C-Arg	Val-Thr-Gly-Leu-Arg-Asn-Ile-Pro-Ser-Ile-Gln-Ser-Arg		
[DArg13]IP	Val-Thr-Gly-Leu-Arg-Asn-Ile-Pro-Ser-Ile-Gln-Ser-Arg-Gly-Leu-Phe-Gly-Ala-Ile-Ala-Gly-Phe-Ile-Glu-Gly		

Scheme 1. Amino acid sequence and abbreviations of the synthetic peptides from the intersubunit region of influenza virus hemagglutinin used in this report (APR8/34; Murata et al. [12]).

eluted with a linear gradient (0 – 76%) of acetonitrile containing 0.1% trifluoroacetic acid. Due to this purification procedure, the peptides are present as trifluoroacetate salts. In order to remove the trifluoroacetate counter ion (which has an infrared band around 1670 cm^{-1}), the peptides were additionally purified by chromatography on an Amberlite IR-45 minicolumn. The purified peptides were characterized by amino acid composition and analytical HPLC in two different solvent systems.

Spectroscopy

Circular dichroism measurements were performed on a Jasco J720 dichrograph at room temperature in a 0.2-mm-path-length cell. Double-distilled water and NMR-grade trifluoroethanol (Aldrich) were used as solvents. Octyl-β-D-glucoside was from Sigma. Each measurement was the average of five repeated scans in steps of 0.2 nm. Unless otherwise stated, the peptide concentration was 1 mg/ml. The mean residue ellipticity ($[\Theta]_{MR}$) is calculated using a mean residue molecular mass of 110 Da.

Aqueous peptide solutions for FT-IR spectroscopy [≈100 µl; 2% (mass/vol.)] were prepared in D_2O and adjusted to pD 7 with NaOD or DCl as needed. Solutions in trifluoroethanol were prepared at similar concentrations. Solid-state spectra were recorded from KBr discs. For temperature studies, the CaF_2 cell was placed in a temperature-controlled holder. Infrared spectra were recorded on a Digilab FTS-60 FT-IR spectrometer at a resolution of 2 cm^{-1}.

RESULTS

Secondary structure prediction

Application of the Chou-Fasman-Prevelige algorithm [9] to a 48-amino-acid segment of the hemagglutinin protein which contains the in positions 18 – 42, shows that the C-terminal part of IP (represented by peptides FP1 and FP3 from the fusion region) has the ability to adopt both α-helical and β-sheet conformations (Fig. 1). The N-terminal fragment of IP, HA1C-Arg, has no propensity for α-helical conformation; however, it contains an additional β-forming core (Ile-Pro-Ser-Ile). The N-terminal part of IP is also predicted to form repeating β-turns (Val-Leu-Gly-Thr, Ile-Pro-Ser-Ile and Gln-Ser-Arg-Gly or Ser-Arg-Gly-Leu, and possibly Leu-Arg-Asn-Ile). Thus, the critical Arg residue at position 329 of hemagglutinin (indicated by an asterisk in Fig. 1), is situated in a region where a β-turn is likely to occur.

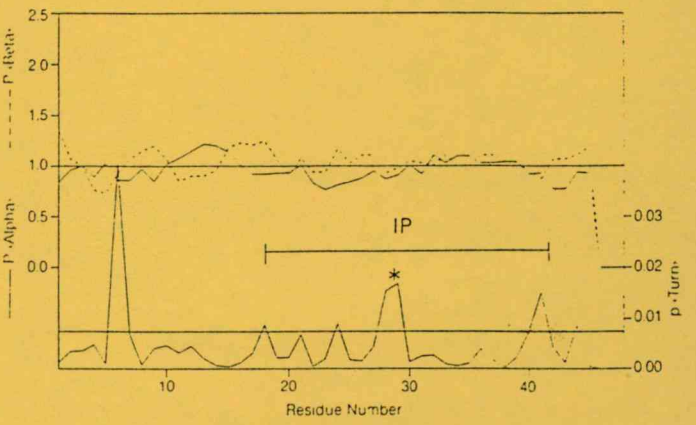

Fig. 1. Secondary structure predictions for a 48-amino-acid segment of hemagglutinin which contains the IP fragment in positions 18 – 42. The asterisk indicates the position of Arg329 in this segment of hemagglutinin. P〈alpha〉, P〈beta〉 and P〈turn〉 represent the probabilities for the respective secondary structural elements; for details see [9].

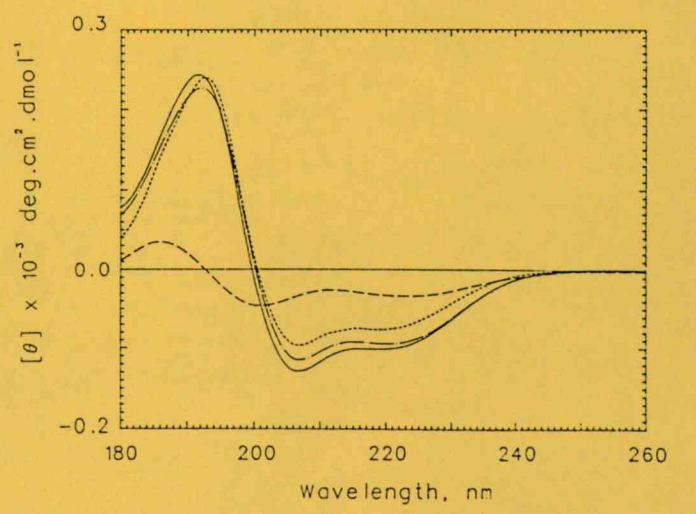

Fig. 2. Circular dichroism spectra, in trifluoroethanol, of the hemagglutinin peptide fragments IP (———), [DArg13]IP (–·–·–·–), FP3 (·····) and HA1C-Arg (– – – –).

Circular dichroism spectroscopic studies

Circular dichroism spectra, in trifluoroethanol, of the hemagglutinin fragments IP, [DArg13]IP, FP3 and HA1C-Arg are illustrated in Fig. 2. IP gives a helical circular dichroism spectrum; the α-helical content, calculated by the procedure of Greenfield and Fasman [10], or by that of Yang et al. [11], is approximately 30%, which corresponds to seven or eight residues (two turns of the helix). Fragment FP3 also gives a spectrum with helical features, which, in agreement with the secondary structure predictions, indicates that the helical component of IP is located in its C-terminal half, represented by FP3. A lower absolute intensity and the different relative

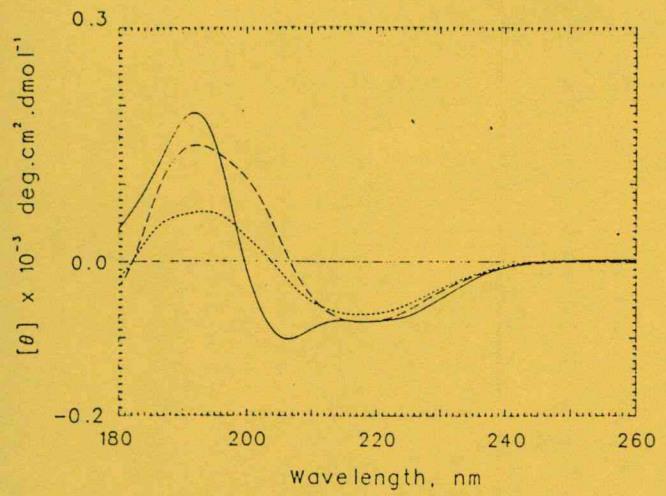

Fig. 3. Circular dichroism spectra of IP in 1:1 trifluoroethanol/D_2O (——), 10/90% trifluoroethanol/D_2O (····) and in D_2O containing 2.5% octyl-β-D-glucoside (– – – –).

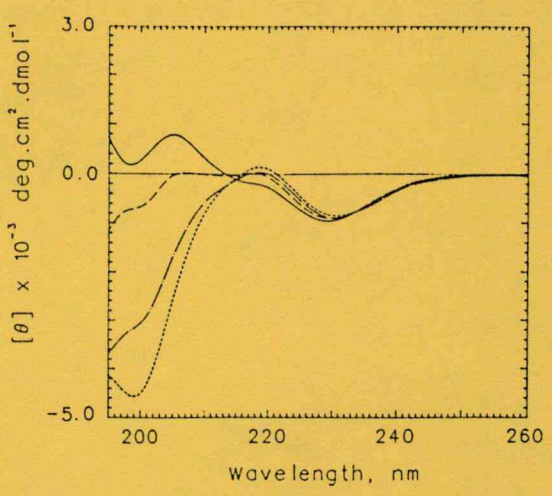

Fig. 4. Circular dichroism spectra of FP3 at different concentrations in water (PH 6): 5.4 mg/ml (——), 2.7 mg/ml (– – – –), 1.35 mg/ml (–·–·–·–) and 0.74 mg/ml (····).

band intensities in the spectrum of FP3 compared to that of IP are compatible with a shorter or looser α-helix in FP3, or with the presence of more than one conformer population of FP3. The fact that IP and [DArg13]IP have very similar spectra suggests that the central arginine in IP, and possibly the adja cent serine and glycine residues, may not play a significant role in determining the chiroptical properties of this peptide. In addition to about 30% α-helix and about 30% unordered conformation, a significant amount of β-sheet (≈35%) was calculated for IP, [DArg13]IP and FP3. The peptide fragments HA1C-Arg and HA1C exhibit blue-shifted, low-intensity helical (class C) spectra which can be correlated with certain subtypes of β-turns or their repeats (distorted helices, e.g. 3_{10} helix) [13–15].

Addition of water to trifluoroethanol results in a gradual change in the circular dichroism spectra of IP and FP3; however, the helical character of the peptide segments is preserved until the water content reaches 50%. The spectrum of IP in pure water (pH 5.5) is indicative of an equilibrium between two or more conformers. In an aqueous solution containing 2.5% octyl-β-D-glucoside, a non-ionic surfactant with secondary-structure-promoting properties, IP shows a spectrum with a negative band at 218 nm and a positive band at 183.5 nm (Fig. 3). The single negative band indicates the predominance of a β-sheet conformation, while the shape of the positive band may be related to a small contribution from an aperiodic structure [14]. Thus, octyl-β-D-glucoside has a similar effect to that of low (<25%) trifluoroethanol concentrations in water, whereby β-structures are favoured. The analysis of the IP spectrum shows that the β-sheet contribution to the spectrum is dominant (≈50%), though a significant amount (≈25%) of α-helix is also present.

While the circular dichroism spectra of IP and FP3 in trifluoroethanol showed no concentration dependence (in the range 0.1–3 mg ml), a definite spectral change with increasing concentration was observed in water. The spectra at higher concentrations are suggestive of the presence of significant amounts of β-conformers. On dilution in water, the spectral contribution of the β-sheet gradually decreased and, below a 0.5 mg/ml, the spectra revealed the predominance of an aperiodic structure (Fig. 4). These results are consistent with β-sheet formation stemming from aggregation of IP and FP3 in water at higher concentration. IP and FP3 are switch peptides with expressed α-helicity in helix-promoting environments, and a preponderant β-sheet character at higher concentrations or in the presence of micelles. Below the critical micelle concentration (≈0.7%), IP and FP3 showed spectra similar to those measured in dilute aqueous solutions. Since the N-terminal fragment of IP also has some β-forming potential, single chains of this peptide have the ability of forming antiparallel β-pleated sheets with strong H-bonds between adja cent chains.

Infrared spectroscopic studies

The infrared spectrum of IP and those of its C-terminal peptides FP1 and FP3 obtained from lyophilized solids reveal that these peptides are highly aggregated. A strong amide-I band at 1628 cm^{-1} in IP and at 1632 cm^{-1} in FP1 and FP3, along with the presence of a weaker component band at about 1690 cm^{-1}, identify these aggregates as antiparallel β-sheets [16–18]. A broad band at 1650–1665 cm^{-1} indicates the presence of other populations (aperiodic conformers, α-helical components and turns). The amide-II band shows peaks at 1523 cm^{-1} (typical for β-type structures) and at 1546 cm^{-1} (characteristic of aperiodic and/or α-helical structures), indicative of the existence of at least two populations effectively frozen in a solid KBr matrix.

In aqueous (D_2O) solution, the infrared spectrum of IP also exhibits the strongest amide-I band at 1626 cm^{-1}, with a weaker band at about 1698 cm^{-1} and a broad unstructured band centred at about 1650 cm^{-1} (Fig. 5). Band narrowing by Fourier self-deconvolution [19] leads to a better visualization of the individual bands (Fig. 5). The 1626/1698 · cm^{-1} band pair reflects the prevalence of the β-sheet conformation in D_2O, which was also detected in the solid state. The broad band at 1650 cm^{-1} is compatible with the presence of some unordered and/or α-helical peptide segments. The weak band at 1585 cm^{-1} is characteristic of the arginine side-chain group. The amide-II band at about 1545 cm^{-1} (due to aperiodic and α-helical amide groups) has shifted to about 1450 cm^{-1} as a consequence of NH to ND exchange; however, the presence of a residual amide-II band at 1526 cm^{-1} indicates that even

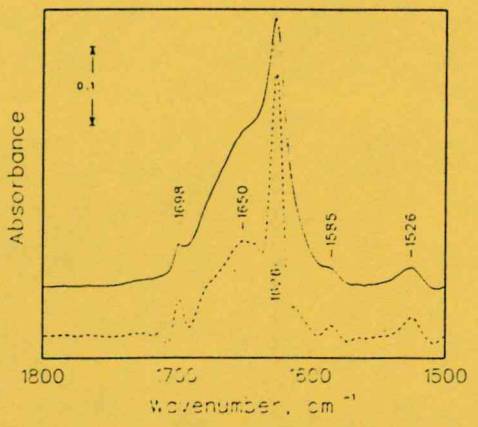

Fig. 5. Infrared spectrum of the hemagglutinin peptide fragment IP in aqueous (D_2O) solution in the region of the amide-I and amide-II bands (———). (----) The same spectrum after reducing the widths of the infrared bands by a factor of 1.5 by use of Fourier self-deconvolution [19].

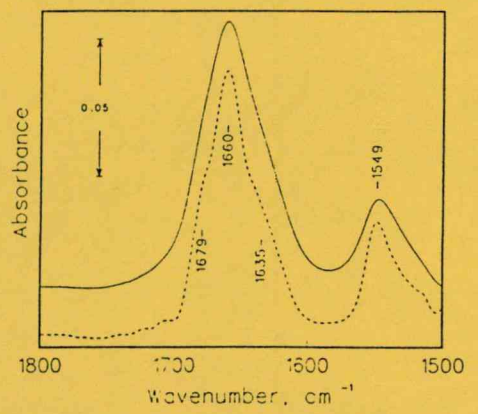

Fig. 6. Infrared spectrum of the hemagglutinin peptide fragment IP in trifluoroethanol solution in the region of the amide-I and amide-II bands (———). (----) The same spectrum after reducing the widths of the infrared bands by a factor of 1.75 by use of Fourier self-deconvolution [19].

after 24 h this exchange is not complete for the β-sheets. However, when a solution of IP was heated from ambient temperature to 80 °C, this band disappeared gradually between 64 °C and 80 °C, and the 1626-cm^{-1} band shifted to 1622 cm^{-1}, reflecting the complete NH to ND exchange of the β-component.

In trifluoroethanol solution (Fig. 6), the infrared spectrum undergoes a radical change. The major amide-I band is at 1660 cm^{-1}, with shoulder bands at 1635 cm^{-1} and 1679 cm^{-1}. The major amide-II band is at 1549 cm^{-1} band can be attributed to a weakly hydrogen-bonded α-helical conformation, the band at 1679 cm^{-1} is in the region of turns, while the 1635-cm^{-1} band reflects the presence of some residual β-structure (possibly β-turns). The change of solvent from trifluoroethanol to a 1:1 trifluoroethanol/D_2O mixture has the net effect of increasing the β-sheet component at the expense of the α-helical component. The spectrum of IP in D_2O solution containing 2.5% octyl-β-D-glucoside also shows an increase in the β-sheet components compared to that in D_2O.

FP1 is only slightly soluble in either D_2O or trifluoroethanol; however, FP3 dissolves more readily both in D_2O and trifluoroethanol and the spectra are similar to those of FP1. The spectrum in D_2O has only a strong band at 1626 cm^{-1} and a weak one at 1688 cm^{-1}. The position of the two bands and their relative intensities are typical of antiparallel β-sheet structures [16–18]. Upon heating an aqueous (D_2O) solution of FP3 to 80 °C, the peak positions did not change. The remarkable stability of this peptide may be attributed to strong hydrogen-bonded β-strands, probably formed between single peptides. The spectrum of FP3 in trifluoroethanol resembles that of IP except that the band at 1635 cm^{-1} is stronger, indicating that FP3 retains a larger proportion of β-sheet conformation.

The infrared spectra in D_2O of the N-terminal peptide fragments HA1C and HA1C-Arg are practically identical and exhibit only a single broad amide-I band centred at approximately 1646 cm^{-1}, typical of unordered peptides proteins in D_2O solution [17, 18].

DISCUSSION

Generally, there is good agreement between the circular dichroism and FT-IR data on the conformation of the hemagglutinin fragments. Minor differences may be related to the nature of the two techniques. While circular dichroism spectra provide information on the relative spatial orientation of the backbone amide groups, the main chromophores of peptides and proteins, FT-IR spectroscopic data obtained from the structure-sensitive C=O stretching vibration (amide I band) reflect the strength of the H-bonding in the different secondary structures. Both type of spectra indicate a significant α-helical content for IP in trifluoroethanol and show an α-to-β conversion in mixtures containing increasing amounts of water. The position of the amide-I band at 1660 cm^{-1} reflects the weakness of the hydrogen bonds in the helix.

Both circular dichroism and FT-IR spectra provide evidence for β-sheet conformation in IP, FP1 and FP3 in aqueous solution; this is probably due to intermolecular association of the peptides in solution, as evidenced by the low frequency (1626 cm^{-1}) of the amide-I band. The position and relative intensity of the amide-I bands is consistent with their assignment to an antiparallel β-sheet conformation [16–18]. This information cannot be derived from the circular dichroism spectra of the peptides.

The presence of β-turns is supported by an X-ray analysis of the cleaved hemagglutinin, which shows that the N-terminal glycine-rich sequence of chain HA2 (comprised by FP1 and FP3) forms a series of four contiguous reverse β-turns [20].

On the other hand, the infrared spectra of HA1C and HA1C[Arg] differ considerably from those of the other peptide fragments. A single strong band at 1646 cm^{-1} is clearly indicative of a conformation without any secondary structure. Indeed, the secondary structure predictions (Fig. 1) and the class-C circular dichroism spectra of these fragments do not support the occurrence of ordered peptide conformation.

A comparison of X-ray diffraction, circular dichroism and FT-IR spectroscopic data suggests that FP1, FP3 and presumably the N-terminal fusogenic region of HA2, can adopt a variety of conformations (α-helix, β-sheet and repeating β-turns). Structural and environmental factors may, however, bring about the prevalence of a single conformational state. The finding that the sugar-coated octyl-β-D-glucoside micelles prompt the formation of β-sheet structure of IP and FP3, even in dilute aqueous solution suggests that an event preceding

membrane fusion might be chain extention (pleating) of the N-terminal domain on the glycoprotein surface of the endosomal membrane. It is also reasonable to suppose that membrane fusion itself is triggered by a subsequent pH-dependent β-to-α conformational transition of the region, which is initiated by the overall pH-dependent conformational change of hemagglutinin trimers. This assumption is supported by previous findings providing evidence for the correlation of helix formation with fusogenicity [5].

The conformational mobility of peptides comprising the intersubunit region of hemagglutinin may be of importance also in immune recognition as it represents the most conservative amino acid sequence [20, 21]. The functionally essential posttranslational modification of this region occurs late in the secretory pathway [22, 23], and is mediated by host-cell proteases. The event triggers membrane fusion but also influences enzymic degradation and antigenic processing [24, 25].

According to its sequence, the C-terminal half of IP (which comprises FP3) may adopt an α-helix with some amphipathic character (repeating occurrence of glycine residues). FP3 is terminated by a Rothbard motif. Thus, this peptide fulfills both the criteria suggested by Berzofsky and Rothbard for potential T-cell epitopes [26, 27]. Notably, no typical Rothbard motif is contained in the N-terminal part of IP (represented by HA1C-Arg and HA1C).

Results of immunological studies on peptides covering the intersubunit area demonstrate that this region of hemagglutinin can be the target of both B-cell and T-cell recognition. A neutralizing monoclonal antibody inhibiting the membrane fusion event could be isolated from the spleen of an influenza virus infected Balb/c mouse. This antibody recognizes the intersubunit peptides IP and [DArg13]IP, but does not react with any of the subunit peptides (Kurucz et al., Rajnavölgyi et al., unpublished results). IP in addition carries T-cell epitopes, available also in HA1C and FP3. The T-cell recognition in the context of major histocompatability class II molecules of d haplotype, however, is influenced by the presence of Arg329 (situated in the center of IP).

According to our comparative spectroscopic approach, both halves of the intersubunit peptide (represented by HA1C, HA1C-Arg and FP1, FP3) are capable of adopting multiple conformations and that different conformations may prevail depending on environmental conditions (nature of solvent, buffer, presence of lipids, pH, etc). It is therefore very likely that the interaction with major histocompatability structures plays an important role in stabilizing peptide conformations suitable for T-cell recognition. In contrast, antibody recognition requires a more defined conformation adopted by the hemagglutinin molecule and maintained in IP. Based on the circular dichroism and FT-IR evidence discussed earlier, IP and also [DArg13]IP adopt a β-sheet conformation in aqueous solution containing octyl-β-D-glucoside micelles. This finding, in correlation with the high β-turn propensity of the central Arg-containing segment, may suggest a β-sheet structure as a common organization essential for monoclonal antibody recognition.

This work was supported, in part, by grants OTKA 2310 (to E.R.), OTKA 1591 (to M.H.) and DMB-90070055 of the National Science Foundation, USA (to G.D.F.). Issued as NRCC No. 32851.

REFERENCES

1. Lamb, R. A. & Choppin, P. W. (1983) *Annu. Rev. Biochem. 52*, 467–506.
2. Matlin, K. & Simons, K. (1983) *Cell 34*, 233–243.
3. Roth, M. G., Getling, M.-J. & Sambrook, J. (1986) in *The influenza viruses* (Krug, R. M., ed.) Plenum Publishing Corp., New York.
4. Lear, J. D. & De Grado, W. F. (1987) *J. Biol. Chem. 262*, 6500–6505.
5. Wharton, S. A., Martin, S. R., Ruigrok, R. W. H., Skehel, J. J. & Wiley, D. (1988) *J. Gen. Virol. 69*, 1847–1858.
6. Westhof, E., Altschuh, D., Moras, D., Bloomer, A. C., Mondragou, A., Klug, A. & Van Regenmortel, M. H. V. (1984) *Nature 311*, 123–126.
7. Geysen, H. M. (1985) *Immunol. Today 6*, 364–369.
8. Cornette, J. L., Margalit, H., De Lisi, C. & Berzofsky, J. A. (1989) *Methods Enzymol. 178*, 611–634.
9. Prevelige, P., Jr. & Fasman, G. D. (1989) in *Prediction of protein structure and principles of protein conformation* (Fasman, G. D., ed.) pp 391–416, Plenum Press, New York.
10. Greenfield, N. & Fasman, G. D. (1969) *Biochemistry 8*, 4108–4116.
11. Yang, J. T., Wu, C.-S. C. & Martinez, H. M. (1986) *Methods Enzymol. 130*, 208–269.
12. Murata, M., Sugahara, Y., Takahashi, S. & Ohnishi, S.-I. (1987) *J. Biochem. (Tokyo) 102*, 957–962.
13. Woody, R. W. (1974) in *peptides, polypeptides and proteins* (Blout, E. R., Bovey, F. A., Lotan, N. & Goodman, M., eds) pp 338–360, Wiley, New York.
14. Woody, R. W. (1985) in *The peptides* (Hruby, V. J., ed.) vol. 7, pp 16–114, Academic Press, Orlando.
15. Perczel, A., Hollosi, M., Foxman, B. M. & Fasman, G. D. (1991) *J. Am. Chem. Soc. 113*, 9772–9784.
16. Miyazawa, T. & Blout, E. R. (1961) *J. Am. Chem. Soc. 83*, 712–714.
17. Krimm, S. & Bandekar, J. (1986) *Adv. Protein Chem. 38*, 183–364.
18. Surewicz, W. K. & Mantsch, H. H. (1988) *Biochim. Biophys. Acta 952*, 115–130.
19. Mantsch, H. H., Moffatt, D. J. & Casal, H. L. (1988) *J. Mol. Struct. 173*, 285–298.
20. Bosch, F. X., Garten, W., Klenk, H.-D. & Rott, R. (1981) *Virology 113*, 725–735.
21. Kawaoka, Y. & Webster, R. G. (1988) *Proc. Natl Acad. Sci. USA 85*, 324–328.
22. Copeland, C. S., Doms, R. W., Bolzau, E. M., Webster, R. G. & Helenius, A. (1986) *J. Cell. Biol. 103*, 1179–1191.
23. Copeland, C. S., Zimmer, K.-P., Wagner, K. R., Healy, A. G., Mellman, I. & Helenius, A. (1988) *Cell 53*, 197–209.
24. Braciale, T. J. & Braciale, V. L. (1991) *Immunol. Today 12*, 124–129.
25. Jackson, D. C. & Brown, L. E. (1991) *Peptide Res. 4*, 114–124.
26. Berzofsky, J. A., Cease, K. B., Cornette, J. L., Spouge, J. L., Margalit, H., Berkower, I. J., Good, M. F., Miller, L. H. & DeLisi, C. (1987) *Immunol. Rev. 98*, 9–52.
27. Rothbard, J. B. & Taylor, W. R. (1988) *EMBO J. 7*, 93–100.

Peptide Research

Branched Polypeptides as Antigens for Influenza Virus Hemagglutinin and T-Cell Receptor Subunits

G.K. Tóth, G. Váradi, Z. Nagy[2], É. Monostori[1], B. Penke, Z. Hegedűs[1], I. Andó[1], G. Fazekas[2], I. Kurucz[4], M. Mák[3] and É. Rajnavölgyi[2]

A. Szent-Györgyi Medical University, Szeged; [1]Biological Research Center of Hungarian Academy of Sciences, Szeged; [2]Eötvös Loránd University, Budapest; [3]Central Research Institute of Chemistry, Budapest; [4]Institute of Drug Research, Budapest, Hungary

ABSTRACT

The multiple antigenic peptide (MAP) method was applied to improve the immunogenicity of synthetic peptides representing distinct regions of the influenza virus hemagglutinin (HA). A tetrameric MAP with multiply incorporated overlapping B- and T-cell epitopes was combined with a particular HA sequence representing the slightly modified fusion peptide on the C-terminus of the Lys core (MAP-1). As a result of repeated injections of BALB/c mice with MAP-1 but not with the monomeric HA1C[Arg] peptide, the appearance of MAP-1-specific antibodies crossreactive with the acid-pretreated virus could be observed. In vitro *studies revealed the potency of the MAP-1 structure to induce proliferation of HA1C[Arg]-primed T-cells, and* in vivo *studies demonstrated the protective feature of the immune response elicited by MAP-1 and to a lesser extent by the monomeric HA1C[Arg]. The increased level of MAP-1-specific antibodies upon viral challenge shows the activation of MAP-1-specific B- and/or T-cells.*

The advantage of the previously verified FP3 helper T-cell epitope included in MAP-1 was further utilized to synthesize chimeric structures comprising short fragments of the ζ (MAP-2) or δ (MAP-3) subunits of the T-cell antigen receptor (TCR) complex. The selected peptides of the ζ- and δ-chain regions failed to elicit an antibody response in BALB/c mice as tetra- or octamers, but the inclusion of the modified fusion region resulted in an immunogenic construction. The chimeric MAP-2 and MAP-3 were successfully used to develop polyclonal and monoclonal antibodies recognizing the corresponding multimeric peptides, but they were unable to bind to the cell membrane-expressed form of the subunits.

The MAP constructions that were designed, including appropriately selected B- and helper T-cell epitopes, were proven to be immunogenic; but the crossreactivity of the induced antibodies with the corresponding native proteins was highly dependent on the individual characteristics of the resultant combinations.

INTRODUCTION

The MAP method was successfully used to increase the immunogenicity of various peptide fragments of different proteins (10,17,32,37,40,42). The most promising approaches were aimed at the enhancement of the protective immune response against distinct pathogens such as the major immunogenic region of the foot-and- mouth disease virus (FMDV) (20), the circumsporozoite antigen of malaria (14,30,38,39), hepatitis (39), *Schistosoma mansoni* (7) or the V3 loop of the human immunodeficiency virus (Levi et al., 22th Eur. Pept. Symp. 1992, A413). This method offers attractive advantages: a) the molar ratio of the peptide epitope to the core molecule is high; b) this kind of structure provides enhanced reproducibility as compared to the previously used peptide–protein carrier conjugates; c) there is no carrier-mediated epitope competition because of the low immunogenicity of the core region.

The effect of copy number was systematically studied with FMDV-derived peptides (20), and tetramers were demonstrated as efficient as octamers. Immunization with MAP in most cases requires adjuvants; however, the widely used but highly toxic Freund's adjuvant can be substituted by other approaches such as $Al(OH)_3$, the only adjuvant licensed for human application (20), or by the involvement of lipopeptides (13,21,24) or other recent immunopotentiators used for viral subunits (15,36).

Recent improvements to this technology (40), including peptide vaccines containing different incorporated adjuvants (12,13,21,24), opened up wide possibilities for eliciting an efficient memory response involving not only IgG-type antibodies, but also helper and cytotoxic T-lymphocytes (15,36) reactive with both the vaccine and the pathogen. A critical consideration in the development of peptide-based subunit vaccines is the inclusion of one or more potent T-cell epitopes to promote the generation of appropriate T-cell help and long-lasting memory (27,50). The limitation of this alternative lies in the critical orientation of the T- and B-cell epitopes included in the immunogen (27,38). If B-epitopes are linked to T-epitopes in the appropriate position, the immunogenicity can be improved. However, the T-cell-dependent immune response is restricted by the polymorphic major histocompatibility gene complex (MHC). Therefore, a valuable vaccine that is immunogenic in all members of an outbred population requires more than one T-cell epitope. The MAP approach was estab-

lished to also overcome the genetic restriction mediated by MHC (14,31).

The first approach in the present study was aimed at increasing the immunogenicity of a previously identified overlapping T/B-epitope of influenza virus (A/PR/8/34: H1N1) hemagglutinin (HA) (22,33). For these studies, an elongated analog of the HA fusion peptide, characterized by a highly hydrophobic conserved sequence (6,22, 33), was grafted by four tridecapeptides comprising the C-terminal 317-329 amino acids of the HA1 subunit (HA1C[Arg]; see Figure 1, MAP-1). The idea to combine these peptides was based on previously published results demonstrating that the C-terminus of the HA1 subunit encompasses multiple T- and B-cell epitopes (10,35), and that the fusion peptide is also recognized by virus-specific antibodies (6). In our previous studies it was shown that the HA1C[Arg] region and the Arg extended fusion peptide FP3 are efficient in inducing a proliferating T-cell response (33 and É. Rajnavölgyi, unpublished observation). Additionally, the HA1C[Arg] region is immunogenic and can be recognized by anti-peptide or anti-influenza monoclonal antibodies only if it is linked to the fusion peptide (References 22 and 33, and Z. Nagy et al., unpublished observation).

The activation of T-lymphocytes, including the T-helper subpopulation, occurs when they are triggered via the T-cell antigen receptor (TCR) complex. The TCR complex consists of the idiotypic α- and β-chains noncovalently associated with the γ-, δ- and ε-polypeptides of the CD3 complex, and additionally with the ζ- and η-chains (23). The α- and β-heterodimers are responsible for the specific recognition and binding of the antigen, while the CD3 complex, as well as the ζ- and η-chains, participates in signal transduction generated by antigen binding. Although a number of studies strongly indicate the participation of the CD3 ε- and ζ-chains in signal transduction (23), the roles of the other polypeptides associated with the TCR have not been revealed so far. Monoclonal antibodies are powerful tools used for studying cell-surface receptors or their subunit function. The production of antibodies against cell-surface receptors encounters several difficulties. Isolation or purification of the membrane-bound proteins are laborious, if not impossible—the antibodies generated against the whole cells, membrane fractions or even the enriched receptor react with a number of uncharacterized epitopes. The close homology of the TCR-related subunits in different species raises further difficulties (47). As the MAP approach was successfully utilized to obtain monoclonal antibodies to the TCR α- and β-chains (32), we applied this method in the development of monoclonal antibodies to the N-terminal extracellular part of the human TCR δ- and ζ-subunits.

In the second part of this study, we synthesized the octameric MAP of the N-terminal extracellular region of the human ζ-chain identical to its murine counterpart. To overcome the inefficiency of this construction to elicit antibodies in BALB/c mice, the tetrameric MAP of these peptides was grafted to the influenza-derived FP3 peptide (Figure 1), introduced as a T-cell epitope and as a hydrophobic region previously shown to support the conformational stability of N-terminal peptide conformation (22). In the MAP-2 and MAP-3 constructions, the orientation of the δ- and ζ-chain peptides was identical to that of the HA1C[Arg] B-cell epitope (Figure 1).

The two approaches applied in this study provided valuable information on the applicability and limitations of the MAP system.

MATERIALS AND METHODS

Chemicals

Dichloromethane (DCM), dimethylformamide (DMF), diisopropylethylamine (DIEA), methanol (MeOH), trifluoroacetic acid (TFA) and HPLC-grade acetonitrile (AcN) were purchased from E. Merck (Darmstadt, Germany) and were used without further purification. Fluka (Buchs, Switzerland) supplied puriss-grade dicyclohexylcarbodiimide (DCC). Protected amino acid derivatives were from Bachem (Torrance, CA). 1-Hydroxy-benzótriazole (HOBt), *p*-cresol and dimethyl sulphide were purchased from Aldrich (Steinheim, Germany). Hydrogen fluoride (HF) was obtained from UCAR (Olen, Belgium).

Peptide Synthesis

The branched peptide antigens were synthesized by a solid-phase technique, utilizing ^{t}Boc chemistry (29). Side-chain protecting groups were as follows: Arg(Tos), Asp(OcHex), Cys(Meb), Thr(Bzl), Lys(2ClZ), Glu(OcHex), Tyr(2BrZ) and Ser(Bzl). The peptide chains were elongated on MBHA resin (0.8 mmol/g) and the syntheses were carried out manually. Couplings were performed with DCC, with the exception of Asn, Gln and Arg, which were incorporated as their HOBt esters. Amino acid incorporation was monitored with the ninhydrin test (25). In the event of incomplete coupling, this step was repeated, but DCM was substituted by DMF. The completed peptide resins were treated with liquid HF/dimethyl sulphide/*p*-cresol (88:6:4, vol/vol), at 0°C for 1 h. HF was removed and the resulting free peptides were solubilized in 10% aqueous acetic acid, filtered and lyophilized.

Peptide Purification and Characterization

The crude peptides were purified by reverse-phase HPLC (RP-HPLC), using an Astec 300 C4 5-μ column (8 × 250 mm). The HPLC apparatus was produced by Knauer (Berlin, Germany). The solvent system used was as follows: 0.1% TFA in water, 0.1% TFA + 80% AcN in water; gradient: 0% → 90% B in 1.5 h; flow 1.5 ml/min. The appropriate fractions were pooled and lyophilized. Purity was checked by RP-HPLC, isoelectrofocusing and SDS polyacrylamide gel electrophoresis (PAGE). The analytical HPLC investigations were made on a Vydac C4 column (4 × 250 mm, 214TP54; The Separations Group, Hesperia, CA), at a flow rate of 0.8 ml/min, with detection at 220 nm; the solvent system used was as follows: A: 0.1% TFA in water, B: 0.1% TFA + 80% AcN in water; gradient: 0% → 90% B in 20 min. Two-dimensional electrophoresis, with isoelectric focusing vs. SDS PAGE, was carried out by using Servalyt Ag 2-11 (Serva, Heidelberg, Germany) in the first dimension and 15% SDS PAGE as the second dimension.

Mass Spectrometry

The FAB-MS experiments concerning the MAP-1 were performed with a VG ZAB-2SEQ hybrid tandem mass spectrometer, equipped with an LSIMS source (Cs^+ ion gun used at 30 keV). The tryptic digestion was carried out

"on tip." The matrix-assisted laser desorption ionization measurements were carried out with MALDI III equipment (Kratos, Manchester, UK) in linear mode.

Immunological Methods

a) Induction of anti-MAP-1 antibodies

BALB/c mice (Institute of Oncology, Budapest, Hungary) were immunized with 100 µg MAP-1 (see Figure 1) or with the tridecamer free HA1C[Arg] or FP3 HA peptides emulsified in complete Freund's adjuvant (CFA) (Sigma Chemical, Deisenhofen, Germany) by s.c. injection into the hind footpads and the base of the tail. Eight weeks later, the mice were challenged with the same amount of peptide emulsified in incomplete Freund's adjuvant (IFA) (Sigma). Blood samples were taken 14 days after the last antigen challenge. Both pooled and individual sera were studied.

b) Induction of anti-MAP-2 and anti-MAP-3 antibodies

BALB/c mice were injected with 100 µg antigen into the footpads with CFA. The injections were repeated twice in monthly periods: first subcutaneously with IFA and finally intraperitoneally in phosphate-buffered saline (PBS). The spleen cells of the immune mice were removed and hybridized with SP2/O murine myeloma cells according to Köhler and Milstein (26). For the production of ascitic fluid in mice, 10^6 hybridoma cells were injected intraperitoneally into BALB/c mice and ascitic fluid was harvested after 2–3 weeks.

After hybrid selection of anti-ζ and anti-δ fusion products, 126 and 89 growing colonies, respectively, were obtained, of which 12 and 4, respectively, produced monoclonal antibodies (MAb), detected by EIA. One of the colonies maintaining the high MAb-producing capacity to ζ or δ was subcloned by the limiting dilution method and further characterized.

Protection experiments

Eight- to ten-week-old male BALB/c mice were preimmunized with s.c. injections of 100 µg MAP-1 or the HA1C[Arg] or FP3 peptides as described above. Five weeks after the second antigen challenge, preimmunized mice were aerosol infected with a 5 LD_{50} dose of the mouse pathogenic A/PR/8/34 influenza virus. Virus dilution corresponding to 50% mortality was determined for each batch of virus in a preliminary survival experiment using different dilutions of the virus for infection. Experimental groups consisted of 5–10 animals. Control mice were treated as described above, but using PBS emulsified in CFA or IFA without the peptides. The number of survivors was given as a percentage of the total number in the groups and was determined daily postinfection.

Antibody detection and quantitation

a) The detection and quantitation of anti-MAP-1 or A/PR/8/34 influenza virus-specific serum antibodies were performed by solid-phase enzyme immunoassay (EIA) using different peptides (10 µg/ml) or purified virus (20 HAU/ml) coated to the solid phase of Maxisorp (NUNC, Roskindale, Denmark) or polyvinyl-chloride (PVC) (Enzy-Plate; Propilen G.M., Pécs, Hungary) plates, respectively. Acidic pretreatment of the virus was performed in a 0.1-M acetate buffer pH = 5.0 for 20 min at RT. Overcoating and antibody dilutions were done with PBS containing 1% bovine serum albumin (BSA) and 2% fetal calf serum (FCS). Excess of reagents was washed out three times with PBS and finally with PBS containing 0.05% Tween 20 (SERVA, Heidelberg, Germany). Bound antibodies were detected with horseradish peroxidase-labeled anti-mouse IgG as a developing second antibody (Sigma Chemical). Ortho-phenylene-diamine (OPD) was used as a substrate (Sigma Chemical). The relative level of polyclonal antibodies was determined by titration of immune sera taken at different points of time after the antigen challenge and characterized by the OD_{492} values corresponding to a defined serum dilution.

b) Monoclonal antibodies against

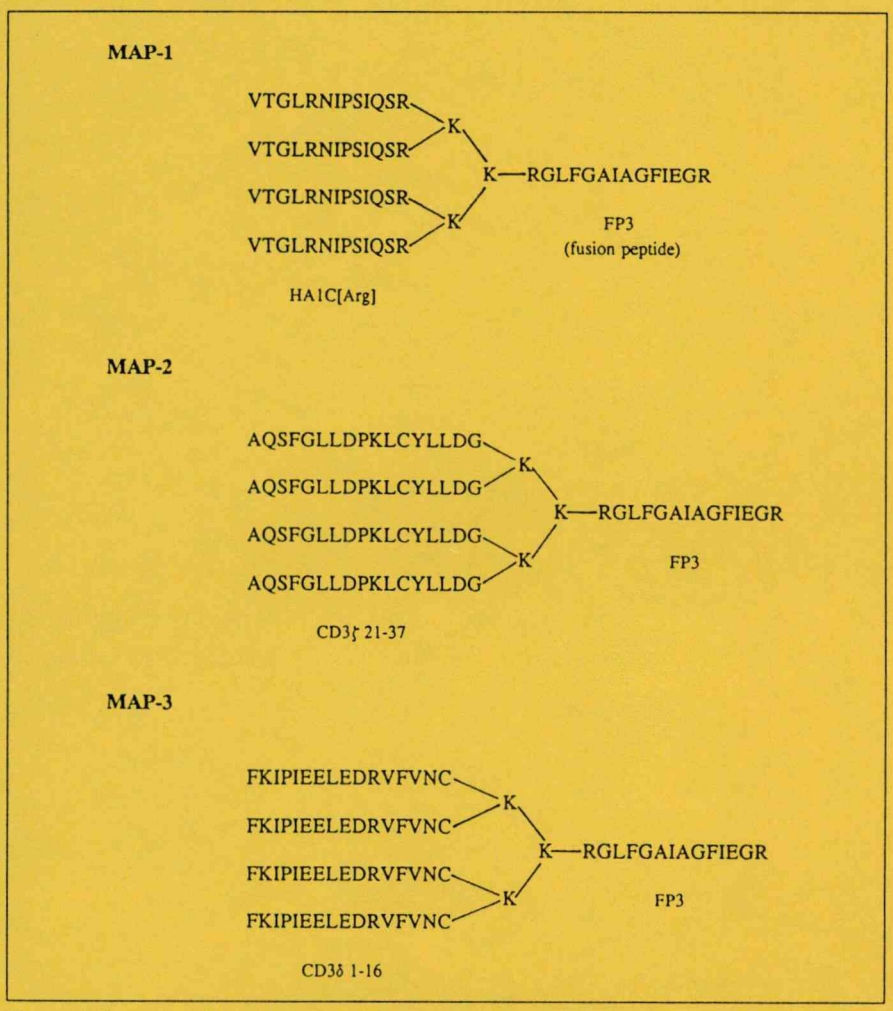

Figure. 1. Structure of the synthesized chimeric "multiple antigenic peptides."

MAP-2 and MAP-3 were tested by EIA. Ninety-six-well microplates were coated with 10 µg/ml antigen overnight at 4°C. After washing the wells with PBS containing 0.05% Tween 20, hybridoma supernatants were added for 1 h at 37°C. Finally, horse radish peroxidase conjugated rabbit-anti mouse Ig (DAKOPATTS, Glostrup, Denmark) was used as a second antibody. The reaction was developed by OPD and H_2O_2 as substrates and measured at 495-nm wavelength on a Titertek Multiscan ELISA Reader (EFLAB OY, Helsinki, Finland). Polyclonal antisera and ascitic fluids were tested at different dilutions starting from a dilution of 1:100 to reduce nonspecific binding to the antigen. Hybridoma supernatants were used undiluted, since these reagents contained low concentrations of specific antibody (5–10 µg/ml).

Immunofluorescence and immunoblot

For immunofluorescence analysis, cells were stained with MAb in the optimal dilution (1:100 for ascites and undiluted for hybridoma culture supernatant), and fluorescein isothiocyanate (FITC)-labeled goat anti-mouse Ig (Sigma Chemical) was diluted 1:100 and analyzed on a FACStar IV instrument (Becton-Dickinson Immunocytometry Systems, Mountain View, CA) for fluorescence intensity using a linear amplifier. Immunoblot analyses were carried out as described by Towbin et al. (43)

T-cell proliferation assay

The T-cell proliferation assay was performed by the standard method of Corradin et al. (11), using T-cell-enriched lymph node cells. B-cell depletion was performed by panning on anti-mouse Ig (prepared in our laboratory)-coated Petri dishes. Briefly, 4×10^5 T-cells were incubated together with 2×10^5 irradiated normal BALB/c spleen cells as antigen-presenting cells (APC) in the presence of different concentrations of the peptides. The reactivity of the T-cells with influenza virus was detected in the presence of APC preinfected with 100 HAU/ml A/PR/8/34 (4 h, 37°C). The APC were washed twice with glucose-containing PBS, irradiated and used as described above. Proliferation was detected by ^{3}H-thymidine (1 µCi, 3.7 kBq/well) incorporation added in the last ten hours of the 4-day culture.

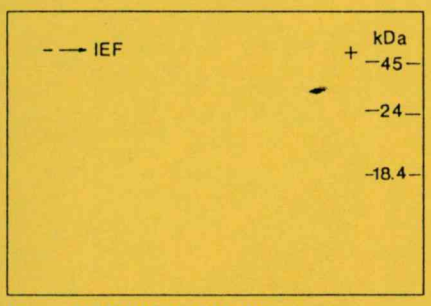

Figure 2. 2D PAGE of MAP-1 structure.

RESULTS

Synthesis and Purification of the Branched Multiple Antigenic Peptides

As specific immune reactions can be mediated by low concentrations of peptides, particular emphasis was put on the purity, homogeneity and compositional studies of the synthetic peptides. The MAPs were synthesized using solid-phase peptide synthesis with Boc methodology. After removing the protecting groups, the solubilized branched peptides were purified by reverse-phase HPLC without any difficulties. The resulting purified peptides were characterized by two-dimensional SDS gel electrophoresis (Figure 2) and analytical HPLC (Figure 3). Since amino acid analysis is almost useless in the case of MAPs, we tried to characterize the MAP-1 by mass spectrometry. The Fab MS wasn't able to determine the molecular ion. The smaller fragments became observable only after tryptic digestion (on probe tip), and the peaks identified were as follows: 1307.7 (GLFGAIAGFIEGR, calc 1307.51); 914.6 (NIPSIQSR, calc 914.03); 545.6 (VTGLR, calc 544.65); 1440.7 (VTGLRNIPSIQSR, calc 1440.66). The Fab MS technique permitted the entire sequence assignment of the branched peptide, with the exception of the branched lysine core. The new matrix-assisted laser desorption ionization mass spectrometry proved to be applicable for determining the molecular ion (Figure 4); however, the accuracy of the method is only 0.5%–0.1%—therefore, alone, it is not applicable for proving the chemical structure. The synthesis and characterization of the control peptides (HA1C[Arg] and FP3) is published elsewhere (22).

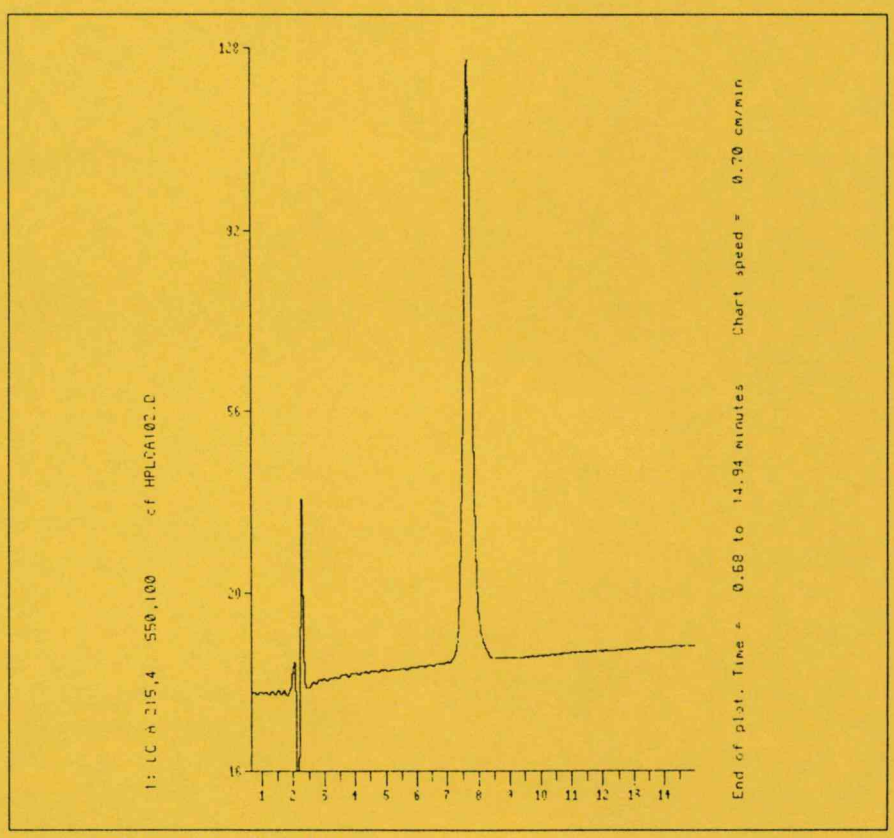

Figure 3. RP-HPLC of purified MAP-1

Table 1. Protection of BALB/c Mice Against a Lethal Dose of A/PR/8/34 Influenza Virus Infection by MAP-1 and HA1C[Arg]

Peptide Used for Preimmunization	Percent of Survivors[a]		
	Control[b]	HA1C[Arg]	MAP-1
Experiment 1 ($n = 5$)	0	40	60
Experiment 2 ($n = 5$)	0	20	60
Experiment 3[c] ($n = 10$)	0	0	22

[a]Data registered on day 16 postinfection are documented. Control mice died on day 8–9 in experiments 1 and 2 and on day 7–8 in experiment 3 postinfection.

[b]Control mice were treated as other groups using PBS emulsified in CFA instead of the peptides.

[c]In experiment 3, a new batch of the mouse pathogenic A/PR/8/34 influenza virus was used.

n = Mice included in experiment groups.

Characteristics of Immune Response Elicited by MAP-1 Comprising Influenza Virus HA Peptides

As summarized in Figure 5A (dotted columns), repeated injections of MAP resulted in the production of IgG-type antibodies recognizing the MAP-1 structure, but the antibodies were inactive and did not bind to the subunit peptides HA1C[Arg] or the Arg extended fusion peptide FP3 (see Figure 1). MAP-1-specific antibodies showed weak binding to the infective A/PR/8/34 influenza virus coated to the solid phase, but their binding could be enhanced significantly by acidic pretreatment of the virus (Figure 5A, PR8pH5). As shown in Figure 5B, no HA1C[Arg]-, FP3- or MAP-1-specific antibodies could be detected after HA1C[Arg] immunization. The high level of influenza virus-specific antibodies, detected only after viral challenge (Figure 5B, dark columns), corresponds to antibodies raised against other epitopes of the virus.

T-Cell Recognition of the MAP-1 Structure

Immunization with the HA1C[Arg] peptide induces a proliferative T-cell response that recognizes virus-infected APC and is fully crossreactive with the MAP-1 structure (Figure 6). These results show that the processing and presentation of HA1C[Arg], MAP-1 or the infective virus result in a common epitope recognized by HA1C[Arg]-primed T-cells. In this assay, MAP was even more efficient than the same concentration of HA1C[Arg] used subsequently (Figure 6). In molar terms, the monomeric HA1C[Arg] contains four times as many copies as the tetrameric MAP-1; but, in the case of identical µg/ml concentrations, the amount of the presumably processed HA1C[Arg] peptide in the *in vitro* cultures or in preimmunized mice is about 20% less in case of MAP-1, taking into consideration the molar masses (FP3 = 1693, HA1C[Arg] = 1481) of HA1C[Arg] and FP3 .

Protection Induced by the MAP-1 Structure

Twenty-two to sixty percent of MAP-1-preimmunized BALB/c mice acquired complete protection against a

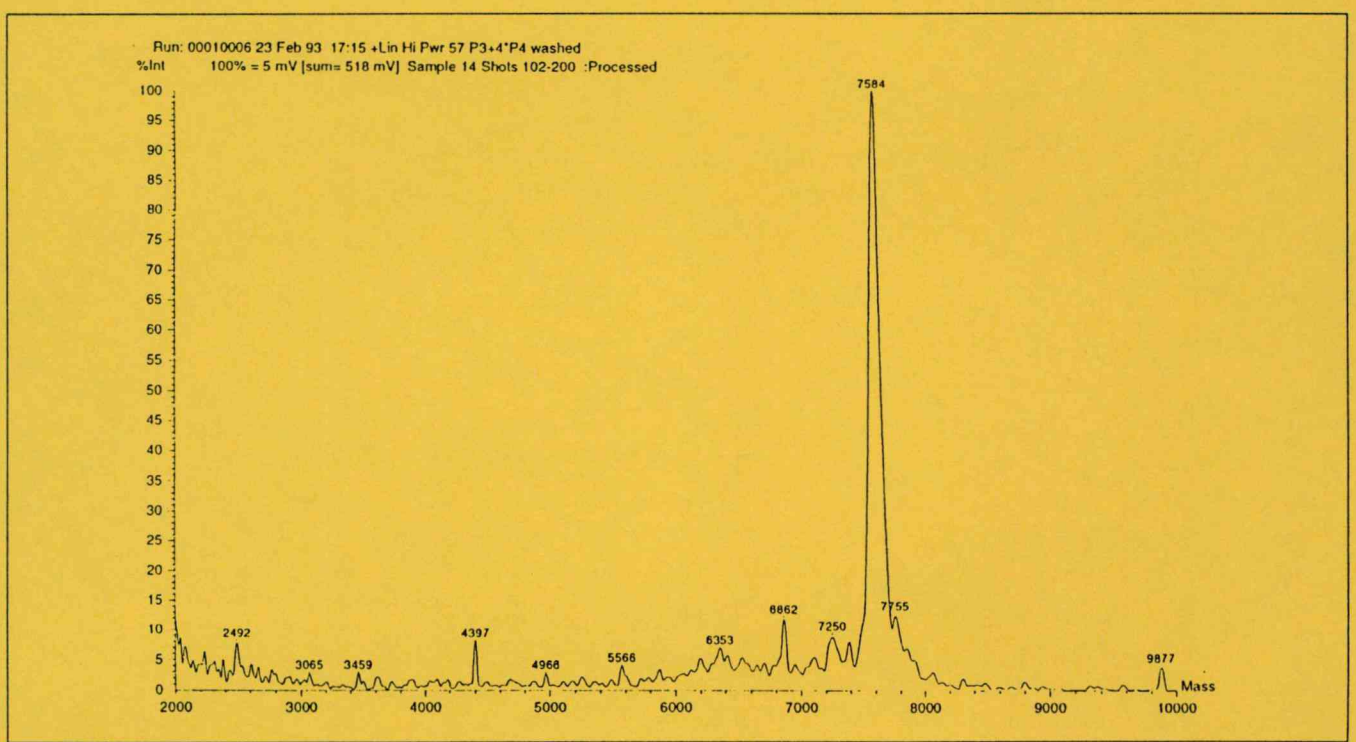

Figure 4. Matrix-assisted laser desorption ionization spectra of MAP-1 structure.

lethal dose of influenza virus as compared to the HA1C[Arg] or control PBS-pretreated mice (Table 1). As summarized in Figure 5B (dark columns), as a result of viral challenge an elevated level of MAP-1-specific IgG-type antibodies could be detected in the serum of the survivors two weeks postinfection. The lack of MAP-1- or HA1C[Arg]-specific antibodies in HA1C[Arg] preimmunized and subsequently infected mice demonstrates that the virus infection itself does not result in the production of MAP-1-specific antibodies (Figure 5B, dark columns). The level of total virus-specific antibodies detected in MAP-1- or HA1C[Arg]-pretreated mice was significantly higher than that in control mice (data not shown).

Table 2. Characterization by EIA of Mouse Antibodies Raised Against TCR ζ- and δ-Peptides

A: $OD495_{sample}-OD495_{control}$[a]

Dilution of the Antisera	Mouse Anti-ζ Serum[b]	Monoclonal Anti-δ Ascitic Fluid
1:100	2.031	>2
1:300	1.678	>2
1:1000	0.557	0.815

B: $OD495_{sample}-OD495_{control}$[c]

Monoclonal Anti-ζ Hybridoma Supernatant	Monoclonal Anti-δ Hybridoma Supernatant
1.185	1.436(1)
	0.960(2)

[a]OD495 value given by preimmune serum at the proper dilution.

[b]Mouse anti-ζ serum was obtained from mice as a test blood prior to using the spleen for hybridoma production. Ascites fluid was produced as described in Materials and Methods.

[c]OD495 value given by PBS–Tween 20 used as a control. Hybridoma supernatants were harvested from the cells producing monoclonal antibodies.

(1) and (2) show the results obtained with supernatants of two independent hybridoma clones producing anti-ζ and anti-δ MAb.

Characterization of Antibodies Produced Against the ζ- and δ-Chains of Human TCR Complex

Monoclonal antibodies were raised against the peptide antigens derived from the TCR ζ- and δ-chains, respectively (see Figure 1). Table 2, A and B, shows the results obtained by EIA. The conventional antiserum or the monoclonal antibodies were highly reactive with the corresponding ζ- or δ-peptide fragments. Higher than 50% inhibition was achieved when ζ-peptide was used as competitor (Figure 7). This experiment proved the peptide specificity of the antiserum raised against the ζ-peptide. In contrast, indirect immunofluorescence or immunoblotting analysis showed that the antipeptide antibodies did not recognize the native ζ-chain (data not shown). The δ-peptide antibodies were also tested for reaction with the native δ-chain and gave similar results to the ζ-chain.

DISCUSSION

The recent improvements in peptide chemistry have made feasible the synthesis of large polypeptides or small proteins. However, the purification and structure and purity verification remain problematic. The originally described MAP system (37), consisting of at least 8 epitopic peptides, can easily lead to a molecule with a molecular mass higher than 10–15 kDa. After purification by means of the conventional techniques (RP-HPLC, size-exclusion chromatography and ion-exchange), we can establish by HPLC and gel electrophoresis that the resulting purified material is homogeneous, that it has the correct amino acid composition, and that the sequencing resulted in the expected structure; but we cannot be sure whether the actual purity is 80% or 90%. The separation power of the conventional purification techniques is not sufficient to investigate the actual homogeneity of the products. Only mass spectroscopy seems applicable for acquiring information concerning the

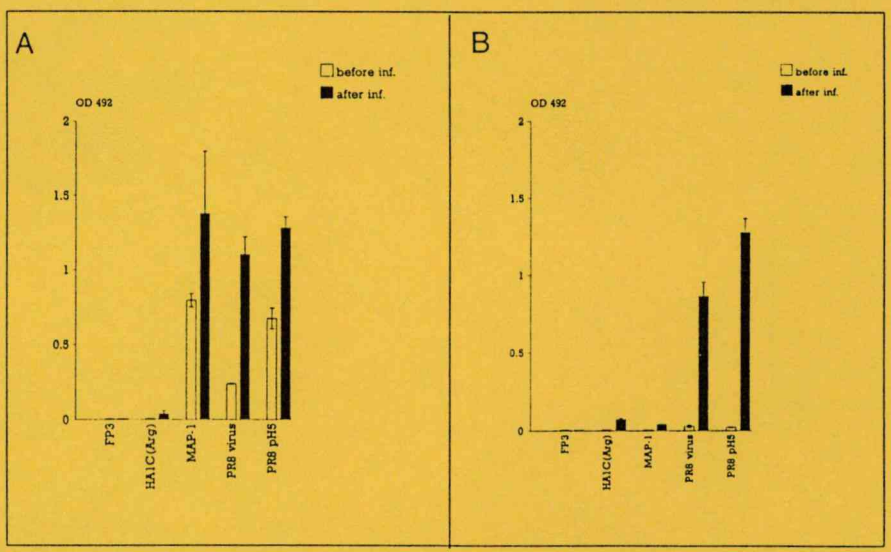

Figure 5. Relative levels of MAP-1- and HA1C[Arg]-induced serum antibodies. BALB/c mice were immunized with MAP-1 (A) or HA1C[Arg] (B), and the relative levels of serum antibodies were measured by EIA, using immune sera taken 14 days after the peptide boost or viral challenge. OD_{492} values (mean value of duplicates obtained for individual sera ± SEM) correspond to 10^3 serum dilutions detected with the solid-phase attached peptides HA1C[Arg], FP3, MAP-1 or with infective (PR8) or acid-pretreated (PR8 pH5) A/PR/8/34 influenza viruses. The number of pretreated mice was 3, the number of MAP preimmunized survivors was 6, and the number of HA1C[Arg] preimmunized survivors was 2.

quality and the side-products formed during the synthesis. If the number of epitopic peptides is decreased to 4–5, the efficiency and qualitative parameters of the synthesis can be increased dramatically.

RP-HPLC may be efficient enough to separate the resulting products and side-products, and, if so, verification of the structure and purity by means of mass spectrometry would be much easier. For example, Figure 4 shows the matrix-assisted laser desorption MS of MAP-1. The calculated mass differs slightly from the measured one; since the accuracy of the MALDI spectrophotometer in linear mode is only 0.1%–0.5%, the measured mass can correspond to the expected molecular mass. The small peaks below the molecular ion can correspond to possible side-products. The more accurate Fab-MS proved to be useless for determining the molecular ion, but after enzymic digestion with trypsin, all the possible fragments were detected—so this method verified the structure.

Influenza virus was one of the first subjects of the subunit vaccination approach, and epitopes of different proteins of the virus were applied to elicit antibodies or T-cells (4). The rationale behind our approach was to combine T- and B-cell epitopes previously identified in the intersubunit region in the HA molecule (22,33). The MAP-1 structure investigated in this study actually mimics the natural sequence of HA present in its uncleaved form in non-infective virions, generated as a result of non-productive infection (16). MAP-1 encompasses two T-cell epitopes (the HA1C[Arg] sequence and the modified fusion peptide (FP3)) in such a way that the overlapping B-cell epitope, localized also in the HA1C[Arg] region, might be able to adopt its appropriate conformation (22). Previous results indicated that the presence of the highly ordered fusion peptide (22,48) is beneficial in stabilizing the overall structure of the less ordered HA1C[Arg] and promotes antibody recognition (33, Z. Nagy et al, unpublished observation). These results, together with the data proving the T-cell-activating capacity of FP3, motivated us to include this peptide in MAP-2 and MAP-3 in order to enhance the immunogenicity of the nonimmunogenic ζ- and δ-chain peptides.

The introduction of an RKKR motif between the two HA epitopes in MAP-1 was designed to provide a sensitive enzyme-susceptibility site, also present in natural sequences of highly pathogenic avian influenza virus strains (45). This sequence can promote the appropriate processing of MAP-1 by trypsin-like enzymes of antigen-presenting cells favoring elaboration of the T-cell epitope previously localized in the HA1C[Arg] region. Our present results, showing the cross-reactivity of HA1C[Arg], MAP-1 and the infective virus in a T-cell proliferation assay (Figure 6), support this possibility. However, it cannot be ruled out that MAP-1 binds to MHC II molecules as a multivalent ligand, therefore increasing the otherwise low affinity of the linear HA1C[Arg] peptide. Nevertheless, the increased activity of MAP-1 in this assay points to the possible role of enhanced helper T-cell activation in mediating protection of MAP-1-preimmunized mice (Table 1).

Protection against a lethal dose of pathogenic influenza virus was attempted by different approaches including the passive administration of antibodies (22); the induction of neutralizing antibodies, helper or cytotoxic T-cells by viral proteins (1,19,24); or by synthetic peptides (2,3,15,35). Data obtained with CD8+ T-cell-depleted mice revealed that the antibody response has a major role in mediating protection against influenza virus infection (18). Passive administration of IgA-type, but not IgG-type, antibodies was demonstrated to confer complete protection (34). In the case of synthetic peptides, the critical point was to elicit T-cells or antibodies crossreactive with the virus and also neutralizing it (3,5).

The data summarized in Figure 5 demonstrate that the MAP-1 structure is immunogenic and is able to induce IgG-type, MAP-1-specific antibodies crossreactive with the acid-pretreated virus. It is well established that the C-terminus of the HA1 subunit of influenza virus hemagglutinin, comprised in the HA1C[Arg] peptide, is buried in the mature, cleaved form of the HA molecule (49), but it can be exposed for antibody recognition by mild acidic treatment (42). This type of IgG antibody can be detected after repeated MAP-1 administration and at an elevated level after viral challenge in all survivors pretreated with MAP-1. In contrast, the monomeric subunit peptides HA1C[Arg] and FP3 were unable to elicit an antibody response directed to the corresponding peptides, to MAP-

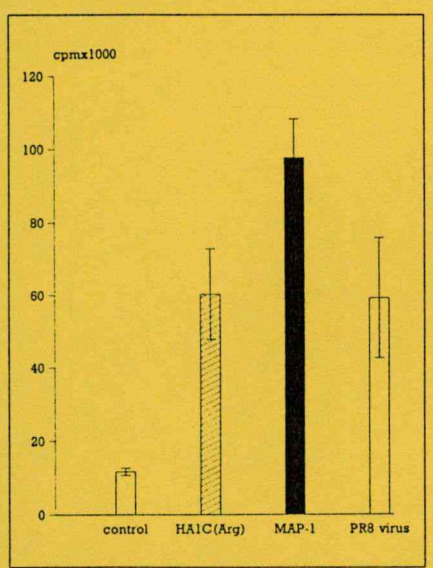

Figure 6. Proliferation of HA1C[Arg]-induced T-cells in presence of HA1C[Arg], MAP-1 or virus preinfected APC. T-cell-enriched lymph node cells of HA1C[Arg]-primed BALB/c mice were stimulated *in vitro* with 20 μg/ml HA1C[Arg] peptide (rising to right), MAP-1 (dark column) or APC preinfected with 100 HAU/ml A/PR/8/34 influenza virus. Empty columns correspond to control cultures incubated without peptides or the virus. Mean values of cpm ± SEM of triplicate cultures obtained in a typical experiment are documented.

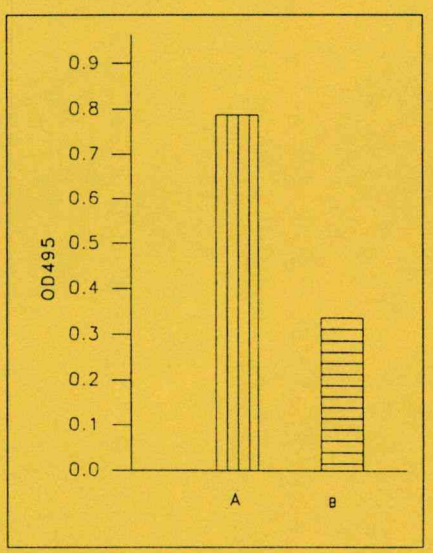

Figure 7. Specificity test of mouse anti-ζ-peptide serum. The plate was coated with 10 μg/ml of MAP-2 overnight at 4°C. It was then washed and left to react with the mouse anti-MAP-2 serum (1:10000 dilution) in the presence (B) or absence (A) of the 22-32 fragment of the ζ-chain (QSFGLLDPKLC, 10 μg/ml) as a competitor for 1 h at 37°C. The assay was completed as described in Materials and Methods.

1 or to any form of the pretreated mice, compared to the HA1C[Arg]-preimmunized animals. This points to the beneficial participation of the MAP-1-specific antibody response in protection, but raises the possibility of other mechanisms as well. As an alternative explanation, protection induced by MAP-1 can be mediated or supported by efficient help delivered by HA1C[Arg] and/or FP3-specific T-cells cross-reactive with the virus (Figure 6) (33).

The previously detailed and promising results motivated us to include in this study the modified fusion peptide in MAP-2 and MAP-3, comprising oligopeptides of the ζ and δ TCR subunits. MAP-2 and MAP-3 resulted in immunogenic structures, compared to their subunit peptides or even to their tetra- or octamers lacking the FP3 HA peptide. However, polyclonal or monoclonal MAP-2 or MAP-3 antibodies did not recognize the cell-membrane-bound or nitrocellulose-attached forms of the corresponding ζ- or δ-subunits.

ACKNOWLEDGMENTS

This work was supported in part by grants OTKA 2734, 2310, 5257, 928, ETT T-80/90 and the Bástyai-Holzer Foundation. The authors are indebted to Dr. T. Janáky and Shimadzu Austria for the LDI MS measurements. The expert technical assistance of Erzsébet Veress and Árpád Mikessy is acknowledged.

REFERENCES

1. **Andrew, M.E. and B.E.H. Coupar.** 1989. Efficacy of influenza haemagglutinin and nucleoprotein as protective antigens against influenza virus infection in mice. Scand. J. Immunol. *28*:81-85.
2. **Arnon, R.** 1992. Development of synthetic vaccines, p. 767-774. *In* Progress in Immunology. Proceedings of the 8th International Congress of Immunology, Budapest, Hungary.
3. **Arnon, R. and M.H. Van Regenmortel.** 1992. Structural basis of antigenic specificity and design of new vaccines. FASEB J. *6*:3265-3274.
4. **Arnon, R. and R.H. Horwitz.** 1993. Synthetic peptides as vaccines. Curr. Topics Immunol. *4*:449-453.
5. **Atassi, M.Z., J.V. Torres and P.R. Wyde.** 1989. Cytotoxic and helper T-lymphocyte responses to antibody recognition regions on influenza virus hemagglutinin. Adv. Exp. Med. Biol. *251*:49-63.
6. **Atassi, M. Z. and R.G. Webster.** 1983. Localization, synthesis, and activity of an antigenic site on influenza virus hemagglutinin. Proc. Natl. Acad. Sci. *80*:840-844.
7. **Auriault, C., I. Wolowczuk, H. Gras-Masse, M. Marguerite, D. Boulanger, A. Capron and A. Tartar.** 1991. Epitopic characterization and vaccinal potential of peptides derived from a major antigen of *Schistosoma mansoni* (Sm28 GST). Pept. Res. *4*:6-11.
8. **Baleux, F. and P. Dubois.** A novel version of multiple antigenic peptide allowing the incorporation of multiple antigenic peptides on a cysteine functionalized lysine tree. Int. J. Pept. Protein Res. (In press).
9. **Briand J. P., C. Barin, M.H.V. Van Regenmortel and S. Muller.** 1992. Application and limitations of the multiple antigen peptide (MAP) system in the production and evaluation of anti-peptide and anti-protein antibodies. J. Immunol. Methods *156*:255-265.
10. **Brown, L. E., J.M. Murray, A.M. Anders, X.-L. Tang, D. White, G.W. Tregear and D.C. Jackson.** 1988. Genetic control and fine specificity of the immune response to a synthetic peptide of influenza virus hemagglutinin. J. Virol. *62*: 1746-1752.

11. **Corradin, G., H.M. Etlinger, and J.M. Chiller.** 1977. Lymphocyte specificity to protein antigens. I. Characterization of the antigen-induced in vitro T cell-dependent proliferative response with lymph node cells from primed mice. J. Immunol. *119*:1048-1053.
12. **Defoort, J.P., B. Nardelli, W. Huang, D.R. Shiu and J.P. Tam.** 1992. Complete synthetic vaccine with built-in adjuvant, p. 845-846. *In* J.A. Smith and J.A. Rivier (Eds.), Peptides; Chemistry and Biology. ESCOM, Leiden.
13. **Defoort, J.P., B. Nardelli, W. Huang and J.P. Tam.** 1992. A rational design of synthetic peptide vaccine with a built-in adjuvant. Int. J. Pept. Protein Res. *40*:214-221.
14. **Del Giudice, G., C. Tougne, J.A. Louis, P.-H. Lambert, E. Biaanchi, F. Bonelli, L. Chiappinelli and A. Pessi.** 1990. A multiple antigen peptide from the repetitive sequence of the Plasmodium malariae circumsporozoite protein induces a specific antibody response in mice of various H-2 haplotypes. Eur. J. Immunol. *20*:1619-1622.
15. **Ders, K., H. Schild, K.H. Wiesmüller, G. Jung and H.-G. Rammensee.** 1989. In vivo priming of virus-specific cytotoxic T lymphocytes with synthetic lipopeptide vaccine. Nature *342*:561-564.
16. **Doherty, P.C., W. Allan and M. Eichelberger.** 1992. Roles of αβ and γδ T-cell subsets in viral immunity. Annu. Rev. Immunol. *10*:123-151.
17. **Drijfhout, J. W. and W. Bloemhog.** 1991. A new synthetic functionalized antigen carrier. Int. J. Pept. Protein Res. *37*:27-32.
18. **Eichelberger, M., W. Allan, M. Zijlstra, R. Jaenisch and P. Doherty.** 1991. Clearance of influenza virus respiratory infection in mice lacking class I major histocompatibility complex-restricted CD8+ T cells. J. Exp. Med. *174*:875-880.
19. **Endo, A., S. Itamura, H. Iinuma, S. Funahashi, H. Shida, F. Koide, K. Nerome and A. Oya.** 1991. Homotypic and heterotypic protection against influenza virus infection in mice by recombinant vaccine virus expressing the haemagglutinin or nucleoprotein of influenza virus. J. Gen. Virol. *72*:699-703.
20. **Francis, M. J., G.Z. Hastings, F. Browm, J. McDermed, Y.-A. Lu and J.P. Tam.** 1991. Immunological evaluation of the multiple antigen peptide (MAP) system using the major immunogenic site of foot-and-mouth disease virus. Immunology *73*:249-254.
21. **Gluck, R.** 1992. Immunopotentiating reconstituted influenza virosomes (IRIVs) and other adjuvants for improved presentation of small antigens. Vaccine *10*:915-919.
22. **Hollósi, M., A.A. Ismail, H.H. Mantsch, B. Penke, G. Váradi, G.K. Tóth, I. Laczkó, I. Kurucz, Z. Nagy, G.D. Fasman and É. Rajnavölgyi.** 1992. Conformational and functional properties of peptides covering the intersubunit region of influenza virus hemagglutinin. Eur. J. Biochem. *206*:421-425.
23. **Isakov, N.** 1993. Tyrosine phosphorylation and dephosphorylation in T lymphocyte activation. Mol. Immunol. *30*:197-210.
24. **Jones, P.D., R. Tha Hla, B. Morein, K. Lovgren and G.L. Ada.** 1988. Immune responses in the murine lung to local immunization with influenza A virus glycoproteins in micelles and immunostimulatory complexes (ISCOMS). Scand. J. Immunol. *27*:645-652.
25. **Kaiser, E., R.L. Colescott, C.D. Bossinger and P.I. Cook.** 1970. Color test for detection of free amino groups in the solid-phase synthesis of peptides. Anal. Biochem. *34*:595-598.
26. **Köhler, G. and C. Milstein.** 1975. Continuous cultures of fused cells secreting antibody of predefined specificity. Nature *256*:495-497.
27. **Löwenadler, B., N. Lycke, C. Svanholm, A.-M. Svennerholm, K. Krook and M. Gidlund.** 1992. T and B cell responses to chimeric proteins containing heterologous T helper epitopes inserted at different positions. Mol. Immunol. *29*:1185-1190.
28. **Migliorini, P., N. Boulanger, B. Betschart and G. Corradin.** 1990. Plasmodium berghei subunit vaccine: repeat synthetic peptide of circumporozoite protein comprising T and B cell epitopes fails to confer immunity. Scand. J. Immunol. *31*:237-242.
29. **Merrifield, R.B.** 1964. The synthesis of a tetrapeptide. Solid phase peptide synthesis. J. Amer. Chem. Soc. *85*:2149-2154.
30. **Munesinghe, D. Y., P. Clavijo, M.C. Calle, R.S. Nussenzweig and E. Nardin.** 1991. Immunogenicity of multiple antigen peptides (MAP) containing T- and B-cell epitopes of the repeat region of the P. falciparum circumporozoite protein. Eur. J. Immunol. *21*:3015-3021.
31. **Pessi, A., D. Valmori, P. Migliori, C. Tougne, E. Bianchi, P.H. Lambert, G. Corradin and G. Del Giudice.** 1991. Lack of H-2 restriction of the Plasmodium falciparum (NANP) sequence as multiple antigen peptide. Eur. J. Immunol. *21*:2273-2276.
32. **Posnett, D.N., H. McGrrath and J.P. Tam.** 1988. A novel method for producing anti-peptide antibodies using a peptide derived from the T cell antigen receptor beta-chain constant region. J. Biol. Chem. *263*:1719-1725.
33. **Rajnavölgyi, É.** 1992. Synthetic peptides in the search for T- and B-cell epitopes. Immunol. Today *13*:17-19.
34. **Renagar, K. B. and P.A. Small.** 1991. Passive transfer of local immunity to influenza virus infection by IgA antibody. J. Immunol. *146*:1972-1978.
35. **Roche, P.A. and P. Cresswell.** 1990. High-affinity binding of an influenza derived peptide to purified HLA-DR. J. Immunol. *144*:1849-1856.
36. **Schild, H., K. Deres, K., K.H. Wiesmüller, G. Jung and H.G. Rammensee.** 1991. Efficiency of peptides and lipopeptides for in vivo priming of virus-specific cytotoxic T cells. Eur. J. Immunol. *21*:2649-2654.
37. **Tam, J.P.** 1988. Synthetic peptide vaccine design: synthesis and properties of a high-density multiple antigenic peptide system. Proc. Natl. Acad. Sci. USA *85*:5409-5413.
38. **Tam, J.P., P. Clavijo, Y.A. Lu, V. Nussenzweig, R. Nussenzweig and F. Zavala.** 1990. Incorporation of T and B epitopes of the circumsporozoite protein in a chemically defined synthetic vaccine against malaria. J. Exp. Med. *171*: 299-306.
39. **Tam, J.P. and Y.A. Lu.** 1990. Synthetic peptide vaccine engineering: Design and synthesis of unambiguous peptide-based vaccines containing multiple peptide antigens for malaria and hepatitis, p. 351-370. *In* R. Epton (Ed.), Innovation and Perspectives in Solid-Phase Synthesis I. Intercept, UK
40. **Tam, J. P. and F. Zavala.** 1989. A novel approach to increase detection sensitivity of synthetic peptides in solid-phase immunoassays. J. Immunol. Methods *124*:53-61.
41. **Tamura, S., H. Funato, Y. Hirabayashi, Y. Suzuki, T. Nagamine, C. Aizawa and T. Kurata.** 1991. Cross-protection against influenza virus infection by passively transferred respiratory tract IgA antibodies to different hemagglutinin molecules. Eur. J. Immunol. *21*:1337-1344.
42. **Tang, X.-L., G.W. Tregear, D. White and D.C. Jackson.** 1988. Minimum requirement for immunogenic and antigenic activities of homologs of a synthetic peptide of influenza virus hemagglutinin. J. Virol. *62*:4745-4751.
43. **Towbin, H., T. Staehelin and J. Gordon.** 1979. Electrophoretic transfer of proteins from polyacrylamide gels to nitrocellulose sheets: Procedures and some applications. Proc. Natl. Acad. Sci. *76*:4350-4354.
44. **Tóth, G.K., G. Váradi, B. Penke, É Monostori, Z. Hegedus, Z. Nagy, I. Kurucz and É. Rajnavölgyi.** 1992. Synthesis of branched polypeptides as antigens for influenza virus hemagglutinin and T-cell receptor subunits, p. 882-884. *In* C.H. Schneider and A. Eberle (Eds.), Peptides 1992. Proceedings of 22nd Eur. Pept. Symp. ESCOM, Leiden.
45. **Vey, M., M. Orlich, S. Adler, H.-D. Klenk, R. Rott and W. Garten.** 1992. Hemagglutinin activation of pathogenic avian influenza viruses of serotype H7 requires the protease recognition motif RXK/RR. Virology *188*: 408-413.
46. **Wang, C.Y., D.J. Looney, M.L. Li, A.M. Walfield, J. Ye, B. Hosein, J.P. Tam and F. Wong-Staal.** 1991. Long-term high-titer neutralizing activity induced by octameric synthetic HIV-1 antigen. Science 285-287.
47. **Weisman, A.M., D. Hou, D.G. Orloff, W.S. Modi, H. Seunaez, S. O'Brien and R. Klausner.** 1988. Molecular cloning and chromosomal localization of the human T-cell receptor zeta chain:Distinction from the molecular CD3 complex. Proc. Natl. Acad. Sci. *85*:9709-9713.
48. **White, J.M.** 1990. Viral and cellular membrane fusion proteins. Ann. Rev. Physiol. *52*:675-697.
49. **Wilson, I.A., J.J. Skehel and D.C. Wiley.** 1981. Structure of the haemagglutinin membrane glycoprotein of influenza virus at 3# resolution. Nature *289*:366-373.
50. **Zegers, N.D., C. van Holten, E. Claassen and W.J.A. Boersma.** 1993. Peptide induced memory (IgG) response requires covalent linkage of a B cell epitope and a T cell epitope, p. 836-837. *In* C. H. Schneider and A. Eberle (Eds.), Peptides 1992. Proceedings of 22th Eur. Pept. Symp. ESCOM, Leiden.

Address correspondence to:

Gábor K. Tóth
Department of Medical Chemistry
A. Szent-Györgyi Medical University
H-6720 Szeged, Dóm tér 8, Hungary

Vol. 193, No. 3, 1993 BIOCHEMICAL AND BIOPHYSICAL RESEARCH COMMUNICATIONS
June 30, 1993 Pages 1247-1254

CIRCULAR DICHROISM AND FOURIER-TRANSFORM INFRARED SPECTROSCOPIC STUDIES ON T-CELL EPITOPIC PEPTIDE FRAGMENTS OF INFLUENZA VIRUS HEMAGGLUTININ

Sándor Holly[1], Zsuzsa Majer[2], Gábor K. Tóth[3], Györgyi Váradi[3], Éva Rajnavölgyi[4], Ilona Laczkó[5] and Miklós Hollósi[2*]

[1]Central Research Institute of Chemistry, H-1525 Budapest, P.O.B. 17, Hungary

[2]Department of Organic Chemistry, Eötvös University, H-1158 Budapest, P.O.B. 32, Hungary

[3]Department of Medical Chemistry, A. Szent-györgyi Medical University, H-6720 Szeged, Hungary

[4]Department of Immunology, Eötvös University, H-2131 Göd, Hungary

[5]Institute of Biophysics, Biological Research Center, 6701 Szeged, P.O.B. 521, Hungary

Received May 17, 1993

Epitopic peptides representing the C-terminal (HA1) region of cleaved hemagglutinin of influenza virus from different serotypes were synthesized. Circular dichroism and Fourier-transform infrared spectroscopic data showed that peptides HS2 and HS3 have a predominantly α-helical conformation in trifluoroethanol. Recently a component band appearing between 1640 and 1635 cm^{-1} in the amide I region of the Fourier-transform infrared spectra of polypeptides has been correlated with strongly H-bonded ß-turns (Ref. 8). Using this assignment, HS1 was found to contain less α-helix but have tendency to adopt ß-turn(s). Interestingly, fragment HS2 with the highest α-helix content proved to be the poorest T-cell epitope among serotypes HS1-HS3.

There is a growing interest in the understanding of the secondary structure of small (<20 residues) epitopic peptides. It has been reported recently that the peptide-binding site of human class I histocompatiblity molecules recognizes 8-11mers (1). Similarly, the antigens recognized by MHC class II-restricted T

*To whom correspondence should be addressed.

0006-291X/93 $4.00

Table 1. Amino acid sequence and abbreviations of the synthetic peptides from the C-terminal region of influenza virus A hemagglutinin from different serotypes

	317.....329
HS1	VTGLRNIPSIQSR
HS2	ATGLRNVPQIESR
HS3	LATGMRNVPEKQTR

cells can be mimicked by small peptides more heterogenous in their size (2). It is well established that MHC-bound peptides are tightly mounted in a groove in extended conformation with a kink in the middle (3,4). Previously, prediction methods suggested amphipathic α-helices for MHC class II restricted T cell epitopes (5).

Small size peptides are expected to adopt multiple conformations in solution. Our earlier spectroscopic studies on synthetic intersubunit fragments of influenza virus hemagglutinin (HA) also demonstrated the presence of conformer mixtures and the dependence of antibody recognition on conformation (6). Circular dichroism (CD) and Fourier-transform infrared (FT-IR) spectroscopies, contrary to NMR, have the capacity of time resolving conformational changes of the peptide chain and therefore both techniques can be applied for the study of conformer mixtures of peptides in solution.

This paper reports CD and FT-IR spectroscopic measurements on peptides (Table 1) comprising the C-terminal of the HA1 subunit of three serotypes of human influenza A viruses. Previous data showed that these peptides were able to elicit MHC II restricted murine T cells cross-reactive with the virus (7).

MATERIALS AND METHODS

The peptides were synthesized by the solid phase technique utilizing Boc chemistry (8). Side chain protecting groups were as follows: Tos(Arg), Bzl(Thr), OcHex(Glu) and Bzl(Ser). The peptide chains were elongated on MBHA resin (0.6-0.8 mmol/g) and the syntheses were carried out manually. Couplings were performed with dicyclohexylcarbodiimide (DCC) (with the exception of Asn, Gln and Arg which were incorporated as their HOBt-esters) using three-fold excess of Boc-amino acids. Amino acid incorporation was monitored by ninhydrin test (9). In case of incomplete couplings this step was repeated, but the dichloromethane (DCM) was substituted by dimethylformamide (DMF). The completed peptide

resins were treated with liquid HF/dimethyl sulphide/p-cresol/p-thiocresol (86:6:4:2, vol/vol), on 0°C, 1 h. HF was removed and the resulted free peptides were solubilized in 10% aqueous acetic acid, filtered and lyophilized.

The crude peptides were purified by reverse-phase HPLC (Knauer; Berlin, Germany) using Lichrosorb RP-18 10 μ column (16 x 250 mm). The following solvent systems were used: 0.1% trifluoroacetic acid (TFA) in water (A); 0.1%TFA, 80% acetonitrile (AcN) in water (B); gradient: 0%-50% B in 1.5 hours, flow rate 3 ml/min. The appropriate fractions were pooled and lyophilized. The purity was checked by RP-HPLC (Nucleosil 5 C 18 column, solvent systems as above, gradient: 30%-60% B in 15 min, flow rate 0.8 ml/min, detection at 220 nm, or Eurosil Bioselect 5 C 18 column, flow rate 1.5 ml/min with solvent systems and detection as previously) and proved to be substantially pure (>97%).

The FAB-MS experiments were performed with a VG ZAB-2SEQ type hybrid tandem mass spectrometer, equipped with an LSIMS source (Cs^+ ion gun used at 30 keV). The results of the MS measurements were in all cases in good agreement with the calculated value.

Circular dichroism spectra were measured on a Jobin-Yvon Mark VI dichrograph calibrated with epiandrosterone. Measurements were carried out in 0.02 cm cells at ambient temperature. NMR grade trifluoroethanol (TFE) (Aldrich) and double distilled water were used as solvents. The concentration of the samples ranged between 0.5-1 mg/ml. Mean residue ellipticity, $[\theta]_{MR}$, is given in deg.cm^2/dmol.

Infrared measurements (at a resolution of 4 cm^{-1}) were performed at room temperature on a Nicolet 170SX spectrometer. Peptide solution (c≈1 mg/ml) were prepared in TFE (see above). The IR spectrum of TFE (containing traces of water) was obtained under identical conditions. The deformation vibrational band of water between 1700-1600 cm^{-1} was removed by substracting the spectrum of TFE on the basis of the combination band of OH stretching and HOH deformation at 5293 cm^{-1}. This procedure allowed an unambiguous comparision of the spectra in the critical 1650-1600 cm^{-1} range. KBr cells of 0.041 cm were used. The spectra were analyzed by a normalized, least-squares curve-fitting program, using products of Gauss and Lorentz curves (Holly et al., unpublished). The selection of component curves was assisted by the Fourier self-deconvolution method of Mantsch et al. (10).

RESULTS AND DISCUSSION

CD studies

In water the CD spectra of peptides HS1-HS3 show a strong negative band between 195-200 nm which is accompanied by a shoulder near 220 nm. In TFE peptides HS1-HS3 adopt helical CD spectra with low intensity bands (Fig. 1). On addition of increasing amounts of water, the spectra (e.g. Fig. 2) are gradually shifted towards the spectrum measured in water. It is the CD spectrum of peptide HS2 which shows the most expressed helical features (Fig. 1). The intensity of the negative and the positive bands of the $\pi\pi^*$ couplet is definitely lower in the CD spectrum of HS1.

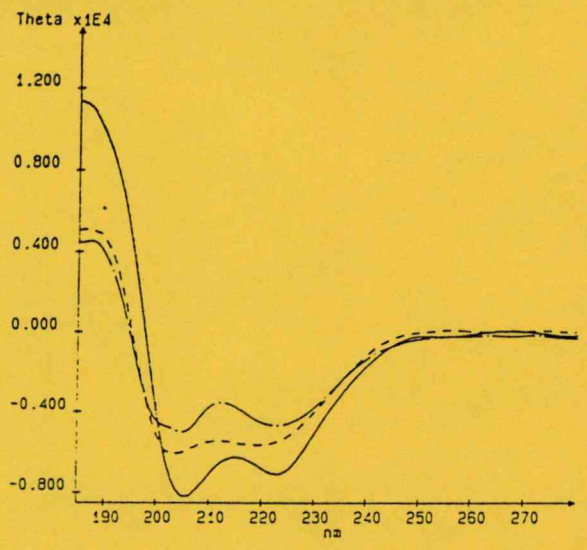

Fig. 1. Circular dichroism spectra in TFE of epitopic peptides HS1-HS3. (— · —) HS1; (———) HS2; (- - - - -) HS3.

FT-IR spectra

Peptides HS1-HS3 are present as TFA salts because of the purification procedure using TFA-containing eluents. The trifluoroacetate anion is known to have an absorption band in the amide I infrared region. In the infrared spectrum of CF_3COONa in KBr pellet the ν_{as} mode of the COO^- group appears at 1694.5 cm^{-1} while the ν_{as} and ν_s vibrations of the CF_3 group at 1218 and 1143

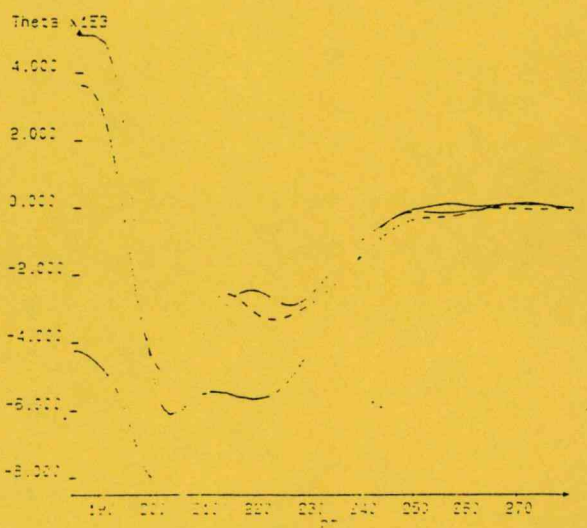

Fig. 2. Circular dichroism spectra of HS3 in TFE/water mixtures. (———) 100%; (- - - - -) 75%; (— · —) 50% TFE.

cm^{-1}, respectively. In the KBr spectra of peptides HS1-HS3 the ν_s CF_3 band shows up at 1135+1 cm^{-1}, accompanied by the ν_{as} band near 1205 cm^{-1}. In the curve-fitted spectra of the peptides in KBr, a component band was found between 1702 and 1699 cm^{-1}. The ratio of band intensities I(~1700)/I(~1135) in the spectra of peptides and I(1694.5)/I(1143) in the spectrum of CF_3COONa in KBr is practically the same (1.55+0.15). On the basis of this, the component band near 1700 cm^{-1} in KBr and at 1691+0.5 cm^{-1} in the TFE spectra of peptides HS1-HS3 was assigned to the COO^- group of the counterion trifluoroacetate.

As reported earlier (6), after substracting the contribution of trifuoroacetate, the IR spectrum of HS1 in D_2O is dominated by a strong band at 1647.5 cm^{-1} (aperiodic conformation).

The FT-IR spectra in TFE of fragments corresponding to serotypes HS1-HS3 are shown in Fig. 3. All three spectra contain a strong amide I component band between 1678-75 cm^{-1}. This band was assigned to the amide I mode of solvent-exposed carbonyls. Peptides HS2 and HS3 show a strong component band, characteristic of weakly H-bonded α-helices, at 1661 and 1659.5 cm^{-1}, respectively (Fig. 3b and c). In the curve-fitted IR spectrum of HS1 (Fig. 3a), a strong component bands appears at 1663 cm^{-1}, above the upper limit of the α-helix (11). (A typical but weak α-helix band is present at 1656 cm^{-1}, Fig. 3a). Weak component bands show up in the spectra near 1645 cm^{-1} (aperiodic conformation) and at 1624-1623 cm^{-1} (ß-sheet). The ß-sheet band is more intensive in the spectra of HS2 and HS3. Component bands between 1639 and 1635 cm^{-1} are also seen in the curve-fitted spectra of the peptides.

Recently an infrared band at 1639 cm^{-1} has been assigned to the repeating 1←4 H-bond of 3_{10} helices (12,13). Similarly, in the FT-IR spectra of the bridged cyclic peptides cyclo[Gly-Pro-Xxx-Gly-NH-$(CH_2)_n$-CO] (Xxx=Gly, Ser(O^tBu), Ser, Thr(O^tBu); n=2,4) a band near 1640 cm^{-1} was assigned to the acceptor C=O of the 1←4 intramolecular H-bond of type I or type II ß-turns (14). It was also shown that in TFE the "ß-turn band" appears down-shifted in the 1640-1635 cm^{-1} amide region. Thus, the low intensity component band between 1641 and 1634 cm^{-1} in the IR spectra of HS1-HS3 (Fig. 3) may be indicative of the presence of H-bonded ß-turns.

According to secondary structure prediction, peptide HS1 tends to adopt ß-turns: the highest turn propensity is predicted for

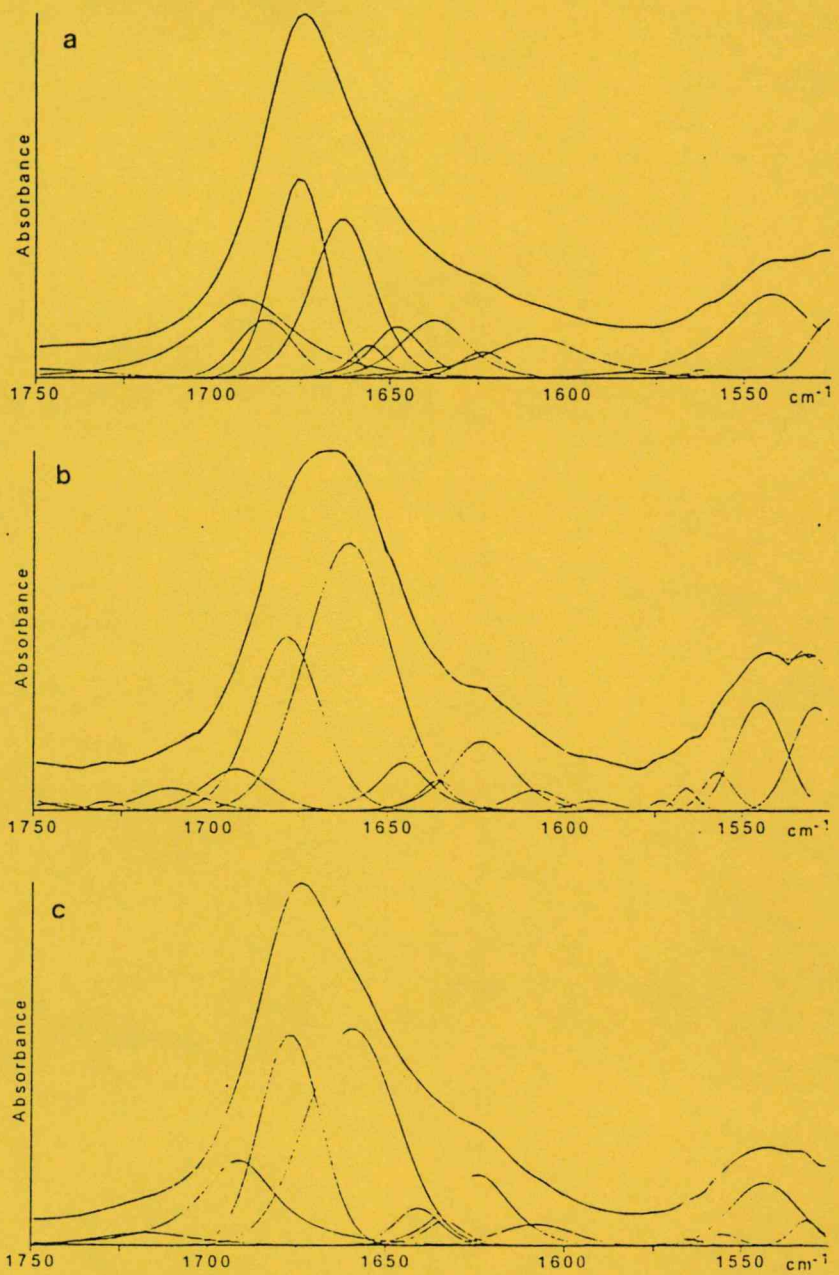

Fig. 3. The amide I and II spectral regions of the FT-IR spectra in TFE of HS1(a), HS2(b) and HS3(c). The measured and curve-fitted (sum) spectra are shown together with the component bands resulting from the analysis (see Materials and Methods).

the Ile-Pro-Ser-Ile tetrapeptide (6). The replacement of Ser for Gln in HS2 and Glu in HS3 destroys the turn-forming Pro-Ser core and increases the helical tendency of these peptides. The structural information inferred from CD and FT-IR studies is in agreement with the prediction. Both methods indicate that the

highest amount of α-helix is present in HS2, but the helicity of HS3 is also significant. The most intensive "ß-turn band" at 1637.5 cm^{-1} can be seen in the curve-fitted infrared spectrum of HS1 (Fig. 3a). As reflected by the weak component band at 1624-23 cm^{-1}, peptides HS2 and HS3 contain definite amount of ß-sheet conformation in TFE solution. Based on the integrated intensities of the α-helix and ß-sheet component bands, it is peptide HS3 in which the ß-sheet content is the highest.

We think that, without overinterpreting the curve-fitted FT-IR spectra, two main conclusions can be drawn:

(1) Peptides HS2 and HS3 in TFE adopt a predominant α-helical conformation which is broken or, more likely loosened at Pro324. Minor conformer(s) or conformational regions with aperiodic and ß-sheet conformation are also present. Contrary to this, HS1 occurs as a multicomponent mixture of conformers even in TFE.

(2) FT-IR spectroscopic data allow the presence of ß-turns in all three peptides. Based on secondary structural prediction and the relative intensity of the ß-turn band in the infrared spectrum, HS1 contains at least one ß-turn which likely encompasses the Pro-Ser dipeptide.

TFE is known to induce α-helical conformation (15). The significant differences in the FT-IR spectra (Fig. 3) clearly indicate that HA fragments HS1-HS3 have different conformational propensities. Interestingly HS2, showing the highest α-helix content on the basis of both CD and FT-IR evidences, was proved to be less potent to induce an *in vivo* T cell response and *in vitro* T cell proliferation compared to peptides HS3 or HS1 corresponding to other serotypes (7). It is reasonable to suppose that in a water rich environment α-helicity does not play a determinant role in the recognition of T cell epitopic peptides from the intersubunit region of influenza virus HA.

ACKNOWLEDGMENTS

The authors are indebted to Dr Mariann Mak for the MS measurements. This work was supported by Hungarian grants OTKA I/3/2245 and 2734.

REFERENCES

1. Rammensee, H.-G., Falk, K., and Rotzschke, H. (1993) Curr. Opinion in Immunol. 5, 35-44.
2. Hunt, D.F., Michel, H., Dickinson, T.A., Shabanowitz,J., Cox, A.L., Sakaguchi, K., Appella, E., Grey, H.M., and Sette, A. (1992) Science 256, 1817-1820.

3. Guo, H.-C., Jardetzky, T.S., Garrett, T.P.J., Lane, W.S., Streminger, J.L., and Wiley, D.C. (1992) Nature 360, 364-366.
4. Madden, D.R., Gorga, J.C., Strominger, J.L., and Wiley, D.C. (1991) Nature 353, 321-325.
5. Cornette, J.L., Margalit, H., DeLisi, C., and Berzofsky, J.A. (1992) In The amphipathic helix (R.M. Epand, Ed.). CRC Press (Boca Raton).
6. Hollosi, M., Ismail, A.A., Mantsch, H.H., Penke, B., Varadi, G., Toth, G., Laczko, I., Kurucz, I., Nagy, Z., Fasman G., and Rajnavolgyi, E., (1992) Eur. J. Biochem. 206, 421-425.
7. Rajnavolgyi, E. (1992) Immunology Today 13, A17-19.
8. Merrifield, R.B. (1963) J. Am. Chem. Soc. 85, 2149-2154.
9. Kaiser, E., Colescott, R.L., Bossinger, C.D., and Cook, P.J. (1970) Anal. Biochem. 34, 595-598.
10 Mantsch, H.H., Moffatt, D.J., and Casal, H.L. (1986) J. Mol. Structure 173, 285-298.
11. Surewicz, W.K., and Mantsch, H.H. (1988) Biochim. Biophys. Acta 952, 115-130.
12. Miick, S.M., Martinez, G.V., Fiori, W.R., Todd, A.P., and Millhauser, G.L. (1992) Nature 359, 653-655.
13. Prestelski, S.J., Byler, D.M., and Thompson, M.P. (1991) Int. Peptide Protein Res. 37, 508-512.
14. Mantsch, H.H., Perczel, A., Hollosi, M., and Fasman, G.D., (1993) Biopolymers 33, 201-207.
15. Urry, D.V., Masotti, L., and Krivacis, J.R. (1971) Biochim. Biophys. Acta 241, 600-612.

Scand. J. Immunol. 40, 281–291, 1994

The Intersubunit Region of the Influenza Virus Haemagglutinin is Recognized by Antibodies During Infection

Z. NAGY, É. RAJNAVÖLGYI, M. HOLLÓSI*, G. K. TÓTH†, G. VÁRADI†, B. PENKE†, I. TÓTH‡, A. HORVÁTH, J. GERGELY & I. KURUCZ§

Department of Immunology, L. Eötvös University, Göd, Hungary
**Department of Organic Chemistry, L. Eötvös University, Budapest, Hungary*
†Department of Medical Chemistry, A. Szent-Györgyi Medical University, Szeged, Hungary
‡Department of Pharmaceutical Chemistry, The School of Pharmacy, University of London, UK
§Institute for Drug Research, Budapest, Hungary

Nagy Z, Rajnavölgyi É, Hollósi M, Tóth GK, Váradi G, Penke B, Tóth I, Horváth A, Gergely J, Kurucz I. The Intersubunit Region of the Influenza Virus Haemagglutinin is Recognized by Antibodies During Infection. Scand J Immunol 1994;40:281–91

The influenza virus haemagglutinin has an important role in the infectious cycle of the virus and carries multiple B and T cell epitopes. It is synthesized as a single polypeptide chain but viral infectivity depends on its post-translational enzymatic cleavage. The cleavage site of a trypsin-like enzyme responsible for this modification is found in the most conserved intersubunit region of the molecule. In this study the role of this region in antibody recognition was investigated. Synthetic peptides comprising the intact and cleaved forms of the intersubunit segment were used to examine the specificity of virus- or peptide-induced antibodies. The immune response elicited by viral infection resulted in the appearance of antibodies capable of neutralizing the virus without interfering with its binding to the receptor. A monoclonal antibody (MoAb) of such functional properties was shown to recognize the intact intersubunit region both in the uncleaved haemagglutinin molecule and in a 25-mer synthetic peptide comprising the intact intersubunit region. Specificity and functional studies revealed the conformation-dependent recognition of the C-terminal segment of the haemagglutinin 1 subunit by this MoAb. The binding of the antibody was shown to inhibit the trypsin-mediated cleavage of the haemagglutinin molecule and the membrane fusion event. The enzymatic cleavage of the haemagglutinin was demonstrated to abolish antibody recognition of the infective virus suggesting an escape mechanism mediated by the functional destruction of this highly conserved region. The synthetic peptide corresponding to the intact intersubunit region is characterized by an ordered structure and is able to elicit an antibody response in BALB/c mice while its subfragments are nonimmunogenic. Furthermore, this peptide elicited a protective immune response demonstrated by *in vivo* experiments.

É. Rajnavölgyi, Department of Immunology, L. Eötvös University, Jávorka S. u. 14., H-2131 Göd, Hungary

INTRODUCTION

The haemagglutinin (HA) molecule of influenza viruses belongs to type I transmembrane proteins and forms envelope spikes on virions or is expressed in the membrane of infected host cells [1]. The HA molecule is one of the major targets of antibody (Ab) recognition and multiple overlapping epitopes have been identified by monoclonal antibodies (MoAb) [2–4]. Four major antigenic subsites eliciting Ab of distinct specificities and functional properties were localized mostly on the outer surface of the molecule [5, 6]. The majority of neutralizing Ab were demonstrated to recognize the head region of HA known to be involved in receptor binding mediated by sialic acid side chains of membrane glycoproteins or glycolipids [5].

Influenza A viruses encompass 14 HA subtypes of related but not identical amino acid sequences [7, 8]. The amino acid sequence of the HA molecule is not only different in diverse influenza virus serotypes but as a consequence of mutations is a subject for continuous changes [9] resulting in frequent antigenic variations of the neutralizing epitopes of haemagglutinin [10, 11]. Amino acid substitutions generated by antigenic drift

in distinct strains of the virus are accumulated in the exposed regions of the HA molecule close to the receptor binding site where the main neutralizing epitopes of HA are located [5]. Therefore, neutralizing Ab raised against one virus strain in most cases are unable to cross-react with other strains of influenza viruses [12].

The most conserved region of the single chain precursor of influenza virus haemagglutinin (HA0) is buried in the hydrophobic intersubunit core region [3, 13] and comprises an enzyme cleavage site as a target for a functionally essential post-translational modification. This event occurs at the late stage of the constitutive secretory pathway [14] and is mediated by host cell related trypsin-like enzymes [15] belonging to the substilisin family [16]. The enzymatic cleavage results in a disulphide bridge-linked dimer of HA1 and HA2 subunits [17]. The cleaved HA molecule is ready to undergo a pH dependent conformational change [17, 18] the consequences of which involve the drastic reorganization of the overall structure of the HA trimers and, as a result the exposure of the so called fusion peptide comprising the N-terminal 1-14 amino acids of the HA2 subunit [3, 19–21]. These changes are the prerequisite for the fusion of viral envelope with the endosomal membrane of the host cell which drives the virus core into the cytoplasm to initiate infection and facilitate uncoating processes essential for viral propagation. Cleavage of HA0 followed by the pH dependent conformational change of HA has been proven to influence recognition by either Ab [3, 12, 17] or T cells [22, 23] of certain specificities.

In this study the effect of the post-translational enzymatic cleavage on antibody recognition of the intersubunit region was studied by different approaches. Our results revealed that the uncleaved intersubunit region can be the target of Ab recognition in the course of influenza virus infection. Antibody directed against this region possess neutralizing activity without interfering with receptor binding but inhibiting the membrane fusion event. A synthetic peptide 25 amino acids in length can substitute the intact form of the intersubunit region in binding to or eliciting Ab.

MATERIALS AND METHODS

Synthetic peptides. The detailed description of peptide synthesis, purification and characterization are published elsewhere [24–27]. The nomenclature and chemical characteristics of the peptides are summarized in Table 1, the amino acid sequence and location of the peptides are given in Fig. 4A. The HPLC conditions for Table 1 are described as follows. Peptides FP, IP and [D-Arg^{13}]IP: Nucleosil 5C 18 column (4 × 250 mm), 1.0 ml/min flow rate, detection at 220 nm, solvent A: 0.1% TFA, solvent B: 0.1% TFA, 80% AcN, gradient 40% → 70% B in 15 min and 20% → 50% in 15 min for peptide HA1C[Arg]. For (HA1C[Arg])$_4$: Vydac 5 C 5 column (4 × 250 mm), 1.5 ml min flow rate, detection at 220 nm, solvent A: 0.1% TFA, solvent B: 0.1% TFA, 80% AcN, gradient 25% → 60% B in 15 min.

Virus preparations. The mouse adapted A PR 8 34 influenza virus (H1N1) stock was grown in the chorioallantoic fluid of 12-day-old embryonated hen eggs. Allantoic fluid was harvested after a 40 h incubation at 35°C and stored in aliquots at −70°C. The A/PR/8/34 virus bearing the uncleaved form of the haemagglutinin molecule was propagated on chicken embryo fibroblast cells in Dulbecco's modified Eagle's medium (SIGMA). The supernatant of cell cultures containing the non-infective virus was collected after a 48–72 h incubation at 37°C and titrated for virus content by the standard haemagglutination method [28] (Section 7.1). Virus purification was performed by the method of Barrett & Inglis [28].

Table 1. Characteristics of the synthetic peptides

Peptide	Mass spectra: Calculated	Mass spectra: Found	HPLCA[a] (time)	Purity[b] (%)
HA1C[Arg]	1438.80[c]	1439.90	8′34″	98
FP	1151.30	1151.50	8′41″	97
IP	2574.00[c,d]	2574.50	10′59″	96
[D-Arg^{13}]IP	2572.97	2573.60	10′04″	97
(HA1C[Arg])$_4$	ND		7′08″	97

[a] HPLC conditions are detailed under Materials and Methods.
[b] Determined by HPLC.
[c] Monoisotopic mass.
[d] C-terminal COOH, the other peptides have $CONH_2$ at the C terminus.
ND, not determined.

Animals. Eight to ten week old male BALB c mice were purchased from LATI (Gödöllő, Hungary). Animals were kept under conventional animal facilities during the immunization period.

Influenza virus infection of BALB/c mice. Groups of 5–10 mice were exposed to the mouse pathogenic A PR/8/34 influenza virus-containing allantoic fluid in an airborne infection apparatus or by intranasal introduction under anaesthesia. Dilution of the allantoic fluid resulting in 50% mortality (LD_{50}) was determined in a preliminary survival experiment using different dilutions of the virus for intranasal infection of BALB/c mice. The virus dose used for infection is given under the different immunization protocols. For the protection experiments preimmunized mice were infected with 5 LD_{50}.

Immunization protocols. Induction of influenza virus specific antibodies: BALB/c mice were infected intranasally with the mouse pathogenic stock of the A/PR/8 34 influenza virus using 0.1 LD_{50} on day 0 and 10 LD_{50} on days 14 and 28 (10 μl/animal), respectively (referred as infection in Fig. 1A,C). Blood samples were taken at different points of time as given in the Figure legends. Three days before cell fusion mice were challenged by an intravenous injection of 50 μg purified virus. In another series of experiments 100 μg purified A PR/8/34 virus emulsified in complete Freund's adjuvant (CFA) was injected subcutaneously in the base of the tail (referred as immunization in Fig. 1B,D).

Induction of peptide-specific antibodies: BALB c mice were immunized with 100 μg of the synthetic peptides dissolved in sterile phosphate buffered saline (PBS) and emulsified in CFA (Sigma Chemical Co., St Louis, MO, USA) by subcutaneous injections into the hind footpads and to the base of the tail. Four weeks later the same amount of peptide emulsified in incomplete Freund's adjuvant (IFA) (Sigma) was injected. A final challenge was given after 4 weeks by 100 μg peptide dissolved in PBS.

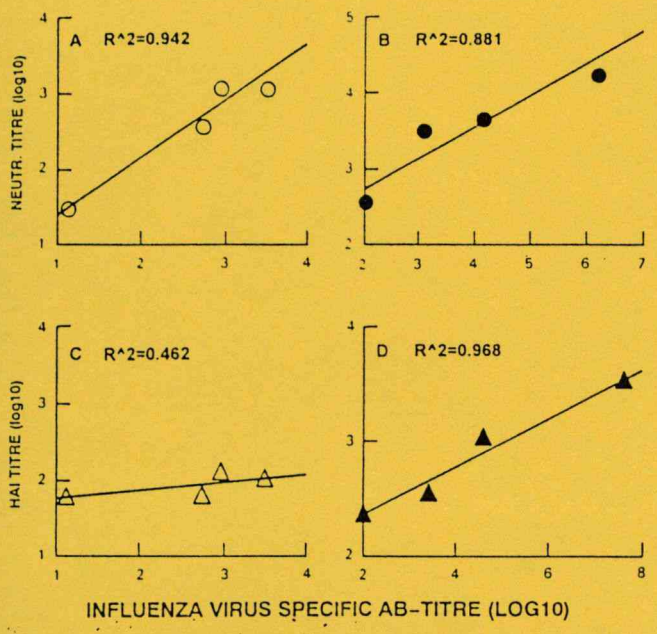

Fig. 1. Correlation of the relative level of influenza virus specific antibodies raised by infection or immunization with the titre of neutralizing or inhibitory antibodies detected by the haemagglutination assay.

BALB c mice were infected (empty symbols) or immunized (dark symbols) with A PR/8/34 influenza virus as described in Materials and Methods. Blood samples were analysed for the relative levels of Ab binding to the influenza virus, inhibitory for haemagglutination or active for *in vitro* neutralization of the virus. Reciprocal serum dilutions effective for 50% virus neutralization (A,B) or inhibition of haemagglutination (C,D) were plotted against the titre of virus-specific antibodies. Correlation was determined by an Apple Macintosh computer using CRICKET GRAF software. Panel A and B compares the relation of neutralizing to virus binding Ab while panels C and D show the comparison of inhibitory Ab detected by the haemagglutination assay as a proportion of virus binding Ab.

In the protection experiments 8 weeks after priming, mice were challenged with 100 or 200 μg peptides emulsified in IFA and 5 weeks later preimmunized mice were intranasally infected with a 5 LD_{50} dose of the mouse pathogenic A/PR 8 34 influenza virus.

Experimental groups consisted of five to 10 animals. Control mice were treated as described above, but using PBS emulsified in CFA or IFA instead of the peptides. The number of survivors was determined daily post infection. Blood samples were taken 14 days after each antigenic challenge.

Production of HA-specific MoAb. Cell fusion was performed with the spleen cells of an influenza virus infected BALB/c mouse using the SP2/0 murine myeloma cells according to the method of Köhler & Milstein [29]. Clones were established by limiting dilution, selection of hybridomas was performed by radio- or enzyme immunoassay (RIA, EIA) and by functional assays. RIA was performed as described previously [30]. For the production of ascites in mice, 10^6 hybridoma cells were injected intraperitoneally into pristane pretreated BALB/c mice and the ascitic fluid was harvested after 2–3 weeks.

Enzyme immunoassay (EIA). Individual sera of immunized BALB/c mice and the fine specificity of selected influenza virus-specific MoAb were analysed by solid phase indirect EIA. The 96-well MaxiSorp immunoplates (Nunc, Roskilde, Denmark) were coated with 50 μl of serial dilution of peptide or virus suspensions. After an overnight incubation at +4°C the plates were saturated with PBS containing 1% BSA and 2% FCS (2 h at 37°C). After washing with PBS containing 0.1% Tween-20 (Serva) (PBS-Tween) dilution of MoAb in PBS-Tween containing 2% FCS and 1% BSA was added and incubated for 2 h at 37°C. HRPO labelled secondary Ab (anti-mouse IgG or IgM) and ortho-phenylenediamine in the presence of H_2O_2 were used to develop the assays. OD_{492} was measured by a MR 700 Microplate Reader (Dynatech, Guernsey, UK). Influenza virus specific Ab titres were determined as described previously [30].

Functional assays. Inhibition of haemagglutination (HAI): Twenty five microlitres of the MoAb dilutions in PBS were added to V bottomed 96 wells of microtitre plates followed by 25 μl of the virus at a concentration of 4 HAU/ml. After incubation for 10 min at room temperature 25 μl of 1 v/v % chicken red blood cells (RBC) were added to the samples, and after 30 min incubation Ab dilutions causing 50% inhibition were determined and their reciprocal values were used as HAI titres [28].

In vitro neutralization of the virus (NEUTR): Different dilutions of MoAb were incubated with a constant, pretitrated amount of the virus (30–100 tissue culture infective dose, $TCID_{50}$) for 30 min at room temperature. The preincubated samples were cultured on chicken embrio chorioallantoic membrane fragments in a rolling drum for 48 h at 37°C [31]. The degree of inhibition of viral growth was determined by quantification of virus content of the supernatants measured by the haemagglutination method as described above. Ab dilutions causing 50% neutralization were determined and their reciprocal values were used as NEUTR titres [28].

Inhibition of the membrane fusion activity (FAI): 50 μl of different dilutions of the MoAb or sera were incubated with the virus at 200 HAU/ml concentration (50 μl) for 10 min at room temperature. 0.8 ml 1% (v/v) guinea-pig RBC were added and incubated for 30 min at +4°C. The samples were centrifuged and the pellets were resuspended in 0.025 M citrate buffer (pH = 5.0) and incubated for a further 30 min at 37°C. The optical density of the supernatants was measured at 540 nm after centrifugation. FAI titres were determined as reciprocal Ab dilutions causing 50% inhibition of the fusion activity.

Inhibition of the trypsin mediated cleavage of immature HA0 molecules: 100 μl of A/PR 8/34 virus bearing uncleaved HA0 molecules at a concentration of 50 HAU/ml were incubated with 100 μl of the different dilutions of MoAb for 45 min at 37°C. Two hundred microlitres (40 μg/ml) trypsin solution (Sigma) was added to the samples and after a further incubation for 15 min at 37°C 20 μl of trypsin inhibitor (50 μg/ml) (Sigma) and 0.8 ml 1 v/v % guinea-pig RBC were added. Haemoglobin release in the supernatant was determined as described above.

RESULTS

Specificity and functional activity of serum Ab induced by infectious influenza virus introduced via different routes

BALB/c mice were intranasally infected or subcutaneously injected with the mouse pathogenic A/PR/8/34 influenza

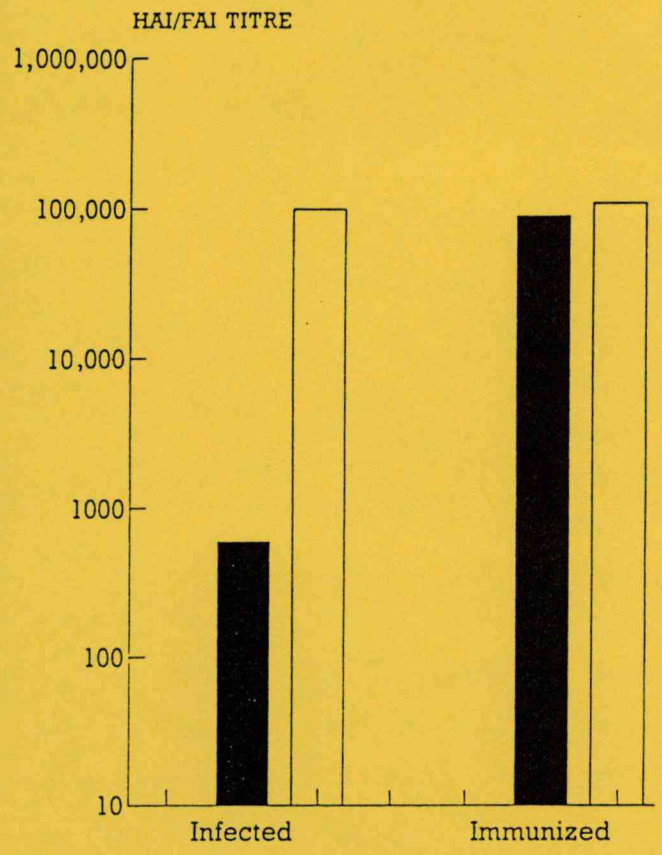

Fig. 2. The relative level of Ab inhibitory in the haemagglutination assay (dark columns) or for the membrane fusion activity of the virus (empty columns) detected in sera of BALB/c mice infected or immunized with A/PR/8/34 influenza virus.

virus. The titre of virus-specific serum Ab was measured and documented in correlation with the relative level of neutralizing Ab (Fig. 1A,B) or with the proportion of inhibitory Ab detected in the haemagglutination assay (Fig. 1C,D). A good correlation between the ability of virus recognition and virus neutralization was found both in influenza virus infected and immunized mice (Fig. 1A,B). In contrast, a weak correlation between the ability to inhibit virus-mediated haemagglutination and the amount of virus-specific Ab could be shown if the characteristics of Ab elicited by influenza virus infection were compared to those induced by immunization (Fig. 1C,D). In addition, a higher level of Ab specifically inhibiting the virus-mediated membrane fusion was observed if intranasal infection was used (Fig. 2).

These results demonstrate that a proportion of Ab interfering with virus replication cannot be restricted to those inhibiting receptor binding detected by the inhibition of haemagglutination.

Recognition of influenza virus by selected influenza virus specific MoAb and their functional properties

As it is summarized in Table 2 a panel of MoAb representing different isotypes, binding properties and functional characteristics was selected from the spleen of a repeatedly infected BALB/c mouse. The screening procedure was focused on the search for hybridomas secreting virus-specific MoAb not inhibitory in the haemagglutination assay. An IgM producing clone Z38 secreting a MoAb of such functional properties (Table 2) was further characterized.

Table 2. Characteristics of the MoAb isolated from a repeatedly, infected BALB/c mouse. BALB/c mice were intranasally infected with A/PR/8/34 influenza virus according to the protocol described in Materials and Methods. Fusion of spleen cells was performed 2 days after a final i.v. injection of the virus. Binding and functional assays were performed as described in Materials and Methods. + +, +, ± and – correspond to the relative activity of MoAb compared in the corresponding assay

		Binding						
MoAb	Isotype peptides					A/PR/8/34		
		IP	D-Arg[13] IP	HA1C [Arg]	FP	HA0	HA	HA (pH5)
Z38	IgM	+ +	+ +	–	–	+ +	–	–
Z48	IgM	–	–	–	–	+	+ +	+
Z50	IgM	–	–	–	–	+	+	+
Z28	IgG2a	–	–	–	–	–	+ +	+ +
Z12	IgG1	–	–	–	–	n.t.	+ +	+ +

		Function		
MoAb	Isotype	HAI[a]	FAI[b]	NEUTR[c]
Z38	IgM	–	+ +	+
Z48	IgM	+	–	–
Z50	IgM	+	–	+
Z28	IgG2a	±	–	±
Z12	IgG1	+	–	+

[a] HAI, inhibition of haemagglutination, [b] FAI, inhibition of fusion activity, [c] NEUTR, neutralization.

Z38 MoAb reacts with the solid phase adsorbed A/PR/8/34 influenza virus expressing uncleaved HA0 molecules but does not bind to solid phase adsorbed virus particles bearing cleaved HA molecules (Fig. 3A). The low pH induced irreversible conformational change of HA molecule does not influence the binding capacity of the Z38 MoAb to the solid phase adsorbed virus.

To study whether the Z38 MoAb is able to interfere with the membrane fusion activity mediated by the HA molecule, the inhibitory activity of the Z38 IgM MoAb was studied measuring the trypsin-induced fusion of the virus, bearing uncleaved HA0 molecules in the presence of different amounts of the antibody. Results summarized in Fig. 3B show that the Z38 MoAb is able to inhibit the fusion activity of the virus in a dose-dependent manner compared to an

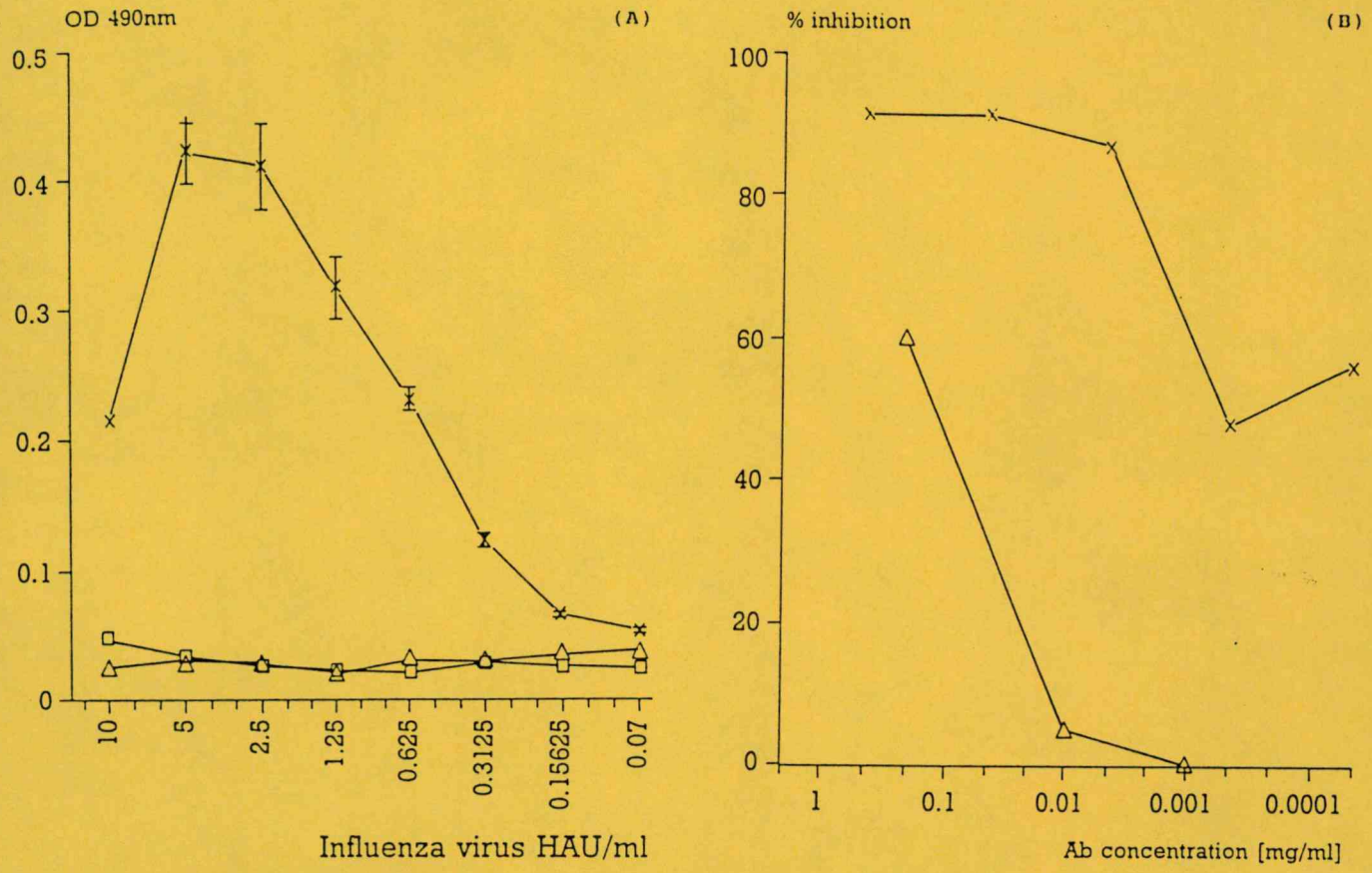

Fig. 3. Binding and functional properties of the Z38 MoAb. (A) Binding of Z38 IgM type MoAb to A PR/8/34 influenza virus expressing different forms of haemagglutinin. The binding of Z38 MoAb (ascitic fluid at 10^3 dilution) to A/PR 8 34 influenza virus expressing uncleaved HA0 molecules (×—×), cleaved (◇—◇) or acid treated HA molecules (△—△) coated to MaxiSorp plates at different concentrations. (B) The inhibitory capacity of MoAb Z38 in the trypsin mediated fusion activity of A PR/8/34 influenza virus bearing uncleaved HA0 molecules. Fusion with guinea pig red blood cells was detected in the presence of different dilutions of Z38 IgM (×—×) or U28 IgM MoAb (△—△) with irrelevant specificity. Inhibition is given as percentage of the fusion activity detected in the absence of MoAb.

isotype matched control MoAb U28. The activity of the U28 MoAb at high concentration can be explained by its partial absorption of the tryptic activity.

These results suggest that the Z38 MoAb is directed against the HA region involved in the membrane fusion event.

Fine specificity of the Z38 MoAb

The fine specificity of the Z38 MoAb was further analyzed by its reactivity with synthetic peptides comprising the intersubunit region of HA. The location and amino acid sequence of the synthetic peptides are summarized in Fig. 4A. Results shown in Fig. 5 demonstrate that the Z38 MoAb binds to the solid phase adsorbed intersubunit peptide IP and its D-Arg^{13} substituted analogue which has been used to exclude the possible *in vitro* degradation of the peptide. None of the other MoAb representing similar or distinct immunoglobulin isotypes but possessing different functional properties are able to recognize these peptides (Table 2).

Figure 5 also demonstrates that the Z38 MoAb shows increased reactivity with solid phase bound $(HA1C[Arg])_4$ developed by the covalent multiplication of the HA1C[Arg] peptide (See Fig. 4A) compared to HA1C[Arg]. This result and the inability to bind to FP (data not shown) demonstrates that the epitope recognized by the Z38 MoAb is localized in the HA1C[Arg] region. These results suggest that the conformation of this region either in the form of synthetic peptides or expressed on the surface of virus particles has influence on Z38 MoAb binding.

Conformational properties of the synthetic peptides comprising the intersubunit region of influenza virus haemagglutinin

The amino acid sequence and localization of overlapping synthetic peptides comprising the intersubunit region of the A/PR/8/34 (H1N1) influenza virus haemagglutinin is given in Fig. 4A. The chemical characteristics of the peptides are summarized in Table 1 and are described elsewhere in more

IP (intersubunit peptide)

317.....**HA1**.....328-329-1.....**HA2**.....12
V T G L R N I P S I Q S - R - G L F G A I A G F I E G
1 25

[D-Arg^{13}]IP

V T G L R N I P S I Q S - D-R - G L F G A I A G F I E G

FP (fusion peptide)

G L F G A I A G F I E G

HA1C[Arg]

V T G L R N I P S I Q S - R

(HA1C[Arg])$_4$ - (HA1C[Arg])$_4$-Lys$_2$-Lys

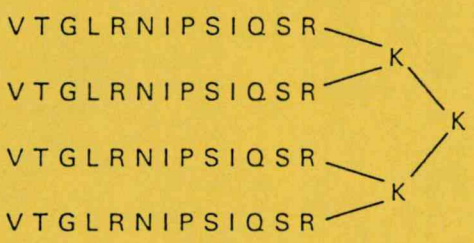

(A)

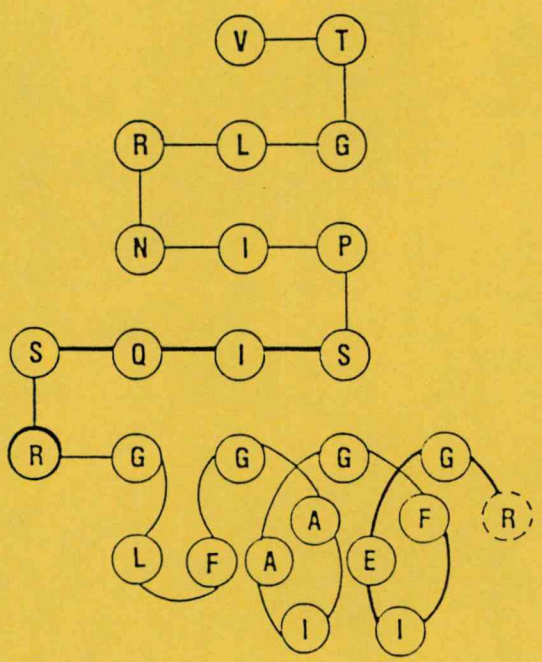

(B)

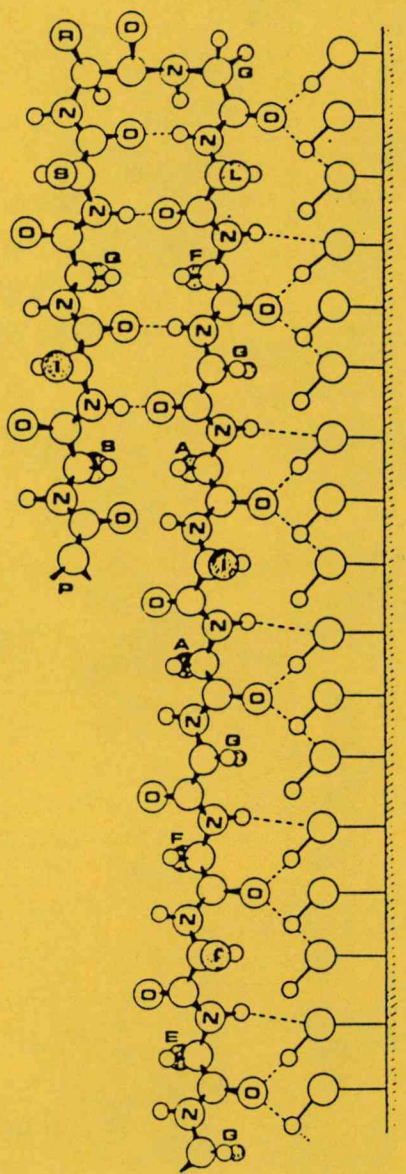

(C)

Fig. 4. Synthetic peptides comprising the intersubunit region. (A) Amino acid sequence of synthetic peptides comprising the intersubunit region of A PR8 34 (H1N1) human influenza A virus haemagglutinin. The detailed description of peptide synthesis, purification and characterization are published elsewhere [24, 26]. (B,C) Schematic representation of the most probable conformations of the intersubunit peptide (IP) adopted in different solvents. (B) The dominant conformation of IP in TFE as suggested by CD and FT-IR [26]. (C) Hypothetical model of the IP in extended conformation on the hydroxyl-rich surface of OG micelles, as suggested by CD and FT-IR measurements [26]. The β-pleated sheet is started with proline 8 of IP which breaks the regular antiparallel structure and folded at a β-turn encompassing the Arg-Gly dipeptide. The amino acid residues are labelled with the one-letter symbols inside or next to the circles (shaded) representing the C^{α} atoms of the side chains.

Fig. 5. Magnitude and specificity of polyclonal serum Ab induced by three immunizations with IP (A), [D-Arg^{13}]IP (B) or (HA1C[Arg])$_4$ (C). Reactivity of serum Ab with synthetic peptides (HA1C[Arg])$_4$ (dark columns), IP (empty columns), [D-Arg^{13}]IP (hatched columns and HA1C[Arg] (dotted columns) is demonstrated. Mean value of titres determined in triplicates ± SD of a typical experiment are documented.

detail [24, 26]. The Chou-Fasman-Prevelige predictive algorithm shows that the C-terminal half of IP has a high propensity to adopt either α-helical or β-sheet conformation [26]. The N-terminal half is predicted to form repeating β-turns. The critical Arg residue at position 329 is situated in a region where a β-turn has a high probability of occurrence. Circular dichroism (CD) and Fourier transform infrared (FT-IR) spectroscopic studies on the intersubunit peptide (See IP in Fig. 4A) in pure water (pH = 6.0), PBS (pH = 7.0) or acidic buffer (pH = 3.0) are indicative of equilibria of two or more conformers. In trifluoroethanol (TFE) a significant α-helix content was revealed and located to the C-terminal half of IP (Fig. 4B). This sequence is also comprised in FP (See Fig. 4A). The C-terminal α-helix has some amphiphilic character, a criterion suggested by DeLisi & Berzofsky [30] and Cornette *et al.* [31] for potential T cell epitopes. Most interestingly, in an aqueous solution containing 2.5% octyl-β-D-glucoside (OG), a non-ionic surfactant, IP and FP showed CD spectra typical for a β-pleated sheet (extended) conformation which according to FT-IR evidences has an antiparallel orientation (Fig. 4C). Thus, the FP peptide and the C-terminal half of IP are able to undergo a conformational switch between α-helix and β-sheet. This transition can be induced by special solvational effects, i.e. presence of an ordered template (Fig. 4C) or very likely by certain microenvironment of cell membranes [32]. On the basis of these results, the potency of this region not only in the membrane fusion but in immune recognition could be assumed.

The antigenic and immunogenic properties of IP representing the intact intersubunit region

To verify the immunogenicity of the synthetic peptides comprising the intersubunit region of influenza virus HA BALB c mice were immunized with the peptides in combination with CFA. As summarized in Fig. 6 the synthetic peptides IP [D-Arg^{13}]IP, and to a much lower extent the (HA1C[Arg])$_4$ branched peptide are immunogenic without the introduction of any carrier. In contrast HA1C[Arg] or FP are inactive to elicit an Ab response (data not shown). Figure 6 also demonstrates the cross-reactivity of polyclonal serum antibodies raised after repeated injections of IP (Fig. 6A) [D-Arg^{13}]IP (Fig. 6B) or (HA1C[Arg])$_4$ (Fig. 6C). Ab react more efficiently with solid phase bound IP or [D-Arg^{13}]IP compared to (HA1C[Arg])$_4$, but are unable to recognize HA1C[Arg]. These results, in good correlation with the conformational studies of the peptides, demonstrate that the covalently linked fusion peptide present in IP and [D-Arg^{13}IP is beneficial for Ab recognition of the HA1C[Arg] region.

Results summarized in Fig. 7 demonstrate the reactivity of serum Ab induced by IP or (HA1C[Arg])$_4$ with the A/PR/8 34 virus bearing uncleaved HA0 or cleaved HA molecules at neutral or acidic conditions. These results show that IP-induced Ab prefer uncleaved HA0 molecules while (HA1C[Arg])$_4$ induced Ab show similar reactivity to both viruses.

Together, these results demonstrate the similar specificity of serum antibodies elicited by IP, [D-Arg^{13}]IP, or (HA1C[Arg])$_4$ to that of the MoAb Z38 and imply that these peptides without any carrier can be applied to induce Ab directing against the intersubunit region.

Protection against lethal influenza virus infection by peptide pre-immunization

On the basis of our previous results it was of particular interest to investigate whether synthetic peptides comprising the intact form of the intersubunit region of HA0, previously proven to be immunogenic, can confer protection against a lethal dose of influenza virus infection. As demonstrated in Fig. 8 pre-immunization with IP or with the (HA1C[Arg])$_4$ results in prolonged survival and complete protection of a considerable number (60%) of the pretreated animals. Despite the similar protective efficiency of 200 μg IP com-

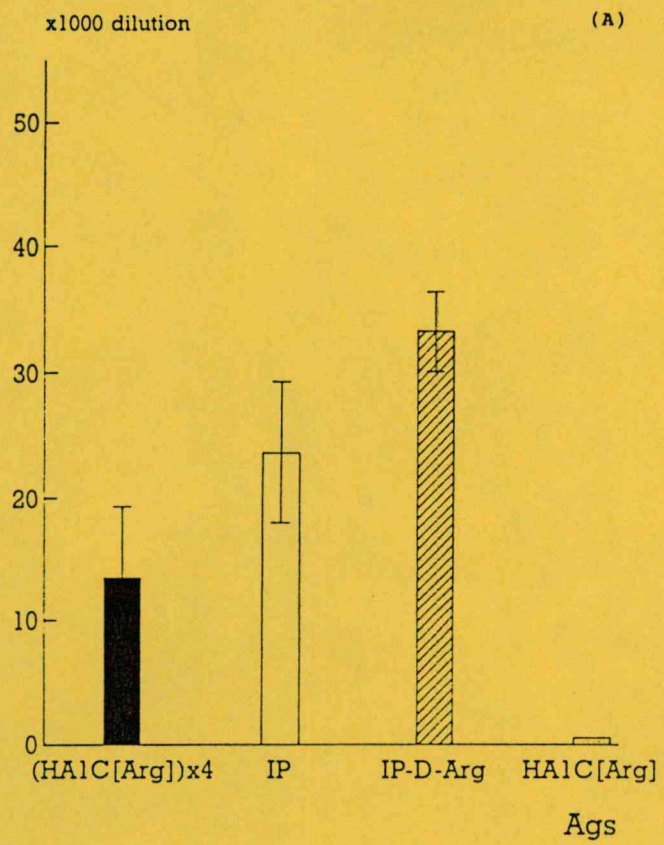

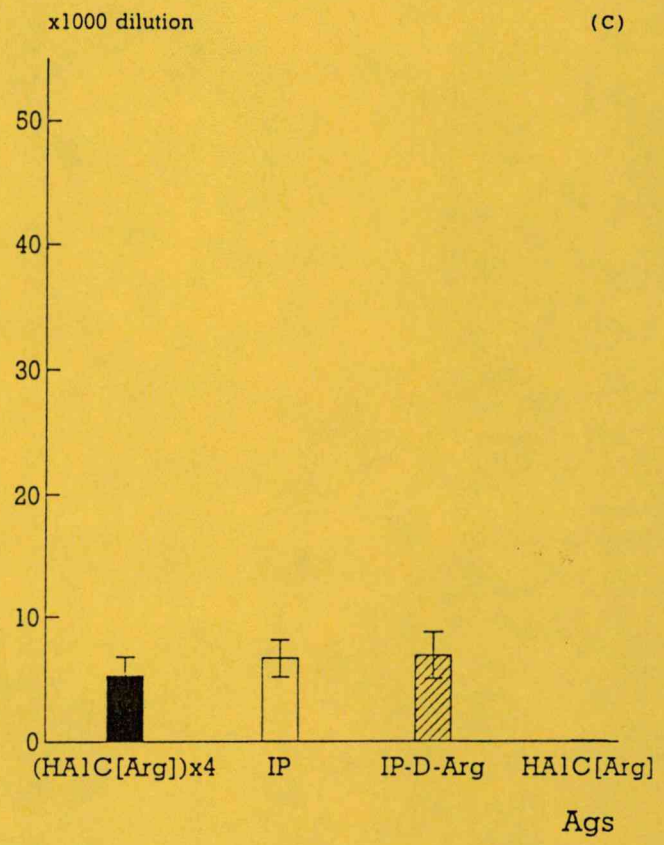

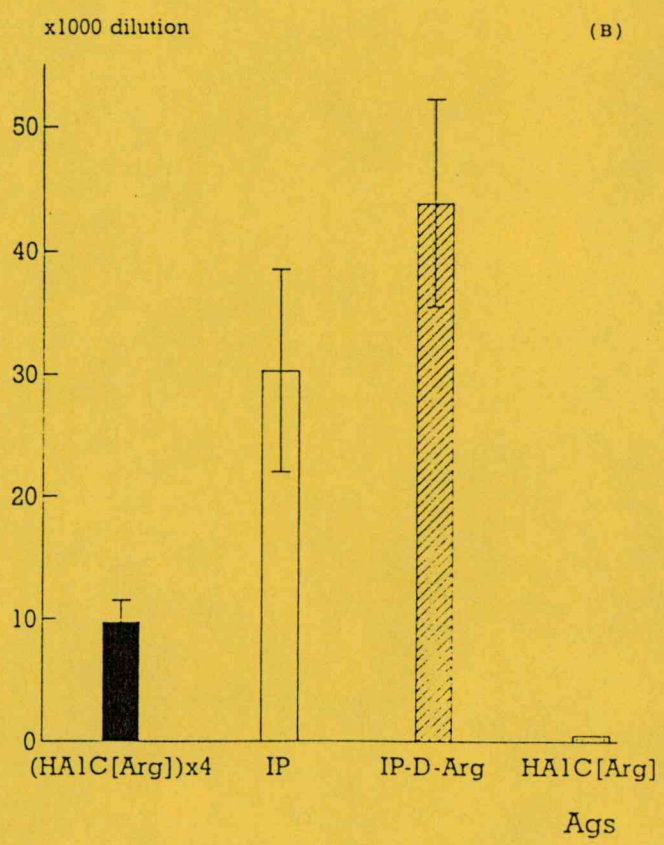

pared with 100 μg $(HA1C[Arg])_4$ the level of peptide-specific Ab in $(HA1C[Arg])_4$ pre-immunized mice is significantly lower (data not shown).

DISCUSSION

The comparison of the level of virus-specific Ab in influenza virus infected BALB/c mice in correlation with their functional properties pointed to the appearance of neutralizing Ab without the ability to inhibit receptor binding (Fig. 1). A relevant target of these HA-specific Ab could be the region attacked by the enzymatic cleavage and subsequently responsible for the membrane fusion [1, 19]. To investigate whether the intact intersubunit region localized between the HA1 and HA2 subunits of the HA molecule has any role in B cell recognition the fine specificity and functional properties of polyclonal and monoclonal Ab were studied. The possible role of the functionally essential post-translational modi-

Fig. 6. Magnitude and specificity of polyclonal serum Ab induced by three immunizations with IP (A), $[D\text{-}Arg^{13}]IP$,(B) or $(HA1C[Arg])_4$ (C). Reactivity of serum Ab with synthetic peptides $(HA1C[Arg])_4$ (dark columns), IP (empty columns), $[D\text{-}Arg^{13}]IP$ (hatched columns), and HA1C[Arg] (dotted columns) is demonstrated. Mean value of titres determined in triplicates ± SD of a typical experiment are documented.

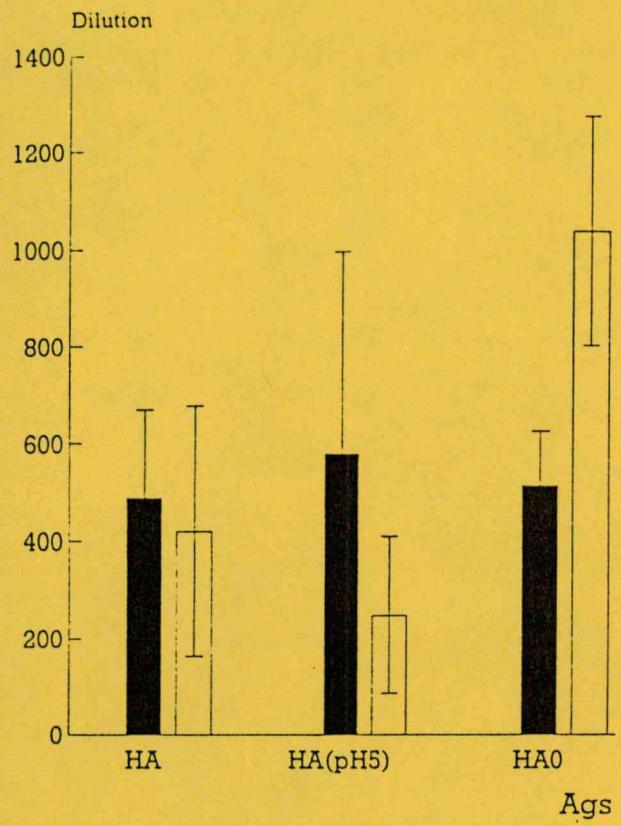

Fig. 7. The relative level of virus reactive serum antibodies of BALB/c mice immunized with IP (empty columns) or $(HA1C[Arg])_4$ (dark columns). Binding of serum Ab to A/PR/8 34 influenza virus expressing cleaved [HA], acid treated HA [HA(pH5)] or uncleaved [HA0] molecules was detected. Mean value of titres determined in triplicates ± SD of a typical experiment are documented.

fication of the HA molecule on Ab binding was of particular interest as the intact intersubunit region is present in non-infectious virions generated as a result of a defective viral growth cycle. In contrast, productive virus replication results in infective viruses bearing cleaved HA molecules. Antigen presenting cells infected by the virus are good candidates as a source of non-infectious viruses as they lack the appropriate enzyme for the enzymatic cleavage of the molecule [33]. So immature uncleaved HA0 molecules may play a role at the initiation of the immune response.

The isolation of an IgM type MoAb (Z38) from an influenza virus infected BALB.c mouse recognizing the uncleaved intersubunit region both in a synthetic peptide and in the uncleaved HA0 molecule (Fig. 3A) clearly demonstrates that this type of Ab can be generated in the course of the adoptive immune response against the virus. The functional properties of this MoAb characterized by its ability to inhibit the membrane fusion event point to the potency of such type of Ab in protection. The fine specificity analysis of the Z38 MoAb demonstrated its reactivity with synthetic peptides comprising the intact intersubunit region and with influenza viruses expressing uncleaved HA0 molecules (Fig. 3A and Fig. 5). Its reactivity pattern with the synthetic peptides IP, $(HA1C[Arg])_4$ and HA1C[Arg] (Fig. 5) points to the localization of a B cell epitope in the C-terminal HA1C[Arg] region of the HA1 subunit. The HA1C[Arg] sequence is presumably hidden in the stem region of the cleaved HA molecule [34,35] providing an explanation for the lack of efficient Z38 MoAb binding to the solid phase adsorbed virus bearing this type of HA molecules. However, adsorption of virus particles to the solid phase may influence the exposure of this epitope. In immature virions with uncleaved HA0 this region must be exposed to the surface of the molecule providing a possibility for the enzymatic cleavage. The relative location of the N-terminus of the fusion peptide to the C-terminus of the HA1 subunit in the known three-dimensional structure of HA [13] strongly suggest a significant local rearrangement of the molecule resulted by the cleavage. The importance of the availability of the cleavage site for enzymes was experimentally verified by Kawaoka & Webster [36] who showed, that glycolisation of avian influenza viruses in the vicinity of this site can interfere with normal cleavage and viral pathogenicity.

The binding of Z38 MoAb inhibits the enzymatic cleavage of the molecule (Fig. 3B) associated with the intersubunit region which is essential for viral infectivity. This observation provides a good explanation for the neutralizing activity of the Z38 MoAb (Table 2) independent of the inhibition of receptor binding. In addition the binding of such type of Ab may influence antigen processing by protecting the intersubunit region from further degradation in the acidic endosomal compartment.

The results of peptide immunization demonstrate that IP representing the intact intersubunit region of the HA0 molecule contains sufficient information to elicit an Ab response resulting in the production of peptide-specific antibodies cross-reactive preferentially with the virus expressing uncleaved HA0 (Fig. 7). This specificity pattern resembles that of the Z38 MoAb and proves that IP [D-Arg^{13}]IP, but less efficiently the $(HA1C[Arg])_4$ comprising multiple copies of HA1C[Arg] are able to induce antibody production against this region (Figs 6 and 7). The increased activity of the $(HA1C[Arg])_4$ artificial construct compared to the monomeric HA1C[Arg] in the binding studies supports the hypothesis that the covalently coupled Lys residues promote adsorption to the solid phase and suggests that multiplied HA1C[Arg] peptides are accessible in an appropriate conformation for antibody recognition in this molecule. On the other hand, this modification does not enhance immunogenicity (Fig. 6) which can be improved by the covalent attachment of the fusion peptide in IP or [D-Arg^{13}]IP.

The detailed analysis of the conformational properties of the IP peptide comprising the intact intersubunit region revealed its characteristic ordered structure supported by the covalently linked fusion peptide (Fig. 4). Our data also demonstrated that the character of the conformational organization (predomi-

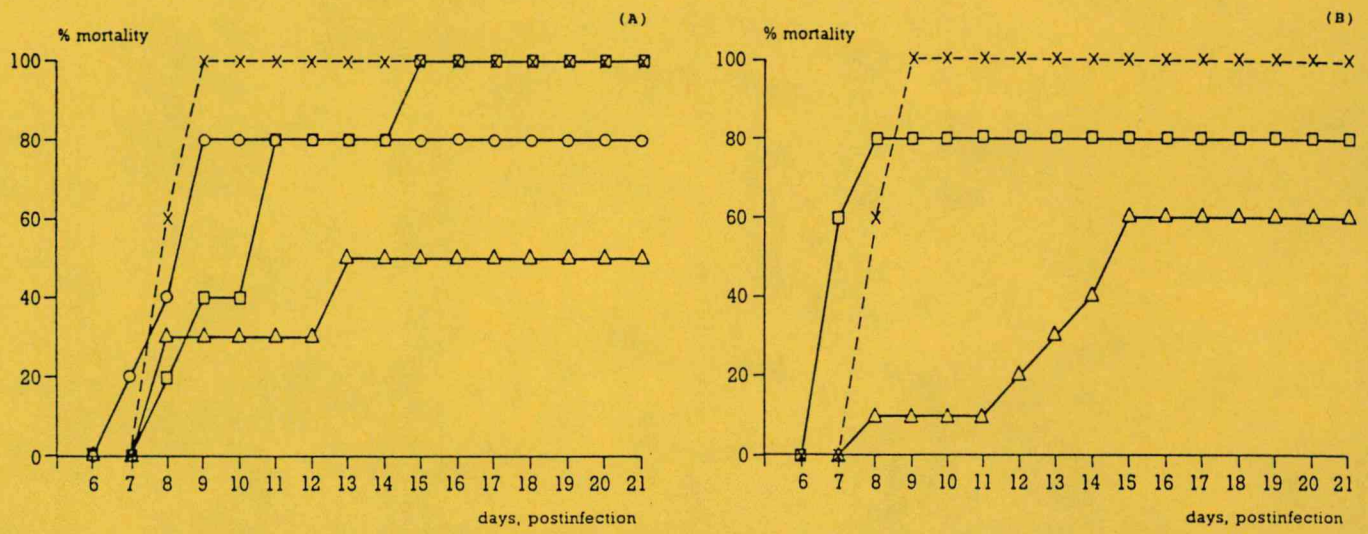

Fig. 8. Sensitivity of BALB/c mice preimmunized with synthetic peptides comprising the intersubunit region to a lethal dose of A/PR/8/34 influenza virus. (A) BALB/c mice were preimmunized with: 100 μg HA1C[Arg] (○–○), FP (□—□) or $(HA1C[Arg])_4$ (△—△) according to the protocol described in Materials and Methods under section 5.2. ×—× corresponds to control mice treated as the other experimental groups except PBS instead of the peptides was used. (B) BALB/c mice were preimmunized with 200 μg (△—△), or 100 μg (□—□) IP. ×—× corresponds to control mice treated as the other experimental groups except PBS instead of the peptides was used.

nantly α-helical or extended β-sheet) of IP or FP was dependent on the solvent used (Fig. 4) [26]. These results imply that natural or synthetic peptides comprising this region have a high tendency to adopt an ordered structure [12, 26, 32, 34] but they can be present in different conformations in aqueous solution or in the vicinity of cell membranes supporting the possibility for both B and T cell recognition [26].

Protection experiments demonstrated the functional potency of the immune response elicited by the IP synthetic peptide or its $(HA1C[Arg])_4$ derivate (Fig. 8). However, there is no direct evidence demonstrating that protection is mediated merely by peptide-specific Ab [37] in spite of the fact that they are present at high concentration in the serum of survivors.

The immunogenicity of the IP and [D-Arg^{13}]IP peptides without the introduction of any carrier point to the simultaneous presence of a T-cell epitope in these peptides. Data on the localization of an overlapping I-E^d restricted helper T cell epitope recognizable both in HA1C[Arg] or IP is described elsewhere (E. Rajnavölgyi *et al.* unpublished observation). In the light of these results the beneficial role of helper T cells induced by peptides comprising the HA1C[Arg] sequence collaborating with IP specific B cells or with those reactive with other HA determinants in protection should be considered. Nevertheless, the major functional importance of Ab directed against a highly conserved, functionally active region of HA might be to focus uncleaved HA0 molecules to specific B cells, internalize and protect them from subsequent enzymatic cleavage at this region and in such a way inhibit membrane fusion. A substantial amount of the virus present in the host has been proven to express uncleaved HA0 which are not able to initiate another virus propagation cycle but are potentially infectious [17]. The constant presence of proteases in the host's sera or the occasional presence of pathogen-derived proteases were demonstrated to result in extracellular processing of uncleaved HA0 molecules giving rise to increased numbers of infectious viruses [38]. Therefore, inhibition of the activation of these potentially infectious virus particles by antibodies specific for the cleavage site might be an efficient strategy in vaccine design. This would result in naturally generated peptides comprising the intact intersubunit region of flexible conformation demonstrated to be active in T as well as B cell recognition. The restricted generation of the intact intersubunit region in the course of viral infection in contrast to the cleaved form point to an efficient escape mechanism of the virus supported by the destruction of the immunologically active form.

ACKNOWLEDGMENTS

The excellent technical assistance of Erzsébet Veress and Árpád Mikessy is acknowledged. The authors are indebted to Dr Marianna Mák for the mass spectroscopy measurements. This work was supported by the OTKA grants 2010 of É.R., F5120 of Z.N. and 2734 of G.K.T.

REFERENCES

1 Wiley DC, Skehel JJ. The structure and function of the hemagglutinin membrane glycoprotein of influenza virus. Ann Rev Biochem 1987;56:365–94.

2 Wilson IA. Structural basis of immune recognition of influenza virus hemagglutinin. Ann Rev Immunol 1990;8:737–71.

3 White JM, Wilson IA. Anti-peptide antibodies detect steps in a protein conformational change: low pH activation of the influenza virus hemagglutinin. J Cell Biol 1987;105:2887–96.

4 Atassi MZ, Webster EG. Localization, synthesis and activity of antigenic sites on influenza virus hemagglutinin. Proc Natl Acad Sci 1983;80:840–4.
5 Weis W, Brown JH, Cusack S, Paulson JC, Skehel JJ, Wiley DC. Structure of the influenza virus haemagglutinin complexed with its receptor, sialic acid. Nature 1988;333:426–31.
6 Kida H, Yoden S, Kuwabara M, Yanagawa R. Interference with a conformational change in the haemagglutinin molecule of influenza virus by antibodies as possible neutralization mechanism. Vaccine 1985;3:219–22.
7 Kawaoka Y, Webster RG. Sequence requirements for cleavage activation of influenza virus hemagglutinin expressed in mammalian cells. Proc Natl Acad Sci 1988;85:324–8.
8 Nobusawa E, Aoyama T, Kato H, Suzuki Y, Tateno Y, Nakajima K. Comparison of complete amino acid sequences and receptor binding properties among 13 serotypes of hemagglutinins of influenza A viruses. Virology 1991;182:475–85.
9 Winter G, Fields S, Brownlee G. Nucleotide sequence of the haemagglutinin gene of a human influenza virus H1 subtype. Nature 1981;292:72–5.
10 Wiley DC, Wilson IA, Skehel JJ. Structural identification of the antibody-binding sites of Hong Kong influenza hemagglutinin and their involvement in antigenic variation. Nature 1981;289: 373–8.
11 Both GW, Sleigh MJ, Cox NJ, Kendal AP. Antigenic drift in influenza virus H3 hemagglutinin from 1968 to 1980: multiple evolutionary pathways and sequential amino acid changes at key antigenic sites. J Virol 1983;48:52–60.
12 Jackson DC, Brown LE. A synthetic peptide of influenza virus hemagglutinin as a model antigen and immunogen. Peptide Res 1991;4:114–24.
13 Wilson IA, Skehel JJ, Wiley DC. Structure of the haemagglutinin membrane glycoprotein of influenza virus at 3A resolution. Nature 1981;289:366–73.
14 Copeland CS, Zimmer KP, Wagner KR, Haeley GA, Mellman I, Helenius A. Folding, trimerization, and transport are sequential events in the biogenesis of influenza virus hemagglutinin. Cell 1988;53:197–209.
15 Bosch FX, Garten W, Klenk H-D, Rott R. Proteolytic cleavage of influenza virus hemagglutinins: primary structure of the connecting peptide between HA1 and HA2 determines proteolytic cleavability and pathogenicity of avian influenza viruses. Virology 1981;113:725–35.
16 Barr PJ. Mammalian substilisins: the long dibasic processing endoproteases. Cell 1991;66:1–3.
17 Nesterowicz AN, White DO, Jackson DC. Conformational changes in influenza virus hemagglutinin and its monomer detected by monoclonal antibodies. Vaccine 1985;3:175–81.
18 Yoden S, Kida H, Kuwarbara M, Yanagawa R, Webster RG. Spin-labelling of influenza virus hemagglutinin permits analysis of the conformational change at low pH and its inhibition by antibody. Virus Res 1986;4:251–461.
19 White JM. Viral and cellular membrane fusion proteins. Ann Rev Physiol 1990;52:675–97.
20 Daniels RS, Downie JC, Hay AJ, Knossow M, Skehel JJ, Wang ML, Wiley DC. Fusion mutants of the influenza virus hemagglutinin glycoprotein. Cell 1985;40:431–9.
21 Marsh M, Helenius A. Virus entry into animal cells. Adv Virus Res 1989;36:107–51.
22 Eisenlohr LC, Gerhard W, Hackett CJ. Acid-induced conformational modification of the hemagglutinin molecule alters interaction of influenza virus with antigen-presenting cells. J Immunol 1988;141:1870–6.
23 Hackett CJ, Eisenlohr LC. Virus entry and antigen biosynthesis in the processing and presentation of Class-II MHC-restricted T-cell determinants of influenza virus. Immunol Res 1990;9:103–14.
24 Tóth GK, Váradi Gy, Penke B, Monostori É, Hegedüs Z, Nagy Z, *et al.* Synthesis of branched polypeptides as antigens for influenza virus hemagglutinin and T-cell receptor subunits. In: Schneider CH, Eberle AN, eds. Peptides. BV: Escom Science Publishers 1993;882–4.
25 Hollósi M, Ismail AA, Mantsch HH, *et al.* Conformational and functional properties of peptides covering the intersubunit region of influenza virus hemagglutinin. Eur J Biochem 1992;206:421–5.
26 Tóth GK, Váradi Gy, Nagy Z, *et al.* Branched polypeptides as antigens for influenza virus hemagglutinin and T-cell receptor subunits. Peptide Res 1993;6:272–280.
27 Mák M, Tamás J. *In situ* enzymatic digestion of oligopeptides on a direct insertion probe tip combined with fast atom bombardment and tandem mass spectroscopy. Organ Mass Spectr 1993;28:542–5.
28 Barrett T, Inglis SC. Growth, purification and titration of influenza virus. In Mahy BWJ, ed. Virology, a practical approach. IRL Press, 1985;119–50.
29 Köhler G, Milsten C. Continuous cultures of fused cells secreting antibody of predefined specificity. Nature 1975;256:495–7.
30 DeLisi C, Berzofsky JA. T cell antigenic sites tend to be amphipatic structures. Proc Natl Acad Sci 1985;82:7048–52.
31 Cornette JL, Margalit H, DeLisi C, Berzofsky JA. The amphipatic helix as a structural feature involved in T-cell recognition. In Epand RM, ed. The Amphipatic Helix. Boca Raton, Ann Arbor London, Tokyo: CRC Press, 1992;333–48.
32 Lear JD, DeGrado WF. Membrane binding conformational properties of peptides representing the NH_2 terminus of the HA-2. J Biol Chem 1987;262:6500–5.
33 Doherty PC, Allan W, Eichelberg M. Roles of $\alpha\beta$ and $\gamma\delta$ T cell subsets in viral immunity. Ann Rev Immunol 1992;10:123–51.
34 Jackson DC, Tang XL, Brown LE, Murray JM, White DO, Tregear GW. Antigenic determinants of influenza virus hemagglutinin. Virology 1986;155:625–32.
35 Wilson IA, Cox NJ. Structural basis of immune recognition of influenza virus hemagglutinin. Ann Rev Immunol 1990;8:737–71.
36 Kawaoka Y, Webster RG. Interplay between carbohydrate in the stalk and the length of the connecting peptide determines the cleavability of influenza virus hemagglutinin. J Virol 1989;63: 3296–300.
37 Renegar KB, Small PA. Passive transfer of local immunity to influenza virus infection by IgA antibody. J Immunol 1991;146: 1972–8.
38 Tashiro M, Ciborowski P, Klenk H-D, Pulverer G, Rott R. Role of *Staphylococcus protease* in the development of influenza pneumonia. Nature 1987;325:536–7.

Received 7 March 1994
Accepted in revised form 26 April 1994

Pergamon

Molecular Immunology, Vol. 31, No. 18, pp. 1403–1414, 1994

0161-5890(94)00130-8
0161-5890/94 $7.00 + 0.00

T CELL RECOGNITION OF THE POSTTRANSLATIONALLY CLEAVED INTERSUBUNIT REGION OF INFLUENZA VIRUS HEMAGGLUTININ

ÉVA RAJNAVÖLGYI,*† ZOLTÁN NAGY,* ISTVÁN KURUCZ,‡ PÉTER GOGOLÁK,* GÁBOR K. TÓTH,§ GYÖRGYI VÁRADI,§ BOTOND PENKE,§ ZOLTÁN TIGYI,‖ MIKLÓS HOLLÓSI¶ and JÁNOS GERGELY*

*Department of Immunology, L. Eötvös University, Göd; ‡Institute for Drug Research, Budapest; §Department of Medical Chemistry, A. Szent-Györgyi Medical University, Szeged; ‖Department of Microbiology, Pécs; and ¶Department of Organic Chemistry, L. Eötvös University, Budapest, Hungary

(*First received* 31 *January* 1994; *accepted in revised form* 24 *August* 1994)

Abstract—The influenza virus hemagglutinin is synthesized as a single polypeptide chain, but upon maturation it will posttranslationally be modified by a host cell related trypsin-like enzyme. The enzymatic cleavage attacks the so-called intersubunit region of the molecule giving rise to covalently linked HA1 and HA2 subunits. An I-E^d-restricted T cell epitope was identified in the highly conserved intact intersubunit region of the influenza virus hemagglutinin. T cell recognition of a 25-mer synthetic peptide comprising the intact intersubunit region does not require further processing and the elimination of the intervening Arg residue coupling the fusion peptide to the C-terminal segment of HA1 does not abolish the T cell activating capacity. The fine specificity pattern of a T cell hybridoma similar to that of the polyclonal T cell response demonstrates that a single T cell receptor is able to recognize peptides of different sizes representing not only the uncleaved but also the cleaved form of this hemagglutinin region. Based on specificity studies the epitope was localized to the C-terminal 11 amino acids of the HA1 subunit. The cross-reactivity of peptide-primed T cells with influenza virus infected antigen-presenting cells shows that fragments comprising the identified epitope of the intersubunit region can be generated as a result of natural processing of the hemagglutinin molecule. As antigen-presenting cells are lacking the enzyme which is responsible for the posttranslational modification of newly synthesized hemagglutinin molecules, the role of immature viral proteins in immune recognition is discussed.

Key words: T cell epitope, antigen processing, influenza virus hemagglutinin.

INTRODUCTION

Intracellular processing of viral proteins raises special possibilities for antigen presentation (Mills *et al.*, 1986; Mills, 1986; Long and Jacobson, 1989; Murray and McMichael, 1992; Driscoll and Finley, 1992). Spike or integral proteins of enveloped viruses are degraded in antigen-presenting cells (APC) as exogeneous antigens upon entry to the host cell via receptor mediated endocytosis. MHC class II molecules play a predominant role in this stage of viral infection presenting viral peptides for virus-specific helper T cells (Doherty *et al.*, 1992; Long, 1992). If infective viruses enter the appropriate host cell, virus replication occurs generating newly synthesized viral proteins which can predominantly be handled as endogenous proteins in terms of antigen processing. In this process, primarily MHC class I but, depending on the type of the host cell, also MHC class II molecules are involved (Brooks *et al.*, 1991; Nuchtern *et al.*, 1990; Jaraguemada *et al.*, 1990; Long, 1992). Influenced by the intracellular destination of viral proteins, MHC class I and class II molecules have the chance to select from different sets of viral peptides, but some fragments of viral proteins might be able to bind to both types of MHC molecules (Sweetser *et al.*, 1989; Perkins *et al.*, 1991).

The hemagglutinin (HA) spike protein of influenza viruses has multiple biological functions and it is one of the main targets of immune recognition (Wilson and Cox, 1990; Thomas *et al.*, 1989; Yewdell and Hackett, 1989). T cell epitopes recognized either by helper or cytotoxic T cells in the context of different H-2

†Author to whom correspondence should be addressed at: Department of Immunology, L. Eötvös University, Jávorka S.u.14, H-2131, Göd, Hungary.

Abbreviations: APC, antigen-presenting cell; CD, circular dichroism spectroscopy; D-FPR, Boc-D-Phe-Pro-Arg-H 1/2 H_2SO_4; FT-IR, Fourier-transform infrared spectroscopy; HA0, immature hemagglutinin; HA, mature hemagglutinin; Ig, immunoglobulin; mAb, monoclonal antibody; MTT, (3-[4,5-dimethylthiazol-2-yl]-2,5-diphenyltetrazolium bromide; PBS, phosphate buffered saline; G-PBS, glucose containing phosphate buffered saline.

(Eisenlohr and Hackett, 1989; Jackson and Brown, 1991) or HLA (Lamb *et al.*, 1982) haplotypes have been localized in distinct regions of the molecule including the C-terminal membrane spanning segment of the HA2 subunit (Braciale *et al.*, 1989) or the head region (HA1) accumulating most of the type- and subtype-specific variations and the corresponding B cell epitopes (Mills *et al.*, 1986; Mills, 1986; Wilson and Cox, 1990).

The most conserved sequence of the HA molecule from different influenza viruses is the functionally essential fusion peptide representing the N-terminal 1–12 amino acids of the HA2 subunit (White, 1990). In newly synthesized, immature hemagglutinin (HA0) molecules, this peptide is covalently linked to the C-terminal of the HA1 subunit via an Arg residue in position 329. This Arg will be deleted in the course of HA0 maturation by subsequent posttranslational enzymatic cleavages (Garten *et al.*, 1991) giving rise to mature HA built up from disulphide-bridge-linked HA1 and HA2 subunits (Webster and Rott, 1987). This event is the prerequisite of viral infectivity ensuring a pH-dependent conformational change of the HA molecule in endosomes where membrane fusion will be catalysed by the exposed fusion peptide (White, 1990). The amino acid sequence of the C-terminal stretch of the HA1 subunit also shows restricted amino acid variations and comprises an enzyme cleavage motif determining enzyme susceptibility and thus influencing tropism of the virus (Nagai *et al.*, 1991; Gotoh *et al.*, 1990; Barr, 1991; Walker and Kawaoka, 1993). The enzyme involved in the posttranslational modification was identified as a trypsin-like serine protease acting in the post-Golgi compartment of defined cell types such as the epithelial cells of the respiratory tract (Webster and Rott, 1987). Professional antigen-presenting cells such as B cells, macrophages or dendritic cells lack the appropriate enzyme for HA0 cleavage and thus upon infection generate immature, uncleaved molecules giving rise to non-infective viruses (Doherty *et al.*, 1992; Webster and Rott, 1987).

As we demonstrated (Rajnavölgyi, 1992; Nagy *et al.*, 1994), the 25 amino acid-long synthetic peptide IP corresponding to the uncleaved form of the intersubunit region of the A/PR/8/34 (H1N1) human influenza A virus hemagglutinin (see Table 1) is able to elicit an IgG response in BALB/c mice without the introduction of any carrier. This result implies that T cell epitope(s) may also be present in this region. This paper reports a study on the possible recognition of the HA1–HA2 intersubunit region by T cells in relation to the influence of the posttranslational modification. This question was approached by the use of synthetic peptides comprising the C-terminal sequence of the HA1 and the N-terminal sequence of the HA2 subunits. These peptides correspond to the covalently linked intact or cleaved forms of the immature HA0 and posttranslationally modified HA molecules, respectively. The conformational properties of these overlapping peptides have been characterized by circular dichroism (CD) and Fourier-transform infrared (FT-IR) spectroscopic methods (Hollósi *et al.*, 1992; Holly *et al.*, 1993; Nagy *et al.*, 1994). They have been used for specificity analysis of peptide or virus-primed T cells. Our results revealed that the intersubunit region encompasses an I-E^d-restricted T cell epitope located in the C-terminal of the HA1 subunit. This epitope can be recognized in peptides corresponding both to the cleaved and uncleaved forms of the hemagglutinin molecule (Table 1). Peptides of different length covering the core region of this epitope are able to prime and activate T cells which also recognize influenza virus-infected APC. These results reveal that the natural hemagglutinin processing pathway can generate peptides comprising this T cell epitope.

MATERIALS AND METHODS

Animals

Eight–ten-week-old female B10 (H-2^b) and CBA (H-2^k) mice were purchased from LATI (Gödöllő, Hungary). Female BALB/c (H-2^d) mice were delivered by the Institute of Oncology (Budapest, Hungary). Animals were housed under conventional conditions.

Virus preparation

The A/PR/8/34 influenza virus (H1N1) stock bearing cleaved hemagglutinin was grown in chorio-allantoic fluid of hen eggs and was prepared as described previously (Nagy *et al.*, 1994). Heat inactivation of the virus was performed at 56°C for 30 min.

Synthetic peptides

The description of peptide synthesis, purification and characterization has been reported elsewhere (Hollósi

Table 1. Description, amino acid sequence and purity of the synthetic peptides

Localization	Code	Sequence	Purity[a] (%)
$HA1_{317-329} + HA2_{1-12}$	IP	VTGLRNIPSIQSRGLFGAIAGFIEG	96
$HA1_{317-329} + HA2_{1-12}$	[D-Arg^{13}]IP	VTGLRNIPSIQS*R*GLFGAIAGFIEG	97
$HA1_{317-329}$	HA1C[Arg]	VTGLRNIPSIQSR	98
$HA1_{317-328}$	HA1C	VTGLRNIPSIQS	99
$HA1_{319-328}$	HAC_{deca}	GLRNIPSIQS	97
$HA_{320-328}$	HAC_{nona}	LRNIPSIQS	98
$HA2_{1-12}$	FP	GLFGAIAGFIEG	97

[a]Determined by HPLC.

et al., 1992; Holly *et al.*, 1993; Tóth *et al.*, 1993). Characteristics of the peptides used in this study are summarized in Table 1.

In vivo *induction of A/PR/8/34 influenza virus-primed T cells*

BALB/c mice were aerosol-infected with 0.03 LD_{50} dose of the mouse pathogenic A/PR/8/34 influenza virus and 3 months later red blood cell lysed spleen cells were enriched with T cells by passing the single cell suspension through a Nylon wool (Fenwal Laboratories) column. In another series of experiments, BALB/c mice were infected as described above but 3 weeks later they were re-challenged with 1 LD_{50}. T cells were isolated 3 months after secondary infection as described above. In a third series of experiments, the A/PR/8/34 virus was injected subcutaneously as 100 μg purified virus emulsified in complete Freund's adjuvant and introduced to the base of the tail.

In vivo *induction of peptide-primed T cells*

B10, CBA or BALB/c mice were immunized subcutaneously at the base of the tail and in the hind footpads with 100 μg peptide dissolved in sterile PBS and emulsified in CFA. Fourteen days later the T cell enriched lymph node cells were used for the proliferation assay. In some experiments, peptide administration was repeated on day 21 in combination with incomplete Freund's adjuvant and the T cell-enriched lymph node cells were isolated 7–10 days after the secondary peptide challenge. T cell enrichment of the popliteal, inguinal and paraaortic lymph node cells of subcutaneously immunized mice was performed either by Nylon wool (Fenwal Laboratories) elimination of adherent cells or by panning on anti-mouse immunoglobulin (Ig) coated Petri dishes. The T cell-enriched, eluted cell population (subsequently termed as T cells) was contaminated with 1–3% B cells detected by cytofluorimetry using FITC-labelled anti-mouse Ig (Sigma, Deisenhofen, Germany).

T cell proliferation assay

The T cell proliferation assay was performed by the method of Corradin *et al.* (1977). Briefly, 5×10^5 enriched lymph node T cells were cultured in the presence of 2% 10^5 irradiated syngeneic spleen cells as APC in the absence or the presence of different concentrations of synthetic peptides. Triplicate microcultures in a final volume of 250 μl were established in flat-bottomed 96-well plates (Greiner) in complete RPMI medium supplemented with 10% fetal calf serum (Gibco), 1 mM sodium pyruvate, 2 mM glutamine, 10 mM HEPES buffer, 5×10^{-5} M 2-mercaptoethanol, antibiotics, non-essential amino acids, and BME-vitamins (all purchased from Sigma).

Influenza virus infection of normal BALB/c spleen cells was performed by a 4 hr preincubation of the cells with different doses of the infective A/PR/8/34 influenza virus. After the preincubation period, cells were washed twice with glucose-containing phosphate saline (G-PBS), irradiated or mytomycin-C (Sigma) treated (25 μg/ml, 37°C, 30 min) and used as APC at 2×10^5 cell/well. Cultures were pulsed with 1 μCi (3.7 kBq) ^{3}H-thymidine for the final 16 hr of the 4-day cultures.

Experiments performed in the presence of the enzyme inhibitor leupeptin (acetyl-Leu-Leu-Arg-SO_3H, Boehringer, Mannheim, Germany) or the tripeptide Boc-D-Phe-Pro-Arg-H 1/2 H_2SO_4 (GKI-14451; D-FPR, the generous gift of S. Bajusz, Institute of Drug Research, Budapest, Hungary) (Bajusz *et al.*, 1978) were performed as described for the T cell proliferation assay except that the inhibitor was present during the whole period of cell culture at 0.5 or 1 mM final concentration.

The inhibitor effect of MHC specific monoclonal antibodies (mAb) I-47 rat IgG2a, anti-H-2D^d (generous gift of G. László, Department of Immunology, L. Eötvös University); 14.4.4 mouse IgG2a, anti-I-E$^{k/d}$ (Ozato *et al.*, 1980); M5/114 rat IgG2b, anti-I-A/D^d (ATCC TIB 120) (Bhattacharya *et al.*, 1981); MKD6 mouse IgG2a, anti-I-A (ATCC HB3) (Kappler *et al.*, 1981) was detected in the presence of 5% hybridoma cell culture supernatants.

Isolation of T cell lines and the IP-12-29 T cell hybridoma

Spleen cells (2×10^6) isolated form virus-infected mice were restimulated weekly with irradiated syngeneic spleen cells and 10 μg HIA virus or 20 μg peptide. Twenty-four hr after the third or fourth restimulation, cell culture supernatants were tested for IL2 production. Three days after restimulation, 200 μl of cell suspensions were tested in triplicate microcultures for proliferation. The IP-12-9 T cell hybridoma was selected from the spleen of a HA1C[Arg]-immunized and virus-challanged BALB/c mouse. HA1C[Arg] immunization was performed as described above and 4 weeks before cell fusion the preimmunized mouse was aerosol-infected with 5 LD_{50} of A/PR/8/34 influenza virus. Spleen cells of the peptide-immunized and subsequently virus-challenged mouse were reactivated *in vitro* with the HA1C]Arg] peptide and 5 days later Ficoll separated T cells were fused with the BW-1100.129.237 alpha-/beta- (White *et al.*, 1989) thymoma cells according to the method of Rock (1985).

Detection of IL2 production

Peptide- or virus-induced IL2 production of activated polyclonal T cells was measured in cell culture supernatants of the proliferation assay harvested after 24 hr incubation in the presence of the peptides or virus-infected APC. The detection of IL2 in the supernatant of the IP-12-29 T cell hybrid was measured in samples taken at 24 or 48 hr of cell cultures containing 1×10^4 hybridoma cells and 2×10^5 irradiated syngeneic normal spleen cells. The relative level of IL2 of cell culture supernatants was quantitated by the proliferation of

Table 2. The *in vitro* IP-specific proliferative response and IL2 production of lymph node T cells isolated from IP-primed BALB/c, B10 or CBA mice

Mouse strain	H-2 K	I-A	I-E	D	IP (μg/ml)	T cell proliferation (cpm $\times 10^{-3}$)	IL2 production (cpm $\times 10^{-3}$)
B10	bb	bb	b-	bb	10	2.8 ± 0.4	0.2 ± 0.1
					4	3.7 + 1.2	0.1 + 0.1
					0.8	5.0 + 1.4	0.8 + 0.2
					—	3.8 + 2.6	0.2 + 0.1
CBA	kk	kk	kk	kk	20	2.0 + 0.7	7.8 + 1.2
					4	1.5 + 0.3	4.9 + 0.7
					0.8	0.7 + 0.1	1.2 + 0.1
					—	0.5 + 0.1	0.3 + 0.1
BALB/c	dd	dd	dd	dd	20	86.3 + 10.7	131.3 + 23.2
					4	45.6 + 8.8	128.2 + 5.1
					0.8	13.5 + 9.4	71.5 + 14.1
					—	1.9 + 0.6	38.8 + 5.4
					20[a]	4.9 + 0.5	n.t.

[a]Tested in the presence of CBA normal spleen cells as APC. n.t., not tested.
T cell proliferation was measured by ^{3}H-thymidine incorporation in the 4-day cultures.
IL2 production was measured by the proliferation of HT2 cells in a secondary culture containing 50 μl of culture supernatant harvested 24 hr after primary culture in the presence of APC and peptide. Mean values of triplicates + S.D. of a typical experiment are documented.

HT2 cells detected by ^{3}H-thymidine incorporation (given as cpm) or by (3-[4,5-dimethylthiazol-2-yl]-2,5-diphenyl-tetrazolium bromide (MTT) uptake (given as OD_{550}) in secondary cultures using a calibration curve in the presence of different amounts of recombinant human IL2 (kindly provided by Hoffman La Roche).

RESULTS

The proliferative response of CBA, B10 and BALB/c mice to the synthetic IP peptide

The proliferative response of *in vivo* primed lymph node T cells of different inbred mouse strains to the

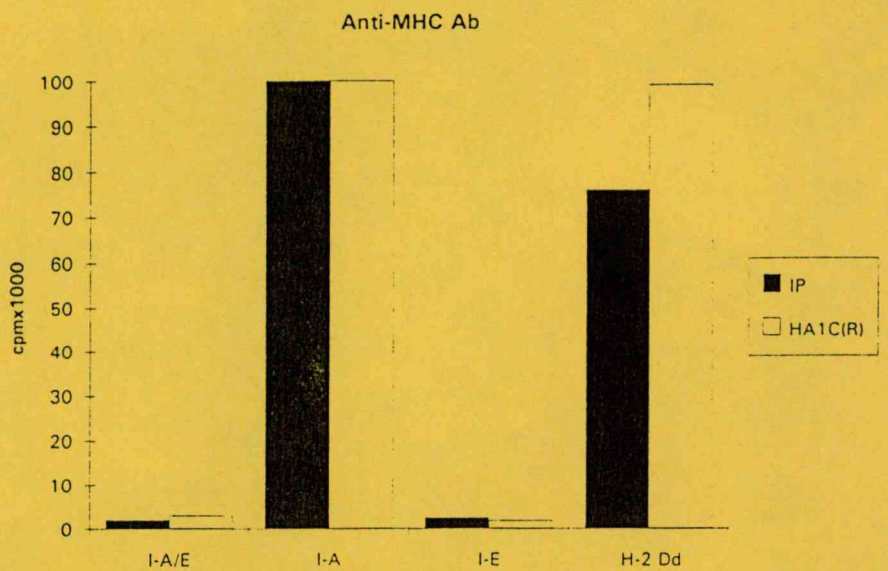

Fig. 1. MHC restriction of the IP- and HA1C[Arg]-primed T cell response. Proliferation of IP-(dark columns) or HA1C[Arg]-(empty columns) primed T cells was studied in the presence of 1 μg/ml IP or HA1C[Arg], respectively in the absence or presence of 5% cell culture supernatants containing mAb reacting with I-A, I-E or H-2D^d molecules. Percentage inhibition was calculated from cpm values obtained for positive cultures (IP, 4696 ± 262, HA1C[Arg], 7316 ± 642) containing the corresponding peptide in the absence of the mAb. Background measured in negative cultures was 982 ± 108.

synthetic IP peptide (see Table 1) representing the uncleaved form of the intersubunit region of the influenza virus hemagglutinin molecule is summarized in Table 2. Data demonstrate that IP is able to induce a peptide-specific, MHC-restricted proliferative response in IP-immunized BALB/c but not in B10 or CBA mice. It is also shown that IP induces proliferation and IL2 production in a dose-dependent manner in the presence of syngeneic APC. Inhibition by MHC-specific antibodies revealed the I-E^d restriction of the IP-specific T cell response (Fig. 1, dark columns).

Specificity of the IP-induced T cell response of BALB/c mice

The reactivity of IP-specific T cells with overlapping synthetic peptides covering the intersubunit region was studied with polyclonal T cells as well as with T cell hybridomas. As shown in Table 3, IP-primed T cells can be activated by the HA1C[Arg] subfragment peptide but not with the FP fusion peptide. This observation points to the location of a T cell epitope to the C-terminal segment of the HA1 subunit. The presence of a T cell epitope in the HA1C[Arg] peptide was also verified by the capability of this peptide, but not of the FP fusion peptide to prime T cells (Table 3). HA1C[Arg]-primed T cells are cross-reactive with the IP peptide (Table 3) and are also recognized in the context of the I-E^d molecule (Fig. 1, plain columns).

To answer the question whether the C-terminal arginine of the HA1C[Arg] peptide has any role in T cell recognition, the capacity of the Arg-truncated HA1C dodecapeptide to induce the activation of HA1C, HA1C[Arg] or IP-primed T cells was studied. Although no striking difference in the T cell priming or activating capacity of HA1C[Arg] or HA1C could be observed (Table 3), it should be noted that the Arg extended peptide gave a higher response in most cases.

The observations obtained with polyclonal T cells raised the possibility that T cells of differing specificity might be responsible for the recognition of IP and HA1C[Arg] and their analogs. The fine specificity pattern of a typical T cell hybridoma (IP-12-29) depicted in Fig. 2 shows full cross-reactivity of IP and HA1C[Arg] supporting the interpretation that HA1C[Arg] can be recognized both in its 13-mer and fusion peptide elongated 25-mer forms. As in the case of polyclonal T cells (Table 3), Arg truncation at the C-terminal of the HA1C[Arg] peptide does not abolish recognition by the IP-12-29 T cell hybridoma (Fig. 2B) demonstrating the identical specificity pattern of polyclonal T cells and that of this monoclonal T cell.

On the basis of these results, a T cell epitope localized in the 317–328 region of the HA1 subunit representing the H1 serotype sequence of influenza virus hemagglutinin could be identified. N-terminally truncated analogs of HA1C up to a deca- ($HA1C_{deca}$) or nonapeptide ($HA1C_{nona}$) are not able to activate the IP-12-29 T cell hybridoma (Fig. 2B).

Processing requirements of IP recognition

The cross-reactivity of IP- and HA1C[Arg]-primed T cells in both directions does not clarify whether IP is recognized in its full length or will be further processed giving rise to a fragment comprising the HA1C[Arg] peptide. The processing requirements of IP were investigated by studying the activity of the D-Arg substituted analog of IP ([D-Arg]^{13}IP) and using different enzyme inhibitors known to interfere with the activity

Table 3. Cross-reactivity of peptide-primed lymph node T cells with the intersubunit IP and subunit peptides HA1C[Arg], HA1C and FP

		In vitro stimulation (cpm × 10^{-3} + S.D.)			
Immunization	μg/ml	IP	HA1C[Arg]	HA1C	FP
IP	20	48.9 + 9.9	36.3 + 6.6	33.4 + 4.3	12.2 + 2.3
	4	63.1 + 2.9	33.5 + 3.0	28.3 + 0.5	14.2 + 6.2
	0.8	50.2 + 4.0	19.9 + 5.3	23.0 + 1.7	12.5 + 1.4
	—	7.1 + 0.7			
HA1C[Arg]	20	43.3 + 3.49	66.1 + 17.4	41.9 + 2.7	n.t.
	4	50.1 + 16.0	41.8 + 10.5	23.8 + 12.4	n.t.
	0.8	65.5 + 4.8	33.4 + 6.3	26.7 + 5.5	n.t.
	—	14.6 + 5.2			
HA1C	20	22.3 + 6.9	34.8 + 2.3	32.9 + 3.9	n.t.
	4	28.0 + 3.9	22.8 + 12.7	24.0 + 9.5	n.t.
	0.8	21.1 + 0.36	18.8 + 5.3	21.8 + 10.4	n.t.
	—	2.8 + 0.3			
FP	20	10.7 + 2.9	n.t.	n.t.	5.9 + 0.5
	4	8.8 + 3.4	n.t.	n.t.	5.4 + 0.7
	0.8	7.2 + 0.8	n.t.	n.t.	5.7 + 2.4
	—	5.5 + 1.1			

T cell proliferation was measured as described under Table 2.

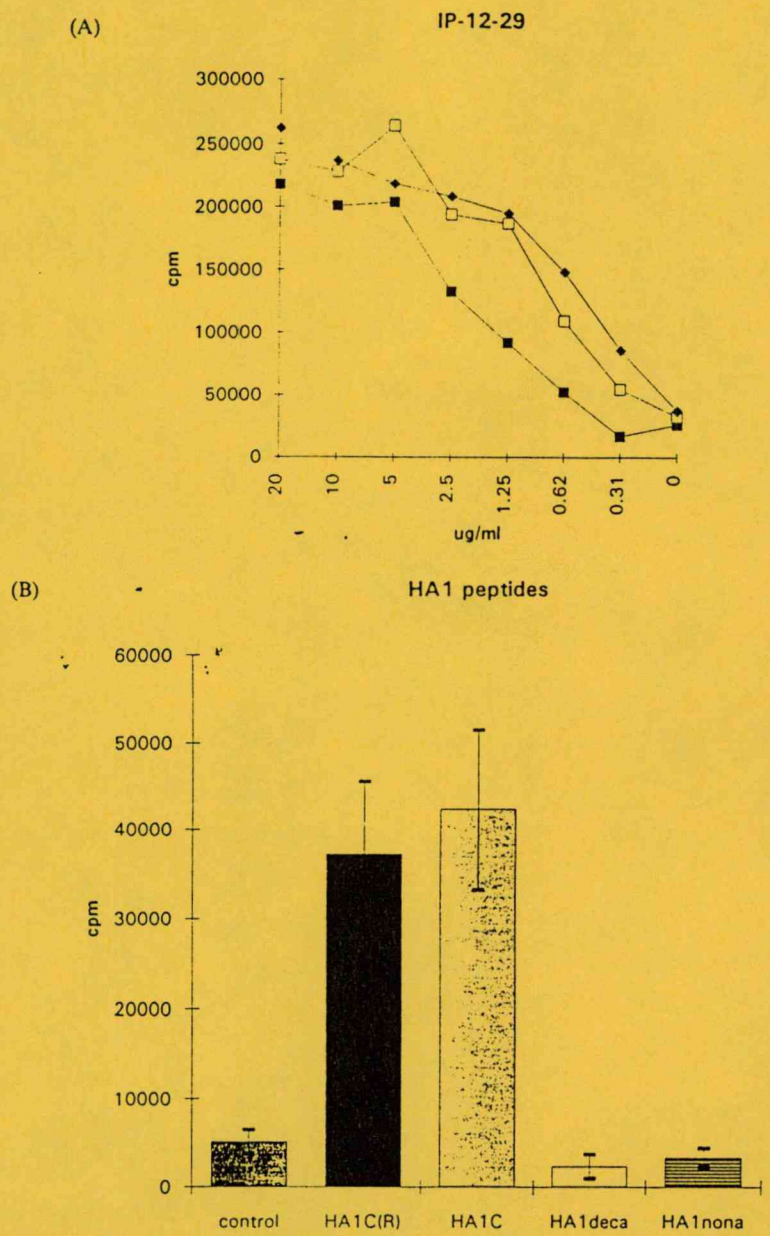

Fig. 2. Reactivity of the IP-12-29 hybridoma with synthetic peptides representing the intersubunit region of influenza virus hemagglutinin. (A) T hybridoma cells were cultured in the presence of irradiated BALB/c spleen cells and different concentrations of the synthetic peptide IP (■—■) [D-Arg[13]]IP (◆—◆) or HA1C[Arg] (□—□). Relative IL2 content of cell culture supernatants was measured by HT2 cell proliferation and given as cpm. Mean values of triplicates of a typical experiment are documented. (B) T hybridoma cells were cultured in the presence of 2.5 μg/ml HA1C[Arg], (HA1C(R), HA1C, $HA1C_{deca}$ or $HA1C_{nona}$ peptides. Negative cultures (control) did not contain peptide.

of trypsin-like enzymes, which have an inhibitory effect for exogenous antigen processing and also for certain viral infection (Andersen, 1983). As shown in Fig. 3 the presence of leupeptin (Fig. 3A, B) or the D-FRP (Fig. 3B) trypsin inhibitor previously shown to inhibit trypsin-mediated fusion of influenza virus (unpublished observation) did not abolish IP recognition by polyclonal (Fig. 3A) or monoclonal (Fig. 3B) T cells, while the same concentration of inhibitors caused complete inhibition of the proliferation of ovalbumin-primed T cells induced by 20 or 4 μg/ml ovalbumin (data not shown). This result, in good accordance with the similar dose–response curves of HA1C[Arg], IP or its [D-Arg[13]]IP analog to activate the IP-12-29 T hybridoma (Fig. 2A) or polyclonal T cells (data not shown) revealed that the IP peptide can be recognized without further processing at the Arg/Gly cleavage site.

Reactivity of HA1C[Arg]- or HA1C-primed T cells with influenza virus

As it is summarized in Fig. 4, syngeneic normal spleen cells preincubated with the infectious virus activate HA1C[Arg]- or HA1C-primed T cells in a dose-dependent

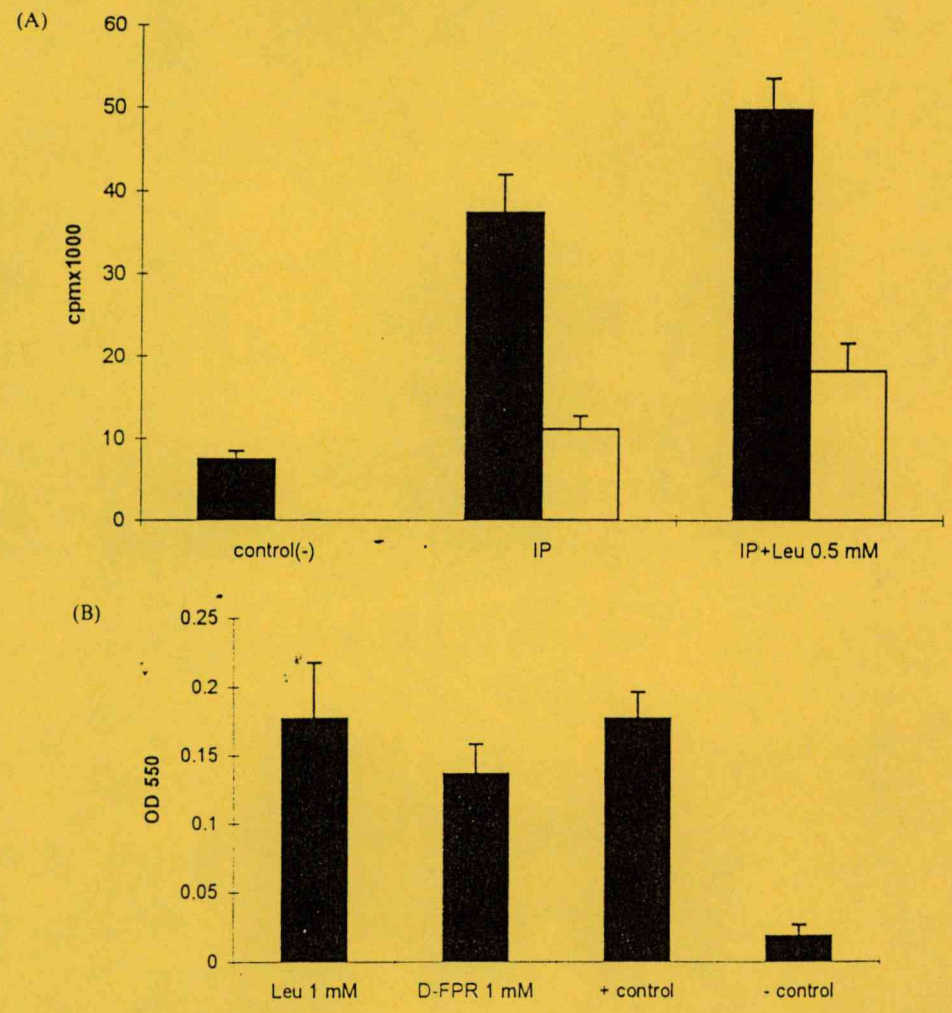

Fig. 3. The activation of IP-specific T cells in the presence of trypsin inhibitors. (A) The T cell proliferation assay was performed in the presence of irradiated syngeneic spleen cells as APC and 4 (dark columns) or 0.8 (open columns) μg ml IP or with the same amount of IP in combination with 0.5 mM leupeptin (Leu). (B) The IP-12-29 T cell hybridoma was cultured in the presence of syngeneic spleen cells as APC and 5 μg ml IP or with the same amount of IP in combination with 1 mM leupeptin (Leu) or D-FPR. Control cultures did not contain peptide (−) or trypsin inhibitor (+). The relative level of IL2 in the culture supernatants was measured by the proliferation of the IL2-dependent HT2 cell line using the MTT assay and given as OD_{550}. Mean values of triplicates of a typical experiment are documented.

manner. These results show that processing of the HA molecule results in fragments comprising the HA1C[Arg] region which is available for MHC class II molecules and can be recognized by peptide-primed T cells.

Occurrence of IP-, HA1C[Arg]- or FP-specific T cells in influenza virus-infected or immunized BALB/c mice

As the HA1C[Arg] epitope was proven to be presented by influenza virus-infected APC, peptide-reactive T cells were searched in influenza virus-infected or immunized BALB/c mice. Synthetic peptides comprising the intersubunit region of influenza virus hemagglutinin were used to activate influenza virus-primed T cells under *in vitro* conditions. As a positive control, APC preinfected with the virus or incubated in the presence of heat inactivated A/PR/8/34 influenza virus were used. As shown in Table 4, primary or repeated viral infections do not result in the activation of a substantial proportion of peptide-specific T cells. Adjuvant combined immunization with a high dose of infectious A/PR/8/34 virus does not induce the priming of these type of T cells either. These results are supported by results obtained with repeatedly restimulated cultures (T cell lines) summarized in Table 4 (lower block). These data demonstrate that repeated influenza virus restimulation results in the development of influenza virus specific T cell lines which recognize epitopes distinct from those located in the intersubunit region while the same procedure does not result in the selection of IP- or FP-specific T cells.

DISCUSSION

The influenza virus hemagglutinin can be present in the infected host in two forms; the single chain HA0 precursor and the posttranslationally modified molecule.

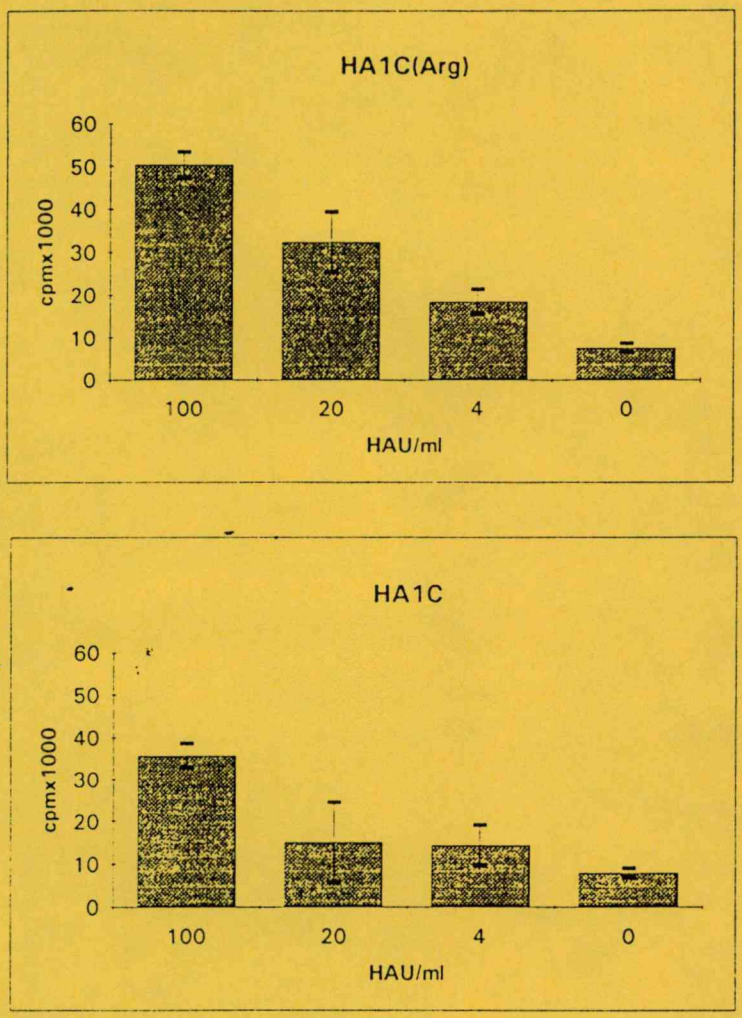

Fig. 4. Proliferation of HA1C[Arg] or HA1C primed T cells in the presence of A/PR/8/34 influenza virus-infected syngeneic ATC. Normal BALB/c spleen cells were preincubated with 100, 20 or 4 HAU/ml dose of A/PR/8/34 influenza virus for 4 hr at 37°C, mytomycin-treated and cultured with HA1C[Arg] or HA1C peptide-primed T cells. Control cultures were set up with the same amount of APC not preincubated with the virus.

Mature, enzymatically cleaved HA molecules are ready to undergo a pH-dependent conformational change, acquire enhanced sensitivity to further enzymatic cleavage and are characterized by increased hydrophobicity compared to the immature uncleaved form (Doms *et al.*, 1985). In this study the question was raised whether the cleaved and/or uncleaved forms of the intersubunit region can be the target of T cell recognition and if so what are the requirements for T cell recognition. To localize and demonstrate the function of T cell epitopes in the intersubunit region of the H1 subtype of influenza virus hemagglutinin inbred mice of different MHC haplotypes were injected with the IP peptide and the polyclonal T cell response against the parental and overlapping synthetic peptides was measured by *in vitro* proliferation and IL2 production. Results revealed that the IP peptide induces an intense T cell response in BALB/c, but not in B10 or CBA mice. The proliferative response of BALB/c mice is I-E^d-restricted and is accompanied by IL2 production. The 24-mer C-terminal segment of the HA1 subunit of the H3 influenza A virus serotype has previously been identified as a region comprising multiple helper T cell epitopes (Jackson and Brown, 1991; Brown *et al.*, 1988). A dominant I-E^d-restricted T cell epitope not cross-reactive with the virus was localized to the 305–317 region together with a subdominant epitope in the 319–328 segment (Brown *et al.*, 1988). It was of particular interest to investigate whether the additional length at the C-terminal of HA1 representing a hydrophobic natural sequence essential for antibody recognition (Nagy *et al.*, 1994) has any effect on T cell recognition of this region. This C-terminal flanking sequence, comprising the fusion peptide has been demonstrated to undergo a conformational switch from alpha-helical to an extended conformation under appropriate conditions (Hollósi *et al.*, 1992). Another crucial question was whether the C-terminal Arg of the HA1 subunit which is eliminated under natural conditions has any effect on T cell recognition. In our studies the 317–329 HA1 fragment representing the H1 serotype sequence of human A type influenza viruses turned out to be a potent MHC class II-restricted T cell epitope used either in its 13-mer or C-terminally elongated 25-mer analog to induce or activate proliferating

Table 4. Reactivity of splenic T cells of influenza virus-infected or immunized BALB/c mice with the synthetic peptides covering the intersubunit region of influenza virus hemagglutinin

(a)

	In vitro stimulation				
	Virus		Peptide		
Immunization	A/PR/8/34	A/PR/8/34 HIA	IP	HA1C[Arg]	FP
Splenic T cells	100 HAU/ml	μg/ml[a/b]	20 μg/ml	20 μg/ml	20 μg/ml
A/PR/8/34 infection primary	102.9 + 14.9	71.9 + 33.4[a]	9.4 + 6.4	4.6 + 4.2	5.0 + 3.6
A/PR/8/34 infection repeated	87.9 + 16.2	86.5 + 4.8[b]	0	0	0
A/PR/8/34 live injection	n.t.	73.7 + 9.4	1.8 + 1.3	n.t.	0

(b)

	In vitro stimulation				
	Virus		Peptide		
Immunization/*in vitro* stimulation	A/PR/8/34	A/PR/8/34 HIA	IP	HA1C[Arg]	FP
T cell lines	100 HAU/ml	μg/ml	20 μg/ml	20 μg/ml	20 μg/ml
A/PR/8/34 infection/A/PR/8/34 HIA proliferation	10.5 + 0.6	54.7 + 1.3	n.t.	0.8 + 0.4	n.t.
IL2 production	48.1 + 3.2	54.1 + 2.1	3.6 + 1.5	6.8 + 1.7	3.1 + 2.1
A/PR/8/34 infection/IP	n.t.	2.2 + 0.2	n.t.	n.t.	n.t.
A/PR/8/34 infection/FP	n.t.	n.t.	n.t.	n.t.	0

HIA, heat inactivated. n.t., not tested.

[a] 4 μg/ml.

[b] 20 μg/ml.

Primary infection of BALB/c mice was performed with 0.03 LD_{50}. Viral challenge was given by 1 LD_{50}. Subcutaneous injection of 100 μg purified live virus was introduced to the base of the tail. Mean cpm values of triplicates + S.D. of a typical experiment are documented. Values are corrected with the corresponding cpm values measured in negative control cultures set up in the absence of the virus or peptides. T cell lines were tested for proliferation or IL2 production after the fourth restimulation with the corresponding antigen in the presence of irradiated syngeneic spleen cells.

BALB/c T cells. The dose–response curves obtained with IP, [D-Arg[13]]IP or HA1C[Arg] to activate the IP-12-29 T cell hybridoma revealed the similar potency of the longer or shorter analogs to activate T cells (Fig. 2A). In addition, the lack of inhibition by serine and thiol protease inhibitors known to interfere with endosomal degradation of certain proteins (Vidard *et al.*, 1991) demonstrated that the longer IP (Fig. 3) or its [D-Arg[13]]IP analog (Fig. 2A) can be recognized without further processing being mediated by trypsin-like enzymes inside or outside of the cell (Fig. 3).

The core region of the epitope was localized to the 317/318–328 region as the N-terminally truncated deca- or nonapeptides were inactive (Fig. 2B). Our results show that overlapping peptides of different length comprising this region are able to activate T cells. The fusion peptide elongated 25-mer peptide is as efficient to activate T cells as the shorter HA1 derived peptides (Fig. 2A, Table 3). Lack of the C-terminal Arg residue in the HA1C subunit peptide, in good correlation with its elimination under physiological conditions by a carboxypeptidase N-like, virus associated host cell derived enzyme (Garten *et al.*, 1991) does not abolish T cell recognition (Fig. 2B, Table 3).

These results are consistent with the recent view of the open binding groove of the class II MHC molecule (Brown *et al.*, 1993). Data on the size of naturally occurring MHC class II associated and eluted peptides of endogenous or exogeneous proteins (Demotz *et al.*, 1989; Rudensky *et al.*, 1991; Srinivasan *et al.*, 1993) revealed a wide size heterogeneity and provided examples for the enhanced binding efficiency of longer peptides (Srinivasan *et al.*, 1993; Nelson *et al.*, 1992). In functional terms our results demonstrate that the epitope identified in the intersubunit region can equally well be recognized as peptides of cleaved or uncleaved hemagglutinin molecules if the appropriate fragments are generated by any route of antigen processing. Lysosomal enzymes are not involved in the posttranslational modification of HA0 and their activity results in abberrant cleavage products of the immature molecule (Klenk *et al.*, 1984). These fragments however, can bind to and be protected from further degradation by MHC molecules. The cross-reactivity of HA1C[Arg]- or HA1C-primed T cells with APC, preincubated with the infective virus which subsequently gives rise to uncleaved HA0 molecules supports this assumption.

The capability of HA1C[Arg]-primed T cells to be activated by influenza virus-infected APC proves that hemagglutinin fragments comprising the studied peptides will be generated in an available form after natural processing of the molecule. The exact pathway of the route of hemagglutinin processing has however, to be elucidated. Input of the infective virus to the exogeneous pathway is much lower compared to the amount of newly synthesized, uncleaved hemagglutinin molecules produced in the course of a single growth cycle (4 hr) (Eisenlohr and Hackett, 1989). This suggests that it is the endogenous pathway which also might be involved in peptide production. This interpretation is consistent with previous results which show that MHC class II molecules can also be efficiently loaded by endogenous influenza virus proteins (Nuchtern *et al.*, 1990; Jaraguemada *et al.*, 1990; Eisenlohr and Hackett, 1989; Hackett *et al.*, 1991; Long, 1992). Previous data showing that re-internalization of non-infectious viruses bearing uncleaved HA0 molecules is unefficient (Scholtissek, 1986) also supports this interpretation.

The cross-reactivity of peptide-primed T cells with virus-infected APC argues against the possibility that the low frequency of T cells directing against this region in virus-primed mice is the consequence of inappropriate processing events. It is more likely that the productive growth cycle of the virus results in strong peptide competition in APC mediated by a large excess of dominant T cell epitopes generated from cleaved HA or from other viral proteins entering the endogeneous processing pathway. Consequently, the epitope defined in this study is not an immunodominant T cell determinant in the course of viral infection. However, primary infection of APC producing uncleaved HA0 precursors might have an important role in the first recruitment of T and B cells (Doherty *et al.*, 1992). As was revealed, the covalent attachment of the highly conserved fusion peptide has a beneficial effect on the expression of the B cell epitope located also in the HA1C[Arg] region (Rajnavölgyi, 1992; Tóth *et al.*, 1992, 1993; Nagy *et al.*, 1994). This is due to the stable conformation of this region which is maintained also in IP as demonstrated by CD and FT-IR spectroscopy (Hollósi *et al.*, 1992). In an *in vivo* situation the concomitant presence of a B cell epitope by itself can be beneficial for T cell recognition by promoting uptake of the protein and protection of a particular region against further degradation. The potency of this region as a subunit vaccine candidate was experimentally demonstrated in survival experiments proving the capability of these peptides and more obviously their modified analogs to elicit a protective immune response (Rajnavölgyi, 1992; Tóth *et al.*, 1992, 1993; Nagy *et al.*, 1994). Based on our results it is reasonable to assume that multiple infections generating cleaved HA molecules does not favour antibody recognition of this region and the subsequent internalization of immature HA0 molecules by specific B cell APC suggesting a functional escape mechanism of the virus.

Acknowledgements—The excellent technical assistance of Erzsébet Veress and Árpád Mikessy is acknowledged. This work was supported by the OTKA grants 2010 of É.R., F5120 of Z.N. and 2734 of G.K.T.

REFERENCES

Andersen K. B. (1983) Leupeptin inhibits retrovirus infection in mouse fibroblasts. *J. Virol* 48, 765–769.

Bajusz S., Barabás É., Tolnai P., Széll E. and Bagdy D. (1978) Inhibition of thrombin and trypsin by tripeptide aldehydes. *Int. J. Pep. Prot. Res.* 12, 217–221.

Barr P. J. (1991) Mammalian substilisins: The long-sought dibasic processing endoproteases. *Cell* **66**, 1–3.

Bhattacharya A., Dorf M. E. and Springer T. A. (1981) A shared alloantigenic determinant on Ia antigens encoded by the I-A and I-E subregions: evidence for I region gene duplication. *J. Immun.* **11**, 2488–2495.

Braciale T. J., Sweetser M. T., Morrison L. A., Kittlesen D. J. and Braciale V. L. (1989) Class I major histocompatibility complex-restricted cytolytic T lymphocytes recognize a limited number of sites on the influenza hemagglutinin. *Proc. natn. Acad. Sci. U.S.A.* **86**, 277–281.

Brooks A., Hartley S., Kjer-Nielsen L., Perera J., Goodnow C., Basten A. and McCluskey J. (1991) Class II-restricted presentation of an endogenously derived immunodominant T-cell determinant of hen egg lysozyme. *Proc. natn. Acad. Sci. U.S.A.* **88**, 3290–3294.

Brown J. H., Jardetzky T. S., Gorga J. C., Stern L. J., Urban R. G., Strominger J. L. and Wiley C. C. (1993) Three-dimensional structure of the human class II histocompatibility antigen HLA-DR1. *Nature* **364**, 33–39.

Brown L. E., Murray J. M., Anders E. M., Tang X.-L., White D. O., Tregear G. W. and Jackson D. C. (1988) Genetic control and fine specificity of the immune response to a synthetic peptide of influenza hemagglutinin. *J. Virol.* **62**, 1746–1752.

Corradin G., Etlinger H. M. and Chiller J. M. (1977) Lymphocyte specificity to protein antigens. I. Characterization of the antigen-induced *in vitro* T cell-dependent proliferative response with lymph node cells from primed mice. *J. Immun.* **119**, 1048–1053.

Demotz S., Grey H. M., Appella E. and Sette A. (1989) Characterization of a naturally processed MHC class II restricted T-cell determinant of hen egg lysozyme. *Nature* **342**, 682–684.

Doherty P. C., Allan W. and Eichelberger M. (1992) Roles of alpha/beta and gamma/delta T-cell subsets in viral immunity. *A. Rev. Immun.* **10**, 123–151.

Driscoll J. and Finley D. (1992) A controlled breakdown: Antigen processing and the turnover of viral proteins. *Cell* **68**, 823–825.

Eisenlohr L. C. and Hackett C. J. (1989) Class II major histocompatibility complex-restricted T cells specific for a virion structural protein that do not recognize exogeneous influenza virus. *J. exp. Med.* **169**, 921–931.

Garten W., Vey M., Ohuchi R., Ohuchi M. and Klenk H.-D. (1991) Modification of the cleavage activation of the influenza virus hemagglutinin by site-specific mutagenesis. *Behring Inst. Mitt.* **89**, 12–22.

Garten W. and Klenk H.-D. (1983) Characterization of the carboxypeptidase involved in the proteolytic cleavage of the influenza hemagglutinin. *J. gen. Virol.* **64**, 2127–2137.

Gotoh B., Ogasawana T., Toyoda T., Inocencio H. M., Hamaguchi M. and Nagai Y. (1990) An endoprotease homologous to the blood clotting factor X as a determinant of viral tropism in chick embryo. *Eur. molec. Biol. Org. J.* **9**, 4189–4195.

Hackett C. J., Yewdell J. W., Bennink J. R. and Wysocka M. (1991) Class II MHC-restricted T cell determinants processed from either endosomes or the cytosol show similar requirements for host protein transport but different kinetics of presentation. *J. Immun.* **146**, 2944–2951.

Hollósi M., Ismail A. A., Mantsch H. H., Penke B., Váradi G., Tóth G. K., Laczkó I., Kurucz I., Nagy Z., Fasman G. and Rajnavölgyi É. (1992) Conformational and functional properties of peptides covering the intersubunit region of influenza virus hemagglutinin. *Eur. J. Biochem.* **206**, 421–425.

Holly S., Majer Zs., Tóth G. K., Váradi Gy., Rajnavölgyi É., Laczkó I. and Hollósi M. (1993) Circular dichroism and Fourier-transform infrared spectroscopic studies on T-cell epitopic peptide fragments of influenza virus hemagglutinin. *Biochem. biophys. Res. Commun.* **193**, 1247–1254.

Jackson D. C. and Brown L. E. (1991) A synthetic peptide of influenza virus hemagglutinin as a model antigen and immunogen. *Peptide Res.* **4**, 114–124

Jaraguemada D., Marti M. and Long E. O. (1990) An endogenous processing pathway in vaccinia virus-infected cells for presentation of cytoplasmic antigens to class II-restricted T cells. *J. exp. Med.* **172**, 947–954.

Kappler J., Skidmore B., White J. and Marrack P. J. (1981) Antigen inducible, H-2 restricted interleukin 2 producing T cell hybridomas. *J. exp. Med.* **153**, 1198–1214.

Klenk H.-D., Garten W. and Rott R. (1984) Inhibition of proteolytic cleavage of the hemagglutinin of influenza virus by the calcium-specific ionophore A23187. *Eur. molec. Biol. Org. J.* **3**, 2911–2915.

Lamb J. K., Echels D. D., Lake P., Woody J. N. and Green N. (1982) Human T-cell clones recognize chemically synthesized peptides of influenza haemagglutinin. *Nature* **300**, 66–69.

Long E. O. and Jacobson S. (1989) Pathways of viral antigen processing and presentation to CTL: defined by the mode of virus entry? *Immun. Today* **10**, 45–48.

Long E. O. (1992) Antigen processing for presentation to CD4+ T cells. *New Biologist* **4**, 274–282.

Mills K. H. G., Skehel J. J. and Thomas D. B. (1986) Extensive diversity in the recognition of influenza virus hemagglutinin by murine T helper clones. *J. exp. Med.* **163**, 1477–1490.

Mills K. H. G. (1986) Processing of viral antigens and presentation to class II-restricted T cells. *Immun. Today* **7**, 260–263.

Murray N. and McMichael A. (1992) Antigen presentation in virus infection. *Curr. Op. Immun.* **4**, 401–407.

Nagai Y., Inocencio N. M. and Gotoh B. (1991) Paramyxovirus tropism dependent on host proteases activating the viral fusion glycoprotein. *Behring Inst. Mitt.* **89**, 34–45.

Nagy Z., Rajnavölgyi É., Hollósi M., Tóth G. K., Váradi Gy., Penke B., Tóth I., Horváth A., Gergely J. and Kurucz I. (1994) The intersubunit region of the influenza virus haemagglutinin is recognized by antibodies during infection. *Scand. J. Immun.* **40**, 281–291.

Nelson C. A., Roof R. W., McCourt D. W. and Unanue E. R. (1992) Identification of the naturally processed form of hen egg white lysozyme bound to the murine major histocompatibility complex class II molecule I-A^k. *Proc. natn. Acad. Sci. U.S.A.* **89**, 7380–7383.

Nuchtern J. G., Biddison W. E. and Klausner R. D. (1990) Class II MHC molecules can use the endogenous pathway of antigen presentation. *Nature* **343**, 74–76.

Ozato K., Mayer N. and Sachs D. J. (1980) Hybridoma cell lines secreting monoclonal antibodies to mouse H-2 and Ia antigens. *J. Immun.* **124**, 533–540.

Perkins D. L., Berriz G., Wang Y., Smith J. A. and Gefter M. L. (1991) Comparison of class I- and II-restricted T cell recognition of the identical peptide. *Eur. J. Immun.* **21**, 2781–2789.

Rajnavölgyi É. (1992) Synthetic peptides in the search for T- and B-cell epitopes. *Immun. Today* **13**, A17–19.

Rock K. L. (1985) Functional T-cell hybridomas. In *Hybridoma Technology in Bioscience and Medicine* (Edited by Springer T.A.) Plenum Press, New York.

Rudensky A. Y., Preston-Hurlburt P., Hong S.-C., Barlow A. and Janeway C. A. Jr (1991) Sequence analysis of peptides bound to MHC class II molecules. *Nature* **353**, 622–627.

Scholtissek C. (1986) Influenza A viruses with noncleaved hemagglutinin are not internalized after adsorption. *Arch. Virol.* **90**, 159–163.

Sette A., Adorini L., Appella E., Colon S. M., Miles C., Tanaka S., Ehrhardt C., Doria G., Nagy Z. A., Buus S. and Grey H. M. (1989) Structural requirements for the interaction between peptide antigens and I-E^d molecules. *J. Immun.* **143**, 3289–3294.

Srinivasan M., Domanico S. Z., Kaumaya P. T. P. and Pierce S. K. (1993) Peptides of 23 residues or greater are required to stimulate a high affinity class II-restricted T cell response. *Eur. J. Immun.* **23**, 1011–1016.

Sweetser M. T., Morrison L. A., Braciale V. L. and Braciale T. J. (1989) Recognition of pre-processed endogenous antigen by class II MHC-restricted T cells. *Nature* **342**, 180–182.

Thomas D. B., Burt D. S., Barnett B. C., Graham C. M. and Skehel J. J. (1989) B- and T-cell recognition of influenza hemagglutinin. *Cold Spring Harbor Symp. on Quant. Biol.* LIV, 487–495.

Tóth G. K., Váradi G., Nagy Z., Monostori É., Penke B., Hegedus Z., Andó I., Fazekas Gy., Kurucz I., Mák M. and Rajnavólgyi É. (1993) Branched polypeptides as antigens for influenza virus hemagglutinin and T-cell receptor subunits. *Peptide Res.* **6**, 272–280.

Tóth G. K., Váradi G., Penke B., Monostori É., Hegedüs Z., Nagy Z., Kurucz I. and Rajnavölgyi É. (1992) Synthesis of branched polypeptides as antigens for influenza virus hemagglutinin and T-cell receptor subunit. In *Peptides* (Edited by Schneider C. H. and Eberle A. N.), p. 882. ESCOM Science Publishers B.V.

Vidard L., Rock K. L. and Benacerraf B. (1991) The generation of immunogenic peptides can be selectively increased or decreased by proteolytic enzyme inhibitors. *J. Immun.* **147**, 1786–1971.

Walker J. A. and Kawaoka Y. (1993) Importance of conserved amino acids at the cleavage site of the haemagglutinin of a virulent avian influenza A virus. *J. gen. Virol.* **74**, 311–314.

Webster R. G. and Rott R. (1987) Influenza virus A pathogenicity: The pivotal role of hemagglutinin. *Cell* **50**, 665–666.

White J., Blackman M., Bill J., Kappler J., Marrack P., Gold D. P. and Born W. (1989) Two better cell lines for making hybridomas expressing specific T cell receptors. *J. Immun.* **143**, 1822–1825.

White J. (1990) Viral and cellular membrane fusion proteins. *A. Rev. Physiol.* **52**, 675–697.

Wilson I. A. and Cox N. J. (1990) Structural basis of immune recognition of influenza virus hemagglutinin. *A. Rev. Immun.* **8**, 737–771.

Yewdell J. W. and Hackett C. J. (1989) Specificity and function of T lymphocytes induced by influenza A viruses. *In The Influenza Viruses* (Edited by Krug R. M.), p. 361. Plenum Press N.Y., London.

ARCHIVES OF BIOCHEMISTRY AND BIOPHYSICS
Vol. 322, No. 1, September 10, pp. 112–118, 1995

3.6.

Mapping the Intersubunit Region of Influenza Virus Hemagglutinin: Comparative CD and FTIR Spectroscopic Studies on Multiple Antigenic Peptides

Zsuzsa Majer,* Sándor Holly,† Gábor K. Tóth,‡ Györgyi Váradi,‡ Zoltán Nagy,§ Attila Horváth,§ Éva Rajnavölgyi,§ Ilona Laczkó,¶ and Miklós Hollósi*,[1]

*Department of Organic Chemistry, Eötvös University, H-1518 Budapest 112, P.O. Box 32, Hungary; †Central Research Institute of Chemistry, H-1525 Budapest, Hungary; ‡Department of Medical Chemistry, Szent-Györgyi University, H-6720 Szeged, Hungary; §Department of Immunology, Eötvös University, H-2131 Göd, Hungary; ¶Biological Research Center, Institute of Biophysics, H-6701 Szeged, Hungary

Received February 22, 1995, and in June 19, 1995

An A/PR/8/34 (IHN1) influenza virus hemagglutinin (HA)-specific monoclonal antibody (Z38) was found to react with the solid phase adsorbed influenza virus expressing uncleaved (HA0) molecules but not to bind to virus particles bearing enzymatically cleaved hemagglutinin. Synthetic peptides corresponding to the uncleaved HA0 317–341 intersubunit region of subtypes H1–H3 (IP1–IP3) or comprising either the C-terminal 317–329 amino acids of HA1 (CP1) or the N-terminal 330–341 of HA2 (fusion peptide, FP) subunits of cleaved HA were used to characterize the fine specificity of Z38 mAb. Circular dichroism and Fourier-transform infrared spectroscopy showed that, compared to IP2 and IP3 comprising the H2 and H3 subtype fragments of the intact intersubunit region, IP1 has relatively low helicity but a tendency to adopt β-turns in trifluoroethanol. The immunological and conformational properties of multiple antigenic peptides (MAPs) containing four copies of CP1 were also studied. Based on the appearance of an infrared component band at 1637 cm^{-1} (β-turn band), the CP1 arms of MAPs also contain repeats of β-turns. However, it is only the MAP1-FP construct comprising also the fusion peptide, which binds Z38 mAb as strongly as IP1 does. This puts emphasis on the role of the fusion region in modifying conformation and consequently the ability of peptides to elicit an antibody response. The results obtained for peptide conformation also suggests a β-turn(s)/β-sheet/β-turn/β-sheet conformational motif in the recognition by the hemagglutinin subtype-specific Z38 monoclonal antibody or by peptide-induced polyclonal antibodies. © 1995 Academic Press, Inc.

Key Words: **antibody recognition; circular dichroism; Fourier-transform infrared; hemagglutinin; β-turn.**

The epidemological success of influenza A viruses is largely due to the variability of their surface glycoproteins. Hemagglutinin (HA),[2] one of these molecules, has two basic functions: (i) it is responsible for receptor binding and (ii) it mediates fusion of the viral and the host cell endosomal membranes (1, 2). HA is also a major target of immune recognition mediated both by antibodies and T cells (3). Influenza A viruses are subdivided into 14 serotypes based on antigenic differences (1). The amino acid sequences of the hemagglutinin subtypes generated by antigenic drift show clustered amino acid changes accumulated in the major antigenic sites (4, 5).

The HA molecule is synthesized in the infected host cell as a precursor polypeptide chain with an intact intersubunit region (HA0) and upon maturation it is cleaved to HA1 and HA2 subunits. (Scheme I). The enzymatic cleavage at Arg^{329} is mediated by host cell proteases (6). This event is the prerequisite of infectivity and permits the pH-dependent conformational change of HA which results in the elaboration of the fusion peptide (FP) comprising the 1–12 amino acids of the HA2 subunit (7). The amino acid sequence of the fusion peptide is identical in all influenza virus

[1] To whom correspondence should be addressed. Fax: 36-1-209-0602. E-mail: hollosi@organ.elte.hu.

[2] Abbreviations used: HA, hemagglutinin; FP, fusion peptide; TFE, trifluoroethanol; FSD, Fourier self-deconvolution.

0003-9861/95 $12.00

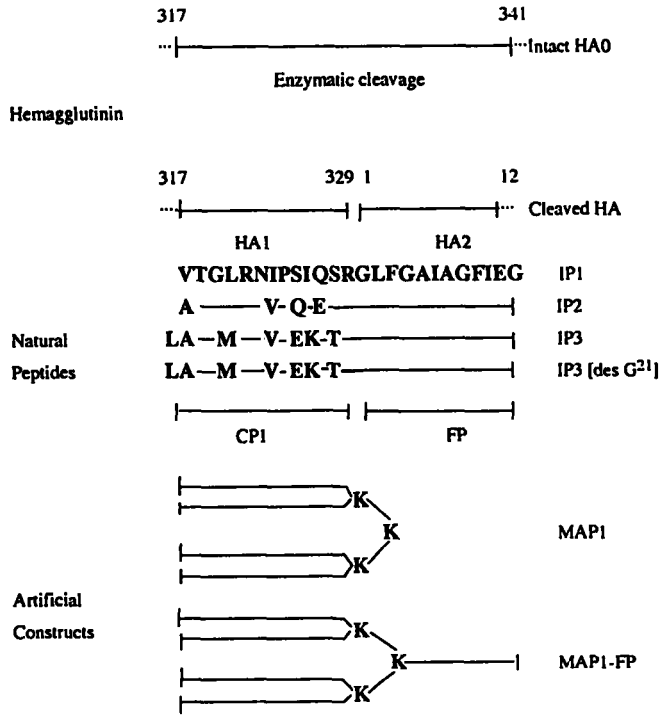

SCHEME I. The intersubunit region of influenza virus hemagglutinin. The 25-mer sequence (IP1) represents the intersubunit region of uncleaved hemagglutinin human subtype 1. IP2 and IP3 are the corresponding intersubunit peptides of subtypes 2 and 3, respectively.

subtypes (Scheme I). The sequence of the C-terminal stretch of the HA1 subunit is also relatively conserved and has an important role in determining the tropism and infectivity of the virus (5, 8).

Recently an IgM producing hybridoma (Z38) was isolated from the spleen of an A/PR/8/34 (H1N1) influenza A virus-infected BALB/c mouse which secretes an HA-specific mAb which is not inhibitory in the hemagglutination assay (9). Z38 mAb reacts with the solid phase adsorbed influenza virus expressing uncleaved (HA0) molecules but does not bind to virus particles bearing cleaved HA. It was also shown that the Z38 mAb is able to inhibit the fusion activity of the virus in a dose-dependent manner (9).

Overlapping synthetic peptides corresponding to linear sequences of the HA1–HA2 intersubunit region were used to characterize the fine specificity of Z38 mAb (9). To clarify the antigenic and immunogenic properties of the HA-derived peptides, multiple antigenic peptides (MAPs) (10, 11) comprising repeated copies of the HA1 317–329 sequence (Scheme I) were also included. The immunological analysis of all these peptides (Table I) suggested that peptide conformation has a pivotal role in determining antibody (Ab) recognition and their capacity to elicit an Ab response. However, peptide conformation does not influence recognition by MHC class II restricted T cells (3, 10).

The design of synthetic immunogens against influenza A viruses which are presumably cross-reactive with different HA subtypes requires the conformational mapping of peptides corresponding to the relatively conserved intersubunit region of HA0. Previous circular dichroism (CD) and Fourier-transform infrared (FTIR) spectroscopic studies revealed a conformational bistability of IP1 and FP (12). An increased α-helicity (>30%) in the helix promoting solvent trifluoroethanol (TFE) was observed while the β-sheet character of the IP1 became predominant in aqueous solution at higher concentration or in the presence of octyl glucoside micelles. CD and FTIR spectroscopy have a "fast time scale" which makes possible the characterization of the static conformation of small, flexible peptides. Recently, an amide I component band between 1640 and 1635 cm^{-1} in the infrared spectrum of peptides has been suggested to be diagnostic of H-bonded β-turns (see Refs. 13 and 19). The detection of β-turns may be of importance in the design and conformational mapping of mid-sized immunogenic peptides functioning as B and/or T cell epitopes.

This paper reports CD and FT-IR spectroscopic studies on peptides covering the intact intersubunit region of HA0 representing the H1, H2, and H3 subtypes (Scheme I). The detailed conformational analysis of highly immunogenic multiple antigenic peptides including HA (H1) sequences has also been performed.

MATERIALS AND METHODS

Materials. The HA peptides IP2, IP3, and IP3[desGly^{21}] were synthesized as described for IP1 (12). The synthesis and characterization of MAP1 and MAP1-FP were reported earlier (10).

Circular dichroism. CD studies were performed on a Jobin-Yvon Mark VI dichrograph calibrated with epiandrosterone. NMR grade TFE (Aldrich) was used as solvent. Measurements were carried out at ambient temperature in 0.01- or 0.02-cm cells. The concentration of the samples ranged between 0.4 and 0.8 mg/ml. No concentration dependence was observed in this range. Molar ellipticity $[\theta]_M$, is given in deg cm^2/dmol. Spectra shown in Figs. 1 and 2 are smoothed by the Savitzky–Golay algorithm of the dichrograph.

Fourier-transform infrared spectroscopy. FTIR spectra (at a resolution of 4 cm^{-1}) were measured at room temperature on Nicolet 170SX and Magna 750 FTIR spectrometers. For experimental conditions see Table II. The analysis of the FTIR spectra was performed by a curve-fitting algorithm (20) which is based on the Fourier self-deconvolution (FSD) method of Mantsch *et al.* (for a review see Ref. 16). The components of the broad amide I band were determined by FSD (in some cases also by second derivation of the spectra). The resulting frequencies and the approaching intensities were given as input parameters into an in-house curve-fitting program which uses Gaussian or Cauchy (Lorentzian) functions or their combinations (sums or products) and a least-squares method (normalized Gauss–Marquardt method). The bending vibrational band of water in the 1700- and 1600-cm^{-1} region was removed by subtracting the spectrum of TFE (containing traces of water) with the help of the combination band of OH stretching and HOH deformation at 5293 cm^{-1}. FTIR spectra were also measured in KBr pellets to determine the

TABLE I

Immunological Characteristics[a] of Synthetic Peptides and Multiple Antigenic Peptides (MAPs) Representing the Intersubunit Region of Influenza A Virus Hemagglutinin

Abbreviated name[b]	Binding of Z38 mAb to the solid phase adsorbed peptides[c]	Binding of IP1 induced polyclonal Ab to solid phase adsorbed peptides	Recognition by CP1 induced T cells[d]	The ability to elicit an Ab response
IP1	+++	+++	+++	+++
IP1[D-Arg^{13}]	+++	+++	+++	+++
IP2	–	++	–	+++
IP3[desG^{21}]	–	–	–	+++
IP3	–	+	–	+++
CP1	–	–	+++	–
FP	–	–	–	–
MAP1	+	NT	++	–
MAP1-FP	+++	++	++	+++

Note. NT, not tested.

[a] For experimental details see Materials and Methods and Refs. 9 and 10. +++/++/+ correspond to relative binding efficiency determined at fixed peptide and Ab concentrations.

[b] Amino acid sequences are shown in Scheme I.

[c] Z38 mAb reacts with solid phase adsorbed A/PR/8/34 human influenza virus expressing uncleaved HA0 molecules but does not bind to virus particles bearing cleaved HA molecules. Z38 mAb is able to inhibit the fusion activity of the virus in a dose-dependent manner.

[d] Reactivity with the IP-12-29 T cell hybrid (11).

COO^- contribution of trifluoroacetate. Using reference spectra of sodium trifluoroacetate in KBr pellets and TFE solution, the contribution of trifluoroacetate could be removed. The spectra of the IP2, IP3, and IP3[desGly^{21}] peptides in Table II are trifluoroacetate corrected. This procedure allowed a direct comparison with the FTIR spectrum of IP1 reported earlier (12). After subtracting the contribution of trifluoroacetate, the deconvolved spectra still showed a component band near 1675 cm^{-1} which was assigned to the nonacceptor CO groups of the β-turn. In the spectra of the MAP peptides, the corresponding feature at ~1673 cm^{-1} is likely a composite of nonacceptor β-turn and trifluoroacetate bands.

Antibody binding assays. The reactivity of synthetic peptides with the Z38 monoclonal Ab and with polyclonal Ab raised against the peptides was studied by solid phase enzyme immunoassay (E/A) as discribed previously (9, 10). Briefly, MaxiSorp plates (Nunc) were coated with the synthetic peptides, incubated with the Ab and bound Ab was detected by biotinylated anti-mouse Ab (Southern Biotechnology). Peptide-specific polyclonal Ab was raised in Balb/c mice as described previously (9, 10).

RESULTS

Immunological Studies

Results of binding studies obtained with the Z38 mAb and with polyclonal Abs raised against the highly immunogenic IP1 peptide are published elsewhere (9, 10) and are summarized in Table I. It was found that both the virus induced Z38 mAb and the IP1 elicited polyclonal Abs bind to the solid phase-adsorbed IP1 and its D-Arg^{13} analog which decreases the possibility of *in vitro* degradation of IP1 by trypsin like endopeptidases. Z38 mAb shows increased reactivity with the solid phase-bound MAP1 compared to CP1 which forms its arms. The binding activity is further increased by linkage of the FP, to MAP1. As it was demonstrated in this study, polyclonal Abs elicited by IP1 cross-react with IP2 but not with IP3 or IP3[desGly^{21}] (Table I). As Abs are unable to bind to the FP, these results suggest that the C-terminal fragment of HA1 (CP1) comprises an Ab epitope. Recognition of this epitope is influenced by the amino acid sequence as revealed by the subtype specificity of Z38 and the cross-reactivity pattern of anti-peptide antibodies. However, the specificity studies suggest the role of peptide conformation in Ab recognition. The localization of an overlapping I-E^d restricted helper T-cell epitope recognizable in all the CP1 containing peptides is described elsewhere (11).

CD Spectroscopic Studies

The peptides IP1, IP2, and IP3 show helical CD spectra in TFE with comparable band intensities (Fig. 1). Deconvolution of the CD spectra by the Provencher–Glöckner method (14) resulted in 36% α-helix content for IP2 and decreasing helicity for IP3 and IP1. The significantly lower band intensities in the spectrum of IP3[desGly^{21}] and CP1 (Fig. 1) and the calculated low (24%) α-helix content of IP3[desGly^{21}] suggest that the helicity of IP peptides originates mainly from the C-terminal amphipathic region. (The expressed helicity in TFE of the intact FP has been confirmed by both CD and FTIR studies (12).) Deletion of Gly^{21} breaks the amphipathic order of the sequence of IP3 which leads to destabilization of the helix. In 50% TFE–water (v/v) the band intensities decrease but the α-helical features of the spectra are preserved (data not shown).

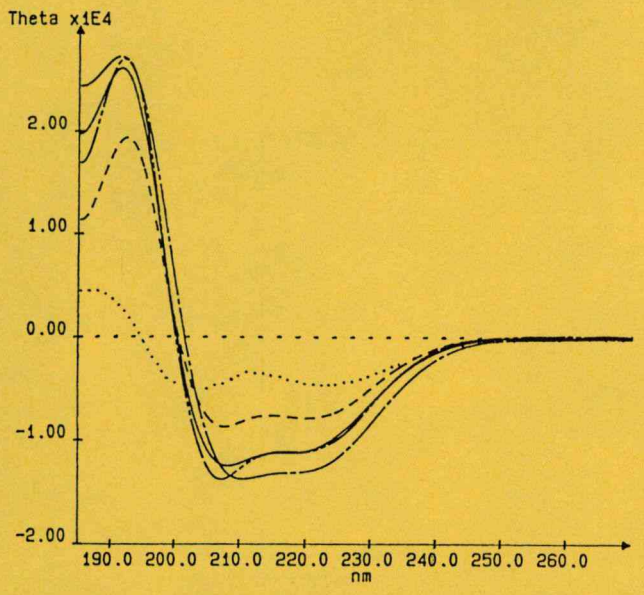

FIG. 1. CD spectra in TFE of the intersubunit peptides and CP1. IP1 (—), IP2 (-· · -), IP3 (-· -), IP3[desGly^{21}] (—-), and CP1 (· · ·). Concentration, 0.4–0.8 mg/ml; path length, 0.02 cm.

As shown in Fig. 2, the branched MAP peptides comprising the corresponding segments of IP1 show CD spectra in TFE which reflect lower amount of α-helix (20% calculated for MAP1-FP and 18% for MAP1). Interestingly, MAP1 lacking the amphipathic helical sequence of FP has a higher helix content than peptide CP1 from which its arms are composed.

FTIR Spectroscopic Studies

Results of FTIR spectroscopic studies are summarized in Table II. The component band which consistently appears in the spectra of the IP peptides between 1658 and 1656 cm^{-1} is indicative of the presence of α-helix (15). The broad component band which is also present in the curve-fitted spectra of IP1, IP2, and IP3 at ~1640 cm^{-1} is at the borderline of aperiodic (~1645 cm^{-1}) and β-turn (1640–1635 cm^{-1}) (13) spectral regions. The weak component near 1620 cm^{-1} likely belongs to some strongly H-bonded β-sheet structure (15, 16). The estimated 25% α-helix content of the IP peptides is compatible with the α-helicity (30–36%) calculated from the CD spectra.

The deconvolution of the CD spectra appears to overestimate the percentage of β-sheet (30–40%) and ignore the presence of aperiodic and β-turn conformer populations. The amino acid sequence of all three IP peptides features the Thr–Gly dipeptide segment at the N-terminus and the Arg–Gly dipeptide at the cleavage site. Both segments have a high propensity to form β-turns (17). Type II β-turns frequently give a class B CD spectrum (low intensity red-shifted variant of the CD of β-sheets) (18) which may obscure the deconvolution of the CD spectra and give rise to higher β-sheet percentages. Likewise, the broad component band at ~1640 cm^{-1} in the infrared spectra may be a composite of two or more bands including the component belonging to the type II β-turn.

Deconvolution of the FTIR spectra of MAP1 and MAP1-FP (Fig. 3) results in different patterns of the amide I component bands. Sharp and intensive components show up in both spectra at ~1661 cm^{-1}. This band reflects the presence of weakly H-bonded α-helix or 3_{10} helix (15, 16). The component bands appearing at 1651 and 1650 cm^{-1}, respectively, are at the borderline of the α-helix and aperiodic conformation. These bands are likely contributed by both the aperiodic and the "typical" α-helical conformations. The appearance of a component band at ~1640 cm^{-1} may be correlated with the type II β-turns (13, 19) predicted at the Thr–Gly core residues. It should be recalled that both MAPs are composed of four CP1 peptides which is expected to enhance the intensity of the component band attributed to the acceptor C=O of H-bonded β-turns (cf. the corresponding infrared spectra in Table II). The component of the nonacceptor amide C=Os of the turn(s) likely shows up above 1670 cm^{-1} (16) and overlaps with the COO^- band of trifluoroacetate. (Note that the trifluoracetate contribution was substracted from the spectra of the IP peptides but not from the spectra of MAPs; Table II.) Again, the weak component at 1623–1624 cm^{-1} is indicative of the presence of some β-sheet conformation.

Apparently, both branched peptides are present as a multicomponent mixture of conformers even in TFE solution. The stronger helical character of the branched peptide MAP1 relative to that of its "arms"; i.e., CP1 (20) can be explained by the cooperativity of side-chain interactions giving rise to an increase of α or 3_{10} helix conformation (Fig. 2).

DISCUSSION

In good correlation with conformational properties, the immunological analysis of peptides with the Z38 mAb and IP1 specific polyclonal antibodies (Table I) revealed a strong cross-reactivity of IP1, MAP1, and MAP1-FP. However, significant differences were found in the capability to elicit an antibody response and the antigenicity of these peptides. MAP1 similarly to CP1 is unable to elicit an Ab response, while IP1 and MAP1-FP are highly immunogenic without any carrier (Table I, last column).

The peptides IP1, IP1[D-Arg^{13}], and MAP1-FP were also found to contain an inscribed helper T-cell epitope (10) which can be recognized in all forms, i.e., CP1, IP1, MAP1, and MAP1-FP. This finding demonstrates that all constructs can be processed in a way which gives rise to CP1 (9, 10).

TABLE II

Amide I Infrared Frequencies of Hemagglutinin Intersubunit Peptides from Subtypes HS1-HS3 and MAP Peptides Subtype HS1[a]

Abbreviated name	Frequency (cm^{-1}) and relative intensity (%) of the component bands (in parentheses)	Assignment of major conformation-dependent amide I bands
IP1[b]	1688, 1674	*c*
	1656	α-Helix
	1642	Aperiodic, β-turn (acceptor)
	1619	β-Sheet
IP2	1689 (10), 1675 (20)	*c*
	1657 (25)	α-Helix
	1640 (16)	Aperiodic, β-turn (acceptor)
	1620 (3)	β-Sheet
IP3	1715 (3), 1680 (27)	*c*
	1660 (34)	α-Helix or 3_{10} helix
	1631 (20)	β-Sheet
IP3[desGly^{21}]	1716 (1), 1688.5 (10), 1675.5 (20)	*c*
	1658 (28.5)	α-Helix
	1639.5 (13)	Aperiodic, β-turn (acceptor)
	1621 (3.5)	β-Sheet
MAP1-FP	1710 (1.5), 1692.5 (7), 1680 (13)	*c*
	1673.5 (15)	TFA[d]
	1660.5 (17.5)	α-Helix (weakly H-bonded) or 3_{10} helix
	1651.5 (17)	α-Helix (or loop), aperiodic
	1637 (8.5)	β-Turn (acceptor C=O)
	1623 (3.5)	β-Sheet
MAP1	1708.5 (2), 1693 (7), 1681 (13.5)	*c*
	1672.5 (15)	TFA[d]
	1661.5 (15)	α-Helix (weakly H-bonded) or 3_{10} helix
	1650 (12)	α-Helix (or loop), aperiodic
	1637 (7.5)	β-Turn (acceptor C=O)
	1624 (2)	β-Sheet
CP1	1690 (12), 1676 (23)	*c*
	1663 (18)	α-Helix (weakly H-bonded) or 3_{10} helix
	1649 (51)	α-Helix (or loop), aperiodic
	1641 (10)	β-Turn (acceptor C=O)
	1623 (5)	β-Sheet

[a] Measurements were performed in TFE in a 0.02-cm KBr cell (IP peptides) or a 0.03-cm NaCl cell (MAP peptides), c = 0.5–1.5 mg/ml.
[b] Ref. 12. Only FSD analysis was performed.
[c] Assignment of high-frequency bands: ≥1710, COOH; ~1690, buried amide C=O or antiparallel β-sheet; 1680–1670, β-turn (non-acceptor C=Os), solvent exposed C=Os.
[d] The contribution of COO^- (trifluoroacetate) near 1675 cm^{-1} was subtracted only from the spectra of IPs and CP1 as described in Materials and Methods. The guanidinium group of Arg has a weak spectral contribution at ~1673 cm^{-1} (ν_{as}) and 1633 cm^{-1} (ν_2s) (16).

Our knowledge on the conformation of T cell epitopic peptides is based now on X-ray diffraction analysis of MHC class I and class II molecules cocrystallized with their peptide ligands (21, 22). Most recently the crystal structure of a monopeptidic complex of the human class II MHC protein HLA-DR1 has been solved to 2.75-Å resolution (23). The synthetic antigenic peptide corresponding to influenza virus hemagglutinin sequence (residues 306–318 of serotype H3, PKYVKQNTLKLAT) was found to bind to HLA-DR1 in an extended but somewhat twisted (polyproline II) conformation. From this picture and the structure of natural peptide ligands reported since 1991, a class II peptide binding groove with open ends can be deduced. The bound peptides extend out of both ends of the site and vary in length from 12 to 35 residues.

Based on comparative CD and FTIR spectroscopic studies, the 25- or 26-mer intersubunit peptides and their N-terminal 13- or 14-mer peptides (CP), shown to bind to I-E^d class II molecules and to HLA-B27 class I molecules (3), have no tendency to adopt α-helical conformation in aqueous solution. The helicity or turn content of the CP peptides from different subtypes is low even in the structure-promoting solvent TFE (12, 20). Conformational data suggest that the *CP peptides,* either free or part of the N-terminal region of IP peptides, have a flexible conformation. They tend to adopt a predominant extended structure: hence they can well

accommodate to the peptide binding groove of MHC molecules.

The *intersubunit peptides* have a more ordered conformation. Under the conditions used in the solid phase indirect immunoassay, they may undergo a surface-induced conformational switch, from α-helix to β-sheet, similar to that observed in the presence of octyl glucoside micelles (9, 12). Considering the predicted and experimentally supported β-turn encompassing the Arg–Gly residues at the cleavage site, the most probable conformation of IP peptides during B cell recognition is an antiparallel β-sheet starting with Ser^{9} and folded at the β-turn encompassing Arg^{13} and Gly^{14}. The N-terminal residues of IPs likely form repeats of β-turns. It is an intriguing question whether the β-turn(s)/β-sheet/β-turn/β-sheet conformational sequence suggested earlier (9) represents an Ab recognition motif or it is the positive charge of the central (or both) arginines of IP peptides which is responsible for the ability to elicit an Ab response. The subtype-independent and outstanding immunogenicity of the IP peptides, relative to the MAP1 peptide containing four central Arg residues, supports the first possibility.

According to the CD and FTIR studies discussed herein, the branched peptides may also adopt β-turn-like 10-membered H-bonded conformation(s). Up to three different types of 10-membered (C_{10}) H-bonded structures may be formed with the participation of the lysine α- and ϵ-amide groups playing the role of either the acceptor or the donor amides of H-bondings. In the MAP1-FP construct the lysine-based β-turns may replace the central Arg–Gly β-turn of the IP peptides. The immunogenicity and activity in a solid phase binding assay of MAP1-FP overrides that of the MAP1 peptide. This lays emphasis on the conformational role of the fusion region in Ab recognition. The cross-reactivity of Z38 mAb with the uncleaved HA0, IP1, and MAP1-FP supports the importance of the putative β-turn(s)/β-sheet/β-turn/β-sheet motive in Ab recognition. It is the higher helicity of IP3 and IP3[$desGly^{21}$] and the concomitant lack of this conformational motif which may prevent the binding of Z38 mAb to them in solid phase adsorbed form (Table I). The ability of the fusion region of IP peptides to form an amphipathic helix may be induced by chaperons and can be beneficial during transport processes.

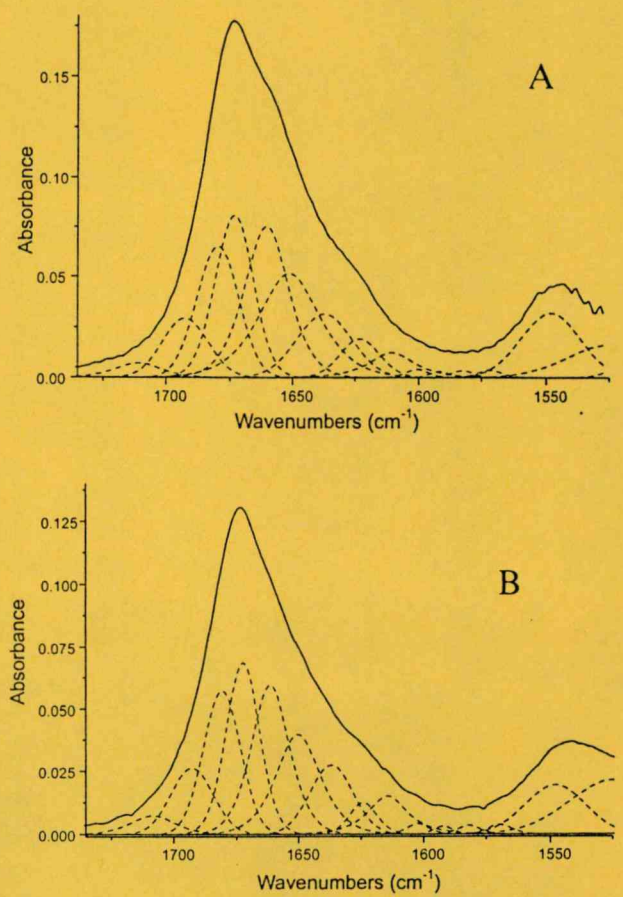

FIG. 3. Amide I region of the decomposed FTIR spectra in TFE of the intersubunit and MAP peptides. MAP1-FP (A), MAP1 (B). For FTIR data on the intersubunit peptides IP1, IP2, IP3, and IP3[des-Gly^{21}] and assignment of the component bands see Table II and Materials and Methods.

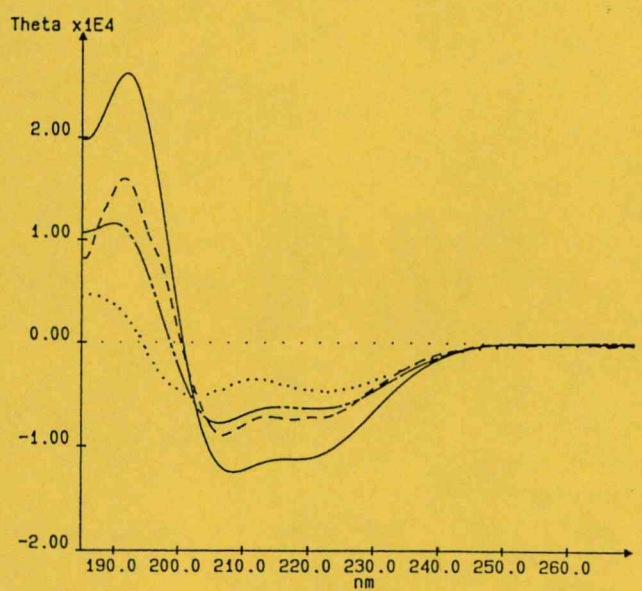

FIG. 2. CD spectra in TFE of the multiple antigenic peptides, MAP1-FP (—·—) and MAP1 (· · · ·). For comparison, the CD spectra of IP1 (—) and CP1 (· · ·) are also shown. Concentration, 0.4–0.8 mg/ml; path length, 0.02 cm.

ACKNOWLEDGMENTS

The authors thank for Judit Máthé for preparing the manuscript. The support of the Hungarian Grants OTKA I/3/2239, 2245, and 5/T017432 are highly appreciated.

REFERENCES

1. Wiley, D. C., and Shehel, J. J. (1987) *Ann. Rev. Biochem.* **56,** 365–394.
2. White, J. (1992) *Science* **258,** 917–924.
3. Rajnavölgyi, É, Nagy, Z., Daser, A., Horváth, A., Gogolák, P., and Kurucz, I. (1994) pp. 173–192 *in* Intelligence Unit Series (Rajnavölgyi, É., Ed.), Biomedical Publishers, Austin, TX.
4. Nobusawa, E., Aoyama, T., Kato, H., Suzuki, Y., Tateno, Y., and Nakajima, K. (1991) *Virology* **182,** 475–485.
5. Kawaoka, Y., Yamnikova, S., Chambers, T. M., Lvov, D. K., and Webster, R. G. (1990) *Virology* **179,** 759–767.
6. Barr, P. J. (1991) *Cell* **66,** 1–3.
7. Bullogh, P. A., Hughson, F. M., Skehel, J. J., and Wiley, D. C. (1994) *Nature* **371,** 37–43.
8. Walker, J. A., and Kawaoka, Y. (1993) *J. Gen. Virol.* **74,** 311–314.
9. Nagy, Z., Rajnavölgyi, É., Hollósi, M., Tóth, G. K., Váradi, Gy., Penke, B., Tóth, J., Horváth, A., Gergely, J., and Kurucz, I. (1994) *Scand. J. Immunol.* **40,** 281–291.
10. Tóth, G. K., Váradi, G., Nagy, Z., Monostori, É., Penke, B., Hegedüs, Z., Andó, I., Fazekas, Gy., Kurucz, I., Mák, M., and Rajnavölgyi, É. (1993) *Peptide Res.* **6,** 272–280.
11. Rajnavölgyi, É., Nagy, Z., Kurucz, I., Gogolák, P., Tóth, G. K., Váradi, Gy., Penke, B., Tigyi, Z., Hollósi, M., and Gergely, J. (1994) *Mol. Immunol.* **31,** 1403–1414.
12. Hollósi, M., Ismail, A. A., Mantsch, H. H., Penke, B., Váradi, Gy., Tóth, G. K., Laczkó, I., Kurucz, Z., Nagy, G. D., Fasman, G. D., and Rajnavölgyi, É. (1992) *Eur. J. Biochem.* **206,** 421–425.
13. Hollósi, M., Majer, Zs., Rónai, A. Z., Magyar, A., Medzihradszky, K., Holly, S., Perczel, A., and Fasman, G. D. (1994) *Biopolymers* **34,** 177–185.
14. Provencher, S. W., and Glöckner, J. (1981) *J. Biochemistry* **20,** 33–37.
15. Byler, M., and Susi, H. (1986) *Biopolymers* **25,** 269–487.
16. Surewicz, W. K., Mantsch, H. H., and Chapman, D. (1993) *Biochemistry* **323,** 389–394.
17. Wilmot, C. M., and Thornton, J. M. (1988) *J. Mol. Biol.* **203,** 221–232.
18. Woody, R. W. (1985) *in* The Peptides (Hruby, V. J., Ed.), Vol. 7, pp. 15–113, Academic Press, New York.
19. Mantsch, H. H., Perczel, A., Hollósi, M., and Fasman, G. D. (1992) *Biopolymers,* **33,** 201–207.
20. Holly, S., Majer, Zs., Tóth, G. K., Váradi, Gy., Rajnavölgyi, É., Laczkó, I., and Hollósi, M. (1993) *Biochem. Biophys. Res. Commun.* **193,** 1247–1254.
21. Falk, K., Rötzschke, O., Stevanovic, S., Jung, G., and Rammensee, H.-G. (1991) *Nature* **351,** 290–296.
22. Rötzschke, O., and Falk, K. (1994) *Curr. Opinion Immunol.* **6,** 45–51.
23. Stern, L. J., Brown, J. H., Jardetzky, Th. S., Gorga, J. C., Urban, R. G., Strominger, J. L., and Wiley, D. C. (1994) *Nature* **368,** 215–221.

3.7.

ELSEVIER

Immunology Letters 54 (1996) 135–144

immunology letters

Collaboration of TCR-, CD4- and CD28-mediated signalling in antigen-specific MHC class II-restricted T-cells

Péter Gogolák[a], Bence Réthy[a], Attila Horváth[a], G.K. Tóth[b], László Cervenák[a], Glória László[a], Éva Rajnavölgyi[a,*]

[a]*Department of Immunology, L. Eötvös University, Jávorka S. 14., H-2131 Göd, Hungary*
[b]*Department of Medical Chemistry, A. Szent-Györgyi Medical University, Szeged, Hungary*

Abstract

A previously developed experimental system was applied to obtain qualitative and quantitative data on the contribution of TCR-, CD4- and CD28-mediated signalling in the activation of an antigen specific T-cell hybridoma. All the three signal transducing receptors were stimulated by their natural ligands, and intermediate and late responses of an I-E^d restricted, $CD4^+$, influenza HA specific murine T-hybridoma (IP-12-7) were monitored by measuring the concentration of intracellular calcium $[Ca^{2+}]_i$ and secreted IL-2. This type of analysis of T-cell activation revealed: (i) calcium mobilization induced by peptide loaded APC requires rapid conjugate formation; (ii) a direct correlation between the magnitude of the intermediate and the late responses was observed as a consequence of differential TCR ligation modulated by peptide dose or by the presence CD4; (iii) considering the APC/peptide and T/APC ratios, the concentration dependence of the intermediate and late responses was similar in both assays but a substantial difference in the sensitivity of the two methods was observed; (iv) CD4 mediated signalling has a co-stimulatory effect predominantly at suboptimal in vitro conditions; and (v) sustained increase of $[Ca^{2+}]_i$ as well as the production of high concentrations of IL-2 is highly dependent on the CD28-B7 interaction. These results demonstrate that distinct peptide doses and the presence or absence of CD4 result in quantitative changes in T-cell responses, while the degree of CD28 mediated signalling has a qualitative affect on the outcome of T-cell activation, revealed by complete or partial inhibition of IL-2 secretion as a result of limited CD28-B7 interaction as well as by alteration in the duration and time kinetics of the calcium response.

Keywords: MHC class II-restricted T-cells; TCR-, CD4- and CD28-mediated signalling; Antigen specific T-cell hybridoma

1. Introduction

T-cells bearing $\alpha\beta$ antigen receptors (TCR) are extremely sensitive to low concentrations of ligands consisting of preformed peptide-MHC complexes [1]. The outcome of APC-T cell interaction is determined by the number of TCR engaged by specific complexes presented on the APC surface [2,3]. Despite of its high sensitivity the TCR binds with an apparent low affinity to its complex ligand although a relatively wide range of differences in TCR affinities have also been demonstrated [4–6], which in combination with TCR density and ligand concentration, has a major influence on T-cell development and function [7–13]. MHC molecules are promiscuous in terms of peptide binding and structurally related peptide ligands can alter the ultimate topology of interactions and consequently influence the mode and degree of T-cell activation [14,15]. The importance of affinity, clustering or conformational change of the TCR in T-cell activation, however, is still controversial [6,9].

The low affinity binding of TCR and the fast off rate of TCR-ligand interactions [13] suggests the involvement of antigen independent interactions in the formation of stable conjugates between APC and T-cells which also exercise an effect on the outcome of T-cell activation [16,17]. A large variety of cell surface molecules involved in this initial contact have been identified [18,19]. The CD4 and CD8 molecules bind to nonpolymorphic regions of MHC class I and II, respec-

* Corresponding author. Tel.: +36 273 45311; fax: +36 273 45147; e-mail: evaraj@alfa.elte.hu

0165-2478/96/$12.00
PII S0165-2478(96)02663-6

tively and function as adhesion molecules as well as co-receptors [20,21]. Signal transduction by these membrane structures is dependent on and closely linked to TCR ligation and coupled to phosphotyrosine kinases (PTK) [22,23]. LFA-1, ICAM-1 and other adhesion molecules of different superfamilies have been shown to be involved in APC T-cell contact [24–27]. The unique contribution of the CD28-B7 interaction in the APC T-cell contact and in providing a secondary signal for specific T-cells has been demonstrated [28,29]. The apparent affinity of the accessory molecules involved in APC T-cell interaction in most cases was suggested to be higher than that of the TCR for its ligand [4].

The well documented polarity and motility of T-cells provides a dynamic view of how T-cells monitor and get activated by APC presenting a sufficient amount of antigen derived peptides [30]. In this process antigen independent adhesion of T-cells to APC precedes and promotes ligation of TCR. The threshold necessary for initiating the signal transduction cascades is achieved if T-cells accumulate a series of ligation and dissociation events via their TCR [2,13]. Receptor mediated activation leads to the assembly of multimolecular signalling complexes at, and in close vicinity to TCR involved in specific interactions [31]. According to the widely accepted two signal model of T-cell activation, signalling events mediated by accessory molecules are dependent on TCR ligation but thereafter may be additive and lower the threshold for activation [12,32].

Based on these data T-cell responses involve a cooperative interaction between the TCR/CD3 complex, the accessory structures CD4/CD8 and the co-stimulatory molecule CD28. Multiple signalling pathways are involved in the initial membrane proximal events of T-cell activation including those mediated by PTK, the phospholipase-calcium-calcineurin pathway, the p21ras G protein mediated cascade and PI 3-kinase induced events [32–34]. The PLC/calcium pathway is predominantly initiated by the TCR, the PI-3 kinase pathway is primarily coupled to CD28 while p21ras and PTK are shared effectors [32].

The CD28 mediated T-cell signalling pathway has been identified as one of the most important costimulatory signals for naive T-cells which are able to augment IL-2 production and proliferation [29,32]. This pathway was also found to protect cells from anergy or apoptosis [35,36]. Combination of TCR and CD28 ligation results in higher levels of IL-2 than signalling via TCR or CD28 alone [32,37]. Whether the pathway initiated by CD28 is unique or merely alters the duration or magnitude of identical biochemical signals is still a question of controversy. Most of the studies performed to clarify these possibilities are based on data using mAb to cross-link TCR, CD4 or CD28 in different combinations [37,38].

In this study the contribution of TCR-, CD4- and CD28-mediated signalling in the activation of an antigen specific, MHC class II restricted, $CD4^+$ T-cell hybridoma was investigated by using natural ligand-mediated signalling via these receptors. To explore these questions we have taken advantage of a well defined system (Fig. 1) where the functional properties of a $CD4^+$ T-cell hybridoma and its $CD4^-$ variant has been characterized and a large set of overlapping peptides of known activity, in combination with APCs carrying different types and densities of adhesion molecules, can be used for T-cell activation [39,40]. To read-out intermediate and late responses of T-cell activation, mobilization of intracellular calcium and secretion of IL-2, respectively, were measured. Our system enabled the parallel monitoring of two T-cell activation signals and provided qualitative and quantitative measures for the relative contribution of TCR, CD4 and CD28 mediated signalling events in antigen specific T-cell activation.

2. Materials and methods

2.1. Synthetic peptides

The synthetic peptide 317–329 H1, covering the C-terminal of the HA1 subunit of the human influenza virus A/PR/34/8 (H1N2 subtype), was synthesized by the classical solid phase tBoc method as described previously [39,41,42]. The peptide was purified by HPLC (peptide purity > 96%) and characterized by amino acid analysis and mass spectroscopy.

2.2. Cell lines and monoclonal antibodies

In the T-cell activation assays the murine B-lymphoma line 2PK3 (ATCC TIB 203) was used as APC. The IP12-7 T-cell hybridoma was developed from a BALB/c mouse pre-immunized with the 317–329 H1 peptide and subsequently infected with the A/PR/8/34 human influenza virus [40]. For IL-2 quantitation the IL-2 dependent CTLL-2 (ATCC TIB 214) T-cell line was used. All cells were cultured in RPMI-1640 supplemented with 2 mM L-glutamine, 1 mM Na-pyruvate, 5×10^{-5} M 2-mercaptoethanol, antibiotics and 5% FCS (complete RPMI).

The monoclonal antibodies (mAb) against murine B7-1 (mAb 1610A1, hamster IgG) [43] and B7-2 (GL1, rat IgG2a) [44] were isolated from cell culture supernatants by protein G affinity chromatography and used in different concentrations as indicated in the corresponding figures. The cell line transfected with the CTLA-4-Ig fusion protein [45] was purified on anti-IgG immunosorbent Sepharose 4B column.

2.3. Monitoring T-cell activation by IL-2 production

IP12-7 T-hybridoma cells (2×10^4) were cultured in

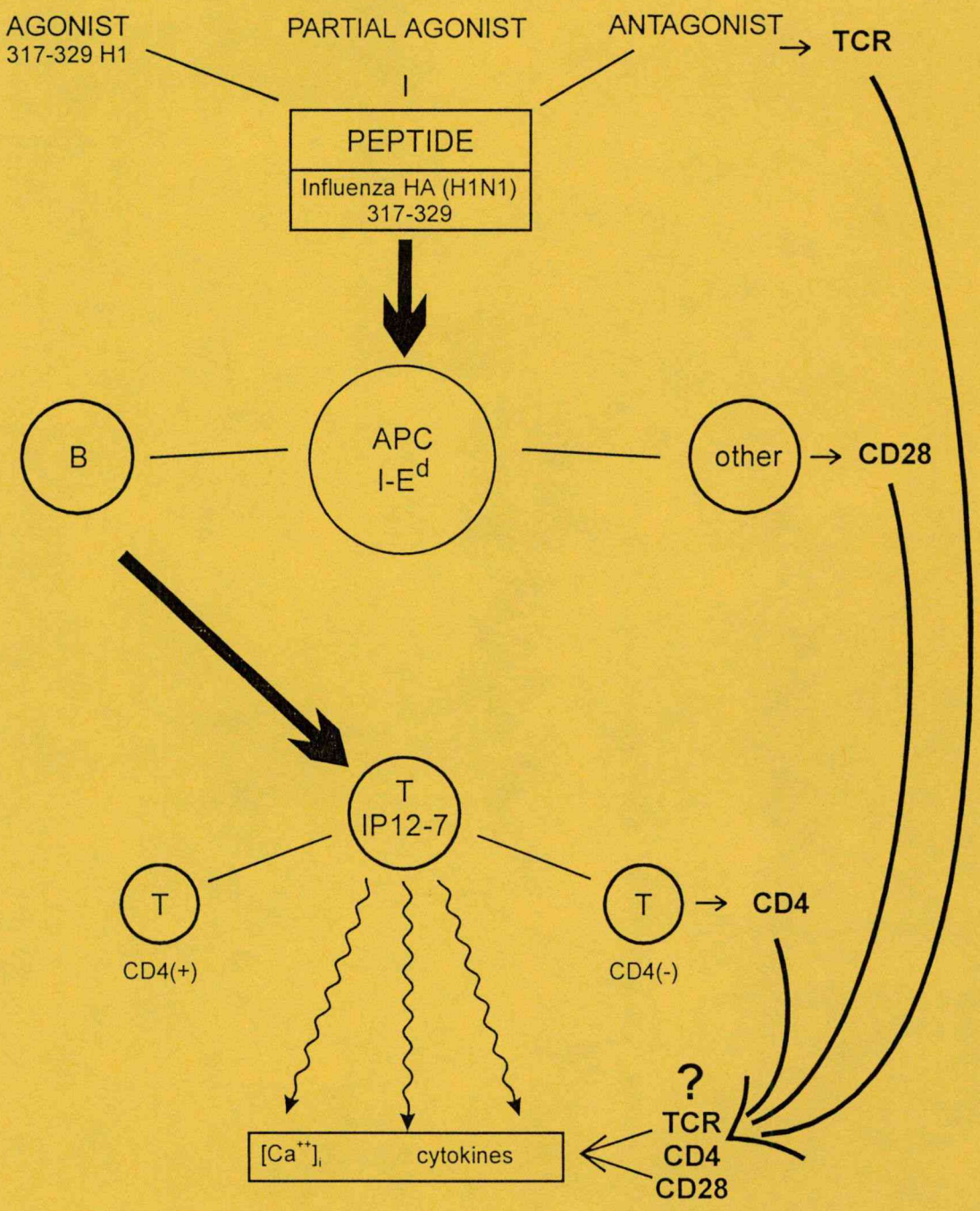

Fig. 1. The experimental system used for monitoring calcium mobilization and IL-2 production of specifically activated T-cells. Characteristics of the IP-12-7 T-cell hybridoma has been previously published [39]. The natural $CD4^-$ variant of the $CD4^+$ IP12-7 T-cell hybridoma was selected by repeated recloning procedures and characterized by the cell surface expression of the $\alpha\beta$ TCR and the CD4 membrane protein detected by flow cytometry. In the present study T-cell activation, induced in the presence of 2PK3 lymphoma cells as APC and of the 317–329 H1 agonist peptide, was measured.

96 well flat bottom tissue culture plates (Nunc) in complete RPMI in the presence of different concentrations of peptides with different numbers of 2PK3 APC. In the competition assay with anti-B7 mAb (equimolar mixture of mAb to B7-1 and B7-2) and CTLA-4-Ig fusion protein, different concentrations of mAb or CTLA-4 were added to the cultures before addition of the peptides. Culture supernatants (75 μl) were removed at 24 h of culture and transferred to secondary cultures where the amount of secreted IL-2 was measured by the proliferation of CTLL-2 detector cells. In this assay, CTLL-2 cells were used at 4×10^3 cells/well starting density and cell proliferation was measured by optical density (OD570) after addition of

(3-[4,5-dimethylthiazol-2-yl]-2,5-diphenyl-tetrazolium bromide (3-[4,5(MTT) or quantitated by ^{3}H-thymidine incorporation as previously described [39].

2.4. Measurement of intracellular calcium

For the measurement of intracellular calcium $[Ca^{2+}]_i$ the IP12-7 T-cell hybridoma cells suspended at 10^7/ml in complete RPMI were loaded with 5 μM fluo-3 in the presence of 100 μg/ml pluronic F-127 (Molecular Probes) at 37°C for 60 min under shaking. Followed by another 60 min incubation at 10^6/ml concentration in RPMI, the cells were washed twice with PBS and resuspended in complete RPMI.

Prewarmed (5 min at 37°C) samples of 5×10^5 fluo-3 loaded T-cells in 1 ml complete RPMI were mixed with 100 μl peptide pre-pulsed 2PK3 APC using different final APC concentrations or peptide doses, used for pre-incubation of APC with the 317–329 H1 peptide at 37°C for 90 min. According to the results of Jameson et al. [46] calcium flux in the T-cells was undetectable under these conditions unless the cells were centrifuged together. After pelleting together APC and T-cells for a short period of time (10–40 s), the mixture was immediately resuspended and $[Ca^{2+}]_i$ was measured for 8–15 min at 37°C. The cells were analysed by Beckton Dickinson FACStar (Beckton Dickinson, Mountain View, CA). The mean values of fluo-3 intensities measured in the whole cell population, calculated by the Becton Dickinson software at different points of time, were given. Dead cells were gated out according to their 7-amino-actinomycin D uptake, and an analysis gate, using forward and side scatter, was used to study a homogenous cell population, which consisted of mostly APC T-cell duplets as verified by light microscope.

3. Results

3.1. Intracellular calcium mobilization of antigen specific T-cells induced by peptide pulsed APC requires rapid conjugate formation

The B-cell lymphoma 2PK3 acts as a potent APC for the IP12-7 T-cell hybridoma when pre-pulsed with the 317–329 H1 peptide. As low as 1 nM concentration of 317–329 H1 is sufficient to induce IL-2 production (Fig. 3A). However, when 5×10^5 fluo-3 loaded IP12-7 cells were mixed with an equal number of peptide pulsed 2PK3 APC, no calcium mobilization was observed (Fig. 2A,B). Short centrifugation (10–20 s) followed by resuspension of the APC-T cell mixture resulted in sustained increase of $[Ca^{2+}]_i$. Fig. 2 demonstrates, that both the magnitude and the duration of the average calcium signal, detected at the population level (mean of $[Ca^{2+}]_i$), can dramatically be increased by elongation of the period of centrifugation or by combination of centrifugation with an additional short incubation period in the pellet (Fig. 2A,B). As revealed by control experiments, conjugation of T-cells with APC alone does not result in intracellular calcium mobilization (Fig. 2A,B). Fig. 2 also shows that higher ratio of APC, pre-pulsed with the 317–329 H1 peptide, results in an increased calcium signal (compare Fig. 3A and B). These results demonstrate that a fixed number of IP-12-7 T-cells can specifically be triggered for intracellular calcium mobilization in an APC and peptide dependent manner if rapid conjugate formation between APC and T-cells is supported by centrifugation.

3.2. The effect of differential TCR ligation on the early and on the late T-cell activation responses modulated by peptide dose

Based on the results demonstrated in Fig. 2, 1:1 APC:T cell ratio was used in further experiments and the cell mixture was pelleted for 30 s. As demonstrated in Fig. 3A, IP-12-7 T-cells responded to IL-2 production at a broad concentration range of the 317–329 H1 peptide. Using 2×10^4 T-cells and an equal number of 2PK3 APC the dose dependent range of IL-2 production was at 0.03–0.004 μg/ml peptide. $[Ca^{2+}]_i$ measured after conjugation of 5×10^5 T-cells with the same amount of 2PK3 APC, pre-pulsed with different concentrations of 317–329 H1 peptide, also resulted in dose dependent activation (Fig. 3B). The threshold for T-cell signalling in the calcium mobilization assay was at 0.1 μg/ml peptide concentration, however, the number of T-cells and APC was 25 times higher than in the functional assay (Fig. 3B). Considering the APC: peptide and T:APC ratios in both assays we conclude that the concentration dependence of the intermediate and late responses of the IP12-7 T-cell hybridoma is similar (0.004 μg/ml for a detectable response in both systems) but there is a substantial difference in the sensitivity of the two methods.

3.3. The effect of CD4 co-receptor on antigen specific T-cell activation

IL-2 production of the $CD4^+$ and $CD4^-$ variants of the IP-12-7 hybridoma was studied in the presence of 2PK3 APC, pre-pulsed with optimal concentration (25 μM) of the 317–329 H1 peptide using different numbers of APC added to 2×10^4 T-cells (Fig. 4A). As few as ~ 10 2PK3 APCs in the microcultures were sufficient to induce a detectable level of IL-2 production in the $CD4^+$ variant, while suboptimal APC numbers resulted in a lower concentration of IL-2 produced by the $CD4^-$ IP-12-7 T-cells under similar conditions. When APC, pre-pulsed with limited concentrations of 317–329 peptide (8–0.5 μM), were added at limited numbers (5000/

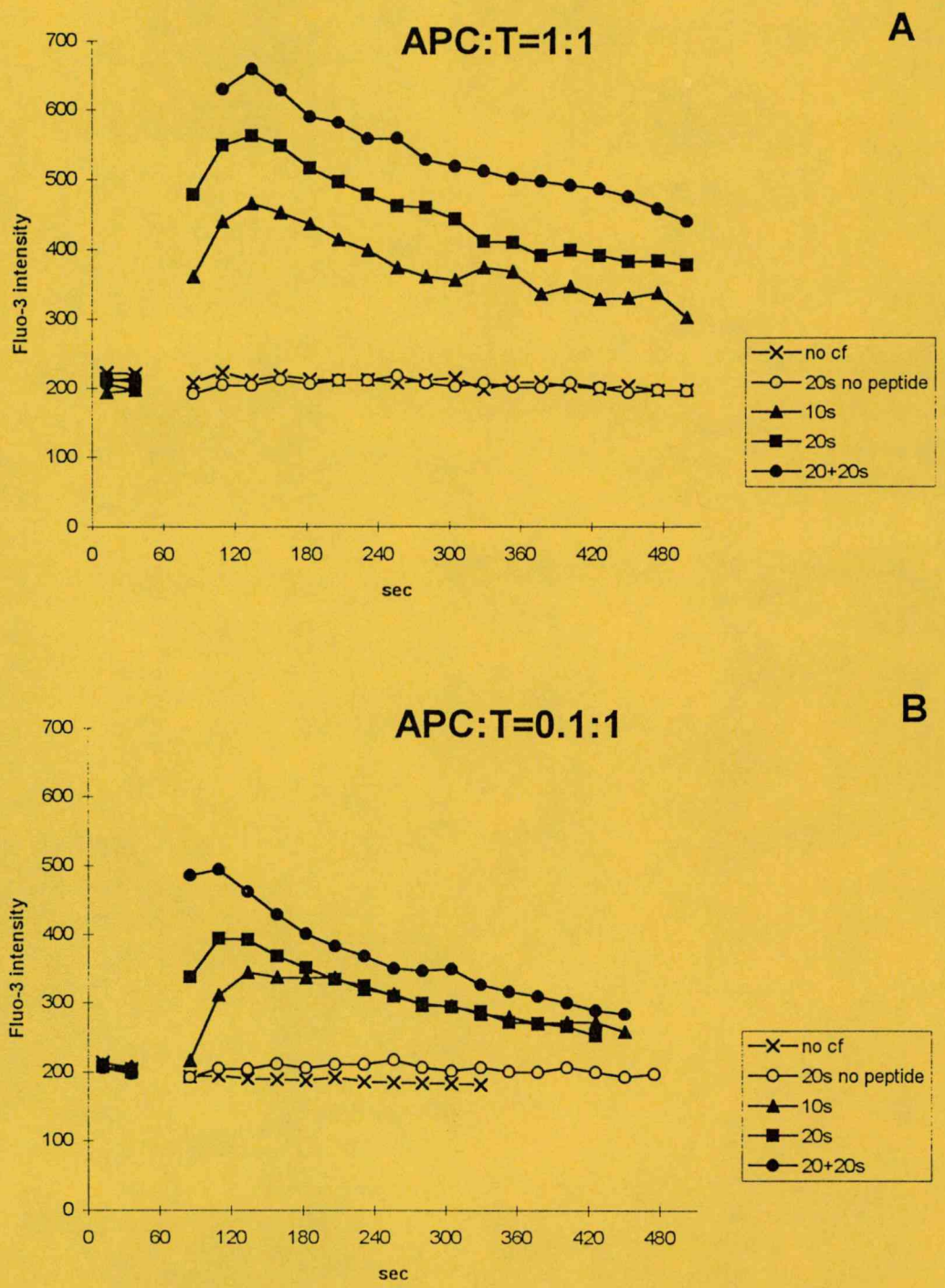

Fig. 2. Intracellular calcium mobilization detected in IP-12-7 T-cells after conjugate formation with peptide loaded APC. 1×10^6 fluo-3 loaded T-cells were mixed with 1×10^6 (A) or 1×10^5 (B) 2PK3 cells prepulsed with 100 μg/ml 317–319 H1 peptide, and centrifuged for 10 (▽) or 20 (■) s or for 20 s followed by an additional 20 s incubation in the pellet (●). As controls, cell mixture without centrifugation (X) or cell mixture containing 2PK3 cells not pulsed with the peptide and centrifuged for 20 s (○), were used.

well and 150/well in Fig. 4B,C, respectively) to 2×10^4 T-cells, marked differences in the amount of IL-2, produced by the $CD4^+$ and $CD4^-$ variants, were detected. These results point to the predominant role of CD4 co-receptors in T-cell activation primarily at limited peptide and APC concentrations.

Ca^{2+} mobilization in the $CD4^+$ and $CD4^-$ IP12-7 T-cell hybridomas was induced at 1:1 APC:T cell ratio and with a peptide pulse carried out at 100 μg/ml concentration (Fig. 4D). Corrected by the cell numbers these conditions correspond to an optimal APC number and 25 times lower but still optimal (0.4 μg/ml) peptide concentration in the functional assay (Fig. 4B). In good correlation with the IL-2

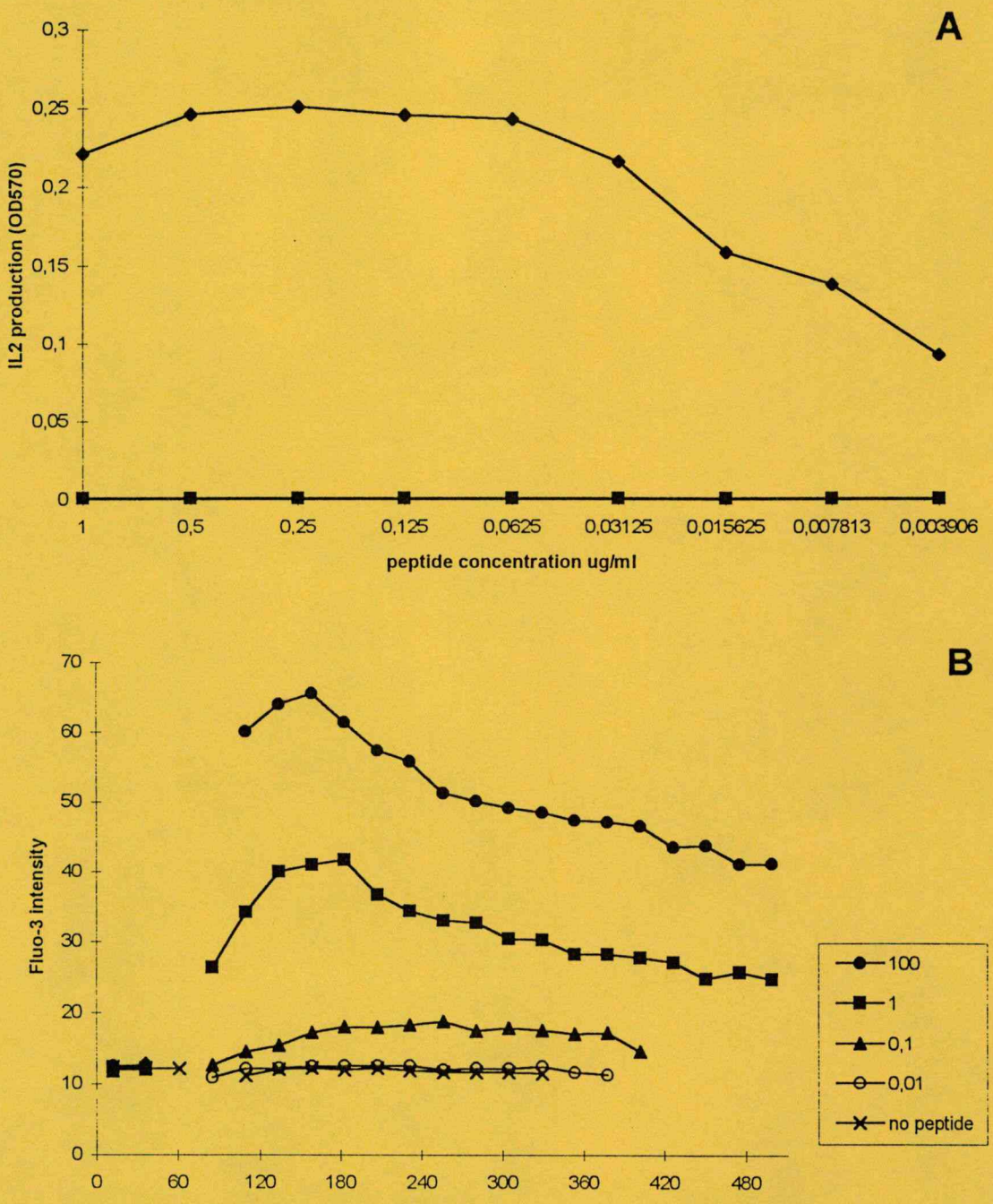

Fig. 3. Dependence of antigen specific T-cell activation on peptide dose. (A) T-cells (2×10^5) were incubated with 2×10^5 2PK3 APC in the presence of different concentrations of 317–329 H1 peptide for 24 h and the amount of secreted IL-2 was detected by using CTLL-2 indicator cells and the MTT assay. (B) Fluo-3 loaded T-cells (1×10^6) were mixed with 1×10^6 2PK3 cells in 100 μl volume which have been prepulsed with 100 (●), 1 (■), 0.1 (▽) or 0.01 (○) μg/ml 317–319 H1 peptide and centrifuged for 30 s. As a negative control, a cell mixture containing 2PK3 cells not pulsed with the peptide and centrifuged for 30 s (X), were used.

response, activation of the $CD4^-$ T-cells resulted in markedly lower calcium flux in terms of its magnitude (Fig. 4D). These data support our previous suggestion that the intensity of the calcium response is proportional to the degree of IL-2 production.

3.4. The role of CD28 accessory molecules in antigen specific T-cell activation

IL-2 production of IP-12-7 T-cells induced by 2PK3 APC, pre-pulsed with limited peptide concentration (0.01 μg/ml) can be inhibited by mAb direct-

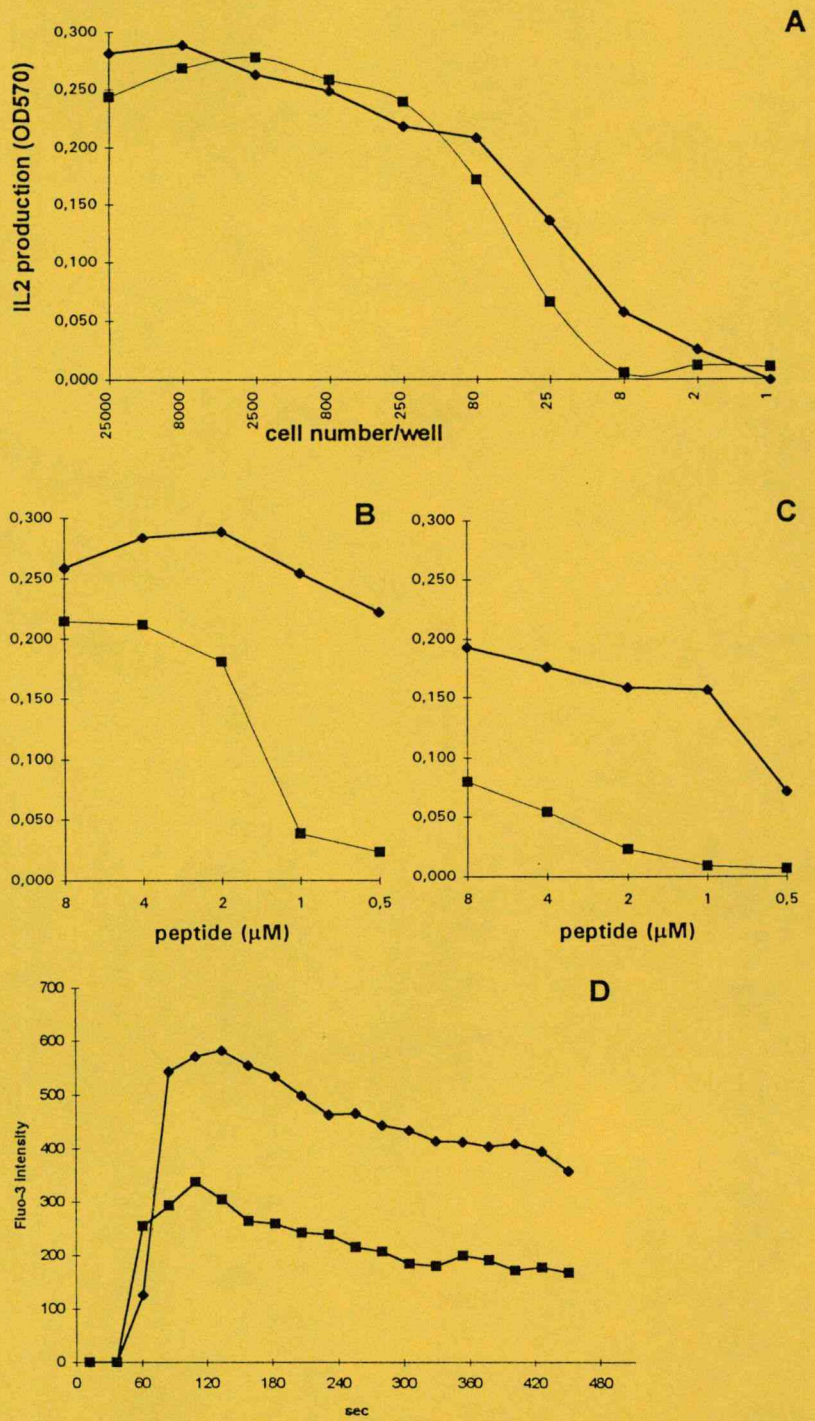

Fig. 4. The contribution of CD4 in antigen specific T-cell activation. (A) 2×10^5 CD4$^+$ (◆) and CD4- (■) IP12-7 T-cells were incubated with different numbers of 2PK3 APC pre-pulsed with 25 μg/ml 317–329 H1 peptide for 24 h and the amount of secreted IL-2 was detected by using CTLL-2 indicator cells and the MTT assay. (B,C) 2×10^5 CD4$^+$ (◆) and CD4$^-$ (■) IP12-7 T-cells were incubated with different concentrations of 317–329 H1 peptide in the presence of 5000 (B) or 150 (C) cell/well 2PK3 APC, and IL-2 production was detected as described above. (D) 1×10^6 fluo-3 loaded CD4$^+$ (◆) or CD4$^-$ (■) T-cells were mixed with 1×10^6 2PK3 cells pre-pulsed with 100 μg/ml 317–319 H1 peptide and centrifuged for 30 s. To compensate the slightly different fluo-3 loading of the two T-cells, mean values of $[Ca^{2+}]_i$ were normalized by the corresponding negative control values obtained with a cell mixture containing 2PK3 cells, which have not been pulsed with the peptide but centrifuged with the loaded T-cells for 30 s.

ing against B7 molecules (equimolar mixture of anti-B71 and anti-B7-2) or by the soluble CTLA4-Ig fusion protein in a dose dependent manner (Fig. 5A). Complete inhibition was achieved at high concentrations of both reagents but the mAb mixture blocking both B7-1 and B7-2 was more efficient when compared with the activity of soluble CTLA4-Ig. When 1×10^6 2PK3 APC were pretreated with these reagents at 10 μg/ml (corre-

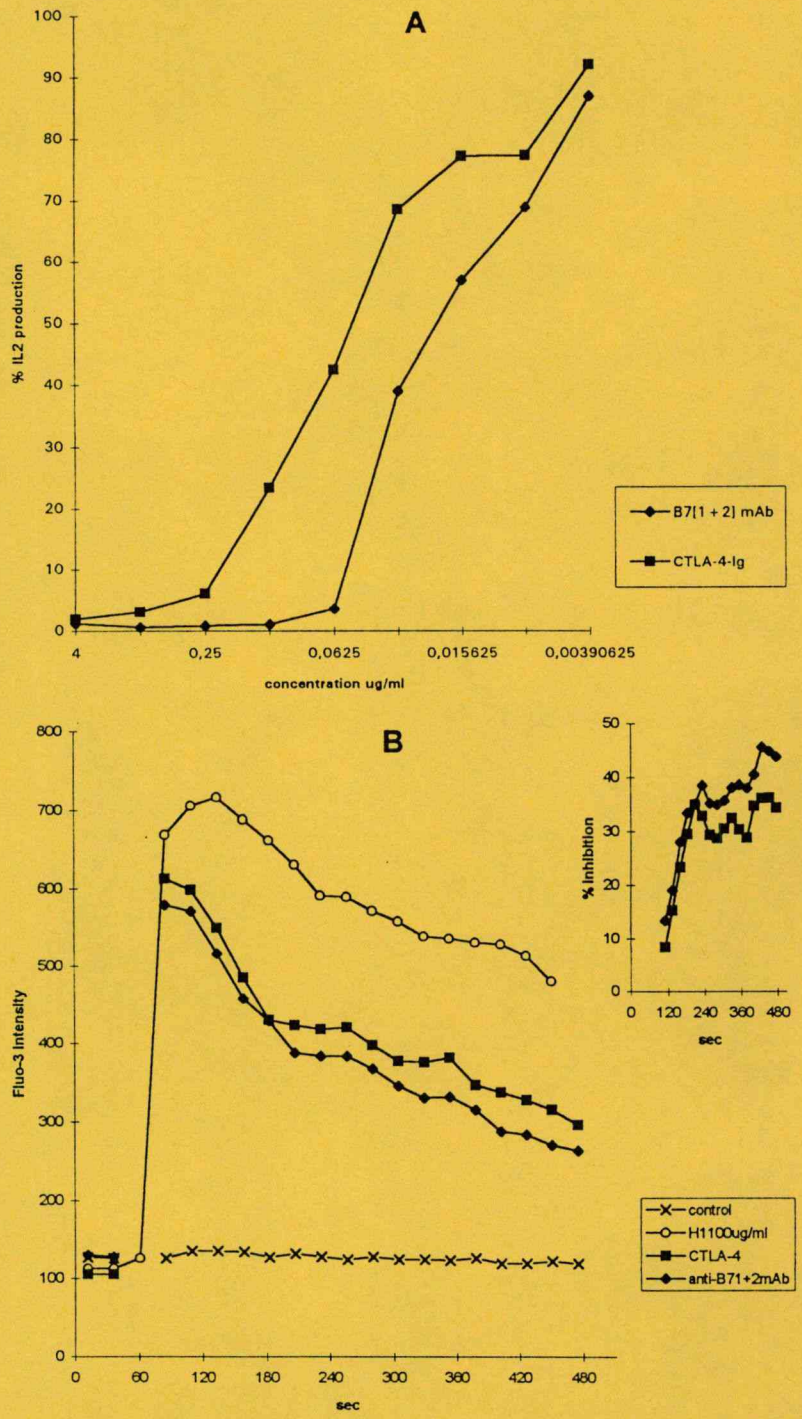

Fig. 5. Contribution of the CD28-B7 interaction in antigen specific T-cell activation. (A) 2×10^4 IP12-7 T-cells were incubated with 0.01 μg/ml 317–329 H1 peptide in the presence of the same amount of 2PK3 APC and different concentrations of equimolar mixture of B71 and B72 specific mAb (◆) or CTLA-4-Ig (■). (B) 1×10^6 fluo-3 loaded T-cells were mixed with 1×10^6 2PK3 cells, pre-pulsed with 100 μg/ml 317–319 H1 peptide, pretreated without (○) or with an equimolar mixture of B7-1 and B7-2 specific mAb (◆) or CTLA-4-Ig (■) and centrifuged with T-cells for 30 s. The insert provides another representation of the data where percentage of inhibition obtained by B7 specific mAb (◆) or CTLA-4-Ig (■) is given.

sponding to 0.2 μg/ml in the functional assay if normalized by cell numbers, Fig. 5A) and pre-pulsed with 100 μg/ml 317–329 H1 peptide (relevant to 0.02 ng/ml in the functional assay), a marked inhibition of the late phase of calcium mobilization was observed. Blocking of B7 molecules on 2PK3 APC conferred a marginal affect on the rapid influx of Ca^{2+} only, but inhibited the sustained increase of $[Ca^{2+}]_i$ at the late phase of the response (4–8 min in the insert of Fig. 5). Similar to the functional assay the slight difference in the inhibitory activity of the same concentrations of the blockers revealed the higher efficiency of anti-B7 mAb as com-

pared to CTLA4-Ig. These results prove the importance of CD28-B7 interaction in both the IL-2 production by and the calcium flux in the IP-12-7 T-cell hybridoma and demonstrate, that CD28 mediated signalling contributes to a large extent to the specific activation of IP-12-7 T-cells triggered by peptide loaded 2PK3 APC.

4. Discussion

The requirements of T-cell activation suggest that only a small fraction of MHC molecules are required to be occupied by the correct peptides [47,48]. The binary complex of peptide-MHC as a ligand for TCR is found in the cell surface of APC in the form of stable complexes (half life 7–12 h) which increases the chance to be recognized [49]. However, these complexes are always present together with a high number of MHC-peptide complexes irrelevant to a particular TCR. Therefore the right combinations are diluted out and the threshold for signalling is highly dependent on the number of successful TCR binding events and simultaneous costimulatory signals.

CD28 mediated activation is triggered by TCR related events [22] and subsequently provides an essential secondary signal required for IL-2 production and proliferation [23]. Lack of co-stimulation by CD28 leads to functional incompetence by induction of anergy or apoptosis [32,35,36]. Coincident ligation of both molecules, however, has additive effects; 2–4% of surface TCRζ/CD3 complexes associate with p59fyn(T), which forms large multimolecular aggregates with CD4-p56lck [50]. PI 3-kinase was shown to associate with both *src* kinases [31] while CD28 can bind about 5% of the total intracellular PI 3-kinase directly via its pYMXM motif [51]. This amount is many times greater than that observed for the TCR associated complex. Thus, CD28 ligation can augment suboptimal activation initiated by the TCR via PI 3-kinase mediated kinase activity and adaptor functions.

Signalling mediated by anti-CD28 mAbs is epitope dependent and is highly influenced by their isotype and cross-linking capacity. Some of these mAbs are able to induce calcium mobilization and p21ras activation in T-cell hybridomas, while B7 ligation by mAbs does not [38,52]. Products of inositol metabolism generated by CD28 associated PI-3-kinase occur with delayed kinetics, greater magnitude and prolonged duration when compared with their accumulation in response to ligation of the TCR [37]. CD28-mediated calcium mobilization and PI 3-kinase activation, however, seems to be restricted to $CD4^+$ T-cells [53,54].

In our studies the involvement and relative contribution of peptide specific TCR signalling, CD4 co-receptor function and CD28 mediated costimulation was investigated. All the three signal transducing receptors were stimulated by their natural ligands and an intermediate and a late response of a T-cell hybridoma was monitored by measuring concentrations of intracellular calcium $[Ca^{2+}]_i$ and secreted IL-2. Our results demonstrate that: (i) the intermediate response of an antigen specific T-cell hybridoma, IP12-7, induced by peptide loaded APC and monitored by the increase of $[Ca^{2+}]_i$ requires rapid conjugate formation; (ii) a direct correlation between the magnitude of the intermediate and the late responses, detected by calcium influx and IL-2 production, respectively, was observed as a consequence of differential TCR ligation modulated by peptide dose; (iii) CD4 mediated signalling has a co-stimulatory effect at suboptimal in vitro T-cell activation, which presumably resembles in vivo situations; and (iv) sustained increase of $[Ca^{2+}]_i$ as well as production of high concentrations of IL-2 is highly dependent on the CD28-B7 interaction.

Calcium mobilization or IL-2 production of the IP12-7 T-cell hybridoma could not be activated by soluble anti-CD3 mAb (data not shown) but if adsorbed to the surface of tissue culture plates, it induced IL-2 production. Peptide specific activation of IP12-7 T-cells was achieved with those APC, which express high density of adhesion molecules, and mAb to LFA-1 or ICAM-1 strongly inhibited IL-2 production (Gogolák et al., unpublished). These results, in good correlation with our present data, suggest that the antigen specific activation of IP12-7 is highly dependent on the firm adhesion to APC and on the secondary signals provided by APC. Under such conditions, fulfilled by a potent APC (2PK3) (Gogolák et al., unpublished), the IP12-7 TCR is extremely sensitive to the recognition of its specific peptide 317-329 H1 (Fig. 3A). In the presence of this APC the mobilization of intracellular calcium, even at high peptide and APC concentrations, could be observed after rapid conjugate formation only, which was ensured by a brief centrifugation of the interacting cells (Fig. 2A,B). If the peptide dose, applied in the two different assays, are corrected to identical T and APC cell numbers, the degree of calcium influx and the amount of secreted IL-2 was modulated to a similar extent by various peptide doses (Fig. 3A,B). This points to a direct correlation between the magnitude of the intracellular calcium signal and the amount of IL-2 production.

The requirement for CD4 mediated costimulation was more pronounced in the case of suboptimal peptide and APC concentrations and resulted in decreased magnitude of both the rapid and the sustained calcium responses (Fig. 4D) as well as in lower amounts of secreted IL-2 (Fig. 4A,B). However, using high peptide and APC concentrations for T-cell activation, the lack of CD4 molecules was completely compensated (Fig. 4A).

The inhibition conferred by blocking B7-CD28 mediated interactions mainly affects sustained $[Ca^{2+}]_i$ which, depending on the relative concentration of the inhibitors, can cause complete inhibition of IL2 production (Fig.

(Fig. 5A,B). This result suggest that a rapid but transient increase of $[Ca^{2+}]_i$ is insufficient for IL-2 production.

The experimental system introduced above enables to provide qualitative and quantitative data on the differential activation of an antigen specific, CD4+ T-cell hybridoma modulated by natural TCR-, CD4- or CD28-mediated signalling. This type of analysis of T-cell activation revealed that peptide dose and the contribution of CD4 results in quantitative changes in the outcome of the studied responses. However, the degree of CD28 mediated signalling has a qualitative affect on T-cell activation revealed by complete inhibition of IL-2 secretion and alteration of the duration and time kinetics of the calcium response.

Acknowledgements

The authors thank E. Veress for skilful technical assistance and G. Fazekas for valuable discussions. The B7-1 specific hamster antibody and the CTLA-4-Ig fusion protein were obtained from R.J. Hodes and K.S. Hatchcock, NIH).

References

[1] Karjalainen, K. (1994) Curr. Opin. Immunol. 6, 9–12.
[2] Valitutti, S., Müller, S., Cella, M., Padovan, E., Lanzavecchia, A. (1995) Nature 375, 148–151.
[3] Viola, A. and Lanzavecchia, A. (1996) Science 273, 104–106.
[4] Davies, M. M. and Chien, Y.- H. (1993) Curr. Opin. Immunol. 5, 45–49.
[5] Sykulev, Y., Brunmark, A, Jackson, M., Cohen, R.J., Peterson, P. A. and Eisen, H. N. (1994) Immunity 1, 15–22.
[6] Ashton-Rickardt, P. G.and Tonegawa, S. (1994) Immunol. Today 15, 362–366.
[7] Sebzda, E., Wallace, V. A., Mayer, J., Yeung, R. S. M., Mak, T. W. and Ohashi, P. S. (1994) Science 253, 1615–1618.
[8] Ashton-Rickardt, P. G., Bandeira, A., Delaney, J. R., Van Kaer, L., Pircher, H. P., Zinkernagel, R. M. and Tonegawa, S. (1994) Cell 76, 593–596.
[9] Janeway, Jr. C.A. (1995) Immunol. Today 16, 223–225.
[10] Groves, T., Katis, P., Madden Z., Manicham, K., Ramsden, D., Wu, G. and Guidos, C. J. (1995) J. Immunol. 154, 5011–5022.
[11] Rabinowitz, J.D., Beeson, C., Lyons, D.S., Davis, M.M., McConnell, H. M. (1996) Proc. Natl. Acad. Sci. 93, 1401–1405.
[12] Kim, D. T., Rothbard, J. B., Bloom, D. D. and Fathman, C. G. (1996) J. Immunol. 156, 2737–2742.
[13] Rothenberg, E. V. (1996) Science 273, 78–79.
[14] Sloan-Lancester, J. and Allen, P.M. (1996) Annu. Rev. Immunol. 14, 1–27.
[15] Madrenas, J., Wange, R. L., Wang, J. L., Isakov, N., Samelson, L. E. and Germain, R. N. (1995) Science 267, 515–518.
[16] Liu, Y. and Linsley, P.S. (1992) Curr. Opin. Immunol. 4, 265–270.
[17] Weiss, A. and Litmann, D.R. (1994) Cell 76, 263–274.
[18] Springer, T. A. (1990) Nature 346, 425–434.
[19] Clark, E. A. and Ledbetter, J. A. (1994) Nature 367, 425–428.
[20] Jenkins, M. K. and Johnson, J. G. (1993) Curr. Oppin. Immunol. 5, 361–367.
[21] Weiss, A. and Littman, D. R. (1994) Cell 76, 263–274.
[22] Chan, A. C. and Shaw, A. S. (1995) Curr. Opin. Immunol. 8, 394–401.
[23] Rudd, C. E., Janssen, O., Cai, Y-C., da Silva, A.J., Raab, M. and Prasad, K. V. S. (1995) Immunol. Today 15, 225–234.
[24] Lecomte, O., Haus, P., Barbat, C., Mazerolles, F., Fischer, A. (1994) Cell Immunol. 158, 376–388.
[25] Lub, M., van Kooyk, Y. and Figdor, C. G. (1995) Immunol. Today 16, 479–483.
[26] Stewart, M. P., Cabanas, C. and Hogg, N. (1996) J. Immunol. 156, 1810–1817.
[27] Linsley, P.S., Ledbetter, J.A. (1993) Immunology 11, 191–212.
[28] Lenschow, D.J., Walunas, T.L. and Bluestone, J. A. (1996) Annu. Rev. Immunol. 14, 233–258.
[29] Hutchcroft, J. E. and Bierer, B. E. (1996) J. Immunol. 156, 4071–4074.
[30] Negulescu, P. A., Kraiseva, T. B., Khan, A., Kerschbaum, H. H. and Cahalan, M. D. (1996) Immunity 4, 421–430.
[31] Wange, R. L. and Samelson, L. E. (1996) Immmunity 5, 197–205.
[32] Ward, S. G., June, C.H. and Olive, D. (1996) Immunol. Today 17, 187–197.
[33] Cantrell, D. A. (1996) Annu. Rev. Immunol. 14, 259–274.
[34] June, C.H., Ledbetter, J.A., Linsley, P.S. and Thompson, C.B. (1990) Immunol. Today 11, 211–216.
[35] Boise, L. H., Noel, P. J. and Thompson, C. B. (1995) Curr. Opin. Immunol. 7, 620–625.
[36] Boise, L. H., Minn, A. J., Noel, P. J., June, C. H., Accavitti, M. A., Lindsten, T., Thompson, C. B. (1995) Immunity 3, 87–98.
[37] Ueda, Y., Levine, B.L., Huang, M.L., Freeman, G.J., Nadler, L.M., June, C.H., Ward, S. G. (1995) Int. Immunol. 7, 957–966.
[38] Nunes, J.A., Collette, Y., Truneh, A., Olive, D. and Cantrell, D.A. (1994) J. Exp. Med. 180, 1067–1076.
[39] Rajnavölgyi, É., Nagy, Z., Kurucz, I., Gogolák, P., Tóth, G.K., Váradi, G., Penke, B., Tigyi, Z., Hollósi, M., Gergely, J. (1994) Mol. Immunol. 31, 1403–1414.
[40] Rajnavölgyi, É., Nagy, Z., Daser, A., Horváth, A., Gogolák, P., Kurucz, I. (1994) in: Synthetic Peptides in the Search for B- and T cell epitopes (É. Rajnavölgyi, Ed.) pp. 173–192, CRC Press, Austin.
[41] Hollósi, M., Ismail, A.A., Mantsch, H.H., Penke, B., Váradi, I.G., Tóth, G.K., Laczkó, I., Kurucz, I., Nagy, Z., Fasman, G.D., Rajnavölgyi, É. (1992) J. Biochem. 206, 421–425.
[42] Tóth, G.K., Váradi, G., Nagy, Z., Monostori, É., Penke, B., Hegedüs, Z., Andó, I., Fazekas, G., Kurucz, I., Mák, M., Rajnavölgyi, É. (1993) Peptide Res. 6, 272–280.
[43] Razi-Wolf, Z., Freeman, G. J., Galvin, F., Benacerraf, B., Nadler, L. and Reiser, H. (1992) Proc. Natl. Acad. Sci. 89, 4210–4214.
[44] Hatchcock, K. S., László, G., Dickler, H. B., Bradshaw, J., Linsley, P. and Hodes, R. J. (1993) Science 262, 905–907.
[45] Lane, P., Gerhard, W., Hubele, S., Lanzavecchia, A. and McConnell, F. (1993) Immunology 80, 56–61.
[46] Jameson, S.C., Carbone, F.R. and Bevan, M. J. (1993) J. Exp. Med. 177, 1541–1550.
[47] Demotz, S., Grey, H. M. and Sette, A. (1990) Science 249, 1028–1030.
[48] Harding, C. V., and Unanue, E. R. (1990) Nature 346, 574–576.
[49] Nelson, C.A., Petzold, S.J. and Unanue, E.R. (1994) Nature 371, 250–252.
[50] Beyers, A.D., Spruyt, L.L. and Williams, A. F. (1992) Proc. Natl. Acad. Sci. USA 89, 2945–2949.
[51] Prasad, K.V.S., Cai, Y.C., Raab, M., Duckworth, B., Cantley, L., Shoelson, S.E. and Rudd, C.E. (1994) Proc. Natl. Acad. Sci. USA 91, 2834–2838.
[52] Vandenberghe, P., Freeman, G.J., Nadler, L.M., Fletcher, M.C., Kamoun, M., Turka, L.A., Ledbetter, J.A., Thompson, C.B. and June, C.H. (1992) J. Exp. Med. 175, 951–960.
[53] Abe, R., Vanderberghe, P., Craighead, N., Smoot, D., Lee, K.P. and June, C.H. (1995) J. Immunol. 154, 985–997.
[54] Ghiotto-Ragueneau, M., Battifora, M., Truneh, A., Waterfield, M.D. and Olive, D. (1996) Eur. J. Immunol. 26, 34–41.

Mikrochim. Acta [Suppl.] 14, 445–447 (1997)

FT-IR Studies on T-cell Epitopic Deletion Peptides of Influenza Virus Hemagglutinin

Sándor Holly[1], Ilona Laczkó[2], Zsuzsa Majer[3], Gábor Tóth[4], and Miklós Hollósi[3,*]

[1] Central Research Institute of Chemistry, 1525 Budapest, P.O.B. 17, Hungary
[2] Institute of Biophysics, Biological Research Centre, 6701 Szeged, P.O.B. 521, Hungary
[3] Department of Organic Chemistry, Eötvös University, 1518 Budapest, P.O.B. 32, Hungary
[4] Department of Medical Chemistry, Szent-Györgyi Medical University, 6720 Szeged, Hungary

Abstract. Fourier-transform infrared spectroscopy was used to compare the conformational mobility of deletion analogues of epitopic peptides from three serotypes (HS1–HS3) of the HA1 sub-unit of the cleaved human influenza virus hemagglutinin. The peptides are present as multicomponent mixtures of conformers even in the structure-promoting solvent trifluoroethanol. Special attention is given to the question whether or not vibrational spectroscopy is capable of monitoring the conformation in solution of mid-size synthetic peptides which may have side-chain and/or counter-ion infrared contributions in the amide I region.

Key words: hemagglutinin, FT-IR spectroscopy, peptide conformation, side-chain absorption, T-cell epitope.

Our recent circular dichroism and Fourier-transform infrared (FT-IR) studies on peptides representing the C-terminal of the HA1 sub-unit of human influenza A virus have demonstrated changes of conformation in dependence on serotype-related differences of the amino-acid sequence [1]. Interestingly, the peptide showing the highest α-helix content has proved to be less potent to induce in vivo T-cell response [2].

According to X-ray crystallographic data epitopic peptides bind to the histocompatibility proteins in extended rather than helical conformation [3]. Since an amphipathic helical structure has been proposed for T-cell epitopic peptides [4], the ability of a switch from α-helix to extended conformation appears to be a prerequisite for good antigenic and immunogenic properties. This paper reports FT-IR spectroscopic studies performed on deletion analogues (Table 1) representing the C terminal epitopic region from different serotypes (HS1–HS3) of hemagglutinin.

* To whom correspondence should be addressed

Experimental

The peptides were synthesized by the solid-phase technique, utilizing Boc chemistry [1]. The crude peptides were purified by reversed-phase HPLC and characterized by HPLC, FAB mass spectrometry and FT-IR spectroscopy. According to the FT-IR measurements in KBr pellets, except for HS1a and HS1b all the peptides were present as trifluoroacetate (TFA) salts. Infrared measurements (at a resolution of 4 cm^{-1}) were performed on a Nicolet 170SX spectrometer. A KBr cell of 0.041 cm path-length was used; the concentration of the samples was ~ 1 mg/ml. The FT-IR spectra were analysed by a normalized least-squares curve-fitting program using products of Gauss and Lorentz curves (Holly et al. personal communication). The position of the component bands is based on Fourier self-deconvolution [5].

Table 1. Amino acid sequence of deletion peptides from C-terminal region of the cleaved influenza virus A hemagglutinin (HA1) from different serotypes

Serotype and location	Abbreviation	Sequence
$HS1_{317-329}$	HS1	VTGLRNIPSIQSR
$HS1_{319-328}$	HS1a	GLRNIPSIQS
$HS1_{320-328}$	HS1b	LRNIPSIQS
$HS1_{320-329}$	HS1c	LRNIPSIQSR
$HS2_{317-329}$	HS2	ATGLRNVPQIESR
$HS2_{319-328}$	HS2a	GLRNVPQIES
$HS2_{320-328}$	HS2b	LRNVPQIES
$HS2_{320-329}$	HS2c	LRNVPQIESR
$HS3_{316-329}$	HS3	LATGMRNVPEKQTR
$HS3_{319-328}$	HS3a	GMRNVPEKQT
$HS3_{320-328}$	HS3b	MRNVPEKQT
$HS3_{320-329}$	HS3c	MRNVPEKQTR

Table 2. Characteristic amide I infrared frequencies of deletion peptides from the C-terminal region of cleaved hemagglutinin (HA1) serotypes HS1–HS3

Component bands (cm^{-1})						
Peptides	Free (shielded) amides	Solvated amides	α-Helix or 3_{10} helix	Aperiodic	β-Turn	β-Sheet
HS1	1677 (26)	1666.5 (12)	1657.5 (18)		1642.5 (12)	1622 (5)
	1675		1660sh			1624
HS1a	1679 (18)		1662 (29)			1632 (27)
(no TFA)	1677		1663			1633
HS1b	1678 (32)		1661 (33)		1637 (6)	1621 (10)
(no TFA)	1673		1665		1634	1623
HS1c	1675.5 (48.5)		1659 (26)			1631.5 (7)
	1675		1662			1634
HS2	1680 (48)	1664 (22)	1651 (21)			1621 (7)
	1674	1662				1622
HS2a	1675 (40)		1658 (14)	1644 (11)		1622
	1676		1663	1647		1623
HS2b	1676 (39)		1659 (11)	1649 (16)		1619 (7)
	1676		1662			1622
HS2c	1676 (48)		1650.5 (11)	1645 (6)		1623 (12.5)
	1676		1660-65sh	1645-50sh		1620
HS3	1677 (22.5)		1659.5 (34)		1641 (3)	1624 (8.5)
HS3a	1676 (31)		1659 (14)		1642 (9)	1621 (9)
	1676		1658		1641	1621
HS3b	1676 (34)		1661 (22)			1626 (15)
	1676		1663			1626
HS3c	1676 (38.5)		1660 (20)			1626.5 (15)
	1676		1662sh			1625.5

In parenthesis: relative intensity in percentage. Only components with ≥5% are listed. The corresponding maximum or shoulder in the FSD spectra is underlined. Weak high frequency component bands at ~1690 cm^{-1} (shielded amide carbonyls or the satellite band of antiparallel β-sheets), ~1700 cm^{-1} (C=O of H-bonded COOH), and ~1715 cm^{-1} (C=O of free COOH) are not listed.

Results and Discussion

The frequencies and assignments of the component bands are listed in Table 2. The deletion peptides are present as mixtures of conformers even in trifluoroethanol (TFE) solution. The removal of the N- and C-terminal residues of the peptide HS1 leads to increased helicity, which is surprisingly high in HS1b. By contrast, truncation of HS2 and HS3 peptides decreases the relative amounts of 3_{10} or weakly H-bonded α-helical conformers. All peptides show some tendency to adopt extended or β-pleated sheet conformation. However, because of the side-chain contribution (band of the guanidinium ion at 1633 cm^{-1}) of the Arg residues to this region, the relative amount of β-sheet is not easy to infer from the curve-fitted spectra containing one or two component bands between 1640 and 1600 cm^{-1}. The $\nu_{as}CO_2^-$ band of the trifluoroacetate counter-ion appears at 1673 cm^{-1} in overlap with the $\nu_{as}NCN$ band of the guanidinium group. The presence of this band in the spectra of HS1a and HS1b containing no trifluoroacetate suggests that linear peptides have a uniform band in this amide I region. Thus, the component band at ~1675 cm^{-1} in the IR spectra of epitopic peptides HS1–HS3c may also be indicative to amide carbonyls exposed to the solvent but not involved in strong oriented intramolecular or intermolecular H-bonds of ordered secondary structures. Our results suggest that an analysis of the high-frequency (> 1660 cm^{-1}) region of the FT-IR spectra of trifluoroacetate salts of small Arg-containing peptides requires special attention.

Acknowledgement. This work was supported by grants OTKA 1995-T017432 (to M. H.) and 1995-T016516 (to I.L.).

erences

S. Holly, Zs. Majer, G. K. Tóth, G. Váradi, É. Rajnavölgyi, I. Laczkó, M. Hollósi, *Biochem Biophys. Res. Comm.* 1993, *193*, 1247.

É. Rajnavölgyi, *Immunology Today* 1992, *13*, A17.

[3] D. R. Madden, J. C. Gorga, J. L. Strominger, D. C. Wiley, *Nature* 1991, *353*, 321.

[4] C. DeLisi, J. A. Berzofsky, *Proc. Natl. Acad. Sci. USA* 1985, *82*, 7048.

[5] H. H. Mantsch, D. J. Moffat, H. G. Casal, *J. Mol. Structure* 1988, *173*, 285.

Immunology Letters

Volume 56, Issue 1-3, pp. 267-267, May, 1997

Differential T cell activation regulated by antigen presenting cells

Authors

P. Gogolak, B. Rethy, A. Horvath, G.K. Toth, E. Buzas, L. Cervenak, G. Laszlo, E. Rajnavolgyi

Abstract

Introduction: To obtain qualitative and quantitative data on the contribution of antigen presenting cell (APC) mediated signals in T cell triggering, the activation of three MHC class II restricted T cell hybridomas of distinct specificity was studied in the presence of various APC. Materials and Methods: The three signal transducing receptors of T cells, i.e. TCR, CD28 and CD4, were stimulated by their natural ligands expressed on the surface of a series of APCs with characterized phenotypes. The intermediate and late responses of T cells to different doses of peptide antigens presented on various APC was monitored by measuring intracellular calcium influx and IL2 production, respectively. The role of CD4 was studied by using a CD4- T cell subclone, contribution of CD28 was studied in the presence or absence of B7-specific antibodies or of soluble CTLA4. Results: Analysis of T cell activation revealed that i) calcium mobilization induced by peptide loaded APC requires rapid conjugate formation highly dependent on the expression pattern of adhesion molecules on APC; ii) a direct correlation was observed between the magnitude of the calcium influx and the concentration of secreted IL2 induced by differential TCR ligation modulated by peptide dose or by the presence or absence of CD4; iii) measured at identical APC/peptide and T/APC ratios, the intermediate and late responses of T cells to different peptide concentrations was similar; iv) a substantial difference in the sensitivity of the two methods, used for monitoring T cell activation, was observed, v) CD4 mediated signalling has a co-stimulatory effect predominantly at suboptimal in vitro conditions; vi) sustained increase of $[Ca^{2+}]_i$ as well as the production of high concentrations of IL2 is highly dependent on the appropriate CD28-B7 interaction determined by the APC; vii) the response of a certain T cell to peptide analogs is highly dependent on APC which can influence the agonistic or antagonistic behaviour of a peptide. Conclusion: These results demonstrate that distinct peptide doses and the presence or absence of CD4 results in qualitative changes of the T cell response, while the degree of CD28 mediated signalling has a qualitative affect on the outcome of T cell activation. This was revealed by the decreased duration and altered time kinetics of the calcium response, by the complete or partial inhibition of IL2 secretion at limited CD28-B7 interaction and by the differential recognition of altered peptide ligands in the presence of different APC.

PII: s0165247897879059

Eur. J. Immunol. 1997. 27: 3105–3114

Éva Rajnavölgyi[1], Attila Horváth[1], Péter Gogolák[1], Gábor K. Tóth[2], György Fazekas[1], Mati Fridkin[3] and Israel Pecht[3]

[1] Department of Immunology, L. Eötvös University, Göd, Hungary
[2] Department of Medical Chemistry, A. Szent-Györgyi University, Szeged, Hungary
[3] The Weizmann Institute of Science, Rehovot, Israel

Characterizing immunodominant and protective influenza hemagglutinin epitopes by functional activity and relative binding to major histocompatibility complex class II sites

In the present study the analysis of functional activity and major histocompatibility complex (MHC) binding of two adjacent MHC class II-restricted epitopes, located in the C-terminal 306–329 region of human influenza A virus hemagglutinin 1 subunit (HA1) conserved with subtype sequences and not affected by antigenic drift, was undertaken to explore the hierarchy of local immunodominance. The functional activity of two T cell hybridomas of the memory/effector Th1 phenotype in combination with *in vivo* immunization studies provided a good tool for investigating the functional characteristics of the T cell resonse. The *in vitro* binding assays performed with a series of overlapping, N-terminal biotinylated peptides covering the 306–341 sequence enabled us to compare the relative binding efficiency of peptides, comprising two distinct epitopes of this region, to I-E^d expressed on living antigen-presenting cells. Our studies revealed that (i) immunization of BALB/c mice with the 306–329 H1 or H2 peptides resulted in the activation and proliferation of T cells recognizing both the 306–318 and the 317–329 epitopes, while the 306–329 H3 peptide elicits predomonantly 306–318-specific T cells, (ii) the 317–329 HA1 epitope of the H1 and H2 but not the H3 sequence is recognized by T cells and is available for recognition not only in the 317–329 peptide but also in the extended 306–329 or 306–341 peptides, (iii) the 306–318 and the 317–329 hemagglutinin peptides encompassing the H1, H2 but not the H3 sequence bind with an apparently similar affinity to and therefore compete for I-E^d binding sites, and (iv) the 317–341, the 317–329 peptides and their truncated analogs show subtype-dependent differences in MHC binding and those with lower binding capacity represent the H3 subtype sequences. These results demonstrate that differences in the binding capacity of peptides comprising two non-overlapping epitopes located in the C-terminal 306–329 region of HA1 of all three subtype-specific sequences to MHC class II provide a rationale for the local and also for the previously observed *in vivo* immunodominance of the 306–318 region over the 317–329 epitope in the H3 but not in the H1 or H2 sequences. In good correlation with the results of the binding and functional inhibition assays, these data demonstrate that in the H1 and H2 subtypes both regions are available for T cell recognition, they compete for the same restriction element with an appearently similar binding efficiency and, therefore, function as co-dominant epitopes. Due to the stabilizing effect of the fusion peptide, peptides comprising the 306–341 or 317–341 H1 sequences are highly immunogenic and elicit a protective immune response which involves the production of antibodies and interleukin-2 and tumor necrosis factor producing effector Th1 cells both directed against the 317–329 region. Based on the similarity of the I-E^d and HLA-DR1 peptide binding grooves and motifs, these results suggest that amino acid substitutions inserted to the H3 subtype sequence during viral evolution can modify the relative MHC binding capacity and invert the local hierarchy of immunodominance of two closely situated epitopes that are able to bind to the same MHC class II molecule.

[I 16269]

1 Introduction

Complex viral proteins carry multiple potential T cell epitopes but the response is focused to only a few immunodominant determinants. The factors dictating immunodominance include peptide affinity to MHC, antigen processing and the repertoire of T cells [1, 2]. In viral infection, demonstrated primarily by cytotoxic T cells, immunodominant epitopes elicit T cells detected during the course of natural infection, while subdominant epitopes evoke little or no response; however, the T cells activated by peptide immunization recognize virus-infected cells [3–5]. This type of limited diversity in specific T cell responses may select for pathogens that carry mutations in the dominant T cell epitopes and, therefore, may support escape from immune control [6, 7].

É.R. and A.H. contributed equally to this work.

Received September 24, 1996; in revised form August 18, 1997; accepted September 11, 1997.

Correspondence: Éva Rajnavölgyi, Department of Immunology, L. Eötvös University, Jávorka S. 14., H-2131 Göd, Hungary
Fax: +36-273-45147;
e-mail: evaraj@alfa.elte.hu

Abbreviations: HA: Hemagglutinin HA0: Immature hemagglutinin **HA1:** Subunit 1 of hemagglutinin HA2: Subunit 2 of hemagglutinin

Key words: Immunodominance / Major histocompatibility complex class II / Peptide binding / Influenza hemagglutinin

0014-2980/97/1212-3105$17.50+.50/0

The membrane protein hemagglutinin (HA) of human influenza A viruses is the major target of neutralizing antibody (Ab) and helper T (Th) cell responses (reviewed in [8–10]). A majority of $CD4^+$ memory T cells elicited by viral infection recognize HA1 regions identified as major Ab binding sites and their recognition is influenced by amino acid substitutions generated by antigenic drift [8, 11, 12]. The major HA1 site of the H3 subtype, recognized by Th cells in BALB/c mice, is covered by the 177–199 sequence comprising both I-A^d- and I-E^d-restricted epitopes [11, 12]. The T cell response against the H1 subtype focuses to three major regions located within the 110–120, 126–138 and 303–313 sequences [9, 13, 14]. In contrast to these variant HA1 regions, the C-terminal 24 amino acids of HA1 are characterized by subtype-specific but conserved sequences within the H1, H2 and H3 subtypes [15, 16]. BALB/c mice are high responders to the 306–329 H3 peptide and the peptide-specific response is directed against the 306–318 region, demonstrating its intrapeptide dominance over the C-terminal fragment [17, 18].

The H3N2 subtypes of human influenza A viruses have been common pathogens of recently occurring epidemics since 1968 [19–21] and the 306–329 sequence of H3 HA1 was also demonstrated to be immunodominant in the human system both at the population and clonal levels when T cells of infected individuals were activated with purified HA [22]. T cell clones isolated from influenza virus-infected individuals recognized both the 306–329 peptide and APC infected with the virus [23, 24]. The dominant epitope, recognized by T cell clones in the context of HLA-DR1 and of the related HLA-DR4 alleles [21, 22] was confined to the 306–318 sequence [25–27]. Analysis of X-ray crystallography data enabled the identification of contact residues of this peptide involved in the binding to HLA-DR1 [28]. Based on the recently described allele-specific motifs determined from the amino acid sequence of peptides eluted from MHC class II molecules [29], the 308–316 minimal core of the H3 sequence of influenza HA1 comprises a motif fitting to the grooves of the highly homologous human HLA-DR1 and murine I-E^d class II molecules, providing an explanation for their functional immunodominance in both species.

The peptide encompassing the 317–329 H1 HA1 sequence was also shown to induce a strong peptide-specific T cell response in BALB/c mice, although this region was identified as a subdominant I-E^d-restricted epitope in the secondary virus-specific response [10, 30, 31]. Extension of this peptide by the 1–13 N-terminal amino acids of the HA2 subunit (encompassing the fusion peptide, FP) gives rise to the intersubunit peptide, which resembles the 317–341 sequence of the immature form of HA0 (Table 1). This peptide, 25 amino acids in length, exhibits significantly increased immunogenicity and is able to elicit a protective immune response against the A/PR/8/34 influenza virus (H1N1) [30–33]. Peptide-specific T and B cells reacted not only with the corresponding peptide but recognized the whole A/PR/8/34 virus and other subtype variants and cross-reacted with peptides corresponding to other subtype sequences ([29, 30, 33] and Horváth et al., in preparation).

Here the following questions were addressed: (i) is local immunodominance of the 306–318 epitope over the 317–329 H3 region in the C-terminal HA1 stretch due to its more efficient binding to I-E^d molecules, (ii) are there subtype related differences in binding of the peptides covering distinct epitopes of the 306–329 region to MHC and/or in activating T cells, and (iii) what are the functional consequences of the close location of two epitopes competing for the same MHC class II peptide binding site. To explore these problems, *in vivo* immunization studies and *in vitro* assays performed with two T cell hybridomas as well as direct binding of N-terminal biotinylated peptides to MHC class II molecules expressed on living murine B cells were studied by flow cytometry [34–37]. Results of the binding assays were compared with those of the functional tests performed with polyclonal T cells elicited by the 306–329 peptides comprising both epitopes and with two T cell hybridomas of the Th1 phenotype characterized by fine specificity patterns identical to that of the 317–329-induced polyclonal T cell response [10, 30]. The binding data, which exhibited a good correlation with results of the functional assays, demonstrated that the 317–329 peptides comprising the H1 or H2 but not the H3 subtype sequences, are as efficient as the 306–318 peptides in binding to I-E^d molecules. These results show that local dominance of the 306–318 over the 317–329 epitope in the H3 sequence is explained by the less efficient binding of H3 317–329 to I-E^d as compared to the H1 and H2 peptides. In contrast to the H3 subtype, the corresponding epitopes comprising the H1 and H2 subtype sequences, have similar binding properties to I-E^d and T cell-activating capacity in context with the same MHC class II molecule. This observation may suggest that amino acid substitutions harbored in the H3 306–329 sequence can modify the relative binding capacity and invert the local hierarchy of immunodominance of two closely situated epitopes that are able to bind to the same restriction element. Based upon the strong similarity of the H-2 I-E^d and HLA-DR1 binding pockets and their corresponding peptide motifs [29, 38], the relevance of this finding to the human system is suggested.

2 Materials and methods

2.1 Synthetic peptides

The synthetic peptides listed in Table 1 were synthesized by the classical solid-phase tBoc method as described previously [30, 32, 33, 39, 40]. Peptides were purified by HPLC (peptide purity >96%) and characterized by amino acid analysis and mass spectroscopy. The 317–329 and 320–329 H3 peptides were synthesized with an automated multiple peptide synthesizer (Abimed model AMS U22, Langenfeld, Germany) using the company's protocols for N-α-fluorenylmethoxycarbonyl (Fmoc) synthesis. Following completion of chain assembly, the N-terminal Fmoc-protecting group was removed and N-terminal biotinylation was performed. Crude peptides were purified by reverse-phase HPLC on a semi-preparative C8 column (Lichrosorb RP-8, 7 μm, 250 × 10 mm, Merck, Darmstadt, Germany). Elution of peptides was achieved by linear gradients established between 0.1% trifluoroacetic acid (TFA) in water and 0.1% TFA in 75% acetonitrite in water (v/v). Purity of peptides was ascertained by analytical HPLC on RP-18 (Merck) and by amino acid analysis following exhaustive acid hydrolysis.

2.2 N-terminal biotinylation of peptides

The peptides listed in Table 1 were biotinylated as described before [35]. Brielfy, 2 mM peptide solution was prepared in 0.1 M $NaHCO_3$ and cooled in ice. 2-N-Hydroxysuccinimide-biotin (NHSB, 2 mg/ml; Sigma) dissolved in dimethylsulfoxide (DMSO) was added to 30% molar excess. The reaction was allowed to proceed at 0°C for 2 h. N-terminal biotinylation of the 317–329 and 320–329 H3 peptides with protected 326 Lys was performed in the resin bound form (Wang-resin, Nova biochem. Calbiochem AG, Laeufelingen, Switzerland). Peptide (11 mg) was suspended in a minimal volume of N-methyl-2-pyrollidone (NMP) and 15 µmol NHSB, and 1.5 µmol diisopropylethylamine were added. After 16 h, the reaction products were washed with NMP, methanol, and dry ether. The biotinylated peptide was deprotected and cleaved from the resin with a cleavage mixture containing 5% triethylsilane (Fluka Chemicals, Buchs, Switzerland), 5% water, and 90% TFA (v/v/v). After 2 h the cleaved peptide was precipitated with ice-cold, peroxide-free ether and following centrifugation the pellett was dissolved in water and subsequently lyophilized. The degree of biotinylation (as compared with non-biotinylated peptide) was estimated by HPLC fractionation on a R18 column using a spectroscopic assay based on the binding of 2(4-hydroxyazobenzene) benzoic acid to biotin [41]. The extent of biotinylation was > 85%.

2.3 Cell lines and monoclonal antibodies

The murine B lymphoma lines A20 (ATCC TIB 208) and 2PK3 (ATCC TIB 203) were used as APC in the T cell activation and in the binding assays. The T cell hybridomas were developed from the spleen of BALB/c mice immunized either with the 317–341 (H1) peptide (H1-9-7-10) or with the 317–329 (H1) peptide and subsequently infected with the A/PR/8/34 influenza A virus (IP12-7 hybridoma) [30]. *In vitro* restimulation was performed with the corresponding peptides used for immunization and 5 days later activated T cells were fused with the BW-1100.129.237 $\alpha^-\beta^-$-thymoma cells [30]. The fusion partner was also used as a control in the cytofluorimetric assays. For IL-2 quantitation, the IL-2-dependent CTLL-2 (ATCC TIB 214) or HT2 T cell lines were used.

The monoclonal antibody (mAb) 14-4-4S (mouse IgG2a; ATCC HB 32) specific for the I-E α-chain, was used in the binding or functional assays to verify MHC restriction. All cell lines were cultured in RPMI supplemented with 2 mM L-glutamine, 1 mM sodium pyruvate, 5×10^{-5} M 2-mercaptoethanol, antibiotics and 5% FCS (complete RPMI).

2.4 Peptide binding assay and cytofluorimetry

A20 or 2PK3 cells (5×10^5–1×10^6 cells suspended in 200 µl RPMI supplemented with 2 mM L-glutamine and 0.1% BSA or FCS) were incubated in standard FACScan tubes (Falcon) with 1–20 µM biotinylated peptides at 37°C for 4 or 14 h. A 4-h incubation is sufficient for peptide internalization to endosomal compartments and substitution of self peptides captured as instabile MHC class II-peptide complexes. A 14-h incubation, however, allows loading of newly synthesized MHC class II molecules [41–43]. Cells were washed twice with PBS containing 0.1% BSA and cooled in ice. Phycoerythrin-labeled streptavidin (Molecular Probes, OR) was added (2 µg/tube) and incubated for 30 min at 0°C. Cells were washed three times with cold PBS-0.1% BSA, resuspended in 0.5 ml washing solution and analyzed by flow cytometry using a FACScan analyzer (Becton Dickinson). Viable cells were gated on the basis of forward and side scatter or of exclusion of 7-amino-actinomycin D. Data are documented either as histograms or as increase in mean fluorescence (arbitrary units). In the latter case, control cells were incubated without biotinylated peptides under the same conditions as those incubated with the labeled ones and mean fluorescence of these samples were taken as background.

Inhibition of peptide binding by mAb, specific for the I-E^d α chain (14-4-4S), was performed by incubating the A20 or 2PK3 cells with biotinylated peptides in the presence of mAb-containing supernatant. In the peptide competition assays, cells were pre-incubated with a 10–100 molar excess of unlabeled competitor peptides for 4 h at 37°C as described above. Bitionylated peptides were added at limited concentration given in the figure legends and the samples were further incubated for another 10 h. Labeling was performed as described for the direct binding assays.

2.5 Monitoring T cell activation by IL-2 production

T hybridoma cells (2×10^5 cells) were cultured in 96-well flat-bottom tissue culture plates (Nunc) in complete RPMI in the presence of different concentrations of peptides and 5×10^4 A20 or 2PK3 APC. In the competition assay with mAb, different dilutions of mAb-containing cell culture supernatants were added together with the peptides. Subsequently 75 µl of culture supernatants were removed at 24 h of culture and transferred to secondary cultures where the amount of secreted IL-2 was measured by the proliferation of CTLL-2 or HT2 detector cells. In this assay, the indicator were used at 4×10^3 (CTLL) or 4×10^4 (HT2) cells/well starting density and cell proliferation was measured by addition of [^{3}H] thymidine or 3-[4,5-dimethylthiazol-2-yl]-2,5-diphenyl-tetrazolium bromide (MTT), respectively [30].

2.6 Polyclonal T cell activation

Spleen and lymph node cells of BALB/c mice immunized with 100 µg peptide were isolated on days 18–21 and the T cell activating capacity of the peptides *in vitro* was measured by the standard proliferation assay as described previously [30]. The titer of peptide-specific Ab was measured by solid-phase indirect EIA as described [30, 31].

Table 1. The location, code, amino acid sequence and activity of the synthetic peptides comprising the 306–341 intersubunit region of immature HA0 to activate the I-E^d restricted H1-9-7-10 and IP12-7 T cell hybridomas[a]

Location	Code subtype	Sequence	Activation H1-9-7-10	IP-12-7
$HA1_{306-318}$	306–318 (H1)	**PKYVRSAKLRMVT**	–	–
$HA1_{306-318}$	306–318 (H2)	**PKYVKSEKLVLAT**	–	–
$HA1_{306-318}$	306–318 (H3)	**PKYVKQNTLKLAT**	–	–
$HA1_{307-329}$+$HA2_{1-12}$	317–341 (H1)	**VTGLRNIPSIQSRGLFGAIAGFIEG**	+++	+++
$HA1_{307-329}$+$HA2_{1-12}$	317–341 (H2)	**ATGLRNVPQIESR GLFGAIAGFIEG**	+++	–
$HA1_{307-329}$+$HA2_{1-12}$	317–341 (H3)	**ATGMRNVPEKQT RGLFGAIAGFIEG**	–	–
$HA1_{306-329}$+$HA2_{1-12}$	306–341 (H1)	**PKYVRSAKLRMVTVTGLRNIPSIQSRGLFGAIAGFIEG**	+++	+++
$HA1_{306-329}$+$HA2_{1-12}$	306–341 (H2)	**PKYVKSEKLVLATATGLRNVPQIESRGLFGAIAGFIEG**	+++	–
$HA1_{306-329}$+$HA2_{1-12}$	306–341 (H3)	**PKYVKQNTLKLATATGMRNVPEKQTRGLFGAIAGFIEG**	–	+
$HA1_{306-329}$	306–329 (H1)	**PKYVRSAKLRMVTVTGLRNIPSIQSR**	+++	+++
$HA1_{306-329}$	306–329 (H2)	**PKYVKSEKLVLATATGLRNVPQIESR**	+++	–
$HA1_{306-329}$	306–329 (H3)	**PKYVKQNTLKLATATGMRNVPEKQTR**	–	N.T.
$HA1_{307-329}$	306–329 (H1)	**VTGLRNIPSIQSR**	+++	+++
$HA1_{307-329}$	317–329 (H2)	**ATGLRNVPQIESR**	+++	–
$HA1_{307-329}$	317–329 (H3)	**ATGMRNVPEKQTR**	–	+
$HA1_{318-327}$	318–327 (H1)	**VTGLRNIPSI**	–	+
$HA1_{319-328}$	319–328 (H1)	**GLRNIPSIQS**	–	–
$HA1_{319-328}$	319–328 (H2)	**GLRNVPQIES**	–	–
$HA1_{319-328}$	319–328 (H3)	**GMRNVPEKQT**	–	–
$HA1_{320-328}$	320–328 (H1)	**LRNIPSIQS**	–	–
$HA1_{320-328}$	320–328 (H2)	**LRNVPQIES**	–	–
$HA1_{320-328}$	320–328 (H3)	**MRNVPEKQT**	–	–
$HA1_{320-329}$	320–329 (H1)	**LRNIPSIQSR**	–	–
$HA1_{320-329}$	320–329 (H2)	**LRNVPQIESR**	–	–
$HA1_{320-329}$	320–329 (H3)	**MRNVPEKQTR**	–	–
$HA2_{1-12}$R	FP3	**GLFGAIAGFIEGR**	–	–

a) Activation of the T cell hybridomas was measured by titration of IL-2 in cell culture supernatants after culturing the cells in the presence of 2PK3 APC at different concentration of the peptides. Relative efficiency of the peptides was characterized by their concentrations required for induction of 50% maximal IL-2 production that was determined from the dose-response curves: 0.1 μM (+++), 1 μM (++) and 50 μM (+).

3 Results

3.1 Biological activity of synthetic peptides covering the 306–341 region of influenza virus HA

Table 1 summarizes the functional activity of the H1-9-7-10 and IP12-7 T cell hybridomas in the presence of unlabeled peptides and of the 2PK3 murine B lymphoma cells expressing I-E^d molecules. Although both T cell hybridomas were elicited by immunization with peptides encompassing the 317–329 H1 sequence, they show a distinct cross-reactivity pattern with the corresponding H2 and H3 peptides. The IP12-7 T cell hybridoma can be activated by peptides comprising the 317–329 H1 sequence. It does not react with the corresponding H2 peptide but shows slight cross-reactivity with the 317–329 H3 peptide (Table 1). The H1-9-7-10 T cell hybridoma recognizes peptides of different length covering both the H1 and H2 317–329 sequences but does not recognize any of the H3 peptides (Table 1).

N-terminal truncation of the 317–329 peptides abolished their T cell-activating capacity but elimination of the C-terminal Arg did not (Table 1). Both hybridomas recognize and can efficiently be activated with peptides extended with the 306–318 sequences, *i.e.* 306–329 and 306–341 (Table 1). These functional properties provided a good tool for analyzing the relative activating and inhibitory activity of peptides covering various regions of the 306–329 subtype sequences.

Synthetic peptides covering the 306–341 sequence of the H1, H2 and H3 HA sequences were biotinylated and their biological activity was tested in comparison to the parental peptides by IL-2 production of the T cell hybridomas (data not shown). No alteration in the functional activity of peptides was observed as a result of N-terminal biotinylation. Therefore, these modified peptides were useful reagents for studying their direct MHC binding.

3.2 Direct binding of peptides to MHC class II molecules of living A20 and 2PK3 cells

Fig. 1 presents results of flow cytometric measurements of peptide binding performed after 14-h incubation at 37 °C. The figure shows the increase in mean fluorescence values (arbitrary units) of A20 or 2PK3 cells incubatd with 20 μM biotinylated 317–329 peptide (H1 subtype) (Fig. 1B) in comparison to cells labeled with the I-Eα-specific monoclonal antibody 14-4-4S (Fig. 1A). Results summarized in Fig. 1C, D show the specificity of peptide binding to A20 or 2PK3 cells. Binding of biotinylated 317–329 peptide to A20 (Fig. 1CIII) is completely inhibited by the mAb 14-4-4S (Fig. 1CI) as compared to the corresponding negative control (Fig. 1CII). Partial inhibition of biotinylated

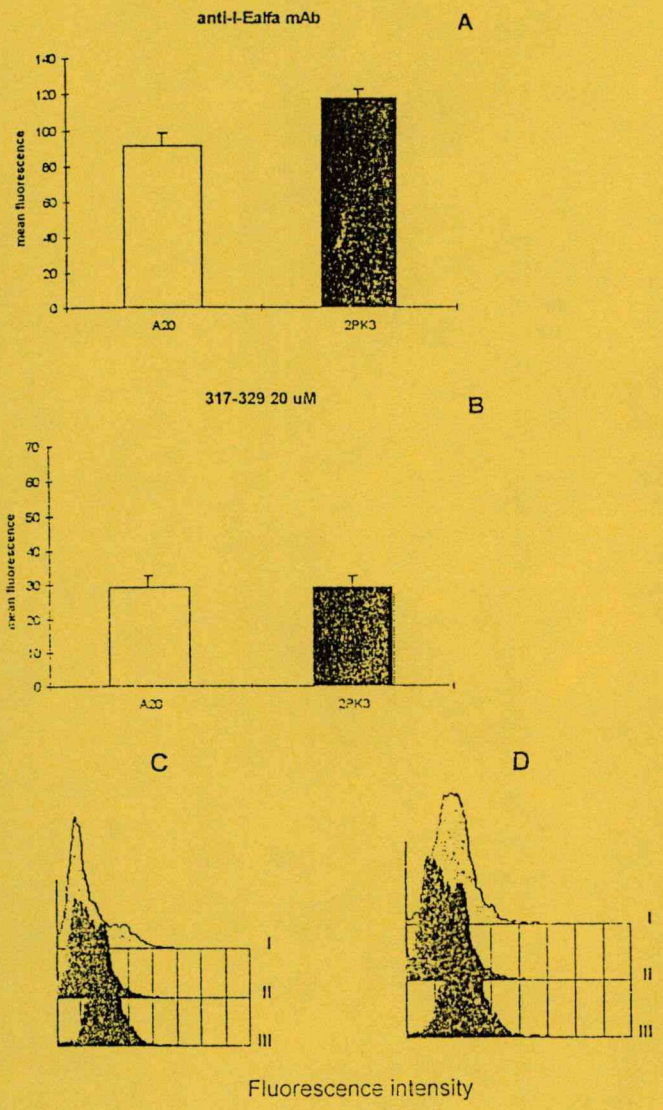

Figure 1. Flow cytometric binding measurements of MHC class II-specific mAb (A) or biotinylated HA peptides (B–D) to A20 and 2PK3 cells. The increase of mean fluorescence was measured after incubation with 1 μg biotinylated 14.4.4 mAb for 1 h on ice (A), with 20 μM N-terminal biotinylated 317–329 (H1 subtype) (B) for 14 h at 37 °C, followed by 30-min incubation with PE-labeled streptavidin on ice. The increase of mean fluorescence was calculated as a difference of antibody treated or peptide loaded samples and negative controls incubated without the antibody or peptides. Mean values of three to five independent experiments ± SD are given. Binding specificity was tested by Ab (C) and peptide (D) competition with A20 or 2PK3 cells, respectively. Binding of 317–329 (H1 subtype) peptide (20 μM) to A20 (C/III) or 2PK3 (D/III) cells is presented with the corresponding negative controls (C/II, D/II) and with cells incubated with the same peptides in the presence of 14.4.4 mAb (C/I) or 20-fold molar excess of 320–328 (H1) peptide (D/I).

317–329 peptide binding (Fig. 1DIII) to 2PK3 cells was found in the presence of a 20-fold molar excess of unbiotinylated 320–328 peptide (Fig. 1DI) as compared to the negative control (Fig. 1DII). As neither the biotinylated 14-4-4S mAb nor the biotinylated peptides bind to BW5147.3 cells (data not shown), these results underscore the binding specificity of N-terminal biotinylated peptides to I-E^d molecules on the surface of living A20 or 2PK3 cells.

3.3 Comparative binding efficiency of peptides comprising various regions of the 306–341 HA subtype sequences

Peptides comprising the three subtype sequences of the 306–318, 317–329 and 317–341 regions bind to 2PK3 cells with slightly different efficiency (Fig. 2). The inability of the H3 IP peptide (IP3) to bind to 2PK3 or A20 cells, however, could be the consequence of biotinylation and functional alteration of the Lys residue at position 326 which is unique in the H3 sequence (Table 1). This possibility was further investigated using shorter peptide analogs of IP. As summarized in Fig. 2C all analogs encompassing the H3 sequence have a detectable but lower binding capacity compared to that of the H2 or H1 sequences. To rule out the involvement of Lys326 modification in binding to I-E^d, binding measurements of the 317–329 and 320–329 peptides, having protected Lys residues during the biotinylation procedure, were also performed. These peptides had similar, low binding activity to living cells as the ones labeled by the standard method (data not shown), suggesting that their lower binding activity is rather due to differences in peptide sequences. This interpretation was further confirmed by the observed similar activity of the unlabeled and biotinylated 317–329 H3 peptide in an activation assay performed with IP 12-7 T cells in the presence of 2PK3 APC (data not shown).

In good correlation with the binding data summarized in Fig. 2 no activation of the H1-9-7-10 hybridoma could be achieved by any of the H3 peptides and the dose-response curve of the 317–329 H1 and H3 peptides revealed that a 100-fold higher concentration of the H3 peptide was required to reach maximal IL-2 production of the IP12-7 hybridoma (data not shown). The reduced ability of the 317–329 H3 peptide compared to its H1 analog to induce IL-2 production can be explained by its lower binding to I-E^d molecules. Still the role of the T cell receptor should also be considered. The results showing that the 317–329 H2 peptide, despite of its efficient binding to MHC class II molecules, does not activate the IP12-7 T cell hybridoma (Table 1) but has comparable activity to the H1 peptide with the H1-9-7-10 hybridoma, clearly point to to the role of subtype-related amino acid substitutions in contact both with the MHC and the T cell receptor.

Data summarized in Fig. 2C show that truncations at both termini of the parental 317–329 peptides result in analogs which still bind to I-E^d despite of their inactivity in the functional assay (Table 1). Furthermore, comparing the binding activity of peptides with or without C-terminal Arg revealed that this additional amino acid increases the efficiency of MHC binding (Fig. 2C). The 320–329 peptides which retained their MHC binding capacity but lost functional activity were used in the functional and binding inhibition assays to assess relative binding to MHC class II molecules.

3.4 Competition between the 306–318 and 319–329 peptides for binding to I-E^d

The relative binding capacity of the 306–318 and 319–329 H1 peptides was studied in both binding and functional competition assays. As is summarized in Fig. 3A, a similar

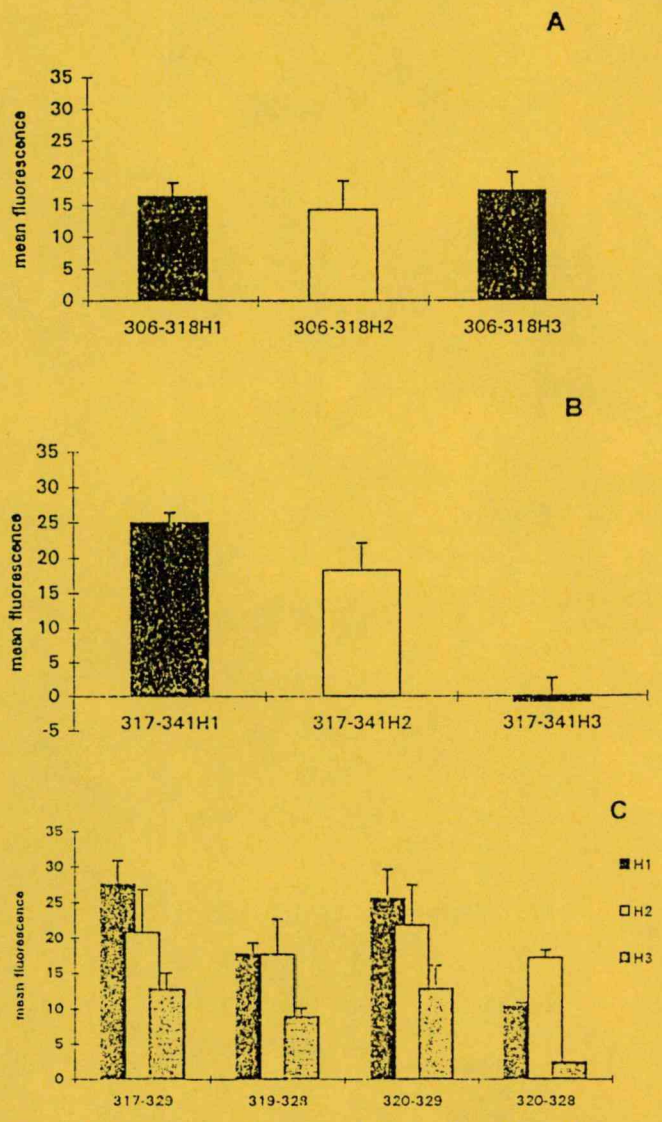

Figure 2. Flow cytometric assay of the binding of peptides comprising subtype sequences of the 306–341 region of HA to I-E^d molecules. The shift in mean fluorescence (arbitrary units) as a result of 14-h incubation at 37 °C of 2PK3 cells with 20 μM N-terminal biotinylated peptides was measured in three independent experiments and mean values ± SD are shown.

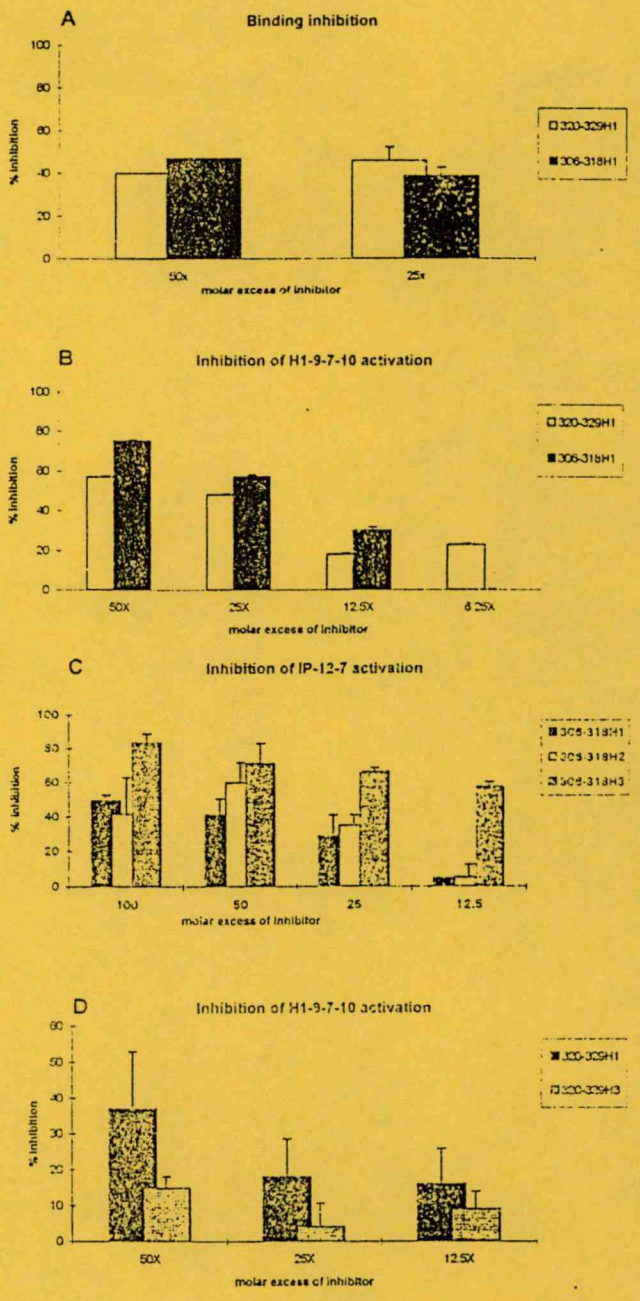

Figure 3. Inhibition of peptide binding to MHC (A) and IL-2 production of T cell hybridomas (B–D) by HA peptides comprising two different epitopes. (A) A20 cells (5×10^5) were preincubated with 25- or 50-fold molar excess of competitor peptides and the binding of 4 μM biotinylated peptide was detected; (□) 320–329 H1, (▩) 306–318 H1. Values shown represent the mean fluorescence intensity (mean ± SD) of three independent experiments and are given as percent inhibition. (B) H1-9-7-10 T cells (10^4–2×10^4) were incubated with 2×10^4 2PK3 cells as APC at a suboptimal concentration (0.5–1 μg/ml) of 317–319 H2 peptide in the presence of increasing concentrations (6- to 100-fold molar excess) of the non-activating 320–329 H1 (□) or 306–318 H1 (▩) peptides. (C) As for (B) using 10^4–2×10^4 IP 12-7 T cells and 2×10^5 A20 cells as APC, with 317–329 H1 peptide and increasing concentrations of 306–318 H1 (▩), 306–318 H2 (□), and 306–318 H3 (▩). (D) As for (B) using H1-9-7-10 T cells with 2PK3 as APC, in the presence of 317–329 H2 peptide and increasing concentrations of 320–329 H1 (▩) and 320–329 H3 (▩) peptides. T cell activation was detected by measuring IL-2 production using CTLL-2 or HT2 indicator cells.

degree of inhibition could be achieved if the binding of 20 μM biotinylated 306–318 or 317–329 peptide was measured in the presence of unlabeled 320–329 and 306–318 peptides, respectively. Competition of non-activating peptides for I-E^d binding sites was also demonstrated in functional assays as demonstrated in Fig. 3B–D. The H1-9-7-10 (Fig. 3B, D) T cell hybridoma was activated in the presence 2PK3 cells with a limited concentration of 317–329 H2 activator peptides together with different concentrations of non-activating 306–318 and 320–329 competitor H1 peptides (Fig. 3B). Similar to the binding inhibition assay, the two peptides possessed similar inhibitory capacity in this assay. The molar excess required for 50 % inhibition in both the binding and functional inhibition assays was in the same order of magnitude (Fig. 3A, B).

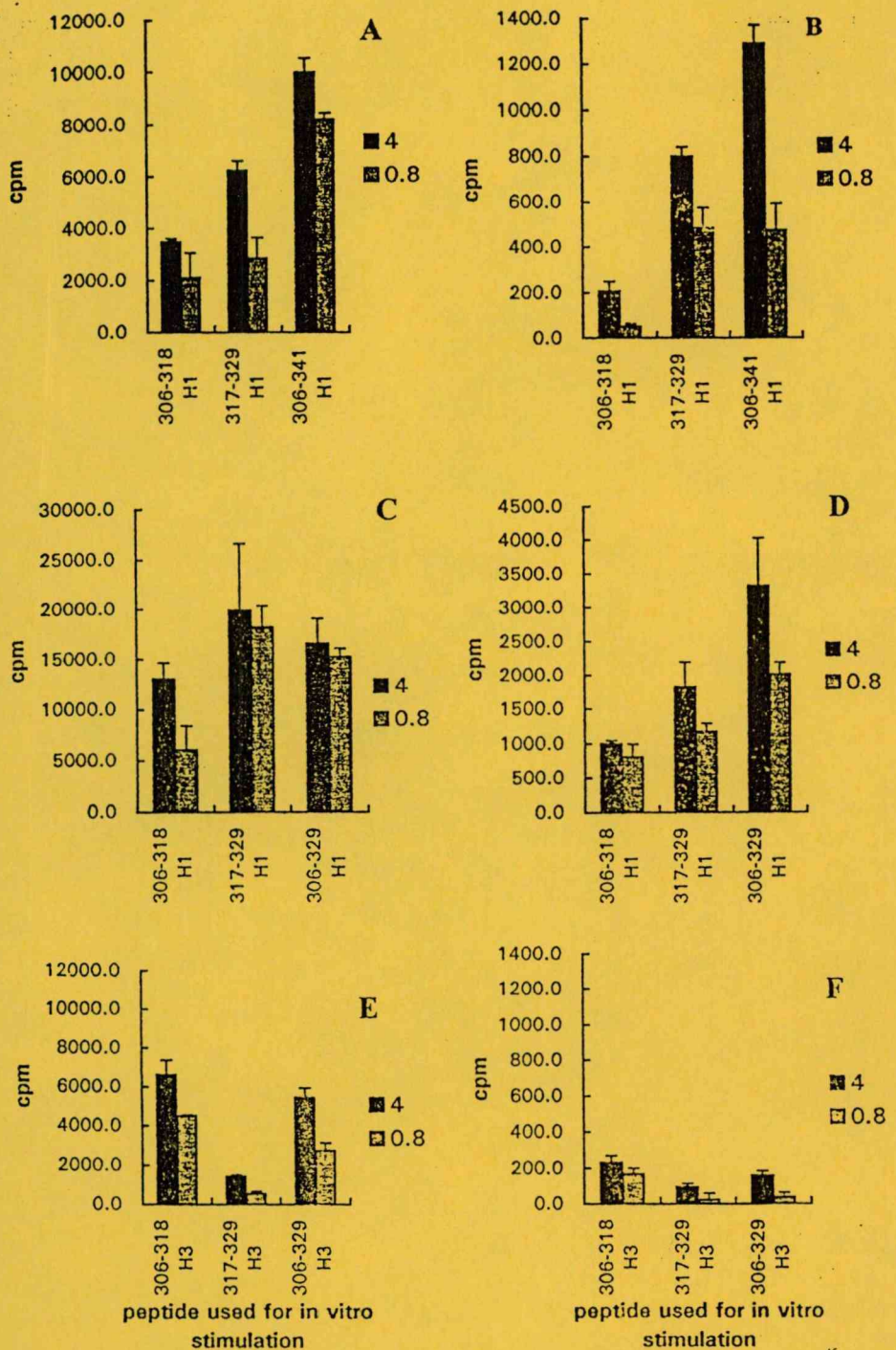

Figure 4. Specificity of *in vivo* activated polyclonal T cells induced by peptides comprising both epitopes. Spleen (A, C, E) and lymph node (B, D, F) cells of BALB/c mice immunized with 100 μg 306–341 (H1 (A, B), 306–329 H1 (C, D) or 306–329 H3 (E, F) peptides were activated *in vitro* by 4 μg/ml (dark columns) or 0.8 μg/ml (gray columns) peptides in the presence of irradiated syngeneic spleen cells. Proliferation was measured by [^{3}H] thymidine incorporation.

Fig. 3C, D demonstrates the relative inhibitory capacity of the 306–318 and 320–329 peptides tested in the sensitive inhibition assay performed with the IP12-7 (Fig. 3C) or the H1-7-9-10 (Fig. 3D) hybridomas. Fig. 3C demonstrates the highest efficiency of the 306–318 H3 peptide in contrast to the low inhibitory activity of the 320–329 H3 peptide (Fig. 3D) in the functional inhibition assay.

3.5 T cell-activating capacity *in vivo* of the 306–318 and 317–329 epitopes

Spleen (Fig. 4A, C, E) and lymph node (Fig. 4B, D, F) cells of peptide immunized BALB/c mice were separated, depleted for B cells and proliferation as well as IL-2 production of *in vitro* re-stimulated T cells was measured. T cells of mice immunized either with the 306–341 (Fig. 4A,

B or 306–329 (Fig. 4C, D) H1 peptides responded to both the 306–318 and the 317–329 peptides and the most intense response was detected with the peptide encompassing both epitopes (Fig. 4A–D). Similar results were obtained with the H2 peptides (data not shown). However, immunization with the 306–329 H3 peptide (Fig. 4E, F) resulted in T cell responses of similar intensity to the 306–329 and to the 306–318 peptides, but no reactivity with the 317–329 peptide was observed. These results demonstrate that under *in vivo* conditions both epitopes, located in the 306–318 and the 317–329 H1 regions, are able to activate peptide-specific T cells. In contrast to H1, the 306–329 H3 sequence has only one functional T cell epitope comprised in 306–318 (Fig. 4E, F).

4 Discussion

Immunodominance of T cell epitopes may have an essential role in the development of T cell responses to pathogens and vaccines. Peptide affinity to MHC has been shown as a major factor in immunogenicity which limits the number of specific peptide/MHC complexes presented to T cells and determines competition among peptides for binding to MHC molecules [1, 44]. However, binding of peptides to MHC with low affinity may have an important role in tolerance induction and shaping immunodominance [45]. The hierarchy of immunodominance in large proteins, however, is a complex interplay of different factors including efficiency and selectivity of antigen processing and presentation, the size of the peripheral T cell repertoire and the local concentration of cytokines required for T cell expansion and differentiation [2].

The influenza HA subunits are generated by a posttranslational modification mediated by host-cell derived subtilisin-like proteases [46, 47]. The C-terminal stretch of HA1, although being embedded in the core of the protein, encompasses an enzyme susceptibility motif which is the target of a special subtilisin-like enzyme [46, 47]. This enzymatic cleavage, which plays a pivotal role in the infectivity of the virus, initiates, in collaboration with the pH-induced conformational change of HA, the further degradation of the C-terminal segment. The C-terminal region of HA1 has been described as a dominant epitope which involves multiple T cell epitopes recognized both in the human and mouse systems [9, 10, 14, 17, 18, 22–24]. The immune response elicited by a conformationally stabilized peptide 317–341, which comprises the HA1 317–329 H1 sequence, confers protection against lethal infection with the A/PR/8/34 virus ([10, 30–32] and Horváth et al., in preparation). The subtype-specific but conserved amino acid sequence and the functional importance of this region in enzymatic cleavage prompted us to study the binding capacity of peptides comprising distinct but not overlapping epitopes of this region to the same murine MHC class II molecule and compare their ability to induce T cell activation *in vitro* and *in vivo*. This study was extended by monitoring the effect of natural amino acid substitutions, evolved during the phylogeny of virus subtypes, on these properties. *In vitro* experiments measuring peptide binding to I-E^d molecules expressed on murine B lymphoma cells and functional assays carried out with two murine T cell hybridomas recognizing the 317–329 region with distinct fine specificity ([30] and this study) as well as *in vivo* immunization studies with peptides comprising both the 306–318 and 317–329 sequences were performed to assess the local immunodominance of these adjacent epitopes.

Our results can be summarized as follows: (i) flow cytometric monitoring of cell surface bound N-terminal biotinylated peptides in combination with binding and functional inhibition assays provides semiquantitative data on their binding capacity, (ii) based on the binding and functional data, the 306–318 and the 317–329 peptides encompassing the H1, H2 but not the H3 sequences bind with an apparent similar affinity to, and therefore, compete for the same restriction element, *i.e.* I-E^d, (iii) the 317–341, the 317–329 peptides and their truncated analogs show subtype-dependent differences in I-E^d binding and (iv) differences in the binding capacity of peptides comprising the three subtype sequences provide a rationale for the local immunodominance of the 306–318 region over the 317–329 epitope upon peptide immunization in the case of the H3 but not in the H1 or H2 sequences.

According to previous experiments [36, 37], all documented binding assays were performed after incubation of living APC with the labeled peptides for 14 h at 37°C. The long-incubation protocol was designed to detect stable MHC class II-peptide complexes (half-life 7–12 h) generated as the net result of different peptide loading pathways [42, 43]. These include direct interaction of peptides with short-lived instable complexes [47–49] as well as the HLA-DM- and invariant chain-dependent peptide binding occurring in endosomal compartments [50, 51].

The local immunodominance of the 306–318 and 317–329 epitopes is determined by the subtype-specific sequence of this region as revealed by the relative binding efficiency, competitor activity and immunogenicity of the corresponding peptides comprising the H1, H2 or H3 subtype sequences. The H1, H2 and H3 306–318 peptides bind to I-E^d with an apperantly similar affinity (Fig. 2) and elicit proliferating T cells *in vivo* in case of all subtype sequences (Fig. 4). The H1 and H2 sequences of 317–329 residues were also shown as potent I-E^d binding epitopes (Fig. 2, Table 1). The 317–329 and 317–341 peptides, however, show subtype related differences in their MHC binding (Fig. 2) and in their efficiency to activate (Table 1), inhibit (Fig. 3A–D) or induce *in vivo* T cell responses (Fig. 4). The discrepancy between the lack and the relatively low, but detectable binding and activating capacity of the 317–341 and 317–329 H3 peptides, respectively (Fig. 2) may be the consequence of the strikingly different solution conformation of the fusion peptide extended analogs [33, 39, 40]. The high propensity of 317–341 to adopt an ordered conformation in these peptides is mediated by FP but may affect the orientation of 317–329 side chains influencing both the occupancy of the corresponding pockets and/or the contact residues with the TCR. This explanation is supported by the finding that the elimination of the fusion peptide from the C-terminal of 317–341 resulted in a tridecapeptide 317–329, which showed some binding to I-E^d (Fig. 2). In addition, both the 306–318 and 317–329 H1 or H2 peptides were recognized by monoclonal (Table 1) or polyclonal T cells (Fig. 4) in longer peptides extended by N- or C-terminal natural sequences, providing evidence that the flanking sequences have no

inhibitory effect on the T cell recognition of the 317–329 epitope. Control experiments ruled out the possibility that the low binding of 317–329 H3 was merely due to the biotinylation of the unique Lys at position 326.

These results demonstrate the similar activity of the 306–318 and 317–329 H1 or H2 peptides and the poor activity of the 317–329 H3 peptide in the binding (Figs. 1, 2), activation (Table 1) or inhibition assays (Fig. 3) and in the immunization experiments (Fig. 4). The sensitive functional inhibition assays demonstrated an inverse rank order of peptides in their relative competitor efficiency of the 306–318 and 317–329 subtype peptides, respectively (Fig. 3D, E). Our results confirm previous data that relative binding efficiency to MHC molecules is a critical factor in determinant selection and ranking peptide immunogenicity [1, 42, 43, 52]. The subdominant feature of the 317–329 peptide upon viral infection may be the consequence of high antigenic competition, inappropriate antigen processing, or the low frequency of T cells of this specificity. This hierarchy, however, can be altered by peptide pre-immunization which may increase the frequency of T cells of the desired specificity. Using the 306–329 or 306–341 peptides for pre-immunization, the ratio of T cells against the two adjacent epitopes was determined by their relative binding efficiencies (Fig. 4).

Extension of the 317–329 peptide by the hydrophobic fusion peptide (306–341 or 317–341) significantly increases the immunogenicity of the subdominant 317–329 epitope ([30–32] and Horváth et al., in preparation) and preimmunization with this peptides results not only in the activation of Th1 cells but also in antibody production and elevated protection against lethal A/PR/S/4 virus infection ([31, 32] and Horváth et al., in preparation). Th1 cells elicited by peptide immunization not only produce IL-2 but also secrete large amounts of TNF upon activation by peptide or virus-pulsed APC (Horváth et al., unpublished results). TNF in combination with IFN-γ was demonstrated to confer strong antiviral activity [53, 54] and mediate apoptosis, and may, therefore, be involved in the elimination of virus-infected cells.

Our results confirm previous data which demonstrated that immunization with the 305–328 H3 peptide resulted in a T cell response mediated primarily by the 305–318 epitope and by an antibody response directed against regions 314–318 and 320–328 [17, 18, 55]. In contrast to H3, immunization with the 306–329 or 317–341 H1 peptides elicited both 306–318- and 317–329-specific T cells and antibodies against the 317–329 region [30, 31]. The importance of this local epitope hierarchy in response to the whole virus may depend on multiple factors. Nevertheless, enhancement of the immune response by peptide preimmunization to a subdominant protective epitope may be a beneficial component of the antiviral immune response and preimmunization with the 306–341 or 317–341 synthetic peptides comprising H1 or H2 sequences confers protection against lethal influenza virus infection ([31, 32] and Horváth et al., in preparation).

This work was supported by the grants OTKA no. 017157, AKP no. 3311/6 and OMFB no. E0028/960202 to É.R and grant B104-CT96-0135 from the European Community to I.P. The expert technical assistance of Erzsébet Veress is acknowledged.

5 References

1 Chen, W., Khilko, S., Fecondo, J., Margulies, D. H. and McCluskey, J., *J. Exp. Med.* 1994. *180:* 1471.
2 Eberl, G., Kessler, B., Eberl, L. P., Brunda, M. J., Valmori, D. and Corradin, G., *Eur. J. Immunol.* 1996. *26:* 2709.
3 Sercarz, E. E., Lehmann, P. V., Ametani, A., Benichou, G., Miller, A. and Moudgil, K., *Annu. Rev. Immunol.* 1996. *11:* 310.
4 Deng, Y., Yewdell, J. W., Eisenlohr, L. C. and Bennink, J. R., *J. Immunol.* 1997. *158:* 1507.
5 Vitiello, A., Yuan, L., Chesnut, R. W., Sidney, J., Southwood, S., Farness, P., Jackson, M. R., Peterson, P. A., Sette, A., *J. Immunol.* 1996. *157:* 5555.
6 Aebischer, T., Moskophidis, D., Rohrer, U. H., Zinkernagel, R. M. and Hengartner, H., *Proc. Natl. Acad. Sci. USA* 1991. *88:* 11047.
7 de Campos-Lima, P. O., Levitsky, V., Brooks, J., Lee, S. P., Hu, L. F., Rickinson, A. B. and Masucci, M. G., *J. Exp. Med.* 1994. *179:* 1297.
8 Wilsin, I. A. and Cox, N. J., *Annu. Rev. Immunol.* 1990. *737.*
9 Yewdell, J. W. and Hackett, C. J., in Krug, R. M. (Ed.), *The Influenza Viruses*, Plenum Press, New York 1989, p. 361.
10 Rajnavölgyi, É., Nagy, Z., Daser, A., Horváth, A., Gogolák, I. and Kurucz, I., in Rajnavölgyi, E. (Ed.), *Synthetic Peptides in the Search for B- and T-cell Epitopes.* CRC Press, Austin 1994, p. 173.
11 Barnett, B. C., Burt, D. S., Graham, C. M., Warren, A. P., Skehel, J. J. and Thomas, D. B., *J. Immunol.* 1989. *143:* 2663.
12 Barnett, B. C., Graham, C. M., Burt, D. S., Skehel, J. J. and Thomas, D. B., *Eur. J. Immunol.* 1989. *19:* 515.
13 Hurwitz, J. L., Heber-Katz, E., Hackett, C. J. and Gerhard, W., *J. Immunol.* 1984. *133:* 371.
14 Gerhard, W., Hackett, C. J., Melchers, F., *J. Immunol.* 1983. *130:* 2379.
15 Scholtissek, C., Rohde, W., von Hoyningen, V. and Rott, R., *Virology* 1978. *87:* 13.
16 Nobusawa, E., Aoyama, T., Kato, H., Suzuki, Y., Tateno, Y. and Nakajima, K., *Virology* 1991. *182:* 475.
17 Ffrench, R. A., Tang, X.-L., Anders, E. M., Jackson, D. C., White, D. O., Drummer, H., Wadw, J., Tregear, W. G. and Brown, L. E., *J. Virol.* 1989. *63:* 3087.
18 Jackson, D. C. and Brown, L. E., *Peptide Res.* 1991. *4:* 114–124.
19 Mitchell, E., Sethi,S., Rowland, M. G., Chakraverty, P., Harris, E. A., Watts, M. R. and White, P. M., *J. Public Health Med.* 1991. *3:* 214.
20 Nakajima, S., Nishikawa, F., Nakamura, K. and Nakajima, K., *Epidemiol. Infect.* 1995. *115:* 591.
21 Barker, W. H., Menegus, M. A., Hall, C. B., Betts, R. F., Freundlich, C. B., Long, C. E., O'Brien, D. H., Weirner, L. B., Cunningham, C., Bonville, C. A., *Am. J. Prev. Med.* 1995. *11:* 149.
22 Lamb, J. R. and Green, N., *Immunology* 1983. *50:* 659.
23 Lamb, J. R., Eckels, D. D., Lake, P., Woody, J. N. and Green, N., *Nature* 1982. *300:* 66.
24 Eckels, D., Sell, T., Bronsen, S., Johnson, A., Hartzman, R. and Lamb, J. R., *Immunogenetics 1984. 19:* 409.
25 Rothbard, J., Lechler, R., Howland, K., Bal, V., Eckels, D., Sekaly, R., Long, E., Taylor, W. and Lamb, J., *Cell* 1988. *52:* 515.
26 Rothbard, J. B., Busch, R., Bal, V., Trowsdale, J., Lechler, R. I. and Lamb, J. R., *Int. Immunol.* 1989. *1:* 487.
27 Rothbard, J. B., Busch, R., Howland, K., Bal, V., Fenton, C., Taylor, W. R. and Lamb, J. R., *Int. Immunol.* 1989. *1:* 479.
28 Stern, L. J., Brown, J. H., Jardetzky, T. S., Gorga, J. C., Urban, R. G., Strominger, J. L. and Wiley, D. C., *Nature* 1994. *368:* 215.
29 Rammensee, H.-G., *Curr. Opin. Immunol.* 1995. *7:* 85.
30 Rajnavölgyi, É., Nagy, Z., Kurucz, I., Gogolák, P., Tóth, G. K., Váradi, G., Penke, B., Tigyi, Z., Hollósi, M. and Gergely, J., *Mol. Immunol.* 1994. *31:* 1403.

31 Nagy, Z., Rajnavölgyi, É., Hollósi, M., Tóth, G. K., Váradi, G., Penke, B., Tóth, I., Horváth, A., Gergely, J. and Kurucz, I., *Scand. J. Immunol.* 1994. *40:* 281.
32 Tóth, G. K., Váradi, G., Nagy, Z., Monostori, É., Penke, B., Hegedüs, Z., Andó, I., Fazekas, G., Kurucz, I., Mák, M. and Rajnavölgyi, É., *Peptide Res.* 1993. *6:* 272.
33 Majer, Zs., Holly, S., Tóth, G. K., Váradi, Gy., Nagy, Z., Horváth, A., Rejnavölgyi, É., Laczkó, I. and Hollósi, M., *Arch. Biochem. Biophys.* 1995. *322:* 112.
34 Kubitscheck, U., Levi, R., Horwitz, R. J., Arnon, R. and Pecht, I., *Scand. J. Immunol.* 1992. *36:* 341.
35 Mozes, E., Dayan, M., Zisman, E., Brocke, S., Licht, A. and Pecht, I., *EMBO J.* 1989. *8:* 4049.
36 Pecht, I., *Isr. J. Med. Sci.* 1993. *29:* 1.
37 Fridkis-Hareli, M., Teitelbaum, D., Gurevich, E., Pecht, I., Brautbar, C., Kwon, O. J., Brenner, T., Arnon, R. and Sela, M., *Proc. Natl. Acad. Sci. USA* 1994. *91:* 4872.
38 Rammensee, H.-G., Friede, T. and Stephanovic, S., *Immunogenetics* 1995. *41:* 178.
39 Hollósi, M., Ismail, A. A., Mantsch, H. H., Penke, B., Váradi, I. G., Tóth, G. K., Laczkó, I., Kurucz, I., Nagy, Z., Fasman, G. D. and Rajnavölgyi, É., *Eur. J. Biochem.* 1992. *206:* 421.
40 Holly, S., Majer, Zs., Tóth, G. K., Váradi, G., Rajnavölgyi, É., Laczkó, I. and Hollósi, M., *Biochem. Biophys. Res. Commun.* 1993. *193:* 1247.
41 Green, N. M., *Biochem. J.* 1965. *4:* 54–59.
42 Sadegh-Nasseri, S., Stern, L. J., Wiley, D. C. and Germain, R. N., *Nature* 1994. *370:* 647.
43 Beeson, C. and McConnell, H. M., *Proc. Natl. Acad. Sci. USA* 1994. *91:* 8842.
44 Oldstone, M. B. A., Lewicki, P., Borst, D., Hudrisier, D. and Gairin, J., *J. Virol.* 1995. *69:* 7423.
45 Fairchild, P. J. and Wraith, D. C., *Immunol. Today* 1996. *17:* 80.
46 Bosch, F. X., Garten, W., Klenk, H.-D. and Rott, R., *Virology* 1981. *113:* 725.
47 Barr, P. J., *Cell* 1991. *66:* 1.
48 Nelson, C. A., Petzold, S. J. and Unanue, E. R., *Nature* 1994. *371:* 250.
49 Pinet, V., Vergelli, M., Martin, R., Bakke, O. and Long, E. O., *Nature* 1995. *375:* 603.
50 Sanderson, F., Thomas, C., Neefjes, J. and Trowsdale, J., *Immunity* 1996. *4:* 87.
51 Busch, R. and Mellins, E. D., *Curr. Opin. Immunol.* 1996. *8:* 51.
52 Sette, A., Vitiello, A., Reherman, B., Fowler, P., Nayersina, R., Kast, W. A., Melief, C. J. M., Oseroff, C., Yuan, L., Ruppert, J., Sidney, J., del Guercio, M.-F., Southwood, S., Kubo, R. T., Chesnut, R. W., Grey, H. M. and Chisar, F. V., *J. Immunol.* 1994. *153:* 5586.
53 Wong, G. H. W. and Goeddel, D. V., *Nature* 1986. *323:* 819.
54 Sarin, A., Conan-Cibotti, M. and Henkart, P. A., *J. Immunol.* 1995. *155:* 3716.
55 Schoofs, P.-G., Geysen, H. M., Jackson, D. C., Brown, L. E., Tang, X.-L. and White, D. O., *J. Immunol.* 1988. *140:* 611.

ELSEVIER

Immunology Letters 60 (1998) 127–136

Immunology Letters

A hemagglutinin-based multipeptide construct elicits enhanced protective immune response in mice against influenza A virus infection

Attila Horváth [a], Gábor K. Tóth [b], Péter Gogolák [a], Zoltán Nagy [a], Istaván Kurucz [a], Israel Pecht [c], Éva Rajnavölgyi [a,*]

[a] *Department of Immunology, L. Eötvös University, Jávorka S. 14., H-2131 Göd, Hungary*
[b] *Department of Medical Chemistry, A. Szent-Györgyi Medical School, Szeged, Hungary*
[c] *The Weizmann Institute of Science, Rehovot, Israel*

Received 18 August 1997; received in revised form 3 October 1997; accepted 7 October 1997

Abstract

Multipeptide constructs, comprising adjacent sequences of the 317–341 intersubunit region of immature influenza A hemagglutinin (H1N1), were designed and the functional properties of these branched peptides were compared to that of the corresponding linear peptides. In vivo studies revealed that the immunogenicity of the peptides was dependent on the presence of the hydrophobic fusion peptide (comprised in FP3), encompassing the N-terminal 1–13 sequence of the HA2 subunit. Antibody and T cell recognition, however, was directed against the 317–329 HA1 sequence, comprised in the P4 peptide. Multiple copies of P4, covalently linked by branched lysine residues, significantly enhanced the efficiency of antibody binding and the capacity of peptides to elicit B- and T-cell responses. A fraction of peptide induced antibodies reacted with immature or with proteolitically cleaved hemagglutinin (HA) molecules pretreated at low pH. Immunization with a multipeptide construct, $(P4)_4$–FP3, not only resulted in elevated antibody and T cell responses but conferred enhanced protection against lethal A/PR/8/34 (H1N1) infection as compared to its subunit peptides. The beneficial functional properties of this artificial peptide antigen may be acquired by multiple properties including: (i) stabilized peptide conformation which promotes strong, polyvalent binding to both antibodies and MHC class II molecules; (ii) appropriate P4 conformation for antibody recognition stabilized by the covalently coupled fusion peptide, resulting in the production of virus cross reactive antibodies which inhibit the fusion activity of the virus; (iii) activation of peptide specific B cells which potentiate antigen presentation and peptide specific T cell responses; and (iv) generation of helper T cells which secrete lymphokines active in the resolution of infection.

Keywords: Hemagglutinin; Immune response; Influenza A virus

1. Introduction

The hemagglutinin (HA) molecule of influenza A viruses is one of the major targets of both the humoral and the T cell-mediated immune responses [1]. The antigenicity of HA, however, is frequently changed by single or multiple mutations of the gene encoding for this membrane protein [2]. These mutations primarily accumulate in or close to epitopes located in the head region of HA being responsible for receptor binding [3,4]. The major problem of efficient vaccination against influenza A viruses originates from this antigenic drift which generates frequently emerging virus variants and consequently alters virus recognition by both antibodies and T cells [5,6].

The amino acid sequence of the intersubunit region of HA0 is conserved within subtypes and can be recognized by both antibodies and T cells in humans as well as in mice [7–10]. The 302–313 region of the H1N1 subtype sequence was described as a major but labile helper T cell epitope in BALB/c mice [11]. The C-termi-

* Corresponding author. Tel.: +36 273 45311; fax: +36 273 45147; e-mail: evaraj@alfa.elte.hu

0165-2478/98/$19.00
PII S0165-2478(97)00137-5

nal 305–329 stretch of HA1 (H3N2 subtype) was characterized as an immunodominant T cell epitope recognized in the context of HLA-DR1 [7,12] and H-2 I-E^d [8] and peptide specific murine and rabbit antibodies directed against its subregions were characterized [9,10,13]. Our previous results demonstrated that a synthetic peptide (IP), covering the 317–341 HA0 sequence (H1N1) is highly immunogenic in BALB/c mice without any carrier and comprises partially overlapping B and T cell epitopes [14,15]. Epitope mapping demonstrated the involvement of the 317–329 sequence in both antibody and MHC binding [14–16] and conformational studies revealed the importance of the fusion peptide (330–341) in stabilizing IP conformation in an immunogenic form [17,18]. Based on these results this region emerged as a candidate for further subunit vaccine design [19].

In this study the magnitude, fine specificity and isotype distribution of antibodies as well as the specificity, cross reactivity and lymphokine production of T cells, elicited by IP and its multipeptide analogs $(P4)_4$ and $(P4)_4$–FP3 (see Table 1), were analysed. The results show that the presence of multiple, covalently linked copies of P4, in combination with the fusion peptide, results in an immunogenic peptide, $(P4)_4$–FP3, which elicits elevated and protective antibody and T cell responses as compared to the parental peptides. Presence of the fusion peptide has a beneficial effect on the immunogenicity of the linear as well as the branched peptides presumably by stabilizing peptide conformation. These effects enhance antibody and MHC binding [14,16], the efficiency of antigen presentation and consequently result in elevated virus specific B and T cell responses.

2. Materials and methods

2.1. Peptide immunization and influenza virus infection of BALB/c mice

Female BALB/c mice 8–10 weeks old were purchased from LATI (Gödöllõ, Hungary). Animals were kept under conventional conditions. BALB/c mice were immunized with 100 μg of the synthetic peptides, emulsified in complete Freund's adjuvant (CFA) (Sigma, St. Louis, MO), by subcutaneous injections into the hind footpads and to the base of the tail. Four weeks later primed mice were challenged with the same amount of peptide emulsified in incomplete Freund's adjuvant (IFA) (Sigma). Blood samples were taken 2 weeks after each antigenic challenge. Influenza virus infection of peptide preimmunized BALB/c mice was performed by aerosol exposure to 2 LD_{50} dose of the mouse pathogenic A/PR/8/34 influenza virus as described previously [14]. This viral dose resulted in the death of all mice at days 7–9.

2.2. Peptides

The description of peptide synthesis, purification and characterization has been reported elsewhere [17–19]. Characteristics of the peptides used in this study are summarized in Table 1.

2.3. Virus preparations

The A/PR8/34 human influenza virus (H1N1) stock, in which virus particles bear cleaved hemagglutinins (PR8), was grown in the chorio-allantoic fluid of 12-day-old embryonated hen eggs and was prepared as described previously [14]. The A/PR8/34 influenza virus, bearing uncleaved hemagglutinins (CEF PR8), was grown in primary chick embryo fibroblast (CEF) cells. The supernatant of the cell culture, containing the virus, was collected and purified by the method described by Barrett and Inglis [20]. Hemagglutination units (HAU/ml) was determined by titration on guinea-pig red blood cells.

2.4. Production of mAb

Spleen cells of immunized BALB/c mice were fused with the Sp2/0 murine myeloma cells according to the method of Köhler and Milstein [21], and clones of the selected hybridomas were established by the limiting dilution technique. The antigens used for immunization and for selection of the hybridomas are summarized in Table 2.

Table 1
Location within the hemagglutinin molecule, designation and amino acid sequence of synthetic peptides comprising the intersubunit region of influenza virus hemagglutinin

Location	Designation	Sequence
$HA1_{320-328}$	320–328	LRNIPSIQS
$HA1_{317-329}$	P4	VTGLRNIPSIQSR
$HA2_{1-12}$-R[a]	FP3	GLFGAIAGFIEGR
$HA0_{317-341}$	IP	VTGLRNIPSIQSRGLF-GAIAGFIEG
$[HA1_{317-329}]_4$	$(P4)_4$-FP3	$(VTGLRNIPSIQSR)_4(K)_3$-GLFDAIAGFIEGR
$HA1[_{317-329}]_4$	$(P4)_4$	$(VTGLRNIPSIQSR)_4(K)_3$
ZAP70(485-499)$_4$-FP3[b]	$(ZAP70)_4$FP3	$(ALGADDSYY-TARSAG)_4(K)_3$-GLFDAIAGFIEGR

[a] The C-terminal extension by Arg was introduced to increase peptide solubility and was shown not to influence FP3 characteristics [18].
[b] The $(ZAP70)_4$FP3 multipeptide construct was used as a specificity control.

Table 2
The generation and functional activity of peptide specific monoclonal antibody secreting clones

Hybridoma code	IP1/2	MAP1/2	PP12
Immunization			
First in vivo antigen challenge	IP	$(P4)_4FP3$	$(P4)_4FP3$
Second in vivo antigen challenge	A/PR/8/34	A/PR/8/34	–
In vitro antigen challenge before fusion	IP	$(P4)_4FP3$	$(P4)_4FP3$
Selection of hybridomas	IP	$(P4)_4FP3$	$(P4)_4FP3$
Isotype	IgG2a	IgG2a	IgM
Binding activity[a]			
Antigens			
IP	++	+	++
$(P4)_4FP3$	++	++	++
FP3	–	–	–
$(P4)_4$	+	–	+
PR8 (CEF)	–	–	+
PR8	–	–	–
PR8 pH5	–	–	–

[a] The binding activity of mAb was analyzed by solid-phase enzyme immunoassay using 10^2 dilution of cell culture supernatants. ++/+/– corresponds to >1.0, >0.4 and <0.1 OD_{492} values.

2.5. Enzyme immunoassay

Pooled or individual sera of immunized mice or the supernatant of hybridoma cells were analyzed for Ab content and specificity by solid-phase enzyme immunoassay (EIA) as described previously [14]. A total of 96-well polyvinyl-chloride (PVC) (EnzyPlate; Propilen G.M., Pécs, Hungary) plates were coated with 50 μl solution of different peptides (10 μg/ml) or with A/PR/8/34 influenza virus (10 HAU/ml) for 1 h at 37°C. Acidic pretreatment of the virus was performed in 0.1 M acetate buffer pH 5.0 for 20 min at room temperature. Bound antibodies were detected by horseradish peroxidase-labeled goat anti mouse IgM, IgG or IgG subclass specific second antibodies (Southern Biotechnology Associates, Birmingham, AL). Titers of virus or peptide specific antibodies were given as reciprocal serum dilutions corresponding to a defined OD_{492} value determined by linear regression analysis. In the inhibition assays pretitrated dilutions of sera were incubated for 2 h at 37°C with different concentrations of the competitor peptides. A total of 50 μl of these samples were dispensed to peptide precoated plates and after 1 h incubation the relative amount of bound Ab was detected as described above.

2.6. Trypsin mediated cleavage of immature HA0 molecules

The ability of peptide specific mAb to interfere with the trypsin-mediated cleavage of HA0 was tested in an in vitro assay as described previously [14]. As immunglobulins are able to consume trypsin activity, isotype matched mAb were used as controls. The peptide specific mAb used in this assay did not inhibit the hemagglutinating capacity of the virus.

2.7. Cell lines and monoclonal antibodies

The murine B lymphoma lines A20 (ATCC TIB 208) and 2PK3 (ATCC TIB 203) were used as APC in the T cell activation and in the binding assays. The IP12-7 T cell hybridoma was developed from a BALB/c mice preimmunized with the P4 peptide and subsequently infected with the A/PR/8/34 influenza A virus [15]. For IL2 quantitation the IL2-dependent CTLL-2 (ATCC TIB 214) T cell line was used. All cell lines were cultured in RPMI supplemented with 2 mM L-glutamine, 1 mM Na-pyruvate, 5×10^{-5} M 2-mercapthoethanol, antibiotics and 5% FCS (complete RPMI). The mAb against the I-E α-chain (14-4-4S, mouse IgG2a; ATCC HB 32) was used as a specificity control in the MHC binding assay.

2.8. Binding of biotinylated peptides to antigen presenting cells bearing MHC class II molecules

The peptides listed in Table 1 were biotinylated as described before [16,22]. Briefly, 2 mM peptide solution was prepared in 0.1 M $NaHCO_3$ and cooled in ice. A sample containing 2 mg/ml *N*-hydroxy-succinimide-biotin (NHSB) (Sigma) dissolved in dimethylsulphoxide (DMSO) was added to 30% molar excess. The reaction was allowed to proceed at 0°C for 2 h. Subsequently 5×10^5–1×10^6 A20 or 2PK3 cells suspended in 200 μl RPMI supplemented with 2 mM L-glutamine and 0.1% BSA were incubated with biotinylated peptides at 1–20 μM concentration at +4 or 37°C for 14 h. Cells were washed twice with ice cold PBS containing 0.1% BSA. In certain experiments peptide incubation was performed in the presence of different enzyme inhibitors present throughout the whole period of incubation.

Leupeptin was used at 2–50 mM final concentrations, mixture of enzyme inhibitors consisted of 1 mM Leupeptin, 0.2 mM phenylmethylsulphonyl fluoride (PMSF), 0.1 mg/ml pepstatin all purchased from Sigma, St. Louis, MO. Phycoerythrin-labelled streptavidin (Molecular Probes, OR) was added at 2 μg/tube and incubated for 30 min at 0°C. Cells were washed three times with cold PBS-0.1% BSA, resuspended in 0.5 ml washing solution and were analysed by flow cytometry using a FACScan analyser (Becton–Dickinson). Viable cells were gated on the basis of forward and side scatter. Data are documented either as histograms or as increase in mean fluorescence (arbitrary units). In the latter case, control cells were incubated without biotinylated peptides under the same conditions as those incubated with the labelled ones. Inhibition of peptide binding by mAb, specific for the I-E^d α-chain (14-4-4S), was performed by incubating the A20 or 2PK3 cells with biotinylated peptides in the presence of mAb-containing supernatant. In the peptide competition assays, cells were pre-incubated with a 10–100 molar excess of unlabelled competitor peptides for 3 h at 37°C and the binding assay was performed as described above.

2.9. In vitro T cell proliferative response

The T cell proliferation assay was performed by the method of Corradin [23], and has been described in detail elsewhere [15,19]. Briefly, 5×10^5 lymph node T cells were cultured with 1×10^5 irradiated syngeneic spleen cells in the absence or presence of different concentration (10–0.08 μg/ml) of synthetic peptides. On day 4 H^3-thymidin incorporation (1 μCi, 3.7 kBq/culture) was measured.

2.10. Quantitation of IL-2 produced by the activated IP12-7 T cell hybridoma

Isolation and characterization of the IP-12-29 T cell hybridoma and the detection of its antigen induced IL-2 production was measured as reported elsewhere [15].

3. Results

3.1. Immunogenicity of peptides and fine specificity of polyclonal antibodies elicited by peptide immunization

BALB/c mice were immunized in combination with CFA with the peptides P4, FP3 and IP, and with their multipeptide constructs $(P4)_4$ and $(P4)_4$–FP3 and the titer of polyclonal peptide specific antibodies was measured on IP and $(P4)_4$–FP3 coated plates. The results summarized in Fig. 1A show that both IP and $(P4)_4$–FP3 administered in CFA are immunogenic and induce high titres of peptide-specific antibodies cross reactive between the IP and $(P4)_4$–FP3. In contrast, the P4 and FP3 peptides were not immunogenic and the multipeptide consturct $(P4)_4$ elicited a poor Ab response, only. Titration of IP and $(P4)_4$–FP3 induced antibodies on IP, $(P4)_4$–FP3 and $(P4)_4$ peptide coated plates demonstrated that $(P4)_4$–FP3 immunization resulted in a slightly higher level of peptide specific Ab than IP injections (Fig. 1B). Although the $(ZAP70)_4$FP3 multipeptide (see Table 1) was immunogenic in CFA (data not shown), binding of IP or $(P4)_4$–FP3 induced Ab to $(ZAP70)_4$FP3 was not detected indicating that $(P4)_4$–FP3 specific Ab were raised against the P4 region and not against the branched lysine residues and/or the FP3

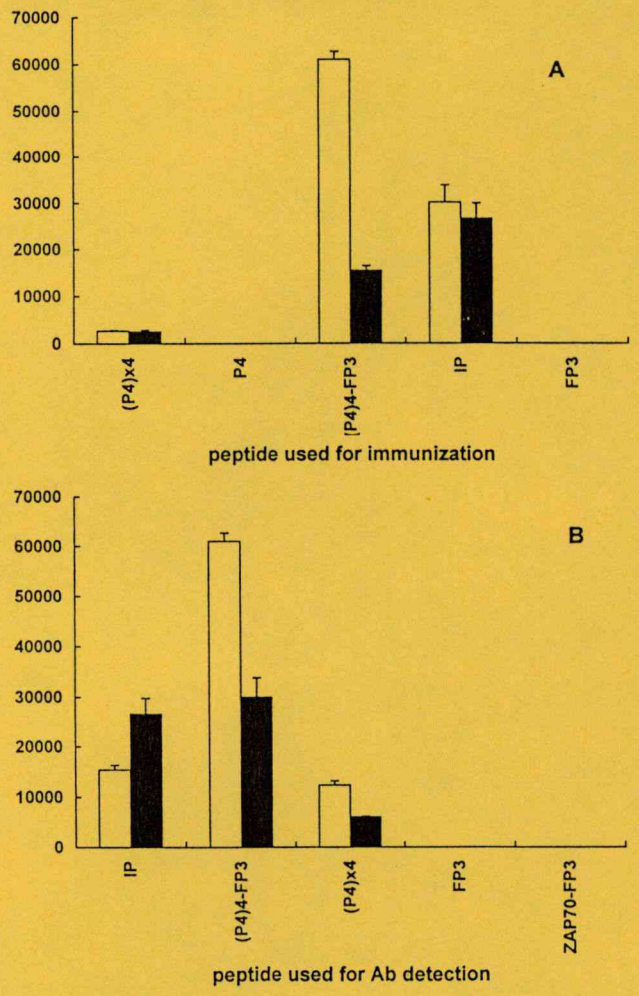

Fig. 1. Magnitude and specificity of peptide induced polyclonal antibodies. The titer of peptide specific antibodies measured on solid phase adsorbed IP (dark columns) or $(P4)_4$–FP3 (empty columns) in pooled sera of BALB c mice. immunized with $(P4)_4$, P4, $(P4)_4$–FP3, IP or FP3 (A). The titer of peptide specific antibodies measured on solid phase adsorbed IP, $(P4)_4$–FP3, $(P4)_4$, FP3 or $(ZAP70)_4$–FP3 in pooled sera of BALB c mice immunized with IP (dark columns) or $(P4)_4$–FP3 (empty columns) (B). Mean values $\pm$ SE of Ab titers measured in the pooled serum of six immunized mice were calculated from triplicate titration curves as described in Section 2.

tail. This interpretation is also supported by the lack of reactivity of IP and $(P4)_4$–FP3 specific Ab with FP3 (Fig. 1B). As revealed by control experiments and by binding inhibition assays, the inability of these Ab to bind to monomeric P4 was due to the weak adsorbtion of this peptide to the solid surface (data not shown). These results demonstrate the enhanced immunogenicity of the $(P4)_4$–FP3 multipeptide to elicit peptide specific Ab as compared to P4 or IP comprising the 317–329 and 317–341 natural sequence of immature HA0, respectively.

Fine specificity analysis of peptide-specific Ab performed by competitive EIA (data not shown) proved that IP and $(P4)_4$–FP3 specific antibodies are directed to the N-terminal 317–329 region of the IP peptide, which is covered by P4. The efficiency of the P4 peptide, calculated from the molar concentrations required for 50% inhibition of IP or $(P4)_4$–FP3 binding was two to three orders of magnitude lower than that of IP, $(P4)_4$ or $(P4)_4$–FP3. The binding (Fig. 1A, 1B) and the inhibition curves (data not shown) demonstrate that despite the cross reactivity of IP and $(P4)_4$–FP3, a substantial fraction of antibodies have unique specificity for the corresponding peptide used for immunization.

3.2. Reactivity of polyclonal peptide specific antibodies with influenza virus hemagglutinin

The presence of those antibodies, which recognize the 317–329 region within the HA molecule, was monitored in the serum of peptide immunized mice by using different virus preparations. A/PR/8/34 virus, grown in chicken embryonic fibroblasts (PR8 CEF) or in embryonated eggs (PR8) was adsorbed to the solid phase in neutral buffer or after acidic treatment at pH 5.0, and specific antibodies were detected by EIA. As summarized in Fig. 2A, 2C a certain fraction of polyclonal, peptide induced Ab does recognize acid pretreated virus particles (PR8 pH 5) but not PR8, suggesting that the pH induced conformational change of the HA molecule favours recognition by IP or $(P4)_4$–FP3 reactive antibodies. The titer of Ab that recognize both the peptide and the acid pretreated A/PR/8/34 virus was much higher in the serum of $(P4)_4$–FP3 than in IP immunized mice (Fig. 2A, 2B).

The isotype analysis of peptide (Fig. 2B) and virus specific (Fig. 2C) IgG Abs revealed that immunization with IP or $(P4)_4$–FP3 resulted in the predominant production of IgG1 and lower levels of IgG2a and IgG2b type antibodies. Significantly higher IgG1, IgG2a and IgG2b titers were measured in the sera of mice immunized with $(P4)_4$–FP3 than with IP detected on both peptide and PR8 pH5 coated plates (Fig. 2B, 2C).

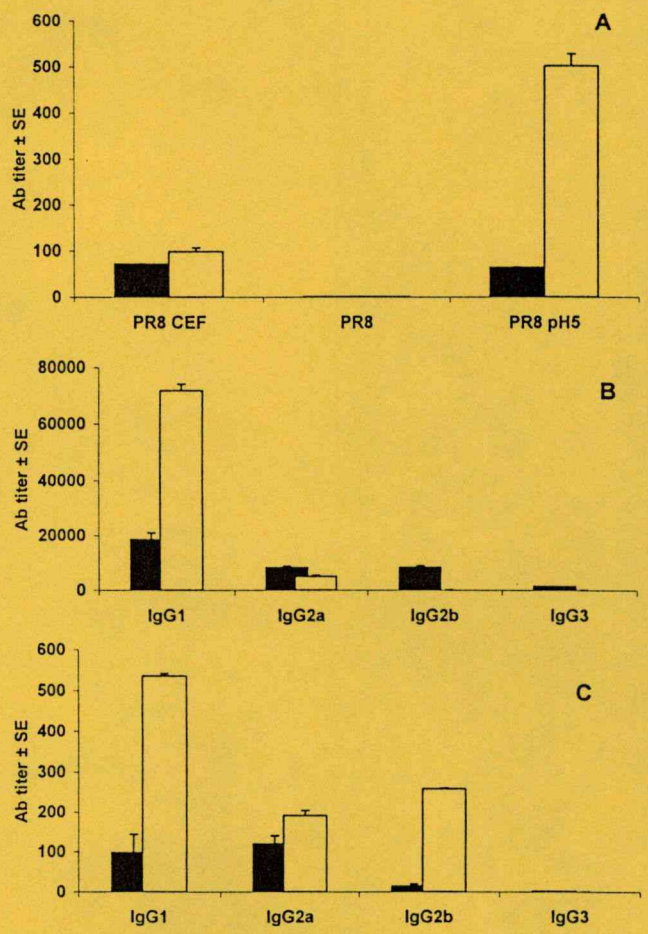

Fig. 2. Reactivity of IP and $(P4)_4$–FP3 induced polyclonal Ab with different forms of influenza virus hemagglutinin and subclass distribution of peptide specific and virus cross reactive polyclonal Ab. (A) A/PR/8/34 (H1N1) virus, grown in chicken embryonic fibroblasts (PR8 CEF) or in embryonated eggs (PR8) and acid pretreated virus (PR8 pH 5) were adsorbed to the solid phase at 10 HAU/ml concentation. Titers ± SE measured in the pooled sera of six IP (dark column) or $(P4)_4$–FP3 (empty column) immunized BALB/c mice are documented. The titers ± SE of peptide (B) and PR8 pH5 virus (C) specific IgG subclasses measured on IP, $(P4)_4$–FP3 (B) or PR8 pH5 (C) coated plates in the sera of IP (dark columns) and $(P4)_4$–FP3 (empty columns) immunized mice, respectively are documented.

3.3. Fine specificity of monoclonal antibodies isolated from IP or $(P4)_4$–FP3 preimmunized BALB/c mice

To compare the fine specificity of IP and $(P4)_4$–FP3 specific Ab at a clonal level monoclonal antibodies were prepared from BALB/c mice immunized by different protocols (Table 2). MAbs were screened for their binding to peptides and to different forms of influenza virus hemagglutinin. Three clones were selected for further characterization and their specificity patterns were summarized in Table 2. As a consequence of its binding to noninfectious virions the PP12 mAb is able to inhibit the trypsin mediated enzymatic cleavage of immature HA0 carried out in an in vitro assay, as described in Section 2 (Table 2). These results, in good

Table 3
The activity of parental peptides and multipeptide constructs to activate polyclonal (A) or monoclonal (B) peptide elicited T cells

	P4	$(P4)_4$	IP	$(P4)_4$–FP3	—
A. Proliferation in the presence of autologous APC and peptide (cpm ± SE)					
Peptide used for immunization					
P4	14 057.8 ± 1125	21 702.7 ± 1444	6504.3 ± 954	18 088 ± 3367	8805.4 ± 1486
$(P4)_4$	19 849.3 ± 5176	22 003.2 ± 4318	11 414.7 ± 2383	33 535.7 ± 701	9022.2 ± 1234
IP	23 175 ± 5906	71 937 ± 4475	40 511.3 ± 6318	85 401.1 ± 2975	10 729.7 ± 943
$(P4)_4$–FP3	22 604.7 ± 5603	31 054.1 ± 5094	15 972.1 ± 4668	66 828.1 ± 3175	10 129.6 ± 615
B. IL-2 production of the IP12-7 hybridoma in the presence of A20 APC and peptide (OD_{550} ± SE)					
Ag used for immunization					
P4 PR8	0.242 ± 0.002	0.378 ± 0.017	0.265 ± 0.007	0.340 ± 0.025	0.004 ± 0.001

A. Proliferation of lymph node derived polyclonal T cells isolated from P4, IP, $(P4)_4$ and $(P4)_4$–FP3 immunized BALB/c mice was measured in the presence of irradiated syngeneic spleen cells and 20 μg/ml stimulator peptides. Mean cpm values of triplicates ± SE of a typical experiment are documented.
B. Activation of the peptide specific T cell hybridoma IP12-7 by different peptides added at 10 μg/ml. Mean values of triplicates ± SE of optical density corresponding to IL2 production detected by the MTT assay are documented.

correlation with data obtained with polyclonal Ab, demonstrate, that certain peptide specific Ab induced by IP or $(P4)_4$–FP3 not only recognize the corresponding peptides, but react with different forms of HA.

3.4. The T cell activating and MHC binding capacity of the linear and branched HA peptides

In vivo experiments revealed that IP and $(P4)_4$–FP3 are more potent to induce an MHC class II restricted T cell response than P4 or $(P4)_4$ (Table 3A). Polyclonal T cells elicited by IP or $(P4)_4$–FP3 recognize all peptides containing P4 but the highest in vitro T cell activation was achieved with $(P4)_4$ or $(P4)_4$–FP3 peptides. These results suggests that polyvalency of $(P4)_4$ or $(P4)_4$–FP3 increases the efficiency of in vitro T cell activation mediated by P4. In good correlation with the Ab data, the enhanced potency of $(P4)_4$–FP3 to prime P4 specific MHC class II restricted T cells in vivo is supported by FP3.

To investigate the possible properties of $(P4)_4$–FP3 responsible for the enhanced activity in the polyclonal T cell activation assays, the efficiency of the HA peptides to interact with MHC class II molecules was measured by direct binding of the biotinylated peptides to living APC. Results summarized in Fig. 4 show the specificity of $(P4)_4$–FP3 binding to 2PK3 cells. Binding of biotinylated $(P4)_4$–FP3 (Fig. 4AIII) is completely inhibited by the I-E^d specific mAb 14-4-4S (Fig. 3AI) as compared to the corresponding negative control (Fig. 4AII). Partial inhibition of biotinylated $(P4)_4$–FP3 binding (Fig. 4BIV) could also be observed in the presence of a 20-fold molar excess of unlabelled $(P4)_4$–FP3 (Fig. 4BII) or by a shorter P4 analog peptide 320–328 (see Table 1, Fig. 4BI). These data demonstrate that $(P4)_4$–FP3, similarly to P4 (data not shown), binds to I-E^d and compete for P4 binding sites. The differences in the optimal concentrations required for binding, and the relative increase in mean fluorescence clearly suggest that the $(P4)_4$–FP3 construct is more efficient in binding to both APCs than its monovalent counterpart P4 (Table 4). The high binding efficiency of the $(P4)_4$–FP3 construct in binding to MHC class II may be the consequence of its ability to form cross-linked MHC class II clusters on the cell surface. To study whether multivalent binding of $(P4)_4$–FP3 can occur at the cell surface or requires internalization and further processing, the binding assay was performed both at 37 and 4°C. A 14 h incubation at 4°C resulted in comparable results with those obtained at 37°C. The serine protease inhibitor leupeptin used at 2, 10 or 50 mM final concentration, or a mixture of enzyme inhibitors (used as described in Section 2) does affect $(P4)_4$–FP3 binding. These data altogether suggest that $(P4)_4$–FP3 binding can occur at the cell surface and the

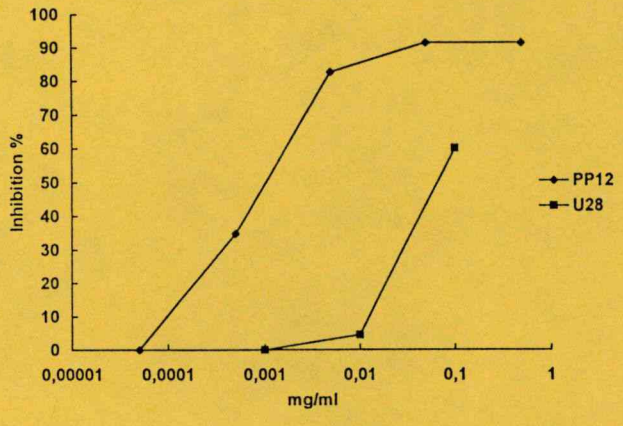

Fig. 3. The effect of PP12 mAb binding on the trypsin mediated enzymatic cleavage of immature HA0. Influenza virus grown on CEF was pre-incubated with PP12 (◆ anti-$(P4)_4$–FP3, IgM) and U28 (■ anti-mouse IgG2a, IgM, isotype matched control) mAb. Inhibition is given as percentage of fusion activity measured in the absence of mAb.

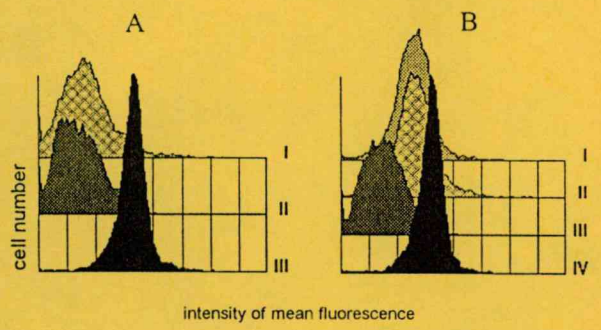

Fig. 4. Specificity of the binding of N-terminal biotinylated peptides to I-E^d molecules of living A20 and 2PK3 cells. Binding of $(P4)_4$–FP3 (5 μM) to 2PK3 cells (A/III, B/IV) is depicted in comparison to 2PK3 cells incubated without the peptide (A/II, B/III) or with $(P4)_4$–FP3 (5 μM) in the presence of 14.4.4 mAb (A/I), 20-fold molar excess of unlabelled $(P4)_4$–FP3 (B/II) or 320–328 (H1) peptides (B/I).

multivalent construct does not require internalization and/or further processing for interacting with the peptide binding groove of MHC class II. However, when investigated with a P4 specific T effector cell (IP12-7 hybridoma), the peptides IP, P4 and $(P4)_4$–FP3 exerted similar activity in inducing IL2 production in the presence of A20 APC (Table 2B). $(ZAP70)_4$FP3 was not effective to induce IL2 production in the same assay demonstrating the P4 specificity of this T cell. These results show that the monovalent P4 comprises the fully active epitope for IP-12-7 and suggest that stabile MHC clusters, formed by polyvalent $(P4)_4$–FP3 but not by P4 on the cell surface, are not essential but may be beneficial for T cell activation. The IP12-7 T cell hybridoma, which recognizes P4, IP and $(P4)_4$–FP3 equally well (Table 2B) can also be activated by the A/PR8/34 virus, grown on CEF, in a dose dependent manner (data not shown). However, infective virions bearing cleaved HA (PR8) resulted in marginal IP12-7 activation. This observation suggests that processing of HA0 but not of cleaved HA via the exogenous route results in the generation of peptides encompassing the P4 sequence.

Table 4
The binding of biotinylated $(P4)_4$–FP3 and P4 peptides to living A20 or 2PK3 cells

Concentration of peptides (μM)		Δ Mean fluorescence ± SE[a]	
		2PK3	A20
P4	20	29.4 ± 3.0	29.2 ± 3.6
IP	20	24.9 ± 1.4	n.t.
$(P4)_4$-FP3	5	59.7 ± 5.2	46.6 ± 5.4
$(P4)_4$-FP3	2.5	46.7 ± 4.6	54.3 ± 5.2
$(P4)_4$-FP3	1	15.7 ± 4.6	16.3 ± 3.7

[a] Mean values of three independent experiments ± SE are documented, n.t.—not tested.

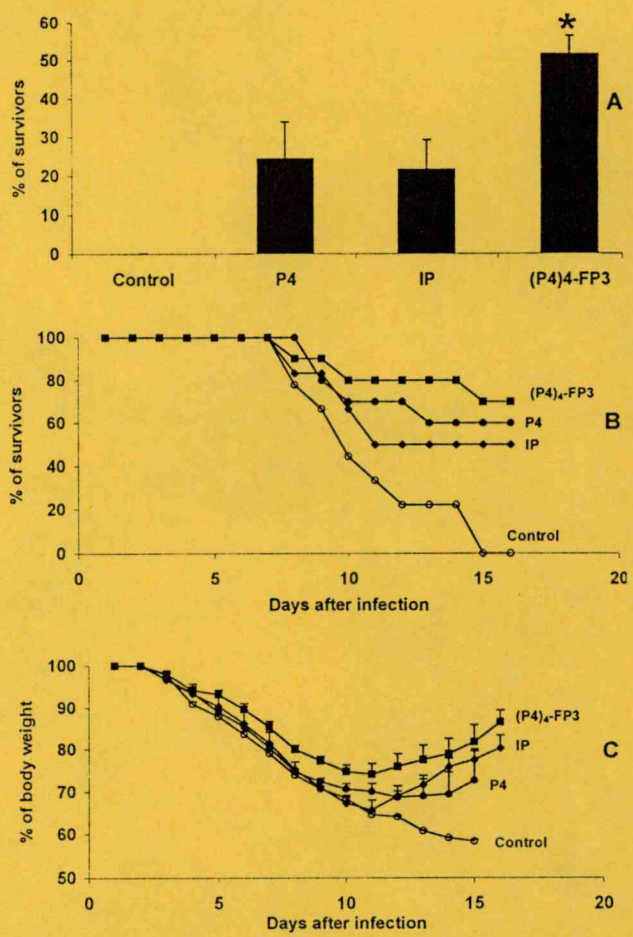

Fig. 5. The effect of P4, IP and $(P4)_4$–FP3 pre-immunization on the survival and body weight loss of BALB/c mice caused by lethal A/PR/8/34 infection. Percent of survivors ± SE, determined in six independent in vivo protection experiments ($n = 36$) are documented. Mice were preimmunized twice with 100 μg peptide and subsequently infected with $2LD_{50}$ mouse pathogenic A/PR/8/34 influenza virus. * $P < 0.05$ as related to P4 or IP (A). Kinetics of death (B) and body weight loss (C) obtained in a typical protection experiment, where six mice of each group were preimmunized with $(P4)_4$–FP3 (■–■), IP (◆–◆) dissolved in PBS and PBS (●-●), all emulsified in CFA, is documented.

3.5. The effect of IP and $(P4)_4$–FP3 preimmunization on the protective immune response of BALB/c mice against a lethal dose of A/PR/8/34 influenza virus

Fig. 5 summarizes the results of six independent in vivo protection experiments in which the body weight loss (Fig. 5C) and survival (Fig. 5B) of peptide pretreated mice, infected with a lethal dose ($2LD_{50}$) of murine adapted A/PR/8/34 influenza virus, was monitored. Preimmunization of BALB/c mice with 100 μg P4 peptide or with its fusion peptide extended analog (IP) conferred some protection against a lethal virus challenge. However, $(P4)_4$–FP3 was significantly more effective to confer protection than the P4 or IP peptides (Fig. 5A). The similar efficiency of P4 and the stochiometric mixtures of P4 and FP3, corresponding to the

composition of IP or $(P4)_4$–FP3, in the protection experiments (data not shown) point to the beneficial effect of covalently linked P4 and FP3 segments.

4. Discussion

The increased efficiency of multipeptide constructs to induce a protective immune response has been demonstrated in different systems [24,25] and the importance of T and B cell epitope orientation has also been shown [26]. In this study a detailed analysis of the immune response induced by different multipeptide constructs (Table 1) was compared with that elicited by the parental monovalent peptides comprising a subdominant protective epitope of influenza virus HA [15,27]. The results obtained with these influenza HA derived peptides not only demonstrated the increased potency of certain multipeptide constructs but shed light on the mechanisms by which increased efficiency could be achieved.

Selection of HA epitopes applied in this study was based on previous results showing the involvement of the intersubunit region of influenza HA, which is not the target of frequent antigenic drifts, in immune recognition [14,15,27]. Epitope mapping of the synthetic peptide IP, encompassing the 317–341 HA0 sequence, revealed the predominant role of P4, comprising the C-terminal of HA1, in both Ab and T cell recognition and postulated the carrier function of FP3, corresponding to the N-terminal fusion region of HA2 [17,28]. Based on this information two multipeptide constructs were designed (Table 1) both containing the P4 peptide in four copies. To study the carrier function of the fusion region, multipeptide constructs with, or without FP3 were also studied. As a specificity control, a similar construct was synthesized which instead of P4 contained an unrelated peptide (ZAP70 485–499) in four copies ($(ZAP70)_4$FP3 in Table 1).

Poly- and mono-clonal Ab, elicited by both IP and $(P4)_4$–FP3, were shown to direct against P4 and were not able to recognize FP3 (Fig. 1). In contrast to IP and $(P4)_4$–FP3, the peptides P4 and $(P4)_4$ were shown to be weak immunogens suggesting the importance of FP3 in maintaining immunogenicity (Fig. 1). The reactivity of IP- and $(P4)_4$–FP3-induced polyclonal Abs with acid pretreated virus and the binding of the monoclonal mAb PP12 to A/PR8/34, grown on CEF, demonstrate that the C-terminal 317–329 region of HA1 is available for Ab recognition either in immature HA0 or after the pH induced conformational change of the mature, enzymatically cleaved HA molecule. Binding of peptide (PP12) or virus induced (Z38) mAb, directed against this region of the molecule, can interfere with the proteolytic cleavage of HA0 [14] (Fig. 3) demonstrating their potential to inhibit the membrane fusion or the enzymatic cleavage of HA mediated by extracellular bacteria [29]. The inability of peptide specific Ab to bind to PR8 at neutral pH shows that the C-terminal of HA1 is not available for Ab binding under such conditions. Therefore the irreversible change of HA conformation, induced at low pH [30], not only exposes the fusion peptide but makes the C-terminal stretch of HA1 available for recognition by certain Ab and also for further enzymatic truncation by carboxy peptidases [31,32]. Based on this consideration P4 specific Ab will be focused to non infectious virions produced by APC or to virions that carry both cleaved and uncleaved HA molecules. Internalization of these particles to acidic endosomal compartments will transfer the bound Ab to the site of fusion [27,31]. Demonstrating the possible in vivo significance of this mechanism, the $(P4)_4$–FP3 induced mAb PP12 has similar specificity and functional activity as the mAb Z38 isolated from the spleen of a virus infected BALB/c mouse [14]. This proves, that a low proportion of virus specific B cells do recognize the C-terminal 317–329 sequence of HA1 during viral infection and on the other hand, $(P4)_4$–FP3 immunization can result in the production of Abs cross reactive with HA0 (mAb PP12, Fig. 3). Another population of virus reactive Abs detected in sera of peptide immunized mice, but not found in our mAb panel (Table 3), reacts with virions carrying conformationally altered HA induced by acidic pH (Fig. 2A, 2C).

The immune response elicited by $(P4)_4$–FP3 is characterized by elevated levels of high affinity IgG type Ab in comparison to that induced by P4 or IP (Fig. 2B). The predominance of the IgG1 isotype in peptide specific Ab is very likely due to the adjuvant used for immunization, however, the fraction of $(P4)_4$–FP3 specific Ab, which is cross reactive with the virus treated at low pH, include IgG2a and IgG2b type Ab as well (Fig. 2B). The IgG2a isotype of peptide specific mAb isolated after preimmunization and viral challenge (Table 3) suggests that viral infection favours isotype switch of peptide specific IgG1 secreting cells. The inability of the selected IgG type mAb to react with any form of the virus points to the relatively low frequency of peptide and virus cross-reactive Ab which is well demonstrated also by the different magnitude of the peptide and virus specific Ab titers (Figs. 1 and 2). Virus infection of peptide immunized mice results in decreased level of peptide specific Ab (data not shown) suggesting high antigenic competition conferred by multiple immunodominant epitopes of HA and other viral proteins. The population of peptide induced virus reactive Ab secreting cells, however, can be challenged by subsequent viral infection.

Peptides, comprising both P4 and FP3, are the ones that are highly potent to induce Ab production and to confer protection against lethal virus infection (Figs. 1 and 5). This observation suggests that peptide specific

Ab and/or peptide specific B cells, by inducing an efficient T helper response, may be involved in mediating protection. However, P4 preimmunization also confers protection without detectable Ab production, which points to the role of peptide specific T cells (Table 2A). The appearance of IgG1, IgG2a and IgG2b type, virus reactive Ab produced as a result of peptide immunization (Fig. 2B) in correlation with the increased potency of IP and $(P4)_4$–FP3 to confer protection (Fig. 5) support the involvement of Ab. As it has been shown previously, both IP and $(P4)_4$–FP3, but not P4 have a high propensity to adopt an ordered conformation in solution [17,27,28] which may protect against rapid degradation and support Ab binding and immunogenicity. Therefore the fusion peptide functions as an efficient stabilizer and/or carrier for P4, however, the fraction of HA-reactive Ab is lower than that of the peptide specific ones. This may explain the less striking differences between the P4-containing and FP3-extended peptides in the protection than in the immunogenicity experiments (Figs. 1, 2 and 5).

Increased copy numbers of P4 within one molecule not only enhances the Ab but also the T cell activating capacity of peptides (Fig. 1, Table 3). The dose dependent binding of the tetravalent $(P4)_4$–FP3 construct to $I\text{-}E^d$ was more efficient than that of P4 (Table 4). This suggests that multivalent interaction of $(P4)_4$–FP3 with MHC class II molecules either on the cell surface or in endocytic compartments is more efficient than monovalent peptide loading and therefore may lower the threshold for in vivo T cell activation by focusing covalently linked T cell epitopes to APC. However, P4, IP and $(P4)_4$–FP3 had similar potency in the activation of a P4 induced effector T cell hybridoma (Table 2B).

P4 can be the degradation product of both immature and mature HA. The enzymatic cleavage and the pH dependent conformational change of HA results in enhanced sensitivity to proteolytic degradation, therefore it is reasonable to assume that processing of HA0 and HA gives rise to different sets of peptides available for MHC class II binding. The reactivity of the IP12-7 T cell hybridoma with A/PR8/34 grown on CEF but not in chicken embryos demonstrates the different processing of the two forms of HA. P4 has been characterized as a subdominant T cell epitope [15], which can be the consequence of the limited generation of the appropriate peptide upon in vivo viral processing. Preimmunization with stabile synthetic peptides of high binding capacity to MHC class II [16] may be a valuable tool to increase the frequency of T cells committed to the required specificity.

As a conclusion, the higher potency of $(P4)_4$–FP3 to confer protection as compared to the monovalent, parental P4 or IP peptides may be due to multiple factors including: (i) stabilized peptide conformation which favours strong, polyvalent Ab and MHC binding [14,16]; (ii) activation of MHC class II restricted helper T cells of the TH1 phenotype, which secrete lymphokines known as potent mediators in the resolution of viral infections (Horváth et al., unpublished results) caused by cytopathic viruses including influenza [16,33,34]; (iii) TH1 cell mediated production of IgG isotypes such as IgG2a, which are highly active in Ab mediated effector functions [35]; (iv) P4 conformation stabilized by FP3 in a structure relevant to its appearance in HA0 and/or in acid treated HA [17,27,28]; (v) activation of peptide specific B cells which function as efficient APC for peptide specific T cells; and (vi) production of Ab which can neutralize by inhibiting intra- or extra-cellular enzymatic cleavage and fusion activity [14,29].

Acknowledgements

This work was supported by the grant OTKA T-017157, AKP 96-43/64 and OMFB EU96-D8-024 to É. Rajnavölgyi. The expert technical assistance of Erzsébet Veress and Árpád Mikesi is acknowledged.

References

[1] I.A. Wilson, N.J. Cox, Annu. Rev. Immunol. 8 (1990) 737–771.
[2] R.A. Lamb, P.W. Choppin, Annu. Rev. Biochem. 52 (1983) 467–506.
[3] D.C. Wiley, J.J. Skehel, Ann. Rev. Biochem. 56 (1987) 365–394.
[4] D.C. Wiley, I.A. Wilson, J.J. Skehel, Nature 289 (1981) 373–378.
[5] K.H. Mills, J.J. Skehel, D.B. Thomas, J. Exp. Med. 163 (1986) 1477–1490.
[6] W. Weis, J.H. Brown, S. Cusack, J.C. Paulson, J.J. Skehel, D.C. Wiley, Nature 333 (1988) 426–431.
[7] J.K. Lamb, D.D. Eckels, P. Lake, J.N. Woody, N. Green, Nature 300 (1982) 66–69.
[8] R.A. Ffrench, X.L. Tang, E.M. Anders, D.C. Jackson, D.O. White, H. Drummer, J.D. Wade, G.W. Tregear, L.E. Brown, J. Virol. 63 (1989) 3087–3094.
[9] P.G. Schoofs, H.M. Geysen, D.C. Jackson, L.E. Brown, X.L. Tang, D.O. White, J. Immunol. 140 (1988) 611–616.
[10] D.C. Jackson, L.E. Brown, Peptide Res. 4 (1991) 114–124.
[11] J.L. Hurwitz, E. Herber-Katz, C.J. Hackett, W. Gerhard, J. Immunol. 133 (1984) 3371–3377.
[12] L.J. Stern, J.H. Brown, T.S. Jardetzky, J.C. Gorga, R.G. Urban, J.L. Strominger, D.C. Wiley, Nature 368 (1994) 215–221.
[13] E.C. Nice, T.L. McInerney, D.C. Jackson, Mol. Immunol. 33 (1996) 659–670.
[14] Z. Nagy, É. Rajnavölgyi, M. Hollósi, G.K. Tóth, G. Váradi, B. Penke, I. Tóth, A. Horváth, J. Gergely, I. Kurucz, Scand. J. Immunol. 40 (1994) 281–291.
[15] É. Rajnavölgyi, Z. Nagy, I. Kurucz, P. Gogolák, G.K. Tóth, Gy. Váradi, B. Penke, Z. Tigyi, M. Hollósi, J. Gergely, Mol. Immunol. 31 (1994) 1403–1414.
[16] É. Rajnavölgyi, A. Horváth, P. Gogolák, G.K. Tóth, Gy. Fazekas, M. Fridkin, I. Pecht, Eur. J. Immunol. 27 (1997) 3105–3110.
[17] M. Hollósi, A.A. Ismail, H.H. Mantsch, B. Penke, G. Váradi, G.K. Tóth, I. Laczkó, I. Kurucz, Z. Nagy, G. Fasman, É. Rajnavölgyi, Eur. J. Biochem. 206 (1992) 421–425.

[18] S. Holly, Zs. Majer, G.K. Tóth, Gy. Váradi, É. Rajnavölgyi, I. Laczkó, M. Hollósi, Biochem. Biophys. Res. Commun. 193 (1993) 1247–1254.
[19] G.K. Tóth, G. Váradi, Z. Nagy, É. Monostori, B. Penke, Z. Hegedûs, L. Andó, Gy. Fazekas, L. Kurucz, M. Mák, É. Rajnavölgyi, Peptide Res. 6 (1993) 272–280.
[20] T. Barrett, S.C. Inglis, in: B.W.J. Mahy (Ed.), Virology, a Practical Approach, IRL Oxford University Press, England, 1985, pp. 119–150.
[21] G. Köhler, C. Milsten, Nature 256 (1975) 495–497.
[22] E. Mozes, M. Dayan, E. Zisman, S. Brocke, A. Licht, I. Pecht, EMBO J. 8 (1989) 4049–4052.
[23] G. Corradin, H.M. Etlinger, J.M. Chiller, J. Immunol. 119 (1977) 1048–1053.
[24] J.P. Tam, Proc. Natl. Acad. Sci. USA 85 (1988) 5409–5413.
[25] E.H. Nardin, G.A. Oliveira, J.M. Calvo-Calle, R.S. Nussenzweig, Adv. Immunol. 60 (1995) 105–149.
[26] J.P. Tam, Y.-A. Lu, Proc. Natl. Acad. Sci. USA 86 (1989) 9084–9088.
[27] É. Rajnavölgyi, Z. Nagy, A. Daser, A. Horváth, P. Gogolák, I. Kurucz, in: É. Rajnavölgyi (Ed.), Synthetic Peptides in the Search for B- and T-cell Epitopes, CRC Press, Austin, TX, 1994, pp. 173–192.
[28] Zs. Majer, S. Holly, G.K. Tóth, G. Váradi, Z. Nagy, A. Horváth, É. Rajnavölgyi, I. Laczkó, M. Hollósi, Arch. Biochem. Biophys. 322 (1995) 112–118.
[29] M. Tashiro, P. Ciborowski, H.-D. Klenk, G. Pulverer, R. Rott, Nature 325 (1987) 536–537.
[30] P.A. Bullough, F.M. Hughson, J.J. Skehel, D.C. Wiley, Nature 371 (1994) 37–43.
[31] J.M. White, I.A. Wilson, J. Cell Biol. 105 (1987) 2887–2896.
[32] W. Garten, H.D. Klenk, J. Gen. Virol. 64 (1983) 2127–2137.
[33] G.H.W. Wong, D.V. Goeddel, Nature 323 (1986) 819–822.
[34] D. Kägi, H. Hengartner, Curr. Opin. Immunol. 8 (1996) 472–477.
[35] Gy. Fazekas, B. Rosenwirth, P. Dukor, J. Gergely, É. Rajnavölgyi, Eur. J. Immunol. 24 (1994) 3063–3067.

3.12.

ELSEVIER

Spectrochimica Acta Part A 56 (1999) 215–223

SPECTROCHIMICA ACTA PART A

www.elsevier.nl/locate/saa

Letter

Effect of chain length on the conformation and T cell recognition of synthetic hemagglutinin fragments

Gábor K. Tóth [a], Sándor Holly [b], Zsuzsa Majer [c], Miklós Hollósi [c], Éva Rajnavölgyi [d], Ilona Laczkó [e,*]

[a] *Department of Medical Chemistry, Szent-Györgyi Medical University, Dóm tér 9, H-6720 Szeged, Hungary*
[b] *Institute of Chemistry, Chemical Research Center, HAS, PO Box 17, H-1518 Budapest, Hungary*
[c] *Department of Organic Chemistry, Eötvös University, PO Box 32, H-1158 Budapest, Hungary*
[d] *Department of Immunology, Eötvös University, H-2131 Göd, Hungary*
[e] *Institute of Biophysics, Biological Research Center, HAS, PO Box 521, H-6701 Szeged, Hungary*

Received 15 June 1999; received in revised form 10 September 1999; accepted 7 October 1999

Abstract

Circular dichroism and Fourier-transform infrared spectroscopies were used to compare the conformational mobility of 13-mer peptides covering the 317–329 region of the envelope protein hemagglutinin of human influenza A virus subtypes H1, H2 and H3 with that of their truncated deca- and nonapeptide analogs. These peptides were demonstrated to bind to the murine I-E^d major histocompatibility complex encoded class II and human HLA-B*2705 class I molecules. Despite the amino acid substitutions in the three 13-mer subtype sequences, no significant differences in the conformational properties could be shown. Deletion of the N-terminal three residues resulted in a shift to an increased α-helical conformer population in the 317–329 H1 peptide and the breakage of the 3_{10} or weakly H-bonded (nascent) α-helix in the H2 and H3 peptides. The conformational change observed upon deletion did not influence the efficiency of I-E^d–peptide interaction, however, the C-terminal Arg had a beneficial effect both on MHC class II and class I binding without causing any remarkable change in solution conformation. © 2000 Elsevier Science B.V. All rights reserved.

Keywords: CD FTIR spectroscopy; Conformation; Hemagglutinin; T-cell recognition

1. Introduction

The presentation of antigenic peptides in the context of the highly polymorphic major histocompatibility complex (MHC) membrane glycoprotein is the prerequisite of specific T-cell

* Corresponding author. Fax: +36-62-433133.
E-mail address: laczko@nucleus.szbk.u-szeged.hu (I. Laczkó)

1386-1425/00/$ - see front matter
PII: S1386-1425(99)00255-3

recognition and effector functions. Antigenic peptides bound to MHC class I molecules are recognized by cytotoxic T-cells while helper T-lymphocytes monitor foreign peptides presented by MHC class II glycoproteins [1–4].

The peptides presented by MHC class I membrane glycoproteins share common characteristic features. They are restricted to a length of 8–10 amino acids and require the presence of conserved amino acid residues at certain positions [3]. The major anchor residues are located close to the chain termini and peptides of different lengths bind similarly at their ends but bulge out in the middle [5]. Despite the general requirements for peptide binding, X-ray crystallographic studies of MHC class I-peptide complexes revealed that the binding affinity of a certain peptide is affected by its individual amino acid sequence [6]. MHC class I epitopic peptides are mounted in the groove of histocompatibility proteins in extended (parallel β-pleated sheet) conformation [7].

MHC class II-restricted epitopes are usually 13–17 residues long and they adopt polyproline II-like semi-extended conformation in MHC bound form. This allows extensive hydrophobic interactions between the peptide and the binding groove thus providing a mode of MHC-peptide interaction independent of the peptide sequence [8–10]. Several side chains are placed within the four to five pockets of unique shape, hydrophobicity and charge characteristic for a given MHC class II allotype.

The C-terminal region of the influenza virus hemagglutinin HA1 subunit comprises B- and T-cell epitopes. The T-cell epitopes are recognized either by helper or cytotoxic T cells in the context of MHC class II (murine I-E^d) [11–14] and class I (HLA-B27) molecules [15,16], respectively. Our earlier circular dichroism (CD) and Fourier-transform infrared (FTIR) spectroscopic studies on peptides comprising the C-terminal 317–329 stretch of the HA1 subunit revealed distinct conformations in dependence on subtype-related differences of the amino-acid sequence [17]. Interestingly, the peptide showing the highest α-helix content has proved to be less potent to induce an in vivo T cell response and in vitro T cell proliferation [18]. Since an amphipathic helical structure has been proposed for T cell epitopic peptides [19], the ability of a switch from α-helix to extended conformation appears to be a prerequisite of good antigenic and immunogenic properties. Indeed, our previous CD spectroscopic studies demonstrated a conformational bistability of the immunogenic 317–341 HA peptide [20].

In order to investigate the conformational constraints of free and of MHC-bound peptides, the conformational properties of the A/PR/8/34 influenza virus hemagglutinin peptides were investigated. CD and FTIR spectroscopic studies were

Table 1
Amino acid sequences and MHC class II (I-E^d) MHC class I (HLA-B*2705) binding of peptides covering the C-terminal region of the HA1 subunit of human influenza A virus subtypes H1–H3

Location	Subtype	Sequence[a]	I-E^d binding	HLA-B*2705 binding
317–329	H1	VTGLRNIPSIQSR	++	+/−
319–328	H1	GLRNIPSIQS	+	−
320–328	H1	LRNIPSIQS	+	+/−
320–329	H1	LRNIPSIQSR	++	++
317–329	H2	ATGLRNVPQIESR	++	−
319–328	H2	GLRNVPQIES	+	−
320–328	H2	LRNVPQIES	+	−
320–329	H2	LRNVPQIESR	++	++
317–329	H3	ATGMRNVPEKQTR	+	−
319–328	H3	GMRNVPEKQT	+/−	−
320–328	H3	MRNVPEKQT	+/−	−
320–329	H3	MRNVPEKQTR	+	++

[a] Changes in the sequence of subtypes H2 and H3, relative to that of H1, are underlined.

performed on peptides 317–329 (H1–H3 subtypes) and on their truncated derivatives (Table 1) and the spectroscopic data were evaluated in the context of the immunological studies on the same peptides.

2. Experimental

The peptides were synthesized by the solid phase technique utilizing Boc chemistry as described earlier [17]. The crude peptides were purified by reverse-phase HPLC and characterized by HPLC, FAB mass spectrometry and FTIR spectroscopy.

CD spectra were measured on a Jobin-Yvon Mark VI dichrograph. Measurements were carried out in 0.02 cm cells in a concentration range of 0.5–1 mg/ml. Mean residue ellipticity, $[\Theta]_{MR}$, is given in deg cm^2/dmol.

Infrared measurements were performed on a Nicolet 170SX spectrometer at a resolution of 4 cm^{-1}. A 0.025 cm cell with CaF_2 windows was used for measuring the FTIR spectra in D_2O. Infrared spectra in trifluoroethanol (TFE) were taken in a KBr liquid cell of 0.041 cm. The concentration of the samples was ~ 1 mg/ml. TFE spectrum obtained under identical condition was subtracted from the sample spectra measured in TFE. The contribution of the H–O–H deformation appearing at ca. 1633 cm^{-1}, due to traces of water, was removed on the basis of the combination band of O–H stretching and H–O–H deformation vibrations at 5293 cm^{-1}. All peptides (except for H1 319–328 and H1 320–328) were present as trifluoroacetate (TFA) salts because of the purification procedure using TFA-containing eluents. The trifluoroacetate anion is known to have an absorption band in the amide I infrared region. In the infrared spectrum of CF_3COONa in KBr pellet the ν_{as} mode of the COO^- group appears at 1694.5 cm^{-1} while the ν_{as} and ν_s vibration of the CF_3 group at 1218 and 1143 cm^{-1}, respectively. In the KBr spectra of the peptides the ν_s CF_3 band shows up at 1135 ± 1 cm^{-1}, accompanied by the ν_{as} band near 1205 cm^{-1}, while the ν_{as} mode of COO^- of TFA anion was found between 1702 and 1699 cm^{-1}. The ratio of band intensities $I(\sim 1700)/I(\sim 1135)$ in the spectra of peptides and $I(1694.5)/I(1143)$ in the spectrum of CF_3COONa in KBr is practically the same (1.55 ± 0.15). On the basis of this the contribution of the ν_{as} (COO^-) vibration of the counterion trifluoroacetate could be removed from the spectra of the peptides in TFE by using the spectrum of CF_3COONa in the same solvent [17,20,21]. The FTIR spectra in TFE were analyzed by a normalized, least-squares curve-fitting program using products of Gauss and Lorentz curves [21]. The position of the component bands is based on Fourier self-deconvolution (Fig. 1) [22].

3. Results and discussion

FTIR and CD spectroscopic measurements were performed in water (D_2O) and in trifluoroethanol. TFE is well known to promote α-helical and β-turn conformations, that is, structures which are stabilized by intramolecular H-bonds. This effect is due to the combination of two properties of the solvent, its high dipole moment and a relatively low dielectric constant [23]. Although, structures detected in halogenated alcohols does not necessarily represent the native conformations of peptides, or its intrinsic ability to adopt folded structures, close correspondence between structures observed for peptides in solution and in bound state was observed in many cases [24,25].

3.1. FTIR studies

In D_2O the full length (317–329) and truncated HA1 peptides show one major broad infrared band between 1650–1640 cm^{-1} which is characteristic of the predominance of unordered (structurless) conformer population(s) and the lack of significant amounts of ordered structures.

In TFE the amide I region below 1675 cm^{-1} of the FTIR spectra contains three or four relatively strong conformation-dependent bands (Table 2). This reflects the presence of conformer mixtures which is in agreement with secondary structural prediction data [20] and the shortness of the frag-

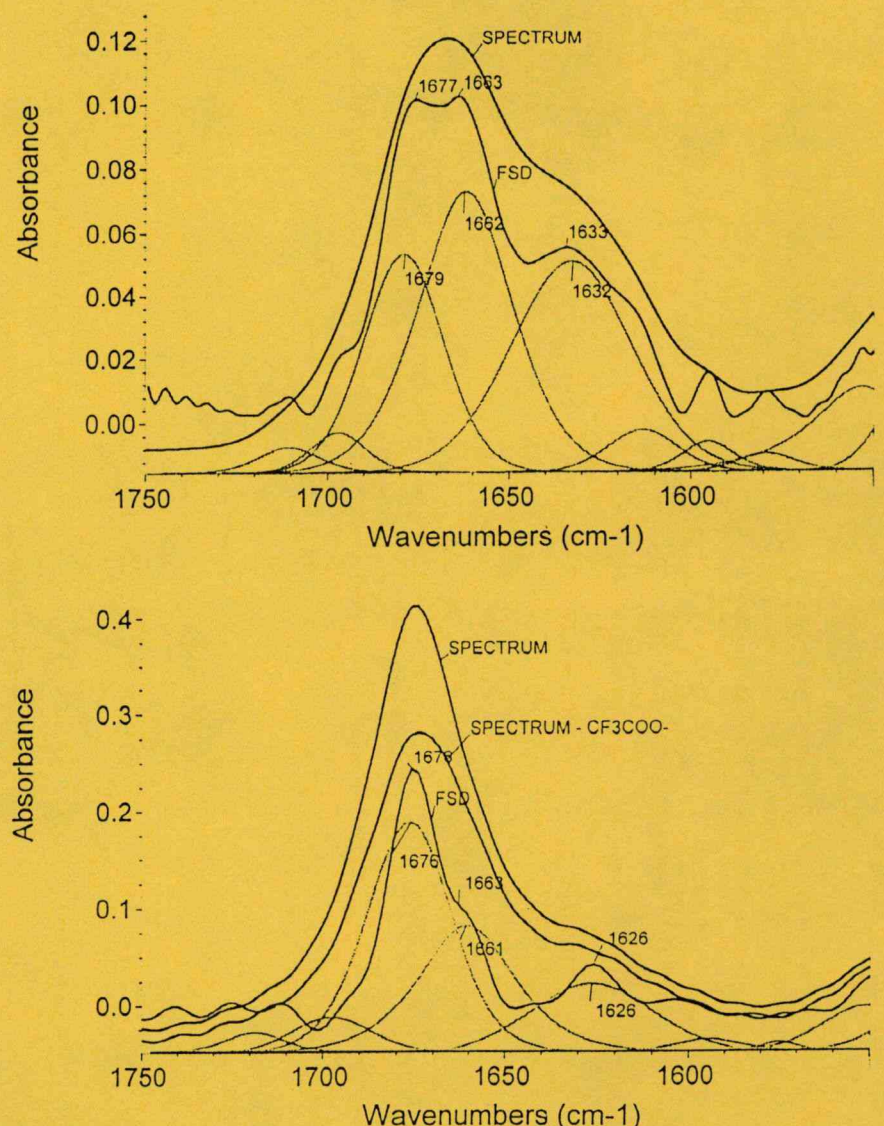

Fig. 1. Amide I region of the FTIR spectra in TFE of hemagglutinin fragments 319–328 H1 (Fig. 1a) and 320–328 H3 (Fig. 1b). The Fourier self-deconvolution (FSD) and curve-fitted spectra are also shown. Peptide 319–328 H1 does not contain CF_3COO^- on the basis of the FTIR spectrum in KBr pellet.

ments. The component between 1640–1620 cm^{-1} indicates the presence of β-pleated sheet conformation. A weak feature at 1613 cm^{-1} in the spectrum of 319–328 H1 peptide likely belongs to aggregated amide groups.

Many spectra contain a band between 1650–1640 cm^{-1}. This component is indicative of unordered conformation. The band shifted to lower frequencies (< 1640 cm^{-1}) may be a sign of the contribution of H-bonded β-turns [26].

The third group of component bands is found in the 1663–1657 cm^{-1} region. Bands between 1657–1650 cm^{-1} in D_2O are generally assigned to α-helix [22]. In TFE the α-helix band has practically the same position [27,28]. In the spectra of peptides containing repeating α-amino isobutyric

acid (Aib) residues a component band at 1663–1662 cm^{-1} was associated with 3_{10} helical conformation [27,28]. Thus, in the case of the HA peptides studied the appearance of the high-frequency component band (1665–1660 cm^{-1}) may reflect a typical 3_{10}, or weakly H-bonded (nascent) α-helical conformation. However, this component may also be due to amides which are solvated by TFE but not involved in intramolecular H-bonding.

For the assignment of amide I components above 1665 cm^{-1} see Table 2. Free or weakly solvated amides were found to give a band above 1670 cm^{-1} in TFE (Table 2) [27,28]. Solvent-shielded amides are expected to absorb at even higher frequencies ($\geq$ 1685 cm^{-1}). The guanidinium group of Arg absorbs at ~ 1673 cm^{-1} (ν_{as}) and 1633 cm^{-1} (ν_s) and the side-chains of asparagine and glutamine which are present in all fragments are also expected to give a constant spectral contibution near 1678, 1670 cm^{-1} (ν) and 1622, 1610 cm^{-1} (δ) [29]. But since a component band near 1675 cm^{-1} was detected in the FTIR spectra of a series of N-Boc protected linear peptides containing no Arg residue(s) [26], furthermore, this band was also present in halogenated alcohols of cyclic peptides containing no basic amino acid residue(s) [30], the component band at ~ 1675 cm^{-1} in the IR spectra of all peptides may be indicative of amide carbonyls exposed to the solvent but not involved in strong oriented intramolecular or intermolecular H-bonds of ordered secondary structures. The spectral region above 1685 cm^{-1} contains the weak

Table 2
Characteristic amide I infrared frequencies of peptides in TFE covering the C-terminal region of the HA1 subunit of human influenza A subtypes[a]

Band frequency (cm^{-1}) Peptides	Free amides[b]	Solvated amides	α-Helix or 3_{10} helix	Aperiodic	β-turn	β-sheet
317–329 H1	1677 (26)	1666 (12)	1657 (18)	–	1642 (12)	1622 (5)
	1675	–	1660sh	–	–	1624
319–328 H1	1679 (18)	–	1662 (29)	–	–	1632 (27), 1613 (5)
	1677	–	1663	–	–	1633, 1613
320–328 H1	1678 (32)	–	1661 (33)	–	1637 (6)	1621 (10)
	1673	–	1665	–	1634	1623
320–329 H1	1675 (48.5)	–	1659 (26)	–	–	1631(7)
	1675	–	1662	–	–	1634
317–329 H2	1680	1664 (22)	1651 (21)	–	–	1621 (7)
	1674	1662	–	–	–	1622
319–328 H2	1675 (40)	–	1658 (14)	1644 (11)	–	1622
	1676	–	1663	1647	–	1623
320–328 H2	1676 (39)	–	1659 (11)	1649 (16)	–	1619 (7)
	1676	–	1662	–	–	1622
320–329 H2	1676 (48)	–	1660 (11)	1645 (6)	–	1623 (12.5)
	1676	–	1660-65sh	1645–50sh	–	1620
317–329 H3	1677 (22.5)	–	1659 (34)	–	1641 (3)	1624 (8.5)
319–328 H3	1676 (31)	–	1659 (14)	–	1642 (9)	1621 (9)
	1676	–	1658	–	1641	1621
320–328 H3	1676 (34)	–	1661 (22)	–	–	1626 (15)
	1676	–	1663	–	–	1626
320–329 H3	1676 (38.5)	–	1660 (20)	–	–	1626 (15)
	1676	–	1662sh	–	–	1625

[a] In parentheses: relative intensities in percentage (see Section 2). Only components of ≥ 5% are listed. The frequency values of the corresponding maximum or shoulder in the FSD spectra are underlined. Weak high frequency component bands at ~ 1690 cm^{-1} (shielded amide carbonyls or the satellite band of antiparallel β-sheets), ~ 1700 cm^{-1} (C=O of H-bonded COOH), and ~ 1715 cm^{-1} (C=O of free COOH) are not listed.

[b] This band also contains the contribution of ν_{as} of guanidinium group of Arg [29].

satellite band of antiparallel β-sheets [31] and that of H-bonded COOH groups (see footnote in Table 2).

Briefly, the truncated peptides from the 317–329 HA1 region are present as multicomponent mixtures of conformers even in the structure promoting solvent TFE. Truncation at one or both termini of the 13-mer 317–329 H2 and H3 peptides results in the breakage of the 3_{10} or weakly H-bonded α-helical conformation (lack or decreased intensity of the component band which appears near 1660 cm^{-1} in the spectra of the parent peptides, Table 2). By contrast, the removal of the first three N-terminal residues of the 317–329 H1 peptide leads to an increased α-helicity which is surprisingly high in the 320–328 peptide. All peptides show some tendency to adopt an extended conformation. However, because of the side-chain contribution (ν_s of guanidinium near 1630 cm^{-1}) of arginine, the relative amounts of β-conformation is not easy to infer from the curve fitted spectra containing one or two component bands between 1640–1600 cm^{-1}. Similarly, the separation of the β-turn band [32] from that of the aperiodic conformation also meets difficulties. It cannot, however, be excluded that the 317–329 H1, and the 319–328 and 320–328 H3 peptides likely adopt one or more β-turns in TFE solution. These latter two analogs were less active in binding to murine I-E^d MHC class II molecules as compared to their H1 and H2 counterparts (Table 1).

3.2. CD studies

The CD spectra in water of the hemagglutinin peptides are marked by a strong negative band below 200 nm which is characteristic of the predominance of aperiodic (structureless) conformer populations. In TFE the 317–329 peptides show low-intensity helical (class C) CD spectra which reflect the presence of ordered conformer populations [27,28]. Upon addition of increasing percentages of water to the TFE solution the spectra change gradually between those measured in TFE and water, respectively.

Fig. 2 shows the CD spectra of the H1 peptides in TFE. The negative $\pi\pi^*$ band of the truncated peptides, compared to the 13-mer, is significantly stronger. The $n\pi^*$ band is also more intense in the spectra of the shortest 320–328 peptide. Except for the left-handed extended helix (polyproline II conformation), all the known ordered secondary structures have CD spectra with a negative $n\pi^*$ band. Thus, the decrease of the intensity ratio of $n\pi^*$ and $\pi\pi^*$ bands together with the blue shift of the negative $\pi\pi^*$ band is indicative of the breakage of ordered conformations. Clearly, deletion of the N-terminal residues (VTG) brings about the stabilization of ordered conformer populations. Due to the shortness of the fragments, deconvolution of the CD curves is not expected to yield realistic amounts of the main ordered secondary structures but the above analysis of the spectral shapes and relative band intensities leads to the conclusion that, in addition to an excess of unordered conformers, small amounts of ordered conformers with helical or β-sheet CD features may account for the CD spectra in TFE of all four H1 peptides.

It is peptide 317–329 of the H2 subtype which has been found to show the highest tendency to adopt an α-helical conformation [17]. The CD spectra in TFE of the truncated H2 peptides 319–328, 320–328 and 320–329 reflect a decrease of α-helicity. The weakest helix-forming tendency is shown by the shortest (9-mer) peptide 320–328 (spectra not shown). This peptide was demonstrated to be a good binder to I-$2E^d$ molecule [33].

Peptides encompassing the full-length (317–329) H2 and H3 subtype sequences were found to have similar helical CD spectra [17]. The decrease of intensity ratio of the $n\pi^*$ and $\pi\pi^*$ bands in the case of the H3 fragments is accompanied by a blue shift of the negative $\pi\pi^*$ band in the spectrum of 320–328 and a red-shift of the negative $\pi\pi^*$ and $n\pi^*$ bands in that of 319–328 (Fig. 3). Taken together, truncation of the 13-mer H3 peptide leads to an increase of unordered conformer populations. The helicity is decreased and the intensive negative $n\pi^*$ band may reflect the contribution of β-sheet conformation. All of the H3 peptides are less efficient in binding to the murine I-E^d molecule as compared to the corresponding H1 and H2 peptides (Table 1).

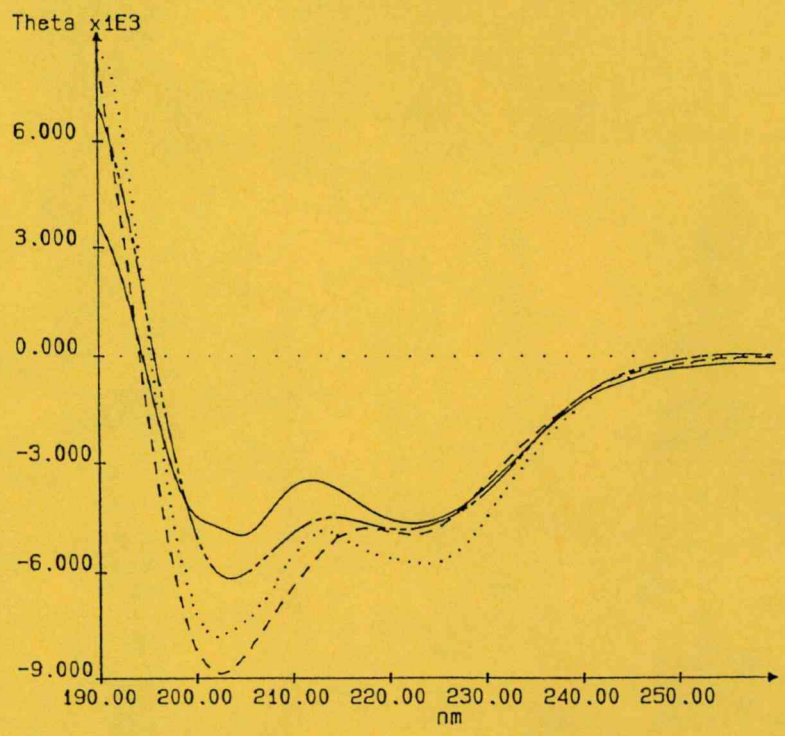

Fig. 2. CD spectra in TFE of peptides representing the C-terminal region of the HA1 subunit of influenza A virus subtype H1 in TFE. 317–329 (—); 319–328 (---); 320–328 (...) and 320–329 (-·-·-).

3.3. Comparison of the results of CD and FTIR spectroscopic studies

Both the FTIR and the CD spectra show that peptides covering the 317–329 subtype-related sequence of HA — as well as their shorter analogues — are present as mixtures of conformers even in TFE solution. It is proline in position 324 which prevents the adoption of longer α-helical or β-sheet stretches. In some cases the data in Table 2 indicate the adoption of turn(s) in addition to α-helix, β-sheet and unordered conformations. It is difficult to estimate the relative amounts of secondary structures from the FTIR spectra because of the contribution of Arg side chain(s) and the ambiguities related to the subtraction of trifluoroacetate contribution. There are two main conclusions which can be drawn from the comparison of FTIR and CD data. (1) The high frequency value (1657–1663 cm^{-1}) of the α-helix band in the infrared spectra of peptides H1–H3 is indicative of weakly H-bonded α-helical structure or the presence of 3_{10} instead of α-helix conformation. (2) There is one band in the β-sheet amide I region (1640–1620 cm^{-1}) of the FSD and curve-fitted FTIR spectra of all peptides except for the spectrum of the 319–328 H1 peptide which contains two bands. The red-shift and increased intensity of the $n\pi^*$ band in the CD spectra also suggest the presence of β-sheet conformer populations.

4. Conclusion

The intersubunit region (317–341) of influenza virus hemagglutinin comprises a conformation-dependent B-cell epitope and also helper and cytotoxic T-cell epitopes which are recognized in the context of murine I-E^d MHC class II and human HLA-B*2705 MHC class I molecules, respectively [11–16].

The region essential for I-E^d binding was located to the 320–325 core sequence [12,33]. All of the N- and C-terminally truncated peptides involved in this study bind to I-E^d in a subtype dependent manner monitored on the surface of viable antigen presenting cells [33]. The C-terminal Arg is not essential for but has a beneficial effect on MHC class II binding and T-cell activation. Neither the switch to a conformer with increased α-helicity upon deletion of the N-terminal 3 residues of the 317–329 H1 peptide nor the breakage of the 3_{10} or weakly H-bonded α-helical conformation in the 317–329 H2 and H3 peptides did influence the I-E^d–peptide interaction.

The N-terminally truncated 320–329 but not the Arg-deleted 320–328 subtype analogs were able to stabilize human HLA-B*2705 class I membrane proteins in transporter deficient cells independent of their subtype-specific sequences [12]. Due to the charged anchor residue important for peptide binding to HLA-B*2705, the truncation of the C-terminal Arg abolished detectable binding to this MHC class I molecule. Despite the few amino acid substitutions in the sequence of the H1, H2 and H3 320–329 decapeptides no differences in HLA-B*2705 binding could be shown and they did not exhibit significant conformational differences either.

Spectroscopic studies reported herein suggest that the solution conformation manifested in the deca- and nonapeptides also comprising the C-terminal Arg, allows efficient interaction with MHC class I and class II molecules and it is not responsible for subtype related differences demonstrated in the binding to I-E^d molecules. The results confirm previous findings based on the characterization of MHC-peptide interactions that different peptide sequences with different population of conformers in solution can adopt an essentially similar extended conformation upon binding to the MHC class II binding groove [9,10].

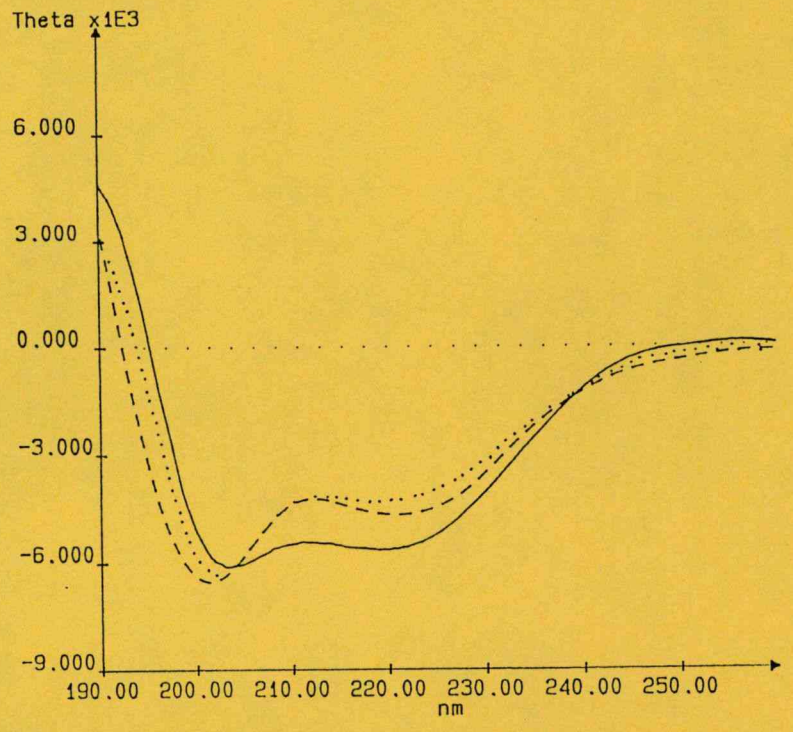

Fig. 3. CD spectra in TFE of peptides representing the C-terminal region of the HA1 subunit of influenza A virus subtype H3. 317–329 (—); 319–328 (---); 320–328 (...).

Acknowledgements

The authors wish to thank for the Hungarian grants OTKA Nr. T022540 (to G.K.T), T025829 (to Zs.M.), T022913 (to M.H.) and T029983 (to I.L.).

References

[1] I.A. York, K.L. Rock, Annu. Rev. Immunol. 14 (1969) 369–396.
[2] J. Pieters, Curr. Opin. Immunol. 9 (1997) 89–96.
[3] H.G. Rammensee, Curr. Opin. Immunol. 7 (1995) 85–96.
[4] D.H. Fremont, W.A. Hendrickson, P. Marrack, J. Kappler, Science 272 (1996) 1001–1004.
[5] H.C. Guo, T.S. Jardetzky, T.P.J. Garrett, W.S. Lane, J.L. Strominger, D.C. Wiley, Nature 360 (1992) 364–366.
[6] D.R. Madden, Ann. Rev. Immunol. 13 (1995) 587–622.
[7] D.R. Madden, J.C. Gorga, J.L. Strominger, D.C. Wiley, Cell 70 (1992) 1035–1048.
[8] T.S. Jardetzky, D.C. Wiley, Proc. Natl. Acad. Sci. USA 93 (1996) 728–734.
[9] L.J. Stern, J.H. Brown, T.S. Jardetzky, J.C. Gorga, R.G. Urban, J.L. Strominger, D.C. Wiley, Nature 368 (1994) 215–221.
[10] A. Dessen, C. Lawrence, S. Cupo, D.M. Zaller, D.C. Wiley, Immunity 7 (1997) 473–481.
[11] É. Rajnavölgyi, Z. Nagy, I. Kurucz, P. Gogolák, G.K. Tóth, G. Váradi, B. Penke, Z. Tigyi, M. Hollósi, J. Gergely, Mol. Immunol. 31 (1994) 1403–1414.
[12] É. Rajnavölgyi, Z. Nagy, A. Daser, A. Horváth, P. Gogolák, I. Kurucz, in: É. Rajnavölgyi (Ed.), Synthetic Peptides in the Search for T and B Cell Epitopes, R.G. Landes Company, Medical Intelligence Unit, Austin, CRC, 1994, p. 173.
[13] Z. Nagy, É. Rajnavölgyi, M. Hollósi, G.K. Tóth, G. Váradi, B. Penke, I. Tóth, A. Horváth, J. Gergely, I. Kurucz, Scand. J. Immunol. 40 (1994) 281–291.
[14] A. Horváth, G.K. Tóth, P. Gogolák, Z. Nagy, I. Kurucz, I. Pecht, É. Rajnavölgyi, Immunol. Lett. 60 (1998) 127–136.
[15] T.S. Jardetzky, W.S. Lane, R.A. Robinson, D.R. Marden, D.C. Wiley, Nature 353 (1991) 326–329.
[16] O. Rötzschke, K. Falk, S. Stevanovic, V. Gnau, G. Jung, H.G. Rammensee, Immunogenetics 39 (1994) 74–77.
[17] S. Holly, Z. Majer, G.K. Tóth, G. Váradi, É. Rajnavölgyi, I. Laczkó, M. Hollósi, Biochem. Biophys. Res. Commun. 193 (1993) 1247–1254.
[18] E. Rajnavölgyi, Immunol. Today 13 (1992) A17–19.
[19] C. DeLisi, J.A. Berzowsky, Proc. Natl. Acad. Sci. USA 82 (1985) 7048–7052.
[20] M. Hollósi, A.A. Ismail, H.H. Mantsch, B. Penke, G. Váradi, G. Tóth, I. Laczkó, I. Kurucz, Z. Nagy, G.D. Fasman, E. Rajnavölgyi, Eur. J. Biochem. 206 (1992) 421–425.
[21] S. Holly, I. Laczkó, G.D. Fasman, M. Hollósi, Biochem. Biophys. Res. Commun. 197 (1993) 755.
[22] W.K. Surewicz, H.H. Mantsch, Biochim. Biophys. Acta 952 (1988) 115–130.
[23] M. Jackson, H.H. Mantsch, Biochim. Biophys. Acta 1118 (1992) 139–143.
[24] H.J. Dyson, P.E. Wright, FASEB J. 9 (1995) 37–42.
[25] I. Laczkó, M. Hollósi, L. Ürge, K.E. Ugen, D.B. Weiner, H.H. Mantsch, J. Thurin, L. Ötvös Jr, Biochemistry 31 (1992) 4282–4288.
[26] M. Hollósi, Z. Majer, A.Z. Rónai, A. Magyar, K. Medzihradszky, S. Holly, A. Perczel, G.D. Fasman, Biopolymers 34 (1994) 177–185.
[27] A. Perczel, M. Hollosi, in: G.D. Fasman (Ed.), Circular Dichroism and the Conformational Analysis of Biomolecules, Ch. 9, Plenum, New York, 1996, p. 285.
[28] D.M. Byler, H. Susi, Biopolymers 25 (1986) 469–487.
[29] S.Y. Venyaminov, N.N. Kalnin, Biopolymers 30 (1990) 1243–1257.
[30] H.H. Mantsch, A. Perczel, M. Hollósi, G.D. Fasman, Biopolymers 33 (1993) 201–207.
[31] S. Krimm, J. Bandekar, Adv. Protein Chem. 38 (1986) 181–364.
[32] H.H. Mantsch, A. Perczel, M. Hollosi, G.D. Fasman, Biopolymers 33 (1993) 201–207.
[33] É. Rajnavölgyi, A. Horváth, P. Gogolák, G.K. Tóth, G. Fazekas, M. Fridkin, I. Pecht, Eur. J. Immunol. 27 (1997) 3105–3114.

Biochemical and Biophysical Research Communications 270, 190–198 (2000)
doi:10.1006/bbrc.2000.2384, available online at http://www.idealibrary.com on IDEAL®

Mapping of a Protective Helper T Cell Epitope of Human Influenza A Virus Hemagglutinin

Péter Gogolák,* Ágnes Simon,* Attila Horváth,* Bence Réthi,* István Simon,† Katalin Berkics,‡ Éva Rajnavölgyi,* and Gábor K. Tóth‡,[1]

*Department of Immunology, L. Eötvös University, Göd, Hungary; †Institute of Enzymology, Hungarian Academy of Sciences, Budapest, Hungary; and ‡Department of Medical Chemistry, University of Szeged, Hungary

Received February 12, 2000

The synthetic peptide comprising the 317–341 region of human influenza A virus (H1N1 subtype) hemagglutinin elicits peptide-specific antibody and helper T cell responses and confers protection against lethal virus infection. Molecular mapping of the 317–329 region, which encompasses the epitope recognized by peptide-specific T cells, revealed that the minimal size required for T cell activation was the 317–326 segment. The most likely peptide alignment, which placed 320Leu to pocket 1 of the I-E^d peptide binding groove, was predicted by molecular mechanics calculations performed with the parental and with the Ala-substituted analogs. In line with the prediction data, the results of the peptide binding assay, where the relative binding efficiency to I-E^d molecules expressed on the surface of antigen-presenting cells was monitored, identified the 320–326 core sequence interacting with the major histocompatibility class II peptide binding groove. Functional analysis of Ala-substituted variants by functional assays and by calculating the surface-accessible areas of the single peptidic amino acids in the I-E^d–peptide complexes demonstrated that 324Pro is a primary contact residue for the T cell receptor. Our results show that this type of analysis offers a suitable tool for molecular mapping of helper T cell epitopes and thus provides valuable data for subunit vaccine design. © 2000 Academic Press

Virus-specific cellular immunity is focused to few immunodominant epitopes the generation of which is governed by the rules of antigen processing and that are selected by major histocompatibility gene complex (MHC) products and by the available T cell repertoire. CD8$^+$ cytotoxic T cells recognize octa- to decapeptides in the context of MHC class I molecules and are the major effectors against virus infected cells (1). Recent data highlighted the importance of their collaboration with virus-specific CD4$^+$ T cells in the development and maintenance of efficient anti-viral immunological memory and thus in therapeutic vaccination (2). CD4$^+$ T cells recognize MHC class II-bound peptide fragments of 15–25 amino acid length (3, reviewed in 4). Identification of potentially active peptides of minimal size, that would fit into a given MHC class II allele, is more difficult than in the case of MHC class I molecules because of the ambiguity in the alignment of peptide sequences of different lengths (5–7).

The C-terminal 306–329 region of human influenza A virus hemagglutinin 1 subunit (HA1) is relatively conserved within subtype sequences and is not affected by antigenic drift (reviewed in 8, 9). In our previous studies we identified the 317–329 region of the A/PR/8/34 (H1N1) influenza virus hemagglutinin (HA) as a subdominant but protective epitope which is the target of both antibody and CD4$^+$ helper T cell recognition (10–12). The synthetic peptide covering the 317–329 sequence induced full activation of peptide-specific T cell hybridomas in an MHC class II-restricted manner in the presence of different antigen presenting cells (APC) as monitored by IL-2 and tumor necrosis factor (TNF) secretion, increase of intracellular free calcium levels and expression of T cell activation markers (13, 14). The 317–329 sequence, elongated by the HA2 $_{1-12}$ fusion peptide, acquired immmunogenicity and elicited both peptide-specific T helper and antibody responses (10, 12).

In this study a detailed mapping of the 317–329 HA1 region was undertaken to determine the minimal peptide size required for full T cell activation and to identify the critical residues which are essential for the

Abbreviations used: APC, antigen presenting cell; CDR, complementary determining region; DCC, dicyclohexyl-carbodiimide; DMSO, dimethyl sulfoxide; FCS, fetal calf serum; HA, hemagglutinin; HA0, immature hemagglutinin; HA1, subunit 1 of hemagglutinin; HA2, subunit 2 of hemagglutinin; HPLC, high-performance liquid chromatography; NHSB, *N*-hydroxysuccinimide biotin, TCR, T cell receptor.

[1] To whom correspondence should be addressed at Department of Medical Chemistry, University of Szeged, Dóm tér 8, H-6720 Szeged, Hungary. Fax: 36-62-425262. E-mail: toth@ovrisc.mdche.u-szeged.hu.

0006-291X/00 $35.00

contact with the I-E^d molecule and with the antigen specific receptor of the IP12-7 T cell hybridoma, which represents the typical specificity pattern of the polyclonal anti-peptide T cell response (9). MHC class II-peptide interaction is attained by evenly distributed H-bonds along the peptide binding groove ensured through broadly conserved MHC residues and by polymorphic allele-specific peptide binding pockets (4, 15). The most likely alignment of the 317–329 peptide in the I-E^d peptide binding groove was predicted by molecular mechanics calculations following energy minimization of the MHC-peptide complexes as described previously (16, 17). It was also shown, that a peptide with most residues substituted to alanine retained binding to HLA-DR1 (5), a human MHC class II allele closely related to murine I-E^d. These data suggested that Ala substitution might not influence significantly the efficiency of peptide binding to MHC class II, but could alter the interaction with the T cell receptor (TCR). Therefore the analysis of systematic Ala substitutions along the peptide was applied for the mapping of primary contact residues with the TCR.

Screening of truncated and site-specific Ala substituted synthetic peptides in functional assays, which measured the magnitude of T cell activation, and relative peptide binding efficiency to the murine I-E^d molecule, revealed that the minimal size of the T cell activating peptide was the 317–326 decapeptide. This analysis also marked those residues which were essential for T cell recognition. Comparison of the surface accessible areas of the peptide amino acids and the number of their atomic contacts with amino acids of the MHC binding pockets enabled us to identify the exposed residues which might contact the IP12-7 TCR. Our results demonstrate that such analysis of structure/function relationships between MHC class II binding and T cell activation may be a useful tool for design of subunit vaccines.

MATERIALS AND METHODS

Peptide synthesis. The 317–329 peptide and its truncated analogs were synthesized as described before (9, 11). The alanine-substituted variants were synthesized by the solid-phase technique utilizing 'Boc chemistry (18). The peptide chain was elongated on a *p*-methylbenzhydrylamine resin (0.48 mmol/g) (19) and the syntheses were carried out using an ABI 430A automatic machine with certain minor modifications of the standard protocol. Side chain protecting groups were as follows: Arg(Tos), Thr(Bzl), and Ser(Bzl). Couplings were performed with DCC, with the exception of Gln and Arg, which were incorporated as their HOBt-esters. The completed peptide resins were treated with liquid HF/dimethyl sulfide/*p*-cresol/*p*-thiocresol (43:3:2:1, v/v), on 0°C, 1 h (20). HF was removed and the resulted free peptides were solubilized in 10% aqueous acetic acid, than filtered and lyophilized. The crude peptides were purified by reverse-phase HPLC. The appropriate fractions were pooled and lyophilized. The purified peptides were characterized by mass spectrometry using a Finnigan TSQ 7000 tandem quadrupole mass spectrometer equipped with electrospray ion source. Peptide purities were above 97% (HPLC) and the measured Mw values were in good agreement with the calculated values in all cases (Table 1).

N-terminal biotinylation of peptides. The peptides listed in Table 1 were biotinylated similarly to described earlier (11). Briefly, 2 mM peptide solution was prepared in 0.1 M $NaHCO_3$ and cooled in ice. Two milligrams per microliter of biotinamidocaproate *N*-hydroxysuccinimide ester (Sigma, Hungary) dissolved in dimethyl sulfoxide (DMSO) was added to 20% molar excess. The reaction was allowed to proceed for 2 h at 0°C.

Cell lines and monoclonal antibodies. The murine B lymphoma line A20 (ATCC TIB 208) and 2PK3 (ATCC TIB 203) was used as APC in the T cell activation and in the binding assays. The IP12-7 T cell hybridoma was developed from the spleen of BALB/c mice immunized with the 317–329 (H1) peptide and subsequently infected with the A/PR/8/34 influenza A virus (9). For IL-2 quantitation the IL-2-dependent CTLL-2 (ATCC TIB 214) cell line was used. All cells were cultured in RPMI supplemented with 2 mM L-glutamine, 1 mM Na-pyruvate, 5×10^{-5} M 2-mercaptoethanol, antibiotics, and 5% FCS (complete RPMI).

Peptide binding assay and cytofluorometry. The peptide binding assay for the truncated peptides was performed as described earlier (11). This procedure was slightly modified for Ala-scanned peptides namely, 5×10^5 2PK3 cells, suspended in 100 μl RPMI supplemented with 2 mM L-glutamine and 0.1% FCS, were incubated in standard FACScan tubes (Falcon) with biotinylated peptides at 20 μM concentrations at 37°C for 2 h. Cells were washed twice with PBS containing 0.1% FCS and cooled in ice. Extravidin R-phycoerythrin conjugate (Sigma, Hungary) was added at 3 μl/tube and incubated for 30 min at 0°C. Cells were washed twice with cold PBS–0.1% FCS, resuspended in 0.5 ml washing solution and fluorescence intensity was measured by FACScan (Fig. 1) or FACScalibur (Fig. 2) equipment. Flow cytometric data were analyzed by using Lysis II or CellQuest software, respectively (Becton–Dickinson). Viable cells were gated out on the basis of their forward and side direction light scatter. Relative peptide binding was given as increase of mean fluorescence in arbitrary units as described previously (11).

Monitoring T cell activation by IL-2 production. T hybridoma cells (2×10^4) were cultured in 96-well flat bottom tissue culture plates (Nunc) in complete RPMI in the presence of different concentrations of peptides and 5×10^4 A20 cells. Seventy-five microliters of culture supernatants was removed at 24 h of culture and transferred to secondary cultures where the amount of secreted IL-2 was measured by the proliferation of CTLL-2 detector cells. In this assay, the indicator cells were used at 5×10^3 cells/well starting density and cell proliferation was measured by addition of [^{3}H]thymidine (9). The amount of secreted IL-2 was given as arbitrary units which were calculated from the cpm values of the titration curves. One arbitrary unit corresponded to 50% of maximal IL-2 secretion.

Molecular mechanics calculations. Simulated 3D structure and the atomic coordinates of the I-E^d molecule were derived from the X-ray data of I-E^k complexed with the murine hemoglobin 64–76 peptide obtained from the PDB code 1iea (21), by replacing the appropriate I-E^d residues in the I-E^k structure. The linker segment B2L–B16L was removed and the peptide residues from B6N to B1L were replaced by the HA317–329 peptide and by the Ala-substituted tridecapeptide variants. The equilibrium conformation of these complexes was determined by conformational energy minimization. Hydrogen atoms were added to the heavy atoms and energy minimization was performed using CVFF force field. Dielectric constant was set to $\epsilon = r\,[\text{Å}]$. The cut-off distance of 15 Å was used for unbound interactions and energy minimization with steepest descent and conjugate gradient algorithms went on until the maximal derivative of the energy function was less than 0.1 kcal/mol/Å. Conformational energy minimization were carried out using the INSIGHT II software package, containing DISCOVER (Biosym Technology, Inc. San Diego, CA) on a Silicon Graphics Indigo Workstation. Contact be-

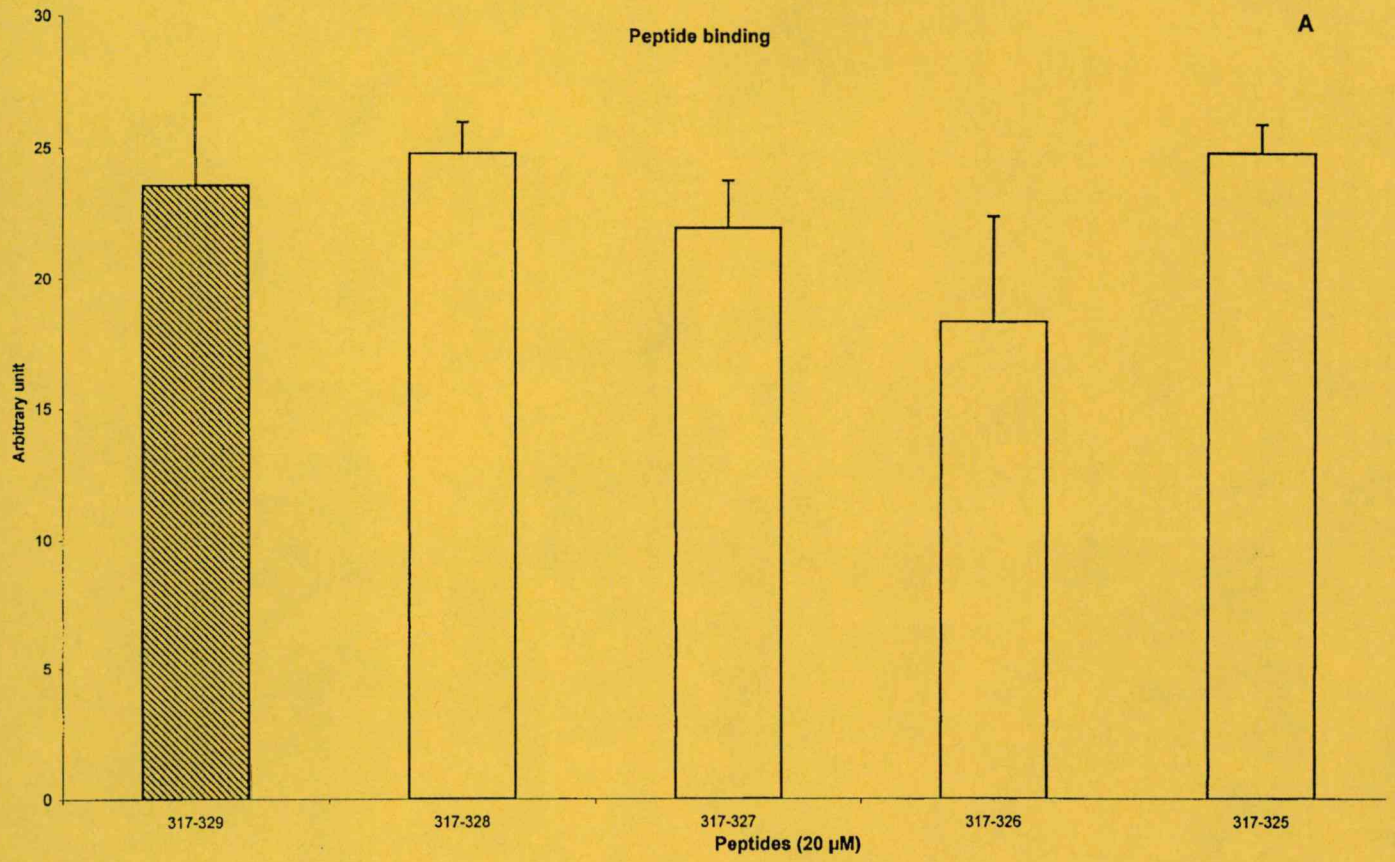

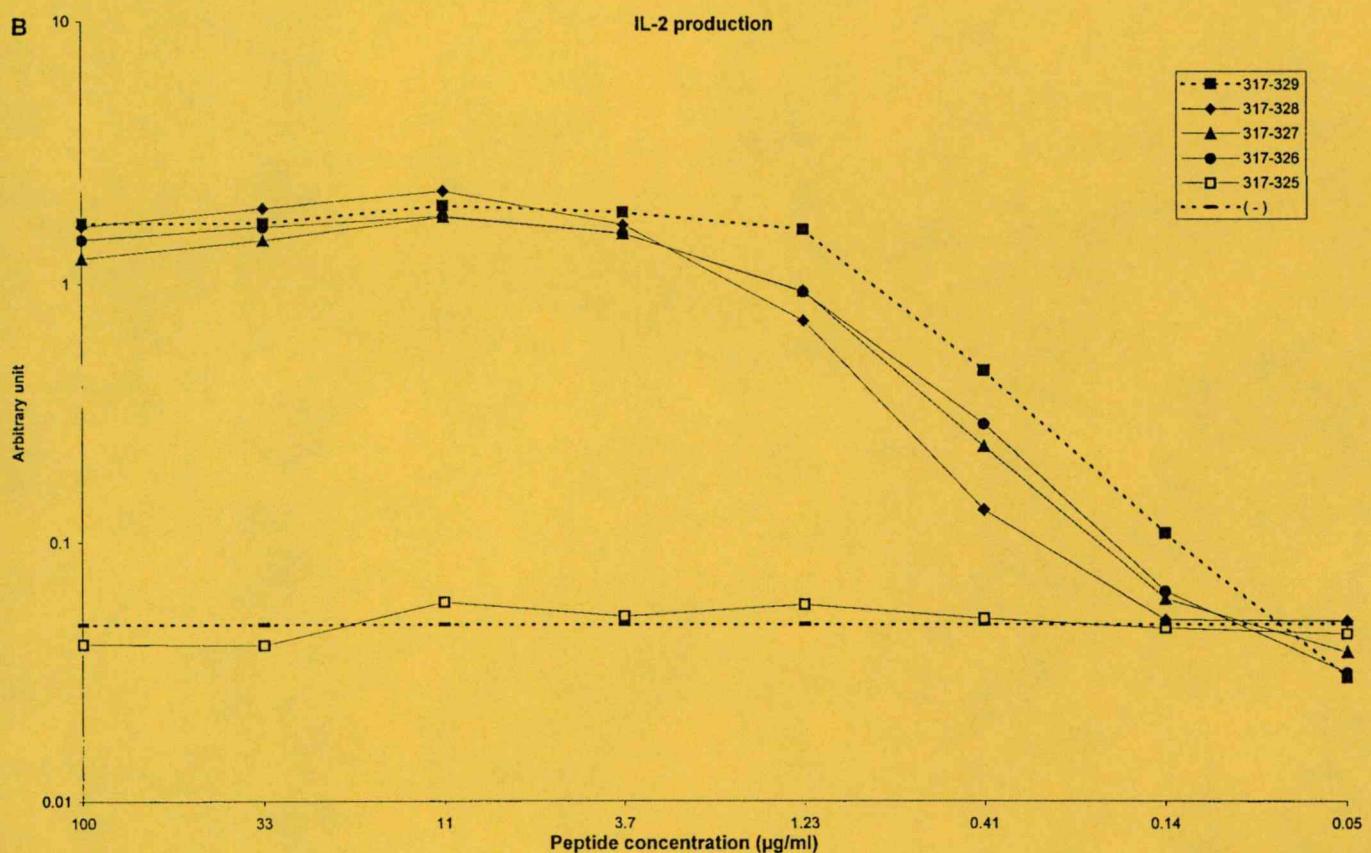

FIG. 1. The effect of C- and N-terminal truncation of the 317–329 peptide on I-E^d binding (A, C) and on the activation of IP-12-7 T cells (B, D). Measurement of T cell activation and the calculation of arbitrary units for the increase of fluorescence intensity (A, C) and for the amount of secreted IL-2 (B, D) was performed as described under Materials and Methods. Mean values of three measurements ± SD are given.

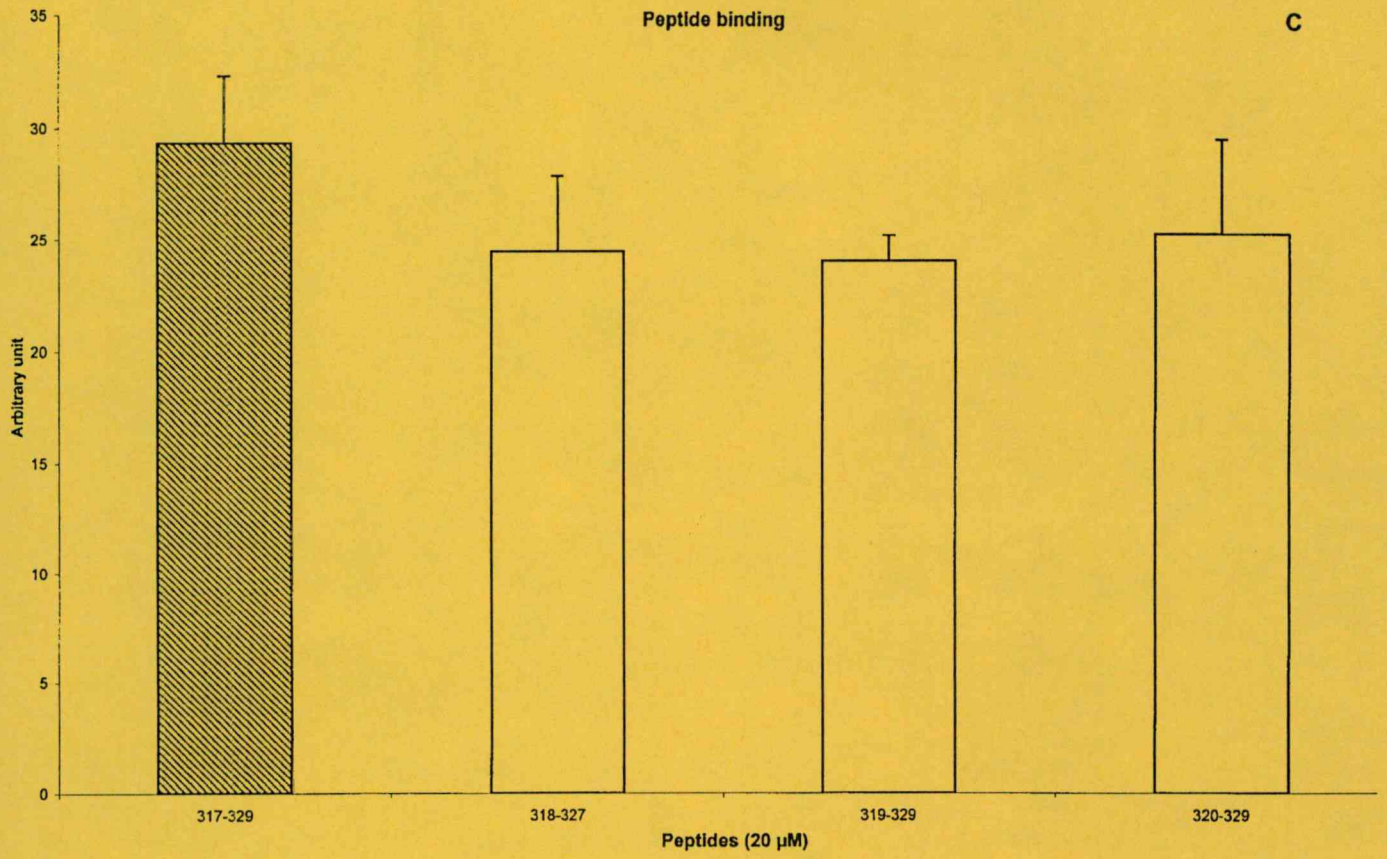

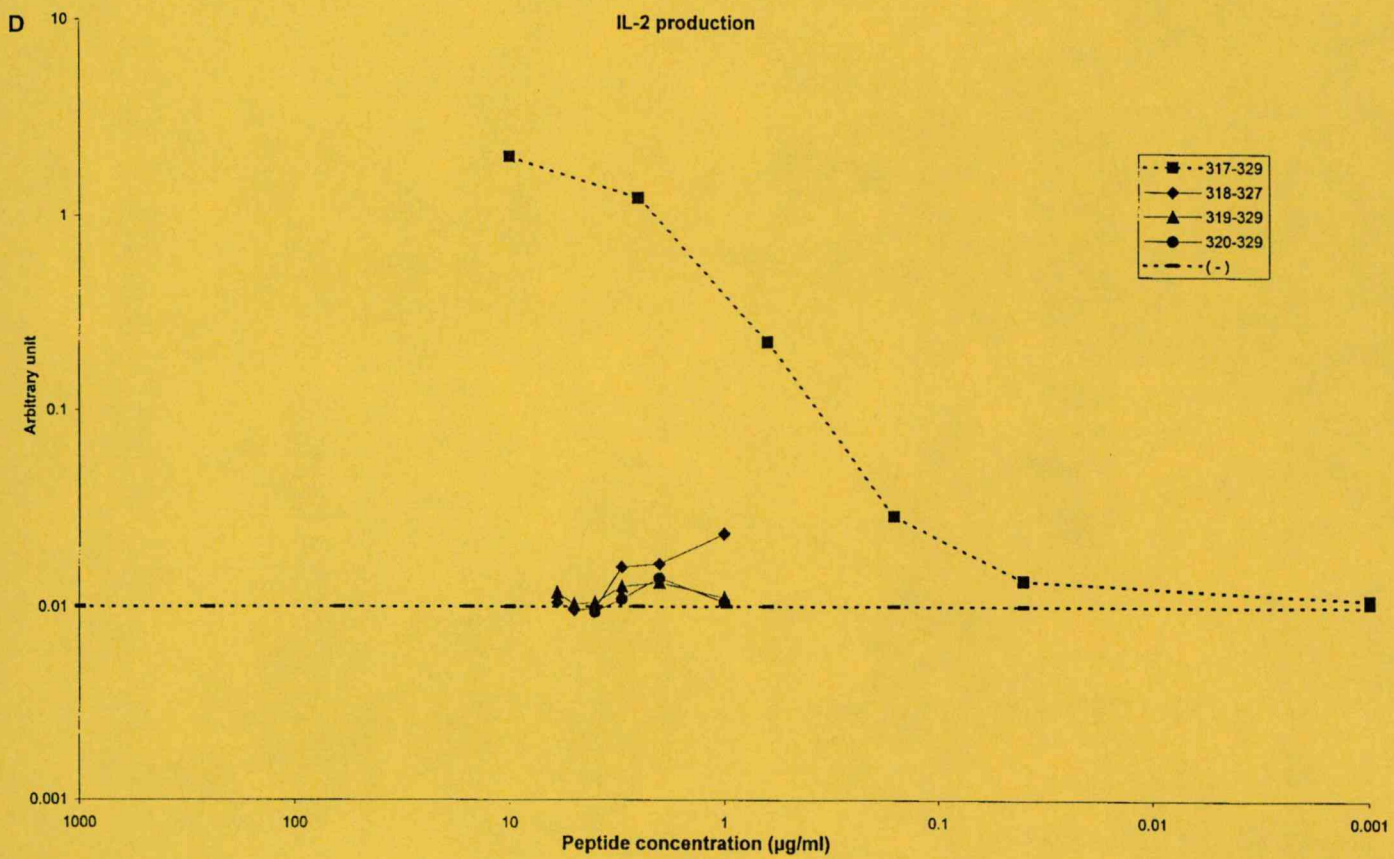

FIG. 1—*Continued*

TABLE 1

Structural and Functional Characteristics of the Alanine-Substituted 317–329 HA1 Peptides

Sequence	Code	MW calculated	MW found	Retention time	MHC binding[j]	T cell activation[k]
VAGLRNIPSIQSR	H1A318	1409.67	1409.3	6.82[a]	+	+++++
VTALRNIPSIQSR	H1A319	1453.72	1453.0	8.49[b]	+	–
VTGARNIPSIQSR	H1A320	1397.61	1398.2	6.26[c]	+	+
VTGLANIPSIQSR	H1A321	1354.58	1354.4	7.86[d]	+	–
VTGLRAIPSIQSR	H1A322	1396.67	1397.2	4.94[e]	+	–
VTGLRNAPSIQSR	H1A323	1397.61	1398.0	5.07[f]	+	–
VTGLRNIASIQSR	H1A324	1413.66	1413.2	10.62[g]	++	–
VTGLRNIPAIQSR	H1A325	1423.63	1423.3	11.05[h]	+	+++++
VTGLRNIPSAQSR	H1A326	1397.61	1397.2	6.66[i]	+	–

[a] 10 → 90% 15 min; [b] 10 → 90% 20 min; [c] 20 → 35% 15 min; [d] 21 → 36% 15 min; [e] 23 → 38% 15 min; [f] 18 → 33% 15 min; [g] 20 → 35% 15 min; [h] 18 → 33% 15 min; [i] 18 → 33% 15 min; [j] measured by flow cytometry with N-terminal biotinylated peptides; [k] measured by IL-2 secretion.

tween atoms was recognized when the distance between the centers of two atoms, belonging to different residues, was less than 4 Å. The solvent accessible area of peptide amino acids, which is indicative of the occupation of the corresponding pockets, was calculated by the MSRoll program, using a probe radius of 1.4 Å (22). The molecule mechanics calculations were performed on various peptide alignments that place different amino acids to pocket 1.

RESULTS

C- and N-Terminal Truncation of the 317–329 Peptide

The functional activity of truncated peptide analogs was monitored by IL-2 secretion of the IP12-7 CD4$^+$ T cell hybridoma. Figure 1 shows that elimination of the C-terminal 329–327 residues does not affect the binding to I-E^d (Fig. 1A) or the secretion of IL-2 when presented on A20 APC (Fig. 1B). Removal of the first Val residues from the N-terminus, however, almost completely abolished the T cell activating capacity of the peptide without substantial change in its peptide binding efficiency (Figs. 1C and 1D). Further truncations of the N-terminal up to 320Leu did not significantly reduced MHC binding but generated functionally inactive peptide analogs (Figs. 1C and 1D). These results show that the minimal size of the epitope, recognized by IP12-7 T cells, is the 317–326 decapeptide but efficient binding to I-E^d can be achieved with shorter overlapping peptides as well (Figs. 1A and 1C).

Ala Scanning of the 317–329 Peptide

Single amino acids of the 317–329 peptide were substituted by Ala starting from residue 317 to 326. Since residues 327, 328, and 329 were shown to be dispensable for T cell activation; therefore, their Ala modification was not tested. As summarized in Table 1 and Fig. 2 substitution of residues 319Gly, 321Arg, 322Asn, 323Ile, 324Pro, and 326Ile by Ala completely abolished T cell activation. The change of 317Val, 318Thr, or 325Ser to Ala did not affect the activating capacity of the peptide while substitution of 320 Leu to Ala resulted in substantial reduction of the T cell activating capacity compared to the parental 317–329 peptide (Figs. 2B and 2C). All these substituted analogs did bind to the I-E^d molecule albeit with slightly different efficiency (Fig. 2A). Therefore these results do not discriminate those amino acids which affect MHC binding, contact directly the TCR or alter the orientation of other TCR contact residues. Interestingly, the 324P → Ala substitution resulted in a functionally inactive peptide (Fig. 2C) despite of its increased relative binding efficiency to I-E^d (Fig. 2A). This suggests that 324Pro may be a primary contact residue for the TCR.

Prediction of Peptide Alignment and Estimation of Amino Acid Accessibility by Molecular Mechanics Calculations

Based on the known I-E^d peptide binding motif (17) several alignments could be predicted for the 317–329 peptide. Placing 320Leu to pocket 1 would define the 320–325 region as an I-E^d binding core sequence, where the surface accessible areas of 320Leu, 323Ile and 325Ser are small, while the number of atomic contacts is large (Table 2). This indicates that these residues accommodate pockets 1, 4, and 6, respectively. In line with the results obtained with the C-terminally truncated peptides none of the Ala substitutions affected the surface accessible areas or the number of atomic contacts of 326Ile, 327Gln, 328Ser, or 329Arg. The 324Pro → Ala change did not affect the surface accessible areas or the atomic contacts of other residues either but completely abolished the T cell activating capacity parallel to increasing binding to I-E^d (Table 2, Fig. 2). In contrast to the 324Pro → Ala changes, Ala modification of 318Thr, 321Arg, 323Ile, and 325Ser substantially altered the surface accessible areas and the atomic contacts of 324Pro (shaded boxes). These calculations suggest that their effect on T cell activa-

TABLE 2

The Effect of Ala Substitutions on the Solvent-Accessible Areas and Atomic Contacts of Single Amino Acids of the 317–329 Peptide

Solvent-accessible area (Å²)

Position	−3	−2	−1	1	2	3	4	5	6	7	8	9	10
Sequence	V	T	G	**L**	**R**	**N**	**I**	**P**	**S**	I	Q	S	R
317–329	161.3	78.3	28.6	**8.7**	**63.1**	**34.6**	**6.2**	**64.9**	**10.0**	18.2	92.5	11.4	187.4
A317	127.[illegible]	82.3	28.9	10.8	65.1	36.7	8.3	63.0	8.4	19.1	93.6	10.7	193.3
A318	134.8	70.[illegible]	49.2	12.9	65.2	38.9	9.9	28.8	10.1	23.8	89.6	10.6	192.2
A319[a]	161.6	76.4	41.[illegible]	4.5	62.4	34.5	6.0	62.0	10.2	21.3	92.8	8.7	187.3
A320	162.3	72.2	31.9	11.[illegible]	66.0	32.6	7.5	69.5	9.1	20.4	92.4	9.4	188.8
A321[a]	157.4	81.4	27.0	13.6	67.[illegible]	48.1	5.5	37.2	11.6	12.6	96.5	14.4	187.4
A322[a]	156.3	77.3	33.7	9.2	67.6	47.[illegible]	7.9	56.6	8.4	20.4	93.2	9.7	186.5
A323[a]	163.2	78.0	25.7	6.9	67.4	39.4	8.[illegible]	31.6	13.4	25.6	90.7	10.8	193.0
A324[a]	160.7	76.7	26.0	10.5	63.2	41.9	11.2	3.[illegible]	10.4	16.4	92.5	13.0	185.2
A325	160.3	75.7	25.4	9.7	60.6	39.2	7.9	45.0	5.[illegible]	12.5	82.8	13.9	179.6
A326[a]	164.5	76.6	26.5	8.5	63.8	34.5	7.5	71.7	9.2	4.[illegible]	95.5	10.5	187.2

Interatomic contacts

Position	−3	−2	−1	**1**	**2**	**3**	**4**	**5**	**6**	7	8	9	10
Sequence	V	T	G	**L**	**R**	**N**	**I**	**P**	**S**	I	Q	S	R
317–329	8	20	18	**64**	**52**	**33**	**50**	**4**	**25**	44	28	37	30
A317	6	21	17	63	52	34	48	4	30	49	26	39	27
A318	24	13	14	56	53	36	51	18	25	50	29	40	28
A319[a]	8	20	20	61	53	35	50	5	28	44	27	37	29
A320	9	22	18	62	49	32	48	4	27	45	27	36	28
A321[a]	8	18	18	60	48	33	52	13	27	52	26	36	29
A322[a]	9	18	16	56	50	23	47	5	26	45	30	33	29
A323[a]	8	20	17	62	51	37	7	23	36	46	26	38	27
A324[a]	8	20	19	59	51	34	48	1	25	46	27	38	30
A325	9	20	19	58	52	35	50	8	20	50	29	34	30
A326[a]	8	20	17	57	52	32	48	4	28	33	29	34	27

[a] Residues of the Ala substitution which abolished T cell activation. Bold defines the I-E^d binding core sequence. Shaded boxes represent changed parameters compared to the parental 317–329 peptide.

tion is rather indirect. The binding and the functional studies together combined with the theoretical approaches strongly suggested that the most probable fitting of the 317–329 peptide to I-E^d was the one that placed 320Leu to pocket 1 and marked 324Pro as a good candidate for a primary TCR contact residue. Molecular modeling studies of other alignments, where 317Val or 318Thr was placed to position 1, showed that the side chain of the residue located to relative position 5 is always pointed away from the MHC molecule. However, the Ala substitution data in these cases did not fit to the binding efficiency and functional activity data.

DISCUSSION

In this study the structural and functional mapping of a ternary complex, composed of the I-E^d MHC class II molecule, the 317–329 HA peptide and the TCR of the IP12-7 hybridoma was analyzed. Our approach applied functional assays performed with the 317–329 HA peptide and with its truncated and single Ala–substituted analogs to identify the most likely fitting of the parental tridecapeptide to the I-E^d peptide binding groove and to determine the residues which may be involved in the contact with the TCR. Our results revealed that the 320–325 HA sequence comprised the minimal core region which accommodated the peptide binding groove of I-E^d, and the 317–326 decapeptide represented the minimal T cell epitope for the IP12-7 hybridoma of the memory/effector Th1 like phenotype.

The overall similarity in the structure of various MHC molecules together with the canonical binding modes of peptides offered theoretical approaches for predicting the MHC class II–peptide interaction (7, 23, 24). Molecular mechanics calculations, combined with the results of the functional assays, predicted that the most likely alignment of the 317–329 peptide would be the one in which 320Leu accommodated pocket 1. In this case the N-terminal amino acids 317Val, 318Thr, and 319Gly, which are implicated in T cell recognition by the functional assays, reside out of the binding groove.

Previous results demonstrated that only a small proportion of the peptide is exposed for interaction with the TCR (24). It was also shown that bound water, the

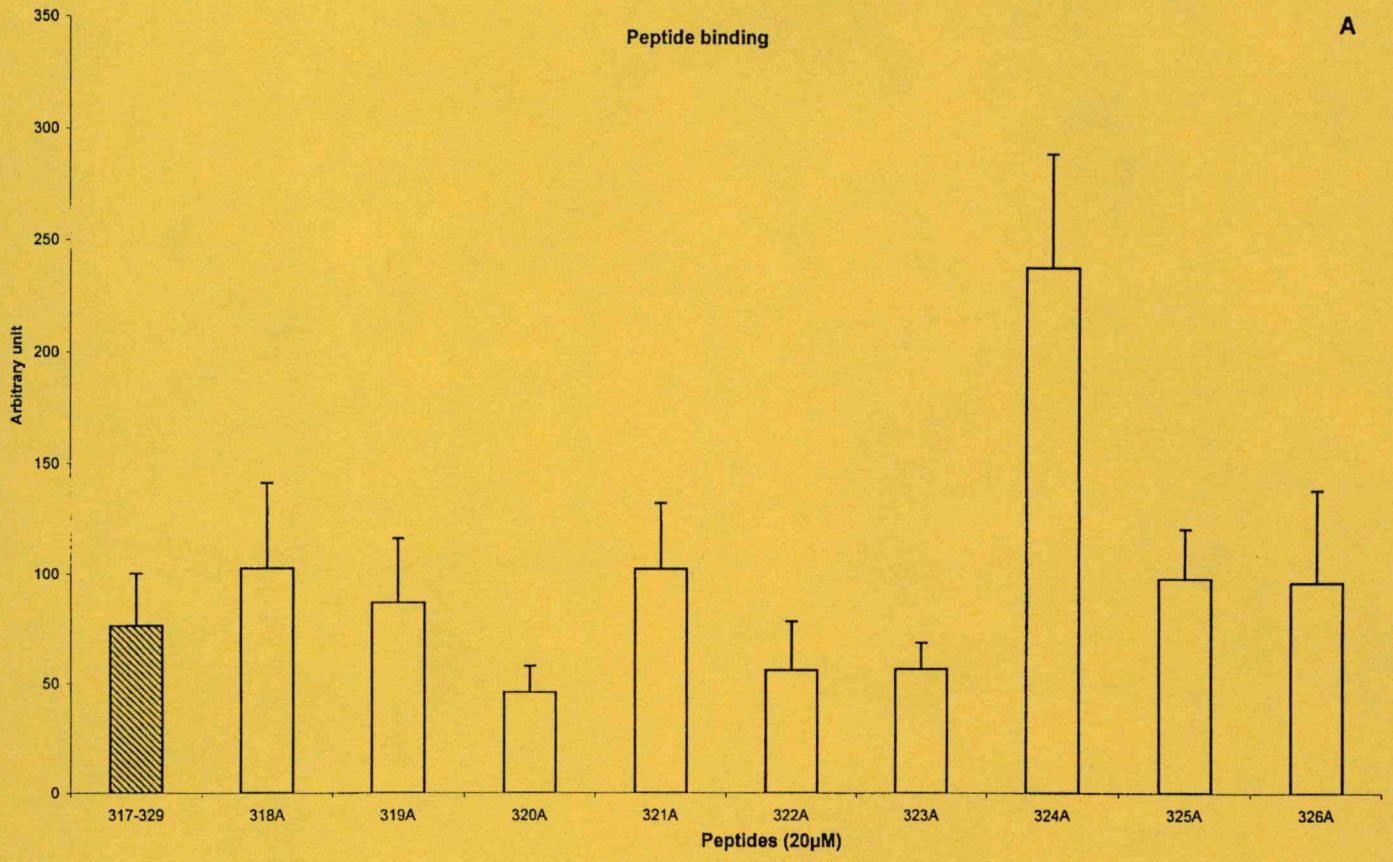

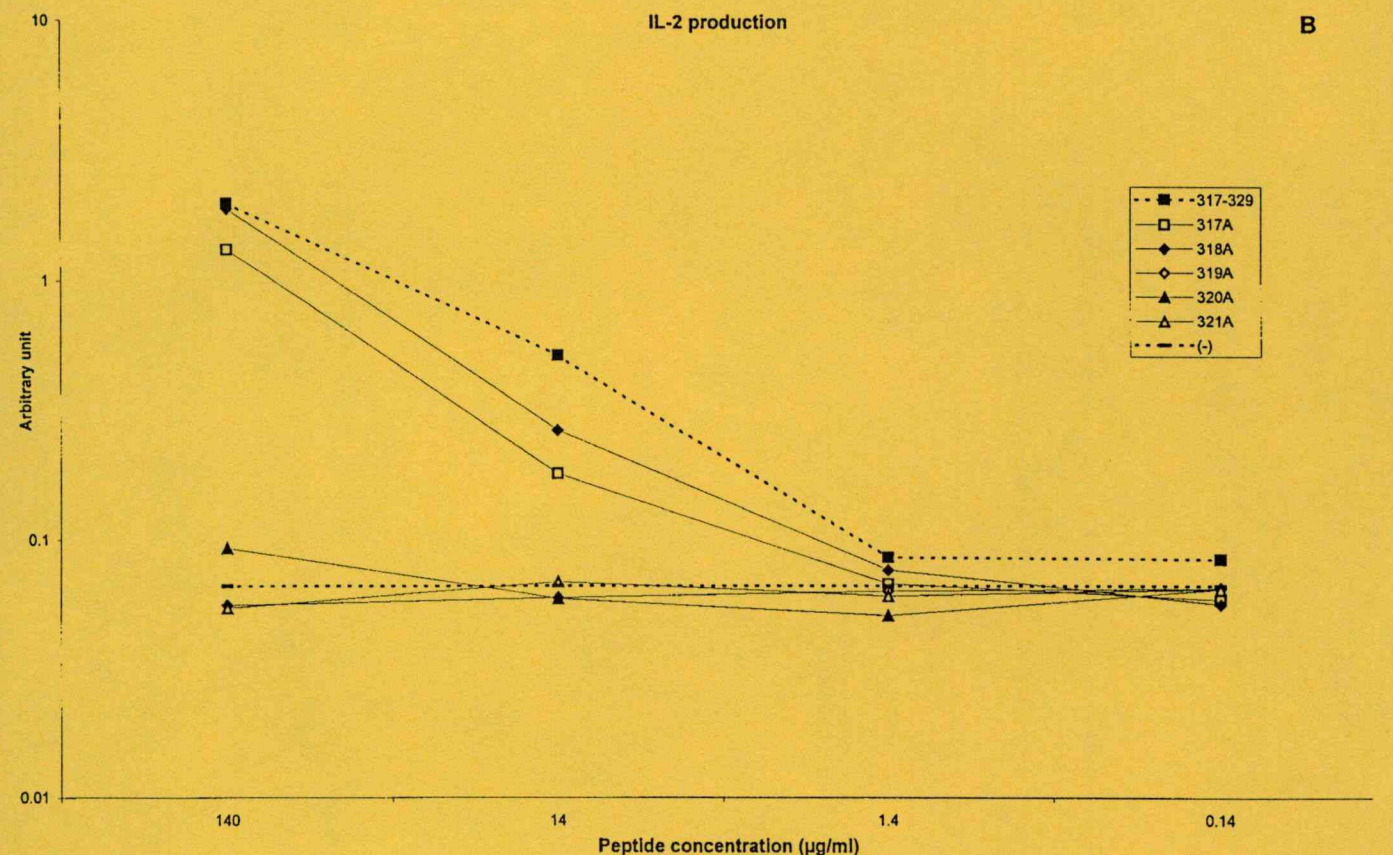

FIG. 2. The effect of Ala substitutions of the 317–329 peptide on I-E^d binding (A) and on the activation of IP-12-7 T cells (B, C). The measurement of peptide binding and of T cell activation was performed as described in the legend to Fig. 1.

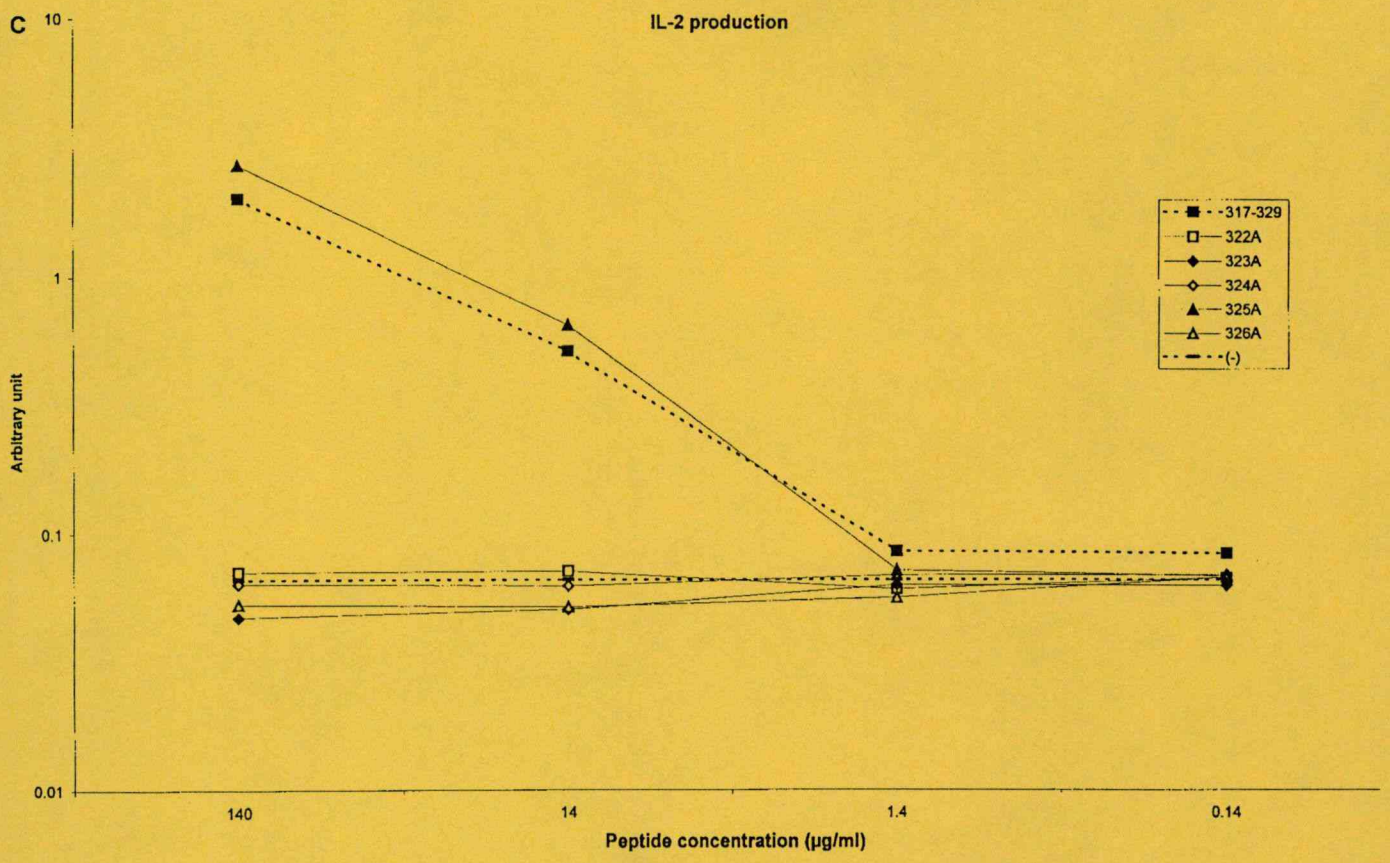

FIG. 2—*Continued*

flexibility of the central portion of the peptide and the dependence of peptidic and MHC side-chain conformations from each other could influence the mode how a given TCR interacts with a defined MHC–peptide complex (25, 26). Since the side-chain function of Ala is neutral, its space filling property offers a good tool to investigate the role of the side-chain functions of other amino acids in T-cell activation.

The TCR binds with low affinity to its ligand and only few complementary determining regions (CDR) contact with the peptide, while others of the flexible binding surface interact with the MHC protein itself (27, 28). The crystal structure of MHC–peptide–TCR complexes suggested a standard docking geometry where the CDR1 of the α- and β-chains face the N- and C-terminal of the peptide, respectively (27). The residue at relative position 5 was identified in several cases to contact with the CDR3 loops of both the α- and β-chains (29). In our system 324Pro at position 5 was identified as a critical residue which did not interact with I-E^d but was essential for T cell recognition. Analysis of the effect of Ala substitutions at positions 318Thr, 321Arg, 323Ile and 325Ser suggested that these residues were important for maintaining the original orientation of 324Pro. The functional inactivity of the peptides substituted by Ala on residues 321Arg and 323Ile could be due to their indirect effect on 324Pro thus identified as a primary TCR contact residue. 319Gly, which was not essential for the right orientation of 324Pro but was required for T cell recognition, might play a role in maintaining the MHC surface around the N-terminal of the peptide which may contact with the TCR. The other amino acids N-terminal to 320Leu may play a similar function.

The present study shows that the classical Ala scanning approach combined with computer assisted prediction methods is a useful tool for mapping MHC class II–peptide–TCR complexes and thus can be applied for subunit vaccine design.

ACKNOWLEDGMENTS

This work was supported by Grants OTKA T022540 (G.K.T.), OTKA T030826 (É.R.), OTKA T030566 (I.S.), FKFP 0186/1999 (É.R.), and AKP 98-13 3,3 (I.S. and É.R.). The expert technical assistance of Erzsébet Veress is acknowledged.

REFERENCES

1. Murali-Krishna, K., Altman, J. D., Suresh, M., Sourdive, D. J. D., Zajac, A. J., Miller, J. D., Slansky, J., and Ahmed, R. (1998) Counting antigen-specific CD8 T cells: A re-evaluation of bystander activation during viral infection. *Immunity* **8**, 177–187.
2. Zajac, A. J., Murali-Krishna, K., Blattman, J. N., and Ahmed, R. (1998) Therapeutic vaccination against chronic viral infection:

The importance of cooperation between CD4+ and CD8+ T cells. *Curr. Opin. Immunol* **10**, 444–449.

3. Chicz, R. M., Urban, R. G., Lane, W. S., Gorga, J. C., Stern, L. J., Vignali, D. A. A., and Strominger, J. L. (1992) Predominant naturally processed peptides bound to HLA-DR1 are derived from MHC-related molecules and are heterogeneous in size. *Nature* **358**, 764–768.
4. Rammensee, H. G., Friede, T., and Stevanovic, S. (1995) MHC ligands and peptide motifs: First listing. *Immunogenetics* **41**, 178–228.
5. Jardetzky, T. S., Gorga, J. C., Busch, R., Rothbard, J., Strominger, J. L., and Wiley, D. C. (1990) Peptide binding to HLA-DR1: A peptide with most residues substituted to alanine retains MHC binding. *EMBO J.* **9**, 1797–1803.
6. Hill, C. M., Liu, A., Marshall, K. W., Mayer, J., Jorgensen, B., Yuan, B., Cubbon, R. M., Nichols, E. A., Wicker, L. S., and Rothbard, J. B. (1994) Exploration of requirements for peptide binding to HLA DRB1*0101 and DRB1*0401. *J. Immunol.* **152**, 2890–2898.
7. Stern, L. J., Brown, J. H., Jardetzky, T. S., Gorga, J. C., Urban, R. G., Strominger, J. L., and Wiley, D. C. (1994) Crystal structure of the human class II protein HLA-DR1 complexed with an influenza virus peptide. *Nature* **368**, 215–221.
8. Jackson, D. C., and Brown, L. E. (1991) A synthetic peptide of influenza virus hemagglutinin as a model antigen and immunogen. *Pept. Res.* **4**, 114–124.
9. Rajnavölgyi, É., Nagy, Z., Kurucz, I., Gogolák, P., Tóth, G. K., Váradi, G., Penke, B., Tigyi, Z., Hollósi, M., and Gergely, J. (1994) T cell recognition of the posttranslationally cleaved intersubunit region of influenza virus hemagglutinin. *Mol. Immunol.* **31**, 1403–1414.
10. Nagy, Z., Rajnavölgyi, É., Hollósi, M., Tóth, G. K., Váradi, G., Penke, B., Tóth, I., Horváth, A., Gergely, J., and Kurucz, I. (1994) The intersubunit region of the influenza virus hemagglutinin is recognized by antibodies during infection. *Scand. J. Immunol.* **40**, 281–291.
11. Rajnavölgyi, É., Horváth, A., Gogolák, P., Tóth, G. K., Fazekas, Gy., Fridkin, M., and Pecht, I. (1997) Characterizing immunodominant and protective influenza hemagglutinin epitopes by functional activity and relative binding to major histocompatibility complex class II sites. *Eur. J. Immunol.* **27**, 3105–3114.
12. Horváth, A., Tóth, G. K., Gogolák, P., Nagy, Z., Kurucz, I., Pecht, I., and Rajnavölgyi, É. (1998) A hemagglutinin-based multipeptide construct elicits enhanced protective immune response in mice against influenza A virus infection. *Immunol. Lett.* **60**, 127–136.
13. Gogolák, P., Réthi, B., Horváth, A., Tóth, G. K., Cervenák, L., László, G., and Rajnavölgyi, É. (1996) Collaboration of TCR-, CD4- and CD28-mediated signaling in antigen-specific MHC class II-restricted T cells. *Immunol. Lett.* **54**, 135–144.
14. Gogolák, P., Réthi, B., Horváth, A., and Rajnavölgyi, É. Antigen presenting cell-induced fine tuning of murine helper T cell activation. Submitted.
15. Rötzschke, O., and Falk, K. (1994) Origin, structure and motifs of naturally processed MHC class II ligands. *Curr. Opin. Immunol.* **6**, 45–51.
16. Rajnavölgyi, É., Simon, Á., Nagy, N., Dosztányi, Zs., Simon, I., Falk, K. I., and Klein, E. (1998) A repetitive sequence of the Epstein–Barr virus nuclear antigen-6 encompasses overlapping regions which bind to various HLA-DR molecules. *In* Peptides 1998 (Bajusz, S., and Hudecz, F., Eds.), pp. 548–549, Akadémiai Kiadó, Budapest, Hungary.
17. Rajnavölgyi, É., Nagy, N., Thuresson, B., Dosztányi, Zs., Simon, Á., Simon, I., Karr, R. W., Ernberg, I., Klein, E., and Falk, K. (2000) A repetitive sequence of EBV nuclear antigen 6 comprises overlapping T cell epitopes, which induce HLA-DR-restricted CD4+ T lymphocytes. *Int. Immunol.* **12**, 281–293.
18. Merrifield, R. B. (1963) The synthesis of a tetrapeptide. Solid phase peptide synthesis. *J. Am. Chem. Soc.* **85**, 2149–2154.
19. Matsueda, G. R., and Stewart, J. M. (1981) A *p*-methylbenzhydrylamine resin for improved solid-phase synthesis of peptide amides. *Peptides* **2**, 45–50.
20. Sakakibara, S., Shimonishi, Y., Kishida, Y., Okada, M., and Sugihara, K. (1996) Use of anhydrous hydrogen fluoride in peptide synthesis. I. Behavior of various protective groups in anhydrous hydrogen fluoride. *Bull. Chem. Soc. Jpn.* **40**, 2164–2167.
21. Fremont, D. H., Hendrickson, W. A., Marrack, P., and Kappler, J. (1996) Structures of an MHC class II molecule with covalently bound single peptides. *Science* **272**, 1001–1004.
22. Connolly, M. L. (1983) Solvent-accessible surfaces of proteins and nucleic acids. *Science* **221**, 709–713.
23. Buus, S. (1999) Description and prediction of peptide-MHC binding: The 'human MHC project.' *Curr. Opin. Immunol.* **11**, 209–213.
24. Stern, L. J., and Wiley, D. C. (1994) Antigenic peptide binding by class I and class II histocompatibility proteins. *Structure* **2**, 245–251.
25. Smith, K. J., Reid, S. W., Harlos, K., McMichael, A. J., Stuart, D. I., Bell, J. I., and Jones, E. Y. (1996) Bound water structure and polymorphic amino acids act together to allow the binding of different peptides to MHC class I HLA-B53. *Immunity* **4**, 215–228.
26. Chelvanayagam, G., Apostolopoulos, V., and McKenzie, F. C. (1997) Milestones in the molecular structure of the major histocompatibility complex. *Protein Eng.* **10**, 471–474.
27. Teng, M. K., Smolyar, A., Tse, A. G., Liu, J. H., Hussey, R. E., Nathenson, S. G., Chang, H. C., Reinherz, E. L., and Wang, J. H. (1998) Identification of a common docking topology with substantial variation among different TCR–peptide–MHC complexes. *Curr. Biol.* **8**, 409–412.
28. Willcox, B. E., Gao, G. F., Wyer, J. R., Ladbury, J. E., Bell, J. I., Jakobsen, B. K., and van der Merwe, P. A. (1999) TCR binding to peptide–MHC stabilizes a flexible recognition interface. *Immunity* **10**, 357–365.
29. Sant'Angelo, D. B., Waterbury, G., Preston-Hurlburt, P., Yoon, S. T., Medzhitov, R., Hong, S., and Janeway, C. A., Jr. (1996) The specificity and orientation of a TCR to its peptide–MHC class II ligands. *Immunity* **4**, 367–376.

MOLECULAR BIOLOGY INTELLIGENCE UNIT

14

SYNTHETIC PEPTIDES IN THE SEARCH FOR B- AND T-CELL EPITOPES

Éva Rajnavölgyi

R.G. LANDES COMPANY
AUSTIN

CHAPTER 6

SYNTHETIC PEPTIDE CONSTRUCTS TO INCREASE THE IMMUNOGENICITY OF B-CELL EPITOPES

Ferenc Hudecz, Gábor K. Tóth

Proteins may carry a large number of overlapping antigenic determinants recognized by B cells. However, it is now apparent that only a limited number of these sites are essential in evoking an effective immune response. Since 1980[1] it has been proven that synthetic peptides comprising epitope sites are able to function as immunogens and/or to react with antibodies (Ab) or with T cells. These observations have provided the basis for the possible application of chemically-defined synthetic oligopeptides such as: (1) immunogens for induction of Ab[2,3] or for stimulation of T cells[4] as protein probes; and (2) antigens in various immunoassays.[5]

The potential of synthetic peptides to induce immune responses is restricted frequently by their lack of immunogenicity. To overcome this problem various attempts have been made. In most cases, as summarized in chapter 6.1, a humoral response has been achieved only by polymerization of the peptide[6] or by prior coupling of small peptides to macromolecules, usually to natural proteins (e.g. keyhole limpet hemocyanin [KLH], bovine serum albumin [BSA], tetanus toxoid [TT]) or synthetic linear or branched (multichain) polypeptide carriers.[2] In most cases these conjugates are used in combination with an adjuvant, Freund's complete adjuvant [FCA], muramyl dipeptide [MDP], alum. The major role of the carrier is the activation of helper T cells, which provide help for peptide specific B cells (chapter 7.3).

It should be noted that one major limitation of such hapten-carrier systems could be antigenic competition, which may result in epitope specific suppression. Thus an ideal carrier would be a molecule that is unable to induce a significant Ab response against itself, while it can provide an efficient helper effect for the hapten-specific Ab response.[7]

Synthetic Peptides in the Search for B- and T-Cell Epitopes, edited by Éva Rajnavölgyi.

Another approach to improve the immunogenic properties of synthetic peptides is the copolymerization with or linking to different T_H cell epitopes[6] (chapter 6.2.). It is based on the observation that, in spite of their short length, a few natural or synthetic peptides which encompass both B- and T-cell epitopes are immunogenic.[8, 9] (chapter 7.3). It has also been shown that the peptide combined for T-cell–B-cell cooperation do not have to be derived from the same protein.[10] For the design of synthetic vaccines, much effort has been concentrated on the search for "promiscuous" T-cell epitopes[11-15] that are able to activate helper T cells, irrespective of the MHC allotype of the immunized individual. Although such epitopes may potentially be active with many covalently bound B-cell epitopes, their use as immunogens requires strong adjuvants for the induction of an intense, long-lasting Ab response directed to the defined B-cell epitopes.[7]

References

1. Walter G, Scheidtmann KH, Carbone H et al. Antibodies specific for the carboxy- and amino-terminal regions of Simian virus 40 large tumour antigen. Proc Natl Acad Sci USA 1980; 77:5197-200.
2. Palfreyman JN, Aitcheson TC, Taylor P. Guidelines for the production of polypeptide specific antisera using small synthetic oligopeptides as immunogens. J Immunol Methods 1984; 75:383-93.
3. Walter G. Production and use of antibodies against synthetic peptides. J Immunol Methods 1986; 88:149-61.
4. Wan AM, Langton BC, Andria ML et al. Antigenic requirements for T-cell activation. Molec Immunol 1986; 23:467-74.
5. Delpierre C, Martin C, Gequiere JC et al. Chemical approach to synthetic immunogens in clinical chemistry. Nucl Med Biol 1987; 14:281-8.
6. Jolivet M, Audibert F, Beachey EH et al. Epitope specific immunity elicited by a synthetic streptococcal antigen without carrier or adjuvant. Biochem Biophys Res Commun 1983; 117:359-65.
7. Del Giudice G. New carriers and adjuvants in the development of vaccines. Current Opinion in Immunology 1992; 4:454-9.
8. Cox JH, Ivanyi J, Young DB et al. Orientation of epitopes influences the immunogenicity of synthetic peptide dimers. Eur J Immunol 1988; 18:2015-9.
9. Leclerc C, Przewlocki G, Schutze MP et al. A synthetic vaccine constructed by co-polymerization of B and T cell determinants. Eur J Immunol 1987; 17:269-73.
10. Levely ME, Mitchell MA, Nicholas JA. Synthetic immunogens constructed from T-cell and B-cell stimulating peptides (T:B chimeras): preferential stimulation of unique T- and B-cell specificities is influenced by immunogen configuration. Cell Immunol 1990; 125: 65-78.
11. Sinigaglia F, Guttinger M, Kilgus J et al. A malaria T-cell epitope recognized in association with most mouse and human MHC class II molecules. Nature 1988; 36:778-80.
12. Panina-Bordignon P, Tan, A, Termijtelen A et al. Universally immunogenic T cell epitopes: promiscuous binding to human MHC class II and promiscuous recognition by T cells. Eur J Immunol 1989; 19: 2237-42.
13. Ho PC, Mutch DA, Winkel KD et al. Identification of two promiscuous T cell epitopes from tetanus toxoid. Eur J Immunol 1990; 20:477-83.

6.1 MACROMOLECULES AS CARRIERS FOR B-CELL EPITOPES

6.1.1 INTRODUCTION

Macromolecular carrier conjugates of B-cell epitopes are used extensively as immunogens in experimental animals to elicit mono- or polyclonal antibody (Ab) responses[1,2] or to induce protectivity against viral, bacterial or parasitic diseases.[3,4] These constructs are also widely applied as antigens in diagnostic assays based on antigen-antibody interaction to detect the presence of Ab directed to the intact protein.[5] Recently it was shown that similarly to Ab, covalent linkage of peptides to protein or synthetic carriers may improve their in vitro T-cell activating capacity[6,7] in solid-phase immunoassays, since peptides shorter than about 15 residues, depending on their amino acid sequence, often do not bind well to the plastic surface of microtitre wells.[8]

Another approach using carrier-bound peptides for immunological studies has been derived from the solid phase technology of peptide synthesis. It has been shown that peptides still attached to a resin support utilized during the synthesis can directly be used as antigens in immunoassays[9] (chapter 4.1.2) and can also be applied as immunogens in experimental animals.[2]

The specificity and the affinity of Ab induced by conjugates carrying B-cell epitopes are influenced by the intrinsic properties of the peptide and carriers as well as by the method of coupling. Palfreyman et al[1] collected data on peptide-carrier conjugates, which were reported in the literature between 1980 and the end of 1983 and used to elicit Ab specific for the corresponding native protein. For this analysis 103 oligopeptides of 20 amino acids or less were included. A total of 83 % of these sequences were successfully used to develop Ab. It should be noted that this set of data is not complete and obviously does not include negative results which remained unpublished.

According to this study the largest group of peptides were coupled to keyhole limpet hemocyanin [KLH] (53) and to bovine serum albumin [BSA] (33). As protein carriers thyroglobulin [THY] (4), tetanus toxoid [TT] and ovalbumin [OVA] have also been applied. Two papers were also included in which synthetic branched (multichain) polypeptide based conjugates were reported. A total of 34% of the peptides were linked to carriers by the heterobifunctional reagent, m-maleimidobenzoyl-N-hydroxysuccinimide ester, [MBS].[10,11] Carbodiimides (11%) and homo-bifunctional compounds, like glutaraldehyde (18%) and bis-diazotized benzidine [BDB] (16%) were also favored as coupling agents (Fig. 6.1).

The data suggest that oligopeptides attached to KLH by MBS linkage have the least chance of producing epitope-specific Ab, though the relatively small number of observations preludes further analysis on a larger data base.[1]

Dyrberg and Oldstone[12] showed that Ab raised against a peptide of the α-chain of the human acetylcholine receptor, conjugated via its N- or C-terminus, do not cross react. In an elegant study, using peptides from the immunogenic region of foot-and-mouth disease virus [FMDV] protein VP1, Schaaper et al[13] observed that the specificity of the polyclonal Ab was affected by not only the orientation of the peptide but also by the position of the attachment site in the epitope. The results obtained with replacement set analysis of epitope peptides by enzyme linked immunoassay [ELISA] clearly showed that the immune response changed when peptides were conjugated by different methods (glutaraldehyde or MBS) to the same carrier and the Ab specificity shifted to the amino acids opposite the amino acid used for attachment.

For the analysis of the influence of coupling strategy on the antigenicity of luteinizing hormone [LH]-OVA conjugates four different conjugation techniques were compared.[14] Two homobifunctional cross-linkers, glutaraldehyde[15] and 1-ethyl-3-(3-dimethylamino-propyl)carbodiimide

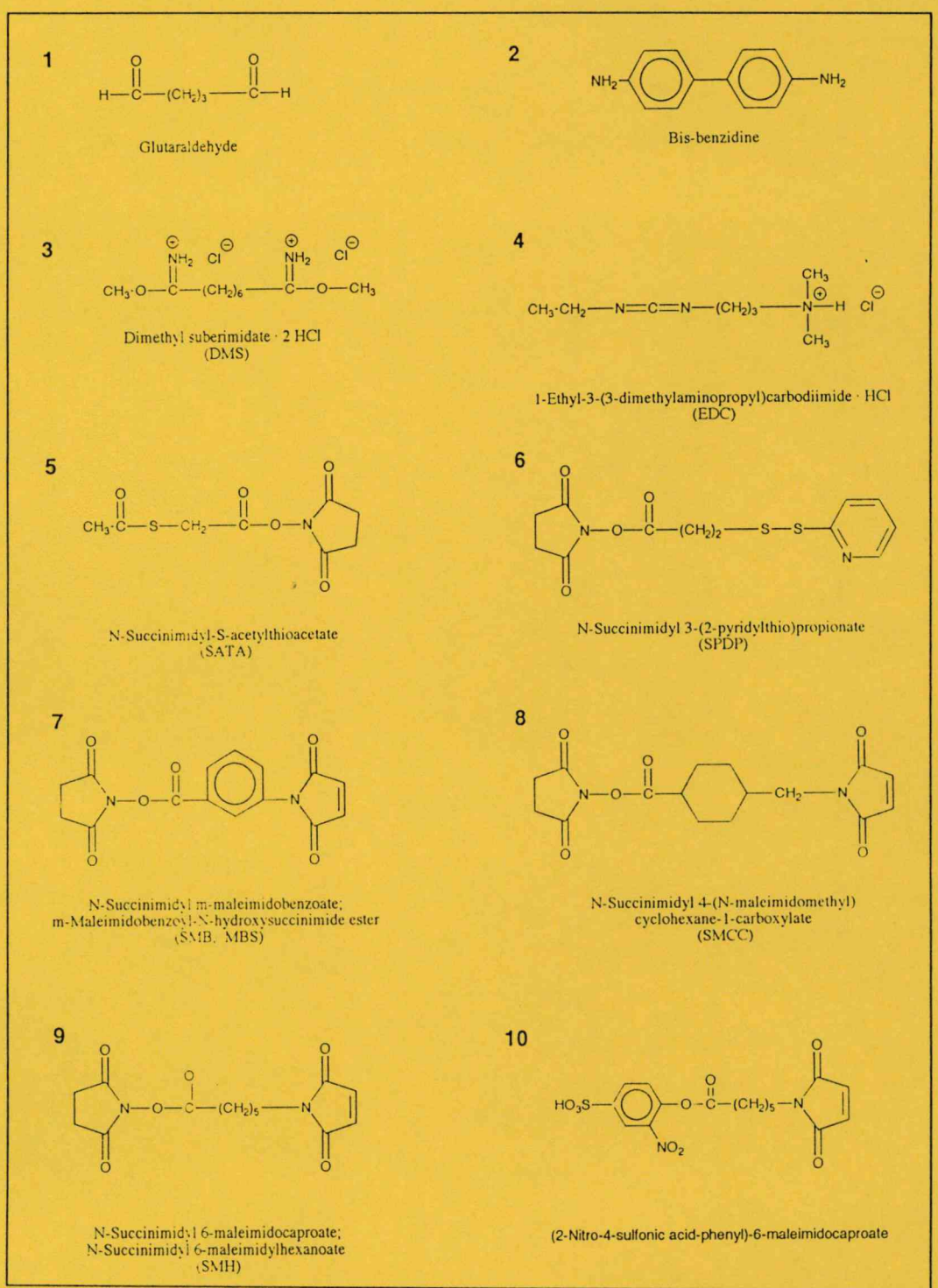

Fig. 6.1. Coupling (cross-linking) reagents frequently used for covalent conjugation of peptide epitopes to macromolecular carriers. 1-3: homobifunctional reagents, 4: heterobifuncional reagent with "zero-length cross linkage", 5-10: heterobifunctional reagents with different linker moiety.

[EDC][16] were evaluated together with one heterobifunctional reagent MBS. It has been concluded that the conjugation technique alters the effectiveness of the LH-OVA conjugates to elicit a hormone specific Ab response. The highest antigenicity has been demonstrated with glutaraldehyde produced conjugate.

Mariani et al[17] studying the influence of the conjugation method on the affinity of Ab observed that the covalent coupling of N-acetylthioglycolyl derivative of peptide corresponding to the sequence of 166-174 of human chorionic somatomammotropin [hCS] to KLH or BSA carriers resulted in monoclonal Ab [MoAb] with 1000-fold enhanced affinity constant as compared to those induced by the free peptide.

6.1.2 Protein Carriers

The classical way of improving the immunogenicity and/or antigenicity of B cell epitopes is their covalent coupling to proteins. In animal studies for the induction of poly- or monoclonal Ab or for preparation antigens for immunoassays, protein carriers have been widely used. Tetanus and diphtheria toxoids and recently tuberculin purified protein derivative [PPD][18] or mycobacterial 65 kD and 70 kD heat shock proteins[19] are largely employed in the development of conjugated vaccines for human use. The data summarized in this section were compiled to provide examples of the application of various protein carriers in inducing peptide specific Ab responses cross reactive with the corresponding protein. Conjugates described here were used as immunogen in experimental animals (mice, rabbits, guinea pigs) in the presence of FCA.

Keyhole Limpet Hemocyanin [KLH]/Limulus Polyphemus Hemocyanin [LPH] Conjugates

For generation of rabbit Ab against the HLA-B27.1 MHC class I protein, peptide 63-84 of the α-chain has been coupled to KLH or BSA using EDC,[16] MBS,[11] or diazo coupling procedures.[20] For the latter one, the peptide was elongated with p-aminophenyl acetic acid at its N-terminal and then attached to proteins after formation of its diazo derivatives. In a similar study peptides of 10-15 amino acid residues from regions of the HLA-DP MHC class II protein were coupled to KLH (or OVA) using glutaraldehyde or MBS.[21]

Conjugates containing the N-terminal 1-39 or C-terminal 95-133 synthetic peptides from interferon-γ[22] or the N-terminal peptide of skeletal muscle α-actin (Ac-DEDETTALVCDNGSGLVK)[23] resulted in polyclonal Ab recognizing the protein.

Neurath et al[24] have shown that synthetic peptide (PSCCCTKPSDGQCTCIPIPSS-[εAc]A, where εAc is ε-aminocaproic acid) corresponding to the hepatitis B surface antigen [HBsAg] conjugated with KLH or LPH was successfully applied to raise protein-specific Ab.

Delpierre et al[5] reported that conjugates of three peptides from lipoproteins (EKLRDLYSKETAA, Apo CII [47-59]; YTGIFTDQVLKGEE, Apo CII [63-79]; RHFWQQDEP, proApo AI) elicited protein specific polyclonal Ab in rabbits useful for the determination of very low density lipoproteins [VLDL] level in serum. Seckler et al[25] conjugated 7 hydrophilic segments of 8-13 amino acid in length to KLH for the development of polyclonal Ab as structural probes to map functional sites of the lactose/H$^+$ transporter protein of E.coli. Based on the binding of peptide-specific Ab to native protein the cytoplasmic side of the protein has been localised.

Human calcitonin specific MoAb were raised by conjugates containing the 32 C- or 34 N-terminal amino acids and KLH or TT.[26] The coupling to carriers was performed by glutaraldehyde.

Bovine Serum Albumin [BSA] Conjugates

Conjugates containing predicted or experimentally verified B cell epitopes like the PSCCCTKPSDGQCTCIPIPSS-[εAc]A peptide corresponding to the HBsAg,[24] two peptides comprising the N-terminal N-acetyl-GDVD tetrapeptide of mammalian cytochrome C,[27] the 56-69 sequence

with an additional Cys at its C-terminal of the HLA-A2 α-chain[28] were prepared and used as antigens in various immunoassays.

Five peptides of 12-43 amino acids from the N-terminal portion of the main merozoite surface polypeptide of *Plasmodium falciparum* were evaluated for their capability to raise Ab that react with the parent protein. Peptides were conjugated by glutaraldehyde either with BSA used for ELISA or with TT for immunization of rabbits or monkeys. When the 43-mer conjugate was used to immunize monkeys in the presence of FCA, three of the four monkeys were partially protected.[29]

To elicit polyclonal protein-specific Ab, BSA-conjugates of the synthetic N-terminal 13-mer peptide of the membrane protein of murine CD8 cytotoxic T cell,[30] seven different 8-11-mer oligopeptides corresponding to the sequence of human renin (EC 3.4.23.15),[31] the N-terminal tetrapeptide (NLAK) of the human platelet-derived growth factor[32] and the synthetic LHRH derived peptide (pGlu-HWSYGLRPG-amide)[33] were reported.

Choppin et al have used methylated BSA as carrier and MBS as a heterobifunctional coupling reagent[11] for the preparation of immunogenic conjugates encompassing four hydrophilic peptides (65-82, 99-118, 138-157 and 164-187) from the variable regions of the HLA-B7 heavy chain.[34]

In mice, neutralizing Ab were elicited by two, BSA attached peptides corresponding to 30-50 and 50-75 regions of the B subunit of cholera toxin.[35] Ghose and Karush induced poly- and monoclonal Ab response against cholera toxin in mice and rabbits by a slightly different approach.[36] Two peptides comprising the 57-69 and 47-60 segments of the B subunit were coupled to BSA through an additional Cys residue at the carboxyl (57-69) or amino terminal (47-60) end using MBS. With Ab induced by BSA-conjugates it has been demonstrated that these peptides are involved in the binding of the cholera toxin molecule to the GM_1 ganglioside receptor.

MoAbs were raised for epitope mapping against the natural peptide apamin, a bee-venom toxin of 18 amino acid residues,[37] and against a neuropeptide (substance P) containing 11 amino acid residues by coupling them to BSA.[38]

Tetanus Toxoid [TT]/Purified Protein Derivative [PPD]

Successful human vaccination against malaria by synthetic sporozoite derived peptides may depend on the choice of an appropriate carrier. TT has been proposed because of its safe and widespread use in humans. Four synthetic peptides, two from the circumsporozoite protein [CSP] of *P. falciparum* [$(NANP)_4$ and $(NANP)_8$], a 24-mer from CSP of *P. knowlesi* and a reference peptide comprising the N-terminal 1-34 amino acids N-terminal of streptococcal M-24 protein[39] were attached to TT by glutaraldehyde. These conjugates were used to investigate the effect of pre-immunization with carrier on the intensity of the peptide specific Ab response induced by peptide-carrier conjugates in mice.[40]

Two peptides covering a sequence near the N-terminal of the S1 subunit of pertussis toxin [PT] were conjugated to PPD of M. tuberculosis by either glutaraldehyde or N-succinimidyl 4-(N-maleimidomethyl) cyclohexane-1-carboxylate [SMCC]/ N-succinimidyl-3-(2-pyridyldithio)-propionate [SPDP] methods and injected into guinea pigs primed with BCG. Each of the conjugates was highly immunogenic producing Ab reacting with the native protein. Interestingly enough no significant cross reactivity between the anti-peptide Ab induced by the two conjugates was observed, which indicated that the specificity of Ab was highly dependent on the conjugation method.[41]

Other Proteins

For polyclonal Ab production in rabbits, a previously mentioned peptide from the HLA-A2 α-chain (56-69)-Cys has been coupled to bovine THY via the heterobifunctional agent MBS.[28] The C-terminal 131-146 peptide (KRKRSQMLFRGRRASQ) of human interferon-γ has been attached to the same carrier by using glutaraldehyde

or EDC and MoAb specific for the protein were raised in BALB/c mice.[42]

For screening purposes,[24] the synthetic peptide (PSCCCTKPSDGQCTCIPIPSS-[εAc]A) corresponding to HBsAg sequence was conjugated with β-galactosidase by using SPDP.

As an example to indicate the use of T-cell epitope-protein conjugates for in vitro T-cell restimulation assay[6] the peptide of 17 amino acids (KPQEEKEKITKEILNGK) from the 28 kD protective antigen of *Schistosoma mansoni* conjugated to OVA should be mentioned.

This review of protein-peptide conjugates indicate the historical development in this field of immunochemistry. As it is demonstrated, the selection of proteins has been based on empirical observations and practical considerations. The use of KLH for immunization or BSA for immunoassays are predominant, while the application of TT or PPD relies on their application in previously developed human vaccines. It should be noted that practically no or very limited chemistry orientated research has been performed to determine molecular structure (average degree of molar substitution etc.) or to optimise reaction conditions for reproducible synthesis. Examples presented here concentrate on successful applications of protein carrier, however the knowledge of unsuccessful attempts is of equal importance for future progress.

6.1.3 Synthetic Polypeptides

Covalent coupling of peptides to natural proteins in most cases lead to the induction of a strong carrier specific immune response, to the appearance of new antigenic determinants on the carrier molecule or inappropriate presentation of the epitope. To overcome these problems it has been suggested that synthetic polymeric peptides with controlled composition could replace protein carriers. To induce an epitope specific Ab response, peptides were first coupled to linear synthetic poly-α-amino acids or branched chain (multichain) polypeptides introduced by Sela et al[43] and recently to polytuftsin.[4] Synthetic polypeptides have also been successfully used as carriers in various immunoassays.[27,32,44]

Polylysine

Two synthetic peptides comprising of the N-terminal N-acetyl-Gly-Asp-Val-Glu tetrapeptide of mammalian cytochrom C were conjugated to polylysine by glutaraldehyde and used successfully for solid phase Ab binding assays.[27] For a similar purpose[32] a tetrapeptide sequence (Asn-Leu-Ala-Lys) of a human platelet-derived growth factor with protected amino-terminal has been coupled to polylysine by DCC/hydroxylbenzotriazole [HOBt] method[45] or by EDC.[16]

Branched Chain Polypeptides

The first completely synthetic immunogen used successfully for generating peptide specific Ab responses contained a peptide corresponding to the amino acid sequence 89-108 [ELTIPIFATNSDCELIVKAM] of MS-2 bacteriophage coat protein and the synthetic branched polypeptide, poly[Lys-(DL-Ala_m)], (m ~20) (AK). This conjugate, prepared by EDC and administered to guinea pigs in Freund's complete adjuvant, elicited phage-neutralizing Ab.[46] Later, using the same carrier, AK, Audibert et al demonstrated that the conjugate of a 14-mer peptide [GNRVRRSVGSSLKC, 188-210] from diphtheria toxin was also able to induce protective immunity. This was achieved in guinea pigs after immunization with conjugate in combination with FCA or with MDP in aqueous solution.[47]

In order to produce peptide-carrier conjugates of predictable composition Lee et al[48] coupled two peptides (111-145 or 109-145) from the C-terminal part of human chorionic gonadotropin [hCG] to AK or poly[Lys-{(Tyr,Glu)-DL-Ala_m}] (TGAL) using N-succinimidyl 6-maleimidylhexanoate [SMH].[49] In a comparative study it has been shown that the levels of hCG specific Ab were similar if rabbit were immunized with the synthetic polymer or TT conjugates.

In a systematic study for the development of macromolecular carriers, two new

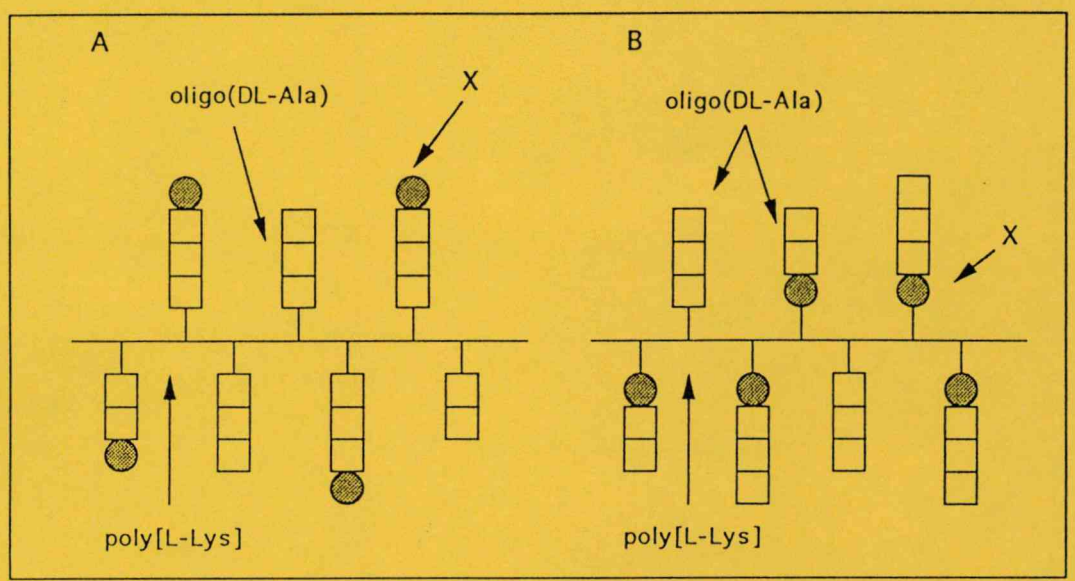

Fig. 6.2. Schematic presentation of branched chain polypeptides with poly[L-lysine] backbone. (A) XAK type polypeptides with the general formula poly[Lys-(X_i-DL-Ala_m)]; and (B) AXK type polypeptides with the general formula poly[Lys-(DL-Ala_m-X_i)]. X = Glu, D-Glu, Ile, Leu, D-Leu, Phe, D-Phe, Pro, His, Lys, D-Lys or Tyr and i<1, m ~3.

groups of branched polypeptides with the general formula poly[Lys-(X_i-DL-Ala_m)] (XAK) and poly[Lys-(DL-Ala_m-X_i)] (AXK) where i<1, m ~ 3, and X = Glu, D-Glu, Ile, Leu, D-Leu, Phe, D-Phe, Pro, His, Lys, D-Lys or Tyr) were introduced by Hudecz and Szekerke.[50-52] These constructs (Fig. 6.2.) represent a significantly modified version of multichain polypeptides used for immunological studies by Sela et al.[43] In order to provide a simple, but versatile model system suitable for primary structure-conformation adopted in different solutions and structure-function analysis, the length of the poly[DL-Ala] side chains has been shortened (from 22-30 to 3-4) and instead of copolymers, only single optically active amino acids (X) were introduced into the branches. Representatives of these polypeptides have been used for the construction of synthetic immunogens and/or antigens with oxazolone[53,54] or peptide epitopes from glycoprotein D of herpes simplex virus type-1[55,56] (chapter 8.1) or from mucin glycoproteins[44] (chapter 9).

In order to investigate the role of macromolecular carrier in inducing epitope specific, protective immune response against HSV-1 infection, branched polypeptides {poly[L-Lys-(DL-$Ala_{3,4}$)], (AK) or poly[L-Lys-($Leu_{0.76}$-DL-$Ala_{2.95}$)] (LAK)} or KLH conjugates of two epitopes [1-23 and 276-284] of gD-1 were used as immunogens.[55,56] Conjugates with carrier AK, induced a significant gD-epitope specific IgG response accompanied by the appearance of a low level of carrier-specific Ab. In contrast negligible epitope specific IgG responses were elicited with LAK-gD peptide. Immunization with the respective peptide-KLH conjugates induced intense carrier-specific response without measurable peptide specificity. In protection experiments repeated administration of [1-23]-LAK conjugate was not able to prolong survival compared to untreated control mice. In sharp contrast, 1-23 or 276-284 peptide conjugated to AK resulted in the production of HSV crossreactive Ab conferred complete protection of a considerable proportion (50%) of preimmunised animals against HSV-1 infection (chapter 8.1.)

An immunodominant epitope peptide (APDTRPAPG) from mucin type 1 glycoprotein has been conjugated with two branched polypeptides AK and D-LAK

containing D-Leu at the side chain terminal position by SPDP. These conjugates containing uniformly orientated epitope peptides were used to study the effect of the carrier upon epitope specific Ab recognition. In this comparative study it has been demonstrated that the secondary structure of the carrier analysed by CD spectroscopy (chapter 5) has a marked influence on the accessibility of the epitope for IgG type monoclonal Ab binding to PDTR or RPA segments[41] (chapter 9).

Polytuftsin [PTF]

Trudelle et al[57] proposed the application of the polymerized form of an immunostimulatory tetrapeptide (Thr-Lys-Pro-Arg) derived from the CH2 domain of IgG. A peptide (10-26) corresponding to the Pre-S2 region of the HBsAg has been cross-linked with PTF by glutaraldehyde, MBS/N-succinimidyl-S-acetylthioacetate [SATA] or by 3-maleimido propionic acid succinimidyl ester [MPS]/SATA. It has been observed that the conjugate prepared by glutaraldehyde elicited significantly enhanced peptide specific Ab production, while the other two conjugates had no detectable activity in mice.[58]

6.1.4 Coupling Chemistry for Peptide Conjugation

Attachment of peptides to protein/polypeptide carriers involves joining of these two components by a covalent bond achieved through the use of coupling (cross-linking) reagents reviewed recently.[59-61] The coupling reagents are bifunctional compounds containing two functional groups with the capability of reacting with the side chains of amino acids of carriers (Fig. 6.1). These compounds may be classified into (a) homobifunctional linkers, which have two identical functional groups (e.g. glutaraldehyde,[15] bis-diazo-benzidine,[63] dimethyl suberimidate[37]); (b) heterobifunctional linkers, which have two different types of reactive functional moieties (e.g. N-succinimidyl-3-(2-pyridyldithio)-propionate [SPDP][62], N-succinimidyl 4-(N-maleimido-methyl) cyclohexane-1-carboxylate [SMCC],[67] N-succinimidyl 6-maleimidylhexanoate [SMH],[49] m-maleimidobenzoyl-N-hydroxysuccinimide ester, [MBS].[11] These linkers form bridges between the carrier and the peptide and therefore conjugates of this kind will contain three moieties: peptide epitope, carrier and linkers. As a special subgroup of heterobifuncional compounds one can regard carbodiimides, which belong to the family of "zero-length cross linkers". These compounds cause the formation of amide bond between amino and carboxyl groups without inserting spacer group (e.g. EDC,[16] DCC/HOBt).[45]

To date over three hundred coupling reagents have been prepared, but only less than a dozen have been used frequently to attach peptide epitopes to carriers.

Since peptides and carriers described in this chapter may contain several functional groups (NH_2, COOH, SH, OH or aromatic ring) simultaneously, conjugation using homobifunctional reagents (e.g. glutaraldehyde, bis-diazotized benzidine) or carbodiimides could generate a large array of different products. In order to obtain well-defined conjugates heterobifunctional reagents should be used.

Peptides having neither a Tyr, nor His, nor Cys, nor Lys may present some difficulties to conjugate. It has also been observed that coupling through the COOH or NH_2 terminus directly to carriers generally results in attaching the peptide close to the carrier molecule so the accessibility of the peptide epitope could be restricted for immunrecognition. The preparation of extended peptides by the introduction of terminal Cys, Tyr, His[1] or a prosthetic group (e.g. acetylthioglycolyl,[17] p-aminophenyl-ethanoyl,[21] sulhydryl[62,68]) is a technique which has been widely used to circumvent these difficulties.

Homobifunctional Coupling Reagents

Because the identical functional end-groups, these reagents are not selective in their cross-linking action.

Glutaraldehyde Method

Reaction with α,ω-dialdehydes, especially glutaraldehyde, has been widely employed for the coupling of peptide epitopes to carriers and also for polymerization of peptide epitopes.[6,14,21-23,25-27,29,31,35,39-42,57] The formation of an intermolecular cross-link, represented by five carbon atoms in a chain between two nitrogen atoms, requires the presence of reactive amino groups in both partner molecules.The first time Richards and Knowles[69] proposed glutaraldehyde as a protein cross-linking reagent. Avremeas[70] demonstrated the conservation of immunological and enzymatic activity of different enzymes coupled to proteins with the aid of a one-step reaction, modified by Reichlin.[15] A major drawback of this method is the crosslinking of peptides in an uncharacterized way, with the formation of homopolymers.

Recently an alternative, two-step conjugation method has been published by Zegers et al[71] which produces peptide-carrier conjugates without formation of homopolymers of either component. The performance of KLH conjugates of eight synthetic peptides from human androgen receptor, human α_1-trypsin and gp120 of HIV-1 in immunization and immunochemistry suggested that these compounds are superior to conjugates prepared by classical glutaraldehyde coupling.

Bis-diazotized Benzidine [BDB] Method

One of the oldest coupling methods is based on the conversion of an aromatic amino group into diazonium group.[63,64] Diazonium functional groups react readily with the phenol (in Tyr), imidazol (in His), amino groups of peptides and proteins. BDB is formed by reaction of amino groups of benzidine with nitrous acid to give bis-diazonium salt, which can react in alkaline solution with the appropriate group in the carrier as well as in the peptide molecule, thus allowing the formation of a benzidine bridge interposed between two moieties. Still quite a few examples can be found in the literature about the successful use of this method. [20,21,24,30,33]

Heterobifunctional Reagents

In contrast, protein linking reagents that possess two different functional groups allow greater control over composition of conjugates.

Carbodiimide Method

Carbodiimides are heterobifunctional reagents which couple an amino group with a carboxyl group to form a peptide bond. In 1964 Goodfriend et al[16] first reported the use of water soluble carbodiimides in immunology. The one-step procedures generally used for carbodiimide coupling of peptides and proteins[5,14,19,31,32,42,46,55,56] could result in conjugates which elicit immunodominant Ab directed against the neodeterminants on the carrier and relatively poor anti-peptide Ab response. To overcome this problem, the two-step cross-linking has also been employed with EDC[65] or with DCC/HOBt method.[45] In this case the peptide was activated first at low pH and than this solution was added to the carrier dissolved in buffer at pH 8-9.

In a recent report Deen et al[66] showed that the presence of N-methyl-imidazol in the buffer of the EDC mediated one-step coupling reaction significantly altered the composition of the conjugate induced polyclonal Ab. Using four different peptides, three protein carriers (KLH, chicken gamma globulin, BSA) and alum gel or water in oil emulsion as adjuvant it has been demonstrated that the proportion of immunodominant neodeterminants introduced during coupling was significantly decreased, while the Ab response against conjugated peptide was enhanced.

MBS and Related Methods

Three active ester type coupling reagent containing maleimide moiety have been used most frequently.[14,17,21,28,34,36,41,48,57] MBS was introduced by Kitagawa and Aikawa [10] and the procedure was modified by Liu et al.[11] SMH was proposed by Keller and Rudinger[49] and SMCC by Yoshitake et al.[67] Conjugation reaction with these compounds is usually a two-step procedure. First, the carriers are modified by acylation

at the ε-amino group of Lys residues and/or at the N-terminal α-amino group. After separation of derivatized protein from unreacted species, the thioether bond are formed between maleimide moiety of the carrier and thiol group of the peptide epitope. The flexibility of the spacer between the peptide and the carrier depends on the coupling reagent selected. SMH contain more flexible, non-aromatic spacer, while the presence of aromatic or saturated ring in MBS or SMCC, respectively makes a much more rigid connection.

SPDP Method

For the preparation of conjugates[23,44,47] in which peptides are coupled to carrier through a disulphide bridge an other heterobifunctional reagent has been introduced by Carlson et al.[62] The disulphide bond is formed in a two-step procedure. First, the carriers are reacted with SPDP to produce an activated disulphide derivative at the amino groups. In the second step the disulphide bond is formed by the thiolysis of SPDP modified carrier using the free thiol group of the peptide.

Another reagent used for the introduction of sulphydryl group into synthetic carriers[48,57] is SATA,[68] which reacts with amino groups of the carrier to yield acetylthio derivative. Hydroxylamine treatment liberates free thiol groups which can be conjugated to peptides with free SH group.

6.1.5 Considerations for Selection of Coupling Agents

The generation of Ab directed to neodeterminants or the linker moiety introduced by the coupling reagent has been investigated by several groups. It has been shown that coupling agents may induce Ab specific for the new antigenic determinants unmasked by the coupling reaction or for linkage moiety. Briand et al[8] prepared epitope-carrier conjugates using 9 synthetic 6-14-mer peptides, four frequently used carrier proteins (KLH, BSA, OVA, THY) and four popular coupling reagents (glutaraldehyde, EDC, BDB and MBS). Most coupling reactions investigated lead to the modification of residues of the carrier that were not involved in the formation of peptide-carrier bond. It has been found that in animals immunized with peptide conjugates, such coupling agent-modified residues, elicited the formation of Ab, specific for the modified carrier molecule, but were unable to recognize the native carrier or the peptide moiety, however reacted strongly with other unrelated carrier proteins treated with the same coupling agent. For the demonstration of the presence of peptide specific Ab in immunoassays, several authors suggest to use as antigen the peptide coupled to another carrier by means of a different coupling agent.[8,69]

In a comparative study Peeters et al[72] investigated the effect of four heterobifunctional coupling reagents on the immunogenicity and antigenicity of the conjugates using angiotensin as epitope peptide and TT as macromolecular carrier. Three coupling reagents were "maleimide" type: SMCC,[67]SMH,[49] MBS[10] and one contained an activated disulphide: SPDP.[62] After immunization of mice in the presence of FCA, constrained linkers derived from the SMCC and MBS induced very high linker-specific Ab titers. In contrast, conjugates prepared by SMH and SPDP elicited almost no detectable linker-specific Ab response. Since the thioether bond is more stable than the disulphide linkage, the authors recommend SMH as the coupling reagent of choice.

In a similar study Aldwin and Nitecki[73] demonstrated by Western blot analysis that a peptide-KLH conjugate cross-linked with a water-soluble reagent, (2-nitro-4-sulfonic acid-phenyl)-6-maleimidocaproate, did not induce detectable Ab specific for the spacer. In this immunogen, peptide from the human macrophage-specific colony stimulating factor (CSF-1) residues 7-21 (CSHMIGDSGHLQSLQR) was used and the immunization was performed with FCA. The same observation was confirmed by the authors with the experience of over 100 peptide-protein conjugates and numerous assays for Ab cross-reactivity between

conjugates of different peptides. In an other study, the coupling reagent maleimidocaproyloxy-succinimide (HMHS) was found to induce a strong immune response.[74]

6.1.6 Adjuvants

It is well known that small molecules including peptides are frequently poorly immunogenic. To improve their immunogenicity, these compounds have to be conjugated to carriers. However, to induce an effective immune response it is generally necessary to further enhance their immunogenicity by simultaneous administration of an adjuvant or immunopotentiator. An alternative approach is to design constructs in which adjuvant is covalently coupled to the peptide epitope ("built in adjuvants", chapter 6.2.3.)[23] or to carriers.[46]

A wide variety of organic as well as inorganic compounds are capable of potentiating immune responses by acting as adjuvants. These can be: (a) water and oil emulsions including mineral oil; (b) microorganisms and their fractions; (c) multimeric complexes such as liposomes, micelles or iscoms; (d) synthetic biodegradable polynucleotides (e) peptides, peptidoglycans; (f) inorganic salts like aluminium hydroxide and phosphate (alum gel).

The most commonly used substance in experimental animals are FCA and FIA adjuvants, which consists of heat-killed cultures of *Mycobacterium tuberculosis*, dried and suspended in mineral oil and lanolin. FCA is still the strongest adjuvant, however its general use is forbidden even in veterinary medicine.[3] FIA is free of bacteria. Metabolizable oil of animal origin, i.e. squalene or shark oil are available for use in FIA-type emulsion and can make this adjuvant available for limited human use.[75] The potentiating capacity of FCA is partly due to a delayed antigen absorption, which provides a prolonged immunogenic stimulus for the immune system.

The smallest biologically active unit of bacterial cell wall peptidoglycan capable of replacing whole Mycobacteria in FCA is muramyl dipeptide, N-acetyl-muramyl-L-alanyl-D-isoglutamine, [MDP].[76] The adjuvant activity of MDP on Ab production is seen with most antigens when injected simultaneously. However, activity is increased when MDP is covalently bound to the immunogenic peptide or carrier or when it is encapsulated in liposomes.[47,76] Clinical evaluation of several muramyl peptide analogs is currently under way. One of them, murabutide (3'-n-propyl-MDP) has completed phases I and II trials as adjuvant for a tetanus vaccine.[77]

Lipopolysaccharide [LPS] from Gram negative bacteria was shown to be a potent stimulator of Ab production, but was highly toxic[3]. It has been found that the adjuvant and toxic effects are largely related to the lipid A fraction. The modification of lipid A to form monophosphoryl lipid A [MPL] resulted in a substance with reduced toxicity and preserved adjuvant activity. The use of MPL alone or combined with trehalose dimycolate has been compared favourably with other adjuvants in experimental animals with protein conjugates,[78] but was not superior in studies with gonadotropin releasing hormone [GnRH]-protein conjugates.[79]

It has been established that the Ab response to a peptide epitope or epitope-carrier conjugate can be enhanced by their incorporation into physically defined multimeric complexes such as liposomes, micelles or iscoms.[80]

Liposomes which consist of one or more concentric lipid bilayers prepared usually from natural phospholipids have been shown to enhance the immune response to peptide epitopes.[81] Initially peptides were encapsulated within the liposome or passively adhering them to the surface via charge-charge interactions, but this approach did not result in a strong Ab response to the peptides even in the presence of FCA.[82,83] Better results were obtained by using acylated peptides, which are lipid soluble, can readily be incorporated into the bilayers of liposomes as demonstrated by Brynestad et al[84] with HSV epitopes (1-23 and 163-178). Using peptides from circumsporozoite protein of

P. falciparum [$(NANP)_3$, $NP(NANP)_5NA$] and 7 peptides corresponding to gp 160 of HIV_{IIIb}, Goodman-Snikoff et al[85] found that a B cell epitope and a T-cell epitope in the form of synthetic peptides presented together and covalently coupled at the surface of phospholipid-liposomes are necessary for the optimal Ab response. The method described represents a significant advance in eliciting an immune response to peptides, because it requires only peptides and phospholipids in the absence of additional adjuvants.

Lövgren et al coupled two different peptides (LHRH and 144-159 sequence of FMDV protein) to preformed iscoms consisting of influenza virus envelope proteins and used for immunization without adjuvant. Peptide specific Ab were produced, but the magnitude of the Ab response was not satisfactory. However, results obtained with biotin-iscom model preparations suggest that conjugates with proper (~10 epitope/carrier) epitope density can induce significantly higher epitope specific Ab responses without FCA, when compared to relevant BSA conjugates or micelles administered with FCA.[86]

The effectiveness of iscoms, liposomes could be correlated with the route of peptide presentation, which could resemble to the native orientation or conformation of the respective protein and for the activation of T cells.

A variety of inorganic compounds, such as aluminium salts (alum) and calcium phosphate have been used as adjuvants. It has been found that immunization of PPD conjugates of epitope peptides from pertussis toxin produced significantly higher level of peptid specific Ab in the presence of aluminium hydroxide in BCG primed guinea pigs.[41] Presumably, the capacity of inorganic salts to act as adjuvants is related to a slower release of antigen at the site of injection and to an inflammatory effect which intensifies the host defence mechanisms to antigens.

The mode of action of adjuvants is under intense investigation. Macrophages are the primary targets for adjuvant action as they are stimulated to release interleukin 1, which promotes T_H cell activation. Adjuvants may stimulate other accessory cells and their cytokine production. Some of the adjuvants are known to have a polyclonal B cell activating capacity.[87]

In a recent study, Karagouni and Hadjipetrou-Kourounakis[88] investigated the class and subclass distribution of hapten specific Ab induced by FITC-carrier conjugates in the absence or presence of nine different adjuvants. It has been found that different IgG subclasses were favoured by different adjuvants. Immunization with antigen alone or with LPS or Li salt, as adjuvant, resulted in the dominance of IgG3. The majority of Ab was IgG1 after immunization with FIA, FCA, alum, poly I:C, poly A:U, Quil A or Be salt. An attempt has also been made to correlate the adjuvant effect with certain T_H-subtypes.

Taken together adjuvant research is still an open territory for scientists in this field. There is a need to gather more empirical information about the optimal use of present adjuvants, but it is also urgent to perform fundamental experiments to correlate chemical structure with adjuvant activity. Based on this knowledge one can not only select the proper adjuvant by fortune, but design molecules for specific needs.

Acknowledgments

The author is very grateful to Professor Mária Szekerke for the stimulating discussions and Dr György Orosz for his editorial contribution. During the course of this work the author was supported by a grant from the Hungarian Ministry of Welfare (ETT No. 017/1993) and by a grant from the World Health Organization (T9/181/133).

References

1. Palfreyman JN, Aitcheson TC Taylor P Guidelines for the production of polypeptide specific antisera using small synthetic oligopeptides as immunogens. J Immunol Methods 1984; 75:383-93.
2. Plaue S, Muller S, Briand JP et al. Recent

advances in solid-phase peptide synthesis and preparation of antibodies to synthetic peptides. Biologicals 1990; 18:147-57.
3. Del Giudice G. New carriers and adjuvants in the development of vaccines. Current Opinion in Immunology 1992; 4:454-9.
4. Riveau GJ, Audibert FM. Synthetic peptide vaccines against pathogens and biological mediators. TiPS 1990; 11:194-8.
5. Delpierre C, Martin C, Gequiere JC et al. Chemical approach to synthetic immunogens in clinical chemistry. Nucl Med Biol 1987; 14:281-8.
6. Marguerite M, Bossus M, Mazingue C et al. Analysis of antigenicity and immunogenicity of five different chemically defined constructs of a peptide. Molec Immunol 1992; 29:793-800.
7. Wan AM, Langton BC, Andria ML et al. Antigenic requirements for T cell activation. Molec Immunol 1986; 23: 467-74.
8. Briand JP, Muller S, Van Regenmortel MHV. Synthetic peptide as antigens: pitfalls of conjugation methods. J Immunol Methods 1985; 78:59-69.
9. Geysen HM, Rodda SJ, Mason TJ et al. Strategies for epitope analysis using peptide synthesis. J Immunol Meth 1987; 102: 259-74.
10. Kitagawa T, Aikawa T. Enzyme coupled immunoassay of insulin using a novel coupling reagent. J Biochem 1976; 79:233-6.
11. Liu FT, Zinnecker M, Hamaoka T et al. New procedures for the preparation and isolation of conjugates of proteins and a synthetic copolymer of D-amino acids and immunochemical characterization of such conjugates. Biochemistry 1979; 18:690-7.
12. Dyrberg T, Oldstone MBA. Peptides as antigens. Importance of orientation. J Exp Med 1986; 164:1344-9.
13. Schaaper WMM, Lankhof H, Puijk WC et al. Manipulation of antipeptide immune response by varying the coupling of the peptide with the carrier protein. Molec Immunol 1989; 26:81-5.
14. Grieger DM, Reeves JJ. Active immunization of beef heifers against luteinizing hormone: II. Evaluation of conjugation technique on antigenicity of LH. J Anim Sci 1990; 68:3747-54.
15. Reichlin M. Use of glutaraldehyde as a coupling agent for proteins and peptides. Methods in Enzymology 1980; 70: 159-65.
16. Goodfriend TL, Levine L, Fasman GD. Antibodies to bradykinin and angiotensin: A use of carbodiimide in immunology. Science 1964; 144:1344-5.
17. Mariani M, Bracci L, Presentini R et al. Immunogenicity of a free synthetic peptide: carrier-conjugation enhances antibody affinity for the native protein. Molec Immunol 1987; 24: 297-303.
18. Lussow AR, Del Giudice G, Renia L et al. Use of tuberculin purified protein derivative-Asn-Asn-Asn-Pro conjugate in Bacillus Calmette Guérin primed mice overcomes H-2 restriction of the antibody response and avoids the need of adjuvants. Proc Natl Acad Sci. USA 1990; 87:2960-4.
19. Lussow AR, Barrios C, Van Embden J et al. Mycobacterial heat shock proteins as carrier molecules. Eur J Immunol 1991; 21: 2297-302.
20. Rojo S, López De Castro JA, Aparicio P et al. HLA-B27 antigenicity: antibodies against the chemically synthesized 63-84 peptide from HLA-B27. I display alloantigenic specificity and discriminate among HLA-B27 subtypes. J Immunol 1986; 137: 904-10.
21. Chersi A, Houghten RA, Morgani MC et al. Recognition of HLA class II molecules by antipeptide antibodies elicited by synthetic peptides selected from regions of HLA-DP antigens. Z Naturforsch 1987; 42c: 1313-8.
22. Russell JK, Hayes MP, Carter JM et al. Epitope and functional specificity of monoclonal antibodies to mouse interferon-γ: the synthetic peptide approach. J. Immunol 1986; 136:3324-8.
23. Bulinski JC, Kumar S, Titani K et al. Peptide antibody specific for the amino terminus of skeletal muscle α-actin. Proc Natl Acad Sci USA 1983; 80:1506-10.
24. Neurath AR, Kent SBH, Strick N. Specificity of antibodies elicited by a synthetic peptide having a sequence in common with a fragment of a virus protein-the hepatitis B surface antigen. Develop Biol Standard 1983; 54:103-12.

25. Seckler R, Möröy T, Wright et al. Anti-peptide antibodies and proteases as structural probes for the lactose/H+ transport of E coli. Biochemistry 1986; 25: 2403-9.
26. Motté P, Alberici G, Ait-Abdellah M et al. Monoclonal antibodies distinguish synthetic peptides that differ in one chemical group. J Immunol 1987; 138:3332-8.
27. Jemmerson R, Morrow PR, Kliman NR et al. Analysis of an evolutionary conserved antigenic site on mammalian cytochrome c using synthetic peptides. Proc Natl Acad Sci USA 1985; 82:1508-12.
28. Ways JP, Rothbard JB, Parham P. Amino acid residues 56 to 69 of HLA-A2 specify an antigenic determinant shared by HLA-A2 and HLA-B17. J Immunol 1986; 137:217-22.
29. Cheung A, Leban J, Shaw AR et al. Immunization with synthetic peptides of a Plasmodium falciparum surface antigen induces antimerozoite antibodies. Proc Natl Acad Sci USA 1986; 83:8328-32.
30. Brunati S, Corradin G, Bron C. Production and characterization of a rabbit antiserum to the mouse CD8 antigenic complex by immunization with a synthetic peptide. J Immunol. Methods 1987; 96:97-105.
31. Bouhnik J, Galen FX, Menard J et al. Production and characterization of human renin antibodies with region oriented synthetic peptides. J Biol Chem 1987; 262:2913-8.
32. Davis LE, Castor CW, Tinney FJ et al. Preparation and characterization of antibodies with specificity for the amino-terminal tetrapeptide sequence of the platelet-derived connective tissue activating peptide-III. Biochemistry International 1985; 10: 395-404.
33. Ellinwood WE, Ronnekleiv OK, Kelly MJ et al. A new antiserum with conformational specificity for LHRH: usefulness for radioimmunoassay and immunocytochemistry. Peptides 1985; 6:45-52.
34. Choppin J, Metzger JJ, Bouillot M et al. Recognition of HLA class I molecules by antisera directed to synthetic peptides corresponding to different regions of the HLA-B7 heavy chain. J Immunol 1986; 136: 1738-44.
35. Guyon-Gruaz A, Delmas A, Pedoussaut S et al. Oral immunization with asynthetic peptide of cholera toxin B subunit. Eur J Biochem 1986; 159:525-8.
36. Ghose AC, Karush F. Induction of polyclonal and monoclonal antibody responses to cholera toxin by synthetic peptide approach. Molec Immunol 1988; 25:223-30.
37. Defendini ML, Pierres M, Regnier-Vigouroux A et al. Epitope mapping of apamin by means of monoclonal antibodies raised against free or carrier-coupled peptide. Molec Immunol 1990; 27:551-8.
38. Couraud JY, Frobert Y, Conrath et al. Monoclonal antibodies to substance P: production, characterization of their fine specificities, and use in immunochemistry. J Neurochem 1987; 49:1708-19.
39. Gras-Masse HS, Jolivet ME, Audibert FM et al. Influence of $CONH_2$ or COOH as C-terminus groups on the antigenic characters of immunogenic peptides. Mol Immunol 1986; 23:1391-95.
40. Lise LD, Mazier D, Jolivet M et al. Enhanced epitopic response to a synthetic human malarial peptide by preimmunization with tetanus toxoid carrier. Infect Immunity 1987; 55:2658-61.
41. Ibsen PH, Holm A, Raaschou-Nielsen M et al. Induction of polyclonal antibodies to the S1 subunit of pertussis toxin by synthetic peptides coupled to PPD: Effect of conjugation method, adjuvant, priming and animal species. APMIS 1992; 100:159-69.
42. Ichimori Y, Kurokawa T, Honda S et al. Monoclonal antibodies to human interferon γ. J Immunol Meth 1985; 80:55-66.
43. Sela M. Chemical synthesis for the understanding of immune response phenomena and for their medical application. In: Larralde C, Wills K, Ortiz-Ortiz L, Sela M, eds. Molecules, cells and parasites in immunology. New York: Acad Press 1980: 215-28.
44. Hudecz F, Price MR. Monoclonal antibody binding to peptide epitopes conjugated to synthetic branched polypeptide carriers. Influence of the carrier upon antibody recognition. J Immunol Methods 1992; 147: 201-10.
45. Rees AR, Offord RE. The semisynthesis of portions of hen's egg lysozyme by fragment

condensation. Biochem J 1976; 159:487-93.
46. Langbeheim H, Arnon R, Sela M. Antiviral effect on MS-2 coliphage obtained with a synthetic antigen. Proc Natl Acad Sci USA 1976; 73:4636-40.
47. Audibert F, Jolivet M, Chedid L et al. Successful immunization with totally synthetic diphtheria vaccine. Proc Natl Acad Sci USA 1982; 79:5042-6.
48. Lee ACJ, Powell JE, Tregear CW et al. A method for preparing β-hCG COOH peptide-carrier conjugates of predictable composition. Mol Immunol 1980; 17:749-56.
49. Keller O, Rudinger J. Preparation and some properties of maleimido acids and maleoyl derivatives of peptides. Helv Chim Acta 1975; 58: 531-41.
50. Hudecz F, Szekerke, M. Coll Czech Chem Commun 1985; 50:103-13.
51. Hudecz F, Votavova H, Gaál D et al. Branched polypeptides with a poly(L-lysine) backbone: synthesis, conformation and immunomodulation. In: Gebelein ChG, Carraher ChE, eds. Polymeric Materials in Medication. New York: Plenum Press, 1985:265-89.
52. Mezö G, Hudecz F, Kajtár J et al. Biopolymers 1990; 28: 1801-26.
53. Hudecz F, Kajtár J, Kurucz I et al. Investigation of the carrier function of polypeptides. Synthesis, conformation and cytotoxicity of oxazolone conjugates of poly(Lys) and poly[Lys-(DL-Ala_m)]. Makromol Chem Macromol Symp 1988; 19: 107-24.
54. Rajnavölgyi É, Hudecz F, Mezö G et al Synthetic branched polypeptides as carriers for low-molecular-weight antigens: Correlation between chemical structure and biological functions. Chimica Oggi 1990; 8: 21-9.
55. Hudecz F, Hilbert Á, Mezö G et al. Epitope mapping of the 273-284 region of HSV glycoprotein D by synthetic branched polypeptide carrier conjugates. Peptide Research 1993; 6:263-71.
56. Hilbert Á, Hudecz F, Mezö G et al. The influence of the branched polypeptide carrier on the immunogenicity of predicted epitopes of HSV-1 glycoprotein D. Scand J Immunol 1994; (in press).
57. Trudelle Y, Brack A, Delmas A et al . Synthesis of a new carrier for immunization: polytuftsin. Two examples of its use with peptides selected in the hepatitis B surface antigen. Int J Pept Protein Res 1987; 30:54-60.
58. Delmas A, Brack A, Trudelle Y. Cross-linking of peptides to synthetic carriers using different reagents: influence on antibody response. In: Giralt E, Andreu D, eds. Peptides 1990. Leiden: ESCOM, 1991:834-5.
59. Feeney RE. Chemical modification of proteins: comments and perspectives. Int. J. Pept. Prot. Res 1987; 29: 145-52.
60. Brinkley M. A brief survey of methods for preparing protein conjugates with dyes, haptens and cross-linking reagents. Bioconjugate Chemistry 1992; 3:2-13.
61. Wong SS. Chemistry of protein conjugation and cross-linking. Boca Raton: CRC Press, 1993.
62. Carlsson J, Drevin H, Axen R. Protein thiolation and reversible protein-protein conjugation. N-succinimidyl-3-(2-pyridyldithio)propionate, a new heterobifunctional reagent. Biochem J 1978; 173: 723-8.
63. Bassiri RM, Utiger RD. The preparation and specificity of antibody to thyrotropin releasing hormone. Endocrinology 1972; 90:722-7.
64. Pressman D, Campbell DH, Pauling L. The agglutination of intact azoerythrocytes by antisera homologous to the attached groups. J Immunol 1942; 44:101-6.
65. Mäkelä O, Seppälä IJT. Haptens and carriers. In: Weir DM ed. Handbook of Experimental Immunology Vol 1. 4th ed. New York: Acad Press, 1986: 3:1-13.
66. Deen C, Claassen E, Gerritse K et al. A novel carbodiimide coupling method for the synthetic peptides. J Immunol Methods 1990; 129:119-25.
67. Yoshitake S, Yamada Y, Ishikawa E et al. Conjugation of glucose oxidase from Aspergillus niger and rabbit antibodies using N-hydroxysuccinimide ester of N-(4-carboxy cyclohexylmethyl)maleimide. Eur J Biochem 1979; 101: 395-9.
68. Duncan RJS, Weston PD, Wrigglesworth R. A new reagent which may be used to introduce sulhydryl groups into proteins, and its use in the preparation of conjugates

for immunoassay. Anal Biochem 1983; 132:68-73.
69. Richards FM, Knowles JR. Glutaraldehyde as a protein cross-linking reagent. J Mol Biol 1968; 37:231-3.
70. Avrameas S. Coupling of enzymes to proteins with glutaraldehyde. Immunochemistry 1969; 6:43-52.
71. Zegers N, Gerritse K, Deen C et al. An improved conjugation method for controlled covalent coupling of synthetic peptides to proteins using glutaraldehyde in a dialysis method. J Immunol Methods 1990; 130: 195-200.
72. Peeters JM, Hazendonk TG, Beuvery EC et al. Comparison of four bifunctional reagents for coupling peptides to proteins and the effect of the three moieties on the immunogenicity of the conjugates. J Immunol Meth 1989; 120:133-43.
73. Aldwin L, Nitecki DE. A water-soluble, monitorable peptide and protein cross linking agent. Anal Biochem 1987; 164:494-501.
74. Jones GL, Edmundson HM, Spencer L et al. The use of maleimidocaproyloxysuccinimide to prepare malarial peptide carrier immunogens. J Immunol Meth 1989; 123:211-6.
75. Zanetti M, Sercarz E, Salk J. The immunology of new generation vaccines. Immunology Today 1987; 8:18-25.
76. Adam A, Lederer E. Muramyl peptides: immunomodulators, sleep factors, and vitamins. Med Res Rev 1984; 4:111-45.
77. Georgiev VST. Immunomodulatory activity of small peptides. TiPS 1990; 11:373-8.
78. Schneerson R, Fattom A, Szu SC et al. Evaluation of monophosphoryl lipid A (MPL) as an adjuvant. Enhancement of the serum antibody response in mice to polysaccharide-protein conjugates by concurrent injection with MPL. J Immunol 1991; 147:2136-40.
79. Roberts AJ, deAvila DM, Gerber JD et al. Active immunization of beef heifers against luteinizing hormone: I. Evaluation of protein carriers and adjuvants on antigenicity of LH. J Anim Sci 1990; 68:3742-6.
80. Morein B, Sundquist B, Hoglund S et al. ISCOM, a cagelike immunostimulating complex of membrane proteins. In: Chanock RM, Lerner RA, eds. Modern approaches to vaccines. Cold Spring Harbor: Cold Spring Harbor, 1984: 363-7.
81. Reddy R, Nair A, Brynestad K et al. Liposomes as antigen delivery in viral immunity. Seminars in Immunology 1992; 4:91-6.
82. Neurath AR, Kent SBH, Strick N. Antibodies to hepatitis B surface antigen (HBsAg) elicited by immunization with a synthetic peptide covalently linked to liposomes. J Gen Virol 1984; 65:1009-13.
83. Dreesman GR, Sparrow JT, Frenchick PJ et al. Synthetic hepatitis B surface antigen peptide vaccine. Adv Exp Med Biol 1985; 185: 129-36.
84. Brynestad K, Babbitt B, Huang L et al. Influence of peptide acylation, immunomodulators on the immunogenicity of a 1-23 peptide of glycoprotein D of herpes simplex virus. J Virol 1990; 64: 680-5.
85. Goodman-Snikoff G, Eisele LE, Heimer EP et al. Defining minimal requirements for antibody production to peptide antigens. Vaccine 1990; 8: 257-82.
86. Lövgren K, Lindmark, Pipkorn R et al. Antigenic presentation of small molecules and peptides conjugated to a preformed iscom carrier. J Immunol Meth 1987; 98:137-43.
87. Allison AC, Byars NE. An adjuvant formulation that selectively elicits the formation of antibodies of protective isotypes and of cell mediated immunity. J Immunol Methods 1986; 95:157-69.
88. Karagouni EE, Hadjipetrou-Kourounakis L. Regulation of isotype immunoglobulin production of adjuvants in vivo. Scand J Immunol 1990; 31:745-54.

6.2 THE MULTIPLE ANTIGENIC PEPTIDE APPROACH

To increase the poor immunogenicity of the relatively short synthetic peptides, numerous methods are available.[1,2] The simplest and oldest procedure is to couple the peptide hapten to an appropriate macromolecular carrier (e.g., bovine serum albumin, thyroglobulin, hemocyanin, tetanus toxoid, etc. See chapter 6.1). Another possibility is to couple the synthetic peptide to a lipid moiety. The resulting lipopeptide conjugates are potent adjuvants and activators of B lymphocytes and macrophages.[3-5]

The multiple antigenic peptide (MAP) approach described by Tam[6-8] offers attractive advantages. The system is based on a small, immunologically inert core matrix of lysine residues bearing radically branching synthetic peptides. This method was successfully applied to increase the immunogenicity of various peptide fragments of different proteins.[9-12] The most promising approaches had the aim of enhancement of the protective immune response against distinct pathogens such as the major immunogenic region of the foot-and-mouth disease virus (FMDV),[13] the circumsporozoite antigen of malaria,[14,15] hepatitis B virus proteins,[16] *Schistosoma mansoni*,[17] influenza virus hemagglutinin[18] or the V3 loop of the human immunodeficiency virus (HIV). The advantages of the method are as follows: (a) the molar ratio of the peptide epitope to the core molecule is high; (b) this kind of structure provides enhanced reproducibility as compared to the previously used peptide-protein carrier conjugates; and (c) there is no carrier-mediated epitope competition because of the low immunogenicity of the core region.

The effect of copy number was systematically studied with FMDV-derived peptides[13] and tetramers were demonstrated to be as efficient as octamers. Immunization with MAP in most cases requires adjuvants (see chapter 6.1.6), though the widely used but highly toxic Freund's adjuvant can be substituted by other approaches, such as $Al(OH)_3$, the only adjuvant licensed for human application,[13] or by the involvement of lipopeptides (chapter 6.2.3) or other immunopotentiators successfully used for peptides of viral origin.[19]

Recent improvements of this technology,[8] including peptide vaccines containing different incorporated adjuvants,[20] have opened up wide-ranging possibilities of eliciting an efficient memory response involving not only IgG-type antibodies, but also helper and cytotoxic T-lymphocytes[21] reactive with both the vaccine and the pathogen. A critical consideration in the development of peptide-based subunit vaccines is the inclusion of one or more potent T-cell epitopes to promote the generation of appropriate T-cell help and long-lasting memory.[22,23] The limitation of this alternative lies in the critical orientation of the T- and B-cell epitopes included in the immunogen.[7] If B-cell epitopes are linked to T-cell epitopes in the appropriate position, the immunogenicity can be improved. However, the T-cell-dependent immune response is restricted by the polymorphic major histocompatibility gene complex (MHC), and therefore a valuable vaccine immunogenic in all members of an outbred population requires more than one T-cell epitope. The MAP approach was established to overcome the genetic restriction mediated by MHC.[14,24]

6.2.1 Carrier-Free Antigens by Epitope Multiplication

The simple multiplication or polymerization of relatively short synthetic peptides by means of either chemical or genetic engineering methods may lead to immunogenic constructs. This technique should result in a "carrier-free" immune response, in contrast with the well-known "carrier" technology reviewed in chapter 6.1., but it has certain disadvantages. The polymerization reaction is practically uncontrollable, and characterization and purification of the resulting polymeric antigen is almost impossible. Stepwise total synthesis of the oligomeric material seems more controllable, but the limitations of preparative peptide chemistry mean that only short

oligomers can be prepared in this way. For example, if we have a medium-size epitope (e.g. 15 amino acids), a pentamer or decamer represents a 75-mer or 150-mer small protein, and such a peptide synthesis is not a routine task even for a well-trained scientist. However, this approach has been successfully applied to raise antibodies against the cholera toxin.[25] In this case, the effects were found to be comparable with those of polymeric epitopes with dipalmityl side-chains (see chapter 6.2.3) or with tetanus toxoid as carrier. Successful attempts have been described for FMDV [26] or diphtheria toxin[27] by epitope multiplication.

6.2.2 Combination of Mixed Epitopes

The epitope multiplication (or the MAP approach) offers the possibility of the "mixed epitope strategy." For an efficient immune response, the incorporation of merely B-cell epitopes into the antigen construction is not enough unless the B-cell epitope can be recognized by T cells as well, or the carrier has T-cell-activating properties. The mixed epitope strategy can lead to immunologically active constructions containing both T- and B-cell epitopes,[28] derived from identical or distinct regions of the same antigen, for example regions of viral proteins representing different serotypes.[29] The different epitopes are not necessarily derived from the same protein, or even not from the same virus. For example, a good TH-cell epitope can be combined with other peptides possessing poor immunogenicity in order to increase the antibody response. The "mixed epitope" strategy of course can be combined with other approaches, such as the MAP approach discussed previously, or the built-in adjuvant approaches described below.

6.2.3 Built-In Adjuvants

Investigation of the outer membrane of different bacteria led to the discovery of lipoproteins with B-lymphocyte-stimulating activity.[3] The N-terminal S-2,3-bis (palmitoxy)-(2-RS)-propyl)-N-palmitoyl-(R)-cysteine proved to be responsible[30] for this activity. The synthesis of this compound[31,32] (its structure is shown in Fig. 6.4) and immunological investigations after its coupling to different viral protein fragments[33] resulted in a very promising approach in the design and preparation of

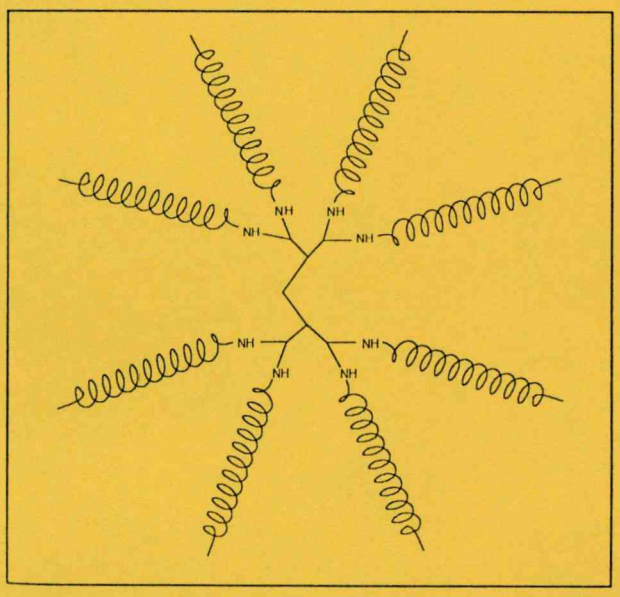

Fig. 6.3. An octameric map with peptide antigens.

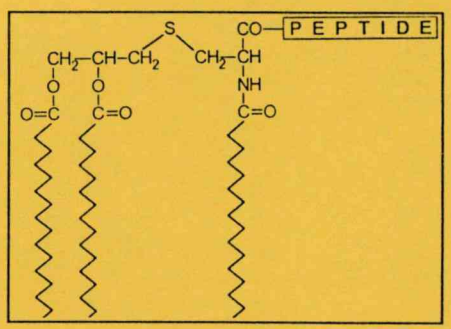

Fig. 6.4

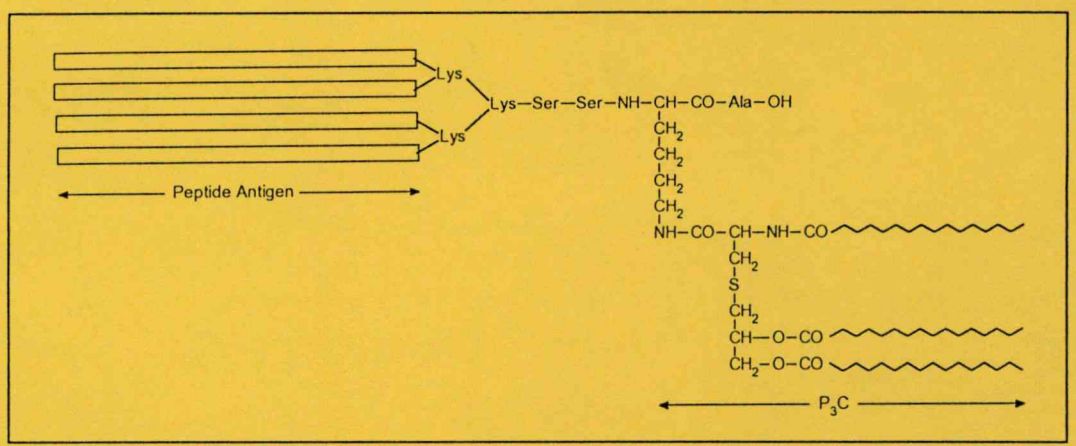

Fig. 6.5. General structure of a MAP-P_3C

synthetic vaccines.[34] The first attempts included FMDV peptide derivatives,[35] but recently many other antigen constructions have been described, such as malaria,[36] *Borrelia burgdorferi*,[37] HIV[38] etc. The induction of virus-specific cytotoxic lymphocyte-mediated responses by using lipopeptides has also been demonstrated.[39,40] The incorporation of lipid moieties into the antigen combination by other methods (epitope multiplication, mixotopes, etc.) seems to be one of the most promising approaches in the design and synthesis of artificial subunit vaccines against infectious diseases. One of such attempts is the design and synthesis of MAP constructions with a built-in lipid moiety[20] (Fig. 6.5).

References

1. Walter G, Scheidtmann KH, Carbone A et al. Antibodies specific for the carboxy- and amino- terminal regions of simian virus 40 large tumor antigen. Proc Natl Acad Sci USA 1980; 77: 5197-200.
2. Neurath R, Kent SBH, Strick N. Specificity of antibodies elicited by a synthetic peptide having a sequence in common with a fragment of a virus protein, the hepatitis B surface antigen. Proc Natl Acad Sci USA 1982; 79: 7871-5.
3. Bessler WG, Cox M, Lex A et al. Synthetic lipopeptide analogs of bacterial lipoprotein are potent polyclonal activators for murine B lymphocytes. J Immunol 1985; 135: 1900-5.
4. Bessler WG, Ottenbreit BP. Studies on the mitogenic principle of the lipoprotein from the outer membrane of Escherichia Coli. Biochem Biophys Res Commun 1977; 76:239-46.
5. Melchers F, Braun V, Galanos C. The lipoprotein of the outer membrane of Escherichia Coli: a B-lymphocyte mitogen. J Exp Med 1975; 142: 473-82.
6. Tam JP, Clavijo P, Lu YA et al. Incorporation of T and B epitopes of the circumsporozoite protein in a chemically defined synthetic vaccine against malaria. J Exp Med 1990; 171: 299-306.
7. Wang CY, Looney DJ, Li ML et al. Long-term high-titer neutralizing activity induced by octameric synthetic HIV-1 antigen. Science 1991; 254:285-7.
8. Tam JP. Synthetic peptide vaccine design: synthesis and properties of a high-density multiple antigenic peptide system. Proc Natl Acad Sci USA 1988; 85: 5409-13.
9. Briand JP, Barin C, Van Regenmortel MHV et al. Application and limitations of the multiple antigen peptide (MAP) system in the production and evaluation of anti-peptide and anti-protein antibodies. J Immunol Meth 1992; 156: 255-65.
10. Posnett DN, McGrrath H, and Tam JP. A novel method for producing anti-peptide antibodies using a peptide derived from the

T cell antigen receptor beta-chain constant region. J Biol Chem 1988; 263: 1719-25.
11. Drijfhout JW, and Bloemhog W. A new synthetic functionalized antigen carrier. Int J Pept Prot Res 1991; 37: 27-32.
12. Tóth GK, Váradi G, Penke B et al. Synthesis of branched polypeptides as antigens for influenza virus hemagglutinin and T cell receptor subunits. In: Schneider CH, Eberle AN. eds. Peptides 1992 Leiden: Escom Science Publishers B.V. 1993: 882-4.
13. Francis MJ, Hastings GZ, Brown F et al. Immunological evaluation of the multiple antigen peptide (MAP) system using the major immunogenic site of foot-and-mouth disease virus. Immunology 1991; 73: 249-54.
14. Del Giudice G, Tougne C, Louis JA et al. A multiple antigen peptide from the repetitive sequence of the plasmodium malariae circumsporozoite protein induces a specific antibody response in mice of various H-2 haplotypes. Eur J Immunol 1990; 20: 1619-22.
15. Munesinghe DY, Clavijo P, Calle MC et al. Immunogenicity of multiple antigen peptides (MAP) containing T- and B cell epitopes of the repeat region of the P. falciparum circumporozoite protein. Eur J Immunol 1991; 21: 3015-21.
16. Tam JP, Lu YA. Synthetic peptide vaccine engineering: design and synthesis of unambiguous peptide-based vaccines containing multiple peptide antigens for malaria and hepatitis. In: Epton R ed. Innovation and Perspectives in Solid Phase Synthesis I. Intercept UK, 1990: 351-70.
17. Auriault C, Wolowczuk I, Gras-Masse H et al. Epitopic characterization and vaccinal potential of peptides derived from a major antigen of Schistosoma mansoni (Sm28 GST). Peptide Research 1991; 4: 6-11.
18. Tóth GK, Váradi G, Nagy Z et al. Branched polypeptides as antigens for influenza virus hemagglutinin and T cell receptor subunits. Peptide Research 1993; 6: 272-80.
19. Deres K, Schild H, Wiesmüller KH et al. In vivo priming of virus-specific cytotoxic T lymphocytes with synthetic lipopeptide vaccine. Nature 1989; 342: 561-4.
20. Defoort JP, Nardelli B, Huang W et al. A rational design of synthetic peptide vaccine with a built-in adjuvant. Int J Pept Prot Res 1992; 40: 214-21.
21. Schild H, Deres K, Wiesmüller KH et al. Efficiency of peptides and lipopeptides for in vivo priming of virus-specific cytotoxic T cells. Eur J Immunol 1991; 21: 2649-54.
22. Zegers ND, Holten C, Claassen E et al. Peptide induced memory (IgG) response requires covalent linkage of a B cell epitope and a T cell epitope. In: Schneider CH, Eberle AN. eds. Peptides 1992 Leiden: Escom Science Publishers B.V. 1993: 836-7.
23. Löwenadler B, Lycke N, Svanholm C et al. T and B cell responses to chimeric proteins containing heterologous T helper epitopes inserted at different positions. Molecular Immunology 1992; 29: 1185-90.
24. Pessi A, Valmori D, Migliori P et al. Lack of H-2 restriction of the Plasmodium falciparum (NANP) sequence as multiple antigen peptide. Eur J Immunol 1991; 21: 2273-6.
25. Jacob CO, Arnon R, Sela M. Effect of carrier on the immunogenic capacity of synthetic cholera vaccine. Molecular Immunology 1985; 22: 1333-9.
26. DiMarchi R, Brooke G, Gale C et al. Protection of cattle against foot-and-mouth disease by a synthetic peptide. Science 1986; 232: 639-41.
27. Audibert F, Jolivet M, Chedid L et al. Successful immunization with a totally synthetic diphtheria vaccine. Proc Natl Acad Sci USA 1982; 79: 5042-6.
28. Tam JP, Zavala F. A novel approach to increase detection sensitivity of synthetic peptides in solid-phase immunoassays. J Immunol Methods 1989; 124: 53-61.
29. Gras-Masse H, Ameisen JC, Boutillon C et al. Synthetic vaccines: The mixotope strategy. In: Smith JA, Rivier JE. eds. Peptides, Chemistry and Biology Leiden: Escom Science Publishers B.V. 1992: 842-3.
30. Jung G, Wiesmüller KH, Becker G et al. Verstärkte Produktion spezifischer Antikörper durch Präsentation der antigenen Determinanten mit kovalent verknüpften Lipopeptid-Mitogenen. Angew Chem 1985; 97: 883-5.
31. Wiesmüller KH, Bessler W, Jung G. Syn-

thesis of the mitogenic S-[2,3-bis(palmitoyloxy)-propyl]-N-palmitoyl pentapeptide from Escherichia coli lipoprotein. Hoppe-Seyler's Z Physiol Chem 1983; 364: 593-606.

32. Metzger JW, Wiesmüller KH, Jung G. Solid-phase peptide synthesis of lipopeptide analogues of bacterial lipoprotein with Fmoc-S-(2,3-dihydroxypropyl)-cysteine. In: Epton R, ed. Innovation and Perspectives in Solid Phase Synthesis II. Intercept UK 1992; 251-[illegible].
33. Wiesmüller KH, Deres K, Shi L et al. Lipopeptide-helper T cell epitope-CTL epitope conjugate induces antibodies against the CTL epitope. In: Epton R, ed. Innovation and Perspectives in Solid Phase Synthesis II. Intercept UK 1992;499-502.
34. Wiesmüller KH, Jung G, Hess G. Novel low-molecular weight ,synthetic vaccine against foot-and-mouth disease containing a potent B cell and macrophage activator. Vaccine 1989; [illegible]: 29-33.
35. Wiesmüller KH, Freund S, Jung G. Novel FMDV vaccine consisting of a T cell epitope and the B cell activating N-terminus of E. coli lipoprotein: synthesis, results of vaccination and molecular dynamics. In: Jung G, Bayer E. eds. Peptides 1988 Berlin-New York: Walter de Gruyter and Co 1989: 695-7.
36. Wiesmüller KH, Jung G, Gillessen D et al. The antibody response in BALB/c mice to the Plasmodium falciparum circumsporozoite repetitive epitope covalently coupled to synthetic lipopeptide adjuvant. Immunology 1991; 72: 109-13.
37. DeOgny L, Pramanik BC, Arndt LL et al. Solid-phase synthesis of biologically active lipopeptides as analogs for spirocheral lipoproteins. Peptide Research 1994; 7: 91-7.
38. Defoort JP, Nardelli B, Huang W et al. Complete synthetic vaccine with built-in adjuvant. In: Smith JA, Rivier JE, eds. Peptides, Chemistry and Biology Leiden: Escom Science Publishers B.V. 1992: 845-8.
39. Deprez B, Gras-Masse, Martinon F et al. Synthesis and evaluation of novel lipopeptide constructs for in vivo induction of virus-specific cytotoxic T-lymphocyte mediated response. In: Hodges RS, Smith JA, eds. Peptides, Chemistry Structure and Biology Leiden: Escom Science Publishers B.V. 1994; 736-7.
40. Deres K, Schild H, Wiesmüller KH et al. In vivo priming of virus-specific cytotoxic T lymphocytes with synthetic lipopeptide vaccine. Nature 1989; 342: 561-4.

3.15.

Peptides 1992
C.H. Schneider and A.N. Eberle (Eds.)

Synthesis of branched polypeptides as antigens for influenza virus hemagglutinin and T-cell receptor subunits

Gábor K. Tóth[a], Györgyi Váradi[a], Botond Penke[a], Éva Monostori[b], Zoltán Hegedűs[b], Zoltán Nagy[c], István Kurucz[d] and Éva Rajnavölgyi[c]

[a]Department of Medical Chemistry, A. Szent-Györgyi Medical University, Dóm tér 8, H-6720 Szeged, Hungary

[b]Institute of Genetics, Biological Research Center of the Hungarian Academy of Sciences, Szeged, Hungary

[c]Department of Immunology, Eötvös Loránd University, Budapest, Hungary

[d]Institute of Drug Research, Budapest, Hungary

Introduction

The activation of T lymphocytes occurs via and is regulated by a number of cell-surface receptors, including T-cell antigen receptor (TCR) complex. These receptors have prime importance in the immune response. However, the role of CD3 subunits of TCR and other receptor-associated proteins (CD3 γ, δ, ε, ζ) are still poorly understood. Monoclonal antibodies are generally used for studying cell-surface receptor functions. Hemagglutinin, the surface glycoprotein of the influenza virus plays an important role in the infectivity and pathogenicity of the virus. The posttranslational enzymatic cleavage mediated by host cell proteases is necessary for the formation of infective virus. The elucidation of the requirements for the T- and B-cell recognition might led to important information for subunit vaccine design. In previous experiments we have localized several T- and B-cell epitopes in the intersubunit part of the influenza virus hemagglutinin, including a very good T helper cell activator [1–3]. The multiple antigen peptide (MAP) method [4–7] emerged into a widely used procedure for the production of a strong immune response against various peptide fragments of different proteins. Our aims were the following:

(1) Raising antibodies against the extracellular part of CD3δ and CD3ζ subunits.
(2) To elucidate the role of hemagglutinin in the immune response.
(3) To investigate the usefulness of the 'multiple antigen peptide'.

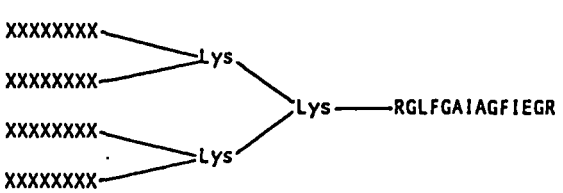

XXXXXXXX = VTGLRNIPSIQSR (HA 317-329), FKIPIEELEDRVFVNC (CD3δ 1-16), AQSFGLLDPKLCYLLDG (CD3ζ 21-37)

Scheme 1. The structure of the synthesized chimeric 'multiple antigenic peptides'.

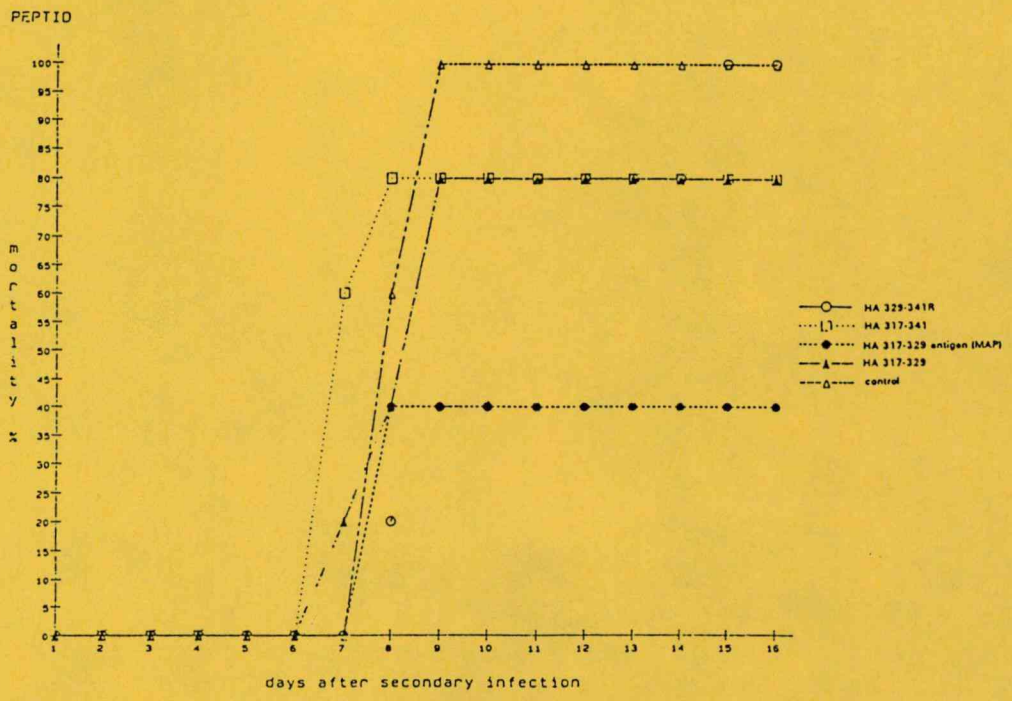

Fig. 1. The effect of the HA antigen construction for the mortality after influenza virus infection.

Peptide Synthesis and Purification

The peptides were synthesized by solid phase technique utilizing *t*-Boc chemistry [8]. Side-chain protecting groups were as follows: Arg(Tos), Asp(OcHex), Cys-(Meb), Thr(Bzl), Lys(2ClZ), Glu(OcHex), Tyr(2BrZ) and Ser(Bzl). The peptide chains were elongated on MBHA resin (0.8 mmol/g) and the syntheses were carried out manually. Couplings were performed with DCC, with the exception of Asn, Gln and Arg which were incorporated as their HOBt esters. Amino acid incorporation was monitored by the ninhydrin test [9]. The completed peptide resins were treated with liquid HF/dimethylsulphide/*p*-cresol (88:6:4, vol/vol), on 0 °C, 1 h. HF was removed and the resulting free peptides were solubilized in 10% aqueous acetic acid, filtered and lyophilized. The crude peptides were purified by RPHPLC using an Astec 300 C4 5 μ column (8 × 250 mm). The solvent system used was the following: 0.1% TFA in water, 0.1% TFA, 80% AcN in water, gradient: 0% → 90% B in 1.5 h, flow 1.5 ml/min. The appropriate fractions were pooled and lyophilized. The purity was checked by RPHPLC, isoelectrofocussing and SDS gel electrophoresis.

Immunological Results

The immunological tests revealed that all the antisera are highly specific against the used synthetic peptides, however, the antisera in the immunne precipitation test do not recognize the native 16 kDa ζ chain. The antisera against the δ chain were able to recognize the native molecule in indirect immunfluorescence using FACS-

star plus. The hemagglutinin antigen construction resulted in a high antibody response after repeated injection into mice. This new MAP construction was highly potent also in TH cell activation. Additionally, in preliminary experiments it showed a protective effect against influenza infection. The MAP system combined with this TH epitope seems to be a promising approach for subunit vaccine design.

References

1. Hollósi, M., Ismail, A.A., Mantsch, H.H., Penke, B., Váradi, G., Tóth, G.K., Laczkó, I., Kurucz, I., Nagy, Z., Fasman, G.D. and Rajnavölgyi, É., Eur. J. Biochem., 206(1992)421.
2. Rajnavölgyi, É., Immunol. Today, 13(1992)17.
3. Rajnavölgyi, É., Nagy, Z., Hollósi, M., Mantsch, H.H., Tóth, G.K., Váradi, G., Penke, B., Fasman, G.D., Gergely, J. and Kurucz, I., submitted for publication.
4. Tam, J.P., Proc. Natl. Acad. Sci. USA, 85(1988)5409.
5. Tam, J.P., Clavijo, P., Lu, Y.A., Nussenzweig, R. and Zavala, F., J. Exp. Med., 171(1990)299.
6. Tam, J.P. and Lu, Y.A., Proc. Natl. Acad. Sci. USA, 86(1989)9084.
7. Defoort, J.P., Nardelli, B., Huang, W., Shiu, D.R. and Tam, J.P., In Smith, J.A. and Rivier, J.E. (Eds.) Peptides: Chemistry and Biology (Proceedings of the 12th American Peptide Symposium), ESCOM, Leiden, 1992, pp. 845–846.
8. Merrifield, R.B., Biochemistry, 3(1964)1385.
9. Kaiser, E., Colescott, R.L., Bossinger, C.D. and Cook, P.I., Anal. Biochem., 34(1970)595.

3.16.

Conformational mapping of the antigenic intersubunit region of influenza virus hemagglutinin: CD and FTIR spectroscopy studies

Zs. Majer[a], S. Holly[b], G.K. Tóth[c], Gy. Váradi[c], I. Laczkó[d], É. Rajnavölgyi[e] and M. Hollósi[a]

[a] Dept. of Organic Chem., Eötvös University, P.O. Box 32, H-1518 Budapest 112, Hungary
[b] Central Research Inst. of Chem., P.O. Box 17, H-1525 Budapest, Hungary
[c] Dept. of Medical Chem., Szent-Györgyi University, H-6720 Szeged , Hungary
[d] Inst. of Biophysics, Biological Research Center, P.O. Box 521, H-6720 Szeged, Hungary
[e] Dept. of Immunology, Eötvös University, H-2131 Göd, Hungary

Introduction

The epidemiological success of influenza A viruses is largely due to the variability of their surface glycoproteins. One of these molecules, the hemagglutinin (HA) is the major target of immune recognition and performs two crucial functions in the early stage of viral infection. It is responsible for receptor binding and mediates fusion of the viral and endosomal membrane of the host cell. Influenza A viruses are subdivided into 14 serotypes based on antigenic differences [1]. The HA molecule of influenza A viruses is synthesized as a precursor polypeptide chain (HA0) and upon maturation it is cleaved to HA1 and HA2 subunits by host cell proteases. The enzymatic cleavage is the prerequisite of infectivity and results in the elaboration of the fusion peptide (FP) comprising the 1-14 amino acids of the HA2 subunit. The amino acid sequence of this motif is identical in all influenza virus serotypes. The amino acid sequence of the C-terminal stretch of the HA1 subunit is also relatively conserved in the different influenza A serotypes. This sequence (CP) plays a crucial role in determining tropism and infectivity of the virus [2]. Fragments of the intersubunit region (IP) of hemagglutinin are capable of adopting multiple conformations in solution, which implies that different conformations may prevail depending on environmental conditions. By contrast, antibody recognition requires a more defined conformation adopted in the hemagglutinin molecule and maintained in IP. Our previous investigations [2] showed that IP is a switch peptide with expressed α-helicity in a helix promoting environment and a preponderant β-sheet character in aqueous solution at higher concentration or in the presence of octyl-β-glucoside (OG) micelles. Synthetic peptides from the C-terminal part of HA1 were reported to have excellent antigenic and immunogenic properties, especially in MAP (multiple antigenic protein) form [3]. This study reports the conformation of IP from three serotypes of influenza A virus and the MAP-1 peptide, with and without the fusion peptide (Table 1), as revealed by comparative circular dichroism (CD) and Fourier-transform infrared spectroscopy measurements.

Results and Discussion

In TFE solution the intersubunit peptides (IPs) show helical CD spectra. The Provencher-Glöckner method [5] results in 36% α-helix content for IP1 and IP2 and decreased helicity for IP3[desGly^{21}]. In TFE the branched MAP peptides also show CD spectra that reflect the presence of significant amounts of α-helix, 34% for MAP1-FP

Table 1 *Structure of peptides and multiple antigenic peptides (MAPs) representing the intersubunit region of influenza virus A hemagglutinin*

Amino acid sequence	Abbreviated name
1 8 13 25 VTGLRN I PS I QSRGLFGA I AGF I EG	IP1
7 9 11 A———V-Q-E———————	IP2
1 4 7 9 10 12 21 LA-M —V-E·K·T ————···——	IP3[desGly^{21}]
1 13 VTGLRN I PS I QSR	CP1
14 25 GLFGA I AGF I EG	FP
[(VTGLRNIPSIQSR)$_2$K]$_2$K	MAP1
[(VTGLRNIPSIQSR)$_2$K]$_2$K-GLFGAIAGFIEG	MAP1-FP

and 18% for MAP1. In the FTIR spectra of the IP peptides in TFE we identified the following component bands by the curve-fitting method of Holly *et al.* (unpublished): 1658-1656 cm^{-1} (α-helix), 1640 cm^{-1} broad band, which is a composite of two or more bands (aperiodic, β-turn, β-sheet) and 1620 cm^{-1} (β-sheet or β-aggregates). Deconvolution of the FTIR spectra of MAP1 and MAP1-FP shows the following component bands: 1661 cm^{-1} (weakly H-bonded α-helix or 3_{10}-helix [6]), 1651-1650 cm^{-1} (α-helix and aperiodic), 1640 cm^{-1} (H-bonded β-turns [7]) and 1623-1624 cm^{-1} (β-sheet). In general, there is a good correlation between the CD and FTIR data on the conformation of the IP and MAP1 peptides. The deconvolution of the CD spectra of IP1 and IP2 shows a high percentage of β-sheet (55% and 64%) in addition to the 30% α-helix content; however, no indication is given of the presence of aperiodic and β-turn conformer populations. Both branched peptides are present as a mixture of conformers even in TFE. A band near 1640 cm^{-1} has been assigned to H-bonded β-turns [7] (in MAP1-FP it may be correlated with type II β-turns predicted at the Thr-Gly and Arg-Gly residues or a pseudo β-turn encompassing a lysine at the branching region). The stronger helical character of MAP1 (18%) compared to CP1 (6% α-helix, 39% β-sheet) [8] can be explained by side chain interactions that stabilize H-bonded α-helix or 3_{10}-helix conformer populations. Results of immunological and conformational studies demonstrate that the CP peptides and the T-cell epitopic N-terminal regions of the IP peptides have a flexible conformation that can adapt to the peptide binding groove of MHC molecules. Our comparative spectroscopy approach lays emphasis on the conformational role of the fusion region in B-cell recognition.

References

1. Kawaoka, Y. and Webster, R.G., Proc. Natl. Acad. Sci. USA, 85(1988)324.
2. Hollósi, M. *et al.*, Eur. J. Biochem., 206(1992)421.
3. Nagy, Z. *et al.*, Scand. J. Immunol., in press.
4. Tóth, G.K. *et al.*, Pept. Res., 6(1993)272.
5. Provencher, S.W. and Glöckner, J., J. Biochem., 20(1981)33.
6. Surewitz, W.K. and Mantsch, H.H., Biochim. Biophys. Acta, 952(1988)115.
7. Hollósi, M. *et al.*, Biopolymers, 34(1994)177.
8. Holly, S., Majer, Zs., Tóth, G.K., Váradi, Gy., Rajnavölgyi, É., Laczkó, I. and Hollósi, M., Biochem. Biophys. Res. Commun., 197(1993)1247.

BIOCHEMICAL AND BIOPHYSICAL RESEARCH COMMUNICATIONS 249, 213–217 (1998)
ARTICLE NO. RC989109

Liposome-Induced Conformational Changes of an Epitopic Peptide and its Palmitoylated Derivative of Influenza Virus Hemagglutinin

Ilona Laczkó,* Miklós Hollósi,† Elemér Vass,† and Gábor K. Tóth‡

*Institute of Biophysics, Biological Research Center, H-6701 Szeged, POB 521 Hungary; †Department of Organic Chemistry, Eötvös University, H-1518 Budapest 112, POB 32; and ‡Department of Medical Chemistry, Szent-Györgyi Medical University, H-6720 Szeged, Dóm tér 8. Hungary

Received June 25, 1998

The conformation of synthetic $HA_{317-329}$-NH_2 representing the major B- and T-cell epitopic region of influenza virus hemagglutinin, its palmitoylated derivative ($HA_{317-329}$-Thr(Pal)-NH_2), and the intersubunit peptide ($HA_{317-341}$-NH_2) comprising also the fusion peptide, were studied in aqueous buffer and in the presence of neutral and negatively charged liposomes. The free peptide is unordered in aqueous solution, even in the presence of liposomes. However, grafting the palmitic acid or the fusion peptide onto the C-terminus of the peptide enables the hydrophilic $HA_{317-329}$ to adopt folded (turn) and β-strand structure on the surface of neutral and negatively charged liposomes, respectively. The results emphasizé the importance of some kind of anchor for achieving a specific conformation of epitopic peptide $HA_{317-329}$-NH_2 on the surface of liposomes. © 1998 Academic Press

Specific immune responses against proteins and viruses can be achieved using synthetic antigenic peptides. However, free peptides are weakly immunogenic when used without carrier molecules [1,2]. Several alternatives have been proposed to improve the immunogenicity of epitopic peptide sequences. Among them, the covalent attachment of fatty acid chain has been shown to enhance the immunogenicity of unmodified peptides [3], and their ability to prime cytotoxic T lymphocytes [4-6]. Recently, many lipopeptides such as the HIV-1 V3(190-211) sequence modified by N$^{\epsilon}$-palmitoyl-L-lysine [3,7] or tripalmitoyl-S-glyceryl-cysteine containing N-acylated peptide derivatives [8] were synthesized and investigated. The synthesis of N-acylated derivatives seems to be simpler compared to that of O-acylated ones, however, the latters are more biodegradable.

The general lack of cross-reactivity between synthetic peptides and native proteins or viruses is believed to be due to the conformational dissimilarity between the peptide and the corresponding sequence within the intact molecule [9]. Experiments with synthetic peptides of influenza virus hemagglutinin (HA) revealed that of a number of peptides, including those representing the major antigenic regions, only the 24 residues fragment 305-328 elicited antibodies which cross-reacted with the virus or intact HA [10]. In the infectious form of the virus HA is cleaved between residues 328 and 329 to form the heavy (HA1) and light (HA2) chains. It is the 305-328 residues sequence of the C-terminus of the HA1 chain which can be recognized by both B and T cells. The shortest peptide which was able to elicit the production of antibodies was a decapeptide corresponding to the 319-328 sequence, subtype H3 (but not subtype H1, H2 or H6) [11]. On the base of our earlier spectroscopic studies on 317-329 fragments from H1-H3 subtypes, we suppose that α-helicity does not play a determinant role in the recognition of T cell epitopic peptides [12].

It is reasonable to suppose that modification by fatty acid promotes the interaction of polypeptides with membranes, however, the effects of these hydrophobic lipid groups on the conformation of peptides have scarcely been studied [13]. This paper reports conformational studies on three synthetic peptides: the C-terminal 13 residues of the HA1 chain, $HA_{317-329}$-NH_2, its O-palmitoylated derivative, $HA_{317-329}$-Thr(Pal)-NH_2 and the intersubunit peptide, $HA_{317-341}$-NH_2. Circular dichroism (CD) and Fourier transform infrared (FTIR) spectroscopic measurements were performed in buffer and in the presence of liposomes to reveal the conformational consequences of covalent attachment of the palmitic acid or the fusion peptide to the 317-329 peptides.

MATERIALS AND METHODS

Peptide synthesis. $HA_{317-329}$-NH_2 (VTGLRNIPSIQSR-NH_2) and $HA_{317-341}$-NH_2 (VTGLRNIPSIQSRGLFGAIAGFIEG-NH_2) were synthesized by solid-phase technique using Boc chemistry [14]. Side-

0006-291X/98 $25.00

chain protecting groups were as follows: Tos (Arg), Bzl (Thr, Ser), cHex (Glu). The peptide chains were elongated on an MBHA resin (0.73 mmoles/g). Couplings were performed with N,N'-dicyclohexylcarbo-diimide (DCC), with the exception of Asn, Gln and Arg which were incorporated as their OBt-esters. As for *the synthesis of the palmitoylated peptide*, $HA_{317-329}$-Thr(Pal)-NH_2 a side-chain unprotected threonine derivative (Boc-Thr-OH) was first attached to the resin and then its hydroxyl function was acylated with palmitoyl chloride in presence of pyridine on the solid phase. After repeated acylation, the peptide chain was elongated further. The completed peptide resins were treated with liquid HF/dimethyl sulphide/p-cresol/p-thiocresol (88:6:4:2, v/v), at −5°C, 45 min. HF was removed and the resulted free peptides were solubilized in 30% aqueous acetic acid, filtered and lyophilized. The crude peptides were purified by semi-preparative reverse phase HPLC on a C-18 column (16 × 250 mm). The peptides were eluted with a linear gradient of aqueous acetonitrile 24% → 80% MeCN, 0.1% trifluoroacetic acid (TFA) in 60 min, 4 ml/min flow rate. The appropriate fractions were pooled and lyophilized. The purified peptides were characterized by amino acid analysis, HPLC and mass spectrometry using a Finnigan TSQ 7000 tandem quadrupole electrospray mass spectrometer. Peptide purity was above 97% (HPLC and capillary zone electrophoresis).

Preparation of phospholipid liposomes. For neutral liposomes 10 mg dipalmitoyl phosphatidylcholine (DPPC) and for negatively charged liposomes 9 mg DPPC+1 mg dipalmitoyl phosphatidic acid (DPPA) were dissolved in 1 ml chloroform and dried by a stream of N_2 gas for 1 h. The dry lipid was hydrated in 3 ml of 5 mM Hepes buffer (pH 7.4) with repeated vortex mixing at 50°C for 20 min. The suspension was sonicated at 50°C for 45 min (until a clear solution was obtained) using a MSE Type 150W ultrasonic disrupter (21 Kc/sec, 10 μ amplitude). The oxygen was expelled by bubbling N_2 through the suspension before sonication. After sonication the suspension was centrifuged for 30 min at 4000 g to remove the titanium dust originated from the probe. For the CD measurements the suspension was diluted with Hepes buffer to a lipid concentration of 1.5 mM. Prior to measurements the peptide-liposome samples were incubated at 25°C for 30 min.

Circular dichroism. CD spectra were monitored using a Jobin-Yvon Mark VI dichrograph. Measurements were carried out at 25°C using an optical cell with a path length of 0.02 or 0.1 cm. Ellipticity is expressed as mean residue ellipticity, $[\Theta]_{MR}$, in units of deg.cm^2.dmole^{-1}.

Infrared spectroscopy. Fourier transform infrared measurements were performed in D_2O (Aldrich, 99.9%) at room temperature on a Bruker IFS-55 FTIR spectrometer at a resolution of 2 cm^{-1} using a 0.05 cm cell with CaF_2 windows. The amide I region of the spectra was decomposed to individual bands by the Levenberg-Marquardt nonlinear curve-fitting method using weighted sums of Lorentz and Gauss functions. The choice of the starting parameters was assisted by Fourier self-deconvolution (FSD) [15]. Since the peptides were eluted with a solvent mixture containing TFA, all peptides were present as trifluoroacetate salts. Thus, in the FTIR spectra the component at 1673 cm^{-1} can be correlated with the ν_{as} (COO^-) vibration of trifluoroacetate [16].

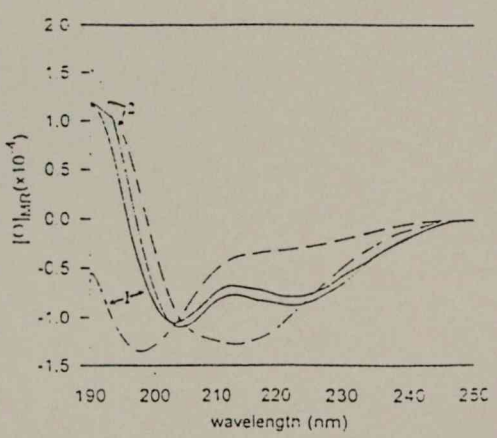

FIG. 1. CD spectra of $HA_{317-329}$ (1) and $HA_{317-329}$-Thr(Pal)-NH_2 (2) in TFE (—) and in 5 mM Hepes buffer, pH 7.4 (---). Peptide concentration: 30 μM.

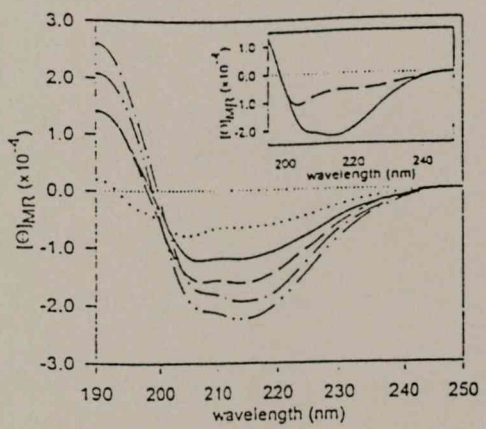

FIG. 2. CD spectra of $HA_{317-329}$-Thr(Pal)-NH_2 at different concentrations in 5 mM Hepes, pH 7.4. 15 μM (· · ·), 30 μM (—), 60 μM (---), 120 μM (-·-), 240 μM (-· · -). *Inset:* CD spectra of $HA_{317-329}$-Thr(Pal)-NH_2 (240 μM) in 5 mM Hepes, pH 7.4 without (—) and with 0.2% (w/v) Triton (---).

RESULTS AND DISCUSSION

Figure 1 presents the CD spectra of $HA_{317-329}$-NH_2 and $HA_{317-329}$-Thr(Pal)-NH_2 in trifluoroethanol (TFE) and in 5 mM Hepes buffer (pH 7.4). The low intensity, blue shifted helical (class C) spectrum of the free peptide in TFE can be correlated with the stabilization of certain subtypes of β-turns [17]. The intensive β-turn acceptor band at 1638 cm^{-1} in the FTIR spectrum also supports the presence of this conformational element [12]. Introducing the palmitoyl moiety into the C-terminus does not result in any significant spectral change in TFE, however, the two peptides show different CD spectra in buffer. In buffer solution the free peptide is present in a predominantly unordered or semiextended (PPII) conformation [18], while the broad negative band in the CD spectrum of $HA_{317-329}$-Thr(Pal)-NH_2 is indicative of a mixture of β-sheet and turn conformers. The increased population of ordered conformations upon introducing palmitoyl group may account for the hydrophobic environment provided by the acyl chain. This may be of significance in the recognition events keeping in mind, that the most structured peptides in solution often correspond to the best immunogens [19].

Characteristic differences in the concentration dependence of the CD spectra of the free and lipoderivative of $HA_{317-329}$ were observed in Hepes buffer. While

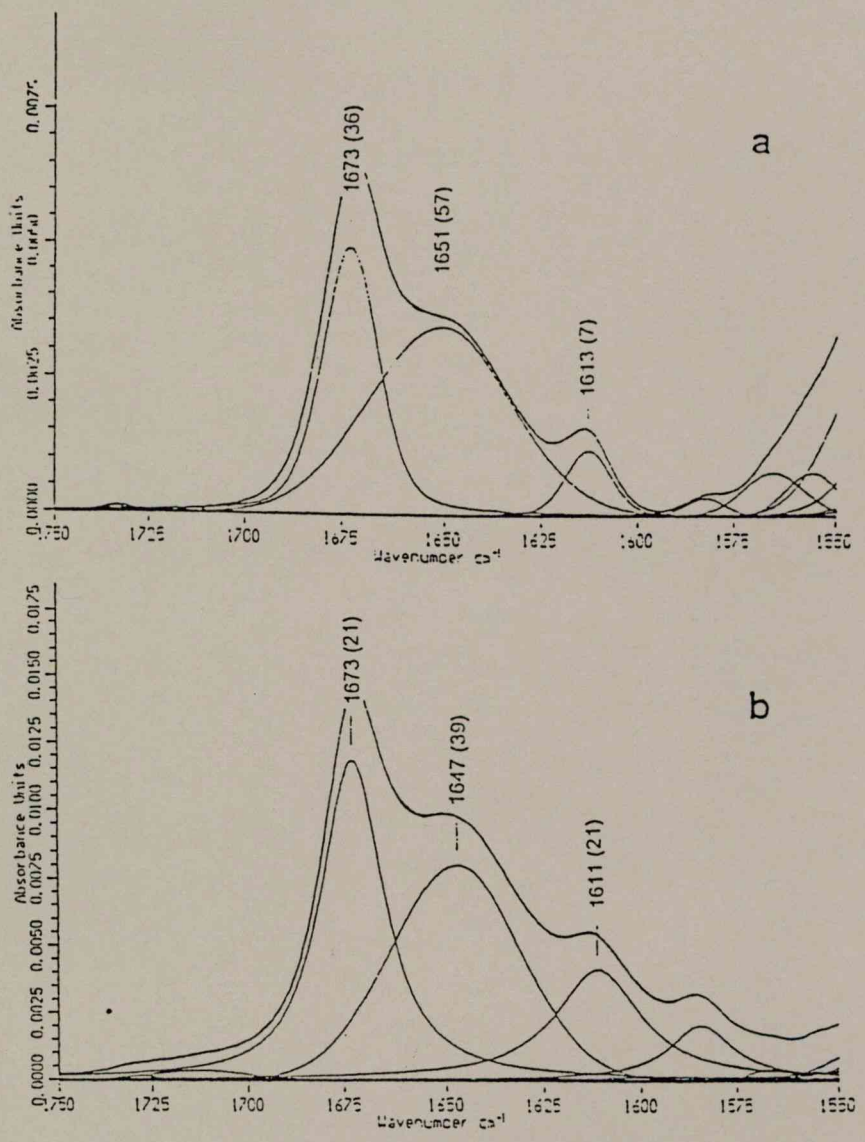

FIG. 3. FTIR spectra of $H_{317-329}$-Thr(Pal)-NH_2 in D_2O at 120 μM (a) and 240 μM (b) peptide concentrations. In parentheses: relative intensities in percentages.

the CD spectrum of the free peptide was practically independent of the concentration in the range of 15-240 μM (data not shown), a definite spectral change was monitored in the case of $HA_{317-329}$-Thr(Pal)-NH_2 (Fig. 2). At the highest concentration (240 μM), the lipopeptide was not fully dissolved (cloudy solution) and the spectrum was suggestive of a mixture of β-sheet (negative band at 215 nm), and folded conformations (shoulder at ~205 nm). On dilution, the spectral contribution of the β-sheet gradually decreases and at 15 μM the spectrum shows enrichment of turn structures, though a significant amount of unordered conformation is also present (low positive band intensity). The FTIR measurements, performed in D_2O at 120 and 240 μM concentrations, support the results of CD spectroscopy. As Fig. 3 shows, two main amide I bands appear: one at 1611 and 1613 cm^{-1} - corresponding to a mixture of β-sheet and β-aggregation - and a stronger component at 1647 and 1651 cm^{-1} which can be correlated with a mixture of helical (or loop) and aperiodic secondary structures [15]. There is a difference, however, in the relative intensity (number in parenthesis in Fig. 3) of the two components. The spectrum of the more concentrated sample suggests higher relative amount of β-sheet conformation or aggregates.

Addition of the solubilizing agent Triton X-100 (0.2% w/v) to the Hepes solution of $HA_{317-329}$-Thr(Pal)-NH_2 at the highest concentration (240 μM), a CD spectrum similar to that of the most diluted (15 μM) sample was obtained (inset in Fig. 2). Apparently, at higher concentrations the lipopeptide forms micelles which are held together by hydrophobic interactions between palmi-

oyl chains. It is unlikely that molecular association initiated by the peptide moieties. However, on the urface of the lipopeptide-micelles part of the peptide noieties gets in close vicinity to each other which leads o the formation of strong H-bonds between neighbour- ng β-strands adopting β-sheet conformation.

The secondary structure of the free, the palmitoy- ated and fusion peptide-coupled $HA_{317-329}$-NH_2 was ompared in the presence of neutral and negatively harged liposomes at [lipid]/[peptide] ratio of 50. As igure 4*a* shows, the CD spectra of the *free* peptide in Hepes buffer and in the presence of *neutral liposomes* re nearly identical: the peptide is disordered or semi- xtended irrespective of the presence or absence of lipo- omes. Interaction between the hydrophylic peptide nd the hydrophylic surface of liposomes is not ex- luded but due to the limited residence time the experi- nental presentation is difficult. Although the electro- tatic attraction between the positively charged pep- ide and the *negatively charged* surface of liposomes esulted in a weak spectral change in the 210-240 nm ange, apparently the induced conformational change vas weak in the absence of some kind of anchor.

On the contrary, the covalently coupled palmitoyl hain greatly modifies the conformation of $HA_{317-329}$ in he presence of both neutral and negatively charged lipo- omes. The 205 nm band in the CD spectrum of the *ipopeptide* in the presence of neutral liposomes suggests nrichment of the population of the folded conformers Fig. 4b). A similar observation was made by Macquaire *t al.* [20] when the conformational change induced by hospholipidic interface of model lipopeptide construc- ions was studied by NMR technique. In the presence f negatively charged liposomes, the shape of the CD pectrum (band at 215 nm) is suggestive of the domi- nance β-sheet conformation. The palmitoyl moiety has no chiral contribution in the spectral range investigated, ence the CD spectra reflect exclusively the change of he peptide conformation. Apparently, the palmitoyl noiety is inserted into the lipophilic interior of the lipo- omes and the peptide on the surface of the liposome adopts an ordered conformation. In the presence of the *neutral* liposomes the adoption of turn structures is most ikely while *negatively charged* liposomes induce an ex- tended conformation. Possibly, the electrostatic interac- ion between the peptide which contains basic amino acids and the acidic phospholipid promotes the exten- sion of the peptide backbone and the stabilization of β-strand or β-sheet structure. Recently Nidome *et al.* reported that peptides with short acyl chain have a fairly strong perturbation activity on DPPC membrane while the peptides with long chain acyl groups (miristoyl or palmitoyl) showed weak membrane-perturbation (peptide was stably anchored to liposomes) and antibac- terial activities [21].

The CD spectra of $HA_{317-341}$-NH_2 (epitopic peptide coupled with the fusion peptide) are illustrated in Fig.

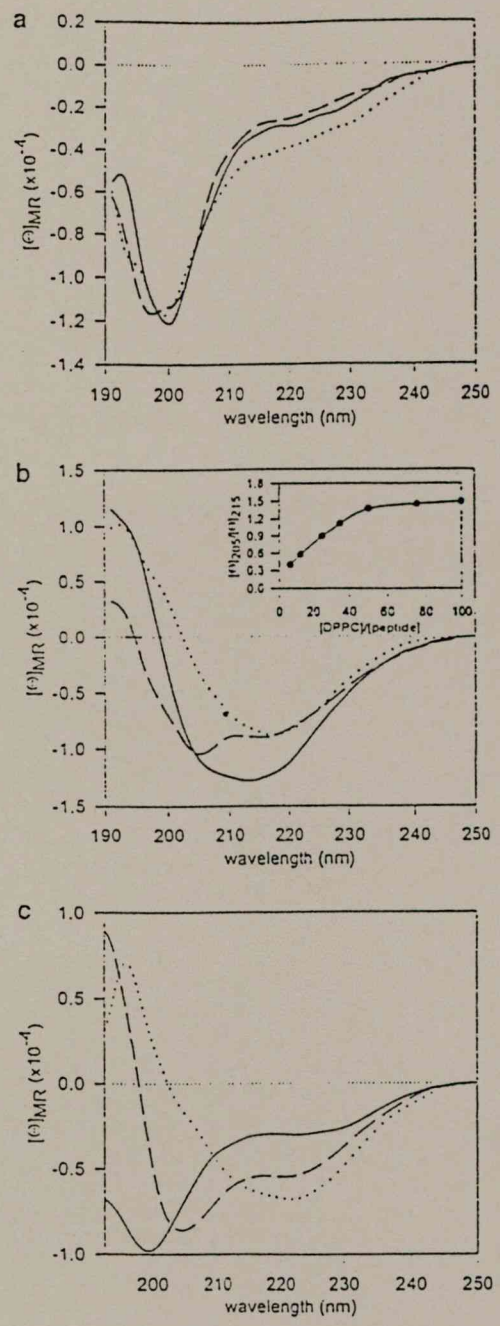

FIG. 4. CD spectra of $HA_{317-329}$ (a), $HA_{317-329}$-Thr(Pal)-NH_2 (b) a $HA_{317-341}$ (c) in 5 mM Hepes buffer, pH 7.4 (—), in the presence neutral DPPC (---) and negatively charged, DPPC:DPPA (0.9:(liposomes (· · ·). Peptides were dissolved at a concentration of μM in 5 mM Hepes buffer containing 1.5 mM liposomes. *Inset* sh the ellipticity ratios measured at 205 and 215 nm in the functio [DPPC]/[peptide] ratios.

4*c*. In buffer, the peptide is mostly unordered althou the relatively intense negative band at longer wa lengths (210-240 nm) indicates the contribution structured forms. In the presence of *neutral* liposor the peptide exhibits a distinctly helical CD spectru while with *negatively charged* liposomes the spectr

; characteristic of β-sheet conformation. It is worth oting that under the latter conditions the negative and is much broader than that of normal β-structure, iggesting that some α-helix and/or nascent helix de- ved from the fusion part is also present. Fusion pep- des were shown to bind to lipid membranes with a ansition of their secondary structure into α-helix [22].

ONCLUSION

This paper reports a definite shift towards ordered condary structures (turn and sheet) of a B and T ll epitopic peptide $HA_{317-329}$-NH_2 of influenza virus magglutinin in solution when covelently coupled to lmitic acid. The relative amount of ordered struc- res was further increased when at higher concentra- ns the *lipopeptide* formed micelles or more impor- ntly in the presence of DPPC liposomes. Contrary to is, no conformational change of the *free* peptide was tected in the presence of liposomes. This work there- e emphasizes (i) the importance of a built-in acyl oup to induce a definite structure of short antigenic ptides in solution and (ii) an increase of the popula- n of ordered conformers by stably anchoring the pep- e to the lipid membrane. This may be of significance achieving the specific conformation necessary for tibody recognition.

KNOWLEDGMENTS

his work was supported by grants OTKA T016516 (to I.L.), 7432 (to M.H.), and T022540 (to G.K. Tóth).

FERENCES

Muller, G., Shapira, M., and Arnon, R. (1982) *Proc. Natl. Acad. Sci. USA* 79, 569–573.

Nimann, H., Houghten, R., Walker, L., Reisfeld, R., Wilson, I., Hogle, J., and Lerner, R. (1983) *Proc. Natl. Acad. Sci. USA* 80, 4949–4953.

3. Hopp, T. (1984) *Mol. Immunol.* 31, 13–16.
4. Deres, K., Schild, H., Wiesmuller, K-H., Jung, G., and Rammensee, H.-G. (1989) *Nature* 342, 561–564.
5. Sauzet, J., Duprez, B., Martinon, F., Guillet, J., Grass-Masse, H., and Gomard, E. (1995) *Vaccine* 13, 1339–1345.
6. Schild, H., Deres, K., Wiesmuller, K-H., Jung, G., and Rammensee, H.-G. (1991) *Eur. J. Immunol.* 21, 2649–2654.
7. Ferru, I., Rollin, C., Estaquier, J., Sutton, P., Delacre, M., Tartar, A., Grass-Masse, H., and Auriault, C. (1996) *Peptide Res.* 9, 136–143.
8. Deprez, B., Sauzet, J. P., Boutillon, C., Martinon, F., Tartar, A., Sergheraert, C., Guillet, J. G., Gomard, E., and Grass-Masse, H. (1996) *Vaccine* 14, 375–382.
9. Nestorowicz, A., Tregear, G. W., Southwell, C. N., Martyn, J., Murray, J. M., White, D. O., and Jackson, D. C. (1985) *Mol. Immunol.* 22, 145–154.
10. Jackson, D. C., and Brown, L. E. (1991) *Peptide Res.* 4, 114–124.
11. Nagy, Z., Rajnavölgyi, É., Hollósi, M., Tóth, G. K., Váradi, G., Penke, B., Tóth, I., Horváth, A., Gergely, J., and Kurucz, I. (1994) *Scandinavian J. Immunol.* 40, 281–291.
12. Holly, S., Majer, Zs., Tóth, G. K., Váradi, Gy., Rajnavölgyi, É., Laczkó, I., and Hollósi, M. (1993) *Biochem. Biophys. Res. Commun.* 193, 1247–1254.
13. Schmidt, M. F. G. (1989) *Biochim. Biophys. Acta* 988, 411–426.
14. Merrifield, R. B. (1963) *J. Am. Chem. Soc.* 85, 2149–2154.
15. Surewicz, W. K., and Mantsch, H. H. (1988) *Biochim. Biophys. Acta* 952, 115–130.
16. Venyaminov, S. Y., and Kalnin, N. N. (1990) *Biopolymers* 30, 1243–1257.
17. Perczel, A., and Hollósi, M. (1996) Turns, *in* Circular Dichroism: Conformational Analysis of Biomolecules (Fasman, G. D., Ed.), pp. 285–380, Plenum Publ Co, New York.
18. Sreerama, N., and Woody, R. W. (1993) *Anal. Biochem.* 209, 32–44.
19. Dyson, J. H., and Wright, P. E. (1995) *The FASEB Journal* 9, 37–42.
20. Macquaire, F., Baleux, F., Giaccobi, E., Huynh-Dinh, T., Neumann, J-M., and Sanson, A. (1992) *Biochemistry* 31, 2576–2582.
21. Niidome, T., Kawakami, R., Okamoto, K., Ohmori, N., Mihara, H., and Aoyagi, H. (1997) *J. Peptide Res.* 50, 458–464.
22. Takahashi, S. (1990) *Biochemistry* 29, 6257–6264.

4.2.

Peptides 1992
C.H. Schneider and A.N. Eberle (Eds.)

Lipidic amino acid based synthetic peptide vaccine adjuvant

Istvan Toth[a], Malcolm Danton[a], Ronald E. Reid[b], Guangming Zhong[c], Robert Brunham[c], Gábor K. Tóth[d] and William A. Gibbons[a]

[a]The School of Pharmacy, University of London, 23–39 Brunswick Square, London WC1N 1AX, U.K.
[b]University of British Columbia, 2146 East Mall, Vancouver, B.C., Canada
[c]University of Manitoba, Canada
[d]Department of Medical Chemistry, A. Szent-Györgyi University, Dóm tér 8, H-6720 Szeged, Hungary

Introduction

Synthetic peptides are widely used to generate antibodies. To induce high antibody response, the peptide must be conjugated to a carrier protein (KLH, BSA) or incorporated into polylysine to form multiple antigenic peptide [1]. Further modification of this procedure was to build in a lipidic anchor [2]. We report here the synthesis and biological evaluation of a novel, lipidic amino acid based Lipid-Core-Peptide (LCP) system.

Results and Discussion

Immunogenicity of MOMP peptides. The B cell antigenicity of 7 MOMP sequences was evaluated using synthetic peptides (Pepscan) and polyclonal antisera from rabbits and mice and monoclonal antibodies from mice. The VDIV of all MOMPS contained multiple cross-reactive, immunodominant, surface exposed epitopes. VDI among C serogroup MOMPs was also immunodominant. T cell antigenicity was evaluated for serovar B MOMP in a lymphocyte proliferation assay using a cloned fragment containing 61 amino acids from B MOMP VDIV (RASFDADTIRLAQPK-SADTIPDVTTLNPTIAGAGDVKTSAEGQLGDTMQIVSLQINKMKSR^{393}). This cloned polypeptide fused with glutathione-S-transferase was able to stimulate an antigen specific T cell proliferation response. Five partially overlapping peptides (designated as P1 to P5) were synthesized with a length of 16 to 22 residues to cover this fragment. Three inbred strains of mice with different H2 haplotypes were used in an in vitro T cell proliferation assay. P1 (with sequence of ^{273}RASFDADTI-RIAQPKSAETIFG) and P5 (^{319}TMQIVSLQLNKMKSRG) were recognised by H-2^{d} strain BALB/c and P2 (^{289}AFTIFDVTTINPTIAG) by both H-2^{k} strain CBA and by H-2^{b} strain C57BL/10. In an in vivo antibody promotion assay, P5 elicited high titer IgG antibody production only in BALB/c, P2 in both CBA and C57BL/10 while P1, P3 and P4 failed to stimulate antibody production in any of the strains. Thus P2 is a potential peptide for incorporation into a candidate *chlamydia* vaccine since its T cell site has the least host genetic restriction and it can promote antibody production to surface exposed B cell epitopes within the peptide.

Table 1 *IgG titers* of mouse antisera raised with P2 preparations*

	B10 ($H\text{-}2^b$)	B10.A ($H\text{-}2^a$)	B10.BR ($H\text{-}2^k$)	B10.D2 ($H\text{-}2^d$)	B10.A(3R) ($H\text{-}2^{13}$)
Tail	1:160	1:1380	1:2860	<1:20	<1:20
I.P.	1:320	1:5160	1:2560	<1:20	<1:20

* IgG antibody titers were assayed against serovar B EBs in an ELISA assay. Pooled sera from 3–5 mice for each group were used.

Synthesis of (Peptide)$_8$Lys$_4$Lys$_2$Lys{HNCH[(CH$_2$)$_{13}$CH$_3$]CO}$_3$NH$_2$ [LCP]. The Boc-NH-CH[(CH$_2$)$_{13}$CH$_3$]COOH was synthesised from 1-bromododecane [3]. The peptides were synthesised stepwise on solid phase using Novabiochem MBHA resin on an Applied Biosystems 430A Automated Synthesizer. Standard HF cleavage was carried out to release peptides from resin. Coupling efficiency of synthesis was monitored by quantitative ninhydrin assay. All of the peptides cleaved from resin were purified by standard FPLC/HPLC techniques involving ion-exchange (e.g. DEAE) and gel filtration (Sephadex G-25 or G-50) chromatography. C4 or C18 RPHPLC was used for large scale purification. The synthesis of (Peptide)$_8$Lys$_4$ Lys$_2$Lys{HNCH[(CH$_2$)$_{13}$CH$_3$]CO}$_3$NH$_2$ was accomplished automatically by a stepwise solid phase procedure. The peptide was removed from the resin support by means of the high or low-high HF method. The crude peptide was then precipitated with ether or ethylacetate and redissolved in 90% acetic acid. The crude peptide was purified by semipreparative HPLC method.

The immunogenicity of P2 sequence was further studied using the synthetic preparation LCP2 which has been proved to enhance immunogenicity of conjugated peptides in other systems. Both preparations were used to immunize five congenic mouse strains. LCP2 elicited high titered antibodies in B10.A($H\text{-}2^a$) and B10.BR($H\text{-}2^k$) strains and low titered antibodies in B10($H\text{-}2^b$) strain. Strains B10.D2($H.2^d$) and B10.A(3R) ($H.2^{13}$) failed to produce antibodies to LCP2. The LCP2 raised antibodies from the strains $H\text{-}2^k$ and $H\text{-}2^a$ were able to recognise native epitopes on chlamydial EBs and displayed similar epitope specificities in Pepscan as antisera raised with whole EBs. These observations suggest that the LCP preparation maximally enhanced immunogenicity of the P2 peptide.

The lipidic amino acids are α-amino acids with a long linear or branched alkyl side chains and can be oligomerised or polymerised using standard solution or solid phase peptide synthetic methods. Different (LAA)$_n$-poly-Lys-(peptide)$_m$ LCP were synthesised on solid phase, with a fully automated procedure, using Boc strategy. Antigene peptides from the major outer membrane protein (MOMP) of *Chlamydia trachomatis* linked to this anchor-polylysine system (LCP2) were greatly enhanced in their immunogenicity when compared to the same peptides with conventional adjuvants.

References

1. Tam, J.P., Proc. Natl. Acad. Sci. USA, 85(1988)5409.
2. Huang, W., Nardelli, B., Shiu, D.R. and Tam, J.P., In Smith, J.A. and Rivier, J.E. (Eds.) Peptides: Chemistry and Biology (Proceedings of the 12th American Peptide Symposium), ESCOM, Leiden, 1992, pp. 847–848.
3. Gibbons et al., Liebigs Ann. Chem., (1990)1175.

4.3.

Peptides 1998
Sándor Bajusz and Ferenc Hudecz (Eds.)

Interaction of an Influenza Virus Hemagglutinin Peptide and its Lipoderivative with Liposomes

ILONA LACZKÓ[1], ELEMÉR VASS[2], MIKLÓS HOLLÓSI[2] and GÁBOR K. TÓTH[3]

[1]*Institute of Biophysics, Biological Research Center, 6701 Szeged, P.O.Box 52.*
[2]*Department of Organic Chemistry, Eötvös University, 1518 Budapest, P.O.Box 32*
[3]*Department of Medical Chemistry, Szent-Györgyi Medical University, 6720 Szeged, Dóm tér 8, Hungary*

Introduction

Specific immune responses against proteins and viruses can be achieved using synthetic antigenic peptides. However, free peptides are weakly immunogenic when used without carrier molecules [1]. The general lack of cross-reactivity between synthetic peptides and native proteins is believed to be due to the conformational dissimalirity between the peptide and the corresponding sequence within the intact molecule [2]. Several alternatives have been proposed to improve the immunogenicity of epitopic peptide sequences. Among them, the covelent attachment of fatty acid chain has been shown to enhance the immunogenicity of unmodified peptides [3,4]. Here we report circular dichroism (CD) and Fourier transform infrared (FTIR) conformational studies to reveal the conformational consequences of covalent attachment of palmitic acid to the 317-329 sequence of the influenza virus hemagglutinin (HA).

Results and Discussion

Figure 1*a* and *b* present the CD spectra of the free $HA_{317-329}$-NH_2(VTGLRNIPSIQSR) and the palmitoylated ($HA_{317-329}$-Thr(Pal)-NH_2) peptides in 5 mM Hepes buffer (pH 7.4), in the presence of neutral (dipalmitoyl-phosphatidyl choline, DPPC) and negatively charged (DPPC/dipalmitoyl-phosphatidic acid, DPPA) liposomes.

In *buffer* solution the free peptide is present in a predominantly unordered or semiextended (PPII) conformation, while the broad negative band in the CD spectrum of the lipopeptide is indicative of a mixture of β-sheet and turn conformers. The increased population of ordered conformation upon introducing palmitoyl group may account for the hydrophobic environment provided by the acyl chain. FTIR measurements also support the data of CD studies.

Secondary structures of the free and palmitoylated peptides were determined in the presence of *liposomes* at a [lipid]/[peptide] ratio of 50. As Figure 1a shows the CD spectra of the free peptide in the presence of neutral and negatively charged liposomes are not much different from that measured in Hepes buffer. On the contrary, a remarkable conformational change was induced by liposomes in the case of palmitoylated peptide. Apparently, the palmitoyl moiety of the lipopeptide is inserted into the lipophilic interior of the liposomes and the peptide adopts an ordered conformation on the surface of the

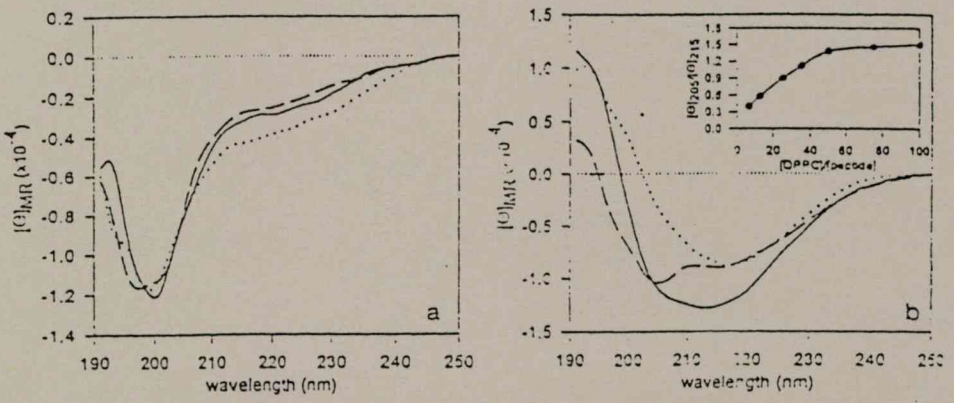

Figure 1. *CD spectra of $HA_{317-329}$-NH_2 (a) and $HA_{317-329}$-Thr(Pal)-NH_2 (b) in 5 mM Hepes buffer, pH 7.4 (———), in the presence of neutral DPPC (- - - - -) and negatively charged, DPPC:DPPA (0.9:0.1) liposomes (·····). Peptides were dissolved at a concentration of 30 µM in Hepes buffer containing 1.5 mM phospholipid*

liposomes.. The 205 nm band in the CD spectrum of the lipopeptide in the presence of neutral liposomes suggests enrichment of the population of the folded conformers, while the band at 215 nm band in the presence of negative liposomes is indicative of the dominance of β-sheet conformation (Figure 1b). In the latter case, the electrostatic interaction between the peptide containing basic amino acids and the acidic phospholipids may promote the extension of the peptide backbone and the stabilization of β-strand or β-sheet structure.

The results demonstrate a definite shift towards ordered secondary structures (turn and β-sheet) of the B and T cell epitopic peptide $HA_{317-329}$-NH_2 in solution when covalently coupled to palmitic acid. The relative amount of ordered structures was further increased in the presence of liposomes. Contrary to this no conformational change of the free peptide was detected in the presence of liposomes. Therefore, this work emphasizes (i) the *importance of a built-in acyl group to induce a definite structure of short antigenic peptide in solution and (ii) an increase of the population of ordered conformers by stably anchoring the peptide to the lipid membrane.* This may be of significance for achieving the specific conformation necessary for antibody recognition.

References

1. Muller, G., Shapira, M. and Arnon, R. *Proc. Natl. Acad. Sci.* USA, 79 (1982) 569.
2. Nestorowicz, A., White, D.O. and Jackson, D.C. *Vaccine*, 3 (1985) 175.
3. Hopp, T. *Mol. Immunol.*, 31 (1984) 4949.
4. Sauzet, J., Duprez, B., Martinon, F., Guillet, J., Grass-Masse, H. and Gomard, E. *Vaccine*, 13 (1995) 1339.

Neuropeptides (1997) 31 (4), 367–372

Synthesis and opioid binding activity of dermorphin analogues containing cyclic β-amino acids

B. Bozó, F. Fülöp*, G. K. Tóth†, G. Tóth, M. Szücs

Biological Research Center, Hungarian Academy of Sciences, Szeged,
*Department of Pharmaceutical Chemistry and
†Department of Medical Chemistry, A. Szent-Györgyi Medical University Szeged, Hungary

Summary In the present work, eight conformationally constrained analogues of the μ specific opioid peptide dermorphin were synthesized by replacing D-Ala^2 with stereoisomers of β-amino-cycloalkane or cycloalkene carboxylic acids. The resulting peptides were tested for their potency to μ and δ opioid binding sites of rat brain membranes labelled with [^{3}H]Tyr^1-D-Ala^2-MePhe^4-Gly-ol, [^{3}H]DAMGO and [^{3}H]Ile^{5,6}deltorphin, respectively. All of the new derivatives displayed highly attenuated binding to both receptor types, albeit the decrease in their potency seemed to be less in the case of δ binding. Trans position of the β-amino groups resulted in higher binding affinities than that of the corresponding cis isomers, the latter being more flexible than the former. It is concluded that conformational constraints caused either by a rigid ring structure or cis isomers instead of D-Ala^2 in dermorphin-derived peptides are unfavourable for binding activity to either opioid receptors. We propose that interaction of the larger heptapeptide derivatives of dermorphins with the μ receptor is distinct from that of the tetrapeptide morphiceptin.

INTRODUCTION

Opioid peptides are a family of structurally related neuromodulators which play a crucial role in controlling the nociceptive pathways via μ, δ and κ opioid receptors. The small peptides are usually highly flexible molecules and they may adopt different conformations required for recognition by different receptor types. Indeed, previous binding experiments performed with rat brain membranes and recent data with recombinant receptors suggest that no opioid peptide family can be exclusively associated with a specific opioid receptor type.[1]

However, mapping the specific structural requirements of individual receptor types and elucidation of their unique physiological role would require highly site-specific ligands. During recent years, enormous synthetic efforts have been made to achieve this goal. More than 1000 analogues of the enkephalins, β-casomorphins, deltorphins, dynorphins and β-endorphin have been synthesized to date[2] (and references cited therein). The pioneering work of Hruby et al and Schiller et al revealed that conformational constraints are absolute requirements for achieving μ-selective peptide binding.[3,4]

Local constraints[5–8] can be introduced in the peptide backbone by employing N$^{\alpha}$-methylated amino acids (which will restrict the Φ torsion angle, $\Phi = -120° \pm 20°$), proline ($\Phi = -70° \pm 20°$,) or cyclic β-amino acids. Formation of mono- or polycyclic structures like disulphide bridges, cyclising the side-chain to the backbone or cyclising the C-terminus to the N-terminus also reduce the conformational freedom of peptides.

In contrast to all mammalian opioid peptides, dermorphin (H-Tyr-D-Ala-Phe-Gly-Tyr-Pro-Ser-NH_2) originally isolated from amphibian skin, contains a D-amino acid in the second position of the sequence and a C-terminal carboxamide group and is therefore relatively stable against enzymatic degradation.[9] The natural heptapeptide shows remarkably high μ selectivity which is comparable to that of β-casomorphins isolated from bovine milk.[10] By substituting Pro for β-aminocyclopentane carboxylic acid (βAc^{5}c) in the N-terminal tetrapeptide of the latter, Tyr-Pro-Phe-Pro-NH_2 (morphiceptin), it was concluded by

Received 28 February 1997
Accepted 1 June 1997

Correspondence to: Dr M. Szücs, Institute of Biochemistry, Biological Research Center, Hungarian Academy of Sciences, H-6701 Szeged, PO Box 521, Hungary. Fax: +36 62 433 506. Email: szücsm@everx.szbk.u-szeged.hu

Mierke et al that Pro² is crucial as part of a constrained topology to maintain the proper orientation of the side chains of Tyr and Phe, but the cis/trans isomerization between Tyr-Pro is not important for biological activity.[11]

In the present study, eight conformationally constrained analogues of dermorphins were synthesized by replacing D-Ala² with β-amino-cyclic carboxylic acids. The resulting peptides were tested for their binding activity to μ and δ opioid receptors in rat brain membranes. It was concluded that the presence of a rigid cyclic ring instead of D-Ala² in dermorphin-derived peptides is conformationally unfavourable for binding activity to either opioid receptor.

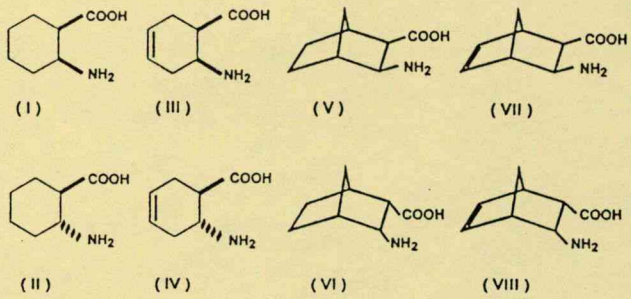

Fig. 1 Structure of cis (upper row) and trans (lower row) β-amino-cyclic-carboxylic acids introduced into the second position of dermorphin.

MATERIALS AND METHODS

Chemicals

Dichloromethane (DCM), dimethylformamide (DMF), diisopropyl-ethylamine (DIEA), methanol (MeOH), trifluoroacetic acid (TFA) and HPLC grade acetonitrile (AcN) were purchased from E. Merck (Darmstadt, Germany) and were used without further purification. Fluka (Buchs, Switzerland) supplied puriss grade dicyclohexylcarbodiimide (DCC). Protected amino acid derivatives and DAMGO (Tyr¹-D-Ala²-MePhe⁴-Gly-ol) were from Bachem Inc. (Torrance, CA, USA). 1-Hydroxy-benzotriazole (HOBt), p-cresol, dimethylsulphide were purchased from Aldrich (Steinheim, Germany). Hydrogen fluoride (HF) was obtained from UCAR (Olen, Belgium).

[³H]naloxone (71.3 Ci/mmol) and [³H]DAMGO (55 Ci/mmol) were obtained from New England Nuclear (Boston, MA, USA). [³H]Ile⁵,⁶-deltorphin (49.5 Ci/mmol) was synthesized by us.[12] Naloxone hydrochloride was kindly donated by S. Hosztafi (Alkaloida Ltd, Tiszavasvári, Hungary). Other chemicals were from Sigma (St Louis, MO, USA).

SYNTHESIS OF THE BUILDING BLOCKS

The alicyclic β-amino acids, namely cis- and trans-2-aminocyclohexane-1-carboxylic acid, cis- and trans-2-amino-4-cyclohexene-1-carboxylic acid, diexo- and diendo-3-aminobicyclo[2.2.1]heptane-2-carboxylic acid and diexo- and diendo-3-aminobicyclo[2.2.1]hept-5-ene-2-carboxylic acid were prepared as described in earlier reports.[13–16] Two methods were used. Compounds I, IV, VII and VIII were prepared from the corresponding dicarboxylic anhydride by ammonolysis and Hofman degradation followed by ion exchange purification. In the case of III, IV and VIII the Hofman degradation was performed using sodium hypochlorite.[14,15] Amino acids V and VI were prepared by cycloaddition of norbornane or norbornadiene and chlorosulphonyl isocyanate, resulting in azetidinones which were transformed to amino acids by aqueous hydrogen chloride treatment.[13,16] The structure of these amino acid derivatives, which were built into the second position of dermorphin (DMF) to gain the new peptides, is shown in Figure 1.

PEPTIDE SYNTHESIS

The peptides were synthesized by solid phase techniques utilizing ᵗBoc chemistry.[17] Side-chain protecting groups were as follows: Tyr(BrZ) and Ser(Bzl). The peptide chains were elongated on MBHA (p-methylbenz-hydrylamine) resin (0.6–0.8 mmol/g) and the syntheses were carried out manually. Couplings were performed with DCC. Incorporation of the amino acids was monitored by the ninhydrin test.[18] In case of incomplete couplings this step was repeated, but the DCM was substituted by DMF. The completed peptide resins were treated with liquid HF/dimethyl sulphide/p-cresol/p-thiocresol (86 : 6 : 4 : 2, vol/vol) at 0°C for 1 h. HF was removed and the resultant free peptides were solubilized in 10% aqueous acetic acid, filtered and lyophilized.

PEPTIDE PURIFICATION

The crude peptides were purified by reverse-phase HPLC with a Lichrosorb RP-18 10 μ column (16 × 250 mm). The HPLC apparatus was made by Knauer (Berlin, Germany). The solvent system following was used: 0.1% TFA in water, 0.1% TFA, 80% AcN in water, gradient: 0% → 50% B in 1.5 h, flow 3 ml/min. The appropriate fractions were pooled and lyophilized. The purity was checked by RP-HPLC (Nucleosil 5 C 18 column, the upper solvent system, gradient: 25% → 45% B in 20 min, flow 1 ml/min detection at 220 nm and proved to be substantially pure (≥ 97%).

Table 1 Structural and analytical characterization of the peptides synthesized in this work based on the structure Tyr[1]-X[2]-Phe[3]-Gly[4]-Tyr[5]-Pro[6]-Ser[7]-NH_2*

Amino acid in position 2	Peptide	Calculated M	Found M	R_t
cis-2-amino-cyclohexane carboxylic acid (I)	DMF 58	857.1	857.8	9.51
trans-2-amino-cyclohexane carboxylic acid (II)	DMF 61	857.1	857.8; 856.4†	11.31
cis-2-amino-cyclohexene carboxylic acid (III)	DMF 59	855.1	855.9	11.17
trans-2-amino-cyclohexene carboxylic acid (IV)	DMF 60	855.1	855.8	10.95
cis-2-amino-norbornane carboxylic acid (V)	DMF 68	869.1	869.8	11.19
trans-2-amino-norbornane carboxylic acid (VI)	DMF 70	869.1	869.8	9.63
cis-2-amino-norbornane carboxylic acid (VII)	DMF 63	867.1	867.8	9.38
trans-2-amino-norbornane carboxylic acid (VIII)	DMF 62	867.1	867.9	9.68

*Dermorphin if X: D-Ala.
†Fab MS measurement, the others are from quadrupole electrospray spectra.

MASS SPECTROMETRY

The FAB-MS experiments were performed with a VG ZAB-2SEQ type hybrid tandem mass spectrometer, equipped with an LSIMS source (Cs^+ ion gun used at 30 keV). The electrospray MS experiments were made on a FINNIGAN TSQ 7000 tandem quadrupole spectrometer equipped with an electrospray ion source. The results of the MS measurements in all cases were in good agreement with the calculated values as shown in Table 1.

MEMBRANE PREPARATION

A crude membrane fraction of Wistar rat brains was prepared as previously described.[19] Briefly, the animals were decapitated, their brains without cerebella rapidly removed and homogenized in 30 volumes of ice-cold 50 mM Tris-HCl (pH 7.4) buffer by a teflon-glass homogenizer. After centrifugation at 20 000 × *g* for 25 min the resulting pellets were resuspended in 30 volumes of buffer and incubated for 30 min at 37°C to remove endogenous opioids. Centrifugation was then repeated as described above. The final pellet was suspended in 5 volumes of 50 mM Tris-HCl (pH 7.4) buffer containing 0.32 M sucrose and stored at – 70°C. Membranes were thawed before use, diluted with buffer and centrifuged at 20 000 × *g* to remove sucrose. The resulting pellets were suspended in 60 volumes of buffer to give a protein concentration of about 0.3–0.5 mg/ml and immediately used in binding experiments. Protein contents of membrane preparations were determined by the method of Bradford using bovine serum albumin as standard.[20]

BINDING ASSAY

800 µl membrane suspension (≈0.2–0.4 mg protein) was incubated with the appropriate [^{3}H]-labelled compounds in 1 nM concentration ([^{3}H]naloxone for 60 min at 0°C, [^{3}H]DAMGO for 60 min at 25°C, [^{3}H]Ile^{5,6}deltorphin II for 45 min at 35°C) in the absence (total binding) or presence of 10^{-10}–10^{-4} M of the peptides to be investigated in a final volume of 1 ml in plastic vials. The non-specific binding was determined with 10^{-5} M naloxone and subtracted from the total value to yield specific binding. The reactions were stopped by filtration through Whatman GF/B ([^{3}H]naloxone) or GF/C filters ([^{3}H]DAMGO and [^{3}H]Ile^{5,6}deltorphin II) utilizing a Brandel M24-R Cell Harvester (Gaithersburg, MD, USA). Filters were washed twice with 10 ml ice-cold 50 mM Tris-HCl (pH 7.4) buffer and dried. Radioactivity was determined in a toluene-based scintillation cocktail in a Beckman LS 5000TD counter. All experiments were carried out as duplicate assays and repeated at least three times. The inhibitory constant, K_i of the peptides was calculated from heterologous displacement curves with the LIGAND computer program.[21]

RESULTS AND DISCUSSION

Figure 1 shows the structures of alicyclic-β-amino-carboxylic acids (β-Acc) which were used to replace D-Ala[2] in dermorphin. While the cis-β-Acc residues (I, III) introduced significant constraints into the peptide, the trans residues of the same substituents (II, IV) were more conformationally flexible.

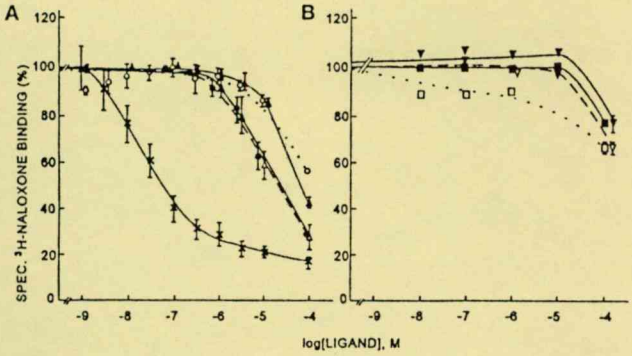

Fig. 2 Competition of dermorphin analogues for rat brain opioid receptors. Crude membrane fraction was incubated with [³H]naloxone (1 nM), and the following unlabelled ligands DMF (×), DMF-58 (○), DMF-59 (▲), DMF-60 (△), DMF-61 (●), DMF-62 (□), DMF-63 (■), DMF-68 (▽), DMF-70 (▼) in 50 mM Tris-HCl (pH 7.4). (A) Symbols represent the mean ± SEM, $n \geq 2$; (B) symbols represent data from a single experiment.

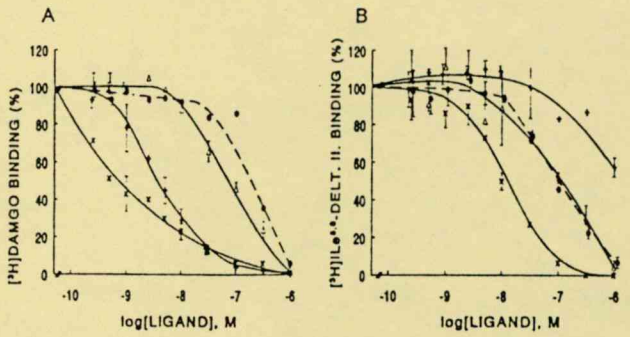

Fig. 3 Displacement of (A) [³H]DAMGO or (B) [³H]Ile^{5,6} deltorphin II binding by various concentrations of DAMGO (+), DMF-60 (△), DMF-61 (●), or DMF (×). Crude membrane fraction of rat brains was incubated with [³H]DAMGO (1 nM), or [³H]Ile-^{5,6}-deltorphin (1 nM), unlabelled ligands and 50 mM Tris-HCl (pH 7.4). For other details see *Materials and methods*. Results are expressed as percentage of control binding, i.e. binding in the absence of displacers. Mean ± SEM, $n = 3$. When the error bars are smaller than the symbols, only the latter are depicted.

The potency of the new ligands in competing for opioid receptors of rat brain membranes was first tested with the general opioid antagonist ligand, [³H]naloxone (Fig. 2). The parent peptide, dermorphin displayed the highest potency to opioid receptors, having an IC_{50} of about 50 nM in this assay. Substitution of its D-Ala^2 by the rigid β-Acc derivatives attenuated opioid binding; all of the new analogues possessed much lower affinity. DMF-*68*,-*70*,-*63*,-*62* – with ligands that contain a bicyclic complex ring structure (cis- or trans-norbornane and norbornene, respectively) – were able to displace [³H]naloxone binding only at very high (100 μM) concentrations (Fig. 2B).

The two relatively most potent new derivatives, DMF-60 and DMF-61 ([trans-β-amino-cyclohexane carboxylic acid]^2 and [trans-β-amino-cyclohexene carboxylic acid]^2-dermorphin) were further tested for their selectivity to μ versus δ opioid binding (Fig. 3, Table 2). The substituted ligands had weak binding (K_i in the micromolar range) to both opioid receptor types, although it seems that the loss of potency to [³H]Ile^{5,6}-deltorphin sites was less than to [³H]DAMGO binding sites, thus conferring some 'δ-preference' to these peptides (Table 2). The K_i values of DAMGO and dermorphin measured in these experiments are in good agreement with reported data[2] (and references cited therein).

The naturally occurring dermorphins contain an N-terminal tripeptide sequence Tyr-D-Xaa-Phe which is also present in deltorphins (delta-specific opioids). A study by Charpentier et al suggests that this common sequence motif is recognized by both μ and δ opioid receptors which is topologically distinct from the region (C-terminal 'address' domain of the ligands) which ensures site-specific interactions with the receptors.[22] Tyr^1, Pro^2 and Phe^3 are the important residues for the biological activity of one of the most selective agonists for the μ-receptor, morphiceptin.[8,11,23] By contrast, the endogenous mammalian opioid peptides (enkephalins, endorphins, dynorphins) are characterized by an identical N-terminal 'message' tetrapeptide sequence Tyr-Gly-Gly-Phe.[1,24] Keeping in mind that besides these structurally diverse μ-receptor preferring peptide ligands the prototypic μ ligands are the morphine-like opiate alkaloids, one might assume that there are multiple factors determining the binding selectivity of μ-specific ligands.

Much has been learned about the structural features of opioid receptors since the first successful cloning by Kieffer et al and Evans et al.[25,26] The amino acid sequences of μ- and δ-receptors are approximately 60–70% similar with the primary variations occurring in the extracellular N-terminus and the intracellular C-terminus domains and the external loops.[27–29] The second and third transmembrane domains of opioid receptors contain conserved aspartate residues[29] that are believed to form an ion pair with the positively charged nitrogen atom, which is a strict structural requirement common to all opioid ligands.[30] In analogy with other G-protein coupled receptors, it was suggested that an opioid 'binding pocket' is formed by the seven putative α helices, while their extracellular loops would discriminate various classes of opioid ligands and define their μ, δ and κ selectivity. However, recent studies utilizing chimeric receptors and mutation studies combined with 3-D computer modelling have revealed the existence of multiple interactions throughout the receptor molecule which display a unique binding pattern for each ligand, at least in the case of δ receptor interaction.[25,31,32] Moreover, the μ and δ

Table 2 Binding affinities of opioid peptides to μ and δ opioid receptors in rat brain membranes

	[^{3}H]DAMGO (μ) K_i (nM)	[^{3}H]Ile^{5,6} deltorphin II (δ) K_i (nM)	K_i (δ)/K_i (μ)
DAMGO	3.3 ± 0.5	634 ± 150*	192
Dermorphin	1.7 ± 0.5	158 ± 21	90
DMF-60	2200 ± 460*	1620 ± 290	0.73
DMF-61	3390 ± 1820	1170 ± 270	0.34

Results (mean ± SEM) of three independent measurements except* where n = 2.

pharmacophore conformations adopted by one and the same compound, namely cyclic β-casomorphins, were also suggested to be distinct in a recent study by Brandt et al utilizing molecular modelling.[33]

An interesting outcome of the present work is that introduction of rigid cyclic β-amino-carboxylic acids in the second positions of the peptide backbone leads to different effects for dermorphins (Figs 1&2, Table 2) than for casomorphins.[11] Here the rigid cyclohexane, norbornane and their unsaturated analogues highly decrease the binding potency of the resulting compounds to μ and δ opioid receptors. In contrast, Pro^2 or other residues causing constrained topology are crucial for proper orientation of Tyr and Phe, thus for the biological activity of morphiceptin.[11] We and others previously reported that introduction of D-Ala in position 2 of morphiceptin leads to an enhancement of the binding affinity to δ-sites, thus resulting in a reduced μ-selectivity.[10,23] Therefore we speculate that interaction of the larger heptapeptide derivatives of dermorphins with the μ-receptor is distinct from that of the tetrapeptide morphiceptin. Indeed, the K_i value for the former was found to be 0.33 nM, while 56 nM was reported for morphiceptin against the cloned μ-opioid receptor by Raynor et al.[34] It cannot be excluded that these ligands would bind to different subtypes of μ-receptor, i.e. to the yet hypothetical μ_1 and μ_2 receptors[35] which might be distinct proteins, or different binding regions of the same protein. The latter was recently demonstrated to be the case with cloned kappa receptors.[36] Although such distinction still awaits in case of the μ-receptor, the results of the present study describing the synthesis and binding characteristics of constrained dermorphin derivatives contribute to the understanding of the structural and topographical requirements of peptide ligand binding.

ACKNOWLEDGEMENTS

B.B. is a PhD student of the Neuroendocrin Program of A. Szent-Györgyi Medical University, Szeged. We are grateful to Mr Zoltán Kele, Pál Szabó (Department of Medical Chemistry, A. Szent-Györgyi Medical University Szeged) and Dr Marianna Mák (Chemical Research Institute, Budapest) for the FAB-MS measurements. The technical assistance of Ildikó Németh is gratefully acknowledged. This work was supported by OTKA T-016084 and ETT 523.

REFERENCES

1. Mansour A, Hoversten M T, Taylor L P, Watson S J, Akil H. The cloned μ, δ and κ receptors and their endogenous ligands: evidence for two opioid peptide recognition cores. Brain Res 1995; 700: 89–98.
2. Schiller P W. Development of receptor-specific opioid peptide analogues. In: Ellis G P, West G B ed. Progress in Medicinal Chemistry. Amsterdam: Elsevier Science Publishers, B.V. 1991; 2: 301–340.
3. Hruby V J, Hadley M E. Binding and information transfer in conformationally restricted peptides. In: Design and Synthesis of Organic Molecules Based on Molecular Recognition. Heidelberg: Springer Verlag, 1986: 269–299.
4. Schiller P W, Weltrowska G, Nguyen T M-D et al. Conformational Restriction of the phenylalanine residue in a cyclic opioid peptide analogue: effects on receptor selectivity and stereospecificity. J Med Chem 1991; 34: 3125–3132.
5. Goodman M, Ro S. Peptidomimetics for drug design. In: Wolff ME, ed. Burger's Medicinal Chemistry and Drug Discovery, Vol 1. John Wiley & Sons 1995: 803–861.
6. Yamazaki T, Zhu Y-F, Probstl A, Chadha R K, Goodman M. Probing a molecular model of taste utilizing peptidomimetic stereoisomers of 2-aminocyclopentanecarboxylic acid methyl ester. J Org Chem 1991; 56: 6644–6655.
7. Deeks T, Crooks P A, Waigh R D. Synthesis and analgesic properties of two leucine-enkephalin analogues containing a conformationally restrained N-terminal tyrosine residue. J Med Chem 1983; 26: 762–765.
8. Yamazaki T, Pröbstl A, Schiller P W, Goodman M. Biological and conformational studies of [Val^4] morphiceptin and [D-Val^4] morphiceptin analogs incorporating *cis*-2 aminocyclopentane carboxylic acid as a peptidomimetic for proline. Int J Pept Protein Res 1991; 37: 364–381.
9. Erspamer V, Melchiorri P. Active polypeptides: from amphibian skin to gastrointestinal tract and brain of mammals. Trends Pharmacol Sci 1980; 1: 391–395.
10. Brantl V, Teschemacher H, Blasig J, Henschen A, Lottspeich F. Opioid activities of β-casomorphins. Life Sci 1981; 28: 1903–1909.
11. Mierke D F, Nöbner G, Schiller P W, Goodman M. Morphiceptin analogs containing 2-aminocyclopentane carboxylic acid as a peptidomimetic for proline. Int J Pept Protein Res 1990; 35: 35–45.

12. Nevin S T, Kabasakal L, Ötvös F, Borsodi A. Binding characteristics of the novel highly selective delta agonist, [^{3}H]Ile^{5,6}Deltorphin II. Neuropeptides 1994; 26: 261–265.
13. Moriconi E J, Crawford W C. The reaction of chlorosulfonyl isocyanate with bridged bi- and tricyclic olefins. J Org Chem 1968; 33: 370–378.
14. Stájer G, Szabó A E, Fülöp F, Bernáth G, Sohár P. Preparation and steric structures of dihydro-1,3-oxanines, 1,3-oxanin-2-ones and -2-thiones fused with norbornane and norbornene. J Heterocyclic Chem 1983; 20: 1181–1185.
15. Bernáth G, Stájer G, Szabó A E, Fülöp F, Sohár P. Preparation and conformational study of partially saturated 3,1-benzoxanines, 3,1-benzoxazin-2-ones and 3,1-benzoxozine-2-thiones. Tetrahedron 1985; 41: 1353–1365.
16. Stájer G, Mód L, Szabó A E, Fülöp F, Bernáth G, Sohár P. Synthesis and kinetic study on the retrodiene decomposition of norbornene-condensed 1,3-oxazin-4-ones. Tetrahedron 1984; 40: 2385–2393.
17. Merrifield R B. The synthesis of a tetrapeptide. Solid phase peptide synthesis. J Am Chem Soc 1963; 85: 2149–2154.
18. Kaiser E, Choleschott R L, Bosshinger C D, Cook P J. Colour test for the detection of free amino groups in the solid phase synthesis of peptides. Anal Chem 1970; 34: 595–598.
19. Szücs M, Coscia C J. Evidence for δ-opioid binding and GTP-regulatory proteins in 5-day-old rat brain membranes. J Neurochem 1990; 54: 1419–1425.
20. Bradford M M. A rapid and sensitive method for the quantitation of microgram quantities of protein utilizing the principle of dye-binding. Anal Biochem 1986; 72: 248–254.
21. Munson P J, Rodbard D. LIGAND: a versatile computerised approach for the characterization of ligand binding studies. Anal Biochem 1980; 107: 220–227.
22. Charpentier S, Sagan S, Delfour A, Nicolas P. Dermenkephalin and deltorphin I reveal similarities within the ligand-binding domains of μ- and δ-opioid receptors and an additional address subsite on the δ-receptor. Biochem Biophys Res Commun 1991; 179: 1161–1168.
23. Liebmann C, Szücs M, Neubert K, Hartrodt B, Arold H, Brath A. Opiate receptor binding affinities of some D-amino acid substituted β-casomorphin analogs. Peptides 1985; 7: 195–199.
24. Portoghese P S. Bivalent ligands and the message-address concept in the design of selective opioid receptor antagonists. Trends Pharmacol Sci 1989; 10: 230–235.
25. Kieffer B L, Befort K, Gaveriaux-Ruff C, Hirth C G. The delta opioid receptor: isolation of a cDNA expression cloning and pharmacological characterization. Proc Natl Acad Sci USA 1992; 89: 12048–12052.
26. Evans C J, Keith D E Jr, Morrison H, Magendzo K, Edwards R H. Cloning of a delta opioid receptor by functional expression. Science 1992; 258: 1952–1955.
27. Thompson R C, Mansour A, Akil H, Watson S J. Cloning and pharmacological characterization of a rat μ opioid receptor. Neuron 1993; 11: 903–913.
28. Reisine T, Bell G. Molecular biology of opioid receptors. Trends Neurosci 1993; 16: 506–510.
29. Surratt C K, Johnson P S, Moriwaki A et al. μ opiate receptor. Charged transmembrane domain amino acids are critical for agonist recognition and intrinsic activity. J Biol Chem 1994; 269: 20548–20553.
30. Morley J S. Structure-activity relationship of enkephalin-like peptides. Annu Rev Pharmacol Toxicol 1980; 20: 81–110.
31. Befort K, Tabbara L, Kling D, Maigret B, Kieffer B. Role of aromatic transmembrane residues of the δ-opioid receptor in ligand recognition. J Biol Chem 1986; 271: 10161–10168.
32. Watson B, Meng F, Thompson R C, Akil H. Structural studies of the mu opioid receptor using chimeric constructs. Analgesia 1995; 1/4–6: 825–828.
33. Brandt W, Stoldt M and Schinke H. A model of the δ opioid receptor pharmacophore conformations of cyclic β-casomorphin analogues. Analgesia 1995; 1/ 4–6: 327–330.
34. Raynor K, Kong H, Chen Y et al. Pharmacological characterization of the cloned κ, δ and μ-opioid receptors. Mol Pharmacol 1993; 45: 330–334.
35. Pasternak G W. Multiple μ opiate receptors: biochemical and pharmacological evidence for multiplicity. Biochem Pharmacol 1986; 35: 361–364.
36. Mansour A, Hoversten M T, Mansson E, Bare L, Watson S J, Akil H. Apparent evidence of receptor subtypes: receptor binding studies with the cloned rat and human kappa receptors. Analgesia 1995; 1/4–6: 553–556.

Pergamon

5.2.

Bioorganic & Medicinal Chemistry Letters 9 (1999) 667–672

BIOORGANIC & MEDICINAL CHEMISTRY LETTERS

SYNTHESIS OF OXYTOCIN ANTAGONISTS CONTAINING CONFORMATIONALLY CONSTRAINED AMINO ACIDS IN POSITION 2

Gábor K. Tóth[a,*], Krisztina Bakos[a], Botond Penke[a], Imre Pávó[c], Csaba Varga[d], Gabriella Török[c], Antal Péter[e] and Ferenc Fülöp[b,*]

[a]*Department of Medical Chemistry,* [b]*Department of Pharmaceutical Chemistry,* [c]*Department of Endocrinology, Albert Szent-Györgyi Medical University, Szeged;* [d]*Department of Comparative Physiology,* [e]*Department of Analytical Chemistry, Attila József University, Szeged, Hungary*

Received 17 November 1998; accepted 19 January 1999

Abstract: Analogues of oxytocin containing *D*-Trp, 2-amino-1,2,3,4-tetrahydronaphthalene-1-carboxylic acid (Atc) or 1,2,3,4-tetrahydro-β-carboline-1-carboxylic acid (Car) with *R* or *S* configurations in position 2 were synthetized, and their receptor bindings were tested on isolated guinea-pig uterus, rat liver and rat kidney inner medulla plasma membranes. The peptides were synthetized in the solid phase by using racemates of Car and Atc. The resulting diastereomeric mixtures were separated by means of RP-HPLC. The binding to the oxytocin receptor was somewhat decreased for the Atc isomers and dramatically decreased for both *R*- and *S*-Car, while the *D*-Trp-containing analogue displayed a relatively high receptor affinity. However, the V_1 receptor affinities were almost the same as those of the parent peptide for the Car-containing analogues and dramatically decreased for the *S*-Atc substituted analogue, which has a relatively high OT/V_1 receptor selectivity of 44.5.

Introduction

There has recently been an increasing tendency towards the rational design of highly active and selective analogues of different peptides. The small peptides are usually highly flexible molecules, and the structures observed in solution depend greatly on the environment. Local constraints are introduced, therefore, in order to restrict the conformational freedom of the parent peptide and to stabilize the desired bioactive conformation.

There are different possibilities for the insertion of definite constraints into a peptide backbone: by introduction of a constrained amino acid, such as an N^{α}-methylated amino acid, which will restrict the torsion angle Φ (Φ=-120° ± 20°), or proline (Φ=-70° ± 20°); the introduction of cyclic amino acids, or side-chain cyclized amino acids, such as like Tic, etc.; the formation of mono- or polycyclic structures involving disulphide bridges; cyclization of the side-chain to the backbone, or cyclization of the C-terminal to the N-terminal.[1,2] The recent increasing interest in posttranslationally modified peptides is due in part to the search for conformationally constrained amino acids. Modulation of the flexibility of a peptide backbone from an extended conformation to a β-turn structure is an important breakthrough in the rational design of highly selective and active peptide or peptidomimetic drugs.

Oxytocin is one of the most well known peptide hormones. In the past few decades, hundreds of oxytocin analogues have been synthetized in an attempt to obtain selective and active analogues, and more information about the structure-activity relationships. One of the main modes of action of oxytocin is its uterus-

* Fax: 36 62 420604; Email: fulop@pharma.szote.u-szeged.hu

0960-894X/99/$ - see front matter
PII: S0960-894X(99)00041-4

contracting action, and therefore its participation in birth.[3] Preterm birth continues to account for the vast majority of cases of neonatal morbidity and mortality. Currently available tocolytic agents suffer from low uterospecificity and prolong pregnancy only marginally, although postponement of birth by merely a few days may naturally be valuable. Effective, early treatment of vaginosis offers particular promise for the prevention of preterm labour. Oxytocin antagonists afford greater specificity than currently used tocolytics and can be expected to exhibit improved efficacy and risk profiles. Such compounds will allow a more effective treatment of preterm labour, with a lower risk of side-effects.[4]

Although the first oxytocin analogues with antagonistic potencies were described by Law and du Vigneaud in 1960,[5] none of the now numerous synthetized analogues have as yet been applied in human medical practice, probably because of their low receptor specificity or low receptor affinity. An attempt was made to introduce 1-deamino-*D*-Tyr(OEt)^2-Thr^4-Orn^8-oxytocin (atosiban) into medical practice as an oxytocin antagonist in the last decade.[3,6] After the successful use of atosiban in clinical studies to treat women in preterm labour, many other analogues were synthetized. Some of them were more potent than the parent peptide. In addition, the conformational background of the inhibitory properties was studied.[7] The results of Hruby *et al.*[8] and Manning *et al.*[9,10] pointed to the importance of the amino acid in position 2 for antagonistic properties, together with the presence of a basic amino acid in position 8.

On the basis of this and our previous work,[11,12] we set out to design and synthetize more selective and more potent antagonistic analogues of oxytocin.

Materials and Methods

Synthesis of conformationally constrained Phe and Trp analogues. The racemic 2-amino-1,2,3,4-tetrahydronaphthalene-1-carboxylic acid (Atc) was prepared from 2-spirohydantointetraline as described earlier.[13,14] The racemic 1,2,3,4-tetrahydro-ß-carboline-1-carboxylic acid (Car) was synthetized from tryptamine with glyoxylic acid according to the literature description.[15] The amino-protecting group (Boc) was incorporated by means of di-tert-butyl dicarbonate in the described manner. The structures of the resulting Boc amino acids were proved by mass spectrometry.

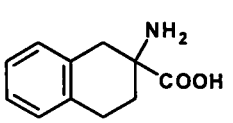

Atc

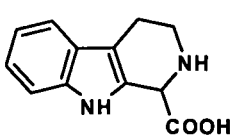

Car

Fig. 1. The structures of the conformationally constrained amino acids used

Peptide synthesis. The peptides were synthetized by a solid-phase technique, utilizing Boc chemistry.[16] Side-chain-protecting groups were as follows: Arg(Tos), Cys(Meb) and Mpa(Meb). The peptide chains were elongated on *p*-methylbenzhydrylamine (MBHA) resin (0.6-0.8 mmol/g) and the syntheses were carried out on an ABI 430 A automatic peptide synthetizer. Couplings were performed with DCC, with the exceptions of Asn, Gln and Arg, which were incorporated as their 1-hydroxybenzotriazole esters. Amino acid incorporation was monitored via the ninhydrin test.[17] The completed peptide resins were treated with liquid HF/dimethyl

sulphide/*p*-cresol/anisole/*p*-thiocresol (93:4:1:1:1, vol/vol) at 0 °C for 1 h. HF was removed and the resulting free peptides were solubilized in 10% aqueous acetic acid (1 mg/10 ml) and folded by stirring with 0.01 M potassium hexacyanoferrate(III). The completion of disulphide formation was monitored by HPLC. After complete folding, the reaction mixture was filtered, the anions were removed by ion-exchange and the remaining solution was lyophilized.

Peptide purification. The crude peptides were purified by reverse-phase HPLC on a Lichrosorb RP-18 10 μ column (16 x 250 mm). The HPLC apparatus was made by Knauer (Berlin, Germany). The solvent system used was as follows: 0.1% TFA in water, 0.1% TFA, 80% CH_3CN in water, gradient: 20% → 45% B in 1 h, flow 4 ml/min. The appropriate fractions were pooled and lyophilized. The purity was checked by RP-HPLC (Lichrosorb 7 C 18 column; the upper solvent system, gradient: 30% → 45% B in 15 min (**a**), or 35% → 50% B in 15 min (**b**), flow 1.4 ml/min, detection at 220 nm). The products proved to be substantially pure (ł 97%), with the exception of peptide **4**, which was rather impure (~90%).

Determination of the absolute configuration. The absolute configuration of Atc in the peptide was determined after acidic hydrolysis (6 M HCl, 110 °C, 24 h) of the peptide, applying precolumn derivatization with fluorenyl ethylchloroformate (FLEC).[18] The FLEC derivatives of amino acids were separated on a Eurosphere 100-C_4 column (Knauer, Berlin), using a NaOAc - CH_3CN mobile phase system and fluorescence detection. The chromatograms of standard racemic Atc and the hydrolysed sample are shown in Fig. 2. For the Car derivatives, due to the extreme acid lability of the β-carboline ring, the determination of the absolute configuration failed.

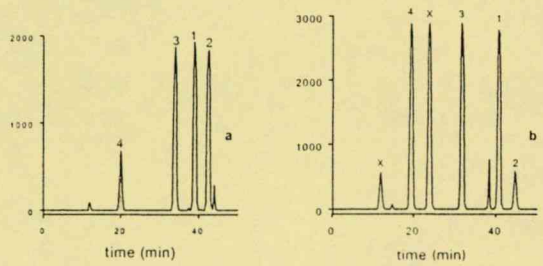

Figure 2. Determination of the absolute configurations of Atc. Column: Eurosphere 100-C_4; flow rate: 0.8 ml/min; detection: fluorescence, Ex. 260 nm, Em. 315 nm; temperature: 40 °C; mobile phase: A: 0.01 M NaOAc (pH 4.2) : CH_3CN = 80 : 20, B: 0.01 M NaOAc (pH 4.2) : CH_3CN = 20 : 80; gradient 0 →10% **B** in 1 min, 10 → 25% **B** in 30 min, 25 → 100% **B** in 40 min; chromatogram **a**: standard (*S*)-Atc and (*R*)-Atc, chromatogram **b**: hydrolysed peptide peaks: 1. (*R*)-Atc 2. (S)-Atc 3. hydrolysed reagent 4. Gly as standard, x product of hydrolysis of peptides. Carboline analysis: Column: Chiradex 250 x 4 mm I.D., 5 μm particle size (Merck, Darmstadt, Germany); flow rate: 0.5 ml/min; eluent: 0.01 M KH_2PO_4 (pH = 3) : CH_3CN = 95 : 5; detection: 220 nm. Column temperature: ambient. Retention factors: → isomer 1: 3.77; isomer 2: 3.99 (resolution: R_s = 0.67)

Mass spectrometry. The MS experiments were performed with a Finnigan Mat TSQ 7000 tandem mass spectrometer equipped with an ESI source. The results of the MS measurements in all cases agreed well with the calculated values, as shown in Table 1.

Table 1. Sequences, abbreviations, retention times (R_t) and mass spectrometric characterization of the synthetized peptides

No.	Peptide (abbreviation)	Gradient	R_t	Mw calcd	Mw found
1	Mpa-*S*-Atc-Ile-Gln-Asn-Cys-Sar-Arg-Gly-NH_2 (Mpa^1,*S*-Atc^2,Sar^{7}AVT)	a	8'28"	1019.86	1019.2
2	Mpa-*R*-Atc-Ile-Gln-Asn-Cys-Sar-Arg-Gly-NH_2 (Mpa^1,*R*-Atc^2,Sar^{7}AVT)	a	9'27"	1019.86	1019.3
3	Mpa-I-Car-Ile-Gln-Asn-Cys-Sar-Arg-Gly-NH_2 (Mpa^1,I-Car^2,Sar^{7}AVT)*	b	7'17"	1044.86	1044.7
4	Mpa-II-Car-Ile-Gln-Asn-Cys-Sar-Arg-Gly-NH_2 (Mpa^1,II-Car^2,Sar^{7}AVT)*	b	8'01"	1044.86	1044.3
5	Mpa-*D*-Trp-Ile-Gln-Asn-Cys-Sar-Arg-Gly-NH_2 (Mpa^1,*D*-Trp^2,Sar^{7}AVT)	a	6'33"	1032.24	1032.8

*I and II Car corresponds to the two stereoisomers but the determination of the absolute configuration has not been done

Receptor assay. Plasma membranes from 60-65 day pregnant guinea-pig uterus containing 1-1.5 pmol of oxytocin receptor/mg of protein were prepared by a modification of the method of Fuchs *et. al.*[19] Uterine tissue was cut into small pieces and suspended in 10 volumes of buffer containing 10 mM Hepes, 1 mM EDTA and 0.5 mM dithiotreitol. After homogenization with a blazer homogenizer and a glass potter, the suspension was filtered and centrifuged at 1000 x g for 30 min. The supernatant was centrifuged at 165,000 x g for an additional 30 min. The resulting pellet was resuspended in assay buffer: 50 mM Hepes, 10 mM $MnCl_2$, pH 7.6, with a concentration of approximately 10 mg of protein in 1 ml. The affinities of oxytocin and its analogues for the receptor were determined by homologue and heterologue displacement, incubating 10 nM tritiated oxytocin (32 Ci/mmol, NEN) and different concentrations of various peptides at 25 °C for 60 min. Membrane-bound radioactivity (total binding) was separated by filtration through a GF/C glass filter and counted. The apparent dissociation constants (K_d values) were calculated by the iterative nonlinear model-fitting program LIGAND.[20]

Rat kidney inner medulla containing V_2 receptors was prepared by differential centrifugation.[21] 50 g of kidney inner medulla was cut into small pieces and homogenized in 500 ml of buffer containing 250 mM sucrose. After filtration, the liquid was centrifuged for 10 min at 1000 x g, and the supernatant was centrifuged for another 30 min at 15000 x g. The pellet was suspended in 100 mM HEPPS, 10 mM $MgCl_2$ pH 8.2 buffer. The protein content of the suspension was approximately 10 mg/ml.

Rat liver plasma membrane was prepared by the method of Lesko *et al.*[22] Briefly, 40 g of rat liver was cut into small pieces and suspended in 250 ml of 1 mM $NaHCO_3$ and 0.5 mM $CaCl_2$, pH=7.5 solution. After homogenization, the resulting suspension was filtered and the filtrate was centrifuged at 800 x g. The pellet was suspended in 1000 ml of buffer, the suspension was centrifuged again, and the resulting pellet was then suspended in a biphase system consisting of 200 g of 20% dextran 500, 103 g of 30% polyethylene glycol 6000, 333 ml of 0.22 M Na_3PO_4, pH=6.5, and 179 ml of distilled water. After centrifugation at 1000 x g for 15 min, the interphase was collected, suspended in 20 ml of 10 mM HEPPS buffer containing 250 mM sucrose (protein content approximately 1 mg/ml) and stored at -70°C. The receptor assay was similar to that of the oxytocin receptor, using tritiated AVP as radiolabelled ligand.

Results and Discussion

Position 2 in oxytocin seems to be crucial for antagonistic activity. We therefore set out to establish the optimal size of the apolar side-chain and in parallel to find the optimal conformational constraints on the basis of the work of Manning and Lebl.[7,8,10,23-25] The use of 1,2,3,4-tetrahydroisoquinoline-3-carboxylic acid for the substitution of tyrosine methyl ether resulted in selective analogues,[9] but the selectivity was not better than that of atosiban. The use of 1 and 2-naphthylalanine resulted in analogues with high uterotonic inhibitory activity, especially in the vasopressin series containing *D*-Har (homoagrinine) in position 8, but the *in vivo* potencies were much lower than the *in vitro* uterotonic activity.[26] Sar^7 AVT derivatives previously proved to be potent and selective antagonistic analogues if the structure of the amino acid in position 2 was appropriate.[11] The high selectivity of the Trp^2 analogue (Mca^1-*D*-Trp^2-Sar^7 AVT undergoes practically no binding to the V_2 receptor, while its affinity for the oxytocin receptor is practically the same as that of the parent peptide) led us to introduce Car, which is a constrained analogue of Trp, in a similar way to 1,2,3,4-tetrahydroisoquinoline-1-carboxylic acid being a constrained analogue of phenylalanine.

The resulting analogues (3 and 4) displayed practically no binding to the uterotonic receptor, while the V_2 receptor affinity was negligible in both cases. The incorporated conformational constraints probably

completely inhibit the interaction with both receptor types. The binding pocket for the apolar side-chain in position 2 does not seem large enough for the rigid tricyclic structure. Interestingly, the V_1 affinities were relatively high in both cases. Thus, with a 3 orders of magnitude decrease in the OT and V_2 binding, these analogues are selective V_1 agonists. Mpa^1-*D*-Trp^2-Sar^7 AVT was also synthetized. Its uterotonic receptor affinity was found to be almost the same as that of native oxytocin, while the V_2 receptor affinity was significantly decreased, but stronger than that of the Mca^1 analogue, which undergoes practically no binding to the V_2 receptor.[11] The only difference lies in the space-filling properties of the first amino acid (Mpa and Mca, respectively). These data indicate that the first amino acid can have a decisive role in the receptor selectivity. This analogue is a 6 times weaker OT agonist than the Mca^1 analogue, but the V_1 binding is 200 times weaker, and the V_1 binding more than 100 times weaker than that of the Mca^1 peptide.

Table 2. Apparent dissociation constants (K_d values in nanomole) of new oxytocin antagonists to guinea-pig myometral oxytocin, rat liver vasopressin (V_1) receptors and rat kidney V_2 receptors

	peptide	OT	V_2	V_1
	AVP		1.5±0.1	0.65±0.04
	oxytocin	6.7±0.5		
	Mpa^1,*D*-Phe^2,Sar^{7}AVT	8±2	421±120	50.1±6
	Mca^1,*D*-Trp^2,Sar^{7}AVT	6±2	$3x10^5$	3.8±0.6
1	Mpa^1,*S*-Atc^2,Sar^{7}AVT	369.5±87	2290±410	17600±1838
2	Mpa^1,*R*-Atc^2,Sar^{7}AVT	1917.7±1682	5340±640	2640±163
3	Mpa^1,I-Car^2,Sar^{7}AVT	8545±3330	$>10^4$	63.5±4.1
4	Mpa^1,II-Car^2,Sar^{7}AVT	57450±1061	$>10^4$	17.8±4.1
5	Mpa^1,*D*-Trp^2,Sar^{7}AVT	37.6±23.2	4960±510	888±210

Because of the good receptor binding of the *p*-chlorophenylalanine-containing analogues[12] and the reported antagonistic properties of some Tic-containing peptides,[27] we additionally replaced the second amino acid (tyrosine in the original oxytocin molecule) by the conformationally constrained analogue of Phe, Atc.

Both Atc and Car were used as racemic mixtures and, after the completion of the synthesis, the resulting diastereomers were successfully separated by reverse-phase HPLC. The configurations of the individual isomers were determined after acidic hydrolysis by using a chiral compound (FLEC) as chromophoric modifier[18] in the case of the Atc-containing peptides. The earlier eluted peak corresponds to the peptide containing the *S* antipode, and the second peak to that containing the *R* antipode. In the case of the Car isomer-containing peptides, the regular acidic hydrolysis completely destroyed the acid-sensitive norharmane ring. Under milder conditions, *e.g.* on application of microwaves or reductive additives which were successfully applied for Trp, the result was practically the same. Since the OT receptor binding for both Car isomers was quite low, we did not make further attempts to determine the absolute configuration. However, we did find appropriate chromatographic conditions for this purpose (see legend to Fig. 2). The OT receptor affinity of Mpa^1-*R*-Atc^2-Sar^7 AVT was 1917 nanomoles, while that of Mpa^1-*S*-Atc^2-Sar^7 AVT was 369 nanomoles, which is moderately less than those of the *D* or *L*-Phe- containing analogues, so the decreased conformational freedom in this case does not support the preferred steric structure.

Although the oxytocic potencies were slightly lower for both antipodes, the even greater decrease in V_2 and V_1 receptor affinity pointed to the possibility of the design and synthesis of selective and potent oxytocin analogues based on determination of the optimal size and steric structure in the second amino acid side-chain in these vasotocin analogues. The *S*-Atc[2] analogue has only 17600 binding to V_1 and 2290 binding to V_2 receptors. Thus, their use for the design of selective OT antagonists could be of interest.

Acknowledgements

This work was supported by the following grants: OTKA 16156 and 14898, and ETT T03/523 and 560. The authors are indebted to Mr Pál Szabó and Mr Zoltán Kele for the MS measurements.

References

1. Hruby, V. J. *Life Sci.* **1982**, *31*, 189.
2. Kazmierski, W.; Wire, W. S.; Lui, G. K.; Knapp, R. J.; Shook, J. E.; Burks, T. F.; Yamamura, H. I.; Hruby, V. J. *J. Med. Chem.* **1988**, *31*, 2170.
3. Akerlund, M.; Carlsson, A. M.; Melin, P.; Trojnar, J. *Acta Obset. Gynecol. Scand.* **1985**, *64*, 449.
4. Keirse, M. J. *Am. J. Obstet. Gynecol.* **1995**, *173*, 618.
5. Law, H. D.; du Vigneaud, V. *J. Amer. Chem. Soc.* **1960**, *82*, 4579.
6. Melin, P.; Trojnar, J.; Johansson, B.; Vilhardt, H.; Akerlund, M., *J. Endocrinol.* **1986**, *111*, 125.
7. Lebl, M.; Hill, P.; Kazmierski, W.; Karaszova, L.; Slaninova, J.; Fric, I.; Hruby, V. J. *Int. J. Peptide Protein Res.* **1990**, *36*, 321.
8. Hruby, V. J.; Chan, W. Y.; Rockway, T. W.; Hlavacek, J.; Ormberg, J. In *Peptides: Design, Synthesis, and Biological Activity* (Channa Basava, G. M. Anantharamaiah eds.), Birkhauser, Boston, 1994, pp. 199-208.
9. Manning, M.; Cheng, L. L.; Stoev, S.; Bankowski, K.; Przybylski, J.; Klis, W. A.; Sawyer, W. H.; Wo, N. C.; Chan, W. Y. *J. Pept. Sci.* **1995**, *1*, 66.
10. Manning, M.; Nawrocka, E.; Misicka, A.; Olma, A.; Klis, W. A.; Seto, J.; Sawyer, W. H. *J. Med. Chem.* **1984**, *27*, 423.
11. Pávó, I.; Slaninova, J.; Klein, U.; Fahrenholz, F. *J. Med. Chem.* **1994**, *37*, 255.
12. Pávó, I.; Varga, C.; Vecsernyés, M.; Bakos, K.; Tóth, G. K.; Herczeg, J.; Slaninova, J.; Fahrenholz, F. *Hanseatic Endocrine Conference. Stade*, **1995**, A. 104.
13. Schiller, P. W.; Weltrowska, G.; Nguyen, T. M.-D.; Lemieux, C.; Chung, N. N.; Marsden, B. J.; Wilkes, B. C. *J. Med. Chem.* **1991**, *34*, 3125.
14. Rastogi, S. N.; Bindra, J. S.; Anand, N. *Ind. J. Chem.* **1971**, *9*, 1175.
15. Vejdelek, Z. J.; Trcka, V.; Protiva, M. *J. Med. Pharm. Chem.* **1961**, *3*, 427.
16. Merrifield, R. B. *J. Amer. Chem. Soc.* **1963**, *85*, 2149.
17. Kaiser, E.; Colescott, R. L.; Bossinger, C. D.; Cook, P. J. *Anal. Biochem.* **1970**, *34*, 595.
18. Einarsson, S.; Josefsson, B.; Möller, P.; Sanchez, D. *Anal. Chem.* **1987**, *59*, 1191.
19. Fuchs, A. R.; Periyasami, S.; Alexandrova, M.; Soloff, M. S. *Endocrinology* **1983**, *113*, 742.
20. Munson, P. J.; Rodbard, D. *Anal. Biochem.* **1980**, *107*, 220.
21. Fahrenholz, F.; Crause, P. *Biochem. Biophys. Res. Commun.* **1984**, *122*, 974.
22. Lesko, L.; Donlon, D.; Marinetti, G. V.; Hare, J. D. *Biochim. Biophys. Acta* **1973**, *311*, 173.
23. Manning, M.; Miteva, K.; Pancheva, S.; Stoev, S.; Wo, N. C.; Chan, W. Y. *Int. J. Pept. Protein. Res.* **1995**, *46*, 244.
24. Manning, M.; Lowbridge, J.; Seto, J.; Haldar, J.; Sawyer, W. H. *J. Med. Chem.* **1978**, *21*, 179.
25. Bankowski, K.; Manning, M.; Seto, J.; Haldar, J.; Sawyer, W. H. *Int. J. Peptide Protein Res.* **1980**, *16*, 382.
26. Procházka, Z.; Slaninová, J. *Collect. Czech Chem. Commun.* **1995**, *60*, 2170.
27. Majer, P.; Slaninova, J.; Lebl, M. *Int. J. Peptide Protein Res.* **1994**, *43*, 62.

ELSEVIER

PEPTIDES

Peptides 20 (1999) 749–751

In vivo effects of 2-substituted [Mpa^{1}Sar^{7}Arg^8]-oxytocin antagonists on postpartum rat[1]

I. Zupkó[a], G.K. Tóth[b], K. Bakos[b], F. Fülöp[c], I. Pávó[d], J. Havass[a], G. Falkay[a,*]

[a]*Department of Pharmacodynamics, Albert Szent-Györgyi Medical University, P.O. Box 121, 6721 Szeged, Hungary*
[b]*Department of Medical Chemistry, Albert Szent-Györgyi Medical University, Szeged, Hungary*
[c]*Department of Pharmaceutical Chemistry, Albert Szent-Györgyi Medical University, Szeged, Hungary*
[d]*Endocrine Unit of the 1st Department of Internal Medicine, Albert Szent-Györgyi Medical University, Szeged, Hungary*

Received 19 November 1998; accepted 19 January 1999

Abstract

A set of oxytocin antagonists consisting of [Mpa^{1}Sar^{7}Arg^8]-oxytocin substituted by various conformationally restricted or bulky D amino acids at position 2 were synthetized and biologically tested. In in vivo pharmacological investigations, the effects of these peptides were examined on the spontaneous motor activity of postpartum rat. Three of the newly prepared peptides proved at least as effective in inhibiting uterine contractions as clinically investigated atosiban. © 1999 Elsevier Science Inc. All rights reserved.

Keywords: Oxytocin antagonists; Conformational restriction; In vivo investigation; Tocolysis; Postpartum rat

1. Introduction

Premature labor (parturition before 37 completed gestation weeks) is currently one of the greatest challenges in obstetrical practice. Some 5 to 10% of fetuses are born prematurely; this comprises ≈13 million cases worldwide annually [19]. The picture is darkened by the fact that 69 to 83% of the neonatal mortalities come from this population [8]. Besides the traditionally used β_2-sympathomimetics and magnesium sulfate, there is a real need for more effective and more tolerable tocolytics. Oxytocin itself and the sensitivity of the uterus to oxytocin play a crucial role in the initiation of both normal and pathologically early delivery. Oxytocin exerts a direct uterotonic effect and also causes the liberation of prostaglandin, which enhances the contractility of the myometrium [2]. The recognition of this complex mechanism of action suggests that specific oxytocin antagonists are of therapeutic value in postponing early contractions of the uterus. This theory is supported by the findings on atosiban ([deamino^1-D-Tyr(OEt)^{2}Thr^{4}Orn^8]-oxytocin), the first clinically tried oxytocin antagonist, which exhibits a much more tolerable side effect profile than those of the tocolytics used today [3]. In this study we report on the synthesis and in vivo pharmacological investigation of new oxytocin antagonists with the general structure [Mpa^{1}Sar^{7}Arg^8]-oxytocin substituted at position 2. Rapidly performable in vitro methods are generally preferred in tests on the reasonably large number of oxytocin antagonists. However, the in vivo results may be inconsistent with the in vitro findings; i.e. compounds found to be effective in vitro may fail to display similar action when tested in vivo [11].

Symbols and abbreviations are in accordance with the recommendations of the International Union of Pure and Applied Chemistry-International Union of Biochemistry (IUB) Commission on Biochemical Nomenclature (J Biol Chem 1972;247:977). All amino acids are in the L configuration unless otherwise noted. Other abbreviations used are as follows: Sar, sarcosine; Orn, ornithine; Atc, 2-amino-2-carboxy-1,2,3,4-tetrahydronaphthalene; Tic, 1,2,3,4-tetrahydroisoquinoline-3-carboxylic acid; Car, 1,2,3,4-tetrahydro-β-carboxylic acid; Dbt, 3,5-dibromotyrosine; Beb, *p*-methylbenzyl; Mpa, β-mercaptopropionic acid; Mca, β-mercapto-β,β-cyclopentamethylenepropionic acid; Pen, β′-dimethylcysteine; Cpa, 4-chlorophenylalanine.

* Corresponding author. Tel.: +36-62-455-567; fax: +36-62-455-567.
E-mail address: falkay@szote.u-szeged.hu (G. Falkay)

[1] This work was supported by a Research Grant from the Hungarian Ministry of Health (ETT Grant T-03-598/96).

PII: S0196-9781(99)00058-3

2. Materials and methods

2.1. Amino acid and peptide synthesis

The racemic 2-amino-2-carboxy-1,2,3,4-tetrahydronaphthalene was prepared from 2-spirohydantointetraline as described earlier [15,16]. The racemic 1,2,3,4-tetrahydro-β-carboline-1-carboxylic acid was synthetized from tryptamine with glyoxylic acid according to the description in the literature [18].

The peptides were synthetized by a solid-phase technique, with tBoc chemistry [13]. Side-chain protecting groups were as follows: Arg(Tos), Cys(Meb), Mca(Meb), and Mpa(Meb). The syntheses were performed on an ABI 430 A automatic peptide synthetizer (Applied Biosystems). The completed peptide resins were treated with liquid hydrogen fluoride (HF)/dimethyl sulfide/*p*-cresol/anisole/*p*-thiocresol (93:4:1:1:1, by volume) at 0°C for 1 h. The HF was then removed and the resulting free peptides were solubilized and folded by stirring with potassium hexacyanoferrate (III). After complete folding, the reaction mixture was filtered, the anions were removed by ion exchange and the remaining solution was lyophilized. The crude peptides were purified by reverse-phase high-performance liquid chromatography. The appropriate fractions were pooled and lyophilized. The purity was checked by reverse-phase high-performance liquid chromatography. The products proved to be substantially pure (≥97%). The structures were proved by mass spectrometry with a Finnigan-Mat TSQ 7000 tandem mass spectrometer equipped with an ESI source (Finnigan-Mat, San Jose, CA). The results of the mass spectrometry measurements in all cases agreed well with the calculated values.

2.2. Measurement of the action on uterine contractility

Female Sprague–Dawley rats were anesthetized with urethane (1 g/kg, intraperitoneally) ≈24 h after spontaneous delivery. After cannulation of the jugular vein, the abdominal cavity was opened and a Millar catheter (Millar Instruments Inc., Houston, Texas, USA) fitted with a liquid-filled latex microballoon was inserted into the uterus through a small section above the cervical part. After a 45-min equilibration period, the intrauterine pressure was recorded (Hewlett-Packard 7702B) and the effects of the given compounds were assessed by expressing the integrated tension relating to a 5-min period after administration of each dose as a percentage of the average for three 5-min periods before the first administration. The maximal inhibition and ED_{50} values were calculated by means of Grafit 3.01. The animals were handled according to a protocol reviewed and approved by the Ethical Committee for the Protection of Animals in Research at Albert Szent-Györgyi Medical University, Szeged, Hungary.

Table 1
Amino acids at position 2, maximal effects, and ED_{50} values of the investigated [Mpa^{1}Sar^{7}Arg^8]-oxytocin peptides

Peptide no.	Amino acid at position 2	Maximal effect (%)	ED_{50} (nmol/kg)	ED_{50} (mg/kg)
1	D-Trp	71.17	2.616	0.0027
2	D-Cpa	43.34	4.282	0.0044
3	*S*-Atc	37.39	1.275	0.0013
4	*R*-Atc	39.99	2.157	0.0022
5	Car-I[a]	27.44	4.785	0.005
6	Car-II[a]	54.05	4.02	0.0042
7	*S*-Tic	66.76	2.587	0.0026
8	Dbt	29.62	5.988	0.007
9	D-Cpa[b]	41.37	1.552	0.0017
10	Atosiban	50.52	0.94	0.00096
	Fenoterol	93.45	2.602	0.001

[a] The absolute configuration of Car has not been determined.
[b] Contains Mca instead of Mpa at position 1.

3. Results

Calculated maximal effects (expressed as percent inhibitions of the spontaneous uterine motility) and ED_{50} values are listed in Table 1. For comparison, in the same system we tested atosiban and the β_2-adrenergic agonist fenoterol, which is extensively used at present (Fig. 1). As indicated, fenoterol exerts a substantially more pronounced inhibitory effect on the postpartum rat uterus. The antioxytocic activities of three of the newly synthetized peptides (nos. 2, 6, and 9) are comparable with that of atosiban, the difference between their maximal inhibitions being <10%. Substitution at position 2 with Dbt and one enantiomer of Car did not lead to significantly effective compounds. Incorporation of the two configurations of Atc resulted in analogs with similarly moderate activity. The peptides containing D-Trp and *S*-Tic proved to be more potent than atosiban, although the differences were not significant statistically.

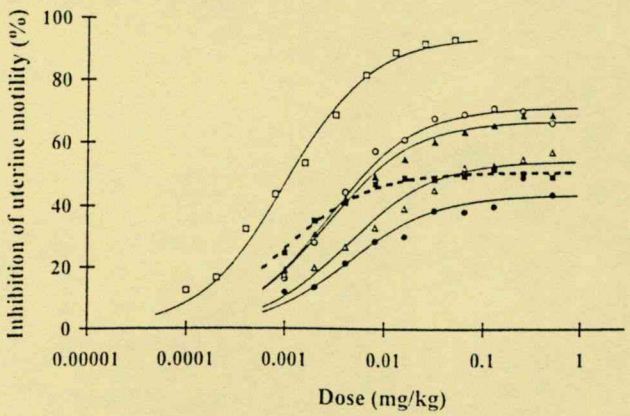

Fig. 1. Representative dose-response curves of peptides nos. 1 (○), 2 (●), 6 (△), and 7 (▲), atosiban (■, dotted line), and fenoterol (□). The data are the averages of the results of six independent experiments. Error bars are not shown, for clarity.

4. Discussion

The available data were used with a view to the design and pharmacological investigation of a series of oxytocin antagonists with conformationally restricted features. The primary aim of the chemical modification was to stabilize peptide conformations with high affinity for oxytocin receptors without activating them. This conformational restriction can be achieved by incorporating a second intramolecular ring or a substituent involving a constrained amino acid [17]. Because peptide-type oxytocin antagonists cannot be given orally, it is a basic expectation to have as long an effect as possible after intravenous administration. As neurohypophyseal hormones lacking an N-terminal amino group are inactivated quite slowly, most of the oxytocin antagonists described to date contain Mpa, Mca, or Pen instead of Cys at position 1 [4]. Substitution of the Pro with Sar at position 7 is known to result in a highly potent oxytocin agonist with practically no antidiuretic activity [6]. The agonist potency of this compound is even higher when it contains Mpa or Mca at position 1 [5]. This considerable selectivity is a characteristic feature of oxytocin analogous with antagonist potency [14]. This change may be connected with the altered conformational mobility of the C-terminal part of the peptides. Another possibility for modification is the Leu at position 8. The most potent oxytocin antagonists contain basic amino acids (Arg/Orn) instead of apolar Leu at this site [9]. The antagonist potency may be further increased by insertion of a bulky lipophilic amino acid at position 2 [12]. This position plays a crucial role in determining the potency and selectivity of the oxytocin antagonist [7]. The most effective of the five new peptides containing constrained amino acids at position 2 is that containing Tic, a frequently used surrogate for Phe and Pro. Oxytocin antagonists containing Tic at position 2 are generally more potent than the adequate Phe analogs, which may be explained by the limited freedom of rotation of Tic [10]. The insertion of D amino acids at position 2 is also known to result in peptides with antioxytocic properties [1]. All these findings indicate that it is rational to investigate the peptides [Mpa^{1}Sar^{7}Arg^8]-oxytocin as oxytocin antagonists. Our in vivo method is closer to the clinical situation in which oxytocin antagonist therapy should be initiated rather than the generally used in vitro techniques. Knowledge of the biological effects of these peptides may contribute to the synthesis of more effective and selective oxytocin antagonists.

Acknowledgments

The authors thank Judit Czinkota for her technical assistance in the experiments.

References

[1] Flouret G, Brieher W, Mahan K. Design of potent oxytocin antagonists featuring D-tryptophan at position 2. J Med Chem 1991;34:642–6.
[2] Fuchs AR, Fuchs F, Husslein P, Soloff MS, Fernstrom M J. Oxytocin receptors and human parturition: a dual role for oxytocin in the initiation of labor. Science 1982;215:1396–8.
[3] Goodwin TM, Valenzuela GJ, Silver H, Creasy G. Dose ranging study of the oxytocin antagonists atosiban in the treatment of preterm labor. Obstet Gynecol 1996;88:331–6.
[4] Grzonka Z, Kasprzykowski F, Lubkowska L, Darlak K, Hahn TA, Spatola AF. In vitro degradation of some arginine-vasopressin analogs by homogenates of rat kidney, liver and serum. Peptides Res 1991;4:270–4.
[5] Grzonka Z, Lammek B, Gazis D, Schwartz IL. Synthesis and some pharmacological properties of [4-threonine,7-sarcosine]oxytocin, a peptide with high oxytocic potency, and of [4-threonine,7-N-methylalanine]oxytocin. J Med Chem 1983;26:1786–7.
[6] Grzonka Z, Lammek B, Kasprzykowski F, Gazis D, Schwartz IL. Synthesis and some pharmacological properties of oxytocin and vasopressin analogues with sarcosine or N-methyl-L-alanine in position 7. J Med Chem 1983;26:555–9.
[7] Hruby VJ, Chow MS, Smith DD. Conformational and structural considerations in oxytocin-receptor binding and biological activity. Annu Rev Pharmacol Toxicol 1990;30:501–34.
[8] Keirse MJNC. New perspectives for the effective treatment of preterm labor. Am J Obstet Gynecol 1995;173:618–28.
[9] Lebl M. Analogs with inhibitory properties. In: Jost K, Lebl M, Brtnik F, editors. Handbook of neurohypophyseal hormone analogs, Vol 2. Boca Raton: CRC Press, 1987. p. 17–74.
[10] Lebl M, Hill P, Kazmierski W, Karaszova L, Slaninova J, Fric I, Hruby VJ. Conformationally restricted analogs of oxytocin: stabilization of inhibitory conformation. Int J Pept Protein Res 1990;36:321–30.
[11] Lowbridge J, Manning M. Synthetic antagonists of in vivo responses by the rat uterus to oxytocin. J Med Chem 1979;22:565–9.
[12] Melin P, Trojnar J, Johansson B, Vilhardt H, Akerlund M. Synthetic antagonists of the myometrial response to vasopressin and oxytocin. J Endocrinol 1986;111:125–31.
[13] Merrifield RB. The synthesis of a tetrapeptide: solid phase peptide synthesis. J Am Chem Soc 1963;85:2149–54.
[14] Pavo I, Slaninova J, Klein U, Fahrenholz F. Enhanced selectivity of oxytocin antagonists containing sarcosine in position 7. J Med Chem 1994;37:255–9.
[15] Rastogi SN, Bindra JS, Anand N. Methyldopa in a rigid framework: 3-amino-3-methyl-6,7-dihydroxy-3,4-dihydrocoumarines 38 2-amino-6,7-dihydroxytetralin-2-carboxylic acids. Ind J Chem 1971;9:1175–82.
[16] Schiller PW, Weltrowska G, Nguyen TM, Lemieux C, Chung NN, Marsden BJ, Wilkes BC. Conformational restriction of the phenylalanine residue in a cyclic opioid peptide analogue: effects on receptor selectivity and stereospecificity. J Med Chem 1991;34:3125–32.
[17] Smith DD, Slaninova J, Hruby VJ. Structure-activity studies of a novel bicyclic oxytocin antagonist. J Med Chem 1992;35:1558–63.
[18] Vejdelek ZJ, Trcka V, Protiva M. Synthetic experiments in the group of hypotensive alkaloids–XXI: chemistry of 1,2,3,4-tetrahydronorharmane-1-carboxylic acid and derivatives. J Med Pharm Chem 1961;3:427–40.
[19] Villar J, Ezcurra EJ, Gurtner de la Fuente V, Campodonico L. Preterm delivery: the unmet need. Res Clin Forums 1994;16:9–38.

5.4.

SYNTHESIS OF CONFORMATIONALLY CONSTRAINED PEPTIDES VIA SOLID-PHASE INCORPORATION OF THE CONSTRAINTS

Gábor K. Tóth[a], Zoltán Kele[a] and Ferenc Fülöp[*,b]

[a]Department of Medical Chemistry and [b]Institute of Pharmaceutical Chemistry, University of Szeged, H-6701 Szeged, POB 121, Hungary

Abstract: A simple solid-phase method has been developed, in which Pictet-Spengler cyclization is applied on the resin for the synthesis of some conformationally constrained tripeptides. This methodology was also used for the synthesis of oxytocin antagonist analogues.

Keywords: Solid-phase chemistry; peptide analogues; combinatorial chemistry.

The small peptides are usually highly flexible molecules, and their structures in solution depend greatly on the environment. In order to restrict the conformational freedom of the parent peptide and to stabilize the desired bioactive conformation, local constraints can be introduced into the molecule. Modulation of the flexibility of a peptide backbone from an extended conformation to a β-turn structure is an important breakthrough in the rational design of highly selective and active peptides or peptidomimetic drugs.[1,2]

The recent developments in combinatorial solid-phase chemistry[3-5] have made feasible the parallel (or one-pot) synthesis of peptides which contain different constrained amino acids, *e.g.* 1,2,3,4-tetrahydroisoquinoline-3-carboxylic acid (Tic), 4,5,6,7-tetrahydroimidazo[4,5-*c*]pyridine-6-carboxylic acid (spinacin) or 3-carboxy-1,2,3,4-tetrahydro-2-carboline (Tcc).[1] In recent years, the Pictet-Spengler reaction has been widely applied in the solid phase in heterocyclic chemistry.[6-11] Although solid phase chemistry originated in the peptide field, as far as we are aware the Pictet-Spengler reaction has not utilized for peptide synthesis. The aim of the present work was to introduce the Pictet-Spengler reaction in the solid phase in the process of oligopeptide synthesis, with a view to the synthesis of conformationally constrained peptides.

The initial goal was the synthesis of tripeptides with the general structure H-Lys-Xxx-Ala-NH_2, where Xxx is methyl-substituted Tic (MeTic), methyl-substituted 7-hydroxy-1,2,3,4-tetrahydroisoquinoline-3-carboxylic acid (MeHat), or methyl-substituted Tcc (MeTcc), derived from Phe, Tyr or Trp. The syntheses were carried out on *p*-methylbenzhydrylamine resin, using *t*-Boc chemistry[12] (see Scheme[13] below).

After the incorporation of the appropriate aromatic amino acids, the resulting dipeptidyl resin was subjected to reaction with acetaldehyde. Under the conditions applied, ring closure with formaldehyde failed. Following completion of the peptide chain, the resulting constrained tripeptide was detached from the resin by means of the standard liquid HF method. Even in the case of Trp, this method led to no serious side-reaction, although the resulting MeTcc, containing a β-carboline ring, is

* Corresponding author. Tel: 36 62 545564; fax: 36 62 545 705; E-mail: fulop@pharma.szote.u-szeged.hu

acid-sensitive in an aqueous environment. The use of standard peptide coupling revealed the presence of a deletion peptide, i.e. the lack of the Lys residue, from one peak in the HPLC trace. The amount of such deletion sequences varied from a few per cent to the majority.[14] The acylation was especially difficult in the case of MeTcc, and the amount of non-acylated dipeptide was high.

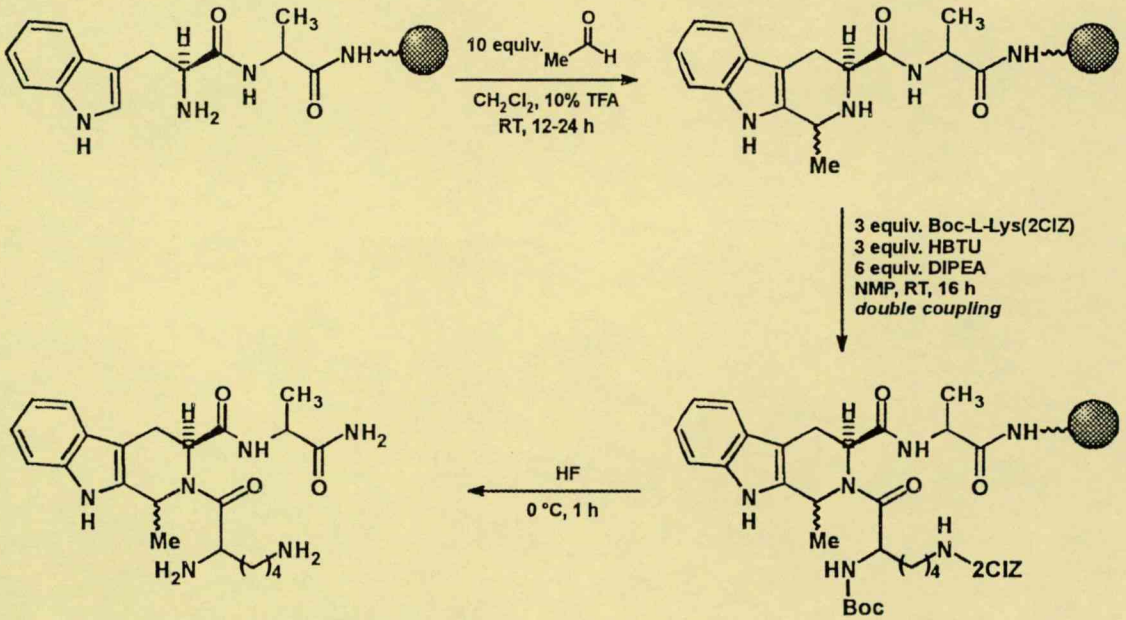

This difficulty in acylation seemed to be the major barrier to the application of the above solid-phase method (in another experiment, we successfully acylated sterically hindered amino acid derivatives, *e.g.* β-carboline derivatives, in the liquid phase). Gilon *et al.*[15] recently published a new bis(trichloromethyl) carbonate (triphosgene, BTC)-mediated coupling for the incorporation of amino acid derivatives into sterically hindered molecules. The main advantage of this method is the *in situ* formation of the highly reactive acid chloride from the protected amino acid with BTC. Our experiments demonstrated that, even in the case of MeTcc, BTC coupling resulted in the desired tripeptide derivatives in acceptable yields[16] (75-80%, based on HPLC results).

During the ring closure, the incorporated substituent introduces a new chiral centre. The crude cleavage mixture therefore contains two diastereomeric peptides; in most cases, these were easily separable by RP-HPLC. The ratio of the diastereomers differed somewhat from 1:1 (based on HPLC analysis).

After the successful synthesis of the model tripeptides, this solid phase method was used to synthetize two oxytocin antagonist analogues containing conformationally constrained amino acids (MeTic or MeTcc) in position 2:[17] Mpa-Xxx-Ile-Gln-Asn-Cys-Sar-Arg-Gly-NH_2, where Xxx is MeTic or MeTcc. The linear peptide was folded without isolation by stirring with $K_3Fe(CN)_6$. After the ring closure only one main product was isolated, the diastereomers were not separable in the applied HPLC conditions.

Electrospray ionization MS of Mpa-MeTcc-Ile-Gln-Asn-Cys-Sar-Arg-Gly-NH_2

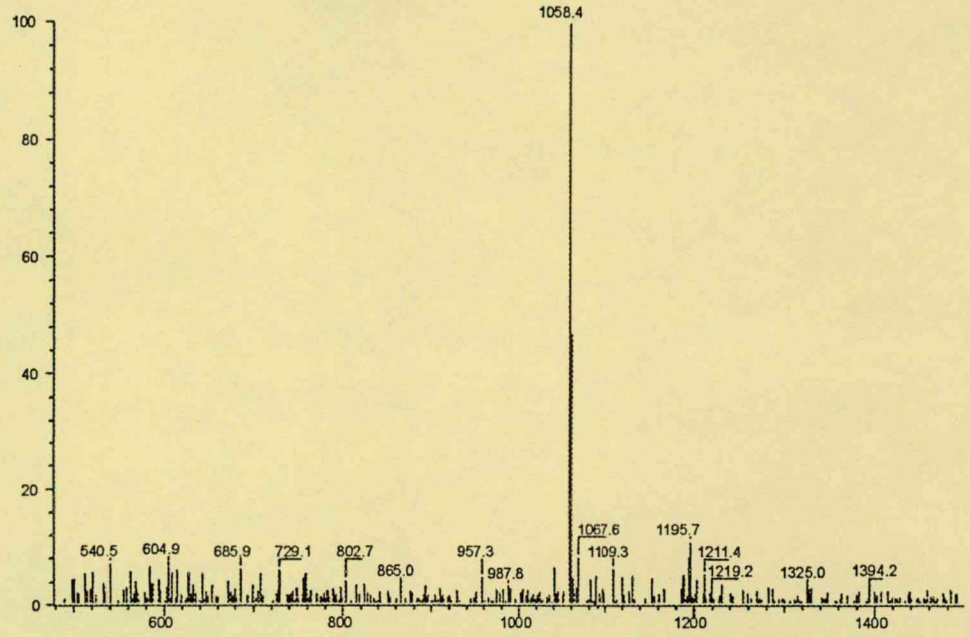

Characterization of the synthesized peptides

Peptide	MW calc.	$M+1^+$	Rt	Gradient^{++}
Lys-MeTcc-Ala-NH_2	428.54	429	7.13	a
Lys-MeTcc-Ala-NH_2	428.54	429	7.28	a
Lys-MeTic-Ala-NH_2	389.50	390	10.37	b
Lys-MeTic-Ala-NH_2	389.50	390	10.62	b
Lys-MeHat-Ala-NH_2	405.50	406	32.8	c
Lys-MeHat-Ala-NH_2	405.50	406	33.9	c
Mpa-MeTic-Ile-Gln-Asn-Cys-Sar-Arg-Gly-NH_2	1019.23	1019.5	9.83	e
Mpa-MeTcc-Ile-Gln-Asn-Cys-Sar-Arg-Gly-NH_2	1058.26	1058.5	8.21	f

$^+$Measured on a Finnigan Mat TSQ 7000 instrument by electrospray ionization. $^{++}$Solvents: *A* = 0.1% TFA in water, *B* = 0.1% TFA in an 8:2 acetonitrile water mixture; gradients (a) 14 → 20% of *B* in 12 min, flow 1.5 ml/min, Lichrosorb 10 RP-18; (b) 10 → 30% of *B* in 20 min, flow 0.8 ml/min, Nucleosil 5 C-18; (c) 0 → 30% in 60 min flow: 0.15 ml/min, Alltech 5 C-18 (d) 24 → 34% of *B* in 15 min, flow: 1.5 ml/min, Lichrosorb 10 RP-18; (e) 30 → 45% of *B* in 15 min, flow: 1.2 ml/min, Lichrosorb 10 RP-18; (f) 26 → 41% of *B* in 15 min, flow: 1.2 ml/min, Lichrosorb 10 RP-18

Acknowledgements. The authors' thanks are due to OTKA (grant No. T 022540) and MKM (grant No. FKFP 0535/1999) for financial support.

REFERENCES AND NOTES

1. Gibson, S. E.; Guillo, N.; Tozer, M. J. *Tetrahedron* **1999**, *55*, 585-615.
2. Kawahata, N. H.; Goodman, M. *Tetrahedron Letters* **1999**, *40*, 2271-2274.
3. Nefzi, A.; Ostresh, J. M.; Houghten, R. A. *Chem. Rev.* **1997**, *97*, 449-472.
4. Loughlin, W. A. *Austr. J. Chem.* **1998**, *51*, 875-893.
5. Houghten, R. A.; Pinilla, C.; Appel, J. R.; Blondelle, S. E.; Dooley, C. T.; Eichler, J.; Nefzi, A.; Ostresh, J. M. *J. Med. Chem.* **1999**, *42*, 3743-3778.
6. Fantauzzi, P. P.; Yager, K. M. *Tetrahedron Letters* **1998**, *39*, 1291-1294.
7. Mayer, J. P.; Bankaitis-Davis, D.; Zhang, J.; Beaton, G.; Bjergarde, K.; Andersen, C.. M.; Burton A.; Goodman, B. A.; Charles, J. *Tetrahedron Letters* **1996**, *37*, 5633-5636.
8. Mohan, R.; Chou, Y. L.; Morrissey, M. M. *Tetrahedron Letters* **1996**, *37*, 3963-3966.
9. Kaljuste, K.; Undén, A. *Tetrahedron Letters* **1995**, *36*, 9211-9214.
10. Yang, L.; Guo, L. *Tetrahedron Letters* **1996**, *37*, 5041-5044.
11. van Loevezijn, A.; van Maarseveen, J. H.; Stegman, K.; Visser G. M.; Koomen G. J. *Tetrahedron Letters* **1998**, *39*, 4737-4740.
12. The peptides were synthetized by a standard *t*-Boc solid-phase procedure. After incorporation of the appropriate aromatic amino acid (Phe, Trp or Tyr(2BrZ)), the free amino group-containing polymer was shaken in 10% TFA/CH_2Cl_2 with 10 equivalents of freshly distilled acetaldehyde for 12-24 h at ambient temperature. After washing of the resin, the elongation of the peptide chain was completed. The peptides were detached from the resin by standard HF cleavage, and the products were characterized by mass spectrometry and RP HPLC.
13. Abbreviations: 2-chlorobenzyloxycarbonyl (2ClZ), *O*-benzotriazol-1-yl-*N,N,N',N'*-tetramethyl-uronium hexafluorophosphate (HBTU), *N,N*-diisopropylethylamine (DIPEA).
14. The yield of this coupling step could be improved by the elongation of the reaction time of the acylation.
15. Falb, E.; Yechezkel, T.; Salitra, Y.; Gilon, C. *J. Peptide Res.* **1999**, *53*, 507-517.
16. 1.25 mmol protected amino acid was dissolved in dry THF, and 0.41 mmol (122 mg) BTC and 3.5 mmol (461 µl) collidine were added to the solution. After stirring for 1 min, the resulting suspension was poured into 0.25 mmol free amino or imino group-containing peptide resin and the mixture was shaken for 6 h at RT. The whole procedure was repeated, and the resin was then washed with MeOH and CH_2Cl_2, dried and subjected to HF cleavage.
17. Tóth, G. K.; Bakos, K.; Penke, B.; Pávó, I.; Varga, C.; Török, G.; Péter, A.; Fülöp, F. *Bioorg. Med. Chem. Lett.*, **1999**, *9*, 667-672.

Synthesis of Conformationally Constrained Peptides via Solid-phase Incorporation of the Constraints

Gábor K. Tóth[a], Zoltán Kele[a] and Ferenc Fülöp[b,*]

[a]Department of Medical Chemistry and [b]Institute of Pharmaceutical Chemistry, University of Szeged, H-6701 Szeged, POB 121, Hungary

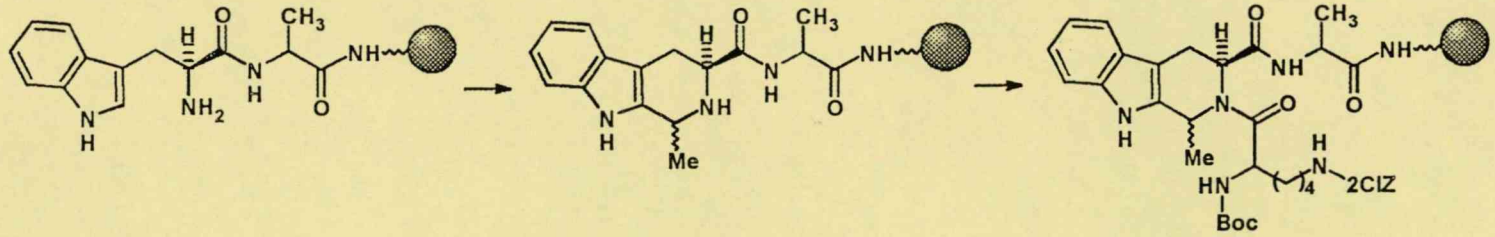

Synthesis and pharmacological properties of oxytocin antagonists containing conformationally constrained amino acids

G.K. TÓTH[1], K. BAKOS[1], I. ZUPKÓ[2], F. FÜLÖP[3], I. PÁVÓ[4] and G. FALKAY[2]

[1]*Department of Medical Chemistry,* [2]*Department of Pharmacodynamics,* [3]*Department of Pharmaceutical Chemistry,* [4]*Department of Endocrinology, A. Szent-Györgyi Medical University, H-6720 Szeged, Hungary*

Introduction

There has recently been an increasing tendency towards the rational design of highly active and selective analogues of different peptides. The small peptides are usually highly flexible molecules, and the structures observed in solution depend greatly on the environment. Local constraints are introduced, therefore, in order to restrict the conformational freedom of the parent peptide and to stabilize the desired bioactive conformation. The recently increasing interest in posttranslationally modified peptides is partly due to the search for conformationally constrained amino acids. Modulation of the flexibility of a peptide backbone from an extended conformation to a β turn structure is an important breakthrough in the rational design of highly selective and active peptide or peptidomimetic drugs.

Results and discussion

Analogues of oxytocin containing D-Trp, D-Cpa (p-chlorophenylalanine), L-Dbt (dibromotyrosine), L-3Tic, 1,2,3,4-tetrahydro-norharman-1-carboxylic acid (Car) and 2-amino-2-carboxy-1,2,3,4-tetrahydronaphthalene (Atc) with R or S configurations in position 2 were synthesized. The Atc and Car containing peptides were synthesized in the solid phase by using racemic mixtures of R and S Atc and Car. After the liquid HF cleavage, the resulting crude diastereomeric mixtures were separated by means of RP-HPLC. The structure and the purity of the resulting analogues were characterized by mass spectrometry, HPLC and CZE investigations. The pharmacological properties of these oxytocin analogues were tested on an *in vivo* system, by their inhibition of uterine motor activity. The intrauterine pressure was measured with a Millar catheter fitted with a latex microballoon inserted into the post partum rat uterus. Atosiban was used as reference material and the results of the pharmacological measurements are shown in Figure 1. According these investigations some of

Y. Shimonishi (ed): Peptide Science – Present and Future, 724–725

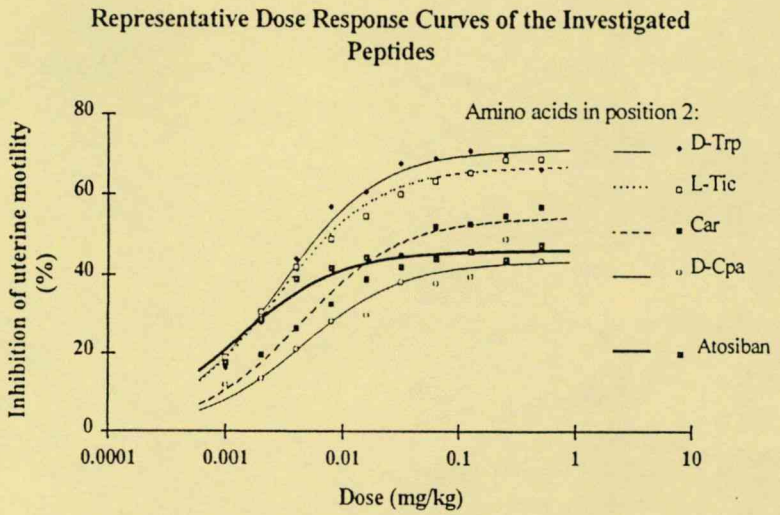

Figure 1. Representative dose response curves of the investigated peptides.

these analogues proved more potent than the reference material. The described investigations are further evidence of the crucial role of the amino acid in position two in case of these oxytocin analogues. The racemic conformationally constrained amino acids can be incorporated into the growing peptide chain and after the synthesis the diastereomeric products can be easily separated by RP HPLC. The inhibitory potency of oxytocin analogues can be increased the incorporation of some conformationally constrained bulky aromatic amino acids instead of the tyrosine in position two.

References

1. Hruby, V.J. Life Sci., 31 (1982) 189.
2. Akerlund, M., Carlsson, A.M., Melin, P., and Trojnar, J. Acta Obset. Gynecol. Scand., 64 (1985) 449.
3. Keirse, M.J., Am. J. Obstet. Gynecol., 173 (1995) 618.
4. Pavo, I., Slaninova, J., Klein, U., and Fahrenholz, F., J. Med. Chem., 37 (1994) 255.
5. Rastogi, S.N., Bindra, J.S., and Anand, N., Ind. J. Chem., 9 (1971) 1175.
6. Vejdelek, Z.J., Trcka, V., and Protiva, M., J. Med. Pharm. Chem., 3 (1961) 427.
7. Bankowski, K., Manning, M., Seto, J., Haldar, J., and Sawyer, W.H., Int. J. Peptide Protein Res., 16 (1980) 382.
8. Lebl, M., Hill, P., Kazmierski, W., Kárászová, L., Slaninová, J., Fric, I., Hruby, V., J. Int. J. Peptide Protein Res., 36 (1990) 321.
9. Manning, M., Cheng, L.L., Stoev, S., Bankowski, K., Przybylski, J., Klis, W.A., Sawyer, W.H., Wo, N.C., and Chan, W.Y., J. Pept. Sci., 1 (1995) 66.
10. Procházka, Z. and Slaninová, J. Collect. Czech Chem. Commun., 60 (1995) 2170.
11. Majer, P., Slaninova, J. and Lebl, M., Int. J. Peptide Protein Res., 43 (1994) 62.

Int. J. Peptide Protein Res. 43, 1994, 29–30
Printed in Belgium – all rights reserved

INTERNATIONAL JOURNAL OF PEPTIDE & PROTEIN RESEARCH
ISSN 0367-8377

A new synthesis of Rink's polymer, 4-(2′,4′-dimethoxyphenylhydroxymethyl)phenoxymethylpolystyrene

GYÖRGYI VÁRADI, GÁBOR K. TÓTH and BOTOND PENKE

Department of Medical Chemistry, Albert Szent-Györgyi Medical University, Szeged, Hungary

Received 15 March, accepted for publication 23 May 1993

For solid-phase peptide synthesis, 2,4-dimethoxy-4′-hydroxybenzhydrol linker was prepared via lithium borohydride reduction of 2,4-dimethoxy-4′-hydroxybenzophenone. The potassium salt of the linker was coupled to chloromethylpolystyrene. This method proved to be better than use of the cesium salt. This new synthesis gave a polymer with appropriate structure and a good degree of substitution. © Munksgaard 1994.

Key words: 2,4-dimethoxy-4′-hydroxybenzhydrol; potassium salt coupling of phenolate; side reactions; substitution level

The solid-phase method introduced by Merrifield is nowadays the most significant process in peptide synthesis. The result of the synthesis depends considerably on the polymer used, especially if the Fmoc strategy is applied. The ideal carrier remains stable during cleavage, and the peptide can be removed by mild acidic treatment after synthesis. Simultaneously, the side-chain protecting groups are also cleaved. Such polymers include the 4-alkoxybenzyl alcohol resin of Wang (1), the 3-xanthydroloxymethylpolystyrene of Sieber (2), the 2-methoxy-4-alkoxybenzyl alcohol resin of Mergler (3) and the 4-(2′,4′-dimethoxyphenylhydroxymethyl)-phenoxymethylpolystyrene of Rink (4).

Rink's polymer is a promising resin. We attempted to synthesize it by following the described method, but two problems arose. Uncontrollable side-reactions occured, the structure of the polymer could not be determined accurately and the described substitution (4) of the resin could not be reproduced: we obtained only approximately 0.1 mmol/g. We tried reducing the time of the reduction, changing the solvent, and using sodium borohydride or lithium aluminium hydride, but an acceptable level of substitution could not be attained.

Because of these difficulties, we decided on an entirely different strategy: preparing the ready linker and coupling it to the polystyrene. Investigation of the reduction of 2,4-dimethoxy-4′-hydroxybenzophenone showed that this reaction proceeded in 15 min instead of the 1 h described in the literature (4). If we continued the reduction, the amount of by-products gradually increased. (One of them is probably a diphenylmethane derivative.) The structure of 2,4-dimethoxy-4′-hydroxybenzhydrol was confirmed by IR and NMR spectroscopy. The linker was coupled to the chloromethylated polystyrene via its cesium salt as described previously. This process resulted in an acceptable degree of substitution. Later we used the potassium salt of the phenolic hydroxy group instead of the expensive cesium salt; the product proved better as regards substitution.

The structure of the resin was proved via its IR spectrum and the degree of substitution by coupling of an Fmoc amino acid to the polymer. We achieved a convenient level of substitution (0.35–0.47 mmol/g), suitable for the synthesis of any peptide.

EXPERIMENTAL PROCEDURES

Melting points were taken with a PHMK apparatus and are uncorrected. Microanalyses were carried out with a Heraeus element analyser. IR spectra were recorded with a Nicolet IR 80 spectrometer, and ^{1}H-NMR spectra with a Bruker Aspect 3000 (400 MHz) spectrometer. Analytical TLC plates were purchased from E. Merck. For TLC, the $CHCl_3$/acetone (9:1) solvent system was used.

2,4-Dimethoxy-4′-hydroxybenzophenone (1). A solution of 4-hydroxybenzoic acid (69 g, 0.5 mol), resorcinol–dimethyl ether (97 mL, 0.75 mol), zinc chloride (150 g, 1.1 mol) and phosphorus oxychloride (326 mL, 3.5 mol) was stirred at 60–65 °C for 1.5 h. The mixture was then poured onto ice (1.5 kg), and solid KOH was added until the deep purple colour turned yellow. Ethyl acetate (300 mL) was then added to the solution, and the organic phase was separated, dried (Na_2SO_4) and con-

centrated at reduced pressure. The precipitated product was isolated by suction and washed with diethyl ether; yield: 92 g (71%); m.p. 134–136 °C, RF = 0.53.

Anal. calc. for $C_{15}H_{14}O_4$: C 69.76, H 5.46; found (258.28): C 69.47, H 5.39. IR (KBr): ν_{max} 1280, 1605, 3330 cm^{-1}. ^{1}H-NMR ($CDCl_3$): δ = 3.70 (s, 3H, 2-OCH_3), 3.85 (s, 3H, 4-OCH_3), 6.52 (m, 1H, 5-H), 6.54 (d, 1H, 3-H), 6.86 (d, 2H, 3′,5′-H), 7.33 (d, 1H, 6-H), 7.72 (d, 2H, 2′,6′-H).

2,4-Dimethoxy-4′-hydroxybenzhydrol (2). Lithium borohydride (6.34 g, 291 mmol) was added in small amounts to a solution of **1** (50.00 g, 194 mmol) in THF (800 mL). The solution was refluxed for 15 min. After removal of the unreacted lithium borohydride with MeOH (200 mL), the solvent was evaporated at reduced pressure and the residue was partitioned between ethyl acetate (600 mL) and H_2O (300 mL). The organic layer was dried (Na_2SO_4) and concentrated at reduced pressure. After this procedure the product could be obtained as a crystalline substance which was washed with diethyl ether; yield 45 g (89%); m.p. 133–135 °C, RF = 0.32.

Anal. calc. for $C_{15}H_{16}O_4$: C 69.22, H 6.19; found (260.29): C 69.16 H 5.77. IR (KBr): ν_{max} 1240, 3240, 3420 cm^{-1}. ^{1}H-NMR ($CDCl_3$): δ = 3.79 (s, 6H, 2,4-OCH_3), 4.795 (s, 1H, CHO*H*), 5.94 (s, 1H, CH), 6.44 (dd, 1H, 5-H), 6.46 (d, 1H, 3-H), 6.77 (d, 2H, 3′,5′-H), 7.06 (d, 1H, 6-H), 7.23 (d, 2H, 2′,6′-H).

Potassium salt of 2,4-dimethoxy-4′-hydroxybenzhydrol (3). K_2CO_3 (23.9 g, 173 mmol) in ethyl alcohol (200 mL) was added to a suspension of **2** (45.0 g, 173 mmol). The solvent was evaporated off at reduced pressure. The resulting oil was taken up in diethyl ether (250 mL) and the solution was agitated with a glass rod until a crystalline solid formed. The suspension was chilled overnight and filtered to give **3** as a pink solid, which was dried at 45–50 °C and reduced pressure; yield 50.5 g (98%).

IR (KBr): ν_{max} 1240, 3240 cm^{-1}.

4-(2′,4′-Dimethoxyphenylhydroxymethyl)phenoxymethylpolystyrene (4). **3** (44.8 g, 150 mmol) in DMF (300 mL) was added to a suspension of chloromethylpolystyrene (150.0 g, 150 mmol Cl) in DMF (500 mL). The suspension was stirred at r.t. for 72 h. The resin was then washed in turn with DMF (800 mL), MeOH (800 mL), H_2O (800 mL), MeOH (800 mL), CH_2Cl_2 (800 mL) and MeOH (800 mL), and dried; yield 156 g.

A mixture of Fmoc-Ala-OH (0.31 g, 1.0 mmol), HOBt (0.14 g, 1.0 mmol), DCC (0.21 g, 1.0 mmol) and 4-dimethylaminopyridine (0.024 g, 0.2 mmol) in DMF (5 mL) was added to **4** (0.41 g) in DMF (5 mL). The suspension was shaken at r.t. for 4 h, and the resin was washed in turn with DMF (5 mL), MeOH (5 mL) and DMF (5 mL). The coupling was repeated with half quantities of the reagents. After removal of the Fmoc group with 20% piperidine in DMF (5 mL) for 5 and 15 min, the degree of substitution of the resin was determined by the method of Gisin (5).

ACKNOWLEDGMENTS

We thank Éva M. Dósai and Katalin Nagy for their careful technical assistance, András Szász for recording the NMR spectra, Dr. György Dombi for microanalyses and recording the IR spectra, and Dr. Sándor Szalma for evaluation of the NMR spectra.

REFERENCES

1. Wang, S.S. (1973) *J. Am. Chem. Soc.* **95**, 1328–1333
2. Sieber, P. (1987) *Tetrahedron Lett.* **28**, 2107–2110
3. Mergler, M., Tanner, R., Gosteli, J. & Grogg, P. (1988) *Tetrahedron Lett.* **29**, 4005–4008
4. Rink, H. (1987) *Tetrahedron Lett.* **28**, 3787–3790
5. Gisin, B.F. (1972) *Anal. Chim. Acta* **58**, 248–249

Address:

Dr. *Gábor Tóth*
Department of Medical Chemistry
A. Szent-Györgyi Medical University
H-6720 Szeged Dóm tér 8
Hungary

6.2.

MAGYAR SZABADALMI HIVATAL

SZABADALMI OKIRAT

A Magyar Szabadalmi Hivatal az okirathoz fűzött leírás alapján

213 459

lajstromszámon a P 93 02231 ügyszámú bejelentésre
szabadalmat adott.

A szabadalmi bejelentés napja és az oltalmi idő kezdete:

1993. augusztus 2.

A találmány címe:
Eljárás peptidszintézishez alkalmazható szubsztituált difenil-metántartalmú polimerek előállítására

A szabadalom jogosultja:
REANAL Finomvegyszergyár Rt., Budapest

Feltaláló:

dr. Penke Botond, Szeged	18%
Gáll Gaszton, Budapest	12%
dr. Szajáni Béla, Budapest	12%
dr. Tóth Gábor, Szeged	12%
Nyerges Levente, Szeged	10%
Váradi Györgyi, Szeged	10%
Sütő Imre, Budapest	8%
Tóth Anna, Budapest	8%
Szabó András, Kiskunfélegyháza	4%
Dósai M. Éva, Szeged	3%
Nagy Katalin, Kiszombor	3%

Budapest, 1998. január 28.

elnök

(19) Országkód:

HU

MAGYAR KÖZTÁRSASÁG

MAGYAR SZABADALMI HIVATAL

SZABADALMI LEÍRÁS

(11) Lajstromszám:

213 459 A

(21) A bejelentés ügyszáma: P 93 02231
(22) A bejelentés napja: 1993. 08. 02.

(51) Int. Cl.[6]

C 07 K 1/04
C 07 B 57/00

(45) A megadás meghirdetésének a dátuma a Szabadalmi Közlönyben: 1997. 10. 28.

(72) Feltalálók:

dr. Penke Botond, 18%, Szeged (HU)
Gáll Gaszton, 12%, Budapest (HU)
dr. Szajáni Béla, 12%, Budapest (HU)
dr. Tóth Gábor, 12%, Szeged (HU)
Nyerges Levente, 10%, Szeged (HU)
Váradi Györgyi, 10%, Szeged (HU)
Sütő Imre, 8%, Budapest (HU)
Tóth Anna, 8%, Budapest (HU)
Szabó András, 4%, Kiskunfélegyháza (HU)
Dósai M. Éva, 3%, Szeged (HU)
Nagy Katalin, 3%, Kiszombor (HU)

(73) Szabadalmas:

REANAL Finomvegyszergyár Rt., Budapest (HU)

(74) Képviselő:

dr. Tóth-Urbán László és dr. Jalsovszky Györgyné, Budapest

(54) Eljárás peptidszintézishez alkalmazható szubsztituált difenil-metántartalmú polimerek előállítására

(57) KIVONAT

A találmány peptidszintézisben alkalmazható /I/ általános képletű szubsztituált difenil-metán-származékot tartalmazó polimer előállítására vonatkozik, mely során a megfelelő /II/ általános képletű vegyületet – ahol R_1 jelentése –OH, $–NH_2$, $–NH–CO/CH_2/_2–COOH$

és R_2, R_3 és R_4 jelentése az /I/ általános képletnél megadott –

a) abban az esetben, ha R_0 jelentése –OH csoport, hidrogénezik, majd ismert módon a szokásosan alkalmazott hordozó polimerhez kapcsolják; vagy

b) abban az esetben, ha R_0 jelentése $–NH_2$ csoport, szokásosan alkalmazott hordozó polimerhez kapcsolják, majd Leuckart reakcióval formilamino-gyantává alakítják és végül hidrazinolízisnek vetik alá.

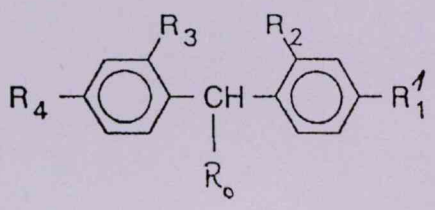

I

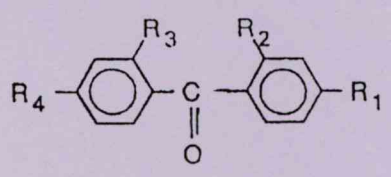

II

HU 213 459 A

A találmány tárgya eljárás peptidkémiai szintéziskben alkalmazható szubsztituált difenil-metán tartalmú polimerek előállítására.

Az /I/ általános képletű vegyületek peptidek szilárd fázisú szintézisére használhatók fel. Az 1964-ben a Nobel díjas R. B. Merrifield által leírt szilárd fázisú peptidszintézis [R. B. Merrifield: Biochemistry *3*, 1385–1390 /1964/; J. M. Stewart és J. D. Young: Solid-Phase Peptide Synthesis Pierce, Illinois 1984] a nyolcvanas évekre gyakorlatilag egyeduralkodóvá vált a peptidek szintézisében. A klasszikus oldalfázisú szintézis csak speciális szerkezetek, illetve ipari méretű szintézisek esetében számít versenytársnak. A szilárd fázisú peptidszintézis sikere döntő mértékben függ az alkalmazott hordozótól [A. R. Mitchell, B. W. Erickson, M. N. Ryabtsev, R. S. Hodges és R. B. Merrifield: J. Amer. Chem. Soc. *98*, 7357 /1976/; The Peptides Vol 2 /Gross, E. és Meienhofer, J. eds/ Academic Press New York, 1980]. Ez különösen az Fmoc-stratégiát alkalmazó eljárások esetén jelent problémát. Az ideális hordozónak stabilnak kell lenni az Fmoc hasítás körülményei között /ismételt bázikus kezelés, pl. 10 tömeg% piperidin-diklór-metánban/ és a szintézis végén a peptid viszonylag enyhe savas kezeléssel eltávolítható kell hogy legyen. Ez utóbbi lépés természetesen együtt jár az oldalfunkciós védőcsoportok eltávolításával és pl. hígított trifluorecetsavval 0 °C-on vagy szobahőmérsékleten végzett rövid idejű /0,5–1 óra/ acidolízist jelent. Az első megemelt savérzékenységű gyantákat már több mint 10 éve leírták, de ezek csak peptidsavak előállítására alkalmasak [S. S. Wang: J. Amer. Chem. Soc. *95*, 1328–1333 /1973/; E. Atherton, H. Fox, D. Harkiss, G. J. Logan, R. C. Sheppard, B. J. Williams: J. Chem. Soc. Chem. Comm. 1978, 537–539] és peptidamidok szintézise enyhe reakciókörülmények között a legutóbbi időkig problematikus volt. A nyolcvanas évek végén számos közlemény jelent meg [G. Breipohl, J. Knolle, W. Stüber: Tetrahedron Letters 1987, 5651–5654; P. Sieber: Tetrahedron Letters 1987, 28. 2107; M. Mergler, R. Nyfeler, R. Tanner, J. Gosteli, P. Grogg: Tetrahedron Letters 1988, 4009; H. Rink: 1987 Tetrahedron Letters 28, 3787–3790; B. Penke, L. Nyerges: Peptide Research 4, 289–295 /1991/] peptidamidok Fmoc stratégiával történő szintézisekhez alkalmas benzhidril alapú hordozók tervezéséről és szintéziséről. Ezek a hordozók természetesen adaptálhatók peptidsavak a korábbiaknál még enyhébb körülmények között történő szintézishez. Néhány ilyen hordozó a következő:

Az /a/ hordozó előállítására Rink az alábbi utat ajánlotta: 4-hidroxi-benzoesavból és rezorcin-dimetiléterből $ZnCl_2$ és $POCl_3$ jelenlétében végzett kondenzáció, majd a kapott benzofenon-származékok kapcsolódása klórmetilezett polisztirol-divinil-benzol kopolimerhez, a kapott „ketongyanta" redukciója $LiBH_4$-el. Azt találjuk, hogy az irodalomban leírt szintézisút számos nehézséggel jár együtt, a gyantán végzett redukció lefutása nem ellenőrizhető, modellkísérleteink tanúsága szerint jelentős mértékű mellékreakcióval kell számolni, a kapott polimer szubsztitúciója alacsony, a megfelelő Fmoc-aminosavval történő észteresítés nehézkes.

A /b/ hordozó előállítására Rink egy meglehetősen komplikáltnak tűnő utat ajánlott. Azt találtuk, hogy az irodalomban leírt szintézisút számos nehézséggel jár együtt, így feleslegesen sok lépésből áll, a gyantán végzett redukció lefutása nem ellenőrizhető, modellkísérleteink tanúsága szerint jelentős mértékű mellékreakcióval kell számolni, a kapott polimer benzhidrol-származék átalakítása Fmoc-aminosavamiddal körülményes, drága és szükségtelen is.

Kutatásaink során új eljárást dolgoztunk ki az /I/ általános képletű vegyületek – ahol

R_o –OH vagy $–NH_2$;

$R_3 = R_4$ jelentése $–OCH_3$;

R_2 jelentése H vagy $–OCH_3$;

R_1 jelentése $–NH–CO–/CH_2/_2–CONH–CH_2–R$ vagy $–O–CH_2–R$

és R jelentése gyanta –

előállítására, mely alkalmas magasabb felületi borítottságú és így a szintézisben előnyösebben alkalmazható polimerek készítésére.

Az /I/ általános képletű vegyületek részben ismertek [/a/–/c/ képletű vegyületek], részben újak.

A találmány szerinti eljárás alapján azon /I/ általános képletű vegyületeket, ahol R_o jelentése –OH csoport úgy állítjuk elő, hogy a /II/ általános képletű vegyületet – ahol

R_1 jelentése –OH, $–NH_2$, $–NH–CO/CH/_2–COOH$,

és R_2, R_3 és R_4 jelentése az /I/ általános képletnél megadott, redukáljuk, majd ismert módon klórmetil polimerhez kapcsoljuk, illetve azon /I/ általános képletű vegyületeket, ahol R_o jelentése $–NH_2$ csoport, úgy állítjuk elő, hogy a /II/ általános képletű vegyületeket ismert módon klórmetil polimerhez kapcsoljuk, majd a kapott „ketongyantát" Leuckart reakcióval formamidban 165 °C-on, ammónium-formát jelenlétében végzett reakcióval formil-amino gyantává alakítjuk, majd formilcsoportot etanolban végzett hidrozinolízissel eltávolítjuk és így peptidszintézisre közvetlenül felhasználható hordozóhoz jutunk.

A Leuckart-reakciót a Chemische Berichte *22*, 1413 /1889/ közlemény ismerteti.

A találmány szerinti eljárással nyert polimerek alkalmasak peptidaminok és peptidsavak előállítására egyaránt.

A találmány szerinti eljárást részletesebben például az alábbiak szerint valósítható meg:

a) abban az esetben, ha R_o jelentése –OH csoport:

a 4-amino-szalicilsav N-acetilezése után elkészítjük a 4-acetamido-szalicilsav metiléterét, majd a közben észteresedett karboxil-csoportot lúgos hidrolízissel felszabadítjuk. Ez után rezorcin-dimetilészterrel kondenzáljuk $ZnCl_2$ és $POCl_3$ jelenlétében, így megkapjuk a 4-acetamido-2,2'4'-trimetoxi-benzofenont, majd az N-acetil-csoportot lúgos hidrolízissel eltávolítjuk. A kapott 4-amino-2,2'4'-trimetoxi-benzofenont $LiBH_4$-el redukáljuk, majd aminocsoportján borostyánkősavval acilezzük és a kapott 4-szukcinilamino-2,2'4'-trimetoxi-benzhidrolt aminometil-gyantához kapcsolva peptidszintézisre közvetlenül felhasználható hordozóvá alakítható. Azt találtuk, hogy a 4-acetamido-benzoesavból kiinduló szintézis terméke, a 2,4-dimetoxi-4'-szukcinilamino-

benzhidrol polimer is kellő savérzékenységgel rendelkezik, viszont lényegesen olcsóbban és egyszerűbben előállítható. Ez esetben első lépésként elkészítjük a 4-acetamido-benzoesavat, majd ezt közvetlenül az előzőekben leírt módon rezorcin-dimetil-éterrel kondenzáljuk, majd a továbbiakban az előzőekben leírtak szerint járunk el.

b) abban az esetben, ha R_0 jelentése $-NH_2$ csoport a 4-amino-szalicilsav N-acetilezése után elkészítjük a 4-acetamido-szalicilsav metiléterét, majd a közben észteresedett karboxilcsoportot lúgos hidrolízissel felszabadítjuk. Ezután rezorcin-dimetil-éterrel kondenzáljuk $ZnCl_2$ és $POCl_3$ jelenlétében, így megkapjuk a 4-acetamido-2,2'4'-trimetoxi-benzofenont, majd az N-acetilcsoportot lúgos hidrolízissel eltávolítjuk, borostyánkősavval acilezzük és a kapott 4-szukcinilamino-2,2'4'-trimetoxi-benzofenont aminometil-gyantához kapcsolva, majd az ezt követő, az előzőekben leírt Leuckart reakcióval a megfelelő formilamino vegyületté alakítjuk. Ez utóbbi hidrazinolizis után a peptidszintézisre közvetlenül felhasználható hordozóvá alakítható /B. Penke, J. Rivier: J. Org. Chem. 1987, *52* 1197–1200/. Azt találtuk, hogy a 4-acetamido-benzoesavból kiinduló szintézis terméke, a 2,4-dimetoxi-4-szukcinilamino-benzhidrilamin polimer is kellő savérzékenységgel rendelkezik, viszont lényegesen olcsóbban és egyszerűbben előállítható. Ez esetben első lépésként előkészítjük a 4-amino-benzoesavat, majd ezt közvetlenül az előzőekben leírt módon rezocin-dimetil-éterrel kondenzáljuk, majd a továbbiakban az előzőekben leírtak szerint járunk el.

Az a) illetve b) eljárásváltozatban a kívánt /I/ általános képletnek megfelelő kiindulási anyagokat alkalmazzuk.

Az eljárást részletesebben az alábbi példákkal szemléltetjük.

1. példa

2,4,4'-Trimetoxi-benzhidrol polimer szintézise

a) 60 g /0,5 mól/ p-hidroxi-benzoesavat és 100 ml /0,75 mól/ rezorcin-dimetilétert 150 g /1,1 mól/ $ZnCl_2$ és 350 ml /3,5 mól/ $POCl_3$ jelenlétében 65 °C-on másfél órán át kevertettünk. Ezután kb. 1 kg jégre öntöttük, 500 ml etil-acetáttal extraháltuk. A szerves fázist 200 ml 10 tömeg%-os Na_2CO_3 oldattal mostuk, Na_2SO_4-en megszárítottuk, szűrtük, bepároltuk. A párlási maradékot kb. 100 ml dietil-éterből kristályosítottuk.

A termelés: 52,2 g /42 %/.

Op.: 138–139 °C,

R_f = 0,4 /benzol : jéceget 7 : 1/. $C_{25}H_{14}O_4$; M = 258,26.

2. példa

2,4,4'-Trimetoxi-benzhidril-amin polimer szintézise

a) 60 g /0,5 mól/ p-hidroxibenzoesavat és 100 ml /0,75 mól/ rezorcin-dimetil-étert 150 g /1,1 mól/ $ZnCl_2$ és 350 ml /3,5 mól/ $POCl_3$ jelenlétében 65 °C-on másfél órán át kevertettünk. Ezután kb. 1 kg jégre öntöttük, 500 ml etil-acetáttal extraháltuk. A szerves fázist 200 ml 10 tömeg %-os Na_2CO_3 oldattal mostuk, Na_2SO_4-en megszárítottuk, szűrtük, bepároltuk. A párolási maradékot kb. 100 ml dietil-éterből kristályosítottuk.

Termelés: 52,2 g /42 %/.

Op.: 138–139 °C;

R_f = 0,4 /benzol: jégecet 7:1/. $C_{25}H_{14}O_4$; M = 258,26.

b) 10 g /39 mmól/ 2,4-dimetoxi-4'-hidroxi-benzofenont 10 g ammónium-formiát és 90 ml formamid jelenlétében 165 °C-on 8 órán át kevertettünk. A reakció lefutását kloroform-metanol 8:2 elegyben vékonyrétegkromatográfiásan ellenőrizzük. A reakció lejátszódása után keverés közben 1,5 liter 2 tömeg%-os $KHSO_4$ oldatba öntöttük a reakcióelegyet, majd háromszor 300 ml etil-acetáttal kimostuk. Az egyesített etil-acetátos fázist kétszer 200 ml 2 tömeg% $KHSO_4$ oldattal és kétszer 200 ml vízzel mostuk, Na_2SO_4-en szárítottuk, majd megszűrtük és bepároltuk. A párlási maradékot 200 ml éter és 100 ml n-hexán elegyéből kristályosítottuk.

Termelés: 8,5 g /77 %/.

Op.: 127–130 °C.

R_f = 0,72 /etilacetát : n-butanol : jégecet: víz 98 : 7,5 : 1 : 2,4/.

c) 28,8 g /100 mmól/ 2,4'-dimetoxi-4-hidroxi-N-formil-benzhidril-amint 100 ml dimetil-formamidban oldottunk, majd hozzáadtunk 27,6 g /150 mmól/ m-klór-toluilsav-metilésztert és 30 g /200 mmól/ cézium-fluoridot. Két napig 70 °C-on kevertettük, majd bepároltuk és 250 ml víz és 250 ml etil-acetát elegyében oldottuk. Az etil-acetátos fázist mostuk 200 ml vízzel, megszárítottuk, bepároltuk, éterből kristályosítottuk.

Termelés: 30 g /69 %/.

Op.: 125–127 °C.

d) 20,1 g /46 mmól/ 2,4-dimetoxi-4'-/3-metoxi-karbonil/-benzil-oxi-N-formil-benzhidril-amint 150 ml metanol és 23 ml 4n NaOH elegyében 60 percig refluxáltunk. A metanolt bepároltuk, a vizes fázis pH-ját 1 : 1 HCl-lel 3-ra állítottuk és háromszor 100 ml etil-acetáttal extraháltuk. Az etil-acetátos fázist szárítottuk; bepároltuk, a maradékot éterből kristályosítottuk.

Termelés: 15,1 g /78 %/.

R_f = 0,63 /etil-acetát : n-butanol : jégecet : víz 98 : 7,5 : 1 : 2,4/.

e) 20 g /17 mmól/ aminometil-polimert 20 percig 100 ml diklór-metánban duzzasztottunk, majd 11 g /26 mmól/ 2,4-dimetoxi-4'-[3-karboxi-benzil-oxi]-N-formil-benzhidril-amint és 5,4 g /26 mmól/ DCC-t adtunk hozzá. Ezután 12 órán át rázattuk, majd 200 ml dimetil-formamiddal, 200 ml diklór-metánnal és 200 ml metanollal mostuk.

f) 26 g, az előzőekben kapott polimert 300 ml metanol és 20 ml hidrazinhidrát, valamint 36 ml jégecet jelenlétében 12 órán át refluxáltattunk, majd 0,5 l metanollal, 0,5 l diklór-metánnal mostuk. A kapott aminocsoport tartalma 0,61 mmól/g/ pikrinsav-tesztből, Gisin B. F.: Helv. Chim. Acta, 56, 1476 (1973)/.

3. példa

/Polimer/ 4-benziloxi-2',4'-dimetoxi-benzofenon

10,32 g /40 mmól/ 4-benziloxi-2',4'-dimetoxi-benzofenont oldottunk 200 ml etanolban és hozzáadtunk 6 g /40 mmól/ CsOH-t, 100 ml metanolban oldva. Az oldatot szárazra pároltuk, egy éjjel exszikkátorban szárítottuk, éterrel eldörzsöltük, a sárgásfehér kristályos anyagot kiszűrtük, éterrel mostuk és szárítottuk. Termelés: 15,6 g benzofenon-fenolát-Cs-só.

40 g /40 mmól/ 1 tömeg% divinil-benzolt tartalmazó klór-metil-polimert /1 mmól Cl /g/ 150 ml DMF-ben duzzasztottunk, hozzáadtunk 15,6 g /40 mmól/ benzo-

fenon-fenolát-Cs-sót 100 ml DMF-ben oldva. A szuszpenziót 3 napig szobahőmérsékleten rázattuk, a gyantát kiszűrtük, a szűrőn kétszer 150 ml DMF-dal, háromszor 100 ml metanollal, háromszor 250 ml diklór-metánnal, végül újból háromszor 100 ml metanollal mostuk, szárítottuk. Termelés: 47,5 g polimer /a Cl-tartalom kb. 50%-a reagált el és cserélődött ki a dimetoxi-benzofenon-származékra/.

/Polimer/ 4-(benzil-oxi)-2',4'-dimetoxi--N-formil-benzhidril-amin

47,5 g /20 mmól/ előző polimert 50 g ammónium-formiát és 450 ml formamid keverékében szuszpendáltunk és 24 órán át 165 °C-on reagáltattuk az elegyet állandó erős keverés közben. A reakcióelegyből 3–4 óránként mintát vettünk és ellenőriztük infravörös spektrum alapján a reakció lejátszódását /a benzofenon keto-csoportjának eltűnését/. A reakcióelegyet 50–55 °C-ra lehűtöttük, a polimert kiszűrtük, ötször 250 ml vízzel, háromszor 150 ml metanollal, háromszor 300 ml diklór-metánnal, végül újabb háromszor 150 ml metanollal mostuk, szárítottuk.

Termelés: 48 g formil-amin-polimer.

/Polimer/ 4-(benzil-oxi)-2,4-dimetoxi-benzhidril--amin /TMBHA-polimer/

48 g /20 mmól/ formil-amin-polimert 1000 ml etanolban szuszpendáltunk, hozzáadtunk 60 ml hidrazin-hidrátot és 112 ml ecetsavat és az elegyet 12 órán át refluxáltuk. A szuszpenziót lehűtöttük, a polimert kiszűrtük, háromszor 200 ml vízzel, háromszor 150 ml metanollal, háromszor 300 ml diklór-metánnal mostuk, végül háromszor 150 ml metanollal mostuk, szárítottuk. Termelés: 46 g. A polimer grammonként 0,43 mmól aminocsoportot tartalmaz a pikrinsavas meghatározás /Gisin-teszt/ szerint.

5. példa

2',4'-Dimetoxi-4-acetamido-benzofenon

12,5 g N-acetil-p-amino-benzoesav (acetil-PABA) /62,2 mmól/, 13 g rezorcin-dimetil-éter /12 cm^3/ és 18,7 g /137 mmól/ vízmentes $ZnCl_2$ keverékéhez 100 cm^3 $POCl_3$-ot adtunk, majd 70 °C-on 1 órán át kevertük, míg a reakcióelegy sötétvörösre színeződött. A $POCl_3$-ot vákuumban bepároltuk. A maradékból sok jég hozzáadása után lila kristályos anyag vált ki. A szilárd anyagot kiszűrtük, vízzel, Na_2CO_3-oldattal és éterrel mostuk. A terméket metanol-H_2O-elegyéből kétszer átkristályosítottuk. Termék: 7 g fehér kristályos anyag /32 %/.

R_f: 0,67 /A/; 0,54 /B/; 0,40 /C/; 0,89 /D/; 0,85 /E/

Elemanalízis:

számított: C % = 68,22; H % = 5,27;
talált: C % = 70,09; H % = 4,51.

6. példa

2',4'-Dimetoxi-4-amino-benzofenon

4,72 g 2',4'-dimetoxi-4-acetamido-benzofenont /15 mmól/ oldottunk 30 cm^3 4 mól KOH és 30 cm^3 metanol elegyében. Az elegyet 1,4 órán át refluxáltuk. A metanolt vákuumban lepároltuk. A vizes oldatból hűtésre sárga kristályos anyag vált ki. Szűrés, vizes mosás és szárítás után 3,5 g anyag keletkezett /86 %/.

Op.: 147–149 °C.

R_f: 0,73 /A/; 0,68 /B/; 0,84 /C/; 0,86 /D/; 0,93 /E/

Elemanalízis:

számított: C % = 70,02; H % = 5,88;
talált: C % = 69,33; H % = 6,27.

7. példa

2',4'-Dimetoxi-4-(szukcinil-amido)-benzofenon

1,9 g /7 mmól/ 2',4'-dimetoxi-4-amino-benzofenont 10 cm^3 piridinben oldottunk, majd hozzáadtunk 1,40 g /14 mmól/ borostyánkősav-anhidridet. Az oldatot 15 percig refluxáltuk. A piridint vákuumban lepároltuk, a kapott olajat EtOAc-0,1 M HCl elegyében vettük fel. A szerves fázist elválasztottuk, vízzel mossuk. Az oldószert felére pároltuk. Éter hozzáadására és hűtésére kristályos anyag vált ki, melynek tömege szűrés, vizes és éteres mosás után 1,6 g /61 %/.

R_f: 0,10 /A/; 0,11 /B/; 0,93 /D/

Elemanalízis:

számított: C % = 63,86; H % = 64,63;
talált: C % = 5,36; H % = 5,69.

8. példa

2',4'-Dimetoxi-4-(szukcinil-amido)-benzofenon-oxim

1,0 g /2,7 mmól/ 2',4'-Dimetoxi-4-(szukcinil-amido)--benzofenont 2 cm^3 piridin és 10 cm^3 EtOH elegyében oldottunk, majd hozzáadtunk 0,5 g /0,7 mmól/ hidroxil-amin-hidrokloridot. Az oldatot 1 órán át forraltuk, majd az oldószert vákuumban lepároltuk. A kapott olajat 5 tömeg% -os $KHSO_4$ oldattal dörzsöltük el. A kiváló kristályos anyagot kiszűrtük, vízzel mostuk, szárítottuk.

Termelés: 0,9 g fehér anyag /87 %/.

R_f: 0,0 /A/; 0,80 % /E/; 0,91 % /D/

Elemanalízis:

számított: C % = 61,28; H % = 61,64;
talált: C % = 5,41; H % = 5,69.

9. példa

2',4'-Dimetoxi-4-amino-difenil-karbinol

1,5 g /5,55 mmól/ 2',4'-dimetoxi-4-amino-benzofenont 35 cm^3 absz. THF-ben oldottunk, majd 0,25 g /11,1 mmól/ $LiBH_4$-et adtunk hozzá. Az oldatot 20 percig refluxáltuk, majd lehűlés után kb. 40 cm^3 metanolra öntöttük. A $LiBH_4$ elbomlása után az oldatot vákuumban bepároltuk. A kapott szilárd maradékot EtOAc–H_2O elegyében felvettük. A szerves fázist elválasztottuk, majd az EtOAc-ot lepároltuk. Sárgásfehér kristályos anyag maradt vissza, ezt éterrel mostuk, szárítottuk.

R_f: 0,46 /A/; 0,36 /B/; 0,93 /E/; 0,33 /C/, 0,86 /D/

Op.: 90–93 °C.

Elemanalízis:

számított: C % = 69,48; H % = 6,61;
talált: C % = 69,79; H % = 6,59.

10. példa

a) 50 g /194 mmól/ 2,4-dimetoxi-4'-hidroxi-benzofenont felvettünk 800 ml THF-ban és 6,34 g /291 mmól/ lítium-borohidridet részletekben hozzáadtunk. A reakcióelegyet 15 percig refluxáltattuk. A $LiBH_4$ feleslegét metanollal elbontottuk. Az oldatot bepároltuk és a párlási maradékot megosztottuk 600 ml etil-acetát és 200 ml víz

között. A szerves fázist Na_2SO_4-tal szárítottuk, szűrtük, betöményítettük. A terméket a bepárlás végén kristályos formában nyertük, majd dietil-éterrel mostuk.
Termelés: 45 g /89 %/.
Op.: 133–135 °C.
R_f = 0,32 /kloroform: aceton 9:1/ $C_{15}H_{16}O_4$; M = 260,29.

b/ 23,9 g /173 mmól/ kálium-karbonát etanolos szuszpenzióját hozzáadtuk 45 g /173 mmól/ 2,4-dimetoxi-4'-hidroxi-benzhidrol etanolos szuszpenziójához, majd az oldószert lepároltuk. A párlási maradékot kb. 250 ml dietil-éterből kristályosítottuk.
Termelés: 50,5 g /98 %/. $C_{15}H_{15}O_4K$; M = 298,37.

c/ 44,8 g /159 mmól/ káliumsót 300 ml DMF-ben felvettünk és 150 g /150 mmól Cl/ klór-metilezett polisztirol gyanta 500 ml DMF-fel készített szuszpenziójához adtuk. Szobahőmérsékleten kevertettük 72 óráig. Mostuk DMF-ral, metanollal, vízzel, metanollal, diklór-metánnal, metanollal /500–500 ml/.
Termelés: 156 g polimer.

11. példa

a) 2,8 g /9,75 mmól/ 2,2'4'-trimetoxi-4'-amino-benzofenont felvettünk 30 ml tetrahidrofuránban és részletekben hozzáadtunk 0,64 g /29,2 mmól/ lítium-borohidridet. Az oldatot 1,5 óráig refluxáltattuk. A $LiBH_4$ feleslegét metanollal elbontottuk, az oldatot bepároltuk, a párlási maradékot megosztottuk 45 ml etil-acetát és 15 ml víz között. A szerves fázist Na_2SO_4-tal szárítottuk, bepároltuk. A terméket kb. 30 ml dietil-éterből kristályosítottuk. Termelés: 2,8 g /100%/.
R_f = 0,67 /1,38 tömeg% n-butanol, 0,18 tömeg% ecetsav, 98,44 tömeg% víz/.
$C_{16}H_{19}NO_4$; M = 289,33.

b) 2,8 g /9,75 mmól/ 2,2'4'-trimetoxi-4'-amino-benzhidrolt felvettünk 15 ml piridinben, hozzáadtunk 0,98 g /9,75 mmól/ borostyánkősav-anhidridet és 1,5 órán keresztül 30–40 °C-on tartottuk. A piridint lepároltuk, a párlási maradékot etil-acetátban felvettük, csontszenet adtunk hozzá és 5 percig refluxáltattuk. A csontszenet kiszűrtük, az oldószert csökkentett nyomáson eltávolítottuk. A terméket dietil-éterből kristályosítottuk.
Termelés: 2,9 g /76,4 %/.
R_f = 0,31 /1,38 tömeg% n-butanol, 0,18 tömeg% ecetsav, 98,44 tömeg% víz/.
$C_{20}H_{23}NO_7$; M = 389,41.

c) 1,75 g /1 mmól/ 0,57 mmól/g borítottságú 4-metil-benzhidrilamin (MBHA) polimert felvettünk 10 ml DMF-ben. Hozzáadtunk 1g /2,57 mmól/ 2,2',4'-trimetoxi-4'-(szukcinil-amido)-benzhidrolt és 0,53 g /2,57 mmól/ diciklohexil-karbodiimidet. A reakcióelegyet egy éjjelen kevertettük. Másnap a polimert mostuk DMF-dal, metanollal, diklór-metánnal, metanollal /10–10 ml/.
Termék: 2,1 g polimer.

SZABADALMI IGÉNYPONT

1. Eljárás peptidszintézisnél alkalmazható /I/ általános képletű szubsztituált difenil-metánt – ahol
R_0 –OH vagy $–NH_2$;
R_3 és R_4 jelentése $–OCH_3$;
R_2 jelentése H vagy $–OCH_3$;
R_1 jelentése $–NH–CO–/CH_2/_2–CONH–CH_2–R$ vagy $–O–CH_2–R$
és R jelentése gyanta –
tartalmazó polimer előállítására, *azzal jellemezve*, hogy a megfelelő /II/ általános képletű vegyületet – ahol
R_1 jelentése –OH, $–NH_2$, $–NH–CO/CH_2/_2–COOH$
és R_2, R_3 és R_4 jelentése az /I/ általános képletnél megadott –

a) abban az esetben, ha R_0 jelentése –OH csoport, hidrogénezzük, majd ismert módon a szokásosan alkalmazott hordozó polimerhez kapcsoljuk; vagy

b) abban az esetben, ha R_0 jelentése $–NH_2$ csoport, szokásosan alkalmazott hordozó polimerhez kapcsoljuk, majd Leuckart reakcióval formil-amino-gyantává alakítjuk és végül hidrazinolízisnek vetjük alá.

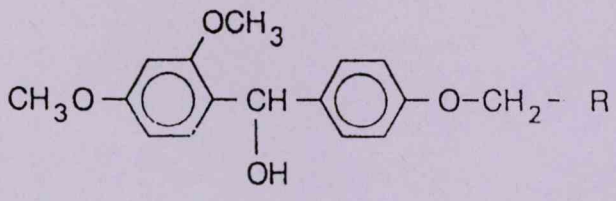

/a/

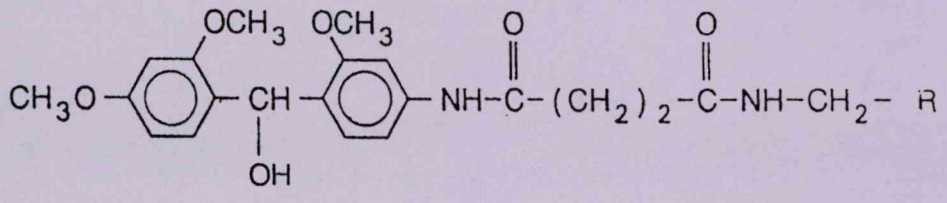

/c/

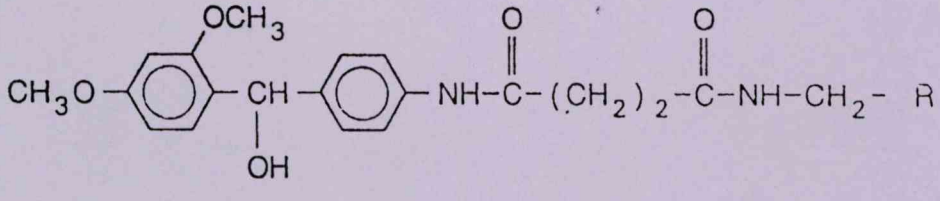

/e/

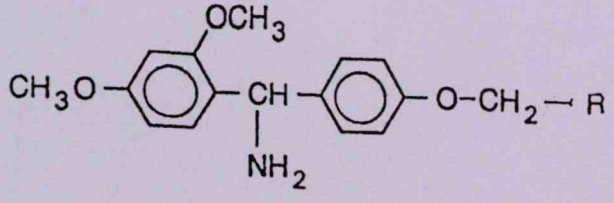

/b/

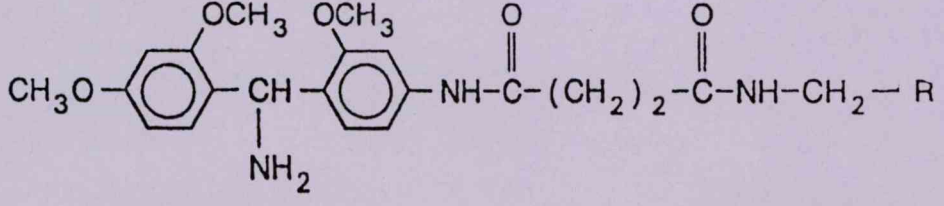

/d/

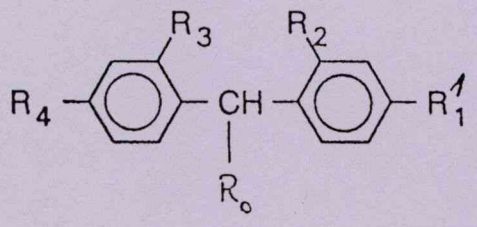

I

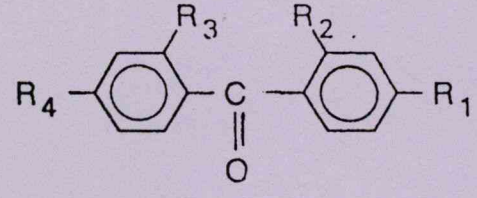

II

Kiadja a Magyar Szabadalmi Hivatal, Budapest
A kiadásért felel: Gyurcsekné Philipp Clarisse osztályvezető
Állami Nyomda Rt. ✆ 260-0451 Fax: 260-3632
E-mail: allami.nyomda@lang.hu – Internet: http://www.lang.hu/allami.nyomda

Peptides 1992
C.H. Schneider and A.N. Eberle (Eds.)

Substituted benzhydrol derivatives as linkers for solid-phase peptide synthesis

György Váradi, Gábor K. Tóth, András Szabó, Levente Nyerges and Botond Penke

Department of Medical Chemistry, A. Szent-Györgyi Medical University, Dóm tér 8, H-6720 Szeged, Hungary

Introduction

A promising resin for the synthesis of peptides with Fmoc chemistry and free carboxyl at the C-terminus is 2,4-dimethoxyphenyl-4'-hydroxymethyl-phenoxymethyl-polystyrene of Rink [1]. Previously we demonstrated the use of 2,4,2'-trimethoxy-4'-succinylamido-benzhydrylamine-polystyrenes for the synthesis of sensitive peptide amides. Based on these results we wanted to design and synthesize a new acid-labile polymer for the synthesis of peptides with free C-terminus. The most commonly used procedure for the preparation of such carriers is the synthesis of the 'keton-resin' and the subsequent reduction. We attempted to synthesize the polymer of Rink by following the above method but we obtained low and unrepeatable substitution. Besides, the structure of the polymer could not be determined accurately.

Results and Discussion

In order to prepare the polymer of Rink we first synthesized the ready linker (2,4-dimethoxy-4'-hydroxy-benzophenone) as described in the literature [1]. Investigation of the reduction showed that it proceeded in 15 min instead of the previously described 1 h. If we continued the reduction, the amount of by-products gradually

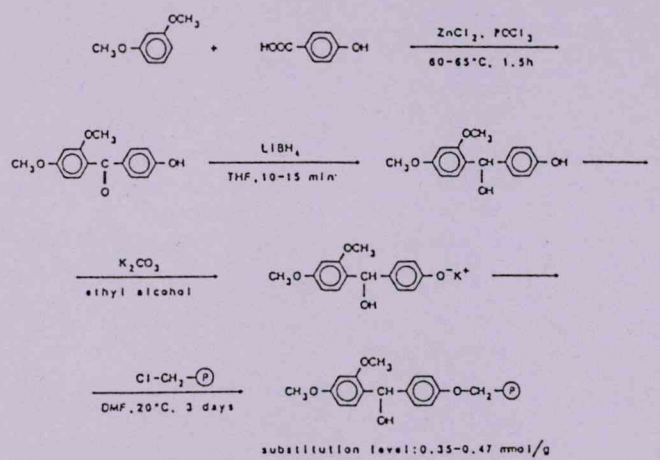

Fig. 1. The new synthesis of 2,4-dimethoxyphenyl-4'-hydroxymethyl-phenoxymethyl-polystyrene of Rink.

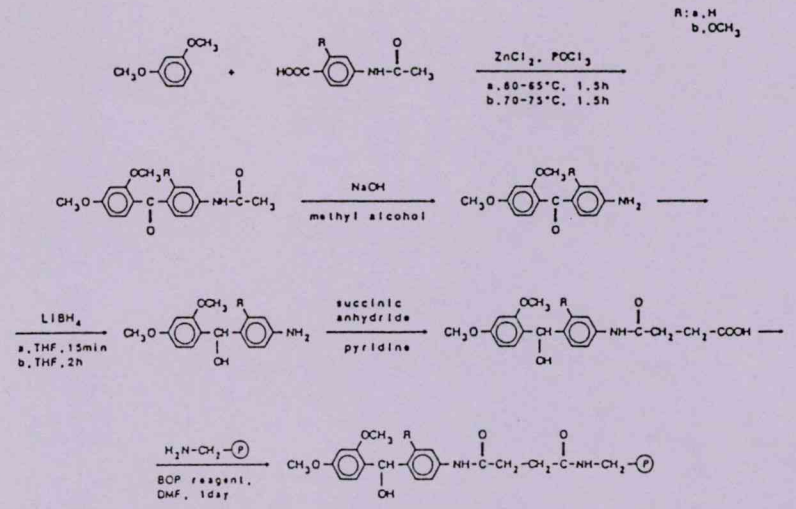

Fig. 2. The synthesis of 2,4-dimethoxy- and 2,4,2'-trimethoxy-4-succinylamido-benzhydrol-polystyrenes.

increased. One of them is probably a diphenylmethane derivative. For the coupling of the linker to chloromethylpolystyrene, beside the known procedure using cesium salt, we tried to use potassium salt of the phenolate too. This latter process resulted in a cheaper method and better resin as regards substitution than the use of cesium salt (Fig. 1). The structure and purity of the substances were proved via NMR, IR spectra and elemental analyses, the substitution degree by coupling of an Fmoc amino acid. We achieved a convenient level of substitution (0.35–0.47 mmol/g). Based on previous experiments we designed two new, even more acid-labile, carriers for the synthesis of peptides with free C-terminus. These are 2,4-dimethoxy- and 2,4,2'-trimethoxy-4'-succinylamido-benzhydrol-polystyrenes.They were synthesized in analogy of the method worked out in the case of the polymer of Rink. The starting materials (2,4-dimethoxy- and 2,4,2'-trimethoxy-4'-acetamidobenzophenone) were prepared from 2-methoxy-4-acetamido-salicylic acid and resorcinol dimethylether. After hydrolysing of the acetyl group the compounds were reduced and the succinyl derivatives of the linkers were coupled then to aminomethylpolystyrene (Fig. 2.). The characterisation of these new resins using model peptide synthesis is in progress.

References

1. Rink, H., Tetrahedron Lett., 28(1987)3787.
2. Penke, B. and Nyerges, L., Pept. Res., 4(1991)289.

6.4.

THE *H*-PHOSPHONATE APPROACH TO THE SYNTHESIS OF PHOSPHOPEPTIDES ON A SOLID-PHASE

Zoltán Kupihár, Zoltán Kele and Gábor K. Tóth*

Department of Medical Chemistry, University of Szeged, H-6720 Szeged, Dóm tér 8., Hungary

Abstract: Ammonium *tert*-butyl *H*-phosphonate was used for the phosphorylation of Tyr- and Ser-containing peptides synthesized by an Fmoc strategy. This reaction, leading to a monoprotected peptide phosphate, was found to be highly efficient and generally applicable. Moreover, the method employed avoids undesired side-reactions during chain elongation (pyrophosphate formation and β-elimination catalysed by piperidine).

Keywords: peptide, solid-phase synthesis, phosphorylation, *H*-phosphonate method, phosphopeptide

The phosphorylation of proteins is probably the most important reversible element of the cell regulation. The involvement of tyrosine phosphorylation/dephosphorylation in this process is well known, and a similar controlling mechanism involving serine/threonine phosphorylation was recently discovered.[1] The isolation of phosphorylated peptides/proteins from biological sources for functional or conformational studies is usually not feasible, and there is therefore a need for efficient chemical phosphorylation methods. Although many papers on phosphopeptide synthesis were published in the past decade, a universal method which can be applied with high efficiency in all cases does not exist. From a chemical point of view, the problems arising during peptide phosphorylation can be divided into two groups:

1. In the case of tyrosine: the decreased nucleophilicity of the phenolic hydroxyl group inhibits the application of phosphoric acid-based phosphorylation reagents (e.g. phosphochloridates[2,3] or phosphoric anhydride[4]). Moreover, pyrophosphate formation may take place if an unprotected phosphate moiety is introduced.[5]

2. In the case of serine or threonine: after incorporation of the phosphate moiety, the molecule can undergo different side-reactions. The most important of these is the β-elimination catalysed by piperidine used for Fmoc deprotection during chain elongation, resulting in a loss of phosphate and formation of the corresponding dehydropeptide.[6]

To overcome these difficulties, many reagents have been tried and introduced into phosphopeptide chemistry.[3,7-13] The routinely used P(III) phosphoramidite derivatives[9-13] can be applied successfully in phosphotyrosine synthesis. However, for phosphoserine/phosphothreonine-containing peptides, application of these symmetrically protected derivatives may lead to the above-mentioned side-reaction.

To eliminate these problems, one of the most widely used and favourable methods makes use of monoprotected phosphate-containing building blocks of Tyr, Ser and Thr.[14] On the other hand, the

*Corresponding author: toth@ovrisc.mdche.u-szeged.hu, fax: +36 62 545971 tel: +36 62545139.

synthesis of these monomers is multistep and tedious. The only reagent that can be applied universally to introduce a monoprotected phosphate into any hydroxyl group-containing peptide is an unsymmetrically protected phosphoramidite.[15] Unfortunately, phosphoramidites are difficult to synthesize, subject to decomposition and oxidation, and expensive to use.

Another alternative to prepare monoprotected peptide phosphates is the use of *H*-phosphonates (phosphonic acid monoesters) that have been applied successfully in oligonucleotide synthesis.[16,17] Subsequent oxidation after phosphorylation of a free hydroxyl function with the corresponding *H*-phosphonate yields the desired monoprotected peptide phosphate. Being P(III) compounds, *H*-phosphonates exhibit the same reactivity as phosphoramidites, but are much less sensitive to oxidation and moisture. To date, the only case where the *H*-phosphonate method has been applied in solid-phase peptide synthesis is the phosphorylation of an *N*-terminal Ser residue with benzyl *H*-phosphonate.[18] We describe here a universally applicable phosphopeptide synthesis involving the *H*-phosphonate approach,

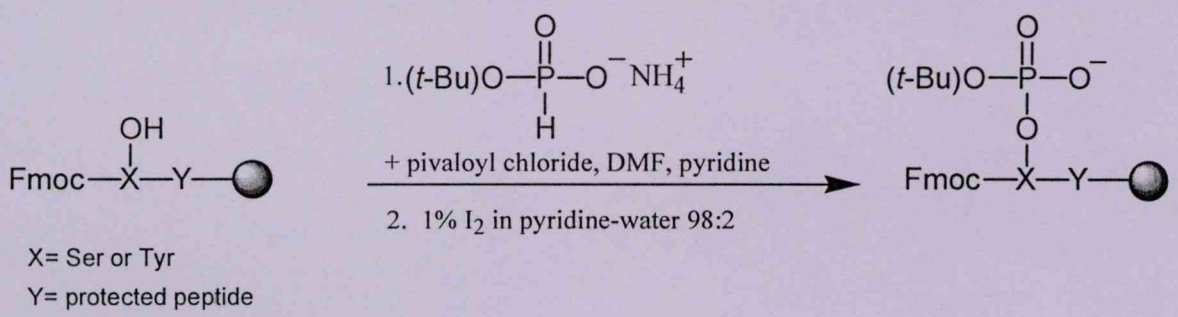

with ammonium *tert*-butyl *H*-phosphonate as phosphorylating agent (Scheme 1).

Scheme 1

1a	S(*P*)ALPG-OH
1b	RKKRIS(*P*)ALPG-OH
2a	Y(*P*)VPMTGP-NH_2
2b	IQEANY(*P*)VPMTGP-NH_2

Table 1

The phosphopeptide sequences synthesized.

(*P*) denotes side-chain phosphorylation

The peptides listed in Table 1 were synthesized by the Fmoc protocol, applying Tentagel SRAM and HMP resins for Tyr- and Ser-containing peptides, respectively. Phosphorylation was performed on the resin directly after incorporation of the free hydroxyl-containing Ser/Tyr residue through the use of 10 equivalents of ammonium *tert*-butyl *H*-phosphonate† and 10 equivalents of pivaloyl chloride in DMF/pyridine 1:1 for 2 h at room temperature. Subsequent oxidation was carried out with 1% I_2 in

†Ammonium *tert*-butyl *H*-phosphonate was prepared from diphenyl phosphite by a literature method.[19]

pyridine/water 98:2 at room temperature for 2 h. After phosphorylation, chain elongation was performed in the usual manner (the carboxamide functions of Gln and Asn were protected with the trityl group). Final cleavage and deprotection were carried out with a TFA/DTT/water 95:2.5:2.5 (v/w/v) mixture.

To monitor the phosphate incorporation and possible side-reactions, after phosphorylation followed by oxidation an aliquot of each peptide (**1a** and **2a**) was cleaved off the resin. LC-MS analyses of the resulting mixtures revealed >90% phosphate incorporation for both Tyr and Ser (illustrated for Tyr in Fig. 1). Surprisingly, iodination of the Tyr aromatic ring could not be detected‡, while oxidation of the Met side-chain was negligible (<1%, Fig. 1, peak a).The desired peptides **1b** and **2b** were obtained in high yield, as determined by HPLC (illustrated on **1b** in Figs 2 and 3). Therefore, significant β-elimination did not take place during chain elongation for the Ser-containing peptide.

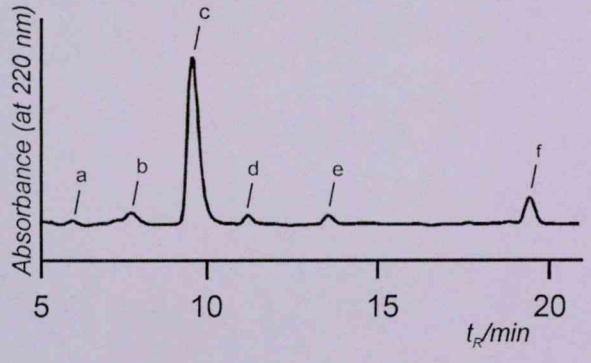

Figure 1

HPLC chromatogram of crude peptide ***2a.***
Peaks were analysed by ESI-MS:
a) *m/z*$^+$ 859.6 $[M+H]^+$ of the Met-oxidized by-product of peptide **2a**
b), d), e) unidentified peaks
c) *m/z*$^+$ 843.1 $[M+H]^+$ of peptide **2a** ($M_{calc.}$ 842.35)
f) *m/z*$^+$ 763.4 $[M+H]^+$ of non-phosphorylated peptide **2a**

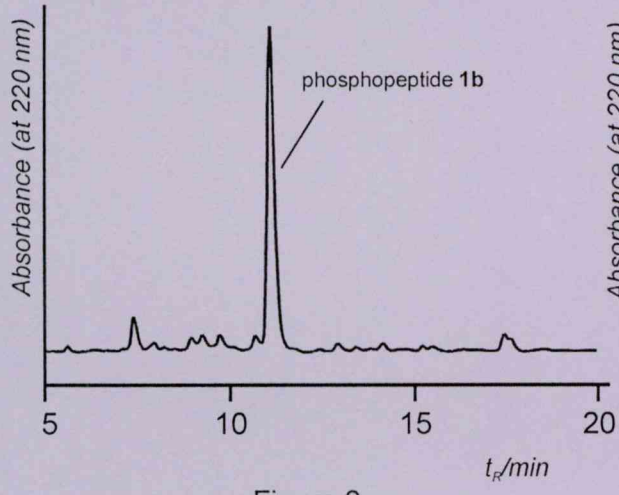

Figure 2

HPLC chromatogram of crude peptide ***1b.***
Major peak identified by ESI-MS
($M_{calc.}$ 1204.69, found *m/z*$^+$ 1205.1 $[M+H]^+$)

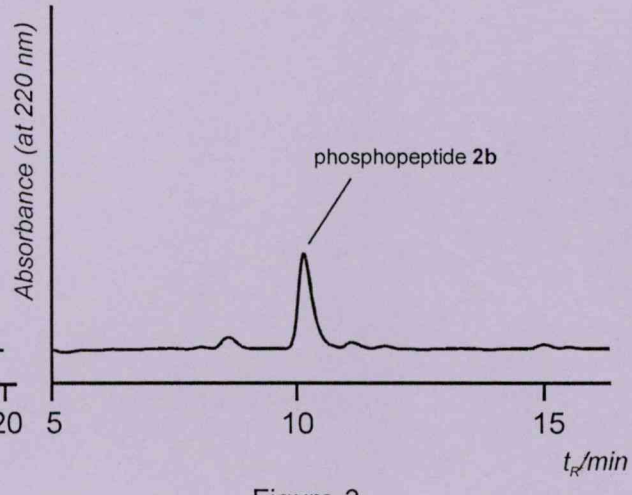

Figure 3

HPLC chromatogram of crude peptide ***2b.***
Major peak identified by ESI-MS
($M_{calc.}$ 1398.49, found *m/z*$^+$ 1399.2 $[M+H]^+$)

‡Although some small peaks (Figure 1, peaks b, c and d) could not be identified, the *m/z* values of M1 (monoiodination) or M2 (diiodination) were not observed by mass screening.

In summary, we have successfully applied the *H*-phosphonate method for the phosphorylation of Ser- and Tyr-containing peptides on solid-phase with high efficiency and without considerable side-reactions during oxidation following phosphorylation and chain elongation. Ammonium *tert*-butyl *H*-phosphonate is inexpensive, easy to synthesize and purify, and less sensitive to oxidation than the phosphoramidite reagents. Furthermore, final removal of the *tert*-butyl group can be performed under milder conditions as compared to the benzyl group in the previously described benzyl *H*-phosphonate. The method published here offers a cheaper and more convenient alternative over the phosphoramidite approach for phosphorylation of any hydroxyl group-containing peptide.

Acknowledgements. This research was supported by grants OTKA T-022540 and FKFP No. 0597/1999.

REFERENCES

1. Hunter, T. *Cell* **2000**, *7*, 113-127.
2. Ötvös, L. Jr.; Elekes, I.; Lee., V. M-Y. *Int. J. Pept. Protein Res.* **1989**, *34*, 129-133.
3. Hoffmann, R.; Wachs, W. O.; Berger, R. G.; Kalbitzer, H. R.; Waidelich, D.; Bayer, E.; Wagner-Redeker, W.; Zeppezauer, M. *Int. J. Pept. Protein Res.* **1994**, *45*, 26-34.
4. Ferrel, R. E.; Olcott, H. S.; Fraenkel-Conrat *J. Am. Chem. Soc.* **1948** *70*. 2101-2107.
5. Ottinger, E. A.; Xu, Q.; Barany, G. *Peptide Res.* **1996**, *9*, 223-228.
6. Lacombe, J.M.; Andriamanampisoa, F.; Pavia, A. A. *Int. J. Pept. Protein Res.* **1990**, *36*, 275-280.
7. Kitas, E. A.; Knorr, R.; Trzeciak, A.; Bannwarth, W. *Helv. Chim. Acta* **1991**, *74*, 1314-1328.
8. Perich, J. W.; Ruzzene, M.; Pinna, L. A.; Reynolds, E. C. *Int. J. Pept. Protein Res.*
9. Bannwarth, W.; Trzeciak, A. *Helv. Chim. Acta* **1987**, *70*, 175-186
10. Perich, J. W.; Johns, R. B. *Tetrahedron Lett.* **1988**, *29*, 2369-2372.
11. de Bont, H. B. A.; van Boom, J. H.; Liskamp, R. M. J. *Tetrahedron Lett.* **1990**, *31*, 2497-2500.
12. Starker, G.; Jakobsen, M. H.; Olsen, C. E.; Holm, A. *Tetrahedron Lett.* **1991**, *32*, 5389-5392.
13. Andrews, D. M.; Kitchin, J.; Seale, P. W. *Int. J. Pept. Protein Res.* **1991**, *38*, 469-475.
14. Wakamiya, T.; Saruta, K.; Yasuoka, J.; Kusumoto, S. *Chemistry Lett.* **1994**, 1099-1102.
15. Kupihár, Z.; Váradi, Gy.; Monostori, É.; Tóth, G. K. *Tetrahedron Lett.* **2000**, *41*, 4457-4461.
16. Garegg, P.J.; Lindh, I.; Regberg, T.; Stawiński, J.; Stromberg, R. *Tetrahedron Lett.* **1986**, *27*, 4051-4054.
17. Froehler, B.C.; Matteucci, M.D. *Tetrahedron Lett.* **1986**, *27*, 469-472.
18. Larsson, E.;Lüning, B. *Tetrahedron Lett.* **1994**, *35*, 2737-2738.
19. Kers, A.; Kers, I.; Stawiński, J.; Sobkowski, M.; Kraszewski, A. *Synthesis* **1995**, *4*, 427-430.

The *H*-Phosphonate Approach to the Synthesis of Phosphopeptides on Solid-Phase

Zoltán Kupihár, Zoltán Kele and Gábor K. Tóth *Department of Medical Chemistry, University of Szeged, Dóm tér 8., H-6720 Szeged, Hungary*

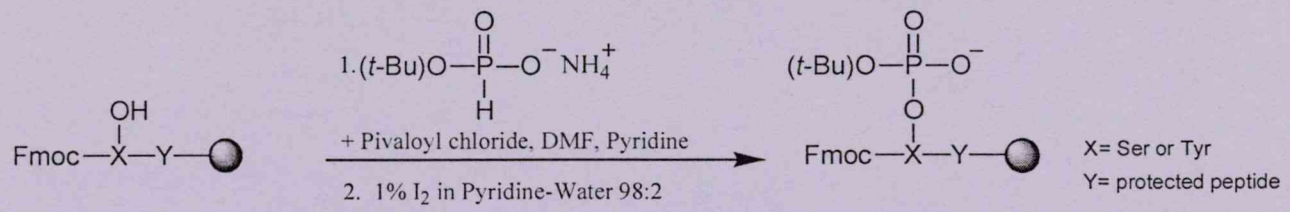

Ammonium--*tert*-butyl *H*-phosphonate was used for phosphorylation of Tyr- and Ser-containing peptides synthesized by an Fmoc strategy.